Development of Solid Supported Glycosyl Phosphonates and their Application Towards the Synthesis of Bioactive Cardiotonic Steroids

by

Ryan Rutkoski

A dissertation submitted in partial fulfillment
of the requirements for the degree of
Doctor of Philosophy
(Medicinal Chemistry)
in the University of Michigan
2024

Doctoral Committee:

Professor Pavel Nagorny, Chair
Assistant Professor Tim Cernak
Research Assistant Professor Martin Clasby
Professor John Montgomery

Ryan Rutkoski

rutkoski@umich.edu

ORCID iD: 0009-0002-1346-750X

© Ryan Rutkoski 2024

Dedication

I dedicate this thesis to all of my friends and family who have supported me throughout my time in school, and to the late Guy Fieri, my noble hedgehog.

Acknowledgements

I would like to especially thank my advisor, Dr. Pavel Nagorny, for his support and guidance over the course of my graduate studies. He has imparted innumerous wisdom and I have developed immensely as a chemist and a person thanks to his guidance.

I'd like to thank the members of my committee, Dr. Martin Clasby, Dr. Tim Cernak, and Dr. John Montgomery for their advice and guidance throughout my dissertation research. I'd also like to thank all members of the Nagorny group, past and present. Nolan Carney, Sungjin Kim and I all joined the lab together circa 2019, and it was a blast progressing through our respective programs over the years. I'd like to acknowledge the rest of the Nagorny lab, Dr. Siyuan Sun, Dr. Sibin Wang, Dr. Zach Fejedelem, Oleskii Zhelavskyi, Dr. Ievgen Zviagin, Colin Tichvon, and Zoey Surma, for their friendship and scientific advice. I will forever cherish the memories.

My family has been greatly supportive of my decision to may over 500 miles away to pursue my graduate degree. I want to thank Beverly Langevin, who took a similar path for her PhD, and probably subconsciously put Michigan higher than any other school I had considered. To my parents Lynne and Joseph, and my brother Jonatham, I am eternally grateful for your unending love and support, I love you all very much.

To all the friends I've made along the way, I couldn't have done it all without you. From a group of engineering students at Rowan University, Warney, Will, Shaggy, Jake, John, Kyle, and Cali, our Dungeons and Dragons adventures, camping excursions, and Independence Day shenanigans have always kept my spirits high. And all of the friends I've had the pleasure to

make in Michigan, especially my cohort-mates, Andrew and Luis, all of football games, camping trips, weddings and movie nights made these past years far more enjoyable than I could've imagined.

A final thank you to Dr. Mery Vet George De la Rosa, for your love and support, I am forever grateful to have you in my life and continue our adventures beyond the thrills of graduate school. I love you very much, and can't wait to explore the world with you now that we're doctors.

Table of Contents

Dedication ii

Acknowledgements iii

List of Tables viii

List of Figures ix

List of Schemes x

List of Appendices xiv

List of Abbreviations xv

Abstract xxii

Chapter 1 Introduction to Glycosylation 1

1.1 Introduction to solid supported glycosylation 1

1.2 Strategies for solid supported glycosylation 4

1.2.1 Polymer Supports 7

1.2.2 Linkers 9

1.2.3 Protecting Groups 11

1.2.4 Analytical Methods 12

1.3 Application of solid supported synthesis to natural product glycosides 13

1.4 Introduction to glycosylated cardiotonic steroids in medicinal chemistry 17

1.4.1 Synthesis of glycosylated cardenolides and bufadienolides 19

1.5 References 27

Chapter 2 Development of Polystyrene Supported Phosphonic Acid Resins for Carbohydrate Immobilization and Glycosylation 40

2.1 Introduction 40

2.2 Development of solid supported glycosyl phosphonates 43
2.2.1 Preparation of polymer supported phosphonic acids 43
2.2.2 Installation of sugars to solid support 45
2.3 Glycosylations with solid supported glycosyl phosphonate donors 50
2.4 Resin bound 2-deoxy glycosides and glycosylation of cardiotonic steroids 58
2.5 Studies towards on-resin glycosylation and protecting group manipulations 64
2.5.1 Protecting group manipulations of resin bound carbohydrates 64
2.5.2 Iterative glycosylation on solid support 65
2.6 Conclusions 75
2.7 Experimental 78
2.7.1 General Methods 78
2.7.2 Preparation of known compounds 80
2.7.3 Preparation of new compounds, resins, and reaction monitoring studies 80
2.8 References 151
Chapter 3 Introduction to Synthesis of Bufadienolide Natural Products 159
3.1 Introduction to bufadienolides 159
3.2 Synthesis of bufadienolides 160
3.2.1 Conversion of butenolides to bufadienolides 174
3.2.2 Synthesis of bufogargarizins 178
3.3 Conclusions 185
3.4 References 186
Chapter 4 Studies Towards the Synthesis of Bufadienolides 193
4.1 Introduction 193
4.2 Oxidative butenolide cleavage and model substrate synthesis 196
4.3 Intermolecular 1,4-addition and cycloaddition strategies 197

4.4 Intramolecular 1,2-addition strategies for bufadienolide synthesis 204

4.4.1 Studies of 1,2-addition via metal-halogen exchange 204

4.4.2 Studies of 1,2-addition via the intramolecular aldol reaction with pyruvate enolates 210

4.5 Reaction of internal alkynes toward the synthesis of bufadienolides 212

4.5.1 Rearrangements of propargyl alcohols towards the synthesis of bufadienolides .. 220

4.6 Conclusions 224

4.7 Experimental 226

4.7.1 General Methods 226

4.7.2 Preparation of known compounds 228

4.7.3 Preparation of new compounds 228

4.8 References 251

Chapter 5 Summary and Future Directions 262

Appendices 272

List of Tables

Table 1.1: Early rhamnosylations with glycosyl bromides 22

Table 2.1: Glycosylation condition optimization[a] 51

Table 2.2: Optimization of glycosylation with 2-deoxyglucose resin **2.18**.[a] 61

Table 2.3: Preliminary on-resin glycosylation studies[a] 67

Table 2.4: Studies of glycosylation of homogenous glycosylphosphonates[a] 69

Table 2.5: Glycosylation on resin bound carbohydrates bearing C6 hydroxyl moiety[a] 71

Table 4.1: Reaction screening of aldehyde **4.35** with 2-sulfanyl silylketene acetals **4.42** and **4.30.**[a] 201

Table 4.2: Investigation of intramolecular 6-*exo*-trig cyclization via 1,2-carbonyl addition[a] 206

Table 4.3: Reductive cyclizations of propiolate ester **4.67**.[a] 209

Table 4.4: Investigations of the intramolecular aldol reaction of pyruvate ester **4.72**.[a] 212

Table 4.5: Semi-hydrogenations of internal alkyne **4.81**.[a] 216

Table 4.6: Semi-reduction of pregnenolone-alkynyl-acetonide **4.84**.[a] 218

Table 4.7: Optimization of acetonide removal and intramolecular lactonization.[a] 219

Appendix Table A.1: Computed relative stabilities of methyl boronic acid esters derived from steroids 1–3 (DFT, B3LYP, 6-31+G*) 278

Appendix Table A.2 Optimization of regioselective rhamnosylation of anhydro-ouabagenin .. 281

Appendix Table A.3: Computed energies for the regioisomeric boronates 296

Appendix Table B.1: Glycosylation of thioglycoside donors **B.8** and **B.11** 312

List of Figures

Figure 1.1: Selected polymer supports in solid-phase carbohydrate synthesis 8

Figure 1.2 Selected linkers for solid phase carbohydrate synthesis 10

Figure 1.3 Medicinally relevant cardiotonic steroids 18

Figure 1.4: Selected examples of various cardenolides containing deoxy sugars. 19

Figure 2.1: Overview of solid supported glycosylation 41

Figure 2.2: Comparison of crude 1H NMR spectra for the reaction of **2.21** with resin **2.16** or corresponding trichloroacetimidate **2.43** as donors. 56

Figure 2.3: Recyclability of resin **2.2** 57

Figure 3.1: Selected examples of naturally occurring bufadienolides 160

Figure 3.2: Cardenolides and bufadienolides with similar steroidal oxygenation patterns. 174

Figure 3.3: Bufogargarizins A-C, *abeo*-steroids with unusual carbon skeletons 179

Appendix Figure A.1: Polyhydroxylated cardiotonic steroid aglycones and challenges with site-selective glycosylation 275

Appendix Figure A.2: Evaluation of anti-inflammatory activity of 200 nM solutions of digoxin and prepared compounds **A.2**, **A.16**, **A.20**, **A.21**, **A.24.** 284

List of Schemes

Scheme 1.1: Recent methods of one-pot regioselective carbohydrate protection 2

Scheme 1.2: Selected methods for stereochemical control of glycosylations on solid support. 3

Scheme 1.3 Strategies for solid support glycosylation 6

Scheme 1.4: Kirshning's polymer supported steroid glycosylations. 15

Scheme 1.5: Bennet's thioglycoside resin for *O*-glycosidation 16

Scheme 1.6: First glycosylation of cardiotonic steroids 20

Scheme 1.7: Rhamnosylation of cardiotonic steroids with trichloroacetimidates 24

Scheme 1.8: Regioselective protecting group strategies enabling regioselective glycosylation of cardenolides. 26

Scheme 1.9: One-pot regioselective glycosylation of strophanthidol 27

Scheme 2.1: Chiral phosphoric acid catalyzed regioselective glycosylation of a macrolactone via a covalent phosphate intermediate 42

Scheme 2.2: Preparation of phosphonic acid resins..... 44

Scheme 2.3: Initial optimization of glycosyl phosphonate formation 46

Scheme 2.4: Phosphonylation of acylated glycosides 47

Scheme 2.5: Preparation of immobilized glycosyl phosphonates 49

Scheme 2.6: Potential mechanism for formation **2.23**..... 52

Scheme 2.7: Glycosylation substrate scope[a]..... 54

Scheme 2.8: Preliminary study of 2-deoxy glycoside transfer from resin **2.18**..... 58

Scheme 2.9: Immobilization of 2-deoxyglycosides..... 59

Scheme 2.10: Notable byproducts from glycosylation of cardiotonic steroids with oleandral 60

Scheme 2.11: Substrate scope for glycosylations with 2-deoxyglycosyl resins.[a]..... 63

Scheme 2.12: Attempts at protect group manipulations on solid supported glycosyl phosphonates.[a] 65

Scheme 2.13: Loading of C4-Fmoc sugars to solid support for carbohydrate elongation. 66

Scheme 2.14: Homogeneous model for carbohydrate protecting group removal and glycosylation[a] 68

Scheme 2.15: Immobilization and deprotection of C6-OFmoc of carbohydrates for on-resin glycosylations[a] 70

Scheme 2.16: Deglycosylation of resin bound disaccharides[a] 72

Scheme 2.17: Studies of on-resin elongation with PMB as the temporary protecting group[a] 73

Scheme 2.18: Studies toward on-resin sulfur-linker disaccharide synthesis[a] 74

Scheme 3.1: Sondheimer's semisynthesis of bufalin **3.3** and resibufagenin **3.5** from 14α-hydroxycortexolone **3.7** 161

Scheme 3.2: Stache's synthesis of scillarenin **3.1** from a cortisone derivative **3.14** 163

Scheme 3.3: Pettit's synthesis of a 5β,14α-bufadienolide 164

Scheme 3.4: Yoshii's synthesis of bufalin **3.3** and resibufagenin **3.5** via transient epoxy cyclopropane **1.33** 165

Scheme 3.5: Wicha's synthesis of 3β-acetoxy-14α-H bufadienolide **3.25** 166

Scheme 3.6: Watt's synthesis of bufadienolide **3.39** 167

Scheme 3.7: Welzel's synthesis of 3-*O*-acetyl bufalin **3.47** from deoxycholic acid 168

Scheme 3.8: Synthesis of butenolides and bufadienolides by cross coupling and hydrogenation 170

Scheme 3.9: Inoue's synthesis of bufalin **3.3** 171

Scheme 3.10: Nagorny's synthesis of cinobufagin **3.6** 173

Scheme 3.11: Pettit's semisynthesis of bufalin **3.3** and resibufagenin **3.5** from digitoxin 175

Scheme 3.12: Wiesner's synthesis of bufalin **3.3** from digitoxigenin **3.67** 177

Scheme 3.13: Li's synthesis of the tetracyclic core of bufogargarizin C **3.84** 180

Scheme 3.14: Li's synthesis of bufogargarizin A **3.82** 183

Scheme 3.15: Li's synthesis of bufogargarizin B **3.83** 184

Scheme 4.1: Selected previous syntheses towards bufadienolides 194

Scheme 4.2: Synthesis of C17 heterocyclic analogs of butenolides and bufadienolides 195

Scheme 4.3: Oxidative cleavage of butenolides to access key hydroxy ketone intermediate **4.2**[a] 196

Scheme 4.4: Synthesis of model pregnenolone-derived hydroxy ketone **4.25**.[a] 197

Scheme 4.5: Previous studies of pyrone formation via cycloaddition and oxidation 198

Scheme 4.6: Synthesis of unsaturated aldehyde **4.35** 199

Scheme 4.7: Preliminary reaction study of aldehyde **4.35** with silyl ketene acetal **4.39**.[a] 200

Scheme 4.8: Enol lactonization studies of **4.44**[a] 202

Scheme 4.9: Cyclization with selenyl ketene acetal **4.50** and ethyl ethynyl ether **4.53**[a] 203

Scheme 4.10: Strategy and substrate for intramolecular cyclization via 1,2-addition 205

Scheme 4.11: Proposed mechanisms for the formation of byproducts **4.25**, and **4.60**-**4.62** 208

Scheme 4.12: Synthesis of propiolate ester substrate **4.67**.[a] 209

Scheme 4.13: Pyruvate aldol strategy for α-pyrone synthesis 211

Scheme 4.14: Alkyne reduction and lactonization strategy towards the synthesis of α-pyrones. 214

Scheme 4.15: Acetonide protection of diol **4.81**.[a] 217

Scheme 4.16: Studies of isomerization and dehydration of lactones **4.83** and **4.59** to α-pyrone **4.86** 220

Scheme 4.17: Au-catalyzed rearrangement of propargylic alcohol **4.81**. 221

Scheme 4.18: Mechanism for formation of furan **4.87**. 221

Scheme 4.19: Phosphine promoted synthesis of allenes and α-pyrones 222

Scheme 4.20: Studies of allene formation and rearrangements toward the synthesis of bufadienolides.[a] 223

Appendix Scheme A.1: Traceless boronic acid protecting group for the selective protection of the C19 position of cardiotonic steroids 277

Appendix Scheme A.2: C3-selective (α)-L-rhamnosylation of strophanthidol **A.3** 279

Appendix Scheme A.3: Initial studies on C3-selective (a)-*L*-rhamnosylation of anhydro-ouabagenin **A.2** 280

Appendix Scheme A.4: One-pot regioselective glycosylation of anhydro-ouabagenin **A.2** 282

Appendix Scheme A.5: Attempts to accomplish the C3-selective glycosylation of ouabagenin **A.1** 282

Appendix Scheme B.1: Computed energies of dioxolenium-type intermediates of galactosylation with C2 and C4 benzoate protecting groups 307

Appendix Scheme B.2: Possible mechanisms for directing group participation in galactosides 308

Appendix Scheme B.3: Synthesis of galactose benzylidene intermediate **B.3** 309

Appendix Scheme B.4: Synthesis of galactosyl donor **B.8**. 310

Appendix Scheme B.5: Synthesis of galactosyl donor **B.11** 311

Appendix Scheme B.6: Glycosylation with an activator with a non-coordinating counterion.[a] 313

List of Appendices

Appendix A: Synthesis and Evaluation of Ouabagenin and Ouabain Analogs and Anti-inflammatory Agents 273

A.1 Introduction 273

A.2 Regioselective synthesis of strophanthidol, anhydro-ouabagenin, and ouabagenin 276

A.3 Biological evaluation of anti-inflammatory activity 283

A.4 Conclusions 287

A.5 Experimental 288

A.6 References 299

Appendix B: Probing the effect on remote participation for galactosylation 304

B.1 Introduction 304

B.2 Synthesis of galactosyl donors and studies on galactosylation diastereoselectivity 308

B.3 Conclusions 313

B.4 Experimental 314

B.5 References 325

List of Abbreviations

α	alpha
β	beta
δ	chemical shift
Δ	reflux
$\Delta^{x,x}$	double bond/olefin
µ	micromoles
6-dEB	6-deoxy-erythronolide B
Ac	acetyl
acac	acetylacetonate
ACS	American Chemical Society
ANOVA	analysis of variance
aq	aqueous
Ar	aromatic
atm	atmosphere (unit)
Bn	benzyl
br	broad
BRSM	based on recovered starting material
BSP	benzenesulfinyl piperidine
Bu	butyl

Bz	benzoyl
CBS	Corey-Bakshi-Shibata
CDI	carbonyldiimidazole
COD	cyclooctadiene
COSY	correlated spectroscopy
CoTPP	5,10,15,20-Tetraphenyl-21H,23H-porphine cobalt(II)
Cp	cyclopentadiene
CPA	chiral phosphoric acid
CSA	camphor sulfonic acid
Cy	cyclohexyl
d	doublet
d	days
d.r.	diastereomeric ratio
DBU	1,8-Diazabicyclo(5.4.0)undec-7-ene
DCC	dicyclohexylcarbodiimide
DCE	1,2-dichloroethane
DDQ	2,3-dichloro-5,6-dicyano-1,4-benozquinone
DFT	density functional theory
DHEA	Dehydroepiandrosterone
DHP	dihydropyran
DiBAl-H	diisobutylaluminum hydride
DIPEA	diisopropylethylamine
DMAP	4-dimethylaminopyridine

DMDO	dimethyldioxirane
DMF	dimethylformamide
DMP	Des-martin periodinane
DMSO	dimethylsulfoxide
DMT	4,4'-dimethoxytrityl
DMTSB	(dimethylmethyl)thio-sulfonium tetrafluoroborate
dppf	1,1′-Bis(diphenylphosphino)ferrocene
DTBMP	di-tert-methylpyridine
DTBP	di-tert-butylpyridine
eq, equiv	equivalent(s)
ESI-TOF	electrospray ionization time-of-flight
Et	ethyl
Et2O	diethylether
EtOAc	ethyl acetate
FDA	Food and Drug Administration
Fmoc	fluorenylmethoxycarbonyl
fod	(6,6,7,7,8,8,8-heptafluoro-2,2-dimethyl-3,5-octanedionato)
FTIR	Fourier transformed infrared
g	grams
h	hours
HMBC	heteronuclear multiple bond correlation
HMDS	hexamethyldisilylamide
HMPA	hexamethylphosphoramide

HPLC	high performace liquid chromatography
HR-MAS	high resolution magnetic angle spinning
HRMS	high resolution mass spectra
HSQC	heteronuclear single quantum coherence
hv	light irridation
IBX	2-iodoxybenzoic acid
IKBKE	inhibitor of nuclear factor kappa-B kinase subunit epsilon
IL-1	interleukin 1
IL-6	interleukin 6
iPr	isopropyl
J	coupling constant
LCMS	liquid chromatography mass spectrometry
LDA	lithium diisopropylamide
LG	leaving group
LPS	lipopolysaccharide
m	multiplet
M	molar
mCPBA	meta-chloroperbenzoic acid
Me	methyl
MeCN	acetonitrile
MeOH	methanol
mg	milligrams
mL	milliliter

mmol	millimole
MHz	megahertz
mL	milliliters
MOM	methoxymethyl
MPEG	polyethylene methyl ether
MS	molecular sieves
MsCl	methanesulfonyl chloride, mesyl chloride
NBS	N-bromosuccinimide
NIS	N-iodosuccinimide
nM	nanomolar
nm	nanometer
NMP	N-methylpiperidine
NMR	nuclear magnetic resonance
p-BrBz	para-bromobenzoate
PCC	pyridinium chlorochromate
PEG	polyethylene glycol
Ph	phenyl
PhH	benzene
PhMe	toluene
Pin	pinnacol
PMB	para-methoxybenzyl
p-NO_2Bz	para-nitrobenzoyl
ppm	parts per million

PPTS	pyridinium para-toluene sulfonate
PS	polymer supported
p-TsOH	para-toluenesulfonic acid, tosylic acid
q	quartet
R	alkyl/aryl
Ra-Ni	Raney nickel
Rf	retention factor
RP	reverse phase
s	singlet
sat	saturated
SET	single electron transfer
SP	solid phase
t	triplet
TBAF	tetrabutylammonium fluoride
TBS	tert-butyl-dimethylsilyl
TBSOTf	tert-butyl-dimethylsilyl trifluoromethanesulfonate
tBu	tert-butyl
tBuOMe	tert-butyl methyl ether
Tc	thiophenecarboxylate
TEOA	triethanolamine
TES	triethylsilyl
Tf	trifluoromethylsulfonyl, triflyl
Tf2O	trifluoromethane sulfonic anhydride, triflic anhydride

TFA	trifluoroacetic acid
TfOH	trifluoromethane sulfonic acid, triflic acid
THF	tetrahyrdofuran
THP	tetrahydropyran
TLC	thin layer chromatography
TMS	trimethylsilyl
TMSOTf	trimethylsilyl trifluoromenthanesulfonate
TNFα	tumor necrosis factor alpha
TolSCl	toluenesulfenyl chloride
Ts	toluenesulfonyl
TsCl	tosylchloride
TTBP	2,4,6-tri-tert-butylpyrimidine
UV	ultraviolet
WHO	World Health Association

Abstract

Carbohydrates play an essential role in biological process including metabolism, energy storage, intercellular communication and immunorecognition. From 2015-2020, of the over 200 FDA approved new small molecule drugs, only nine contained a carbohydrate unit. Carbohydrate drugs and vaccines remain niche due to their complex and labor intensive synthesis, which requires careful regio- and stereocontrol of the glycosidic bond formation. Carbohydrate containing natural products are widely found in traditional and modern medicines as anticancer, antibacterial, antiviral, anti-inflammatory and antiarrhythmic agents, amongst numerous other indications. In Chapter 1, we provide an overview of previous methods and technologies for solid supported carbohydrate synthesis and the glycosylation of cardiotonic steroids. In Chapter 1, we describe the development of novel solid supported glycosyl phosphonate donors. The phosphonic acid resin was prepared from Merrifield resin on decagram scale. Fifteen different protected sugars were immobilized on the solid supported resin in up to 96% yield. The immobilized donors were used to prepare 22 different glycosylated products in up to 96% yield. Reactions conditions were tolerant of natural products containing acid- and base- sensitive functionalities, and oxidation prone substituents. The resins were recyclable, and the same resin could be reloaded with sugar and used for additional glycosylations without reduction in yield or selectivity. The crude reaction profiles of the reactions with immobilized donors were less contaminated with byproducts of donor decomposition than traditional methods with solution phase donors. Finally, the resins were used for solid supported carbohydrate synthesis, and the

immobilized carbohydrates were glycosylated to form disaccharides on the solid support. In Chapter 3, previous strategies for the synthesis of bufadienolide natural products are reviewed. In Chapter 1, we describe the development of methods for the diversification of abundant natural product cardenolides to unnatural heterocyclic analogs. Cardenolides were efficiently converted to a key hydroxy ketone intermediate via oxidative cleavage, and the hydroxy ketone intermediate could be elaborated to lactone-, furan-, and allene-containing analogs. Appendix A describes the synthesis and anti-inflammatory activity of natural and unnatural glycosylated cardiotonic steroids. Carbohydrate containing compounds anhydro-ouabain and convallatoxol were found to reduce LPS induced neuro-inflammation, whereas the aglycone *anhydro*-ouabain was found to exacerbate neuro-inflammation. Appendix B describes an investigation of the factors governing the mechanism of glycosylation based on DFT calculations of the expected reaction intermediates. Based on experimental validation of the computational models, several new glycosyl donors were prepared to evaluate the importance of the thermal stability of the reaction intermediates.

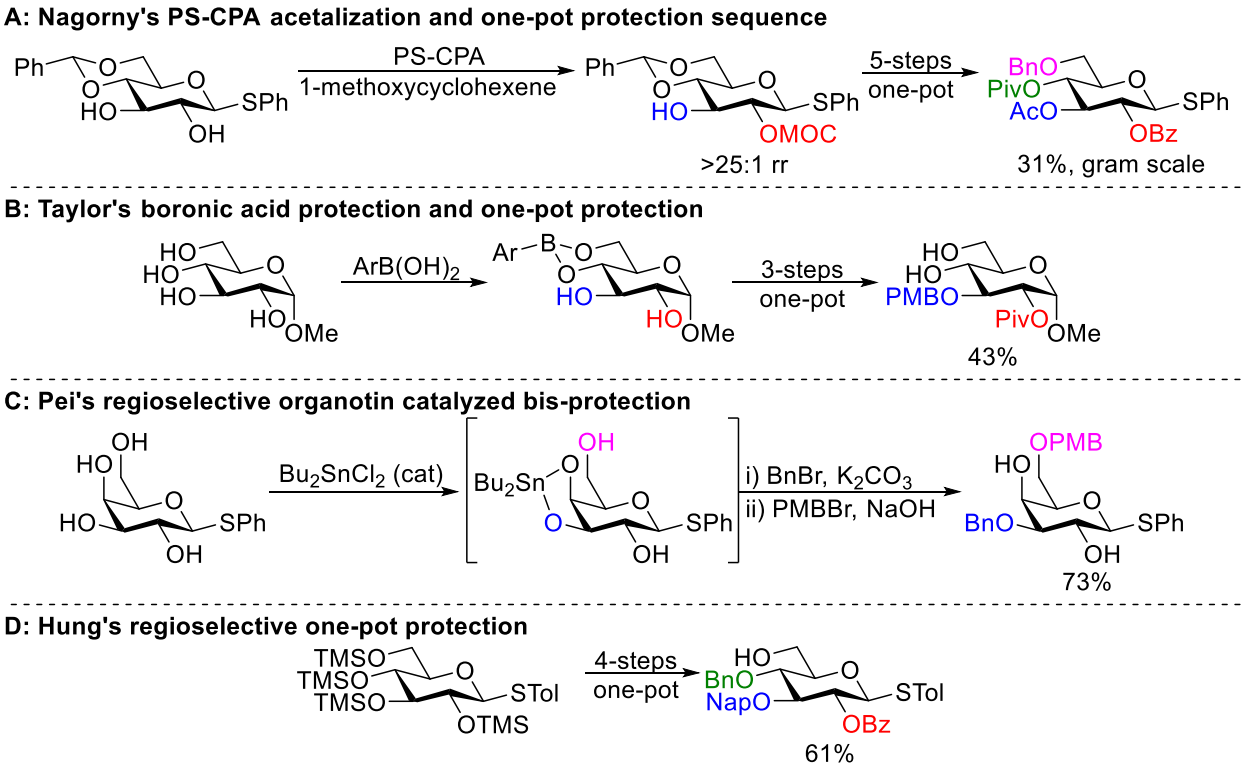
Chapter 1 Introduction to Glycosylation

1.1 Introduction to solid supported glycosylation

Solid supported synthesis was initially developed for the preparation of polypeptides by Merrifield in 1963[1] and its impact on chemistry and biology was highlighted by his Nobel prize in chemistry in 1984.[2] Since then, solid supported synthesis has been expanded for the synthesis of oligonucleotides,[3,4] oligosaccharides,[5,6] and combinatorial libraries.[7,8] The first solid supported synthesis of di- and tri- saccharides was reported in the early 1970's by Fréchet and Scheurch.[9–11] Since then, numerous larger oligosaccharides have been synthesized using solid supported synthesis,[5,6] and the synthesis of oligosaccharides has been automated using high performance liquid chromatography systems[12] as well as dedicated glycan synthesizers,[13] With solid supported synthesis, oligosaccharides up to 151-units have been prepared.[14] Numerous biopolymers have been prepared via solid phase oligosaccharide synthesis including heparins,[15,16] chondroitins,[17] and hyaluronic acids.[18] Combined approaches of solid phase peptide and saccharide synthesis have been used for the preparation of glycopeptides.[19] The synthesis of glycosylated natural products, including cardenolides[20] and aminoglycoside antibiotics,[21] has been performed via solid phase synthesis. These outstanding accomplishments were the culmination of over 50 years of innovation and invention of glycosylation methodology on both solid support and in solution.

Many aspects of the glycosylation reaction can make it more challenging to adapt to solid support compared to peptide coupling or oligonucleotide synthesis. The monosaccharide building blocks contain multiple possible sites for reactivity, and careful selection of protecting groups is needed to selectively activate the desired elongation site. Preparation of orthogonally

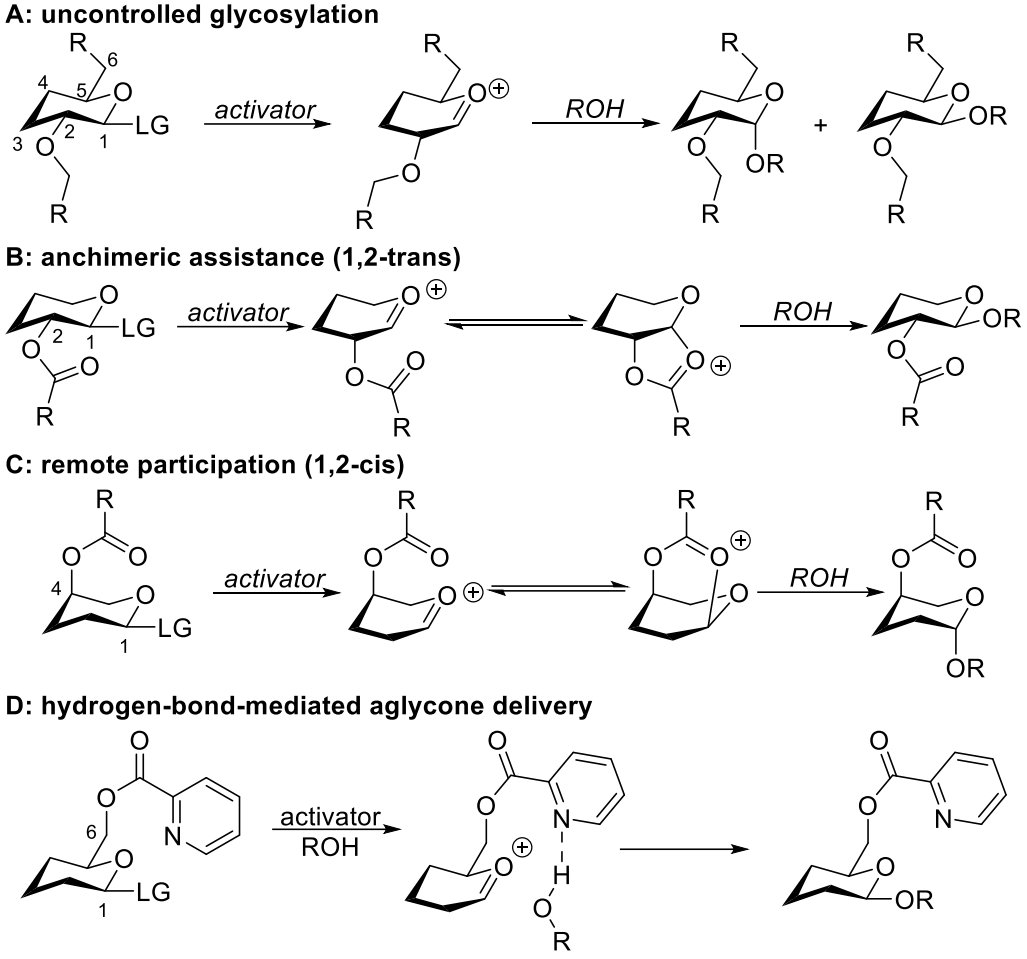
protected building blocks is essential for efficient and regioselective glycosylations. The Nagorny group had previously developed the regioselective acetalization of *cis-1,2*-diols via polymer supported (PS) CPA-catalysis (Scheme 1.1A). This methodology enabled the one-pot regioselective protection of each of the four alcohols of *D*-glucose. Monosaccharide building blocks with orthogonal protecting groups are especially required for branched oligosaccharides, where multiple protecting groups must be removed for sequential glycosylations. Other methodologies employing boronic acid (Scheme 1.1B),[22] organo-tin (Scheme 1.1C) reagents,[23,24] and one-pot procedures (Scheme 1.1D)[25,26] have also greatly expedited the synthesis of orthogonally protected building blocks.



Scheme 1.1: Recent methods of one-pot regioselective carbohydrate protection

For each glycosidic linkage, a new stereogenic center is created, and control of the stereoselectivity is crucial for high yielding sequences. Numerous methods for stereoselective glycosylation have been developed, and some have been applied to solid supported synthesis

including anchimeric assistance (Scheme 1.2B), remote directing group participation (Scheme 1.2C), and hydrogen-bond-mediated aglycone delivery (Scheme 1.2D).



Scheme 1.2: Selected methods for stereochemical control of glycosylations on solid support.

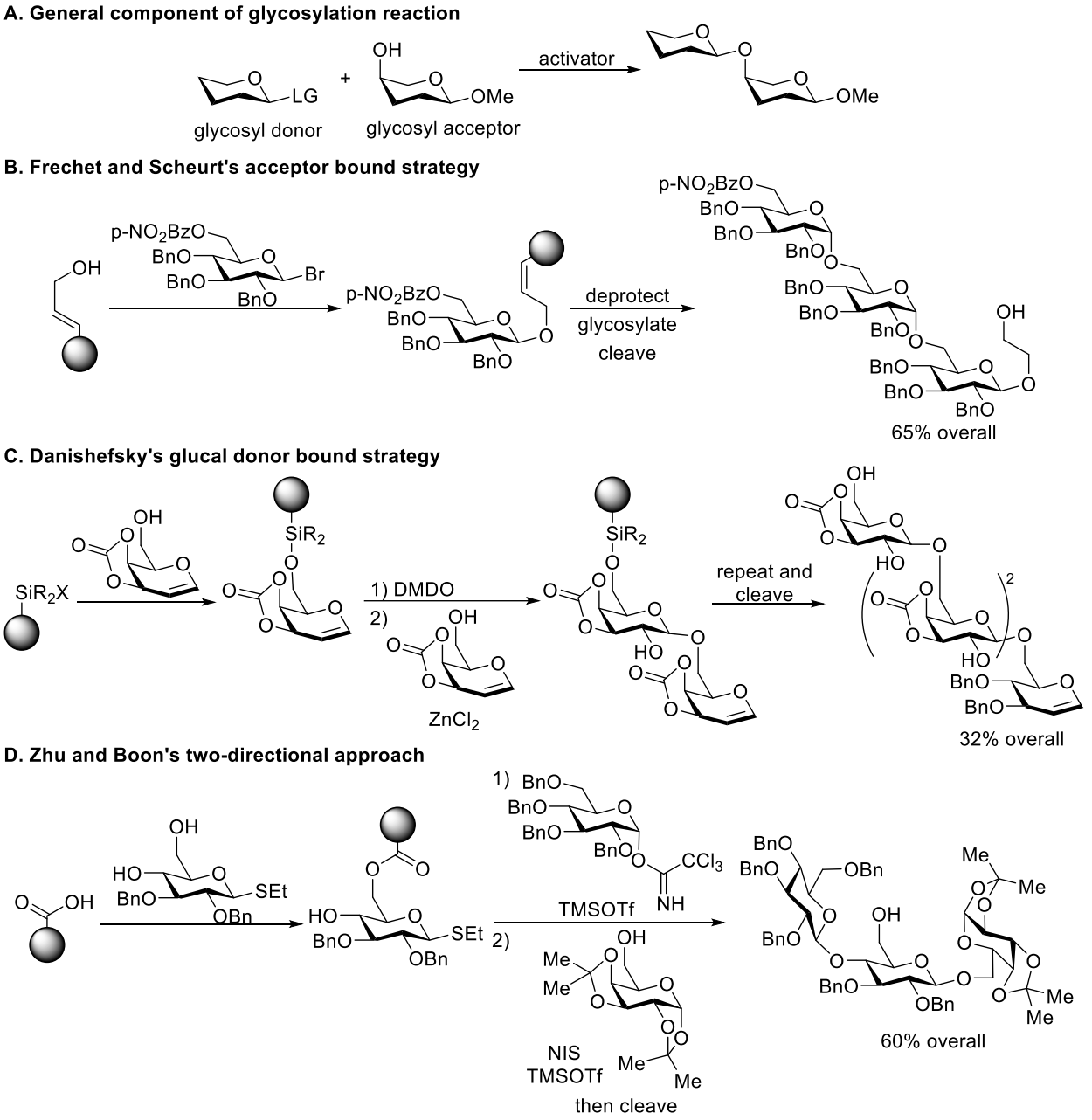
Anchimeric assistance is the oldest and most common strategy employed to facilitate stereocontrol; it allows for fast and selective 1,2-trans glycosylation.[27] Remote participation can occur from the C3-, C4-, or C6- position of the carbohydrate; it results in the glycosyl acceptor approaching from the opposite face of the participating position's directing group. For example, C4-benzoylated galactose, with the directing group on the top face at C4, the acceptor approached from the bottom face, which lead to formation of the 1,2-cis galactoside.[28] Hydrogen-bond-mediated aglycone delivery, like remote participation, can occur from the C3-,

C4-, or C6- position of the carbohydrate. A protecting group bearing a hydrogen bond acceptor, such as picolyl, picoloyl, or 2-diphenylphosphinoyl-acetyl, interacts with the acceptor and delivers it from the same face as the protecting group.[29,30] Synthetic methodology to address the challenges associated with carbohydrate chemistry paved the way for solid supported carbohydrate synthesis to be a vital tool for the preparation of bioactive molecules.

1.2 Strategies for solid supported glycosylation

The general strategy for the glycosylation reaction involves the coupling of a glycosyl donor and glycosyl acceptor. The donor typically is a protected carbohydrate with a leaving group at the anomeric (C1) position. The donor is activated and is displaced by the glycosyl acceptor (Scheme 1.3A). For solid phase glycosylations, either the acceptor or donor can be bound to the solid support, and in some cases, the carbohydrate attached to solid support can function as both the donor and acceptor. The acceptor bound strategy was used by Fréchet and Scheurt during their first report of solid supported glycosylations[9] (Scheme 1.3B). The anomeric position is attached to the solid support, and the resin can be treated with excess of the glycosyl donor, and any undesired side products can simply be removed by filtration. Capping any unreacted acceptor can help improve overall yield by reducing the amount of "deletion" byproducts.[31,32] For the donor bound strategy, the carbohydrate is attached at any position other than the anomeric position. The anomeric position of the carbohydrate is equipped with a leaving group. Upon activation and treatment with a glycosyl acceptor, the carbohydrate chain is extended on the solid support. For this method to be applicable to oligosaccharide synthesis, the anomeric position of the acceptor that is added must have a different leaving group than the resin-bound donor or be equipped with functionality that can be easily converted to a suitable leaving group after the glycosylation reaction. Typically, most common byproducts of the

glycosylation reaction result from the degradation of the glycosyl donor. Since the donor is affixed to the solid support, any unproductive side reaction would lead to chain termination, and result in reduced glycosylation yield. Danishefsky first demonstrated the utility of the donor bound strategy (Scheme 1.3C) with the synthesis of a tetrasaccharide by activation of solid support glycal donors with DMDO, then elongating the sugar-chain by activating the resulting epoxides with $ZnCl_2$.[33] The carbohydrate attached to the solid support can also act as both donor and acceptor. In this case, the carbohydrate is attached to solid support similar to the donor-bound strategy. The carbohydrate chain can be elongated from the anomeric position of the resin-bound carbohydrate ("donor-bound") or from any of the other positions ("acceptor-bound"). Zhu and Boon first demonstrated this strategy for the synthesis of trisaccharides (Scheme 1.3D) using orthogonal glycosyl donors (trichloroacetimidates and thioglycosides).[34]



Scheme 1.3 Strategies for solid support glycosylation

For most methods, the polysaccharide can be cleaved from the solid support with an anchor from the linker remaining at the reducing end. In some cases, these cleaved oligosaccharides can be used as a glycosyl donor to be attached to other oligosaccharides[14] or peptides.[35] Direct activation of the resin bound carbohydrates to be used as donors in glycosylations has not been as thoroughly explored. This strategy would allow for the prepared

polysaccharides to be directly transferred to a natural product or biomolecule without additional intermediate purifications. In some cases, resin bound thioglycosides could be activated and transferred to simple acceptors; however, these typically required a large excess of the acceptor.[36–38] In 2012, Bennet and coworkers reported the use of resin-bound thioglycosides as activatable donors (Scheme 1.5).[39] We developed solid supported glycosylphosphonates as glycosyl donors for the glycosylation of natural products, which will be discussed thoroughly later in this thesis.

1.2.1 Polymer Supports

The choice of the polymer matrix has a great effect on reaction design and substrate compatibility.[40] Merrifield's resin (polystyrene cross-linked with divinylbenzene) (Figure 1.1) was used in first solid supported glycosylation by Fréchet and Schuerch.[9] and has been the most popular amongst other solid phase oligosaccharide synthesizers.[5,41] Merrifield's resin offers high loading efficiency, wide reaction condition compatibility, and is economically priced. It can be adequately swelled in common solvents for solution glycosylation, including CH_2Cl_2, THF, PhMe, DMF, dioxane, MeCN, and Et_2O.[42] Swelling is greatly diminished in highly polar protic solvents, which limits the scope of the on-resin modifications that can be performed. Other polystyrene resins have been developed to improve swelling in especially polar solvents (MeOH, EtOH, DMF). TentaGel[43] and ArgoGel[44] (Figure 1.1) incorporate PEG chains onto the polystyrene backbone. This improves swelling in polar solvents, including water. JandaJel (Figure 1.1) introduced THF-based crosslinkers, which improved swelling in polar solvents (dioxane, THF, DMF) as well as CH_2Cl_2 and benzene.[45] The resin also proved stable to a variety of reagents including: mCPBA, DiBAl-H, aq. NaOH, aq. HCl, and 50% TFA/CH_2Cl_2, and were stable to agitation via magnetic stirring. PanzaGel (Figure 1.1) is another recently developed

resin for oligosaccharide synthesis.[46] It incorporates benzyl-diethylene glycol crosslinkers to improve swelling in polar and non-polar solvents compared to Merrifield resin and JandaGel. Even through structural modifications, polystyrene resins swell significantly less in polar solvents (MeOH, EtOH, water) compared to nonpolar solvents (CH_2Cl_2, PhMe, THF).

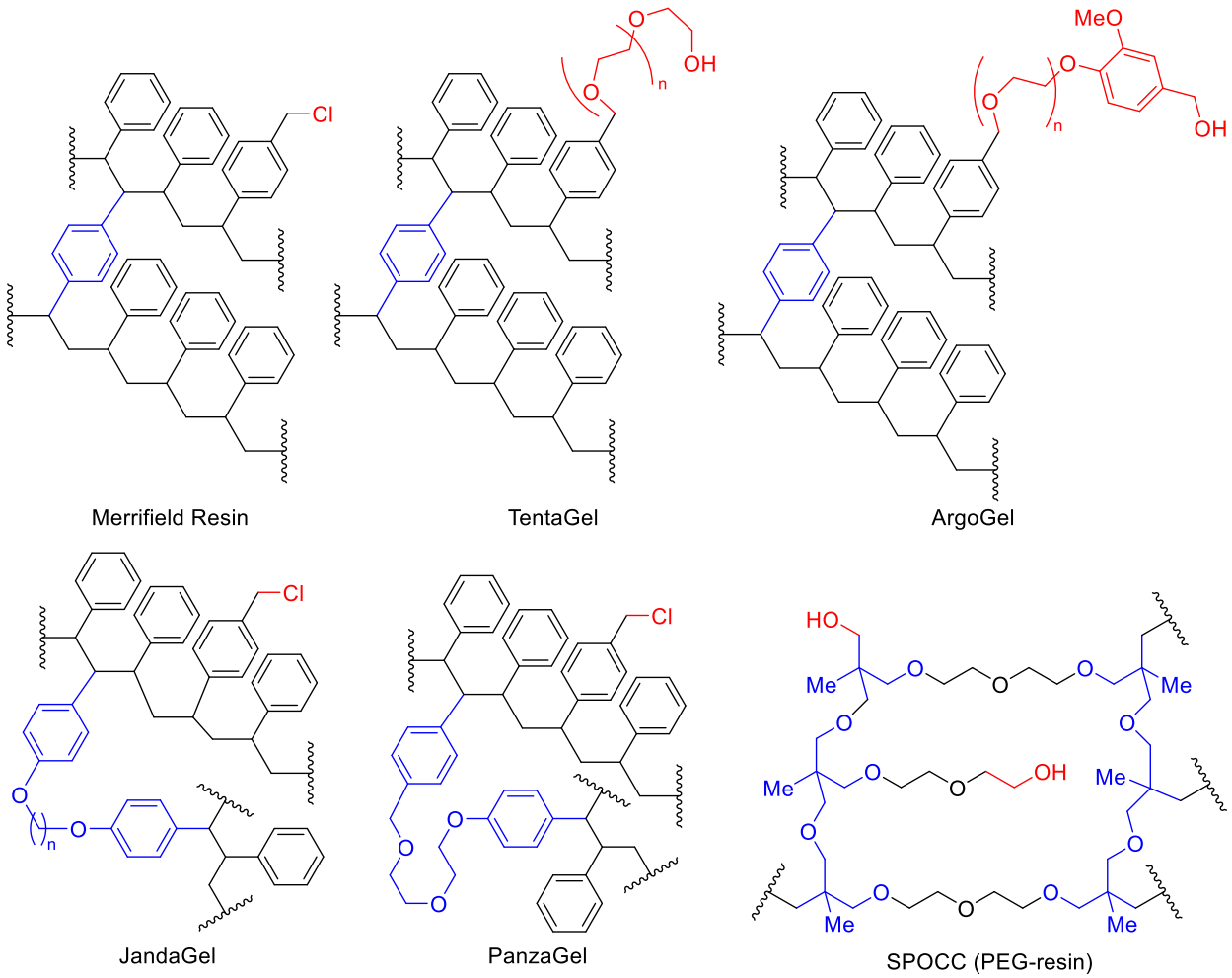


Figure 1.1: Selected polymer supports in solid-phase carbohydrate synthesis

Other polymer backbones have been investigated, including PEG-based resins and controlled pore glass supports. PEG-based (Figure 1.1) resins offer improved swelling in polar solvents, as well as higher loading capacities than Merrifield resins.[47] PEG-resins are less stable to strongly basic conditions and their higher price has inhibited their use in solid phase carbohydrate chemistry. However, they have been used in the synthesis of glycopeptides via

combined solid phase peptide synthesis and solid phase glycosylation.[19] Controlled pore glass supports have had sparing use in solid phase oligosaccharide synthesis.[48,49] The support does not require swelling, so nearly all solvents can be used with this support. Unfortunately, its propensity to fracture during stirring and incompatibility with silyl protecting groups has prevented widespread use in carbohydrate synthesis.

The diverse stability of polystyrene resins has made them the polymer of choice for most chemists performing solid phase glycosylations. Their stability to many organic reagents allows for a diverse selection of protecting groups and glycosylation conditions. Tuning of the cross-linker can improve resin swelling and stability, increasing their value and utility for glycosylations.

1.2.2 Linkers

Direct attachment of a carbohydrate to the benzylic chloride moiety of Merrifield resin is rarely performed due to the difficulty of cleaving the polysaccharide after glycosylations.[50] To make cleavage of the final glycosylated product easier, a diverse array of linkers can be employed.[5] The choice of linker dictates all further protecting groups and glycosylation conditions.[51] The linker must be sufficiently stable and orthogonal to tether the carbohydrate throughout multiple synthetic transformations and can also efficiently release the carbohydrate from the solid support.[52]

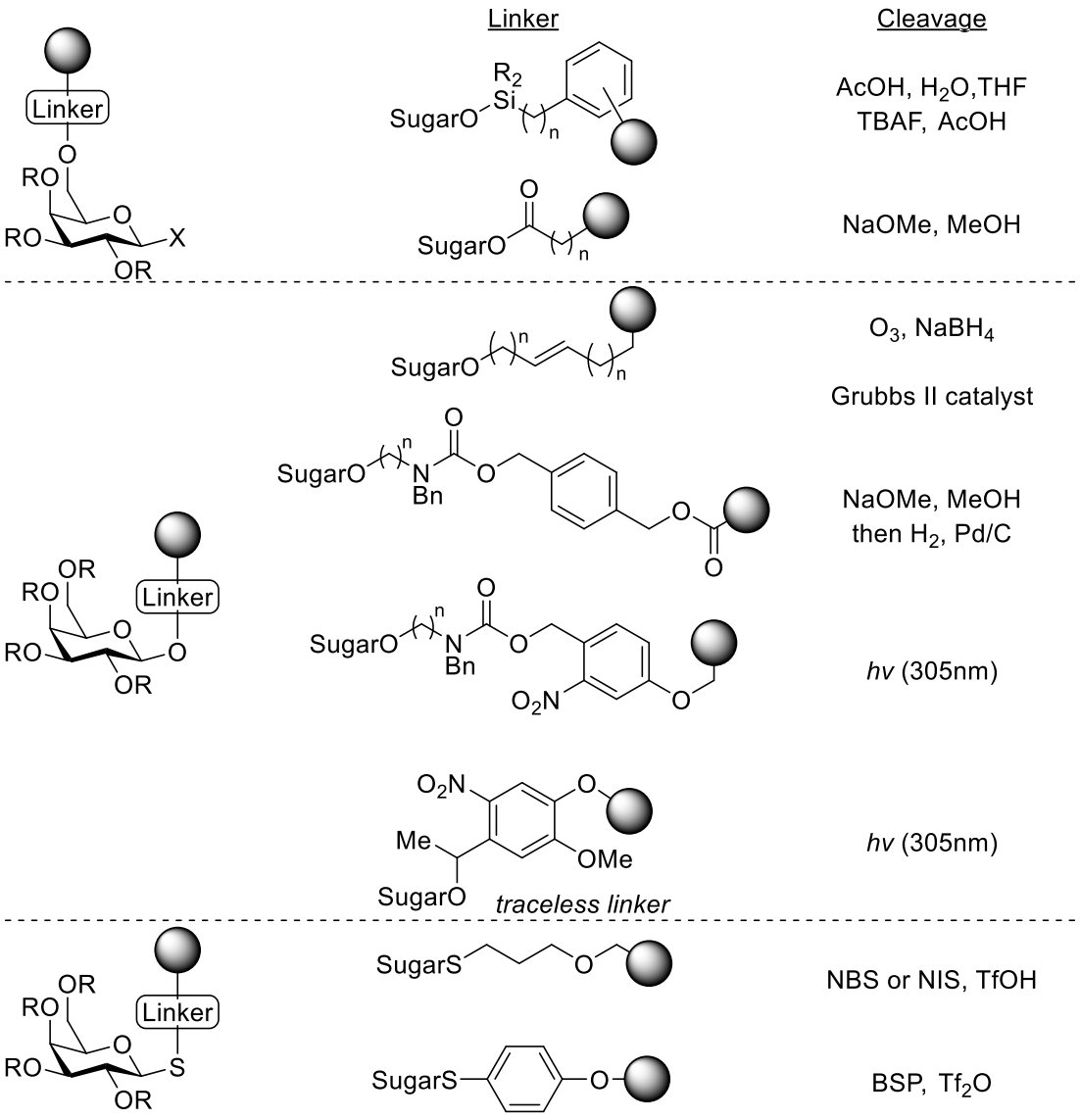


Figure 1.2 Selected linkers for solid phase carbohydrate synthesis

For all strategies of solid phase synthesis, the choice in linker dictates the compatible glycosylation conditions for synthesis on the solid support. The linker must be stable to a wide array of glycosylation conditions and are relatively stable to the mild conditions needed to remove many temporary protecting groups.[50] For the donor bound strategy, silyl groups[51–53] and esters[34,54] (Figure 1.2) have been used to attach the carbohydrate to the solid support. For the acceptor bound strategy, the primary requirement for a linker is that it will not be activated during the subsequent glycosylations. Allyl,[10] alkenyl,[55] and substituted benzyl ethers (Figure

1.2) are the most common linkers used to attach the anomeric position to the solid support. Cleavage of the allyl and alkenyl ethers was achieved by ozonolysis[10] or olefin metathesis.[55] This results in the formation of an anchored polysaccharide with an alkyl chain at the terminal anomeric position.[56] Cleavage of benzyl and substituted benzyl ethers can be achieved by a diverse set of conditions. The benzyl ethers are stable to most glycosylation conditions and mild acidic and basic conditions for protecting group manipulations. Impressively, photolabile linkers offer strong orthogonality for their removal, and have become the linker of choice for automated glycan assembly systems.[13,17] These resins also are capable of releasing the free terminal glycosyl hemiacetals, which can be quickly transformed to glycosyl donors for subsequent glycosylations.[57,58] Thioglycosides can also be attached to the solid support.[59] These solid supported thioglycosides (Figure 1.2) can be directly activated to transfer the polysaccharide to another acceptor.[36,39,59]

1.2.3 Protecting Groups

Orthogonal protecting group manipulations are vital for carbohydrate synthesis to differentiate between the multiple hydroxyl groups. Hydroxyl groups that do not need to be modified during the synthesis are protected with permanent protecting groups. These groups must be stable to many reaction conditions and will only being removed during the final global deprotection. Benzyl ethers are commonly relied upon as permanent protecting groups due to their stability to acidic and basic conditions; they are removed by hydrogenolysis at the end of the synthesis.[14] For stereoselective glycosylations, anchimeric assistance is commonly employed to control the selectivity.[27] Acetate,[60] benzoate,[31] or pivalate[61] esters have been used at the C2-position to direct 1,2-trans-glycosylations. These esters are stable to mild basic and acidic

conditions and can be used as permanent protecting groups. Stereoselective glycosylations on solid support have also been controlled by remote participation[28] and chiral auxiliaries.[62]

Temporary protecting groups are used to selectively unmask specific hydroxy groups to be used as acceptors for solid supported glycosylations. Many protecting groups that are cleaved under mild basic conditions make good temporary protecting groups, as the conditions for their removal do not interfere with glycosidic linkage tethering the carbohydrate to the solid support. They also will survive the acidic conditions typically used for the glycosylation reactions. Conditions for removal of these protecting groups are mild and the reactions are fast. Similar to solid phase peptide synthesis, Fmoc[31] and related carbonates[62] are used due to their fast and mild removal. Levulinic acid esters[63] have similarly been used due to their fast hydrolysis in the presence of hydrazine. PMB ethers[64] are easily removed via mild oxidants such as DDQ. Silyl ethers[65] are readily removed by fluoride (HF/pyridine or TBAF) without interfering with other esters. Acid labile protecting groups are generally shied away from, since the glycosylation reactions typically occur under acidic conditions and may cause competitive deprotection[5]. Some still may be employed, such as DMT,[66] trityl,[67] THP,[38] and benzylidene acetals,[68] when base labile linkers are used to attach the carbohydrates to the solid support and basic conditions are employed for glycosylations.

1.2.4 Analytical Methods

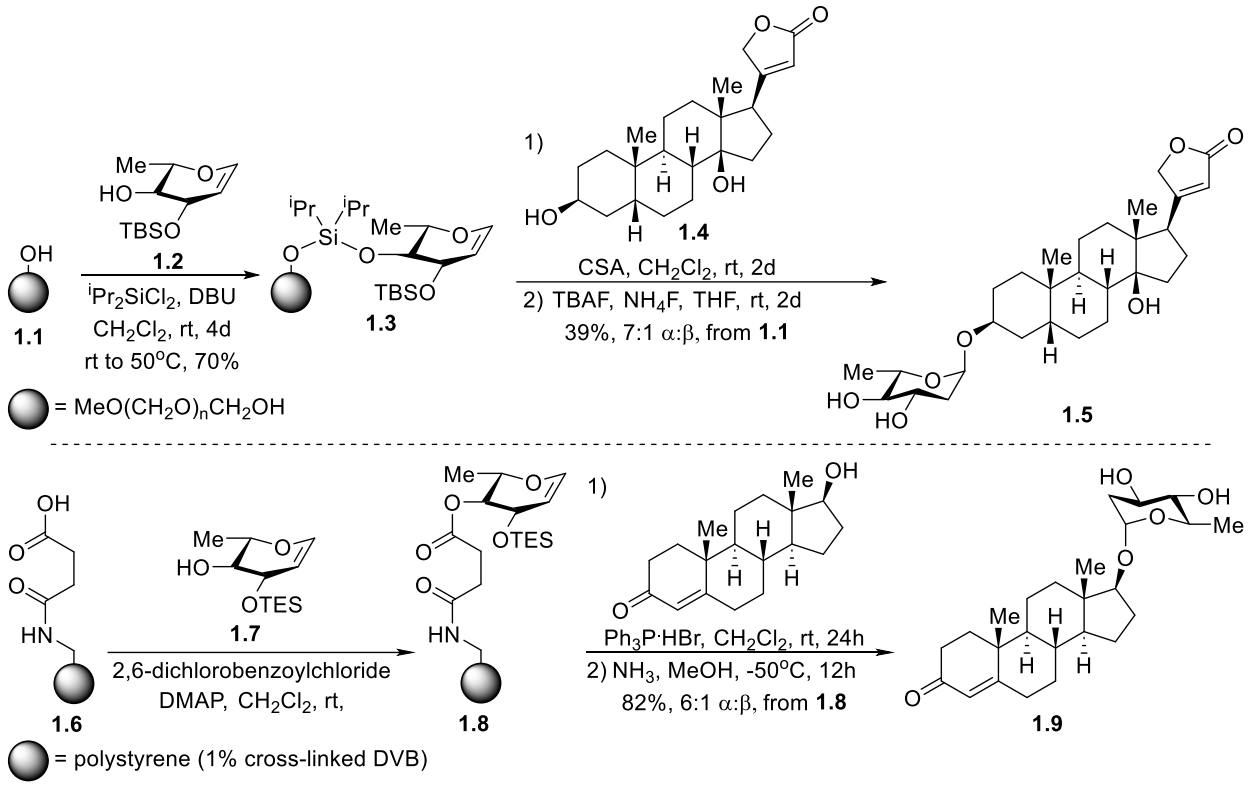
Performing reactions on solid support presents challenges not prevalent during solution phase chemistry. Monitoring reactions often cannot be accomplished by TLC or LCMS, since the products are bound to an insoluble polymer matrix and cannot be detected by these methods.[68] Gravimetric analysis is the simplest way to track reaction completion and efficiency but can be misleading if the product on the solid support undergoes side reactions.[54] In-line FTIR

spectroscopy[69] can be used to track reactions where there is a change in a functional group with a distinct absorption band, such as the carbonyl of esters[54] or terminal alkene[70] of allyl groups. In some cases, NMR can be used to monitor reactions. Gel-NMR has reduced resolution compared to standard 1-D NMR,[71] but for select nuclei (^{13}C, ^{19}F, ^{31}P)[72–78] it can provide insight into reaction progression. Solid-state NMR, namely high-resolution magic angle spinning (HR-MAS) is an impressive tool to observe high resolution spectra of the carbohydrate attached to the solid support.[79–81] This method allows for determination of glycosylation diastereoselectivity directly on the solid support, without the need to cleave the carbohydrate first before analysis.[82] Unfortunately, the high-cost specialty probe required for HR-MAS prohibits the method from being widely used. Inverse gated decoupling ^{13}C-NMR was developed for *in situ* monitoring.[83] This method required ^{13}C-enriched protecting group tags for monitoring and allowed for integration of the ^{13}C-NMR peaks to determine reaction yield.[84] Unlike HR-MAS, no information regarding the glycosylation diastereoselectivity was obtained while the carbohydrate was attached to the solid support. Indirect monitoring of the on-resin reactions is achieved by monitoring the release of protecting group by-products (e.g., dibenzofulvene from Fmoc deprotection,[39] anisaldehyde from PMB deprotection, phthalhydrazide from phthalimide deprotection,[85] triphenylmethanol from trityl deprotection).[39] Direct *in situ* monitoring of reaction progress on the solid support can be challenging and requires specialized methods, however indirect methods can provide sufficient information for method development and reaction optimization.

1.3 Application of solid supported synthesis to natural product glycosides

While widely used for oligosaccharide synthesis, solid supported carbohydrate synthesis has also been explored for the synthesis of glycosylated natural products. The first solid

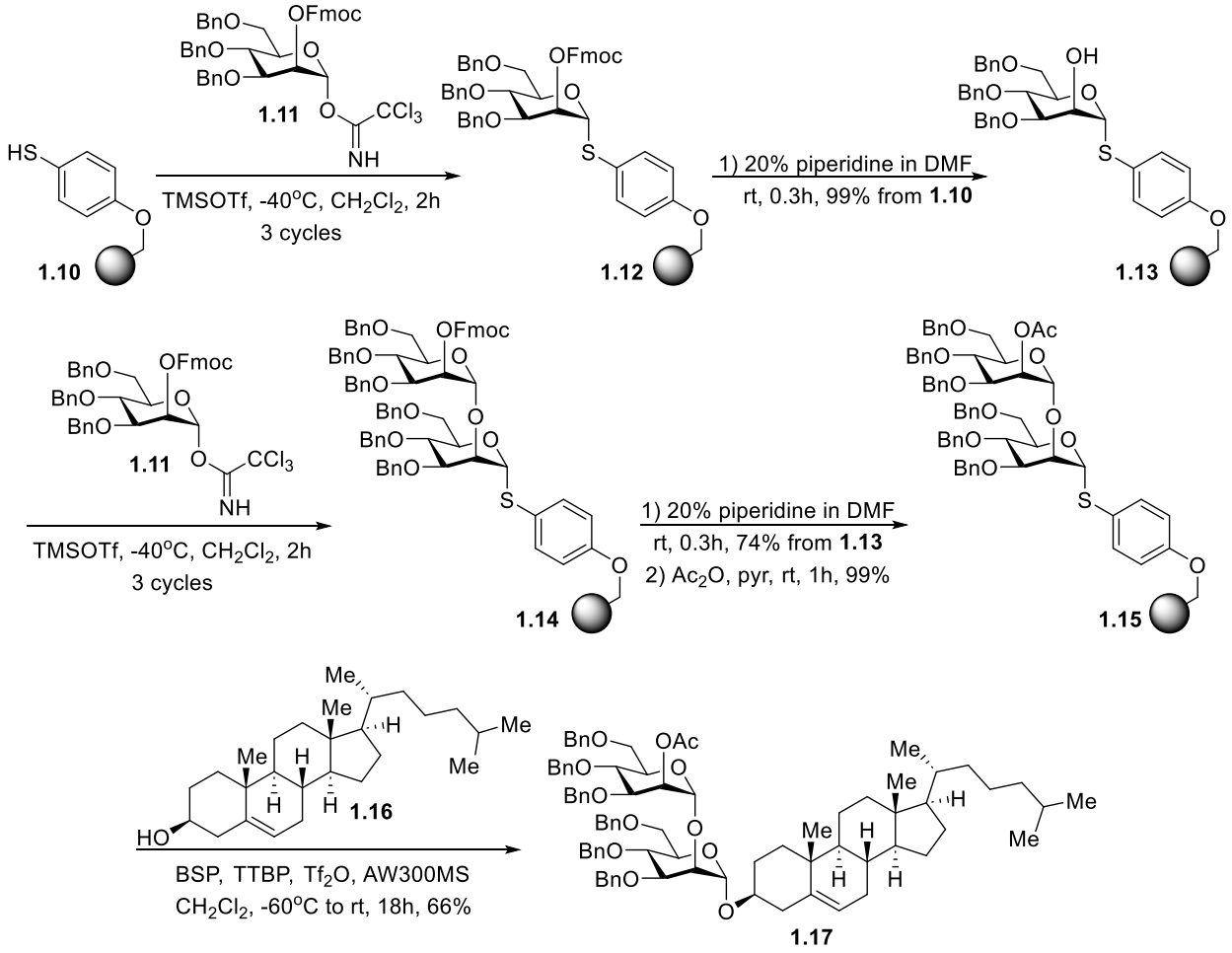
supported synthesis of glycosylated steroids was reported by Kirshning in 2000 (Scheme 1.4).[20] Following the donor bound strategy described above, rhamnal **1.2** was attached to MPEG resin **1.1** via tandem bis-silylation of the C3-alcohol of **1.2** and the alcohol moiety of **1.1** in the presence of DBU. The resin bound rhamnal **1.3** was activated with CSA and treated with digitoxigenin **1.4** to afford the resin bound glycosylated steroid. Tandem silyl deprotection and cleavage from the solid was achieved by treatment of the resin with TBAF in THF, and the resulting glycosylated steroid 3'-desmethyl-beaumontoside **1.5** was obtained in 39% overall yield as a 7:1 mixture of α- and β-glycosides. This was the first, and to date only demonstration of solid supported glycosylation of a cardenolide. Kirshning also demonstrated the utility of polystyrene resin for steroid glycosylation. Rhamnal **1.7** was attached to polystyrene resin **1.6** by esterification to the succinate linker. Activation of resin bound glycal **1.8** with $PPh_3 \cdot HBr$ and treatment with testosterone afforded α-selective glycosylation. The resin was treated with methanolic ammonia to release the deprotected glycosylated steroid **1.9** in 82% overall yield and 6:1 α:β selectivity.



Scheme 1.4: Kirshning's polymer supported steroid glycosylations.

Oligosaccharides could be cleaved from thioglycoside-linker resins by treating with large excess (>20 equiv.) of simple alcohols (MeOH, EtOH, ^{i}PrOH, BnOH) and thiophilic activator (Br_2 or DMTSB).[36,59] For natural product glycosylations, conditions where the acceptor can be used in slight excess as the limiting reagent are desirable. Direct transfer of resin bound thioglycosides to natural product aglycones was reported by Bennet in 2012 (Scheme 1.5).[39] Mannose trichloroacetimidate building block **1.11** was loaded on JandaJel polystyrene resin **1.10** that was affixed with a thiol-containing linker. For complete loading, 3.0 equivalents of donor **1.11** were used, and the cycle was repeated three times (9.0 equivalents total). The temporary Fmoc protecting group was removed by treatment with piperidine in DMF, and the loading was quantified by absorbance of the dibenzofulvene-piperidine adduct at 301 nm (99%). The resin was treated with three more cycles of **1.11** and the Fmoc group was removed in the same manner

as previously. The resulting free alcohol was acetylated to produce disaccharide resin **1.15**. Thioglycoside resin **1.15** was activated with BSP/TTBP/Tf_2O combination in CH_2Cl_2 under anhydrous conditions. Cholesterol **1.16** was added in slight excess (1.5 equivalents) to the activated glycosyl donor and the desired disaccharide containing product **1.17** was obtained as a single diastereomer in 66% yield.



Scheme 1.5: Bennet's thioglycoside resin for *O*-glycosidation

Bennet's work demonstrated the first activation of a resin bound carbohydrate for direct transfer to a natural product aglycone in similar stoichiometry. It also showed the utility of thioglycoside resins for both on-resin elongation and direct glycosylation with the resin bound carbohydrate. The sugar chain was also extended on the solid support for the transfer of a

disaccharide. The loading and elongation of the sugar chain requires a large excess (>9.0 equivalents) of glycosyl donor **1.11**, which is suboptimal for glycosylations with rare glycosyl donors. Cardenolide glycosylation is notoriously challenging, and synthesis of glycosylated cardenolides on solid support can allow for simple and fast diversification of this class of natural products.

1.4 Introduction to glycosylated cardiotonic steroids in medicinal chemistry

Cardiotonic steroids are a diverse class of natural products, with over a thousand unique structures identified.[86] The two main subclasses are cardenolides and bufadienolides, which differ by the heterocycle at the C17 position of the steroidal core (Figure 1.3). Cardenolides have the five-membered butenolide; bufadienolides have the six-membered α-pyrone.[87] Cardenolides are commonly found in plants such as foxglove or lily of the valley, however they are also produced endogenously in humans.[88] Bufadienolides are found in plants as well as in the venom of certain species of toad *(Bufo gargarizans* and *B. melanostictus*). Cardenolides and bufadienolides are both potent inhibitors of Na/K ATPases, and their medicinal use for congestive heart failure is associated with their inhibition of this pathway.[89]

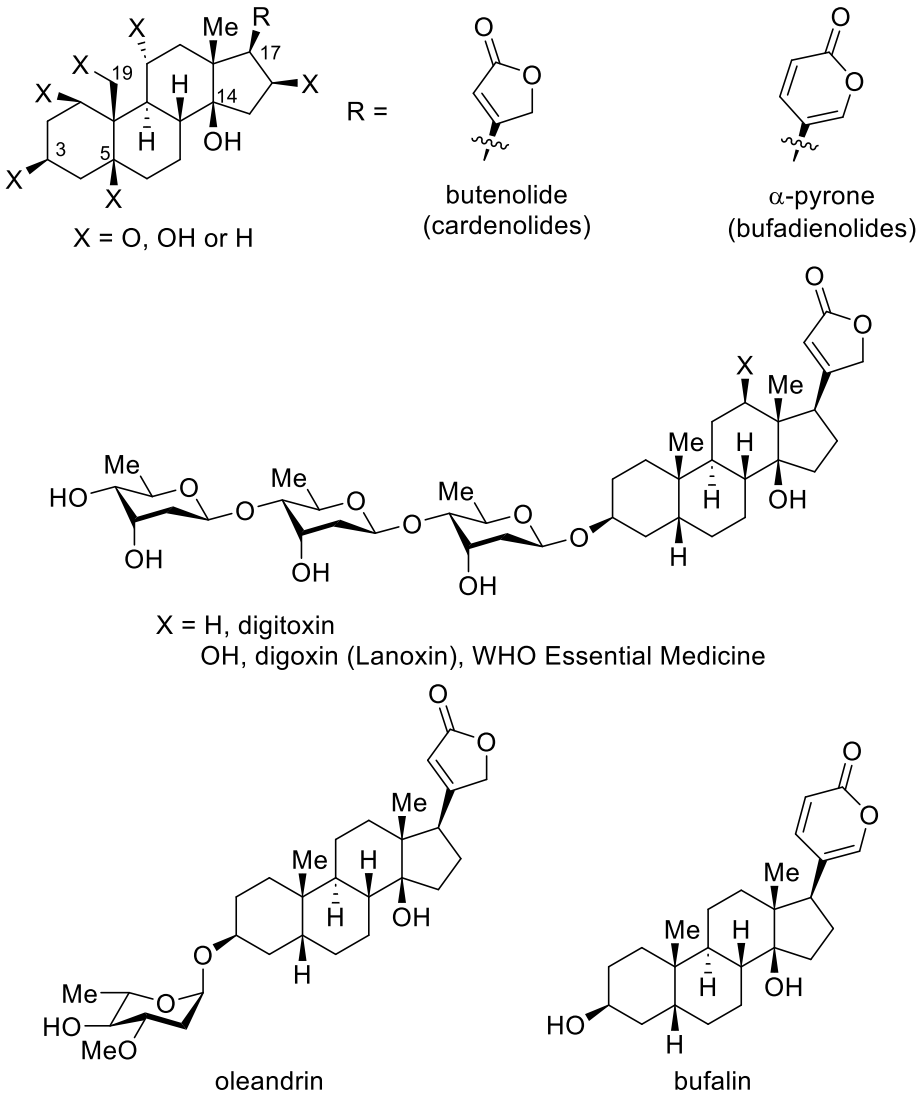


Figure 1.3 Medicinally relevant cardiotonic steroids

Two cardenolides, digitoxin and digoxin (Figure 1.3), are actively prescribed for treatment of cardiovascular disorders, including atrial fibrillation and congestive heart failure. While effective for serious cardiovascular disorders, the limited therapeutic window of digitoxin and digoxin restricts their use for other indications. The cardenolide, oleandrin (Figure 1.3), was evaluated *in vivo* as a possible treatment for COVID-19,[90] and showed promise as an antiviral agent, even garnering the attention and praise of the former President of the United States, Donald Trump. Bufadienolides, including bufalin (Figure 1.3), were also studied for their

antiviral activity against COVID-19.[91] Overall, cardenolides and bufadienolides have been studied as potential therapeutic agents with anti-inflammatory,[92] anticancer,[93] diuretic,[94] antibacterial,[95] immunoregulatory,[96] antihypertensive,[97] neural outgrowth differentiative[98] properties, in addition to the indications mentioned above. However, their toxicity and low therapeutic index has limited their broad application to non-life-threatening conditions. To develop analogs that reduce toxicity and increase the therapeutic window, several total syntheses and medicinal chemistry campaigns have been undertaken. The large focus of medicinal chemistry efforts has been on 1) the degree of oxygenation of the steroid core, 2) the C17-heterocycle, and 3) the C3-carbohydrate.[99] It has been noted that at least one sugar moiety is required to maintain biological activity.[100]

1.4.1 Synthesis of glycosylated cardenolides and bufadienolides

Many cardenolides are found naturally with at least one sugar attached to the aglycone core. Several studies have shown that the sugar is required for potent biological activity.[100–102] Many of the carbohydrates found attached to the steroidal aglycone are deoxyglycosides, with common examples that include digitoxose, rhamnose, and oleandrose (Figure 1.4). Variation of the type of carbohydrate attached to the steroid can change its potency and biological activity.[101]

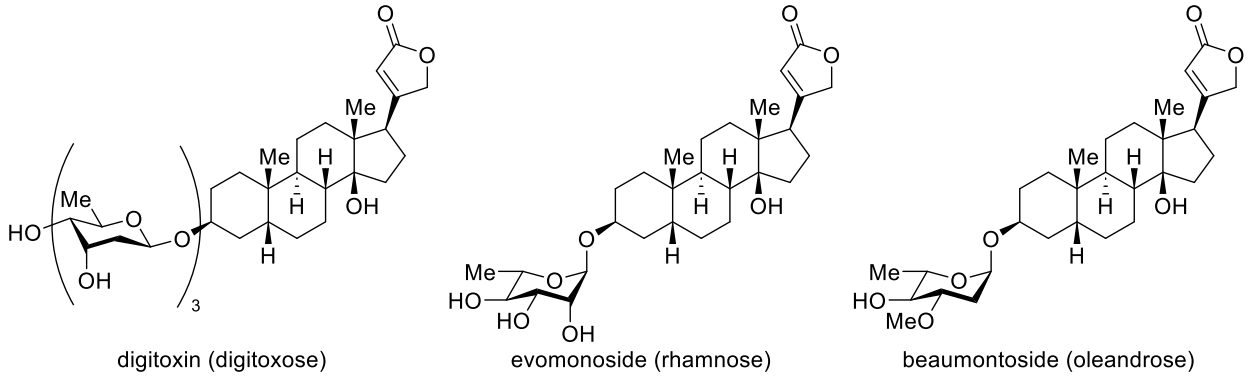
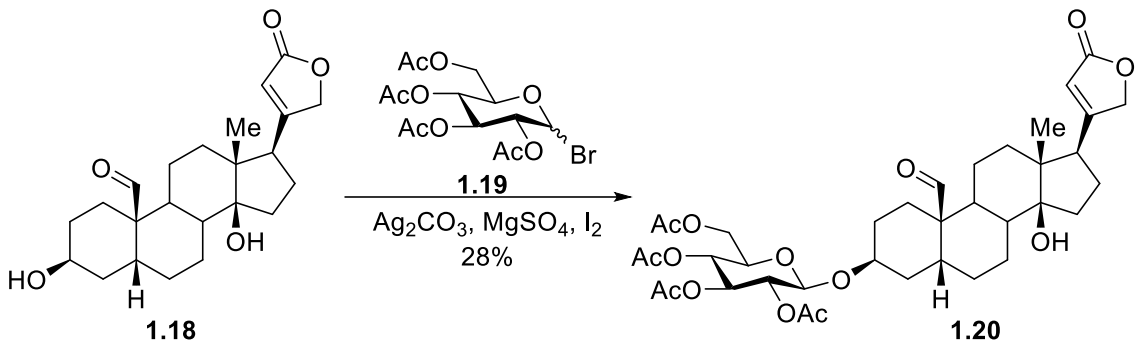


Figure 1.4: Selected examples of various cardenolides containing deoxy sugars.

The first glycosylation reactions were reported in 1901 by Koenigs and Knor[103] and Fischer and Armstrong.[104] The first glycosylation of cardiotonic steroids was reported in 1943 by Uhle and Elderfield.[105] Their first glycosylation of strophanthidin **1.18** was carried out with glucosyl bromide donor **1.19** using the conditions reported by Koenigs and Knor (Scheme 1.6). Uhle and Elderfield were able to prepare β-glycosides of strophanthidin with D-glucose, D-galactose, D-xylose, and L-arabinose in up to 31% yield (Scheme 1.6). The acetylated glycosides were deprotected with either barium methoxide in methanol or methanolic ammonia. Shortly after, they reported the synthesis of the β-glucosides of digitoxigenin, digoxigenin, and periplogenin by the same methodology.[102] Many other groups would adopt glycosyl bromide donors to prepare cardiac glucosides, mannosides, and galactosides for medicinal chemistry studies.[106–110]

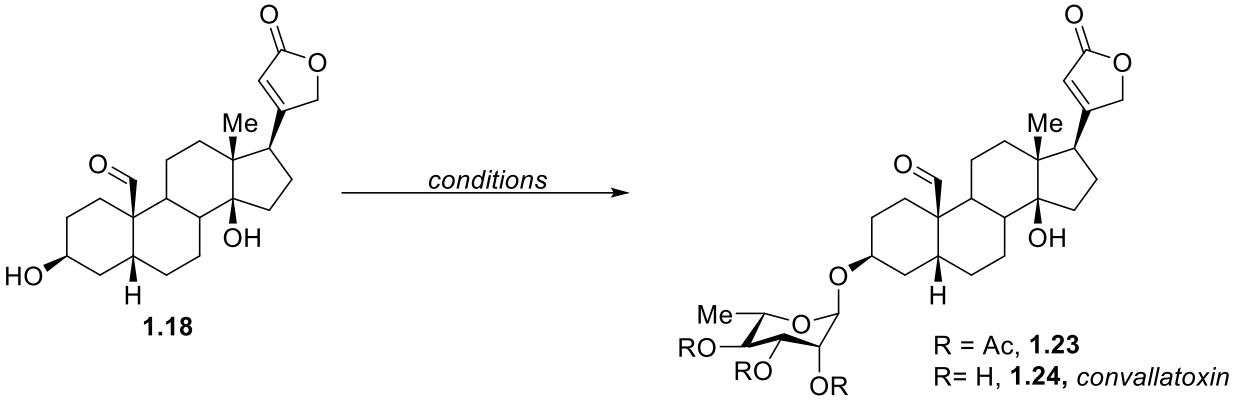


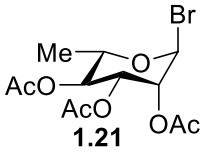
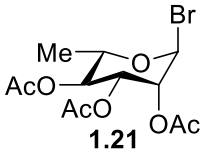
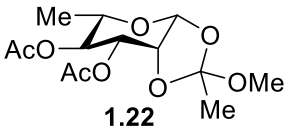
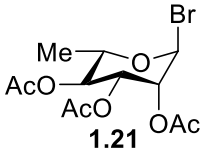
Scheme 1.6: First glycosylation of cardiotonic steroids

Reyle (1950), Chernobai (1964), Pal'yants (1976), and Makarevich (1988) reported syntheses of strophanthin glycosides in moderate to good yields (Table 1.1). Reyle disclosed the first glycosylation of strophanthidin with a deoxy sugar, rhamnose.[111] Acetylated rhamnose bromide donor **1.21** and silver (I) oxide or silver (I) carbonate as activator provided acetylated convallatoxin in 11% or 44% yield, respectively. The acetates were removed by basic hydrolysis with potassium bicarbonate. Chernobai was able to improve the yield by employing strictly

anhydrous conditions and minimizing product decomposition by shortening the reaction time.[112] Pal'yants employed rhamnosyl orthoacetate **1.22** with mercury (II) bromide to facilitate 1,2-trans rhamnosylation.[113] The acetates were removed in a solution of methanolic ammonia to afford convallatoxin in 48% yield. Using this methodology, they were also able to prepare evomonoside and periplogenin-3-*O*-α-L-rhamnoside in 52% and 57% yield, respectively. This was the first time glycosylation of cardenolides was achieved without glycosyl halides. Makarevich further improved upon the Koenigs-Knorr glycosylation of cardenolides by adding mercury (II) oxide to scavenge the *in situ* generated HBr.[114] After protection of the C2' and C3' positions of the rhamnoside moiety of convallatoxin, they performed a second glycosylation with glucosyl bromide donor **1.19** to complete the synthesis of convalloside after removal of the protecting groups. These studies marked the beginning of cardiotonic steroid glycosylation and began to address challenges of working with such complex molecules, such as the propensity of the tertiary hydroxyl groups to undergo elimination, and the extreme lability of the butenolide lactone.

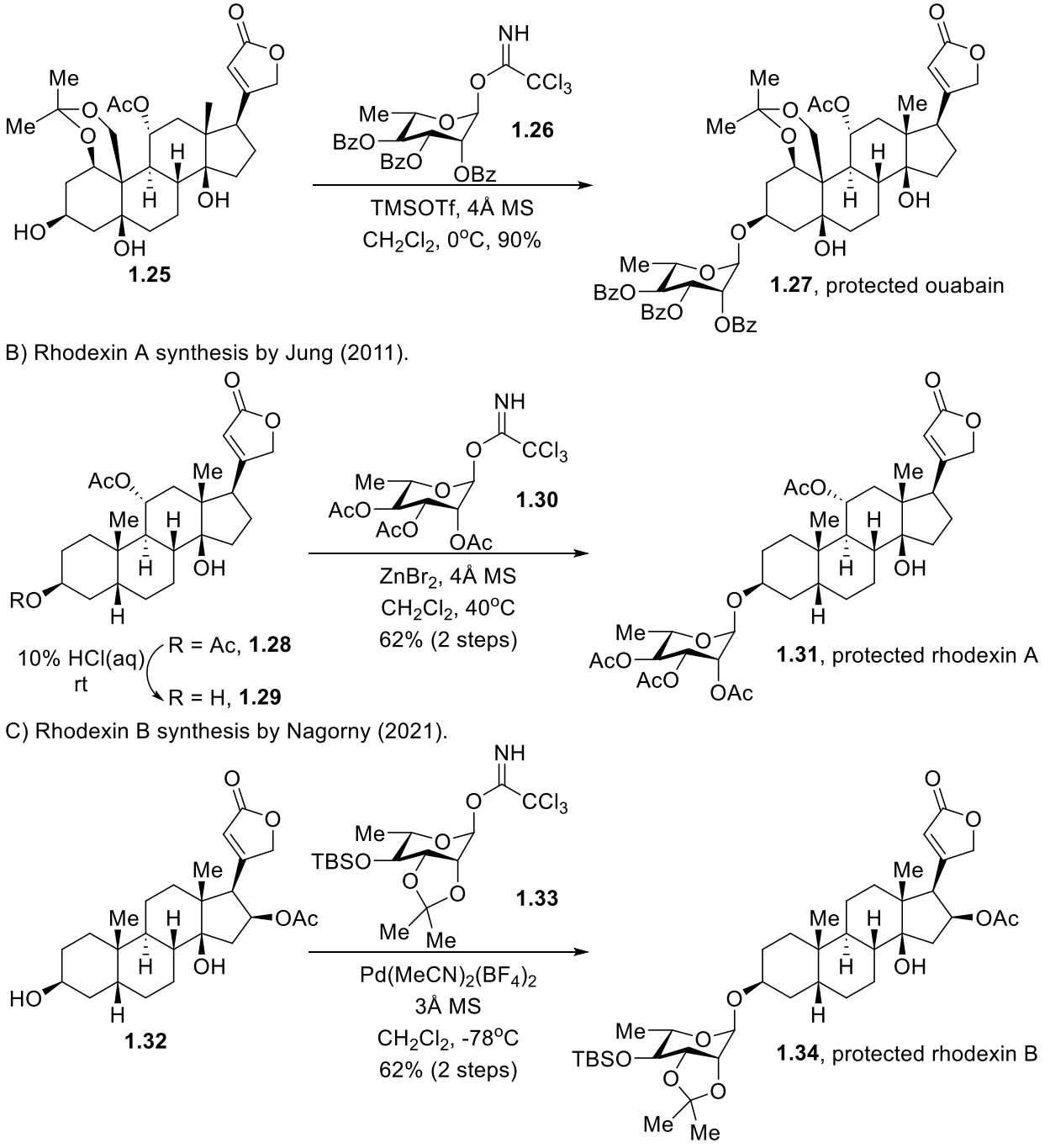
Table 1.1: Early rhamnosylations with glycosyl bromides



entry	donor	conditions	product (yield)
Reyle, et. al. 1950	 1.21	Ag_2O or Ag_2CO_3 dioxane:PhH	**1.23** 11%, AgO 44% Ag_2CO_3
Chernobai, et. al. 1964	 1.21	Ag_2CO_3 PhMe:DCE, Δ then NH_3, MeOH	**1.24** 57% (2 steps)
Pal'yants, et. al. 1976	 1.22	$HgBr_2$ $MeNO_2$, Δ then NH_3, MeOH	**1.24** 48% (2 steps)
Makarevich, et. al. 1988	 1.21	Ag_2CO_3, HgO DCE then NaOH	**1.24** 63% (2 steps)

The invention of new leaving groups greatly enhanced the field of carbohydrate chemistry, and natural product glycosylation, especially for cardiotonic steroids. Glycosyl trichloroacetimidates have emerged as a favorite leaving group (Scheme 1.7), including in our group, due to their ease of preparation and fast reaction times. Although they are not very stable to column chromatography, column-less preparation of these exceptional glycosyl donors is possible.[115] Deslongchamps and coworkers first used trichloroacetimidates for cardenolide glycosylation for their synthesis of ouabain in 2008 (Scheme 1.7A).[116] They employed

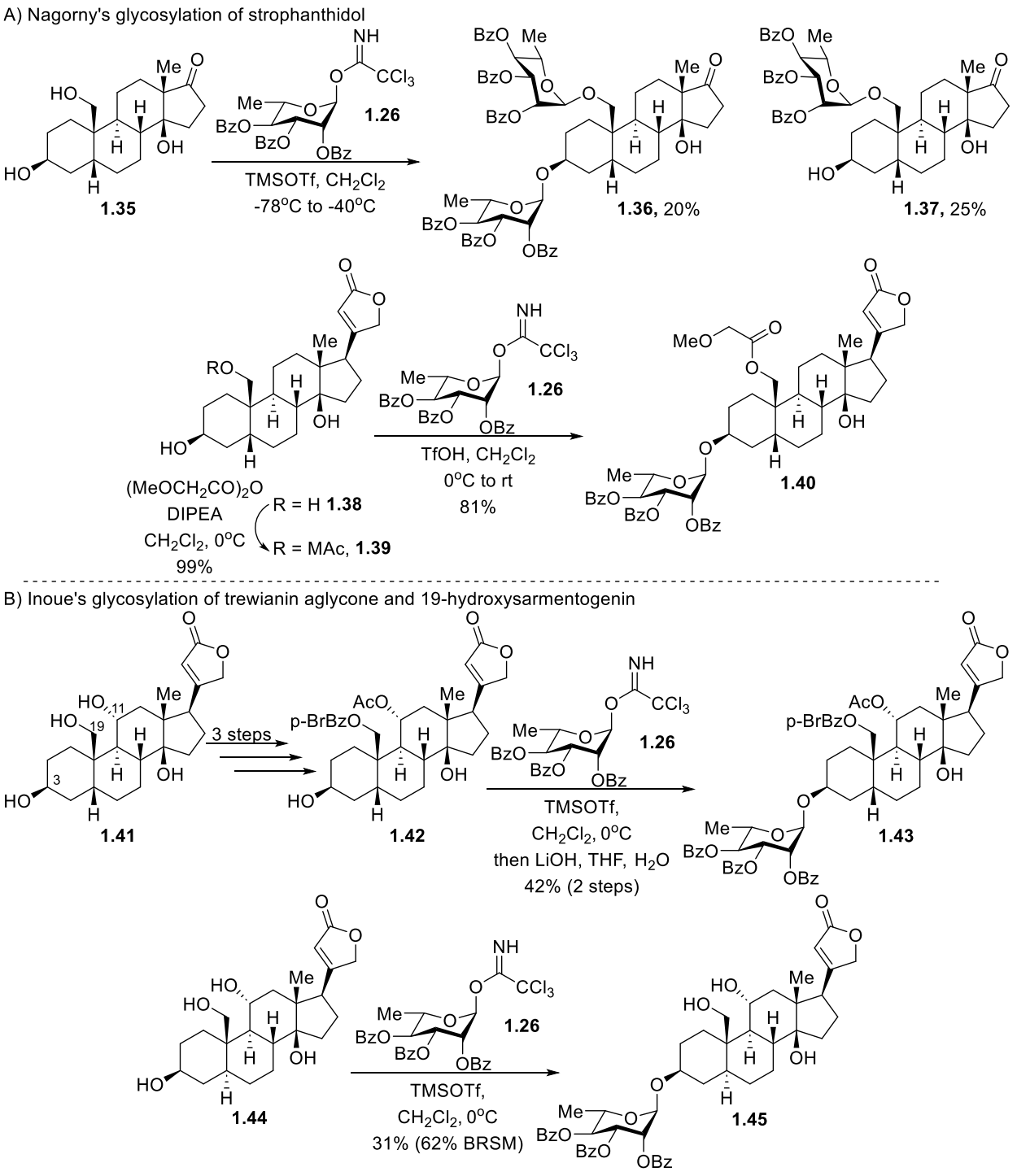
benzoylated rhamnosyl trichloroacetimidate **1.26** for glycosylation of protect ouabagenin intermediate **1.25.** Glycosylation completed within two hours with TMSOTf as promoter; the reaction provided the α-glycoside **1.27** selectively in 90% yield thanks to anchimeric assistance from the C2 benzoate. Jung and coworkers used acetylated rhamnose trichloroacetimidate **1.30** for the glycosylation of sarmentogenin acetate **1.29** (Scheme 1.7B).[117] The less sterically hindered acetate of sarmentogenin diacetate **1.28** was removed with 10% aqueous HCl, and the crude sarmentogenin acetate **1.29** was glycosylated with trichloroacetimidate **1.30** to afford acetylated rhodexin A intermediate **1.31** in 62% yield over two steps. Nagorny and coworkers completed the first total synthesis of rhodexin B and its aglycone oleandrigenin **1.32** in 2021 (Scheme 1.7C).[118] They used rhamnosyl trichloroacetimidate **1.33** bearing acid labile protecting groups, in stark contrast to the base labile acetates and benzoates used previously. The C16 acetate of the aglycone was found to be competitively removed along with the acetates and benzoates of the sugar moiety; thus, selective deprotection of the sugar acetates was not possible. Oleandrigenin **1.32** was glycosylated with trichloroacetimidate **1.33** in 76% yield of the desired α-rhamnoside **1.34**. If the reaction was run at room temperature, exclusive formation of the glycosylate byproduct with the $\Delta^{14,15}$ double bond was observed. These recent advancements highlight the effectiveness of trichloroacetimidates as donors for the glycosylation of cardenolides, but challenges relating to substrate stability and competitive reaction sites still posed problems.



Scheme 1.7: Rhamnosylation of cardiotonic steroids with trichloroacetimidates

Regioselective approaches for the glycosylation of cardenolide aglycones are crucial for medicinal chemistry studies of this class of molecules. The C14 tertiary alcohol is generally unreactive to glycosylation due to steric hindrance, but other primary and secondary alcohols

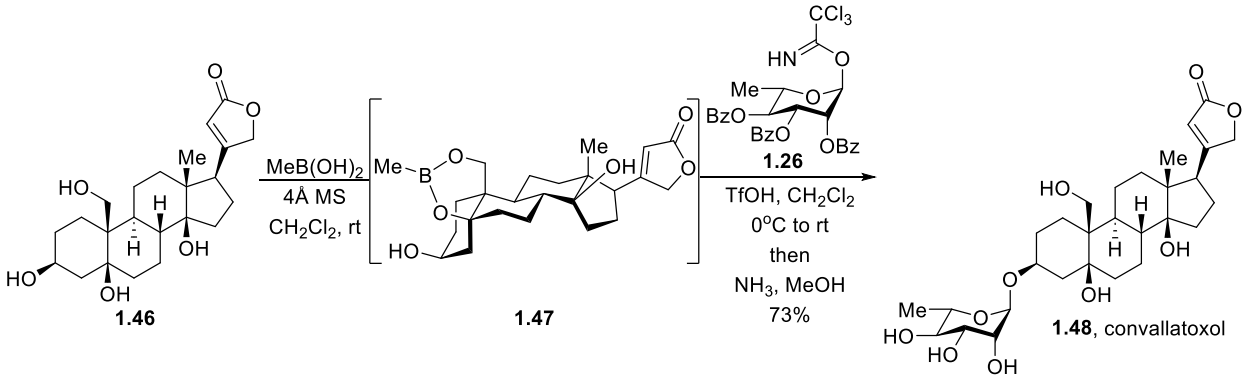
may compete with each other for glycosylation. In their initial studies toward the synthesis of the natural product cannogenol-3-*O*-α-rhamnoside, Nagorny and coworkers observed competitive reactivity between the C19 primary alcohol and secondary axial C3 alcohol of model steroid **1.35**.[119] Reaction of **1.35** with trichloroacetimidate **1.26** afforded a mixture of C3, C19-bisglycosylated **1.36** and C19-monoglycosylated **1.37** products, thus proving the C19 alcohol is more reactive than C3 (Scheme 1.8). Selective protection of cannogenol **1.38** afforded the primary methoxyacetate **1.39.** Glycosylation of **1.39** (Scheme 1.8A) proceeded selectively at the at the C3 position to give the α-rhamnoside **1.40** in 81% yield. Other protecting groups were evaluated at C19 (*p*-BrBz, Ac), however, the deprotection of these esters was slow due to steric hindrance, and multiple side products were observed resulting from opening and isomerization of the butenolide. Inoue reported the synthesis of 19-hydroxysarmentogenin-3-*O*-α-l-rhamnoside **1.43** and trewianin **1.45** in 2018 using a similar strategy (Scheme 1.8B).[120] The C19 alcohol of 19-hydroxysarmentogenin **1.41** was protected as the 4-bromobenzoate ester. The C3 and C11 alcohols were converted to acetate esters, then the C3 acetate was selectively removed to afford C3 alcohol **1.42**. Glycosylation of **1.42** with trichloroacetimidate **1.26** and subsequent global benzoate deprotection afforded α-rhamnoside **1.43** in 42% over two steps. Trewianin aglycone **1.44** was treated directly with trichloroacetimidate **1.26** and TMSOTf to afford the benzoylated 3-O-α-rhamnoside **1.45** in 31% yield as the only observed isomer. It is rationalized that the C3 equatorial alcohol was the most reactive on the molecule, which led to the observed selectivity. Selective protecting group strategies greatly enabled the synthesis of cardenolides; however, the installation and removal adds several steps to the overall sequence.



Scheme 1.8: Regioselective protecting group strategies enabling regioselective glycosylation of cardenolides.

In 2019, the Nagorny group reported the regioselective glycosylation of strophanthidol by using methyl boronic acid as a traceless protecting group.[121] Strophanthidol **1.46** was treated with methyl boronic acid to form cyclic boronate **1.47** *in situ* as a single regioisomer (Scheme

1.9). To cyclic boronate **1.47**, donor **1.26** was added, and glycosylation occurred selectively at the C3 alcohol. The benzoates were removed in a one-pot manner to afford convallatoxol **1.48** in 73% yield. Using this methodology, a total of five glycosides of strophantidol were prepared in up to 77% yield. Later in 2019, the Nagorny group published the total synthesis of ouabagenin and other cardiotonic steroid aglycones and glycosides.[101] They discovered that the glycosides were more potent as anticancer agents than their respective aglycones, and that L-rhamnosides were most active of the evaluated glycosides.



Scheme 1.9: One-pot regioselective glycosylation of strophanthidol

The glycosylation of bufadienolides has been underexplored compared to their cardenolide counterparts. Glycosylation of bufadienolides by enzymatic methods have been studied.[122–127] however most only produce small quantities, and the glycosyl substrates are limited to glucosides. Nagorny reported the only chemical synthesis of bufalin 3-O-α-rhamnoside in 59% yield using trichloroacetimidate donor **1.70** with triflic acid as promoter.[101] Simple and efficient methods for glycosylations of cardiotonic steroids including bufadienolides are needed for medicinal chemistry studies of these compounds.

1.5 References

(1) Merrifield, R. B. Solid Phase Peptide Synthesis. I. The Synthesis of a Tetrapeptide. *J. Am. Chem. Soc.* **1963**, *85* (14), 2149–2154. https://doi.org/10.1021/ja00897a025.

(2) Merrifield, R. B. Solid Phase Synthesis (Nobel Lecture). *Angew. Chem. Int. Ed. Engl.* **1985**, *24* (10), 799–810. https://doi.org/10.1002/anie.198507993.

(3) Guzaev, A. P. Solid-Phase Supports for Oligonucleotide Synthesis. *Curr. Protoc. Nucleic Acid Chem.* **2013**, *53* (1), 3.1.1-3.1.60. https://doi.org/10.1002/0471142700.nc0301s53.

(4) Lönnberg, H. Solid-Phase Synthesis of Oligonucleotide Conjugates Useful for Delivery and Targeting of Potential Nucleic Acid Therapeutics. *Bioconjugate Chem.* **2009**, *20 (6),* 1065–1094. https://doi.org/10.1021/bc800406a.

(5) Seeberger, P. H.; Haase, W.-C. Solid-Phase Oligosaccharide Synthesis and Combinatorial Carbohydrate Libraries. *Chem Rev.* **2000**. *100 (12).* 4349–4394. https://doi.org/10.1021/cr9903104.

(6) Bennett, C. S. Principles of Modern Solid-Phase Oligosaccharide Synthesis. *Org. Biomol. Chem.* **2014**, *12* (11), 1686–1698. https://doi.org/10.1039/C3OB42343C.

(7) Gopi, C.; Krupamai, G.; Sri, C. S.; Dhanaraju, M. D. An Overview of Recent Progress in Modern Synthetic Approach—Combinatorial Synthesis. *Beni-Suef Univ. J. Basic Appl. Sci.* **2020**, *9* (1), 57. https://doi.org/10.1186/s43088-020-00083-7.

(8) Gordon, K.; Balasubramanian, S. Solid Phase Synthesis – Designer Linkers for Combinatorial Chemistry: A Review. *J. Chem. Technol. Biotechnol.* **1999**, *74* (9), 835–851. https://doi.org/10.1002/(SICI)1097-4660(199909)74:9<835::AID-JCTB130>3.0.CO;2-Z.

(9) Schuerch, C.; Frechet, J. M. Solid-Phase Synthesis of Oligosaccharides. I. Preparation of the Solid Support. Poly[p-(1-Propen-3-Ol-1-Yl)Styrene]. *J. Am. Chem. Soc.* **1971**, *93* (2), 492–496. https://doi.org/10.1021/ja00731a031.

(10) Frechet, J. M.; Schuerch, C. Solid-Phase Synthesis of Oligosaccharides. II. Steric Control by C-6 Substituents in Glucoside Syntheses. *J. Am. Chem. Soc.* **1972**, *94* (2), 604–609. https://doi.org/10.1021/ja00757a047.

(11) Frechet, J. M.; Scheurch, C. Solid-Phase Synthesis of Oligosaccharides. III. Preparation of some Derivatives of Di- and Tri- Saccharides via a Simple Alcoholysis Reaction. *Carbohy. Res.* **1972**. *22 (2),* 399–412. https://doi.org/10.1016/S0008-6215(00)81291-4

(12) Panza, M.; Pistorio, S. G.; Stine, K. J.; Demchenko, A. V. Automated Chemical Oligosaccharide Synthesis: Novel Approach to Traditional Challenges. *Chem Rev.* **2018**. *118 (17),* 8105–8150. https://doi.org/10.1021/acs.chemrev.8b00051.

(13) Guberman, M.; Seeberger, P. H. Automated Glycan Assembly: A Perspective. *J. Am. Chem. Soc.* **2019**. *141 (14),* 5581–5592. https://doi.org/10.1021/jacs.9b00638.

(14) Joseph, A. A.; Pardo-Vargas, A.; Seeberger, P. H.; Total Synthesis of Polysaccharides by Automated Glycan Assembly. *J. Am. Chem. Soc.* **2020**. *142 (19).* 8561–8564. https://doi.org/10.1021/jacs.0c00751.

(15) Ojeda, R.; Terentí, O.; de Paz, J.-L.; Martín-Lomas, M. Synthesis of Heparin-like Oligosaccharides on Polymer Supports. *Glycoconj. J.* **2004**, *21* (5), 179–195. https://doi.org/10.1023/B:GLYC.0000045091.18392.a8.

(16) Ojeda, R.; De Paz, J.-L.; Martín-Lomas, M. Synthesis of Heparin-like Oligosaccharides on a Soluble Polymer Support. *Chem Commun.* **2003**, *19*, 2486–2487. https://doi.org/10.1039/B307259B.

(17) Eller, S.; Collot, M.; Yin, J.; Hahm, H. S.; Seeberger, P. H. Automated Solid-Phase Synthesis of Chondroitin Sulfate Glycosaminoglycans. *Angew. Chem. Int. Ed.* **2013**. *52 (22)*, 5858–5861. https://doi.org/10.1002/anie.201210132

(18) Walvoort, M. T. C.; Volbeda, A. G.; Reintjens, N. R. M.; van den Elst, H.; Plante, O. J.; Overkleeft, H. S.; van der Marel, G. A.; Codée, J. D. C. Automated Solid-Phase Synthesis of Hyaluronan Oligosaccharides. *Org. Lett.* **2012**, *14* (14), 3776–3779. https://doi.org/10.1021/ol301666n.

(19) Paulsen, H.; Schleyer, A.; Mathieux, N.; Meldal, M.; Bock, K. New Solid-Phase Oligosaccharide Synthesis on Glycopeptides Bound to a Solid Phase. *J. Chem. Soc. Perkin 1* **1997**, No. 3, 281–294. https://doi.org/10.1039/a604123j.

(20) Jesberger, M.; Jaunzems, J.; Jung, A.; Jas, G.; Schönberger, A.; Kirschning, A. Soluble versus Insoluble Polymers as Supports for the Preparation of New Glycosteroids - a Practicability Study. *Synlett* **2000**, *2000* (9), 1289–1293. https://doi.org/10.1055/s-2000-7128.

(21) Nicolaou, K. C.; Cho, S. Y.; Hughes, R.; Winssinger, N.; Smethurst, C.; Labischinski, H.; Endermann, R. Solid- and Solution-Phase Synthesis of Vancomycin and Vancomycin Analogues with Activity against Vancomycin-Resistant Bacteria. *Chem. – Eur. J.* **2001**, *7* (17), 3798–3823. https://doi.org/10.1002/1521-3765(20010903)7:17<3798::AID-CHEM3798>3.0.CO;2-6.

(22) Mancini, R. S.; Lee, J. B.; Taylor, M. S. Boronic Esters as Protective Groups in Carbohydrate Chemistry: Processes for Acylation, Silylation and Alkylation of Glycoside-Derived Boronates. *Org. Biomol. Chem.* **2017**, *15* (1), 132–143. https://doi.org/10.1039/C6OB02278B.

(23) Xu, H.; Ren, B.; Zhao, W.; Xin, X.; Lu, Y.; Pei, Y.; Dong, H.; Pei, Z. Regioselective Mono and Multiple Alkylation of Diols and Polyols Catalyzed by Organotin and Its Applications on the Synthesis of Value-Added Carbohydrate Intermediates. *Tetrahedron* **2016**, *72* (24), 3490–3499. https://doi.org/10.1016/j.tet.2016.04.076.

(24) Bruce Grindley, T. Applications of Tin-Containing Intermediates to Carbohydrate Chemistry. In *Advances in Carbohydrate Chemistry and Biochemistry*; Horton, D., Ed.; Academic Press, 1998; Vol. 53, pp 17–142. https://doi.org/10.1016/S0065-2318(08)60043-8.

(25) Wang, C.-C.; Lee, J.-C.; Luo, S.-Y.; Kulkarni, S. S.; Huang, Y.-W.; Lee, C.-C.; Chang, K.-L.; Hung, S.-C. Regioselective One-Pot Protection of Carbohydrates. *Nature* **2007**, *446* (7138), 896–899. https://doi.org/10.1038/nature05730.

(26) Kulkarni, S. S.; Wang, C.-C.; Sabbavarapu, N. M.; Podilapu, A. R.; Liao, P.-H.; Hung, S.-C. *"One-Pot" Protection, Glycosylation, and Protection–Glycosylation Strategies of Carbohydrates*. **2018**. *118 (17)*. 8025–8104. https://doi.org/10.1021/acs.chemrev.8b00036.

(27) Sati, G. C.; Martin, J. L.; Xu, Y.; Malakar, T.; Zimmerman, P. M.; Montgomery, J. Fluoride Migration Catalysis Enables Simple, Stereoselective, and Iterative Glycosylation. *J. Am. Chem. Soc.* **2020**, *142* (15), 7235–7242. https://doi.org/10.1021/jacs.0c03165.

(28) Hahm, H. S.; Hurevich, M.; Seeberger, P. H. Automated Assembly of Oligosaccharides Containing Multiple Cis-Glycosidic Linkages. *Nat. Commun.* **2016**, *7* (1), 12482. https://doi.org/10.1038/ncomms12482.

(29) Yasomanee, J. P.; Demchenko, A. V. Effect of Remote Picolinyl and Picoloyl Substituents on the Stereoselectivity of Chemical Glycosylation. *J. Am. Chem. Soc.* **2012**, *134* (49), 20097–20102. https://doi.org/10.1021/ja307355n.

(30) Liu, X.; Lin, Y.; Liu, A.; Sun, Q.; Sun, H.; Xu, P.; Li, G.; Song, Y.; Xie, W.; Sun, H.; Yu, B.; Li, W. 2-Diphenylphosphinoyl-Acetyl as a Remote Directing Group for the Highly Stereoselective Synthesis of β-Glycosides. *Chin. J. Chem.* **2022**, *40* (4), 443–452. https://doi.org/10.1002/cjoc.202100865.

(31) Naresh, K.; Schumacher, F.; Hahm, H. S.; Seeberger, P. H. Pushing the Limits of Automated Glycan Assembly: Synthesis of a 50mer Polymannoside. *Chem. Commun.* **2017**, *53* (65), 9085–9088. https://doi.org/10.1039/C7CC04380E.

(32) Yu, Y.; Kononov, A.; Delbianco, M.; Seeberger, P. H. A Capping Step During Automated Glycan Assembly Enables Access to Complex Glycans in High Yield. *Chem. – Eur. J.* **2018**, *24* (23), 6075–6078. https://doi.org/10.1002/chem.201801023.

(33) Danishefsky, S. J.; McClure, K. F.; Randolph, J. T.; Ruggeri, R. B. A Strategy for the Solid-Phase Synthesis of Oligosaccharides. *Science*. **1993**. *260 (5112)*. 1307–1309. https://doi.org/10.1126/science.8493573.

(34) Zhu, T.; Boons, G.-J. A Two-Directional Approach for the Solid-Phase Synthesis of Trisaccharide Libraries. *Angew. Chem. Int. Ed.* **1998**, *37* (13–14), 1898–1900. https://doi.org/10.1002/(SICI)1521-3773(19980803)37:13/14<1898::AID-ANIE1898>3.0.CO;2-T.

(35) Roberge, J. Y.; Beebe, X.; Danishefsky, S. J. A Strategy for a Convergent Synthesis of N-Linked Glycopeptides on a Solid Support. *Science* **1995**, *269* (5221), 202–204. https://doi.org/10.1126/science.7618080.

(36) Pfäffli, P. J.; Hixson, S. H.; Anderson, L. Thioglycosides Having O-Benzyl Blocking Groups as Intermediates for the Systematic, Sequential Synthesis of Oligosaccharides. Synthesis of Isomaltose. *Carbohydr. Res.* **1972**, *23* (2), 195–206. https://doi.org/10.1016/S0008-6215(00)88025-8.

(37) Rademann, J.; Schmidt, R. R. A New Method for the Solid Phase Synthesis of Oligosaccharides. *Tetrahedron Lett.* **1996**, *37* (23), 3989–3990. https://doi.org/10.1016/0040-4039(96)00763-0.

(38) Wunberg, T.; Kallus, C.; Opatz, T.; Henke, S.; Schmidt, W.; Kunz, H. Carbohydrates as Multifunctional Chiral Scaffolds in Combinatorial Synthesis. *Angew. Chem. Int. Ed.* **1998**, *37* (18), 2503–2505. https://doi.org/10.1002/(SICI)1521-3773(19981002)37:18<2503::AID-ANIE2503>3.0.CO;2-R.

(39) Nguyen, S. H.; Trotta, A. H.; Cao, J.; Straub, T. J.; Bennett, C. S. Direct O-Glycosidation of Resin Bound Thioglycosides. *Org. Biomol. Chem.* **2012**, *10* (12), 2373–2376. https://doi.org/10.1039/C2OB06883D.

(40) Collot, M.; Eller, S.; Weishaupt, M.; Seeberger, P. H. Glycosylation Efficiencies on Different Solid Supports Using a Hydrogenolysis-Labile Linker. *Beilstein J. Org. Chem.* **2013**, *9*, 97–105. https://doi.org/10.3762/bjoc.9.13.

(41) Plante, O. J.; Palmacci, E. R.; Seeberger, P. H. Automated Solid-Phase Synthesis of Oligosaccharides. *Science* **2001**, *291* (5508), 1523–1527. https://doi.org/10.1126/science.1057324.

(42) Forns, P.; Albericio, F. Merrifield Resin. In *Encyclopedia of Reagents for Organic Synthesis (EROS)*; John Wiley & Sons, Ltd, 2003. https://doi.org/10.1002/047084289X.rn00197.

(43) Bayer, E. Towards the Chemical Synthesis of Proteins. *Angew. Chem. Int. Ed. Engl.* **1991**, *30* (2), 113–129. https://doi.org/10.1002/anie.199101133.

(44) Fukase, K.; Nakai, Y.; Egusa, K.; Jr, J. A. P.; Kusumoto, S. A Novel Oxidatively Removable Linker and Its Application to α-Selective Solid-Phase Oligosaccharide Synthesis on a Macroporous Polystyrene Support. *Synlett* **1999**, *1999* (07), 1074–1078. https://doi.org/10.1055/s-1999-2779.

(45) Toy, P. H.; Janda, K. D. New Supports for Solid-Phase Organic Synthesis: Development of Polystyrene Resins Containing Tetrahydrofuran Derived Cross-Linkers. *Tetrahedron Lett.* **1999**, *40* (35), 6329–6332. https://doi.org/10.1016/S0040-4039(99)01251-4.

(46) Panza, M.; Neupane, D.; Stine, K. J.; Demchenko, A. V. The Development of a Dedicated Polymer Support for the Solid-Phase Oligosaccharide Synthesis. *Chem. Commun.* **2020**. *56 (72),* 10568–10571. https://doi.org/10.1039/D0CC03885G.

(47) Rademann, J.; Grøtli, M.; Meldal, M.; Bock, K. SPOCC: A Resin for Solid-Phase Organic Chemistry and Enzymatic Reactions on Solid Phase. *J. Am. Chem. Soc.* **1999**, *121* (23), 5459–5466. https://doi.org/10.1021/ja984355i.

(48) Heckel, A.; Mross, E.; Jung, K.-H.; Rademann, J.; Schmidt, R. R. Oligosaccharide Synthesis on Controlled-Pore Glass as Solid Phase Material. *Synlett* **1998**, *1998* (2), 171–173. https://doi.org/10.1055/s-1998-3127.

(49) Adinolfi, M.; Barone, G.; De Napoli, L.; Iadonisi, A.; Piccialli, G. Use of Controlled Pore Glass in Solid Phase Oligosaccharide Synthesis. Application to the Semiautomated Synthesis of a Glyconucleotide Conjugate. *Tetrahedron Lett.* **1998**, *39* (14), 1953–1956. https://doi.org/10.1016/S0040-4039(98)00103-8.

(50) Guillier, F.; Orain, D.; Bradley, M. Linkers and Cleavage Strategies in Solid-Phase Organic Synthesis and Combinatorial Chemistry. *Chem. Rev*. **2000**. *100 (6)*, 2091–2158. https://doi.org/10.1021/cr980040+.

(51) Doi, T.; Sugiki, M.; Yamada, H.; Takahashi, T.; Porco, J. A. Glycosidation of Solid-Supported Glycosyl Donors Tethered by a Trialkylsilane Linker. *Tetrahedron Lett.* **1999**, *40* (11), 2141–2144. https://doi.org/10.1016/S0040-4039(99)00133-1.

(52) Weigelt, D.; Magnusson, G. A Linker for Solid Phase Carbohydrate Synthesis, Permitting the Introduction of Variable Anomeric Functionality in the Release Step. *Tetrahedron Lett.* **1998**, *39* (18), 2839–2842. https://doi.org/10.1016/S0040-4039(98)00312-8.

(53) Seeberger, P. H.; Danishefsky, S. J. Solid-Phase Synthesis of Oligosaccharides and Glycoconjugates by the Glycal Assembly Method: A Five Year Retrospective. *Acc. Chem. Res.* **1998**, *31* (10), 685–695. https://doi.org/10.1021/ar9600648.

(54) Ganesh, N.V.; Fujikawa, K.; Tan, Y. H.; Stine, K. J.; Demchenko, A. V. HPLC-Assisted Automated Oligosaccharide Synthesis. *Org. Lett*. **2012**. *14 (12)*. 3036–3039. https://doi.org/10.1021/ol301105y.

(55) Andrade, R. B.; Plante, O. J.; Melean, L. G.; Seeberger, P. H. Solid-Phase Oligosaccharide Synthesis: Preparation of Complex Structures Using a Novel Linker and Different Glycosylating Agents. *Org. Lett.* **1999**, *1* (11), 1811–1814. https://doi.org/10.1021/ol991071+.

(56) Czechura, P.; Guedes, N.; Kopitzki, S.; Vazquez, N.; Martin-Lomas, M.; Reichardt, N.-C. A New Linker for Solid-Phase Synthesis of Heparan Sulfate Precursors by Sequential Assembly of Monosaccharide Building Blocks. *Chem Commun* **2011**, *47* (8), 2390–2392. https://doi.org/10.1039/C0CC04686H.

(57) Wilsdorf, M.; Schmidt, D.; Bartetzko, M. P.; Dallabernardina, P.; Schuhmacher, F.; Seeberger, P. H.; Pfrengle, F. A Traceless Photocleavable Linker for the Automated Glycan Assembly of Carbohydrates with Free Reducing Ends. *Chem. Commun.* **2016**, *52* (66), 10187–10189. https://doi.org/10.1039/C6CC04954K.

(58) Le Mai Hoang, K.; Pardo-Vargas, A.; Zhu, Y.; Yu, Y.; Loria, M.; Delbianco, M.; Seeberger, P. H. Traceless Photolabile Linker Expedites the Chemical Synthesis of Complex Oligosaccharides by Automated Glycan Assembly. *J. Am. Chem. Soc.* **2019**, *141* (22), 9079–9086. https://doi.org/10.1021/jacs.9b03769.

(59) Rademann, J.; Schmidt, R. R. Repetitive Solid Phase Glycosylation on an Alkyl Thiol Polymer Leading to Sugar Oligomers Containing 1,2-Trans- and 1,2-Cis-Glycosidic Linkages. *J. Org. Chem.* **1997**, *62* (11), 3650–3653. https://doi.org/10.1021/jo970087f.

(60) Roussel, F.; Takhi, M.; Schmidt, R. R. Solid-Phase Synthesis of a Branched Hexasaccharide Using a Highly Efficient Synthetic Strategy. *J. Org. Chem.* **2001**, *66* (25), 8540–8548. https://doi.org/10.1021/jo016018p.

(61) Werz, D. B.; Castagner, B.; Seeberger, P. H. Automated Synthesis of the Tumor-Associated Carbohydrate Antigens Gb-3 and Globo-H: Incorporation of α-Galactosidic Linkages. *J. Am. Chem. Soc.* **2007**, *129* (10), 2770–2771. https://doi.org/10.1021/ja069218x.

(62) Boltje, T. J.; Kim, J.-H.; Park, J.; Boons, G.-J. Chiral Auxiliary Mediated 1,2-Cis Glycosylations for the Solid Supported Synthesis of a Biologically Important Branched α-Glucan. *Nat. Chem.* **2010**, *2* (7), 552–557. https://doi.org/10.1038/nchem.663.

(63) Walvoort, M. T. C.; van den Elst, H.; Plante, O. J.; Kröck, L.; Seeberger, P. H.; Overkleeft, H. S.; van der Marel, G. A.; Codée, J. D. C. Automated Solid-Phase Synthesis of β-Mannuronic Acid Alginates. *Angew. Chem. Int. Ed.* **2012**, *51* (18), 4393–4396. https://doi.org/10.1002/anie.201108744.

(64) Tang, S.-L.; Linz, L. B.; Bonning, B. C.; Pohl, N. L. B. Automated Solution-Phase Synthesis of Insect Glycans to Probe the Binding Affinity of Pea Enation Mosaic Virus. *J. Org. Chem.* **2015**. *80 (21),* 10482 –10489. https://doi.org/10.1021/acs.joc.5b01428

(65) Pitsch, S.; Weiss, P. A.; Wu, X.; Ackermann, D.; Honegger, T. Fast and Reliable Automated Synthesis of RNA and Partially 2′-O- Protected Precursors (`Caged RNA') Based on Two Novel, Orthogonal 2′-O-Protecting Groups, Preliminary Communication. *Helv. Chim. Acta* **1999**, *82* (10), 1753–1761. https://doi.org/10.1002/(SICI)1522-2675(19991006)82:10<1753::AID-HLCA1753>3.0.CO;2-Y.

(66) Adinolfi, M.; Barone, G.; Napoli, L. D.; Iadonisi, A.; Piccialli, G. Solid Phase Synthesis of Oligosaccharides. *Tetrahedron Lett.* **1996**, *37* (28), 5007–5010. https://doi.org/10.1016/0040-4039(96)01020-9.

(67) Wang, Y.; Zhang, H.; Voelter, W. A New Base-Labile Anchoring Group for Polymer-Supported Oligosaccharide Synthesis. *Chem. Lett.* **1995**, *24* (4), 273–274. https://doi.org/10.1246/cl.1995.273.

(68) Douglas, S. P.; Whitfield, D. M.; Krepinsky, J. J. Polymer-Supported Solution Synthesis of Oligosaccharides Using a Novel Versatile Linker for the Synthesis of D-

Mannopentaose, a Structural Unit of D-Mannans of Pathogenic Yeasts. *J. Am. Chem. Soc.* **1995**, *117* (7), 2116–2117. https://doi.org/10.1021/ja00112a035.

(69) Haase, W.-C.; Seeberger, P. H.; Pochapsky, S. S. Tools for "On-Bead" Monitoring and Analysis in Solid-Phase Oligosaccharide Synthesis. In *Solid Support Oligosaccharide Synthesis and Combinatorial Carbohydrate Libraries*; John Wiley & Sons, Ltd, 2001; pp 165–174. https://doi.org/10.1002/0471220442.ch8.

(70) Chan, T. Y.; Chen, R.; Sofia, M. J.; Smith, B. C.; Glennon, D. High Throughput On-Bead Monitoring of Solid Phase Reactions by Diffuse Reflectance Infrared Fourier Transform Spectroscopy (DRIFTS). *Tetrahedron Lett.* **1997**, *38* (16), 2821–2824. https://doi.org/10.1016/S0040-4039(97)00496-6.

(71) Knerr, L.; Schmidt, R. R. Application of a Ring Closing Metathesis Based Linker to the Solid Phase Synthesis of Oligosaccharides. *Synlett* **1999**, *1999* (11), 1802–1804. https://doi.org/10.1055/s-1999-2930.

(72) Giralt, E.; Rizo, J.; Pedroso, E. Application of Gel-Phase 13c-Nmr to Monitor Solid Phase Peptide Synthesis. *Tetrahedron* **1984**, *40* (20), 4141–4152. https://doi.org/10.1016/0040-4020(84)85095-4.

(73) Rodebaugh, R.; Joshi, S.; Fraser-Reid, B.; Geysen, H. M. Polymer-Supported Oligosaccharides via n-Pentenyl Glycosides: Methodology for a Carbohydrate Library,1. *J. Org. Chem.* **1997**, *62* (17), 5660–5661. https://doi.org/10.1021/jo970216s.

(74) Mogemark, M.; Gårdmo, F.; Tengel, T.; Kihlberg, J.; Elofsson, M. Gel-Phase 19F NMR Spectral Quality for Resins Commonly Used in Solid-Phase Organic Synthesis; a Study of Peptide Solid-Phase Glycosylations. *Org. Biomol. Chem.* **2004**, *2* (12), 1770–1776. https://doi.org/10.1039/B404802D.

(75) Mogemark, M.; Elofsson, M.; Khilberg, J. Monitoring Solid-Phase Glycoside Synthesis with 19F NMR Spectroscopy. *Org. Lett.* **2001**. *3 (10),* 1463–1466. https://doi.org/10.1021/ol015759+.

(76) Mogemark, M.; Elofsson, M.; Kihlberg, J. Fluorinated Protective Groups for On-Resin Quantification of Solid-Phase Oligosaccharide Synthesis with 19F NMR Spectroscopy. *ChemBioChem* **2002**, *3* (12), 1266–1269. https://doi.org/10.1002/1439-7633(20021202)3:12<1266::AID-CBIC1266>3.0.CO;2-6.

(77) Mogemark, M.; Elofsson, M.; Kihlberg, J. Solid-Phase Synthesis of α-Gal Epitopes: On-Resin Analysis of Solid-Phase Oligosaccharide Synthesis with 19F NMR Spectroscopy. *J. Org. Chem.* **2003**, *68* (19), 7281–7288. https://doi.org/10.1021/jo034581x.

(78) Bardella, F.; Eritja, R.; Pedroso, E.; Giralt, E. Gel-Phase 31P-NMR. A New Analytical Tool to Evaluate Solid Phase Oligonucleoside Synthesis. *Bioorg. Med. Chem. Lett.* **1993**, *3* (12), 2793–2796. https://doi.org/10.1016/S0960-894X(01)80766-6.

(79) Melean, L. G.; Haase, W.-C.; Seeberger, P. H. A Novel 4,5-Dibromooctane-1,8-Diol Linker for Solid-Phase Oligosaccharide Synthesis. *Tetrahedron Lett.* **2000**, *41* (22), 4329–4333. https://doi.org/10.1016/S0040-4039(00)00663-8.

(80) Hany, R.; Rentsch, D.; Dhanapal, B.; Obrecht, D. Quantitative Determination of Resin Loading in Solid-Phase Organic Synthesis Using 13C MAS NMR. *J. Comb. Chem.* **2001**. *3 (1)*, 85–89. https://doi.org/10.1021/cc000066q.

(81) Loening, N. M.; Kanemitsu, T.; Seeberger, P. H.; Griffin, R. G. Solid-Phase Synthesis and 1H and 13C High-Resolution Magic Angle Spinning NMR of 13C-Labeled Resin-Bound Saccharides. *Magn. Reson. Chem.* **2004**, *42* (5), 453–458. https://doi.org/10.1002/mrc.1364.

(82) Warrass, R.; Lippens, G. High-Resolution Magic Angle Spinning (MAS) NMR Spectroscopy for On-Bead Analysis of Solid-Phase Synthesis. In *Combinatorial Chemistry*; John Wiley & Sons, Ltd, 1999; pp 533–542. https://doi.org/10.1002/9783527613502.ch18.

(83) Seeberger, P. H.; Beebe, X.; Sukenick, G. D.; Pochapsky, S.; Danishefsky, S. J. Monitoring the Progress of Solid-Phase Oligosaccharide Synthesis by High-Resolution Magic Angle Spinning NMR: Observations of Enhanced Selectivity for β-Glycoside Formation from α-1,2-Anhydrosugar Donors in Solid-Phase Couplings. *Angew. Chem. Int. Ed. Engl.* **1997**, *36* (5), 491–493. https://doi.org/10.1002/anie.199704911.

(84) Kanemitsu, T.; Kanie, O.; Wong, C.-H. Quantitative Monitoring of Solid-Phase Synthesis Using Gated Decoupling 13C NMR Spectroscopy with a 13C-Enriched Protecting Group and an Internal Standard in the Synthesis of Sialyl LewisX Tetrasaccharide. *Angew. Chem. Int. Ed.* **1998**, *37* (24), 3415–3418. https://doi.org/10.1002/(SICI)1521-3773(19981231)37:24<3415::AID-ANIE3415>3.0.CO;2-8.

(85) Ko, K.-S.; Park, G.; Yu, Y.; Pohl, N. L. Protecting-Group-Based Colorimetric Monitoring of Fluorous-Phase and Solid-Phase Synthesis of Oligoglucosamines. *Org. Lett.* **2008**, *10* (23), 5381–5384. https://doi.org/10.1021/ol802229b.

(86) Heasley, B. Chemical Synthesis of the Cardiotonic Steroid Glycosides and Related Natural Products. *Chem. – Eur. J.* **2012**, *18* (11), 3092–3120. https://doi.org/10.1002/chem.201103733.

(87) Michalak, M.; Michalak, K.; Wicha, J. The Synthesis of Cardenolide and Bufadienolide Aglycones, and Related Steroids Bearing a Heterocyclic Subunit. *Nat. Prod. Rep.* **2017**, *34* (4), 361–410. https://doi.org/10.1039/C6NP00107F.

(88) Nesher, M.; Shpolansky, U.; Rosen, H.; Lichtstein, D. The Digitalis-like Steroid Hormones: New Mechanisms of Action and Biological Significance. *Life Sci.* **2007**, *80* (23), 2093–2107. https://doi.org/10.1016/j.lfs.2007.03.013.

(89) Laursen, M.; Gregersen, J. L.; Yatime, L.; Nissen, P.; Fedosova, N. U. Structures and Characterization of Digoxin- and Bufalin-Bound Na+,K+-ATPase Compared with the

Ouabain-Bound Complex. *Proc. Natl. Acad. Sci.* **2015**, *112* (6), 1755–1760. https://doi.org/10.1073/pnas.1422997112.

(90) Plante, K. S.; Dwivedi, V.; Plante, J. A.; Fernandez, D.; Mirchandani, D.; Bopp, N.; Aguilar, P. V.; Park, J.-G.; Tamayo, P. P.; Delgado, J.; Shivanna, V.; Torrelles, J. B.; Martinez-Sobrido, L.; Matos, R.; Weaver, S. C.; Sastry, K. J.; Newman, R. A. Antiviral Activity of Oleandrin and a Defined Extract of Nerium Oleander against SARS-CoV-2. *Biomed. Pharmacother.* **2021**, *138*, 111457. https://doi.org/10.1016/j.biopha.2021.111457.

(91) Jin, Y.-H.; Jeon, S.; Lee, J.; Kim, S.; Jang, M. S.; Park, C. M.; Song, J. H.; Kim, H. R.; Kwon, S. Broad Spectrum Antiviral Properties of Cardiotonic Steroids Used as Potential Therapeutics for Emerging Coronavirus Infections. *Pharmaceutics* **2021**, *13* (11), 1839. https://doi.org/10.3390/pharmaceutics13111839.

(92) Orellana, A. M.; Kinoshita, P. F.; Leite, J. A.; Kawamoto, E. M.; Scavone, C. Cardiotonic Steroids as Modulators of Neuroinflammation. *Front. Endocrinol.* **2016**, *7*.

(93) Babula, P.; Masarik, M.; Adam, V.; Provaznik, I.; Kizek, R. From Na+/K+-ATPase and Cardiac Glycosides to Cytotoxicity and Cancer Treatment. *Anticancer Agents Med. Chem. 13* (7), 1069–1087.

(94) Arnaud-Batista, F. J.; Costa, G. T.; de Oliveira, I. M. B.; Costa, P. P. C.; Santos, C. F.; Fonteles, M. C.; Uchôa, D. E.; Silveira, E. R.; Cardi, B. A.; Carvalho, K. M.; Amaral, L. S.; Pôças, E. S. C.; Quintas, L. E. M.; Noël, F.; Nascimento, N. R. F. Natriuretic Effect of Bufalin in Isolated Rat Kidneys Involves Activation of the Na+-K+-ATPase-Src Kinase Pathway. *Am. J. Physiol.-Ren. Physiol.* **2012**, *302* (8), F959–F966. https://doi.org/10.1152/ajprenal.00130.2011.

(95) Akhtar, N.; Malik, A.; Ali, S. N.; Kazmit, S. U. Proceragenin, an Antibacterial Cardenolide from Calotropis Procera. *Phytochemistry* **1992**, *31* (8), 2821–2824. https://doi.org/10.1016/0031-9422(92)83639-G.

(96) Jacob, P. L.; Leite, J. A.; Alves, A. K. A.; Rodrigues, Y. K. S.; Amorim, F. M.; Néris, P. L. N.; Oliveira, M. R.; Rodrigues-Mascarenhas, S. Immunomodulatory Activity of Ouabain in Leishmania Leishmania Amazonensis-Infected Swiss Mice. *Parasitol. Res.* **2013**, *112* (3), 1313–1321. https://doi.org/10.1007/s00436-012-3146-9.

(97) Ferrari, P.; Ferrandi, M.; Valentini, G.; Bianchi, G. Rostafuroxin: An Ouabain Antagonist That Corrects Renal and Vascular Na+-K+- ATPase Alterations in Ouabain and Adducin-Dependent Hypertension. *Am. J. Physiol.-Regul. Integr. Comp. Physiol.* **2006**, *290* (3), R529–R535. https://doi.org/10.1152/ajpregu.00518.2005.

(98) Yoneyama, T.; Arai, M. A.; Akamine, R.; Koryudzu, K.; Tsuchiya, A.; Sadhu, S. K.; Ahmed, F.; Itoh, M.; Okamoto, R.; Ishibashi, M. Notch Inhibitors from Calotropis Gigantea That Induce Neuronal Differentiation of Neural Stem Cells. *J. Nat. Prod.* **2017**, *80* (9), 2453–2461. https://doi.org/10.1021/acs.jnatprod.7b00282.

(99) Schönfeld, W.; Weiland, J.; Lindig, C.; Masnyk, M.; Kabat, M. M.; Kurek, A.; Wicha, J.; Repke, K. R. H. The Lead Structure in Cardiac Glycosides Is 5 β,14 β-Androstane-3 β,14-Diol. *Naunyn. Schmiedebergs Arch. Pharmacol.* **1985**, *329* (4), 414–426. https://doi.org/10.1007/BF00496377.

(100) López-Lázaro, M.; Pastor, N.; Azrak, S. S.; Ayuso, M. J.; Austin, C. A.; Cortés, F. Digitoxin Inhibits the Growth of Cancer Cell Lines at Concentrations Commonly Found in Cardiac Patients. *J. Nat. Prod.* **2005**, *68* (11), 1642–1645. https://doi.org/10.1021/np050226l.

(101) Khatri, H. R.; Bhattarai, B.; Kaplan, W.; Li, Z.; Long, M. J. C.; Aye, Y.; Nagorny, P. Modular Total Synthesis and Cell-Based Anticancer Activity Evaluation of Ouabagenin and Other Cardiotonic Steroids with Varying Degrees of Oxygenation. *J. Am. Chem. Soc.* **2019**, *141* (12), 4849–4860. https://doi.org/10.1021/jacs.8b1287.

(102) Chen, K. K.; Elderfield, R. C.; Uhle, F. C.; Fried, J. Synthetic Glycosides of Digitoxigenin, Digoxigenin and Periplogenin. *J. Pharmacol. Exp. Ther.* **1943**, *77* (4), 401–406.

(103) Koenigs, W.; Knorr, E. Ueber Einige Derivate Des Traubenzuckers Und Der Galactose. *Berichte Dtsch. Chem. Ges.* **1901**, *34* (1), 957–981. https://doi.org/10.1002/cber.190103401162.

(104) Fischer, E.; Armstrong, E. F. Ueber Die Isomeren Acetohalogen-Derivate Des Traubenzuckers Und Die Synthese Der Glucoside1. *Berichte Dtsch. Chem. Ges.* **1901**, *34* (2), 2885–2900. https://doi.org/10.1002/cber.190103402251.

(105) Uhle, F. C.; Elderfield, R. C. Synthetic Glcyosides of Strophanthidin. *J. Org. Chem.* **1943**, *08* (2), 162–167. https://doi.org/10.1021/jo01190a007.

(106) Fullerton, D. S.; Kihara, M.; Deffo, T.; Kitatsuji, E.; Ahmed, K.; Simat, B.; From, A. H. L. Cardiac Glycosides. 1. A Systematic Study of Digitoxigenin D-Glycosides. *J. Med. Chem.* **1984**, *27* (3), 256–261. https://doi.org/10.1021/jm00369a004.

(107) Harreus, A.; Kunz, H. Stereoselektive Glycosylierung von Steroidalkoholen mit 2,3,4,6-Tetra-O-privaloyl-α-D-glucopyranosylbromid (Pivalobromglucose) und 2,3,4,6-Tetra-O-(o-toluoyl)-α-D-glucopyranosylbromid. *Liebigs Ann. Chem.* **1986**, *1986* (4), 717–730. https://doi.org/10.1002/jlac.198619860411.

(108) Wulff, G.; Röhle, G.; Krüger, W. Untersuchungen zur Glykosidsynthese, IV. Neuartige Silbersalze in der Glykosidsynthese. *Chem. Ber.* **1972**, *105* (4), 1097–1110. https://doi.org/10.1002/cber.19721050403.

(109) Kihara, M.; Yoshioka, K.; Kitatsuji, E.; Hashimoto, T.; Fullerton, D. S.; Rohrer, D. C. Cardiac Glycosides: 2. Synthesis of Glucose and Galactose Analogs. *Steroids* **1983**, *42* (1), 37–53. https://doi.org/10.1016/S0039-128X(83)90072-7.

(110) Li, X.; Ren, Y.; Bao, Y.; Liu, J.; Zhang, X.; Zhang, Y.; Sun, X.-L.; Yao, X.; Tang, J.-S. Synthesis of C3-Neoglycosides of Digoxigenin and Their Anticancer Activities. *Eur. J. Med. Chem.* **2018**, *145*, 252–262. https://doi.org/10.1016/j.ejmech.2017.12.086.

(111) Reyle, K.; Meyer, K.; Reichstein, T. Partialsynthese von Convallatoxin. Glykoside und Aglykone, 61. Mitteilung. *Helv. Chim. Acta* **1950**, *33* (6), 1541–1546. https://doi.org/10.1002/hlca.19500330621.

(112) Chernobai, V. T. Partial Synthesis of Cardiac Glycosides. Convallatoxin and Convallatoxol. *Zhurnal Obshchei Khimii* **1962**, *34* (3), 1018–1020.

(113) Pal'yants, N. Sh.; Bochkov, A. F.; Abubakirov, N. K. Glycosylation of Cardenolides III. Partial Syntheses of Convallatoxin, Evomonoside, and Periplorhamnoside. *Chem. Nat. Compd.* **1976**, *12* (1), 48–49. https://doi.org/10.1007/BF00570180.

(114) Makarevich, I. F.; Terno, I. S. Synthesis of convalloside. *Chem. Nat. Compd.* **1988**. *24*, 323–325. https://doi.org/10.1007/BF00598579.

(115) Ikeuchi, K.; Murasawa, K.; Yamada, H. A Simple Method for the Preparation of Stainless and Highly Pure Trichloroacetimidates. *Synlett* **2019**, *30* (11), 1308–1312. https://doi.org/10.1055/s-0037-1611551.

(116) Zhang, H.; Sridhar Reddy, M.; Phoenix, S.; Deslongchamps, P. Total Synthesis of Ouabagenin and Ouabain. *Angew. Chem. Int. Ed.* **2008**, *47* (7), 1272–1275. https://doi.org/10.1002/anie.200704959.

(117) Jung, M. E.; Yoo, D. First Total Synthesis of Rhodexin A. *Org. Lett.* **2011**, *13* (10), 2698–2701. https://doi.org/10.1021/ol200796r.

(118) Fejedelem, Z.; Carney, N.; Nagorny, P. Synthesis of Cardiotonic Steroids Oleandrigenin and Rhodexin B. *J. Org. Chem.* **2021**, *86* (15), 10249–10262. https://doi.org/10.1021/acs.joc.1c00985.

(119) Bhattarai, B.; Nagorny, P. Enantioselective Total Synthesis of Cannogenol-3-O-α-l-Rhamnoside via Sequential Cu(II)-Catalyzed Michael Addition/Intramolecular Aldol Cyclization Reactions. *Org. Lett.* **2018**, *20* (1), 154–157. https://doi.org/10.1021/acs.orglett.7b03513.

(120) Urabe, D.; Nakagawa, Y.; Mukai, K.; Fukushima, K.; Aoki, N.; Itoh, H.; Nagatomo, M.; Inoue, M. Total Synthesis and Biological Evaluation of 19-Hydroxysarmentogenin-3-O-α-l-Rhamnoside, Trewianin, and Their Aglycons. *J. Org. Chem.* **2018**, *83* (22), 13888–13910. https://doi.org/10.1021/acs.joc.8b02219.

(121) Tay, J.-H.; Dorokhov, V.; Wang, S.; Nagorny, P. Regioselective Single Pot C3-Glycosylation of Strophanthidol Using Methylboronic Acid as a Transient Protecting Group. *J. Antibiot. (Tokyo)* **2019**, *72* (6), 437–448. https://doi.org/10.1038/s41429-019-0172-1.

(122) Ye, M.; Dai, J.; Guo, H.; Cui, Y.; Guo, D. Glucosylation of Cinobufagin by Cultured Suspension Cells of Catharanthus Roseus. *Tetrahedron Lett.* **2002**, *43* (47), 8535–8538. https://doi.org/10.1016/S0040-4039(02)02078-6.

(123) Zhang, X.; Ye, M.; Dong, Y.; Hu, H.; Tao, S.; Yin, J.; Guo, D. Biotransformation of Bufadienolides by Cell Suspension Cultures of Saussurea Involucrata. *Phytochemistry* **2011**, *72* (14), 1779–1785. https://doi.org/10.1016/j.phytochem.2011.05.004.

(124) Zhou, M.; Hou, Y.; Hamza, A.; Zhan, C.-G.; Bugni, T. S.; Thorson, J. S. Probing the Regiospecificity of Enzyme-Catalyzed Steroid Glycosylation. *Org. Lett.* **2012**, *14* (21), 5424–5427. https://doi.org/10.1021/ol3024924.

(125) Zhu, X.-L.; Wen, C.; Ye, Q.-M.; Xu, W.; Zou, D.-L.; Liang, G.-P.; Zhang, F.; Chen, W.-N.; Jiang, R.-W. Probing the Stereoselectivity of OleD-Catalyzed Glycosylation of Cardiotonic Steroids. *RSC Adv.* **2018**, *8* (10), 5071–5078. https://doi.org/10.1039/C7RA11979H.

(126) Fu, Z.-H.; Wen, C.; Ye, Q.-M.; Huang, W.; Liu, X.-M.; Jiang, R.-W. An Efficient Strategy for the Glycosylation of Total Bufadienolides in Venenum Bufonis. *ACS Omega* **2019**, *4* (4), 6819–6825. https://doi.org/10.1021/acsomega.9b00386.

(127) Liu, Y.; Xu, W.; Huang, Z.-H.; Guo, J.; Jiang, R.-W. An Efficient Strategy for the Chemo-Enzymatic Synthesis of Bufalin Glycosides with Improved Water Solubility and Inhibition against Na+, K+-ATPase. *Chemistry & Biodiversity **2020**, 17 (11)*, e2000529. https://doi.org/10.1002/cbdv.202000529.

Chapter 2 Development of Polystyrene Supported Phosphonic Acid Resins for Carbohydrate Immobilization and Glycosylation

This chapter in part was published in:

Rutkoski, R.; Arguelles, A. J.; Huang, Q.; Nagorny, P. *J. Org. Chem*. 2023. 2023, 88, 23, 16467–16484.

DOI: https://doi.org/10.1021/acs.joc.3c01985

2.1 Introduction

Since the work by Fréchet and Schuerch in the early 1970s,[1] solid-phase synthesis has been of great importance to carbohydrate chemistry[2,3] As demonstrated by the pioneering studies of Seeberger and coworkers[4] and others,[5-7] automated solid-phase synthesis has transformed the assembly of complex oligosaccharides and greatly impacted various fields of chemistry, biology, and material science.[8-13] The developments in the aforementioned areas would not be possible without the emergence of new methods for loading and cleaving the glycosyl moiety to/from the resin during the various stages of solid-phase carbohydrate synthesis. The position of carbohydrate attachment may happen at both the anomeric position or other hydroxyl groups, and a variety of linkers at the anomeric position, including thioglycosides, photocleavable benzyl glycosides, allylic alcohol glycosides and esters have been developed.[2,8-13] These methods are tailored to the on-resin oligosaccharide assembly and do not directly involve the use of the acetal end of the linked oligosaccharide for glycosylation reactions (Figure 2.1A and 2.1B). At the same time, the transformations resulting in the direct use of the immobilized carbohydrate as a donor may offer many advantages in the synthesis of glycoconjugates and natural products,

especially if the released solid matrix could be recycled and reused. Such on-resin glycosylations may simplify the purification of the resultant glycosides, shorten the post solid phase synthetic sequences, and have potential for automation and continuous flow applications.[14-18]

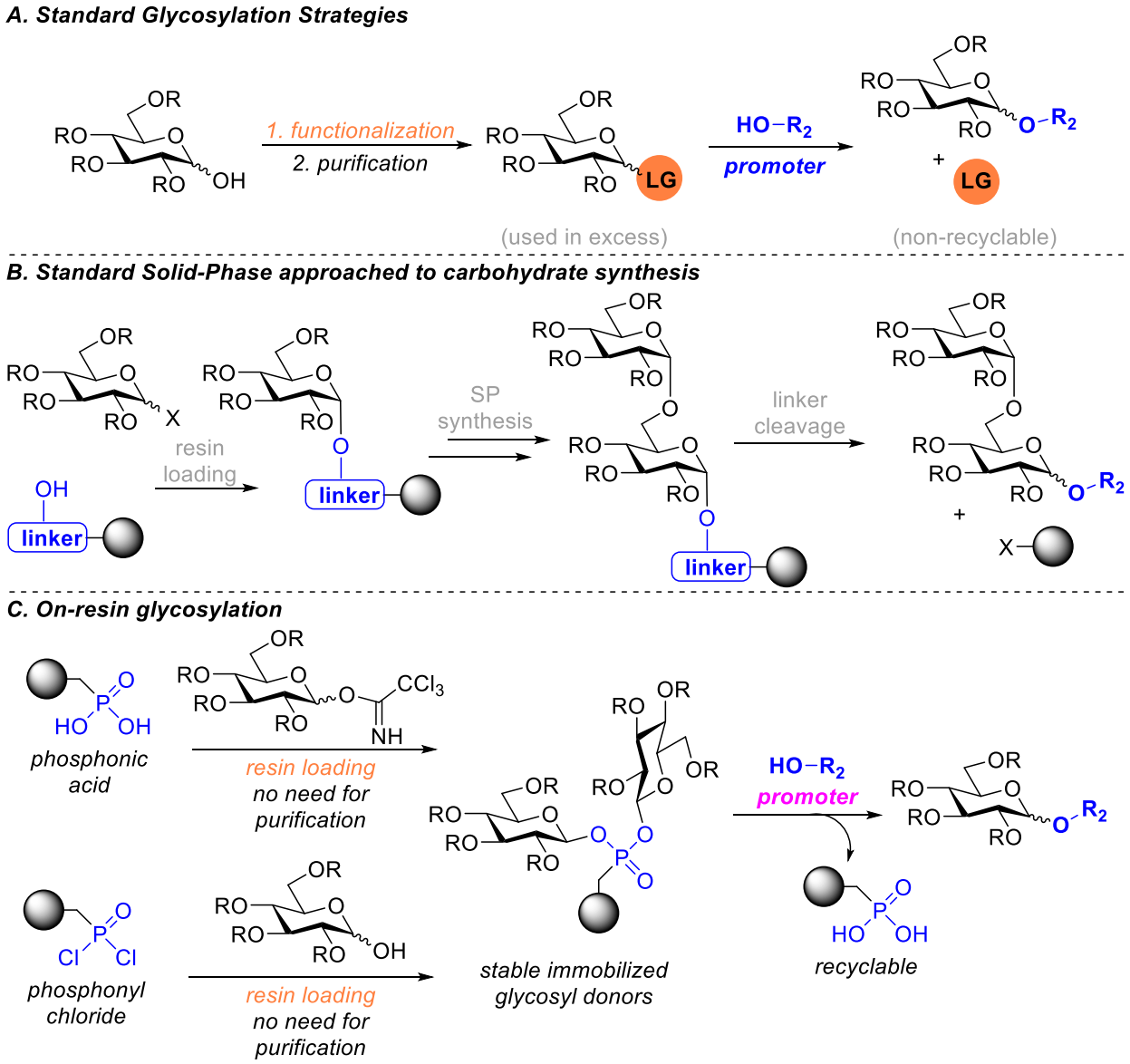
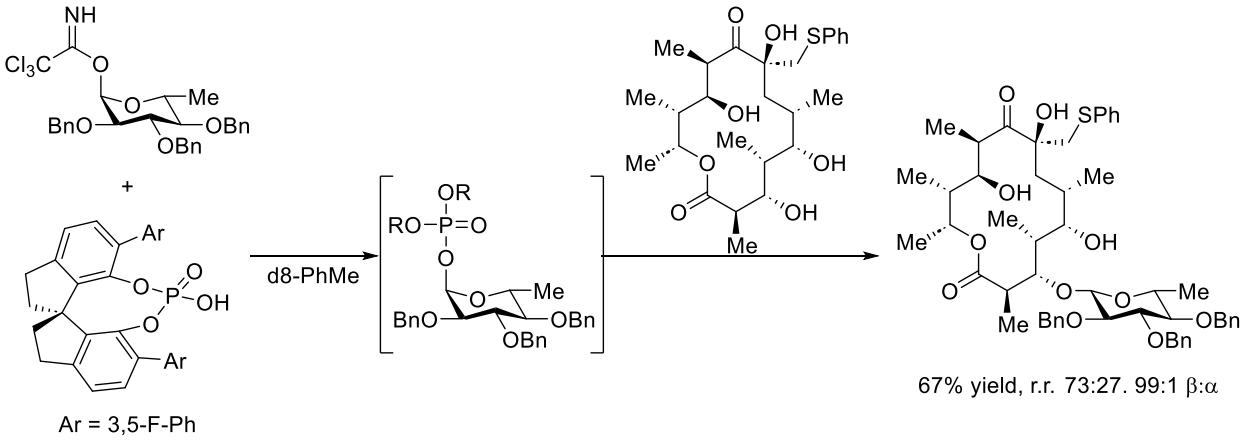


Figure 2.1: Overview of solid supported glycosylation

Most previous methods of solid supported carbohydrate synthesis had focused on the elongation of carbohydrates on the solid support (Scheme 1.3), and the application of solid supported carbohydrate synthesis to natural product synthesis had been relatively underexplored (Scheme 1.4, Scheme 1.5), despite the potential advantages previously outlined (Figure 2.1). The Nagorny group has had long-standing interests in developing new methods and strategies for the synthesis of carbohydrate derivatives[19-23] and glycosylated natural products.[24-26] As a part of these efforts, they have explored the use of chiral phosphoric acids (CPAs) as the catalysts that control both the site-selectivity and diastereoselectivity of complex natural product glycosylations.[24,25]



Scheme 2.1: Chiral phosphoric acid catalyzed regioselective glycosylation of a macrolactone via a covalent phosphate intermediate

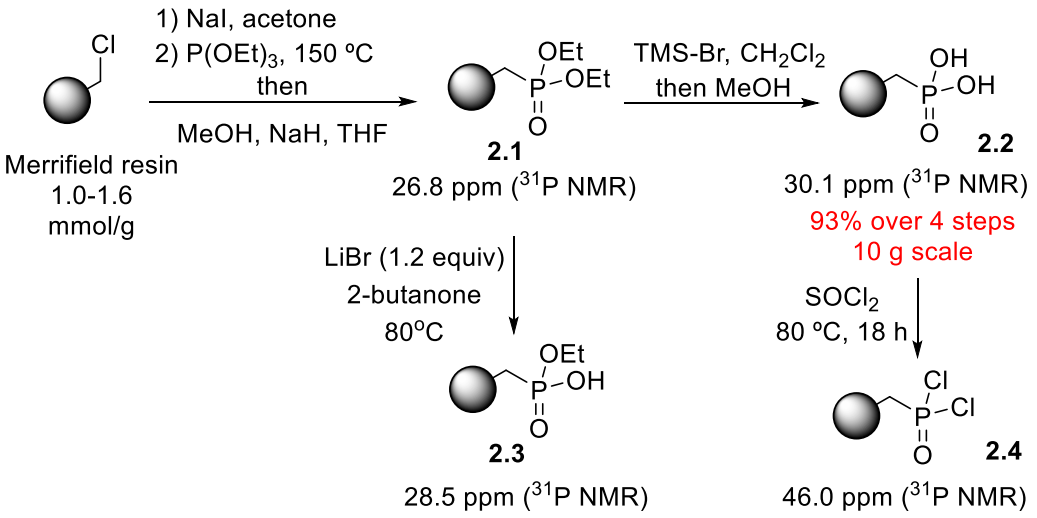
Their recent studies focused on site-selective glycosylation of natural macrolactone-based polyols with trichloroacetimidate donors (Scheme 2.1); they observed fast reactions of CPA catalysts and glycosyl trichloroacetimidates resulting in persistent glycosyl phosphate intermediates that subsequently transferred the carbohydrate moiety to macrolactone acceptors.[24] These observations were not completely unexpected considering that glycosyl trichloroacetimidates are known to react with hydrogen phosphate moiety to produce glycosyl phosphates[27] that are excellent donors for glycosylation reactions.[28] Based on these observations,

they surmised that covalently linked to polystyrene support hydrogen phosphate or phosphonate moieties would capture carbohydrates under mild conditions and provide stable immobilized donors (Figure 2.1C).[29] Upon activation, these donors could be used to glycosylate various acceptors including natural products. The use of such immobilized donors might offer several advantages that include improved stability, cleaner crude reaction mixture profiles and simpler purification, and recyclability of the leaving group (i.e., phosphonate). Such features are particularly useful for the development of automated glycosylations in continuous flow since the resins could be recycled and reloaded.

2.2 Development of solid supported glycosyl phosphonates

2.2.1 Preparation of polymer supported phosphonic acids

Exploration of solid-supported glycosyl phosphonates commenced with the preparation of known, but not well-characterized diethylphosphonate resin **2.1** starting with the commercially available Merrifield resin as the polymer backbone for our solid support (Scheme 2.2).[30-33] Previously, this resin had been applied to the sorption of heavy metals (europium[30-31] and uranium[32]) from wastewater streams. This work marked the inaugural use of polystyrene based phosphonic acid resins for organic synthesis.



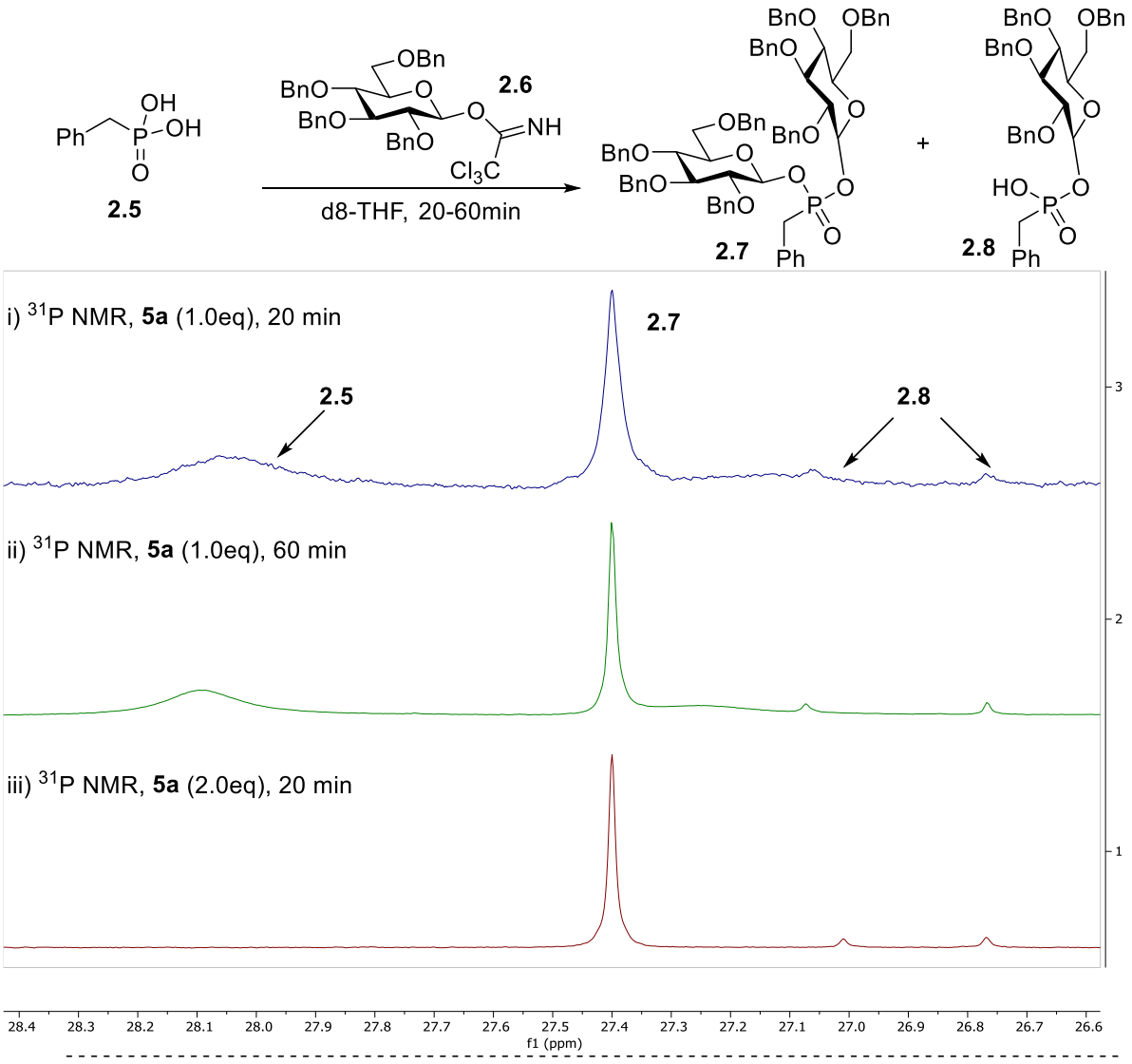
Scheme 2.2: Preparation of phosphonic acid resins

A modified protocol was developed that included transforming the benzylic chloride to the more reactive benzylic iodide (NaI, acetone, rt) followed by the Arbuzov reaction with triethyl phosphite at 150 ºC to provide **2.1**. With the introduction of phosphorous, the formation of the phosphonated resin was monitored and characterized by ^{31}P-gel NMR (δ 26.8 ppm, $CDCl_3$). A capping step was implemented using *in situ* generated methoxide to cap any remaining benzylic chlorides or iodides that were not converted to **2.1** during the Arbuzov reaction. Subsequently, **2.1** was used as the platform for accessing new functionalized resins **2.2-2.3**. The initial attempts at hydrolyzing **2.1** under strongly acidic conditions (12M HCl) or basic conditions (3M NaOH, DMSO/acetone) failed even at reflux, and degradation of the resin was observed in the latter case. This was not unexpected, as it is known that a swollen polymeric matrix is critical for the reactions to occur. Therefore, subsequent studies focused on the transformations in the solvents that are known to solvate the polystyrene beads. While the use of NaI or KI in 2-butanone was not suitable, the use of LiBr (1.2 equivalents) in 2-butanone at 80 ºC led to selective cleavage of one ethoxy group and provided resin **2.3** in quantitative yield (δ 28.5 ppm, ^{31}P-gel NMR). In addition, the treatment of resin **2.1** with bromotrimethylsilane in

dichloromethane at room temperature and subsequent methanolysis afforded phosphonic acid **2.2** (δ 30.1 ppm, ^{31}P-gel NMR). Importantly, the synthesis of phosphonic acid resin **2.2** was conveniently carried out on a decagram scale in excellent yield (93%, 4 steps). Finally, the formation of dichlorophosphonylated resin **2.4** was also achieved by heating **2.2** with excess of thionyl chloride at 80 ºC for 18 hours.[34] Resin **2.4** was found to have a characteristic ^{31}P-gel NMR signal at 46.0 ppm, and it had to be generated and immediately used in the next step due to its propensity to hydrolyze in the presence of moisture.

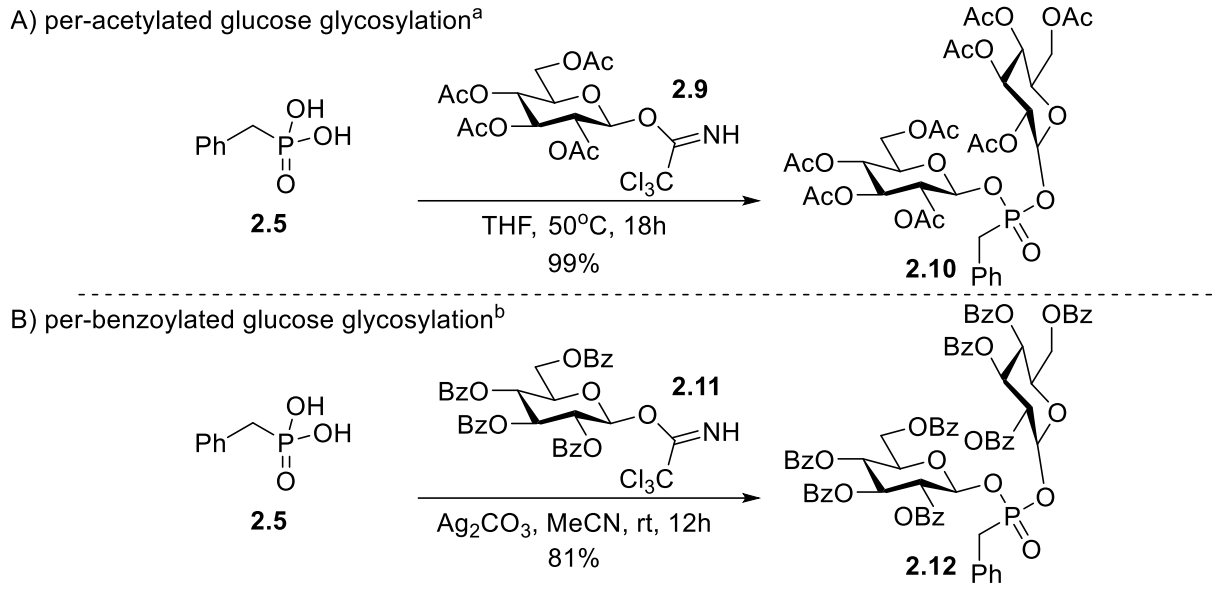
2.2.2 Installation of sugars to solid support

Next, glycosylation reactions on the phosphonic acid moiety were explored. Based on the Nagorny group's prior observation that trichloroacetimidate sugars could rapidly react with CPAs (Scheme 2.1),[24,25] the reaction of benzylphosphonic acid and perbenzylated D-glucose-derived trichloroacetimidate **2.6** was investigated in d^8-THF (Scheme 2.3). This reaction was monitored by ^{1}H and ^{31}P NMR, and it was observed that even with 1:1 stoichiometry, *bis*-glycosylated product **2.7** was formed as the major product along with the minor quantities of monoglycosylated diastereomeric acids **2.8** and unreacted benzylphosphonic acid. The treatment of benzylphosphonic acid **2.5** with 2.0 equivalents of **2.6** for 20 minutes produced **2.7** as the major product along with minor quantities of monoglycosylated diastereomeric acids **2.8**. The formation of **2.8** was minimized when **2.5** was treated with 2.2 equivalents of **2.6** to afford **2.7** in quantitative yield.



Scheme 2.3: Initial optimization of glycosyl phosphonate formation
[a]**2.6** (60 or 120 µmol,1.0 or 2.0 equiv), **2.5** (60 µmol,1.0 equiv), d8-THF(0.4 mL), rt, 20−60min.

Similarly, bis-glycosylation of **2.5** with per-acetylated D-glucose trichloroacetimidate **2.9** in THF at room temperature afforded bis-glycosylated phosphonate **2.10** in 81% yield. The conversion of this reaction was improved when the reaction was run at 50°C, to provide **2.10** in quantitative yield (Scheme 2.4A). While bis-glycosylation of **2.5** with per-benzoylated D-glucose trichloroacetimidate was unsuccessful; bis-glycosylation of **2.5** was accomplished with benzoylated glucosyl bromide **2.11** in MeCN at room temperature to provide phosphonate **2.12** in 81% yield (Scheme 2.4B).

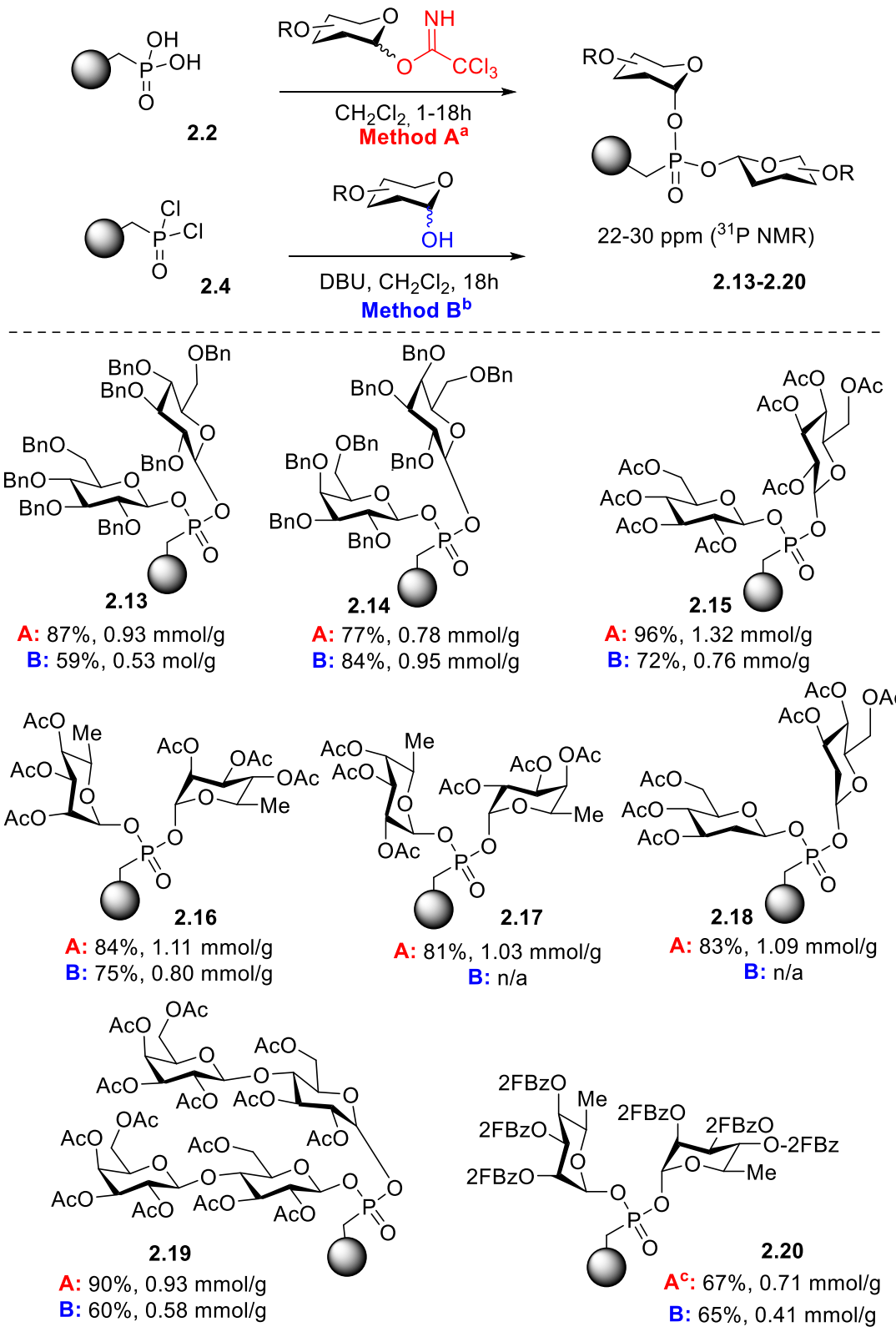


Scheme 2.4: Phosphonylation of acylated glycosides
[a]**2.9** (110 μmol, 2.2 equiv), **2.5** (50 μmol,1.0 equiv), THF (0.5 mL), 50 °C, 18 h. [b]**2.11** (110 μmol, 2.2 equiv), **2.5** (50 μmol,1.0 equiv), Ag_2CO_3 (110 μmol, 2.2 equiv), MeCN (0.5 mL), rt, 12h

These conditions were selected to load carbohydrates on to resins **2.2** and **2.3** for the subsequent studies. Similar to the model studies above, both **2.2** and **2.3** underwent rapid carbohydrate loadings to quantitatively provide the corresponding immobilized glycosyl phosphonates in less than one hour. However, based on the subsequent observations that the ethoxy moiety in glycosylated **2.3** is not stable to Lewis acidic conditions required for the glycosylations of acceptors, subsequent studies were focused on exploring resin **2.2** to obtain bis-glycosylated resins **2.13-2.20** (Scheme 2.5).[35]

The simple stirring of **2.2** in dichloromethane solutions containing 2.2 equivalents of armed perbenzylated D-glucose and D-galactose trichloroacetimidates (method A) efficiently provided difunctionalized glycosylphosphonate resins **2.13** and **2.14** in 87% and 77% yield correspondingly within one hour. The reactions with disarmed (peracetylated) carbohydrates proceeded at slower rates and required 18 hours to achieve full loadings, but still provided bis-functionalized resins **2.15-2.19** in excellent yields (96% for **2.15**, 84% for **2.16**, 81% for **2.17**,

83% for **2.18**, and 90% for **2.19**). Importantly, these transformations are not limited to CH_2Cl_2 as the solvent, and the syntheses of resins **2.15-2.19** via method A were successfully carried out in THF (81%), 1,2-dichloroethane (84%), and toluene (86%) to give similar loading. While *ortho*-fluorobenzoate protected sugars are of great utility in organic synthesis,[36] initial attempts to generate **2.20** from the corresponding trichloroacetimidate were unsuccessful even when carried in refluxing dichloromethane, THF, and dichloroethane. However, refluxing **2.2** with the corresponding trichloroacetimidate in toluene for 18 hours successfully provided resin **2.20** in 67% yield.



Scheme 2.5: Preparation of immobilized glycosyl phosphonates

[a]MethodA: glycosyl trichloroacetimidate (2.2 equiv), resin **2.2** (1.0 equiv), CH_2Cl_2 (2 mL/0.1g), rt, 1 h (**2.13 - 2.14**) or 18 h (for **2.15 – 2.20**). [b]Method B: glycosyl hemiacetal (2.2 equiv), resin **2.4** (1.0 equiv), DBU (4.0 equiv),

CH_2Cl_2 (2 mL/0.1g), rt, 18 h.. [c]The synthesis of **2.20** via Method A was performed in toluene at 110°C for 18 h. The resin loadings have been estimated gravimetrically and confirmed by elemental analysis (resin **2.19**).

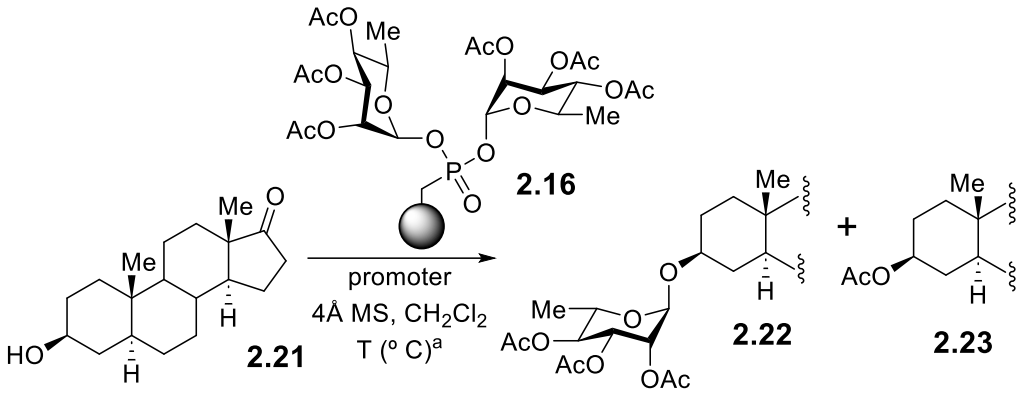
Alternatively, phosphonate resins **2.13-2.20** could be obtained directly from the unfunctionalized reducing sugars and resin **2.4** using Method B (Scheme 2.5). This method works best if fresh resin **2.4** is obtained from **2.2** through the functionalization with thionyl chloride (Scheme 2.2). Freshly formed **2.4** was reacted with sugar hemiacetals (2.2 equiv.) and DBU (4 equiv.) in CH_2Cl_2 for 18 hours, and the resultant phosphonate resins **2.13-2.20** were obtained in similar yields and loadings (59-84% yield). It is important to emphasize, that the formation of resins **2.13-2.20** involves simple mechanical manipulations and convenient purification through filtration and washing. Moreover, all of the immobilized donors **2.13-2.20** were found to be bench stable at room temperature for at least four years.

2.3 Glycosylations with solid supported glycosyl phosphonate donors

With these developments in hand, subsequent studies were focused on identifying the conditions for efficient glycosyl transfer. For this purpose, peracetylated *L*-rhamnose containing resin **2.16** was selected as the donor and *trans*-androsterone **2.21** was chosen as the acceptor (Table 2.1). The initial reaction with TMSOTf (1.8 equiv.) as the promoter,[28] and excess of resin **2.16** (2.5 equiv.) at 0 ºC to room temperature (Table 2.1, entry 1) afforded the desired glycosidic product in only 12% yield. Switching to super-stoichiometric $BF_3{\cdot}Et_2O$ as the promoter (entry 4) led to an increase in yield to 19%, but also resulted in significant formation of the acetylated byproduct **10** (9% yield). Attempts to lower the loading of $BF_3{\cdot}Et_2O$ to catalytic (entry 2) or stoichiometric (entry 3) amounts proved unsuccessful, possibly due to the Lewis basic nature of the phosphonate moiety poisoning the promoter. Based on these observations, it was surmised that longer reaction times with a super-stoichiometric $BF_3{\cdot}Et_2O$ may lead to better conversions,

and, indeed, stirring the reaction mixture for 72 hours led to 34% yield of **2.22** and 13% of **2.23**, even with only 1 equivalent of resin **2.16** (entry 5).

Table 2.1: Glycosylation condition optimization[a]

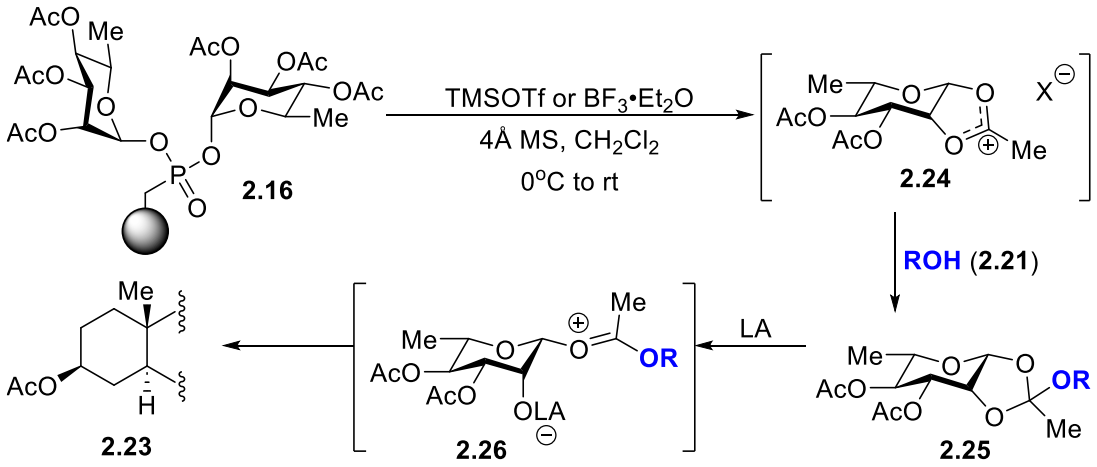


entry	promoter (equiv.)	**2.16** (equiv.)	T (°C)	time (h)	yield of **2.22** (%)	yield of **2.23** (%)
1	TMSOTf (1.8)	2.5	0 to rt	24	12%	-
2	$BF_3{\cdot}Et_2O$ (0.5)	2.5	0 to rt	18	<5%	-
3	$BF_3{\cdot}Et_2O$ (1.0)	2.5	0 to rt	18	<5%	-
4	$BF_3{\cdot}Et_2O$ (1.5)	2.5	0 to rt	18	19%	9%
5	BF_3Et_2O (1.5)	1.0	0 to rt	72	34% (α-only)	13%
6	$BF_3{\cdot}Et_2O$ (1.5)	1.0	-10	18	n.d	-
7	$BF_3{\cdot}Et_2O$ (1.5)	1.0	40	18	78% (α-only)	<5%
8[b]	$BF_3{\cdot}Et_2O$ (1.5)	1.0	80	1	85% (α-only)	<5%
9	$B(C_6F_5)_3$ (0.2)	1.0	0 to rt	24	n.d	-

[a]The reactions were carried out with 0.05 mmol of **2.21** and 0.05−0.125 mmol of pre-swelled **2.16** (i.e., 0.1−0.25 mmol active sugar donor).Upon full consumption of **2.21**, the reaction mixture was filtered, washed, and quenched with Et_3N (50μL) prior to concentration. [b]This reaction was carried using dichloroethane (DCE) as a solvent.

The side-product **2.23** may potentially originate as the result of the undesired pathway involving the formation of an orthoester intermediate **2.25** from the dioxolenium ion **2.24** followed by its rearrangement to **2.26** and cleavage to form acetate **2.23** (Scheme 2.6).[37] In order to render the formation of intermediate **2.26** leading to **2.23** reversible, the glycosylation at elevated temperature (40 ºC) was considered next (entry 7). Indeed, this led to the significantly improved and faster formation of **2.22** (78% yield), and suppressed the formation of **2.23**. Further increase of temperature to 80 ºC required the use of higher boiling solvent (1,2-

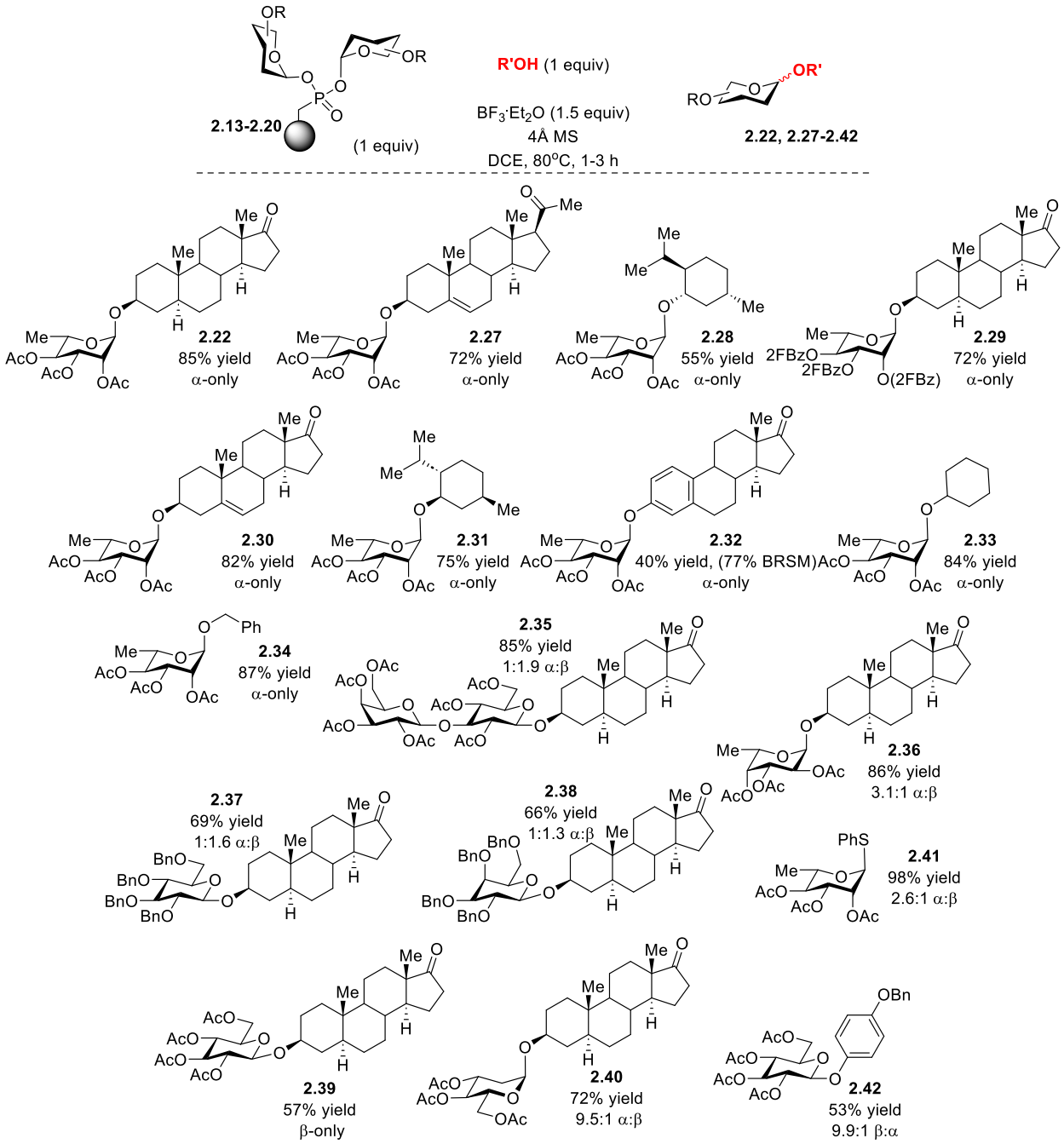
dichloroethane) and resulted in a significantly faster formation of **2.22** (entry 8). Thus, refluxing the reaction in 1,2-dichloroethane for 1 hour led to selective formation of the α-glycoside **2.22** in 85% yield and only trace quantities of **2.23** were observed (<5% yield). While tris(pentafluorophenyl)borane has often demonstrated excellent catalytic activity in glycosylation reactions[38,39] its use as a Lewis acid instead of BF_3•OEt_2 (entry 9) did not lead to any desired product formation at room temperature. In addition to the aforementioned conditions, examination of various Fe(III), Cu(II), Yb(III), Ti(IV), Zn(II), Ag(I), and Zr(IV) salts, molecular iodine, and combination of *bis*-*p*-nitrophenylphosphoric acid with Schreiner's thiourea did not lead to the significant formation of **2.22**. Based on this, the conditions for entry 8 were selected for the subsequent studies (Scheme 2.7).



Scheme 2.6: Potential mechanism for formation **2.23**

Our subsequent studies were focused on demonstrating that resins **2.13–2.20** could be used as donors for glycosylation of various acceptors (Scheme 2.7). Glycosylations with the phosphonic acid resins as glycosyl donors were carried out using various natural and unnatural alcohols, phenols and thiophenol as nucleophiles. Considering that α-L-rhamnose moiety is present in a variety of steroidal natural products, resin **2.16** was used for the generation of α-*L*-rhamnosylated products **2.22**, **2.27-2.31**, and **2.33-2.34** in excellent to good yields (87-75%).

Importantly, products **2.22, 2.27, 2.29-2.31** and **2.34** contained acid sensitive or enolizable functionalities that survived the reaction conditions. At the same time, the α-*L*-rhamnosylation of estrone did not proceed well, probably, due to the lability of the product **2.32** under the reaction conditions. In contrast, the reaction of **2.16** with thiophenol proceeded completely and provided the desired product **2.41** in 98% yield albeit 2.6:1 α:β ratio. The reaction of aglycone **2.21** was subsequently investigated with other resins **2.13-2.15** and **2.17-2.20** to provide glycosylated products **2.35-2.42**. The reaction with **2.19** led to the efficient transfer of peracetylated lactose moiety without cleavage of the glycosidic linkage providing **2.35** in 85% yield and 1.9:1 β:α selectivity, which is consistent with the yields previously observed for the β-glycosylations with peracetylated lactose donors.[40]



Scheme 2.7: Glycosylation substrate scope[a]

[a]The reactions were carried out using 0.05 mmol acceptor with resins **2.13-2.20** (1.0 equiv, i.e., 2.0 equiv of active sugar donor) at 80°C for 3 h in the presence of $BF_3{\cdot}OEt_2$(1.5 equiv) and 4 Å MS. Upon full consumption of the acceptor, the reaction mixture was filtered, washed, and quenched with Et_3N (50μL) prior to concentration.

Similarly, labile L-fucoside **2.36** was obtained in excellent 86% yield and 3.1:1 α:β selectivity. As expected, perbenzylated D-glucose and D-galactose-based donors **2.13** and **2.14** resulted in efficient formation of **2.37** and **2.38**, albeit with no selectivity. Notably, the reaction

with 2-deoxyglucose donor **2.18** proceeded in 72% yield with 9.5:1 α:β selectivity. This transformation is of significance as the selective formation of α-2-deoxyglucosides is often challenging,[41] but important to the synthesis of natural products.[42] Finally, β-selective reactions of **2.15** provided *D*-glucosylated products **2.39** and **2.42** (57% and 53%, respectively). Importantly, these results correlate well with the selectivities and yields obtained for the standard donors of this type and further optimization of the donor protecting groups and Lewis acids will lead to the improvement of these parameters.

One of the important features noted during the studies above was that crude ^{1}H NMR and TLC reaction profiles of the reactions run with donors **2.13-2.20** were significantly cleaner than typical crude glycosylation mixtures for the reactions with trichloroacetimidates as well as other donors (Figure 2.2). Standard glycosylation protocols require using an excess of trichloroacetimidates, and the crude reaction mixtures are contaminated with the unreacted, hydrolyzed, or decomposed donors. In contrast, the excess of unreacted glycosylated resins **2.13-2.20** could be removed by filtration and subsequently recycled, and, therefore, the filtrate would not be contaminated as much with the residual trichloroacetimidate and its decomposition products. Figure 2.2 provides the comparison of ^{1}H NMR profiles of the crude reaction mixture resulting from the reaction of resin **2.16** (2.2 equiv. of active donor) and aglycone **2.21** (Figure 2.2B) and similar solution reactions of trichloroacetimidate donor **2.43** with **2.21** catalyzed by BF_3•OEt_2 (Figure 2.2C) and TMSOTf (Figure 2.2D). As evident from this analysis, both control experiments (Figure 2.2C and Figure 2.2D) are significantly more contaminated with the decomposition side-products such as **2.23** than the reaction in Figure 2.2B, which contains primarily product **2.22**.

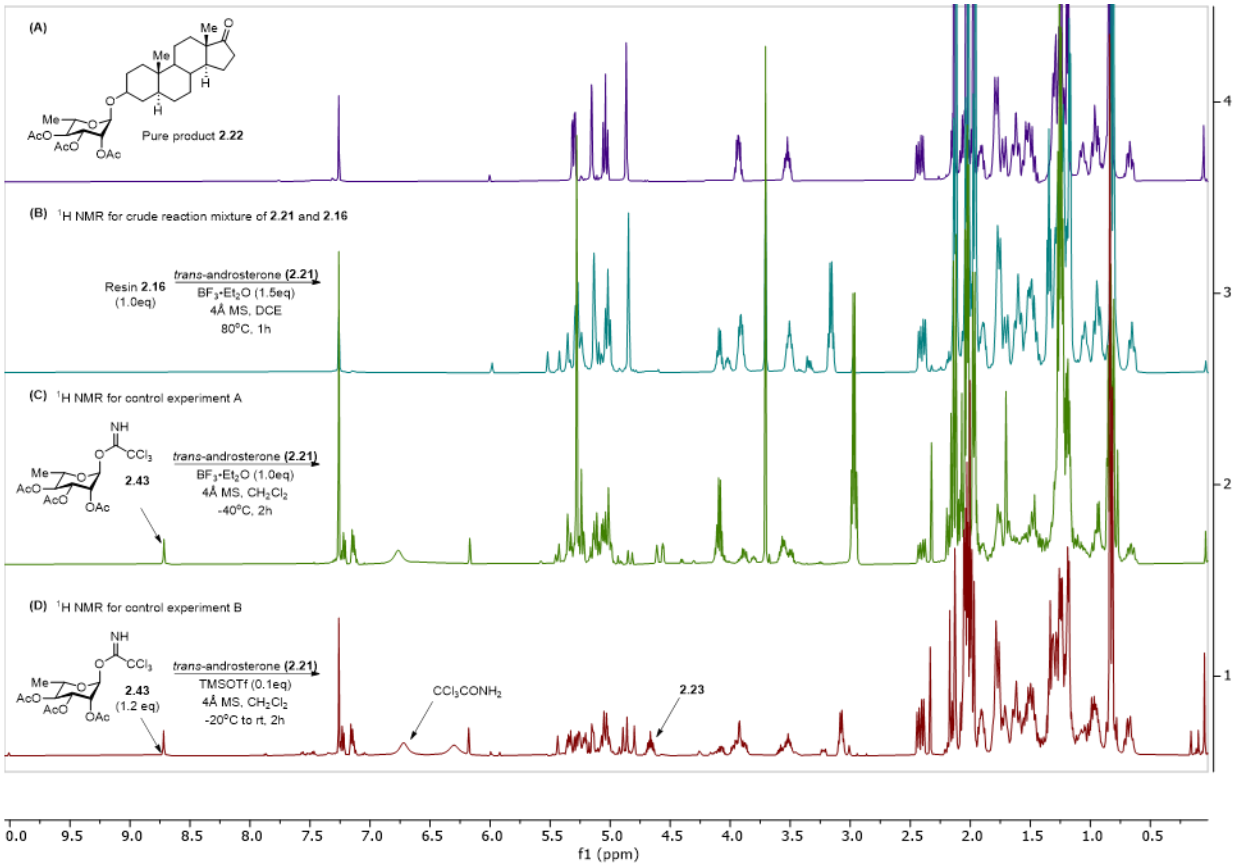
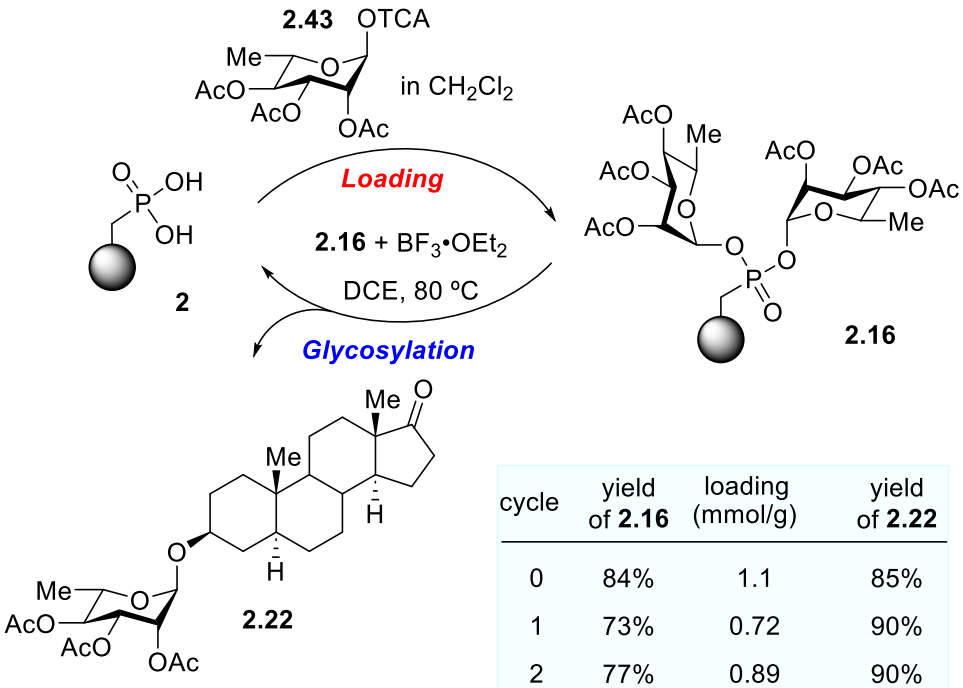


Figure 2.2: Comparison of crude 1H NMR spectra for the reaction of **2.21** with resin **2.16** or corresponding trichloroacetimidate **2.43** as donors.

[a]All spectra were recorded in $CDCl_3$ at 500 MHz; (A) ^{1H} NMR spectrum of pure product **2.22**; (B) ^{1}H NMR spectrum of the crude reaction mixture obtained by reacting resin **2.16** (1.0 or 2.0 equiv of active glycosyl donor), **2.21** (1.0 equiv), $BF_3{\cdot}OEt_2$ (1.5 equiv), dichloroethane, 80°C, 4 Å MS, 1 h; (C) **2.43** (2.0equiv), **2.21** (1.0 equiv), $BF_3{\cdot}OEt_2$ (1.0 equiv), DCM, −40°C, 4 Å MS, 2 h; (D) **2.43** (1.2 equiv), **2.21** (1.0 equiv), TMSOTf (0.1 equiv), DCM, −20°C to rt, 4Å MS, 2 h.

In addition to their excellent bench stability and cleaner crude reaction mixtures, another important feature of donors **2.13-2.20** is that the recovered by filtration polystyrene support consisting of unreacted **2.13-2.20** and **2.2** might be potentially recycled and reused. To demonstrate this, the studies summarized in Figure 2.3 were performed.



cycle	yield of **2.16**	loading (mmol/g)	yield of **2.22**
0	84%	1.1	85%
1	73%	0.72	90%
2	77%	0.89	90%

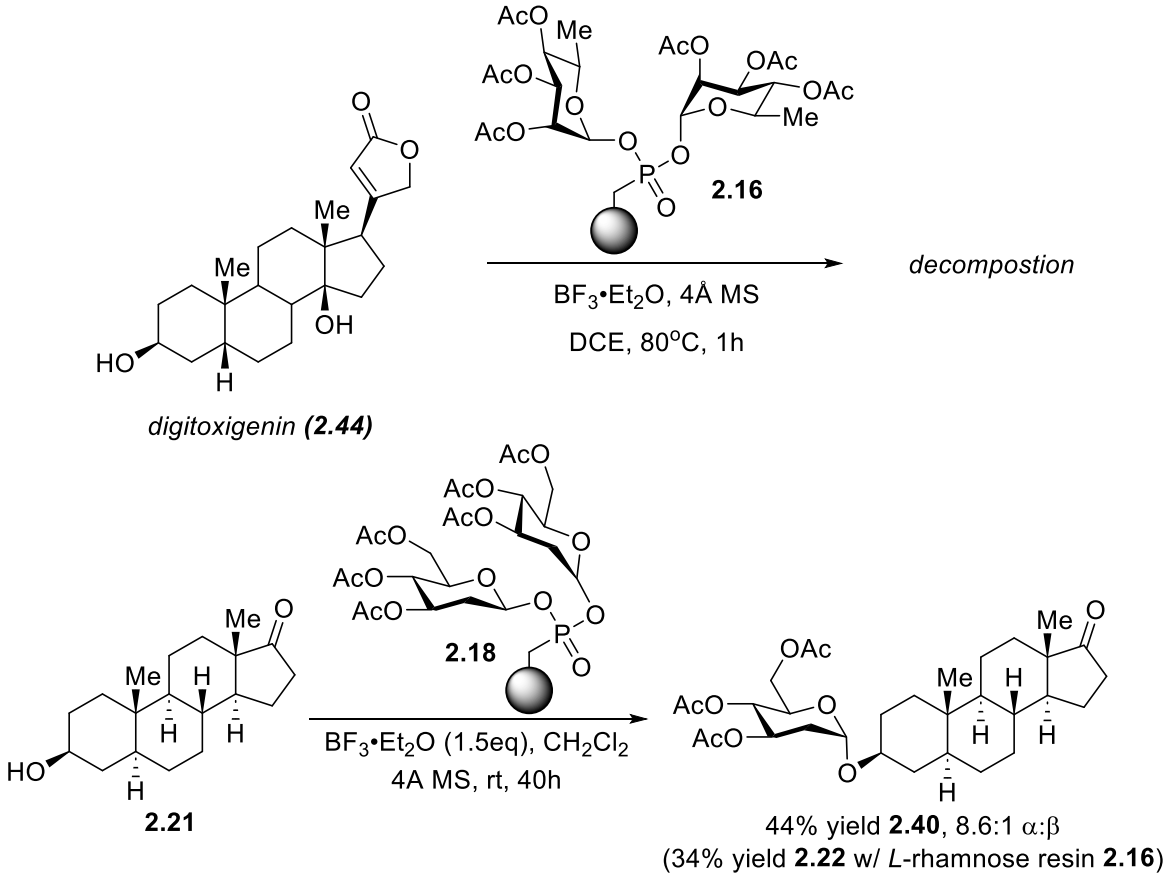
Figure 2.3: Recyclability of resin **2.2**

[a]The loading was achieved using Method A (Scheme 2.5), and glycosylation was performed as described in Scheme 2.7**.** Resin **2.2** was washed and dried between the cycles.

Thus, following the standard work-up of the glycosylation reaction, reacted resin **2.16** was filtered off and treated with aqueous HCl and CH_2Cl_2 for 18 hours. Upon filtering and washing the resin, it could be loaded again with peracetylated *L*-rhamnose-derived trichloroacetimidate. The resultant resin **2.16** was subsequently employed for the glycosylation of steroid acceptor **2.21**, and this reaction was carried out using the established conditions to stereoselectively produce a-**2.22** in 90% yield. Importantly, the immobilized resin **2.16** was conveniently recovered by filtration, recycled, and re-used twice without any noticeable impact on the loading and glycosylation yields (Figure 2.3). This, combined with cleaner crude reaction mixture profiles (Figure 2.2), suggests that the excess donor **2.16** could be recovered and recycled thus minimizing the costs associated with the glycosylation process and making this process potentially amenable to automation.

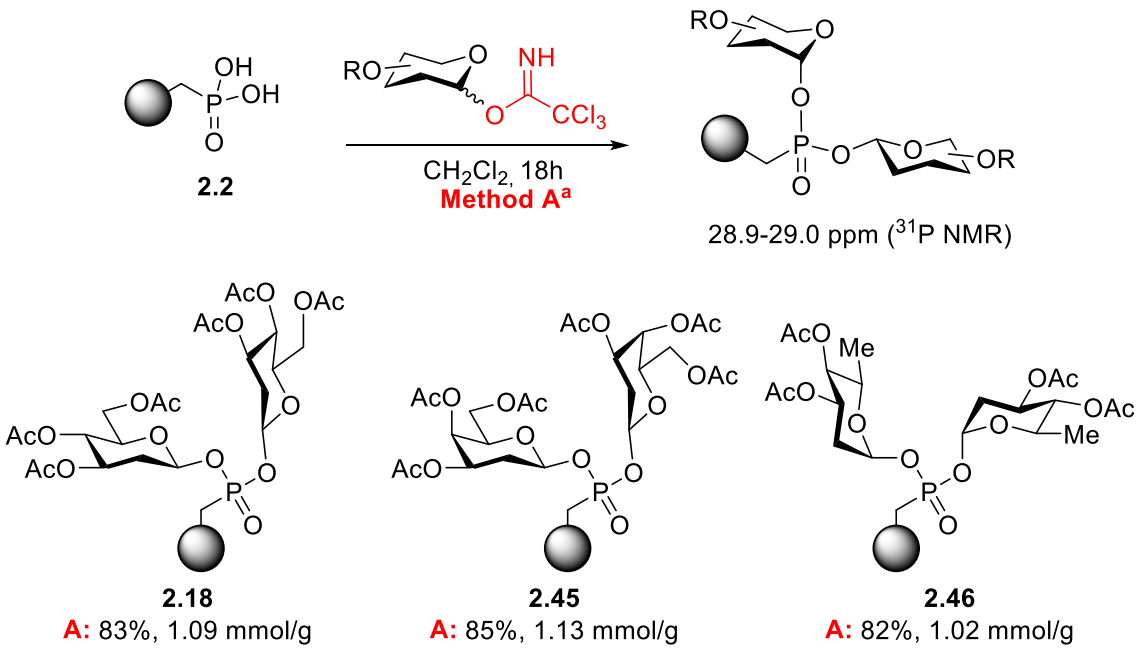
2.4 Resin bound 2-deoxy glycosides and glycosylation of cardiotonic steroids

Initial studies of glycosylation of cardiotonic steroids with resin **7.16** under the established conditions (Scheme 2.8) resulted in decomposition of the delicate aglycone acceptor. It was surmised that the excess quantity of strong Lewis acid and high temperatures were the cause of the incompatibility. Performing the reaction at lower temperatures resulted in lower yield of rhamnosylated product **2.22** (Table 2.1, entry 5). With 2-deoxyglucose resin **2.18**, we observed a slightly in yield for the desired glycoside **2.40** (Scheme 2.8) when the reaction was carried at room temperature. With this initial discovery in hand, the development of reaction conditions for glycosylation with 2-deoxy glycoside resins was investigated.



Scheme 2.8: Preliminary study of 2-deoxy glycoside transfer from resin **2.18**

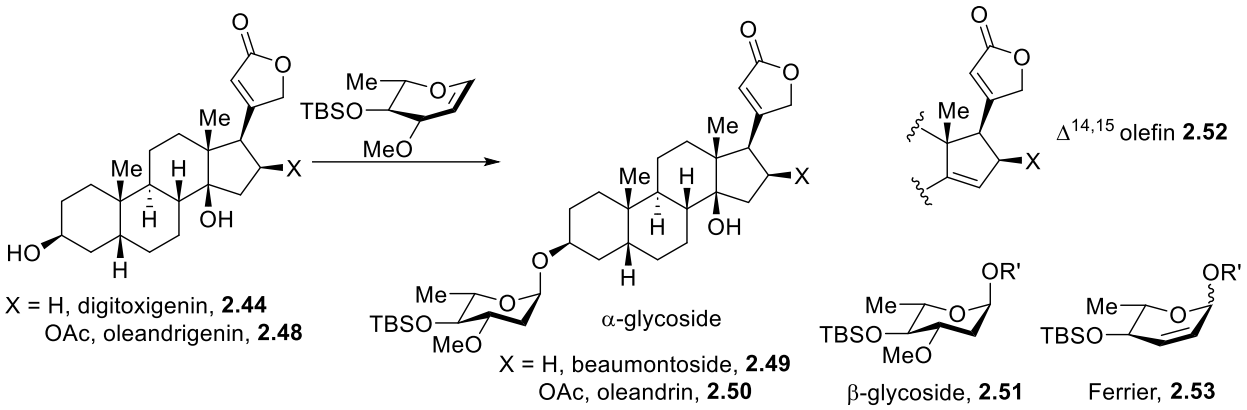
Glycosyl trichloroacetimidates of 2-deoxy-*D*-glucose, 2-deoxy-*D*-galactose, and 2-deoxy-*L*-rhamnose were loaded on the solid support (Scheme 2.9) following the general method A described previously in good yields (82-85%). Attempts to install deoxy sugars directly to resin **2.2** from their corresponding glycals were unsuccessful under both neutral and acidic conditions (TFA, Ph_3P•HBr).



Scheme 2.9: Immobilization of 2-deoxyglycosides

[a]Method A: glycosyl trichloroacetimidate (2.2 equiv), resin **2.2** (1.0 equiv), CH_2Cl_2 (2 mL/0.1g), rt, 18 h. The resin loadings have been estimated gravimetrically and confirmed by elemental analysis (resin **2.19**).

Having successfully installed multiple 2-deoxyglycosides to solid support, we looked to develop glycosylation conditions to maximize yield and diastereoselectivity, while minimizing byproduct formation. In previous studies by our group[43] on the α-glycosylation of cardiotonic steroids with *L*-oleandral, the most common by-products observed were the β-glycosylation product **2.50** $\Delta^{14,15}$ alkene containing cardenolide **2.51** and the product **2.52** resulting from the Ferrier rearrangement (Scheme 2.10).

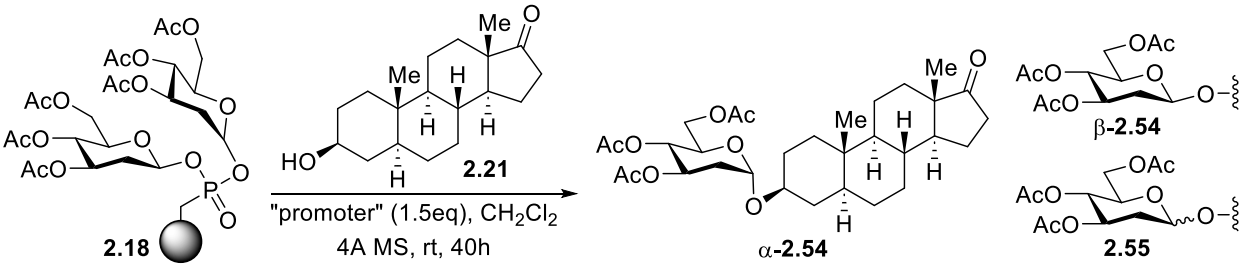


Scheme 2.10: Notable byproducts from glycosylation of cardiotonic steroids with oleandral

The studies commenced by first evaluating the efficiency of BF_3•OEt_2 to promote the reactions at various temperatures (Table 2.2, entry 1-3). The standard conditions for glycosylation with BF_3•OEt_2 afforded glycosides **2.40** in 72% yield and 9.5:1 d.r. (α:β). As the temperature was decreased (80°C to room temperature), a significant drop off in yield was observed, however, there was an increase in the diastereoselectivity, and the formation of Ferrier product **2.53** was nearly completely suppressed at room temperature. Next, the ability of various Lewis acids to promote the glycosylation was evaluated (Table 2.2, entry 5-12, 15). Reactions promoted by $Bi(OTf)_3$ (entry 8) and $Cu(OTf)_2$ (entry 9) were unable to promote any glycosylation. Reactions with $B(C_6F_5)_3$ (entry 5) and $AlCl_3$ (entry 7) favored formation of Ferrier product **2.53** over the desired glycosylation products **2.40**. TMSOTf (entry 6), $Sc(OTf)_3$ (entry 10), and $Hf(OTf)_4$ afford desired products **2.40** in low yields (<40%) and low diastereoselectivity. Excitingly, $Yb(OTf)_3$ (entry 12) and $FeCl_3$ (entry 15) were able to promote the desired glycosylation in good yields (71% for $Yb(OTf)_3$, 76% for $FeCl_3$). The effect of temperature for the best performing promoters, $Yb(OTf)_3$ and $FeCl_3$ was then evaluated. No reaction observed for either promoter at -78°C (entry 14, 17), and at 0°C (entry 13, 16), the yield of **2.40** was modestly improved (5-10% increase), but the diastereoselectivity was slightly decreased. Ultimately the optimization was progressed with $FeCl_3$ at 0°C, as the lower

temperature may help minimize the C14 elimination byproducts previously observed during glycosylation of cardenolides.

Table 2.2: Optimization of glycosylation with 2-deoxyglucose resin **2.18**.[a]



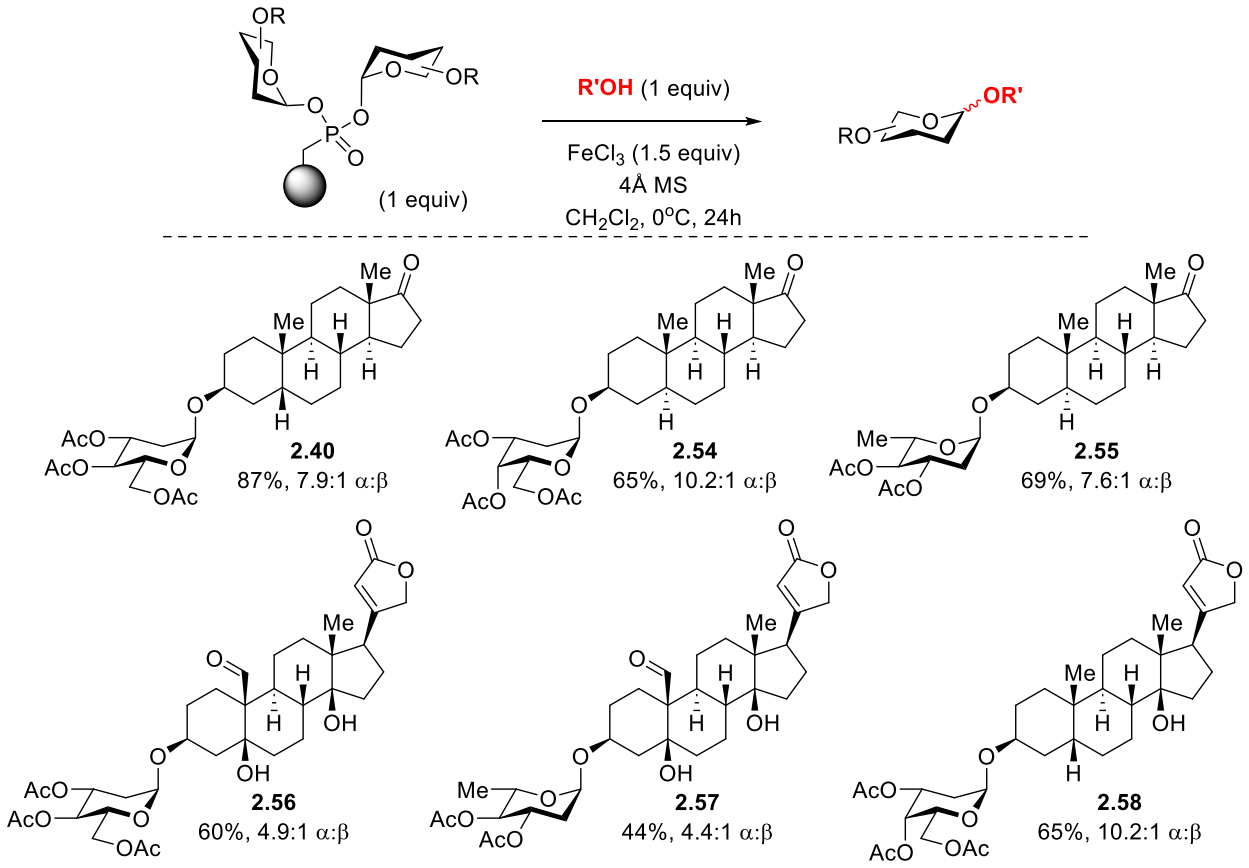
entry	promoter	NMR yield **2.54**[b]	d.r (α-**2.54**:β-**2.54**)[c]	**2.54**:**2.55**[e]	yield **2.54**[f]
1	$BF_3{\cdot}Et_2O$ (80°C, DCE, 3h)	-	9.5:1	6.6:1	72%
2	$BF_3{\cdot}Et_2O$ (40°C, DCE, 24h)	-	7.5:1	13.3:1	53%
3	$BF_3{\cdot}Et_2O$ (rt, DCE, 24h)	-	8.6:1	-	44%
4	$BF_3{\cdot}Et_2O$	40%	6.0:1	2.3:1	-
5	$B(C_6F_5)_3$	-	-	0:1 (112%)	-
6	TMSOTf	35%	-[d]	3.1:1	-
7	$AlCl_3$	25%	3.3:1	0.3:1	-
8	$Bi(OTf)_3$	n.r.	-	-	-
9	$Cu(OTf)_2$	n.r	-	-	-
10	$Sc(OTf)_3$	31%	-[d]	2.4:1	-
11	$Hf(OTf)_4$	24%	-[d]	1.8:1	-
12	$Yb(OTf)_3$	71%	7.0:1	2.8:1	-
13	$Yb(OTf)_3$ (0°C)	82%	2.5:1	4.5:1	-
14	$Yb(OTf)_3$ (-78°C)	n.r.	-	-	-
15	$FeCl_3$	76%	10.8:1	7.2:1	77%
16	$FeCl_3$ (0°C)	82%	7.9:1	4.5:1	87%
17	$FeCl_3$ (-78°C)	n.r.	-	-	-
18	$FeCl_3$ (0°C, 0.05eq)	n.r	-	-	-
19	$FeCl_3$ (0°C, 0.1eq)	n.r	-	-	-
20	$FeCl_3$ (0°C, 0.2eq)	n.r	-	-	-
21	$FeCl_3$ (0°C, 0.5eq)	40%	2.9:1	5.5:1	-
22	$FeCl_3$ (0°C, 1.0eq)	72%	5.5:1	2.5:1	68%
23	$FeCl_3$ (0°C, 2.0eq)	84%	8.3:1	7.5:1	73%
24	$FeCl_3$ (0°C, DCE)	69%	6.0:1	1.7:1	-
25	$FeCl_3$ (0°C, THF)	49%	1.4:1	1:0	-
26	$FeCl_3$ (0°C, Et_2O)	10%	2.6:1	1.3:1	-
27	$FeCl_3$ (0°C, tBuOMe)	n.r.	-	-	-
28	$FeCl_3$ (0°C, MeCN)	50%	1.6:1	1:0	-
29	$FeCl_3$ (0°C, PhMe)	13%	1.8:1	2.0:1	-

[a]The reactions were carried out with 34 µmol of **2.21** and 0.034 µmol of pre-swelled **2.18** (i.e., 68 mmol active sugar donor). Upon full consumption of **2.21**, the reaction mixture was filtered, washed, and quenched with Et_3N (50 µL) prior to concentration. [b]NMR yields were obtained from ^1H NMR (500 MHz, $CDCl_3$) with CH_2Br_2 (5.0 µL) as internal standard. [c]diastereomeric ratios were determined by ^1H NMR of the crude reaction mixtures. [d]The diastereomeric ratio could not be determined due overlapping of the β-product peak with an undetermined impurity. [e]The ratios of **2.40:2.53** were determined by ^1H NMR of the crude reaction mixtures. [f]Isolated yield. n.r. = no reaction.

Attempts to lower the catalyst loading below stoichiometric amounts (Table 2.2, entry 18-21) led to no reaction whatsoever (5-20mol% $FeCl_3$), or greatly reduced yield (50mol%, 40% yield). Reactions with stoichiometric $FeCl_3$ all proceeded in comparable yield (entry 22-23), and higher catalyst loading generally resulted in higher diastereoselectivity. Finally, the effect of solvent was investigated (entry 24-29). The reaction in DCE (entry 24) proceeded in slightly lower yield and diastereoselectivity of **2.40**, and more of the Ferrier product **2.53** was produced. Ethereal solvents THF (entry 25), Et_2O (entry 26), and ^{t}BuOMe (entry 27) led to significant drop-off in yield and diastereoselectivity, and with ^{t}BuOMe, the no reaction was observed. The reaction in THF showed no formation of the Ferrier product **2.53.** In MeCN (entry 28), a solvent shown to promote β-selective glycosylations,[44,45] lower yield of **2.40** was observed, and the reaction was still mildly α-selective. Formation of the Ferrier product was also completely suppressed. The reaction in toluene (PhMe, entry 29) afford very small amounts of nearly unselective glycosylation. We settled upon stoichiometric $FeCl_3$ (1.5 eq) at 0^{o}C in CH_2Cl_2 (entry 16) as optimal conditions for its high yield and selectivity of **2.40** (87%, 7.9:1 α:β).

With optimal conditions in hand, the utility of the 2-deoxyglycosyl resins (**2.18, 2.45, 2.46**) for glycosylation of natural product acceptors, such as androsterone **2.21** and cardiotonic steroids, was demonstrated. First, the glycosylation of *trans*-androsterone acceptor **2.21** with each of the solid supported donors **2.18, 2.45,** and **2.46** was performed. Glycosylation of **2.21** with resin **2.18** afforded 2-deoxy-glucoside **2.40** in 87% yield and 7.9:1 α:β selectivity, and glycosylation with 2-deoxygalactoside resin **2.45** provided 2-deoxygalactoside **2.54** in 65% yield and 10.2 α:β selectivity. Generally, 2-deoxy-galactosides are formed in higher α-selectivity than their glucoside counterparts, and a similar trend was observed in this example. Resin **2.46** derived from *L*-rhamnal was employed to furnish 2,6-dideoxy glycoside **2.55** in 69% yield and

7.6:1 α:β selectivity. These examples demonstrate the ability of the solid supported donors to transfer 2-deoxy glycosides in a high yielding and stereoselective manner.



Scheme 2.11: Substrate scope for glycosylations with 2-deoxyglycosyl resins.[a]

[a]The reactions were carried out using 30 µmol acceptor with resins **2.18, 2.45,** and **2.46** (1.0 equiv, i.e., 2.0 equiv of active sugar donor) at 0 °C for 24 h in the presence of $FeCl_3$ (1.5 equiv) and 4 Å MS. Upon full consumption of the acceptor, the reaction mixture was filtered, washed, and quenched with Et_3N (50µL) prior to concentration.

To further demonstrate the broader impacts of the resin bound donors, we employed the donors for the glycosylation of natural product aglycones strophanthidin and digitoxigenin. Strophanthidin was glycosylated with resins **2.18** and **2.46** to provide **2.56** (60% yield, 4.9:1 α:β) and **2.57** (44%, 4.4:1 α:β) in moderate yields and diastereoselectivity. To our knowledge, these are the first reported chemical glycosylation of strophanthidin with 2-deoxy-glycosides. There are several naturally occurring strophanthidin glycosides with this motif, and this methodology could be further applied to their synthesis and medicinal chemistry evaluation. Finally,

digitoxigenin **2.44** was glycosylated with resin **2.45** to afford 2-deoxygalactoside **2.58** in 65% yield and 10.2:1 α:β selectivity. In total, 10 different glycosides were loaded to the solid support and were used to glycosylate 12 different acceptors ranging from simple alcohols and thiols to complex natural products.

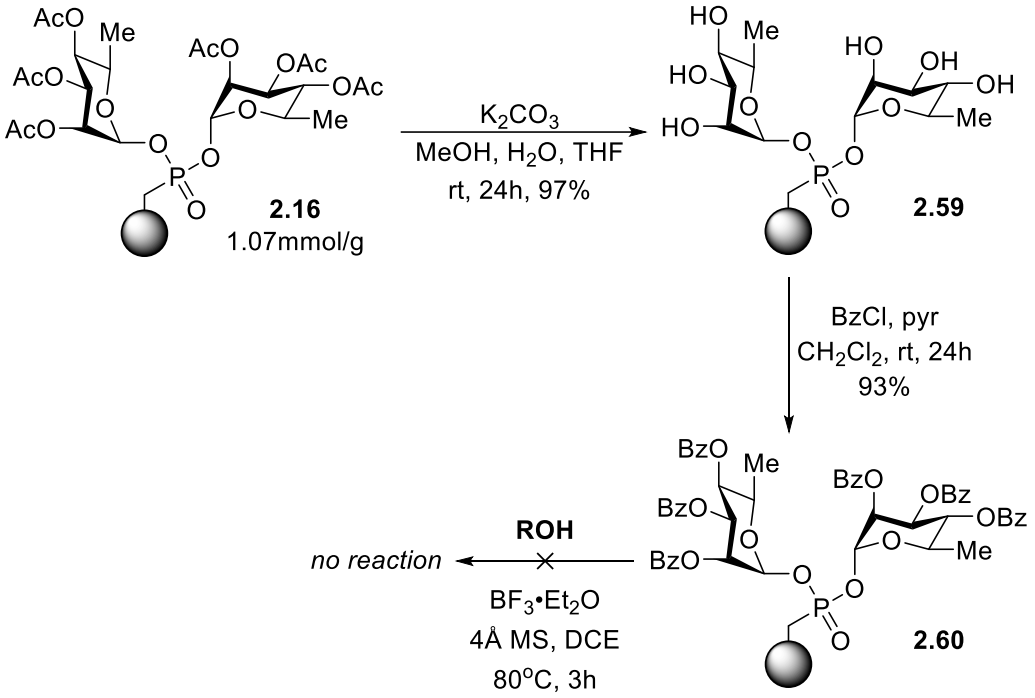
2.5 Studies towards on-resin glycosylation and protecting group manipulations

These prior studies demonstrated the possibility of directly transferring glycosides from the phosphonate resin to complex aglycones. However, this protocol could be even more powerful if combined with carbohydrate elongation on the solid support. The utility of the resin to be used for the on-resin transformations leading to oligosaccharides was probed next. Considering that the successful transfer of lactose disaccharide to form **2.35** was observed (Scheme 2.7), the possibility of forming the disaccharide on resin and then transferring it to aglycone was also investigated. It was vital to find optimal conditions for protecting group removal and glycosylation that would not cleave the glycosylphosphonates moiety.

2.5.1 Protecting group manipulations of resin bound carbohydrates

The studies of on-resin carbohydrate manipulations began by evaluation the stability of the resins to different protecting group manipulations. Installation of benzyl and acetyl protected glycosyl trichloroacetimidates was simple and fast, but benzoylated substrates required refluxing conditions to facilitate loading. Swapping protecting groups after the sugar is loaded to the solid support could also provide a combinatorial approach to monosaccharides with multiple functionalities or protecting groups. Starting from resin **2.16**, deacetylation with K_2CO_3 in a mixture of MeOH, H_2O and THF led to complete deacetylation without cleaving the monosaccharide from the solid support (Scheme 2.12) to afford resin **2.59** in 97% yield. Strong

bases, such as KOH, led to competitive cleavage of the monosaccharides from the solid support; however, deacetylation with weak bases such as KCN, guanidine, and DBU led to incomplete deprotection. The triol monosaccharide resin **2.59** was benzoylated by treatment with benzoyl chloride and pyridine in CH_2Cl_2 to afford **2.60** in 93% yield as judged by gravimetric analysis. Attempts to use resin **2.60** in glycosylation proved to be unsuccessful, likely due to an unremovable insoluble impurity from deacetylation or benzoylation poisoning the promoter.



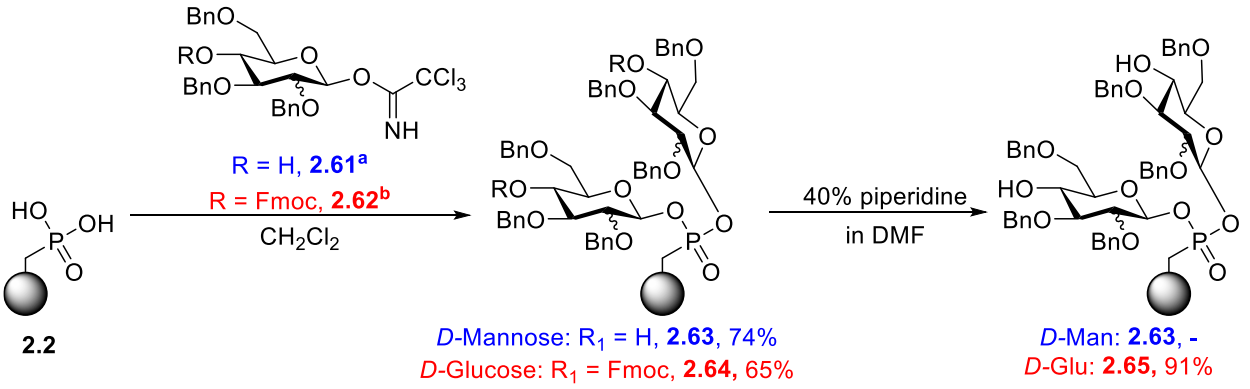
Scheme 2.12: Attempts at protect group manipulations on solid supported glycosyl phosphonates.[a]
[a]Deacetylation was carried out on a 0.3g (0.2 mmol) scale of **2.16**.

While glycosylation was unsuccessful, the ability to manipulate protecting groups on the solid supported phosphonates was key accomplishment towards the ultimate goal of on-resin iterative glycosylation. The stability of the resin bound carbohydrates to mild bases allows for a vast variety of potential protecting groups to be used.

2.5.2 Iterative glycosylation on solid support

The key to solid phase oligosaccharide synthesis is the ability to manipulate the sugar on

the solid support selectively without interfering with the linker that binds it to the polymer matrix. Having already established the stability of the resin bound phosphonates to mild base, we chose to employ Fmoc as the temporary leaving group for on-resin glycosylations. Glycosyl trichloroacetimidates **2.61** and **2.62** were loaded onto the solid support via the established protocol to generate resins **2.64** and **2.65** in 74% and 65% yield, respectively (Scheme 2.13). The Fmoc protecting group of resin **2.65** was removed by treating the resin with a 40% solution of piperidine in DMF at room temperature for one hour to afford resin **2.66** in 91% yield. Removal of the Fmoc-group was confirmed by the formation of dibenzofulvene, which is the byproduct of this reaction.[46]

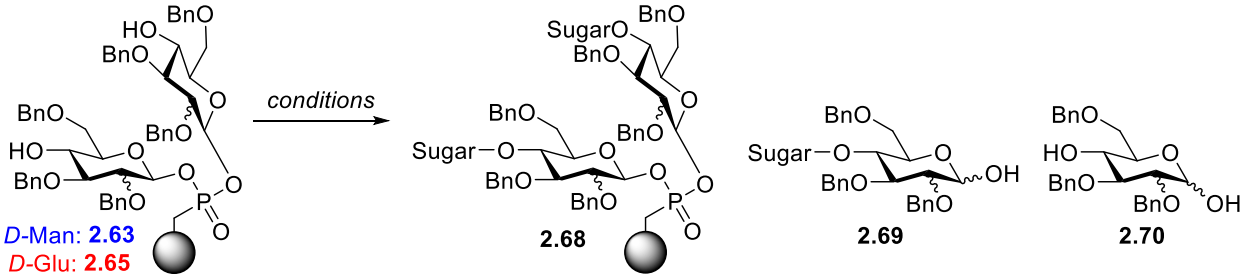


Scheme 2.13: Loading of C4-Fmoc sugars to solid support for carbohydrate elongation.
[a]The loading of **2.61** was carried out on a 145 mg (200 μmol) scale of **2.2**. [b]The loading of **2.62** was carried out on a 100 mg (130 μmol) scale of **2.2**.

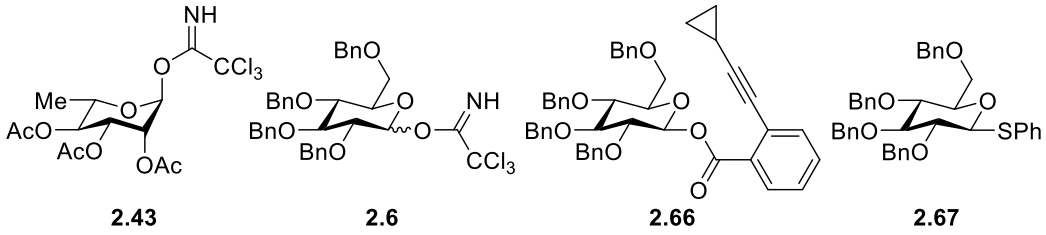
Resins **2.63** and **2.65** were subjected to several conditions to attempt to glycosylate the resin bound monosaccharide to form a disaccharide on the solid support. For resin **2.63**, various Lewis acids were employed to elongate the sugar chain with trichloroacetimidate donor **2.43** (Table 2.3, entry 1-3). After filtration of the resin from the reaction solvents, the filtrate was concentrated by HRMS to identify any sugar cleavage that occurred during the glycosylation reaction. Additionally, a small aliquot of resin was subjected to cleavage with excess BF_3•Et_2O in methanol and the crude product was analyzed by HRMS to determine the carbohydrates that

were bound to the solid support after the elongation reactions. In each of these attempts, the glycosylation of the resin bound monosaccharide was incomplete, and evidence of the starting monosaccharide **2.70** and desired disaccharide **2.69** were found to be cleaved from the solid support. It is possible that the reaction of the resin bound acceptor **2.63** with disarmed donor **2.43** was too slow, and there was competing reaction between the desired glycosylation and hydrolysis of the sugar from the resin triggered by the trichloroacetamide byproduct from the desired glycosylation.[47]

Table 2.3: Preliminary on-resin glycosylation studies[a]



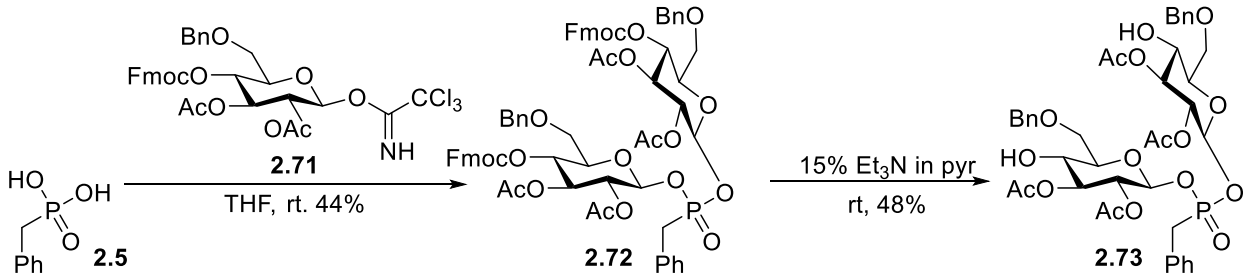
entry	*Resin*	*donor (eq)*	*conditions*	products	resin yield
1	**2.63**	**2.43** (5.0)	TMSOTf (0.2eq), rt, 3h, CH_2Cl_2	**2.63, 2.68-2.70**	67% (**2.63** + **2.68**)
2	**2.63**	**2.43** (5.0)	$B(C_6F_5)_3$ (0.1eq), rt, 1h, CH_2Cl_2	**2.63, 2.68-2.70**	79% (**2.63** + **2.68**)
3	**2.63**	**2.43** (5.0)	$B(C_6F_5)_3$ (0.1eq), -78°C, 1h, CH_2Cl_2	**2.63, 2.68-2.70**	77% (**2.63** + **2.68**)
4	**2.65**	**2.6** (5.0)	$B(C_6F_5)_3$ (0.1eq), -10°C, 1h, CH_2Cl_2	**2.65, 2.68-2.70**	77% (**2.65** + **2.68**)
5	**2.65**	**2.66** (5.0)	$Ph_3PAuOTf$ (2.5eq), rt, 1h, CH_2Cl_2	**2.68, 2.69**	56% (**2.68**)
6	**2.65**	**2.67** (5.0)	$(BrC_6H_4)_3NSbCl_6$ (6.3eq), rt, 1h, MeCN	**2.68, 2.69**	60% (**2.68**)



[a]Glycosylations were carried out on 50 mg (20-40 µmol) scale of **2.63.** After filtration of the resin from the reaction solvents, the filtrate was concentrated by HRMS to identify any sugar cleavage that occurred during the glycosylation reaction. Additionally, a small aliquot of resin was subjected to cleavage with excess BF_3•Et_2O in methanol and the crude product was analyzed by HRMS to determine the carbohydrates that were bound to the solid support after the elongation reactions. Yield of the resin was estimated by gravimetric analysis based on total expected yield of the disaccharide resin.

Armed donor **2.6** was employed in an effort to enhance the reaction rate with resin bound acceptor **2.65**. With $B(C_6F_5)_3$ as a Lewis acid promoter (Table 2.3, entry 4) similar results to

entry 3 were observed. The next set of conditions aimed to address two concerns: 1) changing the donor leaving group to avoid nucleophilic byproducts that may help facilitate sugar cleavage and 2) adopting conditions with milder or non-Lewis acidic promoters to minimize competitive reactivity between the glycosyl phosphonate and the elongation donor. Alkynyl benzoates have emerged as popular glycosylation donors due to their activation under mild conditions with π-acids such PPh_3AuOTf.[48,49] Glycosylation of resin **2.66** with *o*-alkynylbenzoate donor **2.67** led to full conversion to disaccharide, but the disaccharide was competitively cleaved from the solid support under the reaction conditions (entry 5). Sinay's reagent allows for mild and facile activation of thioglycosides without harsh acidic conditions.[50] Glycosylation of resin **2.66** with thioglycoside **2.68** led to full conversion to disaccharide, but the disaccharide was competitively cleaved from the solid support under the reaction conditions (entry 6). The competitive cleavage of the disaccharide resulted in the diminished yields for resin **2.69** (entry 5 and 6). The armed monosaccharide attached directly to the solid support may be more reactive than the elongation donor, so the next study was conducted with a disarmed monosaccharide bound to the solid support, and armed donor was used for elongation.[51]

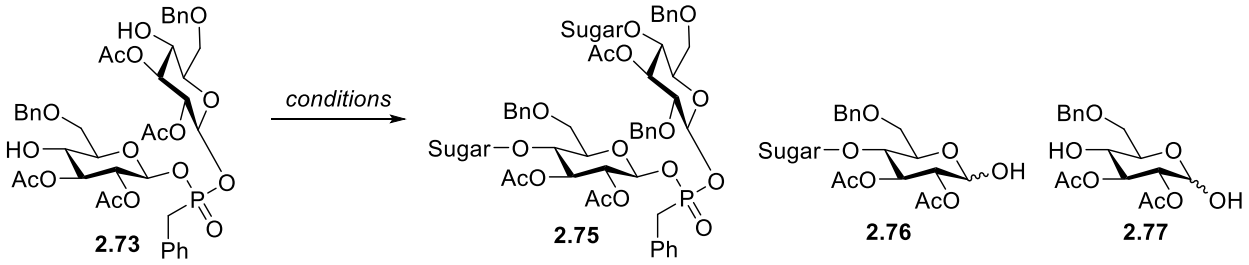


Scheme 2.14: Homogeneous model for carbohydrate protecting group removal and glycosylation[a]
[a]The phosphonylation of **2.71** was carried out on a 10 mg (58 μmol) scale of **2.5**.

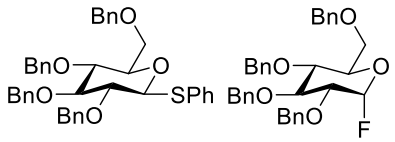
In an effort to glean a more precise picture of the competing reaction surrounding the glycosylphosphonates, we prepared bis-functionalized benzylphosphonate **2.73** (Scheme 2.14). Glycosylation of benzylphosphonic acid **2.5** with glucosyl trichloroacetimidate donor **2.71**

afforded bis-functionalized benzyl phosphonate **2.72** in 44% yield. Removal of the Fmoc group was achieved by stirring **2.72** ion a 15% solution of Et_3N in pyridine at room temperature for one hour to afford resin **2.73** in 48% yield.

Table 2.4: Studies of glycosylation of homogenous glycosylphosphonates[a]



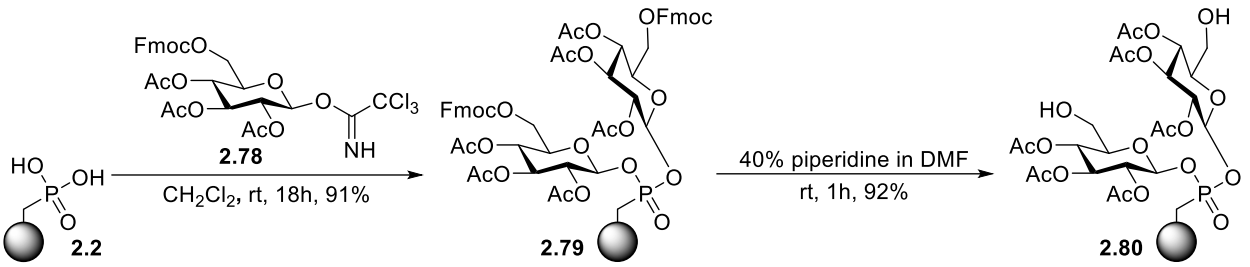
entry	*donor (eq)*	*conditions*	products	yield **2.68**
1	**2.67** (2.4)	$(BrC_6H_4)_3NSbCl_6$ (3.0eq), rt, 1h, MeCN	**2.73, 2.75-2.77**	*trace*
2	**2.74 (5**.0)	Cp_2ZrCl_2 (1.0eq), rt, 1h, PhH	**2.73, 2.75-2.77**	*trace*
3	**2.74** (5.0)	$SnCl_2$ (1.0eq), $AgBF_4$ (2.0eq), rt, 1h, PhH	**2.73, 2.75-2.77**	*trace*



2.67 **2.74**

[a]Glycosylations were carried out on 2.0 mg (2.4 µmol) scale of **2.73.** The products of the reaction were identified by HRMS analysis. Yields were estimated based on TLC and ^1H NMR analysis of the crude reaction mixture. Trace yield is < 5% as judged by ^1H NMR.

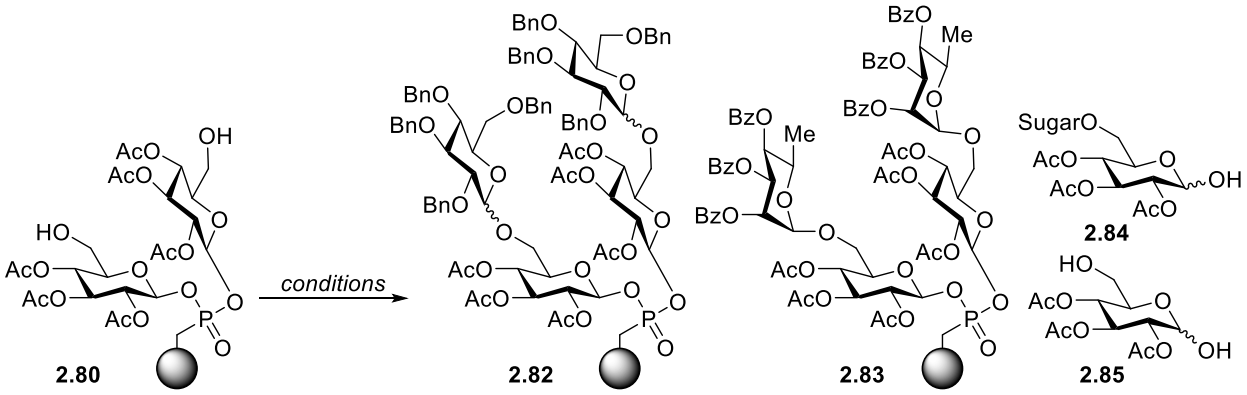
Glycosylation of resin **2.73** with donor **2.68** resulted in incomplete conversion and competitive hydrolysis of the mono- and disaccharide phosphonates (Table 2.4, entry 1). Next, glycosyl fluorides were evaluated with fluorophilic activators as potential donors for on resin glycosylations. Glycosyl phosphonate **2.73** was treated with glycosyl fluoride **2.74** with fluorophilic Lewis acid activators Cp_2ZrCl_2 (entry 2) or $SnCl_2$ (entry 3). Both conditions resulted in incomplete conversion and partial cleavage of the resulting mono- and disaccharides from the solid support. Glycosylations using the C4 alcohol of the resin bound sugar had led to incomplete conversions and slow glycosylation rate leading to undesired competitive hydrolysis of the glycosyl phosphonate.



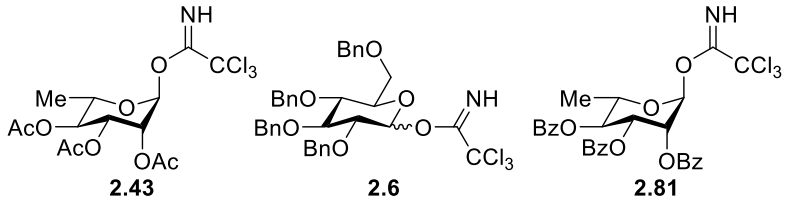
Scheme 2.15: Immobilization and deprotection of C6-OFmoc of carbohydrates for on-resin glycosylations[a]
[a]The loading of **2.78** was carried out on a 134 mg (170 μmol) scale of **2.2**.

We turned our attention to resin bound carbohydrates with the temporary leaving group affixed to the C6 alcohol. The primary C6 alcohol is a less hindered nucleophile than the C4 alcohol, and may lead to faster glycosylation, with fewer undesired byproducts.[52] Acetates were used as the permanent protecting groups so that the first resin bound monosaccharide would be disarmed, and the C2 acetate would direct future glycosylation of the prepared resin-bound disaccharide donor.[38] Trichloroacetimidate **2.78** was loaded onto the solid support via the established protocol to generate resin **2.79** in 91% yield (Scheme 2.15). The Fmoc protecting group of resin **2.79** was removed by treating the resin with a 40% solution of piperidine in DMF at room temperature for one hour to afford resin **2.80** in 92% yield. Resin **2.80** was subjected to several conditions to attempt to glycosylate the resin bound monosaccharide with trichloroacetimidates to form a disaccharide on the solid support (Table 2.5, entry 1-6). After filtration of the resin from the reaction solvents, the filtrate was concentrated by HRMS to identify any sugar cleavage that occurred during the glycosylation reaction. Additionally, a small aliquot of resin was subjected to cleavage with excess BF_3•Et_2O in methanol and the crude product was analyzed by HRMS to determine the carbohydrates that were bound to the solid support after the elongation reactions.

Table 2.5: Glycosylation on resin bound carbohydrates bearing C6 hydroxyl moiety[a]



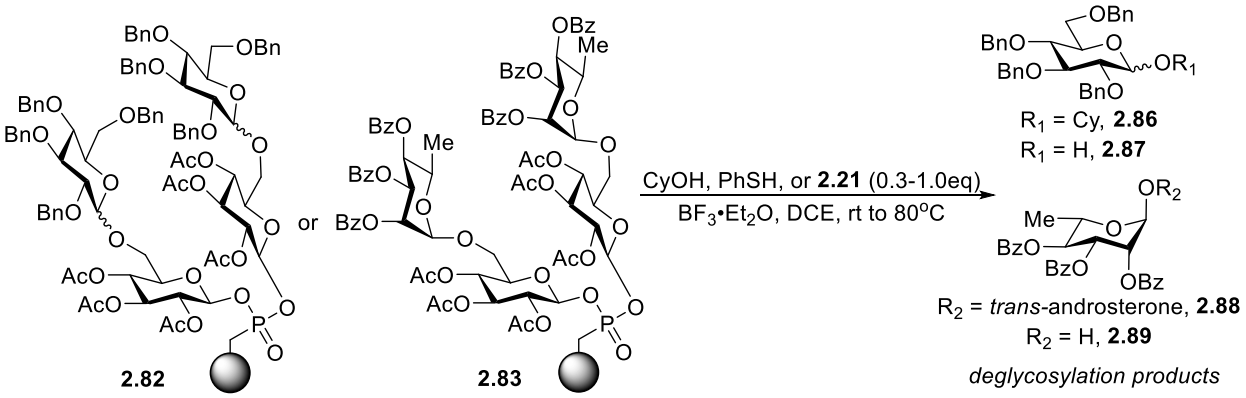
entry	donor (5.0eq)	conditions	products	resin yield
1	**2.43**	$B(C_6F_5)_3$ (0.1eq), rt, 1h, CH_2Cl_2	**2.80, 2.82, 2.84-2.85**	-
2	**2.6**	$B(C_6F_5)_3$ (0.1eq), rt, 1h, CH_2Cl_2	**2.80, 2.82, 2.84-2.85**	-
3	**2.6**	AgOTf (5.0eq), rt, 7h, CH_2Cl_2	**2.82, 2.84**	114%[b] (**2.82**)
4	**2.6**	AgOTf (5.0eq), DTBP (10eq), rt, 7h, CH_2Cl_2	**2.82**	98%[b] (**2.82**)
5	**2.81**	AgOTf (5.0eq), DTBP (10eq), rt, 7h, CH_2Cl_2	**2.80, 2.83**	102%[b] (**2.83**)
6	**2.81**	AgOTf (5.0eq), DTBP (10eq), rt, 17h, CH_2Cl_2	**2.83**	93%[b] (**2.83**)



[a]Glycosylations were carried out on 50-100 mg (30-90 µmol) scale of **2.80.** After filtration of the resin from the reaction solvents, the filtrate was concentrated by HRMS to identify any sugar cleavage that occurred during the glycosylation reaction. Additionally, a small aliquot of resin was subjected to cleavage with excess BF_3•Et_2O in methanol and the crude product was analyzed by HRMS to determine the carbohydrates that were bound to the solid support after the elongation reactions. Yields of the resins were estimated by gravimetric analysis based on total expected yield of the disaccharide resin.

Initial experiments with acetylated rhamnose donor **2.43** (Table 2.5, entry 1) and benzylated glucose donor **2.6** (entry 2) with $B(C_6F_5)_3$ promoter led to incomplete conversion to the disaccharide, but also resulted in cleavage of the disaccharide from the solid support. After switching to a silver(I) trifluoromethanesulfonate (AgOTf, entry 3), the reaction progressed to completion in seven hours; however, the newly formed disaccharide was partially cleaved from the solid support under the reaction conditions. Additionally, the resin was discolored to a brownish color, likely due to an insoluble silver(I) impurity that was unable to be removed by standard washing conditions. This impurity also likely contributed to the inflated yields observed

(>100%, entry 4 and 6). To neutralize the triflic acid formed during the glycosylation, and hopefully suppress the acidic hydrolysis of the glycosylphosphonates, the reaction was buffered with super stoichiometric di-*tert*-butyl-pyridine (DTBP, entry 4),[53] which led to the desired resin-bound disaccharide **2.82**. The presence of DTBP was found to be essential for minimizing the competitive cleavage of mono- and disaccharide off the polystyrene matrix during the glycosylation. Attempts to transfer the resin-bound disaccharide from the resin to cyclohexanol or thiophenol resulted in only trace disaccharide glycosylated products.

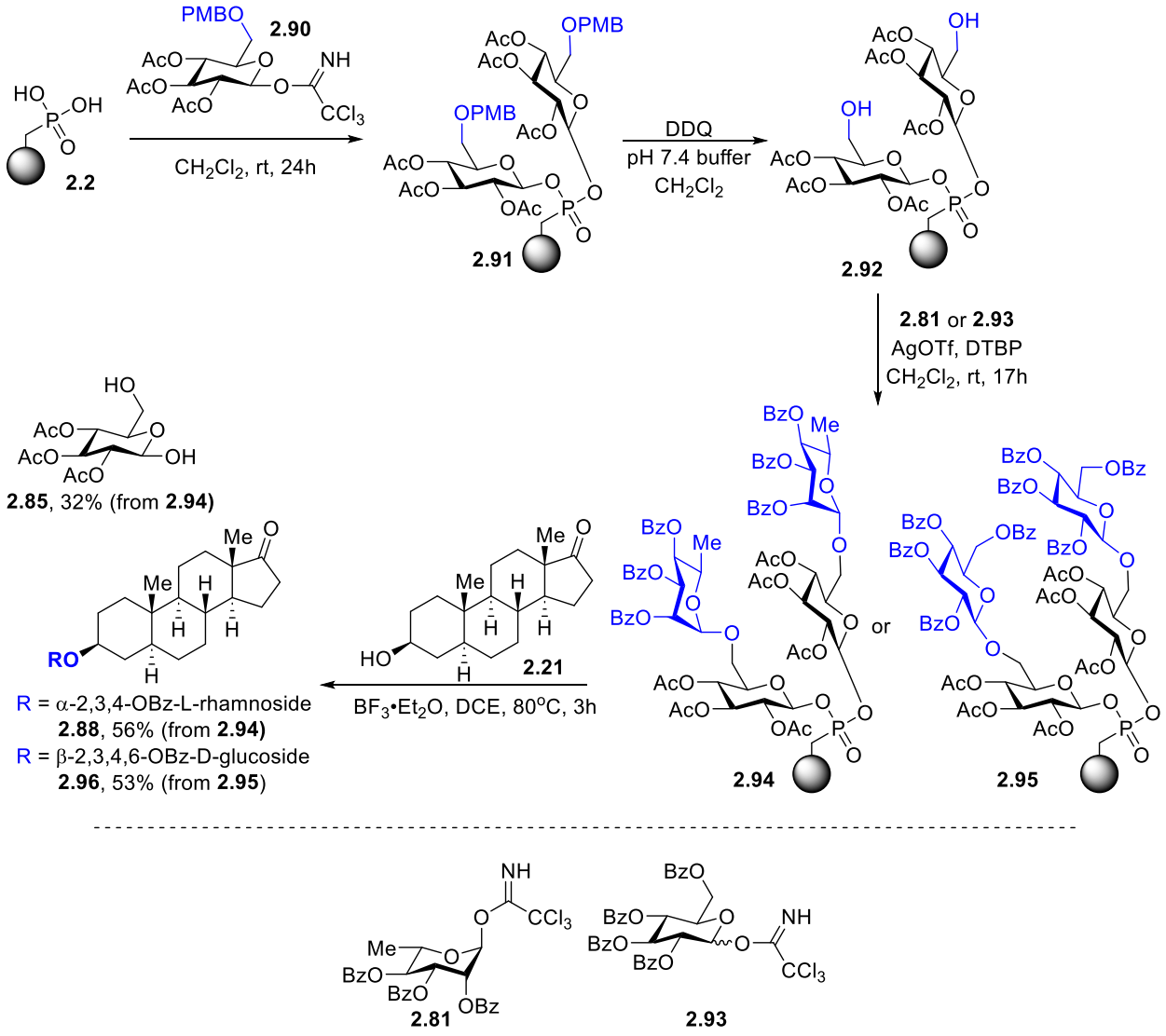


Scheme 2.16: Deglycosylation of resin bound disaccharides[a]

[a]Glycosylations with resins **2.82** or **2.83** (60 µmol, 1.0 equiv) were carried out with acceptors (0.5-1.0 equiv) in DCE (2.0mL). The products were identified by TLC, ^{1}H NMR, and HRMS analysis of the crude reaction mixtures. Conversions were approximated by TLC and ^{1}H NMR analysis. Yields were determined after isolation of products by flash column chromatography.

During the cleavage, with cyclohexanol and thiophenol, products **2.86** and **2.87** resulting from the deglycosylation of the disaccharide were observed (Scheme 2.16). Overall, the reactions were sluggish, and only provided small amounts of the deglycosylated products (11% yield of **2.87** from **2.82** with thiophenol). Deglycosylation has been previously observed when one of the monosaccharide units of the disaccharide is more reactive (armed vs. disarmed).[39] To combat this, disarmed benzoylated rhamnose donor **2.81** was employed for on-resin elongation (Table 2.5, entry 5-6). Disarmed donor **2.81** required longer a reaction time (entry 6) to reach full conversion to the disaccharide resin **2.83**. Attempts to transfer the disaccharide to thiophenol or

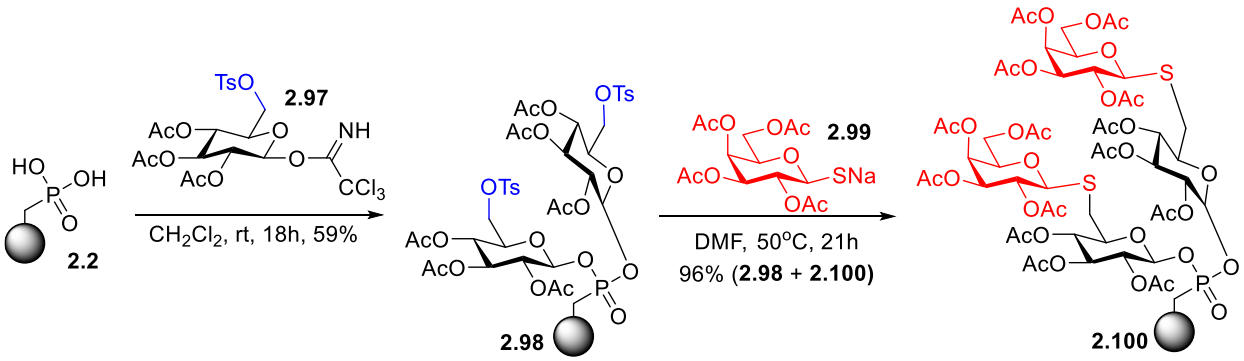
trans-androsterone **2.21** acceptors resulted in formation of only trace amounts of deglycosylation products (Scheme 2.16). The mass recovery of disaccharide glycosides and deglycosylation products were quite low based on the calculated loading of the sugar. To probe whether impurities from the Fmoc deprotection step hampered the glycosylation, we attempted to wash the resin with dilute acid (1% MsOH, TMSOTf, or TFA in CH_2Cl_2), but no improvement in yield was observed.



Scheme 2.17: Studies of on-resin elongation with PMB as the temporary protecting group[a]

[a]The loading of **2.90** was carried out on a 50 mg (65 μmol) scale of **2.2**. Yields of the resins were estimated by gravimetric analysis based on total expected yield of the desired product.

To eliminate potential incompatibility between byproducts from the bases used in Fmoc deprotection, we swapped the C6-protecting group to PMB, which could be removed under neutral conditions via oxidation with DDQ.[54] Thus, resin **2.91** containing a temporary protecting group (PMB) was generated from phosphonic acid **2.2** and trichloroacetimidate **2.90** using the standard protocol A in 68% yield (Scheme 2.17). The immobilized glycosylated resin **2.91** was subjected to the oxidative removal of the PMB group with buffered DDQ to provide **2.92**. This transformation proceeded in 92% yield based on gravimetric analysis. Removal of the PMB-group was confirmed by the formation of *p*-methoxybenzaldehyde, which is the byproduct of this reaction. Elongative glycosylation of **2.92** with trichloroacetimidates **2.81** or **2.93** leading to disaccharide containing resins **2.94** and **2.95** was carried by using AgOTf in combination with DTBP in >90% yield as determined by the increase in the resin mass. The transfer of thus formed disaccharides from **2.94** and **2.95** using *trans*-androsterone **2.21** as an acceptor was hindered by competitive deglycosylation of the disaccharide with BF_3•OEt_2. The formation of the desired products were observed in trace quantities, the major side-products detected in the reaction mixture were glycosylated products **2.89** and **2.96** and monosaccharide **2.85** (Scheme 2.17)



Scheme 2.18: Studies toward on-resin sulfur-linker disaccharide synthesis[a]
[a]Loading of **2.97** was carried out on 100 mg (130 µmol) scale of **2.2**. Yields of the resins were estimated by gravimetric analysis based on total expected yield of the disaccharide resin.

Sulfur-linked oligosaccharides (i.e., thioglycosides) have been used in biological and therapeutic studies due to their resistance to enzymatic degradation.[55] The sulfur-based linkage

may also prove to be more stable to our Lewis acid promoted cleavage of the resin bound sugar.[56] Tosylated glucose trichloroacetimidate **2.97** was loaded to resin **2.2** to give resin **2.98** bearing a tosylate leaving group at the C6 position of the monosaccharide. Resin **2.98** was treated with excess galactosyl thiolate nucleophile **2.99** in DMF at 50°C to facilitate S_N2-displacement of the tosylated. Based on FTIR-analysis of the resulting filtered and washed resin **2.100**, the reaction was incomplete as judged by the presence of the S=O stretch of the tosylate[57] observed at 1365cm^{-1}. Some disaccharide product was formed as judged by gravimetric analysis. The transfer of disaccharide from **2.97** using *trans*-androsterone **2.21** produce only trace amounts of desired disaccharide, and products resulting from deglycosylation (2,3,4,6-tetra-*O*-acetyl-D-galactopyranose) were observed during HRMS analysis.

The presence of the deglycosylation products suggests that further optimization of the ultimate glycosyl transfer conditions is necessary to adopt this chemistry for the transfer of di- and oligosaccharides with sensitive glycosidic linkages. Neutral conditions must be employed for all transformation, as acidic and strongly basic conditions cleaved the carbohydrate from the solid support.

2.6 Conclusions

We developed a decagram synthesis of recyclable polystyrene-based phosphonic acid resin **2.2** from commercially available Merrifield's resin. The immobilized donors could be prepared from their corresponding trichloroacetimidates or hemiacetals to furnish phosphonate donors **2.13**-**2.20**. These glycosylphosphonate-containing resins were obtained in 59-96% yields and were found to be bench-stable at room temperature for periods of at least four years. Optimization of the reaction conditions to transfer the solid supported donors to natural product-like aglycones. Ultimately, these donors could be activated using trifluoroborane etherate at 80

ºC to react with various alcohol and thiol-based acceptors to provide 17 different glycosides in good-to-excellent yields (53-98%). The crude reaction profiles with the solid supported donors were cleaner than traditional trichloroacetimidate donors in solution. To develop a broadly applicable application of these solid supported, the glycosylation of resin-bound 2-deoxyglycosylphosphonates was developed. Additional reaction condition screening identified $FeCl_3$ at 0ºC to be the optimal condition to maximize yield and diastereoselectivity while minimizing undesired byproducts formed due to the competing Ferrier-rearrangement reaction pathway. Resin-bound 2-deoxyglycosylphosphonates were used to transfer 2-deoxy-glucosides, 2-deoxy-glacatosides, and 2-deoxy rhamnosides to natural product and natural product like aglycones in good to excellent yields (44-87%) and good diastereoselectivity for the α-glycoside (up to 10.2:1 α:β). Three protected glycosylated cardiotonic steroids (**2.56**-**2.58**) were prepared using the optimized conditions. In addition, it was demonstrated that **2.2** could be recovered and recycled multiple times without significant decrease in the yields for the subsequent steps. Extensive investigation into the use of the phosphonate resins for solid phase polysaccharide synthesis was performed. Frist, resin bound monosaccharides bearing a temporary Fmoc protecting group were installed to the solid support in good yields (65-91%). Removal of the Fmoc was quick and facile and proceeded in high yields (91-92%), and was monitored by the release of dibenzofulvene (^{1}H NMR, HRMS). Glycosylation of the resin bound monosaccharide acceptor to from a resin bound disaccharide could be achieved with various glycosyl donors (**2.6**, **2.43**, **2.66**, **2.67**, **2.74**, **2.81**) and promoters (Table 2.3-Table 2.5), however, competitive cleavage of the resulting disaccharide was observed under the reaction conditions. Attempts to transfer the disaccharide attached to the solid support to an acceptor proceeded in low yields, possibility to the trace amounts of base from the Fmoc deprotection interfering with the reaction promoter.

Use of PMB as the temporary protecting allow for base-free on-resin deprotection, and conversion of the deprotection reaction was also monitored by the release of *p*-anisaldehyde (^{1}H NMR, HRMS). On-resin glycosylation with glycosyl trichloroacetimidates (**2.81**, **2.93**) proceeded in high yields (<90%) determined by increase in resin mass. Suppression of the cleavage of the disaccharide from the solid support was achieved by using AgOTf as a mild promoter and adding stoichiometric DTBP to neutralize any strong acid formed during the reaction. Transfer of the newly formed disaccharide was found to be challenging and led to the cleavage of newly formed glycosidic linkage. Further efforts to optimize the transfer of the on-resin formed disaccharide can minimize the deglycosylation pathway; the use of the 2-deoxy glycosides as the resin bound monosaccharide acceptor and subsequent cleavage of the 2-deoxy sugar containing disaccharide with $FeCl_3$ may prove fruitful for the elongation and disaccharide transfer. Additionally, the mild conditions and good selectivity for 2-deoxyglycoside transfers offers an enticing approach for the synthesis of natural products bearing similar motifs. The heterogenous nature of the solid support allows for future applications in flow chemistry and automated synthesis. A column packed with phosphonic acid resin **2.2** could be loaded by continuous flow of a solution of 2-deoxy-glycosyltrichloroacetimidate bearing a PMB temporary protecting group. The PMB could be removed and the cleavage could be monitored by in-line UV-Vis spectroscopy. The resin could then be subjected to glycosylation to grow the carbohydrate chain on the solid support, and final transfer of the resin-bound polysaccharide could be achieved with a saturated solution of $FeCl_3$. Careful consideration for regent solubility must be taken to avoid mechanical issues within the flow system. As method for singular glycosylation, the α-selective glycosylation with 2-deoxyglycosides has been notoriously challenging, and a simple high yielding protocol utilizing the solid supported donors could

simplify the synthesis for future medicinal chemistry studies. Given then simple preparation of the solid support and the relatively high loadings achieved for glycoside immobilization (up to 1.1mmol/g), the resins could be used for gram scale synthesis of glycosylated natural products or polysaccharides.

2.7 Experimental

2.7.1 General Methods

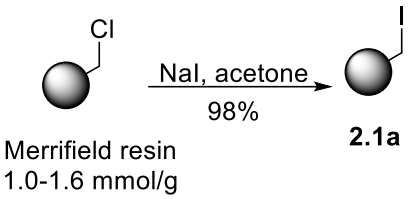
All reagents and solvents were purchased from commercial sources and were used as received without further purification unless otherwise specified. CH_2Cl_2, DMF, Et_2O, THF, PhMe, were purified by Innovative Technology's Pure-Solve System using basic alumina. All reactions were carried out under a positive pressure of nitrogen in flame- or oven-dried glassware with magnetic stirring. Reactions were cooled using a cryocooler or external cooling baths (ice water (0 °C), sodium chloride/ice water (–20 °C), dry ice/acetonitrile (–40 °C), or dry ice/acetone (–78 °C). Heating was achieved by use of a silicone oil bath with heating controlled by an electronic contact thermometer. Deionized water was used in the preparation of all aqueous solutions and for all aqueous extractions. Solvents used for extraction and chromatography were ACS or HPLC grade. Purification of reaction mixtures was performed by flash chromatography using SiliCycle SiliaFlash P60 (230-400 mesh). Yields indicate the isolated yield of the title compound with ≥95% purity as determined by ^{1}H NMR analysis. Diastereomeric ratios were determined by ^{1}H NMR analysis. ^{1}H NMR spectra were recorded on a Varian vnmrs 700 (700 MHz), 600 (600 MHz), 500 (500 MHz), 400 (400 MHz), Varian Inova 500 (500 MHz), 400 (400 MHz), or a Bruker Avance Neo 500 (500 MHz) spectrometer and chemical shifts (δ) are reported in parts per million (ppm) with solvent resonance as the internal standard ($CDCl_3$ at δ 7.26, D_3COD at δ 3.31, C_6D_6 at δ 7.16). Tabulated ^{1}H NMR Data are reported as s = singlet, d = doublet, t = triplet,

q = quartet, qn = quintet, sext = sextet, m = multiplet, ovrlp = overlap, and coupling constants in Hz. Proton-decoupled ^{13}C NMR spectra were recorded on Varian vnmrs 700 (700 MHz) spectrometer and chemical shifts (δ) are reported in ppm with solvent resonance as the internal standard ($CDCl_3$ at δ 77.16, D_3COD at δ 49.0, C_6D_6 at δ 128.06). High resolution mass spectra (HRMS) were performed and recorded on Agilent 6230 TOF or VG (Micromass) 70-250-S Magnetic sector mass spectrometers in the University of Michigan mass spectrometry laboratory. Infrared (IR) spectra were recorded as thin films a Perkin Elmer Spectrum BX FT-IR spectrometer. Absorption peaks are reported in wavenumbers (cm^{-1}). Optical rotations were measured at room temperature in $CHCl_3$ or H_3COH on a Jasco P-2000 polarimeter. Structural assignments were made with additional information from gHMBC experiments. For glucose, galactose, fucose, and lactose, the newly formed glycosidic linkage stereochemistry was assigned based on J^{H1-H2} coupling constants. For coupling constants less than 7Hz, the α-diastereomer was assigned. For coupling constants greater than 7Hz, the β-diastereomer was assigned. For rhamnose, the newly formed glycosidic linkage stereochemistry was assigned based on J^{C-H} coupling constant. The α-diastereomer was assigned to J^{C-H} of approximately 170Hz, and the β-diastereomer was assigned to J^{C-H} of approximately 160Hz. Phosphonic acid resins were characterized by ^{31}P-gel NMR. To a clean, dry NMR tube, 20-50mg of resin was added. $CDCl_3$ (0.6mL) was added and the tube was gently shaken. The resin was allowed to swell in the solvent for 20 minutes, and then the swelled resin was inserted to NMR spectrometer and the ^{31}P NMR spectra was obtained. For resins, longer acquisition times (>100 scans) were needed due to the decreased sensitivity of NMR on the solid support. Peaks generally appeared broader than for soluble phosphonic acids, and as such the diastereoselectivity for resin glycosyl phosphonates could not be determined directly.

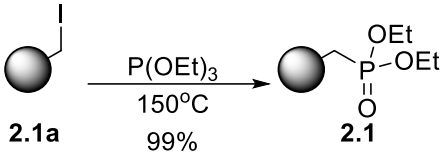
2.7.2 Preparation of known compounds

Compounds **2.6**[58], **2.9**[59], **2.9a**[59], **2.11**[60], **2.14a**[44], **2.17a**[18], **2.18a**[61], **2.43**[18], **2.43a**[66], **2.45a**[67], **2.46a**[68], **2.61a**[69], **2.62a**[70], **2.66**[49], **2.67**[71], **2.71a**[72], **2.74**[73], **2.81**[26], **2.93**[75], **2.97a**[78], and **2.99**[79] were prepared according to the previously reported procedures. The spectra of the prepared compounds matched the reported spectra data.

2.7.3 Preparation of new compounds, resins, and reaction monitoring studies

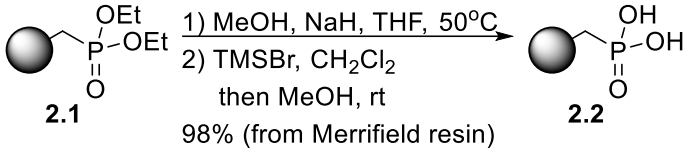


Resin 2.1a: Merrifield resin (10 g, 1.3 mmol/g, 100-200 mesh, 13 mmol, 1 eq) was added to an oven dried flask equipped with magnetic stir bar. Degassed acetone (100 mL) was added, and the suspension was stirred for 20 minutes. NaI (3.9 g, 26 mmol, 2 eq) was added and the reaction was stirred in the dark for 20 hours at room temperature. The reaction mixture was filtered, and the resin was washed with acetone (3x100 mL), 1:1 acetone:H_2O (3x100 mL), H_2O (3x100 mL), 1:1 acetone:H_2O (3x100 mL), acetone (3x100 mL), and CH_2Cl_2 (3x100 mL) and dried under vacuum to afford **2.1a** as a white solid (11 g, 98% yield). **FTIR** (thin film, cm^{-1}): 1492, 1451, 755, 696.

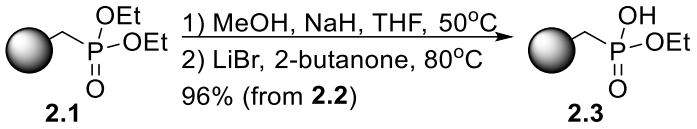


Resin 2.1: Iodinated resin **2.1a** was suspended in $P(OEt)_3$ (45 mL, 260 mmol, 20 eq) and the mixture was heated to 150°C. The reaction was allowed to stir at 150°C for 4 days. The reaction mixture was filtered, and the resin was washed with acetone (3x100 mL), 1:1 acetone:H_2O

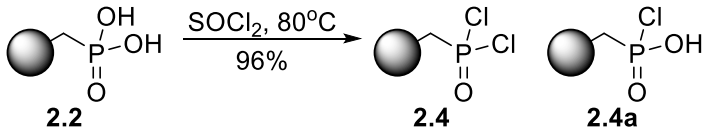
(3x100 mL), H_2O (3x100 mL), 1:1 acetone:H_2O (3x100 mL), acetone (3x100 mL), and CH_2Cl_2 (3x100 mL) and dried under vacuum to afford **2.1** as a white solid (11g, 99%). The installation of the phosphonate was confirmed by ^{31}P NMR. **^{31}P NMR** (162 MHz, $CDCl_3$) δ 26.8.



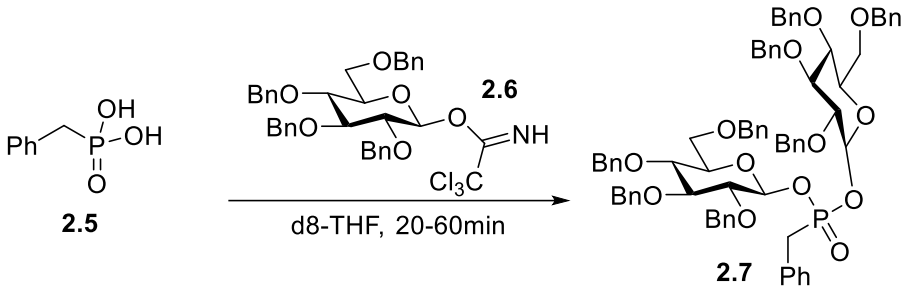
Resin 2.2: Phosphonate resin **2.1** was suspended in THF (50 mL) and stirred for 20 minutes. At the same time, NaH (60% suspension in mineral oil, 5.2 g, 130 mmol, 10 eq) was suspended in THF (50 mL). Anhydrous methanol (5.3 mL. 130 mmol, 10 eq) was added dropwise to NaH suspension. Once gas evolution had stopped, the resulting suspension of methoxide was added to the suspension of resin. The reaction was heated to 50°C and stirred for 20 hours. The reaction mixture was filtered, and the resin was washed with methanol (3x100 mL), acetone (3x100 mL), 1:1 acetone:H_2O (3x100 mL), H_2O (3x100 mL), 1:1 acetone:H_2O (3x100 mL), acetone (3x100 mL), and CH_2Cl_2 (3x100 mL) and dried under vacuum. The capped resin was suspended in CH_2Cl_2 (100 mL) under N_2 and stirred for 20 minutes. TMS-Br (6.9 mL, 52 mmol, 4 eq) was added to the suspension and the reaction was stirred at room temperature for 3 hours. Anhydrous methanol (100 mL) was added to the reaction and was stirred for an additional 17 hours. The reaction was filtered and washed with methanol (3x100 mL), acetone (3x100 mL), 1:1 acetone:H_2O (3x100 mL), H_2O (3x100 mL), 1:1 acetone:H_2O (3x100mL), acetone (3x100 mL), and CH_2Cl_2 (3x100 mL) and dried under vacuum to afford **2.2** as a beige solid (9.8g, 93% yield) over four steps (from Merrifield resin). **^{31}P NMR**: (203 MHz, $CDCl_3$) δ 30.1. **FTIR** (thin film, cm-1): 2918, 1601, 1511, 1493, 1452, 1206, 1180, 1029, 982, 962, 908, 841, 755, 696.



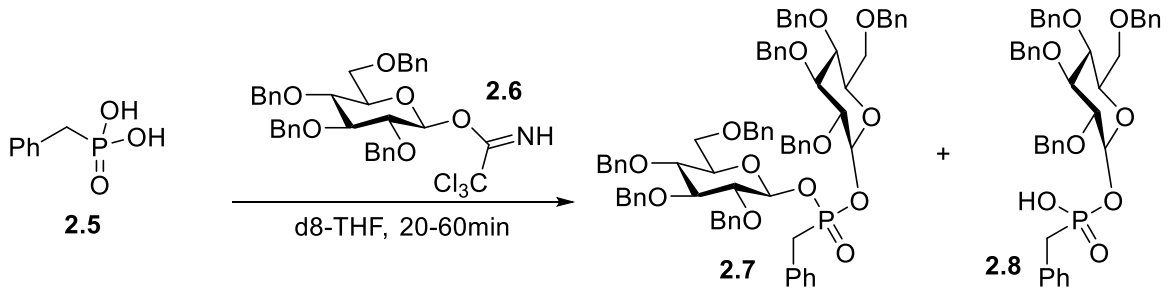
Resin 2.3: Phosphonate resin **2.1** (500 mg, 0.65 mmol, 1.0 eq) was suspended in THF (15 mL) and stirred for 20 minutes. At the same time, NaH (60% suspension in mineral oil, 260 mg, 6.5 mmol, 10 eq) was suspended in THF (10mL). Anhydrous methanol (0.28 mL. 6.5 mmol, 10 eq) was added dropwise to NaH solution. Once gas evolution had stopped, the resulting suspension of methoxide was added to the suspension of resin. The reaction was heated to 50°C and stirred for 20 hours. The reaction mixture was filtered, and the resin was washed with methanol (3x10 mL), acetone (3x10 mL), 1:1 acetone:H_2O (3x10 mL), H_2O (3x10 mL), 1:1 acetone:H_2O (3x10 mL), acetone (3x10 mL), and CH_2Cl_2 (3x10 mL) and dried under vacuum. The capped resin was suspended in 2-butanone (10 mL) and stirred for 20 minutes). LiBr (70 mg, 0.78 mmol, 1.2 eq) was added to the swelled resin and the reaction was heated to 80°C and stirred at that temperature for 20 hours. The reaction was filtered, washed with 1:1 1N HCl (aq):THF (3x10 mL), THF (3x10 mL), and CH_2Cl_2 (3x10 mL) and dried under vacuum to afford **2.3** as a slightly orange solid (491mg, 96%). **^{31}P NMR**: (162 MHz, $CDCl_3$) δ 28.5.



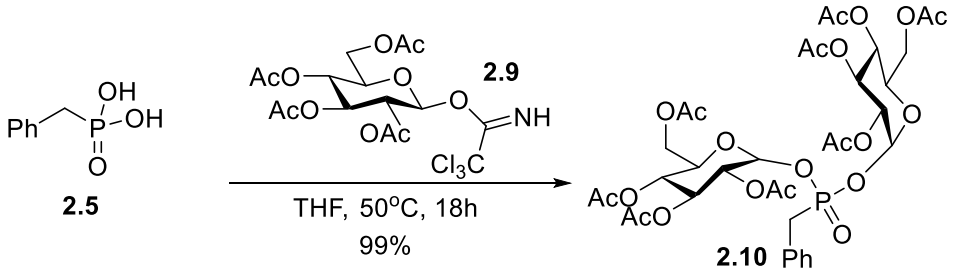
Resin 2.4: Phosphonic acid **2.2** (100mg) was suspended in $SOCl_2$ (5 mL, 500 eq). The reaction was stirred at 80°C for 18 hours. The reaction was filtered and dried under vacuum to afford **2.4** as an orange solid (100mg, 96%). The bis-chlorinated resin was used immediately for loading due to its propensity to rapid instability in the presence of moisture. **^{31}P NMR:** (162 MHz, $CDCl_3$) δ 46.0. The mixed chlorination product **2.4a** was also observed. **^{31}P NMR:** (162 MHz, $CDCl_3$) δ 39.1.



Compound 2.7: Benzylphosphonic acid **2.5** (20 mg, 0.12 mmol, 1.0 eq) and **2.6**[58] (175 mg, 0.26 mmol, 2.2 eq) were stirred in THF (1.0mL) at room temperature for 18 hours. The solvent was removed under reduced residue and product **2.7** was isolated after flash column chromatography (60% EtOAc/hexanes) as a clear viscous liquid (123 mg, 85% yield). **HRMS** (ESI-TOF) (m/z): $[M+Na]^+$ calcd for $C_{75}H_{77}O_{13}PNa$ 1239.4994, found 1239.4975. **^{1}H NMR** (401 MHz, C_6D_6) δ 7.39 – 7.12 (m, 23H), 7.09 – 6.89 (m, 22H), 5.72 (s, 1H), 5.52 (dt, *J* = 8.7, 4.4 Hz, 1H), 5.00 – 4.86 (m, 1H), 4.84 – 4.57 (m, 8H), 4.52 (dd, *J* = 12.7, 10.6 Hz, 2H), 4.45 – 4.38 (m, 1H), 4.38 – 4.30 (m, 3H), 4.23 (dd, *J* = 11.9, 2.3 Hz, 1H), 3.71 (d, *J* = 8.3 Hz, 1H), 3.64 – 3.21 (m, 13H). **^{13}C{^{1}H}** (126 MHz, C_6D_6) δ 139.5, 139.3, 139.19, 139.19, 139.1, 139.0, 138.9, 138.74, 132.0, 131.9, 130.63, 130.57, 128.7, 128.63, 128.61, 128.55, 128.52, 128.50, 128.49, 128.4, 128.17, 128.15, 128.0, 127.9, 127.71, 127.65, 127.6, 127.10, 127.07, 98.6, 98.0, 84.6, 82.6, 82.5, 82.3, 82.2, 77.8, 77.7, 75.7, 75.6, 75.5, 75.4, 74.9, 74.8, 74.7, 74.4, 73.7, 73.6, 73.4, 69.2, 68.9, 36.6, 35.6, 30.2. **^{31}P NMR** (162 MHz, C_6D_6) δ 25.9.

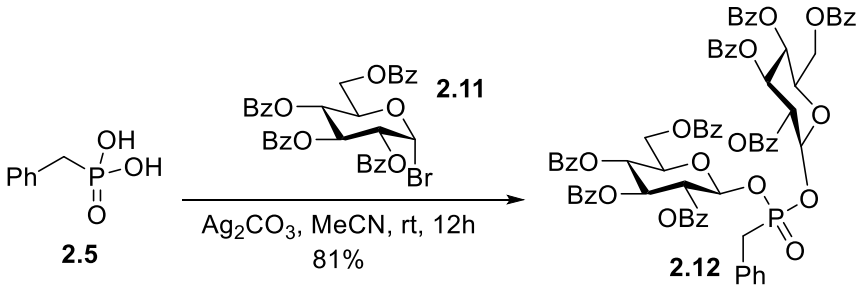


Homogeneous reactions of benzylphosphonic acid (Scheme 2.3) Phosphonated 2.7: Per-benzylated glucose trichloroacetimidate **2.6**[58] (40 mg, 0.06 mmol, 1.0 eq) was added to a stirred solution of benzylphosphonic acid **2.5** (10 mg, 0.06 mmol, 1.0 eq) in d8-THF (0.4 mL). The reaction progress was monitored by ^{31}P-NMR. After stirring for 20 minutes, one new major peak appeared by ^{31}P-NMR, and the benzylphosphonic acid was not consumed. The reaction was allowed to stir for an additional 40 minutes but no further progression was observed. Another aliquot of **2.6** (50 mg, 0.07 mmol, 1.2 eq) was added, and the reaction was stirred for 20 minutes. The ^{31}P-NMR (d8-THF) indicated conversion to a single diastereomer of bisglycosylated product **2.7** (δ 27.3) and trace amounts of a 1:1 diastereomeric mixture of monoglycosylated phosphonates **2.8** (δ 26.9 and 26.7).



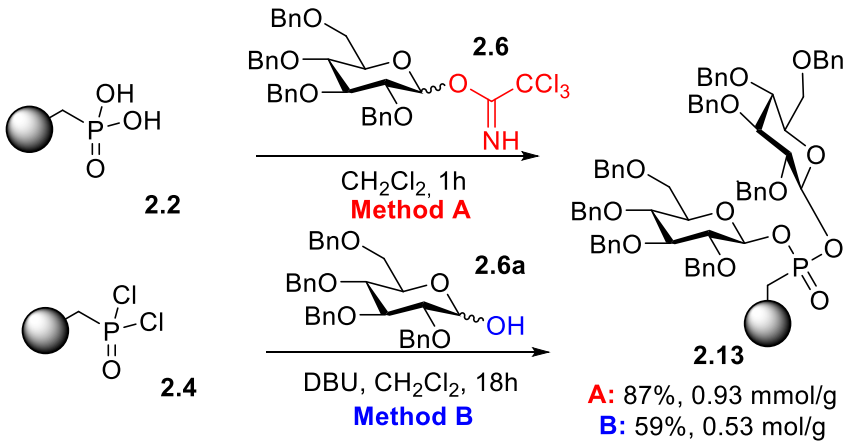
Phosphonate 2.10: Trichloroacetimidate **2.9**[59] (50 mg, 0.11 mmol, 2.2 eq) was added to a stirred solution of **2.5** (8.0 mg, 0.05 mmol. 1.0 eq) in THF (0.5mL). The reaction was heated to 50°C and stirred for 18 hours at that temperature. Upon full consumption of **2.5**, the reaction mixture was concentrated *in vacuo* and the crude reaction was purified by flash column chromatography (40-100% EtOAc/hexanes) to afford **2.10** as a viscous oil (39 mg, 99% yield). The α-glycosidic linkage was assigned for both attached sugars by $J_{C\text{-}H}$ coupling (δ 94.9 ($J_{C\text{-}H}$ = 168.5 Hz)). **HRMS** (ESI-TOF) (m/z): $[M+Na]^+$ calcd for $C_{35}H_{45}PO_{21}Na$ 855.2084, found 855.2078. **^{1}H NMR** (400 MHz, $CDCl_3$) δ 7.26 – 7.18 (m, 5H), 5.35 – 4.91 (m, 9H), 4.32 – 4.11 (m, 3H), 3.77 (tdd, J = 11.5, 4.3, 2.3 Hz, 2H), 3.22 (d, J = 22.6 Hz, 2H), 2.08 (s, 3H), 2.00 (d, J = 2.0 Hz, 9H),

1.98 (s, 3H), 1.95 (d, J = 4.4 Hz, 6H), 1.88 (s, 3H). **^{13}C{^{1}H}** (126 MHz, $CDCl_3$) δ 170.6, 170.5, 170.0, 169.9, 169.42, 169.36, 169.1, 129.8, 129.8, 128.7, 128.6, 127.3, 127.3, 95.0, 95.0, 94.9, 94.9, 72.8, 72.4, 72.3, 72.2, 71.1 (dd, J = 28.3, 7.9 Hz), 67.7, 67.5, 61.4, 61.0, 60.4, 35.0, 33.9, 20.7, 20.7, 20.6, 20.5, 20.5, 20.5. **^{31}P NMR** (202 MHz, $CDCl_3$) δ 26.7

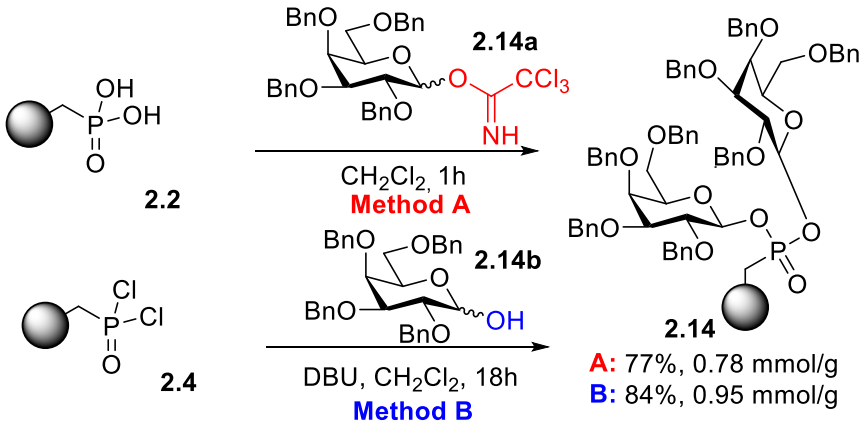


Phosphonate 2.12: Glycosyl bromide **2.11**[60] (67 mg, 0.10 mmol, 2.2 eq) was added to a foil wrapped vial containing **2.5** (8.0 mg, 0.05 mmol, 1.0 eq) and Ag_2CO_3 (28 mg, 0.10 mmol, 2.2 eq) suspended in MeCN (0.5mL). The reaction was stirred in the dark until **2.5** was consumed based on TLC analysis. The reaction mixture was filtered through celite and concentrated; then the crude residue was purified by flash column chromatography (10-30% EtOAc/hexanes) to afford **2.12** (50 mg, 81% yield) as a viscous oil. **^{1}H NMR** (500 MHz, $CDCl_3$) δ 8.21 (d, *J* = 7.7 Hz, 2H), 8.07 (dd, *J* = 11.0, 7.9 Hz, 4H), 8.01 – 7.84 (m, 7H), 7.78 (dd, *J* = 11.4, 7.8 Hz, 4H), 7.69 – 7.20 (m, 25H), 7.01 (d, *J* = 7.4 Hz, 2H), 6.93 (t, *J* = 7.5 Hz, 1H), 6.86 (t, *J* = 7.4 Hz, 2H), 5.89 (t, *J* = 9.6 Hz, 1H), 5.67 (dt, *J* = 21.3, 8.8 Hz, 2H), 5.56 (t, *J* = 9.2 Hz, 2H), 5.42 (t, *J* = 7.2 Hz, 1H), 5.32 (q, *J* = 9.3 Hz, 1H), 5.13 (s, 1H), 4.61 – 4.47 (m, 2H), 4.40 (dd, *J* = 12.4, 6.0 Hz, 1H), 4.29 (dd, *J* = 12.4, 5.1 Hz, 1H), 3.94 (dd, *J* = 10.1, 5.9 Hz, 1H), 3.85 (dt, *J* = 9.0, 3.9 Hz, 1H), 3.20 (dq, *J* = 22.5, 15.2 Hz, 2H). **^{13}C{1H} NMR** (126 MHz, $CDCl_3$) δ 166.0, 165.9, 165.5, 165.4, 165.2, 165.1, 165.0, 164.6, 133.7, 133.6, 133.5, 133.4, 133.3, 133.2, 133.1, 130.1, 130.0, 129.9, 129.9, 129.9, 129.8, 129.8, 129.7, 129.7, 129.6, 129.6, 129.3, 129.2, 129.2, 128.9, 128.8, 128.7, 128.6, 128.5, 128.4, 128.4, 128.3, 128.3, 126.9, 126.9, 95.3 (d, *J* = 166.0 Hz), 95.3 (d, *J* =

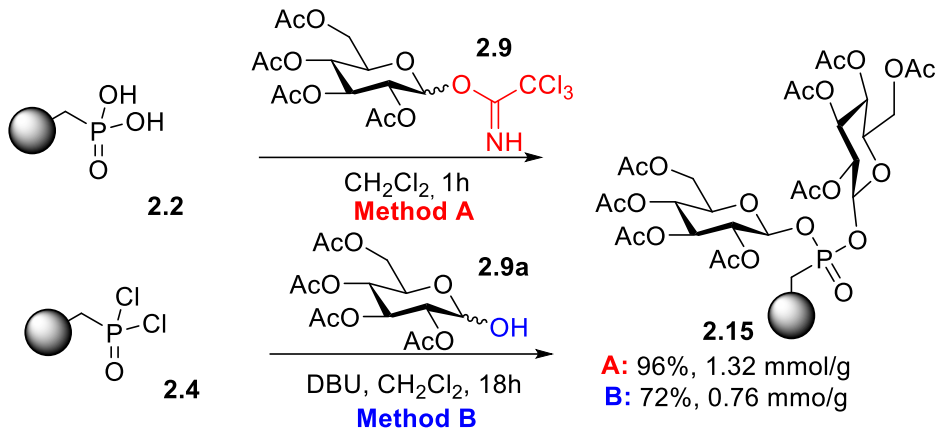
166.0 Hz), 95.2, 73.2, 72.6, 72.3, 72.0, 71.9, 71.4, 71.3, 68.9, 68.7, 62.5, 62.4, 34.7 (d, J = 137.9). **^{31}P NMR** (202 MHz, $CDCl_3$) δ 27.7.



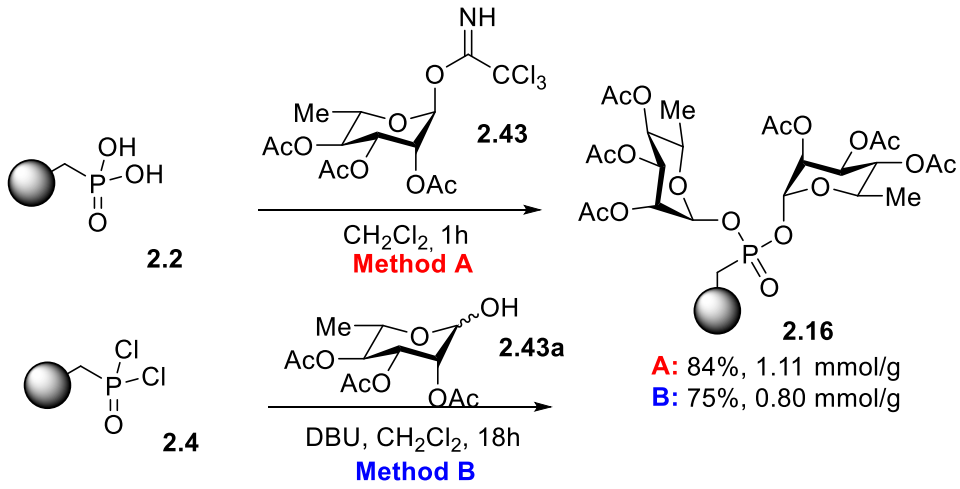
Resin 2.13: (Method A) Phosphonic acid resin **2.2** (200 mg, 0.26 mmol, 1.0 eq) was suspended in anhydrous CH_2Cl_2 (2.0 mL). Glucosyl trichloroacetimidate **2.6**[58] (360 mg, 0.53 mmol, 2.2 eq) was added and the reaction was stirred at room temperature for 1 hour. The reaction was filtered, washed with CH_2Cl_2 (3x10 mL), and dried under vacuum to afford resin **2.13** (391 mg, 87%, 0.93 mmol/g) as a pale orange solid. **(Method B)** Phosphonic acid resin **2.4** (100 mg, 0.13 mmol, 1.0 eq) was suspended in CH_2Cl_2 (2.0 mL). Glucosyl hemiacetal **2.6a** (281 mg, 0.52 mmol, 4.0 eq) and DBU (77 µL, 0.52 mmol, 4.0 eq) were added and the reaction was stirred at room temperature for 18 hours. The reaction was filtered, washed with CH_2Cl_2 (3x5 mL), and dried under vacuum to afford resin **2.13** (139 mg, 59%, 0.54 mmol/g) as a pale orange solid. **^{31}P NMR** (203 MHz, $CDCl_3$): δ 28.0. **FTIR** (thin film, cm^{-1}): 1494, 1452, 1070, 1027, 965, 907, 865, 735, 696.



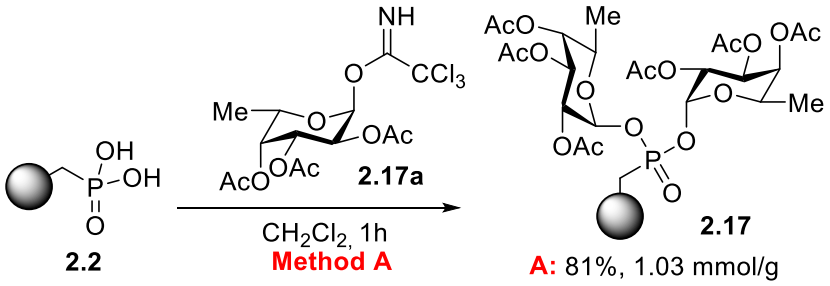
Resin 2.14: **(Method A)** Phosphonic acid resin **2.2** (100 mg, 0.13 mmol, 1.0 eq) was suspended in anhydrous CH_2Cl_2 (2.0 mL). Galactosyl trichloroacetimidate **2.14a**[44] (180 mg, 0.26 mmol, 2.2 eq) was added and the reaction was stirred at room temperature for 1 hour. The reaction was filtered, washed with CH_2Cl_2 (3x5 mL), and dried under vacuum to afford resin **2.14** (183 mg, 77%, 0.78 mmol/g) as a pale orange solid. **(Method B)** Phosphonic acid resin **4** (100 mg, 0.13 mmol, 1.0 eq) was suspended in CH_2Cl_2 (2.0mL). Galactosyl hemiacetal **2.14b** (281 mg, 0.52 mmol, 4.0 eq) and DBU (77 µL, 0.52 mmol, 4.0 eq) were added and the reaction was stirred at room temperature for 18 hours. The reaction was filtered, washed with CH_2Cl_2 (3x5 mL), and dried under vacuum to afford resin **2.14** (19 5mg, 84%, 0.95 mmol/g) as a pale orange solid. **^{31}P NMR** (203 MHz, $CDCl_3$): δ 27.8. **FTIR** (thin film, cm^{-1}): 1493, 1452, 1097, 1059,1027, 965, 910, 847, 734, 696, 641.



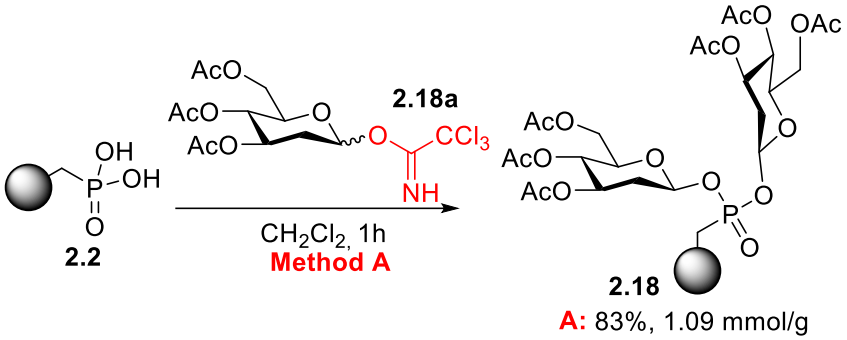
Resin 2.15: **(Method A).** Phosphonic acid resin **2.2** (200 mg, 0.26 mmol, 1.0 eq) was suspended in anhydrous DCM (2.0 mL). Glucosyl trichloroacetimidate **2.9**[59] (282 mg, 0.57 mmol, 2.2 eq) was added and the reaction was stirred at room temperature for 18 hours. The reaction was filtered, washed with CH_2Cl_2 (3x10 mL), and dried under vacuum to afford resin **2.15** (356 mg, 96%, 1.3 mmol/g) as a pale orange solid. **(Method B).** Phosphonic acid resin **2.4** (100 mg, 0.13 mmol, 1.0 eq) was suspended in CH_2Cl_2 (2.0 mL). Glucosyl hemiacetal **2.9a**[59] (181 mg, 0.52 mmol, 4.0 eq) and DBU (77 µL, 0.52 mmol, 4.0 eq) were added and the reaction was stirred at room temperature for 18 hours. The reaction was filtered, washed with CH_2Cl_2 (3x5 mL), and dried under vacuum to afford resin **2.15** (134 mg, 72%, 0.76 mmol/g) as a pale orange solid. **^{31}P NMR** (202 MHz, $CDCl_3$): δ 28.3. **FTIR** (thin film, cm^{-1}): 1751, 1216, 1031, 758, 698.



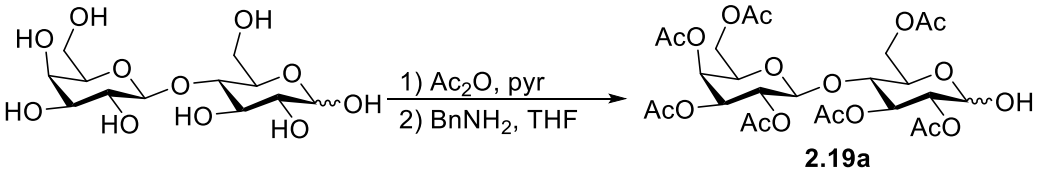
Resin 2.16: **(Method A)** Phosphonic acid resin **2.2** (205mg, 0.27mmol, 1.0eq) was suspended in anhydrous CH_2Cl_2 (2.0 mL). Rhamnosyl trichloroacetimidate **2.43**[18] (254 mg, 0.59 mmol, 2.2 eq) was added and the reaction was stirred at room temperature for 18 hours. The reaction was filtered, washed with CH_2Cl_2 (3x10 mL), and dried under vacuum to afford resin **2.16** (294 mg, 84%, 1.1 mmol/g) as a pale orange solid. **(Method B)** Phosphonic acid resin **2.4** (100 mg, 0.13 mmol, 1.0 eq) was suspended in CH_2Cl_2 (2.0 mL). Rhamnosyl hemiacetal **2.43a**[66] (150 mg, 0.52 mmol, 4.0 eq) and DBU (77 µL, 0.52 mmol, 4.0 eq) were added and the reaction was stirred at room temperature for 18 hours. The reaction was filtered, washed with CH_2Cl_2 (3x5 mL), and dried under vacuum to afford resin **2.16** (128 mg, 75%, 0.80 mmol/g) as a pale orange solid. **^{31}P NMR** (203 MHz, $CDCl_3$): δ 22.6. **FTIR** (thin film, cm^{-1}): 1746, 1646, 1217, 1045, 757, 698.



Resin 2.17: (Method A) Phosphonic acid resin **2.2** (165 mg, 0.21 mmol, 1.0 eq) was suspended in anhydrous CH_2Cl_2 (2.0 mL). Fucosyl trichloroacetimidate **2.17a**[18] (200 mg, 0.46 mmol, 2.2 eq) was added and the reaction was stirred at room temperature for 18 hours. The reaction was filtered, washed with CH_2Cl_2 (3x10 mL), and dried under vacuum to afford resin **2.17** (230 mg, 81%, 1.0 mmol/g) as a pale orange solid. **^{31}P NMR** (203 MHz, $CDCl_3$): δ 29.9. **FTIR** (thin film, cm^{-1}): 2361, 2338, 1217, 698, 668.

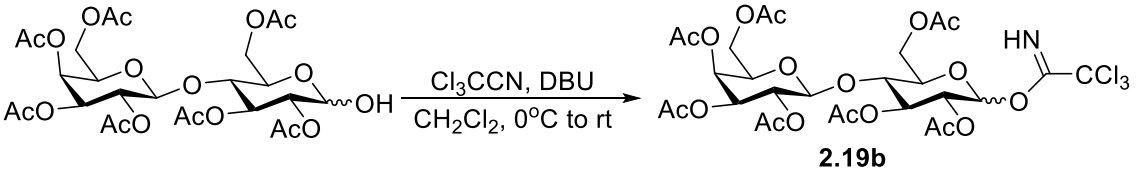


Resin 2.18: Phosphonic acid resin **2.2** (225 mg, 0.29 mmol, 1.0 eq) was suspended in anhydrous CH_2Cl_2 (2.0 mL). 2-deoxy-glucosyl trichloroacetimidate **2.18a**[61] (280 mg, 0.64 mmol, 2.2 eq) was added and the reaction was stirred at room temperature for 18 hours. The reaction was filtered, washed with DCM (3x10 mL), and dried under vacuum to afford resin **2.18** (320 mg, 83%, 1.1 mmol/g) as an orange solid. **^{31}P NMR** (203 MHz, $CDCl_3$): δ 28.9. **FTIR** (thin film, cm^{-1}) 3059, 3025, 2922, 2849, 1740, 1601. 1493, 1452, 1367, 1223, 1130, 1045, 983, 842, 757, 698.



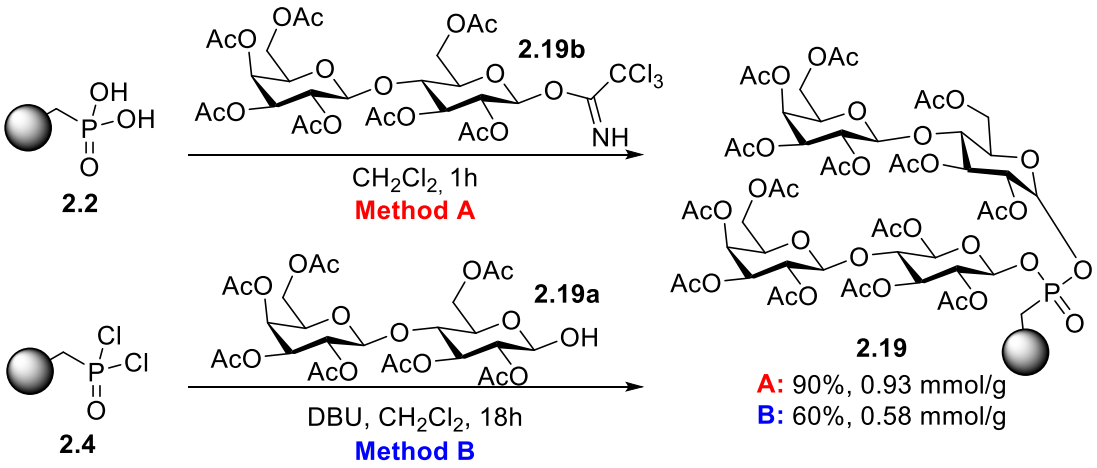
Compound 2.19a: D-Lactose (2.0 g, 5.8 mmol, 1.0 eq) was added to an oven dried flask. The flask was charged with pyridine (20 mL) and acetic anhydride (8.8 mL, 93 mmol, 16 eq). The reaction was stirred at room temperature for 20 hours. The reaction mixture was diluted with 1 N HCl (aq) (100 mL) and extracted with EtOAc (3x50 mL). The combined organics were washed with sat aq $NaHCO_3$ and brine, then dried over Na_2SO_4 and concentrated *in vacuo*. The crude residue was added to a flask containing THF (20 mL). Benzyl amine (0.77 mL, 7.0 mmol, 1.2 eq) was added and the reaction was allowed to stir at room temperature for 20 hours. The solvent was then evaporated, and the resulting residue was diluted with 1 N HCl (aq) (50 mL) and extracted with EtOAc (3x50 mL). The combined organics were washed with sat aq $NaHCO_3$

(2x50 mL) and brine (2x50mL), then dried over Na_2SO_4 and concentrated *in vacuo*. The crude residue was purified by flash column chromatography (50% EtOAc/Hexanes) to afford **2.19a** (2.2 g, 1:2.7 α:β, 59% yield, mixture of diastereomers) as a white solid over two steps. $\mathbf{R_f}$ = 0.05 (30% Acetone/hexanes). **HRMS** (ESI-TOF) (m/z): $[M+Na]^+$ calcd for $C_{26}H_{36}O_{18}Na$ 659.1794, found 659.1801. **^{1}H NMR** (500 MHz, $CDCl_3$) (major diastereomer) δ 5.52 (t, *J* = 9.7 Hz, 1H), 5.36 (dd, *J* = 11.4, 3.6 Hz, 2H), 5.11 (dt, *J* = 10.5, 7.8 Hz, 1H), 4.96 (dt, *J* = 10.4, 3.4 Hz, 1H), 4.49 (dd, *J* = 13.2, 7.9 Hz, 2H), 4.21 – 4.03 (m, 5H), 3.92 – 3.85 (m, 1H), 3.78 (q, *J* = 9.2 Hz, 1H), 2.15 (s, 3H), 2.13 (s, 3H), 2.08 (s, 3H), 2.06 (s, 3H), 2.06 (s, 3H), 2.04 (s, 3H), 1.96 (s, 3H); (minor diastereomer) δ 5.24 (t, *J* = 9.3 Hz, 1H), 5.11 (dt, *J* = 10.5, 7.8 Hz, 1H) (overlapping), 4.96 (dt, *J* = 10.4, 3.4 Hz, 1H) (overlapping), 4.84 (dd, *J* = 10.2, 3.6 Hz, 2H), 4.79 (dd, *J* = 9.7, 8.0 Hz, 1H), 4.72 (d, *J* = 8.0 Hz, 1H), 4.49 (dd, *J* = 13.2, 7.9 Hz, 2H) (overlapping), 4.21 – 4.03 (m, 2H), 3.92 – 3.85 (m, 1H), 3.78 (q, *J* = 9.2 Hz, 1H) (overlapping), 3.66 (ddd, *J* = 10.0, 5.2, 2.1 Hz, 1H), 2.17 (s, 3H), 2.15 (s, 3H), 2.13 (s, 3H), 2.08 (s, 3H), 2.06 (s, 3H), 2.06 (s, 3H), 2.04 (s, 3H). ^{13}C NMR (126 MHz, $CDCl_3$) (major diastereomer) δ 170.6, 170.5, 170.4, 170.3, 170.2, 169.8, 169.1, 100.9, 90.0, 76.3, 71.4, 71.0, 70.6, 70.6, 70.3, 69.6, 69.1, 68.1, 66.7, 61.9, 60.8, 30.9, 20.9, 20.7, 20.6, 20.5; (minor diastereomer) **^{13}C{^{1}H} NMR** (126 MHz, $CDCl_3$) δ 170.6, 170.4, 170.2, 170.2, 170.1, 169.7, 169.2, 101.0, 95.1, 76.2, 73.3, 72.9, 72.3, 71.0, 69.1, 68.1, 66.6, 62.1, 60.8, 34.6, 31.6, 22.6, 20.9, 20.8, 20.5, 14.1. **FTIR** (thin film, cm^{-1}): 3472, 2957, 1739, 1432, 1367, 1214, 1171, 1037, 954, 903. **$[\alpha]_D^{20}$** = +32.7 (c = 2.22, $CHCl_3$). **MP.** 95-98°C.

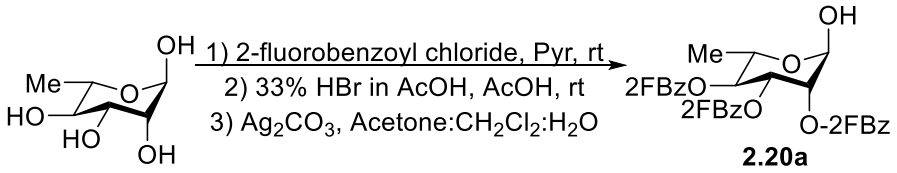


2.19b

Compound 2.19b: Cl_3CCN (0.24 mL, 2.4 mmol, 3.0eq) was added dropwise to a solution of **2.19a** (500 mg, 0.79 mmol, 1.0 eq) and DBU (0.035 mL, 0.24 mmol, 0.3 eq) in CH_2Cl_2 (5 mL) at 0 °C. The reaction was warmed to room temperature and stirred for 20 hours. The solvent was removed *in vacuo*. The crude residue was purified by flash column chromatography (50:50:5 EtOAc:Hexanes:Et_3N) to afford **2.19b** (0.49 g, 79% yield) as a yellow oil. $\mathbf{R_f}$ = 0.14 (30% Acetone/hexanes). **HRMS** (ESI-TOF) (m/z): $[M+Na]^+$ calcd for $C_{28}H_{36}Cl_3NO_{18}Na$ 802.0891, found 802.0820. **^{1}H NMR**: (500 MHz, $CDCl_3$) δ 8.65 (s, 1H), 6.48 (d, *J* = 3.8 Hz, 1H), 5.55 (t, *J* = 9.7 Hz, 1H), 5.35 (d, *J* = 3.4 Hz, 1H), 5.12 (dd, *J* = 10.4, 7.9 Hz, 1H), 5.06 (dd, *J* = 10.1, 3.8 Hz, 1H), 4.95 (dd, *J* = 10.4, 3.4 Hz, 1H), 4.53 – 4.40 (m, 2H), 4.19 – 4.03 (m, 4H), 3.91 – 3.84 (m, 2H), 2.15 (s, 3H), 2.11 (s, 3H), 2.06 (s, 3H), 2.05 (s, 3H), 2.04 (s, 3H), 2.00 (s, 3H), 1.96 (s, 3H). **^{13}C{^{1}H} NMR**: (126 MHz, $CDCl_3$) δ 170.4, 170.3, 170.2, 170.1, 170.1, 169.4, 169.1, 161.0, 101.2, 92.9, 75.9, 71.1, 70.9, 70.7, 70.0, 69.6, 69.1, 66.6, 61.5, 60.8, 43.8, 20.9, 20.8, 20.7, 20.5, 20.5. **FTIR** (thin film, cm^{-1}): 3312.12, 2974.10, 1743.59, 1675.26, 1571.73, 1453.83, 1367.77, 1213.59, 1173.43, 1145.78, 1044.13, 903.96, 797.50, 736.45, 696.00, 641.78. $\mathbf{[\alpha]_D^{20}}$ = +24.0 (c = 1.54, $CHCl_3$).



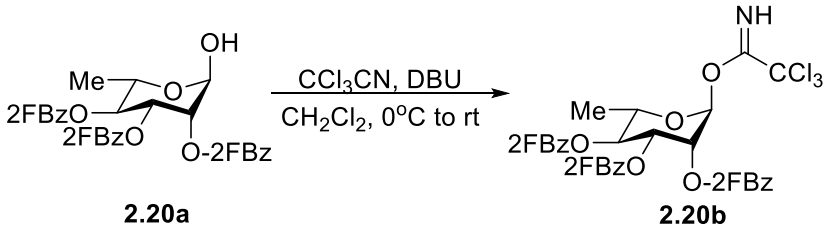
Resin 2.19: (Method A) Phosphonic acid resin **2.2** (220 mg, 0.29 mmol, 1.0 eq) was suspended in anhydrous CH_2Cl_2 (2.0 mL). Lactosyl trichloroacetimidate **2.19b** was added and the reaction was stirred at room temperature for 18 hours. The reaction was filtered, washed with CH_2Cl_2 (3x10 mL), and dried under vacuum to afford resin **2.19** (517 mg, 90%, 0.93 mmol/g) as a pale orange solid. **(Method B)** Phosphonic acid resin **2.4** (100 mg, 0.13 mmol, 1.0 eq) was suspended in CH_2Cl_2 (2.0 mL). Lactosyl hemiacetal **2.19a** (331 mg, 0.52 mmol, 4.0 eq) and DBU (77 µL, 0.52 mmol, 4.0 eq) were added and the reaction was stirred at room temperature for 18 hours. The reaction was filtered, washed with CH_2Cl_2 (3x5 mL), and dried under vacuum to afford resin **7g** (156 mg, 60%, 0.58 mmol/g) as a pale orange solid. **^{31}P NMR** (203 MHz, $CDCl_3$): δ 28.1. **FTIR** (thin film, cm^{-1}): 1750, 1734, 1718, 1215, 1045, 757, 699. **Elemental Analysis**: Calcd for $C_{115}H_{133}O_{37}P$: C, 64.61, H, 6.267. Found: 64.43%, H: 6.305%.



2.20a

Compound 2.20a: L-Rhamnose monohydrate (1.0 g, 5.8 mmol, 1.0 eq) was added to an oven dried flask. The substrate was dissolved in pyridine (20 mL) at room temperature. 2-fluorobenzoyl chloride (5.6 mL, 47 mmol, 8.0 eq) was added dropwise at room temperature. When the addition was complete, the reaction was stirred for 20 hours at room temperature. The reaction mixture was diluted with EtOAc, and washed with 1 N HCl (3x100 mL), conc. aq. $NaHCO_3$ (3x100 mL) and brine (3x100 mL) and dried over Na_2SO_4 and concentrated *in vacuo.* The crude residue was dissolved in CH_2Cl_2 (20 mL). 33% HBr in AcOH (5 mL) was added dropwise at room temperature. The reaction was stirred for 20 hours at room temperature. The reaction mixture was diluted with CH_2Cl_2 (100 mL), washed with $NaHCO_3$ (3x100 mL) and brine (3x100 mL), dried over Na_2SO_4 and concentrated *in vacuo.* The crude mixture was

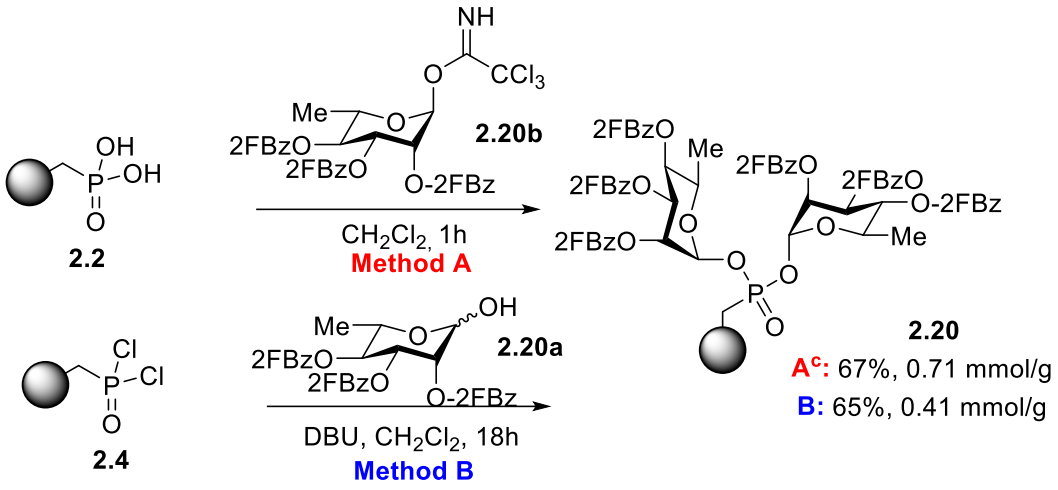
dissolved in a mixture of Acetone/CH_2Cl_2/H_2O (60 mL/10 mL/6 mL). Ag_2CO_3 (2.4 g, 8.7 mmol, 1.5 eq) was added and the reaction was stirred at room temperature in the dark for 20 hours. The reaction mixture was filtered through celite, and the filtrate was concentrated *in vacuo*. The crude mixture was purified by flash column chromatography (30% EtOAc/Hexanes) to afford **2.20a** (2.2 g, 80% yield) as a white solid over three steps. $\mathbf{R_f}$ = 0.26 (30% EtOAc/hexanes). **HRMS** (ESI-TOF) (m/z): $[M+Na]^+$ calcd for $C_{27}H_{21}F_3O_8Na$ 553.1081, found 553.1129.**^{1}H NMR** (600 MHz, $CDCl_3$) δ 7.97 (td, *J* = 7.5, 1.9 Hz, 1H), 7.86 (s, 0H), 7.79 (tt, *J* = 7.5, 3.9 Hz, 1H), 7.56 (s, 1H), 7.49 (tdd, *J* = 8.6, 5.8, 1.8 Hz, 1H), 7.25 – 7.22 (m, 1H), 7.20 – 7.15 (m, 3H), 7.12 – 7.05 (m, 2H), 6.99 (dd, *J* = 10.7, 8.2 Hz, 1H), 5.91 (dd, *J* = 10.1, 3.3 Hz, 1H), 5.73 (dd, *J* = 3.4, 1.9 Hz, 1H), 5.70 (t, *J* = 10.0 Hz, 1H), 5.44 (s, 1H), 4.41 (dq, *J* = 9.8, 6.2 Hz, 1H), 1.37 (d, *J* = 6.3 Hz, 3H). **^{13}C{^{1}H} NMR**: (151 MHz, $CDCl_3$) δ 163.4, 163.1, 162.9, 161.4, 161.2, 161.1, 135.0 (d, *J* = 8.8 Hz), 134.7 (d, *J* = 7.0 Hz), 134.6, 132.2, 132.1, 131.9, 124.1 (d, *J* = 3.9 Hz), 124.0 (d, *J* = 3.8 Hz), 123.9 (d, *J* = 3.9 Hz), 117.2, 117.1 (d, *J* = 3.9 Hz), 117.0, 116.9, 116.8, 107.2, 92.1, 72.0, 71.2, 69.7, 66.8, 17.7. **^{13}C NMR** (126 MHz, $CDCl_3$) δ 92.3 (d, *J* = 172.3 Hz). **^{19}F NMR** (564 MHz, $CDCl_3$) δ –108.5 (dt, *J* = 11.3, 5.9 Hz), –108.9 (dt, *J* = 11.6, 5.6 Hz), –109.4 (ddd, *J* = 11.3, 7.1, 4.9 Hz). **FTIR** (thin film, cm^{-1}): 3460, 2983, 1719, 1612, 1585, 1488, 1456, 1345, 1288, 1244, 1159, 1120, 1069, 1034, 975, 916, 868, 837, 815, 782, 752, 691, 655. **$[\alpha]_D^{20}$** = +65.5 (c = 0.90, $CHCl_3$). **MP.** 65-67°C.



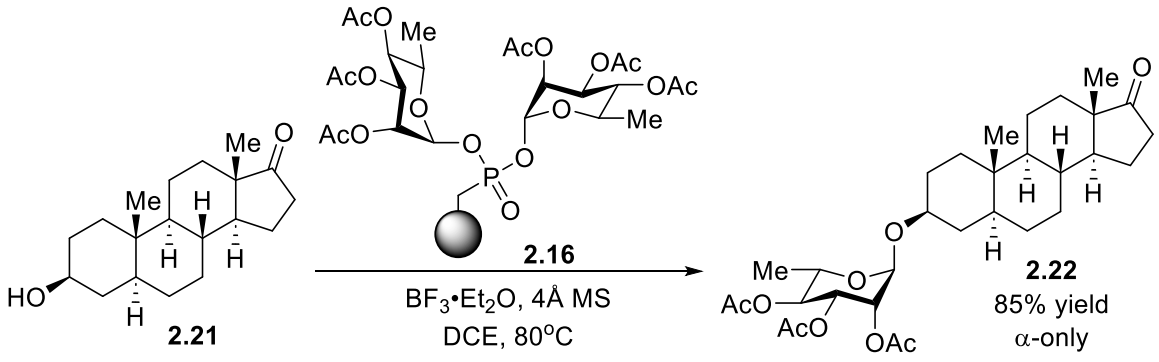
2.20a **2.20b**

Compound 2.20b: CCl_3CN (1.3 mL, 13 mmol, 3 eq) was added dropwise at 0 °C over 20 minutes to a solution of **2.20a** (2.2 g, 4.2 mmol, 1.0 eq) and DBU (190 mL, 1.26 mmol, 0.3 eq)

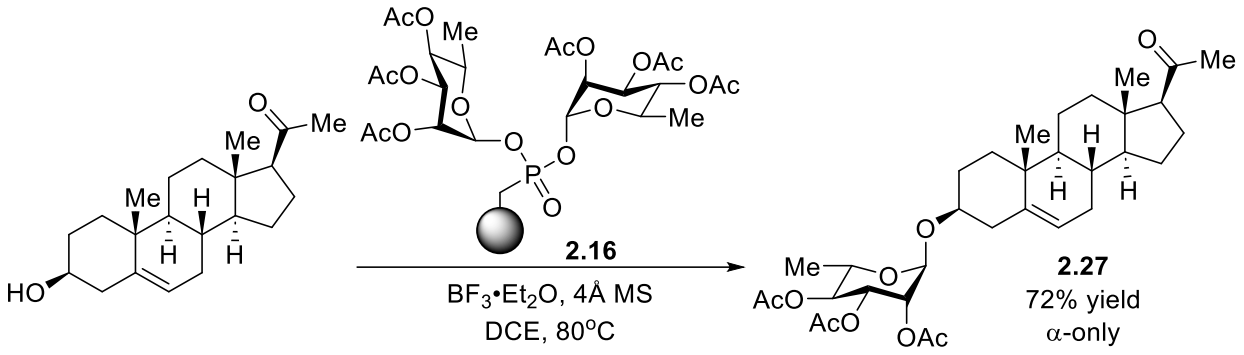
in CH_2Cl_2 (25mL) under an N_2 atmosphere. Upon complete addition, the reaction was warmed to room temperature and stirred for 20 hours. The solvent was evaporated, and the crude material was purified by flash column chromatography (0-50%EtOAc/hexanes + 5% Et_3N) to afford **2.20b** (1.6 g, 57% yield) as an orange solid. $\mathbf{R_f}$ = 0.60 (30% EtOAc/hexanes). **HRMS** (ESI-TOF) (m/z): $[M+Na]^+$ calcd for $C_{29}H_{21}Cl_3F_3NO_8Na$ 696.0178, found 696.0162. **^{1}H NMR** (600 MHz, $CDCl_3$) δ 8.81 (s, 1H), 7.97 (td, *J* = 7.5, 1.8 Hz, 1H), 7.84 (td, *J* = 7.5, 1.9 Hz, 1H), 7.79 (td, *J* = 7.6, 1.9 Hz, 1H), 7.61 – 7.54 (m, 1H), 7.50 (tdd, *J* = 7.8, 4.8, 1.8 Hz, 1H), 7.43 (tdt, *J* = 6.9, 4.7, 1.8 Hz, 1H), 7.24 (d, *J* = 7.8 Hz, 1H), 7.22 – 7.15 (m, 2H), 7.11 – 7.06 (m, 2H), 7.00 (dd, *J* = 10.6, 8.3 Hz, 1H), 6.47 (d, *J* = 1.9 Hz, 1H), 5.92 (dd, *J* = 3.3, 2.0 Hz, 1H), 5.88 (dd, *J* = 10.1, 3.3 Hz, 1H), 5.79 (t, *J* = 10.0 Hz, 1H), 4.36 (dq, *J* = 9.7, 6.2 Hz, 1H), 1.43 (d, *J* = 6.2 Hz, 3H). $^{13}C\{^1H\}$ NMR (151 MHz, $CDCl_3$) δ 163.3, 163.0, 161.4, 161.3, 160.0, 135.2 (d, *J* = 9.2 Hz), 134.9 (d, *J* = 6.0 Hz), 134.8, 132.3, 132.1, 131.8, 124.1 (d, *J* = 4.0 Hz), 124.0 (d, *J* = 4.2 Hz), 124.0 (d, *J* = 3.7 Hz), 117.3, 117.2, 117.1, 117.0, 116.9, 116.9, 107.2, 94.6, 90.7, 71.2, 69.8, 69.6, 69.2, 17.7. ^{13}C NMR (151 MHz, $CDCl_3$): δ 94.6. (d, J = 180.0 Hz). **^{19}F NMR** (564 MHz, $CDCl_3$) δ –108.0 (dt, *J* = 11.5, 5.8 Hz), –108.9 (dt, *J* = 11.8, 5.6 Hz), –109.3 (ddd, *J* = 11.3, 7.1, 4.9 Hz). **FTIR** (thin film, cm^{-1}): 3340, 2986, 1724, 1676, 1612, 1585, 1488, 1456, 1288, 1243, 1158, 1118, 1071, 1034, 974, 867, 843, 795, 751, 690, 642. $\mathbf{[\alpha]_D^{20}}$ = +90.0 (c = 2.86, $CHCl_3$).



Resin 2.20: **(Method A)** Phosphonic acid resin **2.2** (100 mg, 0.13 mmol, 1.0 eq) was suspended in anhydrous toluene (2.0 mL). Rhamnosyl trichloroacetimidate **2.20b** was added and the reaction was stirred at 100°C for 18 hours. The reaction was cooled to room temperature, filtered, washed with CH_2Cl_2 (3x10 mL), and dried under vacuum to afford resin **2.20** (157 mg, 67%, 0.71mmol/g) as an orange solid. **(Method B).** Phosphonic acid resin **2.4** (100 mg, 0.13 mmol, 1.0 eq) was suspended in CH_2Cl_2 (2.0 mL). Rhamnosyl hemiacetal **2.20a** (276 mg, 0.52 mmol, 4.0 eq) and DBU (77 µL, 0.52 mmol, 4.0 eq) were added and the reaction was stirred at room temperature for 18 hours. The reaction was filtered, washed with CH_2Cl_2 (3x5 mL), and dried under vacuum to afford resin **2.20** (113 mg, 65%, 0.41 mmol/g) as a pale orange solid. **^{31}P NMR** (203 MHz, $CDCl_3$): δ 27.2. **FTIR** (thin film, cm^{-1}): 1734, 1456, 1288, 1243, 1117, 1074, 753, 697.

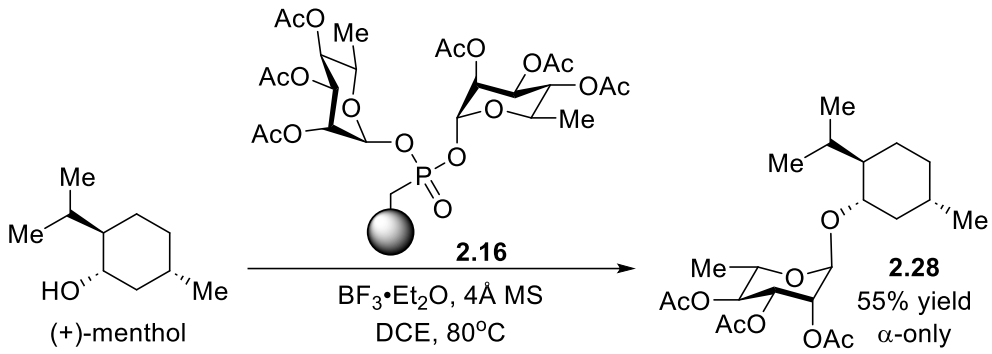


Glycoside product 2.22: Resin **2.16** (93 mg, 0.10 mmol, 2.0 eq), DCE (2.0 mL), and 4Å molecular sieves were added to a plastic vial. The resin was swelled at room temperature for 20 minutes. Glycosyl acceptor *trans*-androsterone (15 mg, 0.05 mmol, 1.0 eq) was added, and the reaction was heated to 80 °C. $BF_3{\cdot}Et_2O$ (10 µL, 0.08 mmol, 1.5 eq) was added and the reaction progress was monitored by TLC for 1 hour. Upon full consumption of the acceptor, the reaction mixture was filtered, and the resin was washed with CH_2Cl_2 (3x5 mL), EtOAc (3x5 mL), and CH_2Cl_2 (3x5 mL), and the filtrate was then quenched with Et_3N (50 mL). The filtrate was concentrated, and the crude residue was purified by flash column chromatography (30% EtOAc/hexanes) to afford **2.22** (24.7 mg, α-only, 85% yield) as a white solid. $\mathbf{R_f}$ = 0.33 (30% EtOAc/hexanes). R_f = 0.33 (30% EtOAc/hexanes). **HRMS** (ESI-TOF) (m/z): $[M+Na]^+$ calcd for $C_{31}H_{46}O_9Na$ 585.3035, found 585.3022. **^{1}H NMR** (500 MHz, $CDCl_3$) δ 5.30 (dd, *J* = 10.1, 3.5 Hz, 1H), 5.15 (dd, *J* = 3.5, 1.8 Hz, 1H), 5.04 (t, *J* = 9.9 Hz, 1H), 4.86 (d, *J* = 1.8 Hz, 1H), 3.93 (dq, *J* = 9.9, 6.3 Hz, 1H), 3.52 (tt, *J* = 10.8, 4.8 Hz, 1H), 2.42 (dd, *J* = 19.3, 8.8 Hz, 1H), 2.13 (s, 3H), 2.09 – 2.05 (m, 1H), 2.03 (s, 3H),1.97 (s, 3H), 1.91 (ddd, *J* = 11.7, 8.6, 5.9 Hz, 1H), 1.78 (dt, *J* = 12.6, 3.2 Hz, 3H), 1.72 (dt, *J* = 13.2, 3.7 Hz, 1H), 1.62 (ddd, *J* = 14.8, 9.2, 3.1 Hz, 2H), 1.57 – 1.45 (m, 2H), 1.40 – 1.21 (m, 7H), 1.19 (d, *J* = 6.3 Hz, 3H), 1.07 (tt, *J* = 11.5, 3.7 Hz, 1H), 0.96 (td, *J* = 13.9, 4.1 Hz, 2H), 0.85 (s, 3H), 0.82 (s, 3H), 0.67 (td, *J* = 9.7, 8.0, 5.2 Hz, 1H). **^{13}C{^{1}H} NMR** (126 MHz, $CDCl_3$) δ 221.3, 170.3, 170.1, 95.5, 76.8, 71.4, 70.6, 69.2, 66.3, 54.4, 51.4, 47.8, 44.7, 37.0, 35.9, 35.8, 35.0, 33.9, 31.6, 30.9, 29.1, 28.4, 21.8, 21.0, 20.8, 20.8, 20.5, 17.4, 13.8, 12.2. **^{13}C NMR** (176 MHz, $CDCl_3$): δ 95.4 (d, *J* = 171.0 Hz). **FTIR** (thin film, cm^{-1}): 1735, 1370, 1244, 1219, 1127, 1076, 1055, 1041. 1017, 982. $\mathbf{[\alpha]_D^{20}}$ = +71.8 (c = 2.50, $CHCl_3$). **MP.** 145-148°C. By-product **2.23** was identified and confirmed by comparison with reported spectra.[62]



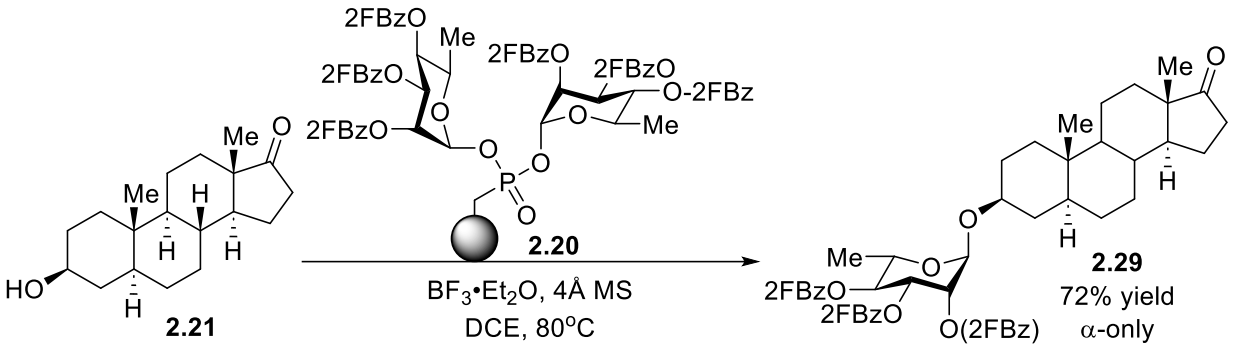
Glycoside product 2.27: Resin **2.16** (91 mg, 0.10 mmol, 2.0 eq), DCE (2.0 mL), and 4Å molecular sieves were added to a plastic vial. The resin was swelled at room temperature for 20 minutes. Glycosyl acceptor pregnenolone (16 mg, 0.05 mmol, 1.0 eq) was added, and the reaction was heated to 80°C. $BF_3{\cdot}Et_2O$ (10 µL, 0.08 mmol, 1.5 eq) was added and the reaction progress was monitored by TLC for 1 hour. Upon full consumption of the acceptor, the reaction mixture was filtered, and the resin was washed with CH_2Cl_2 (3x5 mL), EtOAc (3x5 mL), and CH_2Cl_2 (3x5 mL), and the filtrate was then quenched with Et_3N (50 mL). The filtrate was concentrated, and the crude residue was purified by flash column chromatography (30% EtOAc/hexanes) to afford **2.27** (21.4 mg, α-only, 72% yield) as a white solid. $\mathbf{R_f}$ = 0.39 (30% EtOAc/hexanes). **HRMS** (ESI-TOF) (m/z): $[M+Na]^+$ calcd for $C_{33}H_{48}O_9Na$ 611.3191, found 611.3179. **^{1}H NMR** (500 MHz, $CDCl_3$) δ 5.35 (dt, *J* = 10.0, 3.0 Hz, 2H), 5.21 (dd, *J* = 3.5, 1.8 Hz, 1H), 5.07 (t, *J* = 9.9 Hz, 1H), 4.90 (d, *J* = 1.9 Hz, 1H), 3.97 (dq, *J* = 9.7, 6.2 Hz, 1H), 3.49 (tt, *J* = 11.3, 4.1 Hz, 1H), 2.55 (t, *J* = 9.0 Hz, 1H), 2.35 (ddd, *J* = 13.4, 5.0, 2.1 Hz, 1H), 2.25 (td, *J* = 10.8, 2.6 Hz, 1H), 2.22 – 2.18 (m, 1H), 2.17 (s, 3H), 2.14 (s, 3H), 2.07 (s, 3H), 2.05 – 2.02 (m, 1H), 2.01 (s, 3H), 1.92 – 1.84 (m, 2H), 1.77 – 1.42 (m, 9H), 1.32 – 1.25 (m, 2H), 1.22 (d, *J* = 6.3 Hz, 3H), 1.20 – 1.14 (m, 1H), 1.10 (td, *J* = 14.4, 4.4 Hz, 1H), 1.03 (s, 3H), 0.99 (dd, *J* = 11.3, 4.5 Hz, 1H), 0.65 (s, 3H). **^{13}C{^{1}H} NMR** (126 MHz, $CDCl_3$) δ 209.6, 170.3, 170.1, 140.2, 121.8, 95.7, 77.6, 71.4, 70.5, 69.2, 66.3, 63.7, 56.9, 50.0, 44.0, 38.8, 38.3, 37.3, 36.7, 31.8, 31.8, 31.6,

29.3, 24.5, 22.8, 21.1, 21.0, 20.9, 20.8, 19.4, 17.4, 13.2. **^{13}C NMR** (176 MHz, $CDCl_3$): δ 95.4 (d, J = 171.0 Hz). ^{13}C-H NMR (176 MHz, $CDCl_3$): δ 95.7 (d, J = 170.7 Hz). **FTIR** (thin film, cm^{-1}): 1751, 1700, 1365, 1250, 1214, 1126, 1088, 1078, 1041, 984. **$[\alpha]_D^{20}$** = –11.9 (c = 1.86, $CHCl_3$). **MP.** 167-168°C.



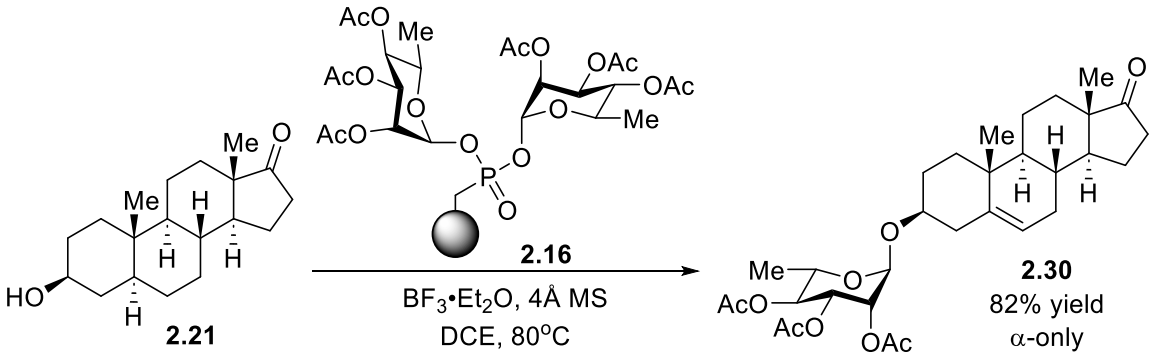
Glycoside product 2.28: Resin **2.16** (70 mg, 0.10 mmol, 2.0 eq), DCE (2.0 mL), and 4Å molecular sieves were added to a plastic vial. The resin was swelled at room temperature for 20 minutes. Glycosyl acceptor (+)-menthol (8.0 mg, 0.05 mmol, 1.0 eq) was added, and the reaction was heated to 80°C. $BF_3{\cdot}Et_2O$ (10 µL, 0.0 8mmol, 1.5 eq) was added and the reaction progress was monitored by TLC for 1 hour. Upon full consumption of the acceptor, the reaction mixture was filtered, and the resin was washed with CH_2Cl_2 (3x5 mL), EtOAc (3x5 mL), and CH_2Cl_2 (3x5 mL), and the filtrate was then quenched with Et_3N (50 mL). The filtrate was concentrated, and the crude residue was purified by flash column chromatography (25% EtOAc/hexanes) to afford **2.28** (12.0 mg, α-only, 55% yield) as a white solid. **R_f** = 0.53 (30% EtOAc/hexanes). **HRMS** (ESI-TOF) (m/z): $[M+Na]^+$ calcd for $C_{22}H_{36}O_8Na$ 451.2303, found 451.2303. **^{1}H NMR** (500 MHz, $CDCl_3$) δ 5.32 (dd, *J* = 10.1, 3.4 Hz, 1H), 5.16 (dd, *J* = 3.5, 1.8 Hz, 1H), 5.05 (t, *J* = 9.9 Hz, 1H), 4.80 (d, *J* = 1.9 Hz, 1H), 4.01 (dq, *J* = 9.8, 6.3 Hz, 1H), 3.33 (td, *J* = 10.7, 4.4 Hz, 1H), 2.15 (s, 3H), 2.09 (td, *J* = 7.0, 2.6 Hz, 1H), 2.04 (s, 3H), 1.99 (s, 3H), 1.73 – 1.53 (m, 3H), 1.38 (ddt, *J* = 8.6, 5.4, 2.6 Hz, 0H), 1.30 – 1.23 (m, 2H), 1.20 (d, *J* = 6.3 Hz, 3H), 1.05 (q, *J* =

11.8 Hz, 1H), 0.96 (dd, *J* = 12.8, 3.3 Hz, 1H), 0.90 (dd, *J* = 6.8, 2.5 Hz, 6H), 0.84 (td, *J* = 12.6, 12.0, 3.8 Hz, 1H), 0.76 (d, *J* = 6.9 Hz, 3H). **^{13}C{^{1}H} NMR** (176 MHz, $CDCl_3$) δ 170.3, 170.1, 170.0, 99.0, 82.0, 71.4, 70.4, 69.2, 66.4, 48.4, 42.7, 34.2, 31.6, 25.7, 23.2, 22.3, 20.99, 20.97, 20.81, 20.75, 17.2, 16.2. **^{13}C NMR** (176 MHz, $CDCl_3$): δ 99.0 (d, *J* = 172.7 Hz). **FTIR** (thin film, cm^{-1}): 1741, 1243, 1232, 1216, 1124, 1082, 1070, 1040, 1021. **$[\alpha]_D^{20}$** = –14.3 (c = 1.20, $CHCl_3$). **MP.** 68-72°C.



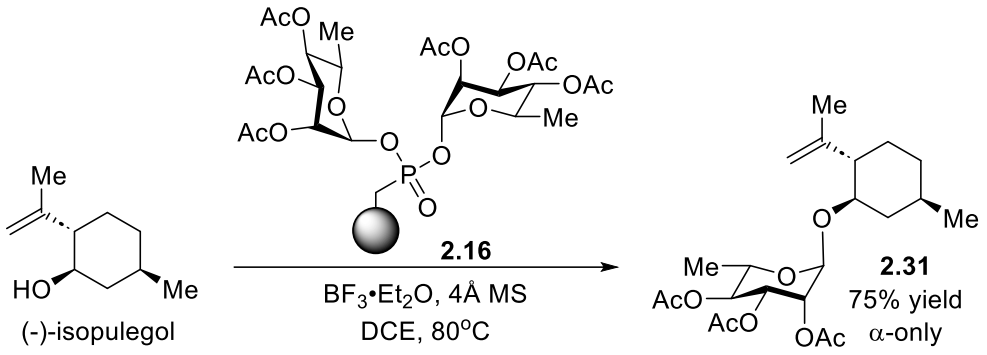
Glycoside product 2.29: Resin **2.20** (146 mg, 0.10 mmol, 2.0 eq), DCE (2.0 mL), and 4Å molecular sieves were added to a plastic vial. The resin was swelled at room temperature for 20 minutes. Glycosyl acceptor *trans*-androsterone (15 mg, 0.05 mmol, 1.0 eq) was added, and the reaction was heated to 80°C. $BF_3{\cdot}Et_2O$ (10 µL, 0.08 mmol, 1.5 eq) was added and the reaction progress was monitored by TLC for 3 hours. Upon full consumption of the acceptor, the reaction mixture was filtered, and the resin was washed with CH_2Cl_2 (3x5 mL), EtOAc (3x5 mL), and CH_2Cl_2 (3x5 mL), and the filtrate was then quenched with Et_3N (50 µL). The filtrate was concentrated, and the crude residue was purified by flash column chromatography (30% EtOAc/hexanes) to afford **2.29** 30.9 mg, α-only, 75% yield) as a yellow-brown solid. **R_f** = 0.36 (30% EtOAc/hexanes). **HRMS** (ESI-TOF) (m/z): $[M+Na]^+$ calcd for $C_{46}H_{49}F_3O_9Na$ 825.3221, found 825.3206. **^{1}H NMR** (500 MHz, $CDCl_3$) δ 7.99 (td, *J* = 7.5, 1.8 Hz, 1H), 7.86 (td, *J* = 7.6, 1.8 Hz, 1H), 7.80 (td, *J* = 7.6, 1.8 Hz, 1H), 7.57 (tdd, *J* = 7.3, 4.6, 1.8 Hz, 1H), 7.51 (tdd, *J* = 7.4,

4.7, 1.8 Hz, 1H), 7.47 – 7.40 (m, 1H), 7.26 (dd, *J* = 15.4, 7.8 Hz, 1H), 7.22 – 7.15 (m, 2H), 7.10 (q, *J* = 9.0, 7.5 Hz, 2H), 7.01 (dd, *J* = 10.7, 8.3 Hz, 1H), 5.87 (dd, *J* = 10.1, 3.3 Hz, 1H), 5.69 (t, *J* = 10.0 Hz, 1H), 5.64 (t, *J* = 2.6 Hz, 1H), 5.18 (d, *J* = 1.8 Hz, 1H), 4.24 (dq, *J* = 12.4, 6.3 Hz, 1H), 3.67 (tt, *J* = 10.9, 4.9 Hz, 1H), 2.46 (dd, *J* = 19.3, 8.8 Hz, 1H), 2.09 (dt, *J* = 18.8, 9.0 Hz, 1H), 1.95 (ddd, *J* = 15.8, 12.5, 6.1 Hz, 1H), 1.85 – 1.79 (m, 2H), 1.79 – 1.49 (m, 5H), 1.43 (d, *J* = 12.6 Hz, 1H), 1.37 (d, *J* = 6.2 Hz, 3H), 1.34 – 1.22 (m, 6H), 1.14 (tt, *J* = 11.8, 9.1, 3.5 Hz, 1H), 1.01 (dtd, *J* = 24.4, 12.7, 12.1, 4.8 Hz, 2H), 0.90 (s, 3H), 0.89 (s, 3H), 0.73 (td, *J* = 11.3, 4.0 Hz, 1H). **^{13}C{^{1}H} NMR** (126 MHz, $CDCl_3$) δ 221.4, 163.4 (t, *J* = 3.2 Hz), 163.3, 163.20 – 163.11 (m), 163.0, 161.2, 161.1, 160.9, 135.0 (d, *J* = 8.9 Hz), 134.7 (dd, *J* = 9.0, 3.5 Hz), 132.2, 132.0, 131.9, 124.1 (dd, *J* = 9.3, 3.9 Hz), 123.9 (d, *J* = 3.7 Hz), 118.3 (d, *J* = 9.5 Hz), 118.1 (d, *J* = 9.3 Hz), 117.9 (d, *J* = 9.2 Hz), 117.3, 117.1, 117.0, 116.9 (d, *J* = 7.3 Hz), 95.5, 77.3, 72.2, 71.7, 70.2, 66.7, 54.4, 51.4, 47.8, 44.7, 37.0, 35.9, 35.8, 35.1, 34.1, 31.6, 30.9, 29.2, 28.5, 21.8, 20.5, 17.7, 13.8, 12.3. **^{13}C NMR**: (151 MHz, $CDCl_3$): δ 95.5 (d, *J* = 169.5 Hz). **^{19}F NMR** (564 MHz, $CDCl_3$): δ –108.7 (dt, J = 11.3, 5.6 Hz), –109.0 (dt, *J* = 11.3, 5.5 Hz), –109.5 (dt, *J* = 11.2, 5.6 Hz). **FTIR** (thin film, cm^{-1}): 1734, 1718, 1288, 1246 1122, 1073, 1056, 1035, 1018, 754. **$[\alpha]_D^{20}$** = +64.3 (c = 3.09, $CHCl_3$). **MP.** 90-95°C.



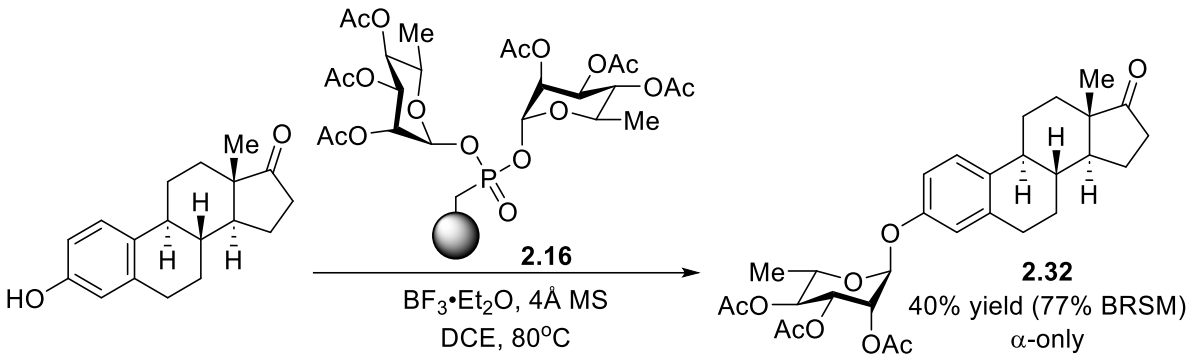
Glycoside product 2.30: Resin **2.16** (14 5mg, 0.10 mmol, 2.0 eq), DCE (2.0 mL), and 4Å molecular sieves were added to a plastic vial. The resin was swelled at room temperature for 20

minutes. Glycosyl acceptor DHEA (15 mg, 0.05 mmol, 1.0 eq) was added, and the reaction was heated to 80°C. $BF_3{\cdot}Et_2O$ (10 µL, 0.08 mmol, 1.5 eq) was added and the reaction progress was monitored by TLC for 1 hour. Upon full consumption of the acceptor, the reaction mixture was filtered, and the resin was washed with CH_2Cl_2 (3x5 mL), EtOAc (3x5 mL), and CH_2Cl_2 (3x5 mL), and the filtrate was then quenched with Et_3N (50 µL). The filtrate was concentrated, and the crude residue was purified by flash column chromatography (10% EtOAc/hexanes) to afford **2.30** (23.9 mg, α-only, 82% yield) as a white solid. $\mathbf{R_f}$ = 0.34 (30% EtOAc/hexanes). **HRMS** (ESI-TOF) (m/z): $[M+Na]^+$ calcd for $C_{31}H_{44}O_9Na$ 583.2878, found 583.2877. **^{1}H NMR** (500 MHz, $CDCl_3$): δ 5.36 (d, *J* = 5.1 Hz, 1H), 5.32 (dd, *J* = 10.1, 3.5 Hz, 1H), 5.18 (dd, *J* = 3.4, 1.8 Hz, 1H), 5.05 (t, *J* = 9.9 Hz, 1H), 4.88 (d, *J* = 1.8 Hz, 1H), 3.95 (dq, *J* = 12.5, 6.3 Hz, 1H), 3.47 (tt, *J* = 11.3, 4.4 Hz, 1H), 2.45 (dd, *J* = 19.3, 8.8 Hz, 1H), 2.34 (ddd, *J* = 11.6, 5.1, 2.0 Hz, 1H), 2.28 – 2.19 (m, 1H), 2.15 (s, 3H), 2.13 – 2.05 (m, 1H), 2.04 (s, 3H), 1.98 (s, 3H), 1.94 (ddd, *J* = 14.4, 8.9, 6.2 Hz, 1H), 1.90 – 1.80 (m, 3H), 1.71 – 1.58 (m, 3H), 1.58 – 1.43 (m, 2H), 1.33 – 1.22 (m, 3H), 1.19 (d, *J* = 6.3 Hz, 3H),1.09 (dd, *J* = 13.6, 3.8 Hz, 1H), 1.03 (s, 3H), 1.01 – 0.94 (m, 1H), 0.87 (s, 3H), 0.86 – 0.79 (m, 1H). **^{13}C{^{1}H} NMR** (126 MHz, $CDCl_3$): δ 221.1, 170.3, 170.1, 170.1, 140.4, 121.4, 95.7, 77.4, 71.4, 70.5, 66.3, 51.8, 50.2, 47.5, 38.3, 37.2, 36.9, 35.9, 31.5, 31.4, 30.8, 29.3, 21.9, 21.0, 20.8, 20.8, 20.4, 19.4, 17.4, 13.6. **^{13}C NMR** (176 MHz, $CDCl_3$): δ 95.7. (d, *J* = 171.4 Hz). **FTIR** (thin film, cm^{-1}): 2930, 2854, 1739, 1454, 1370, 1245, 1218, 1132, 1075, 1049, 980, 951, 797, 752, 667. $\mathbf{[\alpha]_D^{20}}$ = –34.4 (c = 1.27, $CHCl_3$). **MP.** 137-138°C.



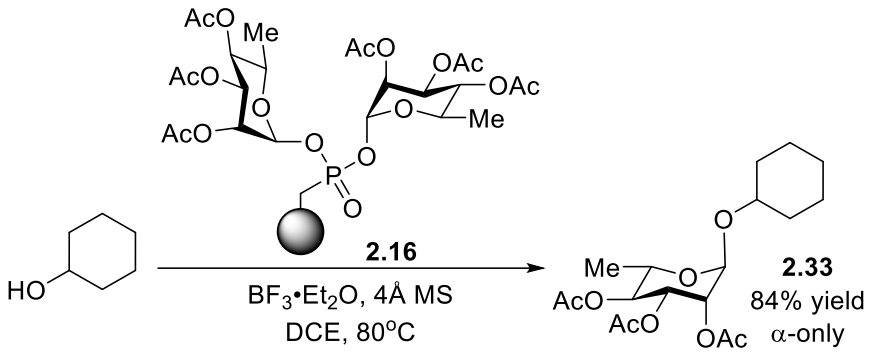
Glycoside product 2.31: Resin **2.16** (145 mg, 0.10 mmol, 2.0 eq), DCE (2.0 mL), and 4Å molecular sieves were added to a plastic vial. The resin was swelled at room temperature for 20 minutes. Glycosyl acceptor (-)-isopulegol (8.2 mg, 0.05 mmol, 1.0 eq) was added, and the reaction was heated to 80°C. $BF_3{\cdot}Et_2O$ (10 µL, 0.08 mmol, 1.5 eq) was added and the reaction progress was monitored by TLC for 1 hour. Upon full consumption of the acceptor, the reaction mixture was filtered, and the resin was washed with CH_2Cl_2 (3x5 mL), EtOAc (3x5 mL), and CH_2Cl_2 (3x5 mL), and the filtrate was then quenched with Et_3N (50 µL). The filtrate was concentrated, and the crude residue was purified by flash column chromatography (25% EtOAc/hexanes) to afford **2.31** (16.9 mg, α-only, 75% yield) as a clear oil. $\mathbf{R_f}$ = 0.47 (30% EtOAc/hexanes). **HRMS** (ESI-TOF) (m/z): $[M+Na]^+$ calcd for $C_{22}H_{34}O_8Na$ 449.2146, found 449.2187. **^{1}H NMR** (500 MHz, $CDCl_3$) δ 5.20 (dd, *J* = 10.2, 3.4 Hz, 1H), 5.12 (dd, *J* = 3.4, 1.8 Hz, 1H), 5.02 (t, *J* = 10.0 Hz, 1H), 4.84 (dd, *J* = 7.0, 2.0 Hz, 2H), 4.81 (t, *J* = 1.8 Hz, 1H), 3.96 (dq, *J* = 9.8, 6.3 Hz, 1H), 3.51 (td, *J* = 10.6, 4.3 Hz, 1H), 2.13 (s, 3H), 2.09 – 2.05 (m, 1H), 2.04 (s, 3H), 2.03 – 1.98 (m, 1H), 1.97 (s, 3H), 1.73 (d, *J* = 1.4 Hz, 3H), 1.65 (tt, *J* = 11.9, 2.5 Hz, 2H), 1.47 – 1.27 (m, 2H), 1.25 (s, 1H), 1.13 (d, *J* = 6.3 Hz, 3H), 1.00 – 0.93 (m, 1H), 0.92 (d, *J* = 6.6 Hz, 3H). **^{13}C{^{1}H}** NMR (126 MHz, $CDCl_3$) δ 170.3, 170.2, 167.0, 147.6, 111.6, 94.1, 77.2, 71.1, 70.9, 69.3, 66.3, 50.8, 39.7, 34.2, 31.3, 30.7, 22.2, 21.0, 20.9, 20.8, 20.4, 17.2. **^{13}C NMR**

(176 MHz, $CDCl_3$): δ 94.1 (d, *J* = 169.3 Hz). **FTIR** (thin film, cm^{-1}): 1747, 1735, 1653, 1559, 1244, 1217, 1040. **$[\alpha]_D^{20}$** = +65.3 (c = 1.39, $CHCl_3$).



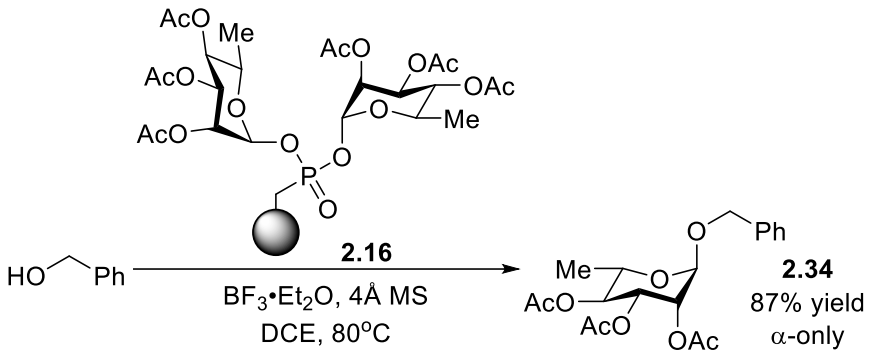
Glycoside product 2.32: Resin **2.16** (145 mg, 0.10 mmol, 2.0 eq), DCE (2.0 mL), and 4Å molecular sieves were added to a plastic vial. The resin was swelled at room temperature for 20 minutes. Glycosyl acceptor estrone (14mg, 0.05mmol, 1.0eq) was added, and the reaction was heated to 80°C. $BF_3{\cdot}Et_2O$ (10 µL, 0.08 mmol, 1.5 eq) was added and the reaction progress was monitored by TLC for 1 hour. Upon full consumption of the acceptor, the reaction mixture was filtered, and the resin was washed with CH_2Cl_2 (3x5 mL), EtOAc (3x5 mL), and CH_2Cl_2 (3x5 mL), and the filtrate was then quenched with Et_3N (50 µL). The filtrate was concentrated, and the crude residue was purified by flash column chromatography (30% EtOAc/hexanes) to afford **2.32** as a white solid (11.3 mg, α-only, 40% yield). Some of the starting material estrone was also recovered (6.7 mg, 77% BRSM). **R_f** = 0.28 (30% EtOAc/hexanes). **HRMS** (ESI-TOF) (m/z): $[M+Na]^+$ calcd for $C_{30}H_{38}O_9Na$ 565.2409, found 565.2397. **^{1}H NMR** (500 MHz, $CDCl_3$) δ 7.21 (d, *J* = 8.6 Hz, 1H), 6.87 (dd, *J* = 8.6, 2.7 Hz, 1H), 6.82 (d, *J* = 2.7 Hz, 1H), 5.51 (dd, *J* = 10.1, 3.5 Hz, 1H), 5.42 (d, *J* = 1.9 Hz, 1H), 5.40 (dd, *J* = 3.5, 1.9 Hz, 1H), 5.14 (t, *J* = 10.0 Hz, 1H), 4.00 (dq, *J* = 9.8, 6.2 Hz, 1H), 2.89 (dd, *J* = 9.1, 4.2 Hz, 2H), 2.50 (dd, *J* = 19.0, 8.7 Hz, 1H), 2.40 (dq, *J* = 12.1, 3.5 Hz, 1H), 2.30 – 2.22 (m, 1H), 2.18 (s, 3H), 2.14 – 2.07 (m, 1H), 2.06 (s, 3H), 2.02 (s, 3H), 2.01 – 1.93 (m, 1H), 1.69 – 1.36 (m, 6H), 1.24 (d, *J* = 10.8 Hz, 2H), 1.20

(d, *J* = 6.3 Hz, 3H), 0.91 (s, 3H). **^{13}C{^{1}H} NMR** (126 MHz, $CDCl_3$): δ 220.9, 170.1, 170.1, 170.0, 154.0, 138.1, 134.2, 126.5, 116.4, 113.8, 95.7, 71.0, 69.8, 68.9, 67.1, 50.4, 48.0, 44.0, 38.2, 35.9, 31.6, 29.6, 26.5, 25.9, 21.6, 20.9, 20.8, 20.8, 17.5, 13.9. **^{13}C NMR** (126 MHz, $CDCl_3$) δ 95.7 (d, *J* = 173.4 Hz). **FTIR** (thin film, cm^{-1}): 1739, 1243, 1217, 1124, 1082, 1055, 1032, 754. **$[\alpha]_D^{20}$** = +149 (c = 1.14, $CHCl_3$). **MP.** 187-190°C.

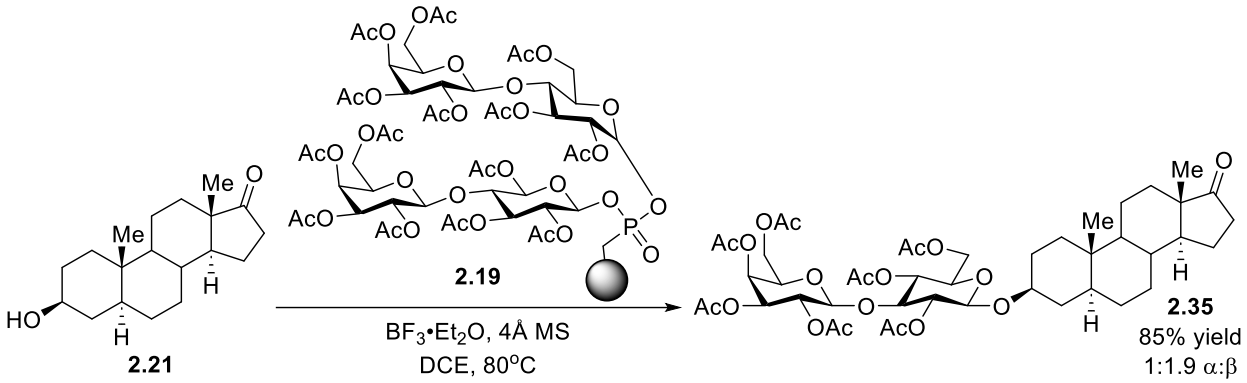


Glycoside product 2.33:[63] Resin **2.16** (148 mg, 0.19 mmol, 2.0 eq), DCE (2.0 mL), and 4Å molecular sieves were added to a plastic vial. The resin was swelled at room temperature for 20 minutes. Glycosyl acceptor cyclohexanol (9.6 mg, 0.10 mmol, 1.0 eq) was added, and the reaction was heated to 80°C. $BF_3{\cdot}Et_2O$ (18 µL, 0.14 mmol, 1.5 eq) was added and the reaction progress was monitored by TLC for 1 hour. Upon full consumption of the acceptor, the reaction mixture was filtered, and the resin was washed with CH_2Cl_2 (3x5 mL), EtOAc (3x5 mL), and CH_2Cl_2 (3x5 mL), and the filtrate was then quenched with Et_3N (50 µL). The filtrate was concentrated, and the crude residue was purified by flash column chromatography (15% EtOAc/hexanes) to afford **2.33** (30.1 mg, α-only, 84% yield) as a clear oil. **^{1}H NMR** (500 MHz, $CDCl_3$) δ 5.31 (dd, *J* = 10.1, 3.5 Hz, 1H), 5.21 – 5.16 (m, 1H), 5.03 (t, *J* = 10.0 Hz, 1H), 4.85 (d, *J* = 1.9 Hz, 1H), 3.94 (dq, *J* = 9.7, 6.3 Hz, 1H), 3.56 (ddt, *J* = 13.2, 9.0, 3.8 Hz, 1H), 2.13 (s, 3H), 2.03 (s, 3H), 1.97 (s, 3H), 1.86 – 1.78 (m, 2H), 1.71 (dd, *J* = 10.8, 5.9 Hz, 2H), 1.50 (dq, *J* = 9.3, 4.1 Hz, 1H), 1.46 – 1.36 (m, 1H), 1.34 – 1.20 (m, 4H), 1.19 (d, *J* = 6.3 Hz, 3H). **^{13}C{^{1}H}** NMR

(126 MHz, $CDCl_3$) δ 170.3, 170.1, 170.0, 95.5, 76.0, 71.4, 70.6, 69.3, 66.3, 33.2, 31.3, 25.5, 24.0, 23.8, 21.0, 20.8, 17.4.

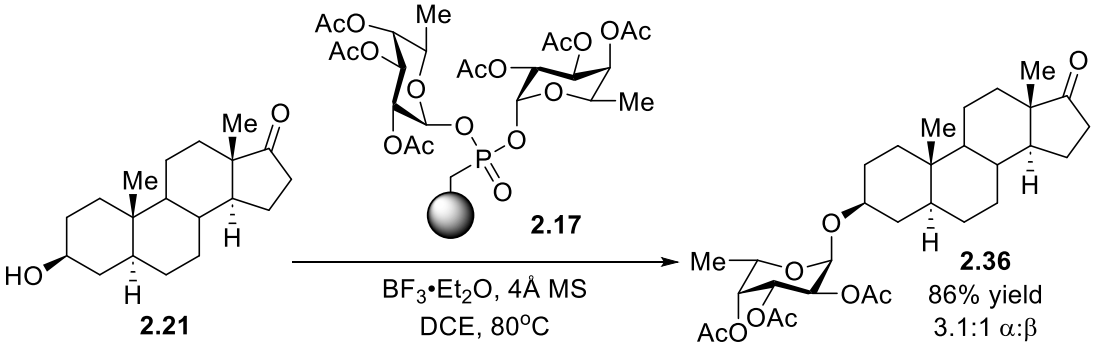


Glycoside product 2.34:[64] Resin **2.16** (148 mg, 0.19 mmol, 2.0 eq), DCE (2.0 mL), and 4Å molecular sieves were added to a plastic vial. The resin was swelled at room temperature for 20 minutes. Glycosyl acceptor benzyl alcohol (10 mg, 0.10 mmol, 1.0 eq) was added, and the reaction was heated to 80°C. $BF_3{\cdot}Et_2O$ (18 µL, 0.14 mmol, 1.5 eq) was added and the reaction progress was monitored by TLC for 1 hour. Upon full consumption of the acceptor, the reaction mixture was filtered, and the resin was washed with CH_2Cl_2 (3x5 mL), EtOAc (3x5 mL), and CH_2Cl_2 (3x5 mL), and the filtrate was then quenched with Et_3N (50 µL). The filtrate was concentrated, and the crude residue was purified by flash column chromatography (15% EtOAc/hexanes) to afford **2.34** (31.9 mg, α-only, 87% yield) as a white solid. **^{1}H NMR** (500 MHz, $CDCl_3$) δ 7.49 – 7.28 (m, 5H), 5.33 (dd, *J* = 10.1, 3.5 Hz, 1H), 5.28 (dd, *J* = 3.6, 1.8 Hz, 1H), 5.07 (t, *J* = 9.9 Hz, 1H), 4.80 (d, *J* = 1.8 Hz, 1H), 4.70 (d, *J* = 12.0 Hz, 1H), 4.54 (d, *J* = 12.0 Hz, 1H), 3.90 (dq, *J* = 9.8, 6.3 Hz, 1H), 2.13 (s, 3H), 2.04 (s, 3H), 1.98 (s, 3H), 1.20 (d, *J* = 6.3 Hz, 3H). **^{13}C{^{1}H} NMR** (126 MHz, $CDCl_3$) δ 170.1, 170.0, 167.0, 136.6, 128.5, 128.1, 128.0, 96.7, 71.2, 69.9, 69.5, 69.2, 66.5, 20.9, 20.8, 17.4.



Glycoside product 2.35: Resin **2.19** (111 mg, 0.10 mmol, 2.0 eq), DCE (2.0 mL), and 4Å molecular sieves were added to a plastic vial. The resin was swelled at room temperature for 20 minutes. Glycosyl acceptor *trans*-androsterone (15 mg, 0.10 mmol, 1.0 eq) was added, and the reaction was heated to 80°C. $BF_3{\cdot}Et_2O$ (10 µL, 0.08 mmol, 1.5 eq) was added and the reaction progress was monitored by TLC for 1 hour. Upon full consumption of the acceptor, the reaction mixture was filtered, and the resin was washed with CH_2Cl_2 (3x5 mL), EtOAc (3x5 mL), and CH_2Cl_2 (3x5 mL), and the filtrate was then quenched with Et_3N (50 µL). The filtrate was concentrated, and the crude residue was purified by flash column chromatography (50% EtOAc/hexanes) to afford **2.35** (40.0 mg, 85% yield, 1:1.9 α:β) as a white solid. $\mathbf{R_f}$ = 0.34 (50% EtOAc/hexanes). **HRMS** (ESI-TOF) (m/z): $[M+Na]^+$ calcd for $C_{45}H_{64}O_{19}Na$ 931.3939, found 931.3931. **^{1}H NMR** (500 MHz, $CDCl_3$) (major diastereomer) δ 5.33 (d, *J* = 3.2 Hz, 1H), 5.17 (t, *J* = 9.3 Hz, 1H), 5.09 (dt, *J* = 10.5, 6.0 Hz, 1H), 4.94 (dt, *J* = 10.4, 3.3 Hz, 1H), 4.83 (dd, *J* = 9.6, 8.0 Hz, 1H), 4.54 (d, *J* = 8.0 Hz, 1H), 4.46 (d, *J* = 8.2 Hz, 1H), 4.43 – 4.34 (m, 1H), 4.18 – 4.05 (m, 3H), 3.86 (t, *J* = 6.9 Hz, 1H), 3.76 (t, *J* = 9.5 Hz, 1H), 3.57 (ddd, *J* = 9.9, 5.3, 2.1 Hz, 1H), 3.54 – 3.41 (m, 1H), 2.42 (dd, *J* = 19.3, 8.8 Hz, 1H), 2.14 (s, 3H), 2.09 (s, 3H), 2.07 (d, *J* = 3.6 Hz, 1H), 2.04 (s, 6H), 2.03 (s, 6H), 1.95 (s, 3H), 1.93 – 1.88 (m, 1H), 1.84 – 1.74 (m, 2H), 1.74 – 1.66 (m, 2H), 1.65 – 1.36 (m, 4H), 1.33 – 1.17 (m, 7H), 1.06 (ddt, *J* = 12.3, 9.0, 3.3 Hz, 2H), 0.93 (m, 2H), 0.84 (s, 3H), 0.79 (s, 3H), 0.66 (td, *J* = 11.2, 3.9 Hz, 1H). (minor diastereomer). δ

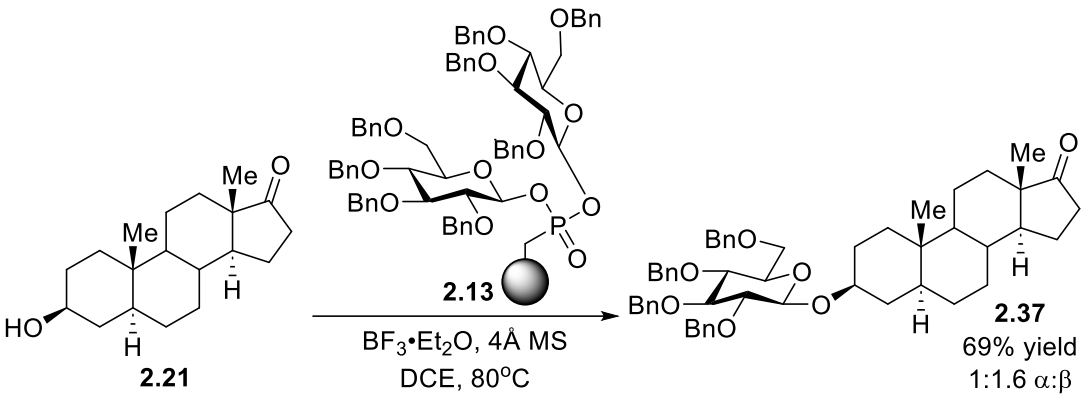
5.44 (t, *J* = 9.7 Hz, 1H), 5.33 (d, *J* = 3.2 Hz, 1H), 5.09 (d, *J* = 10.5, 2.9 Hz, 2H), 4.93 (t, *J* = 3.3 Hz, 1H), 4.69 (dd, *J* = 10.2, 3.8 Hz, 1H), 4.46 (d, *J* = 8.2 Hz, 1H), 4.45 – 4.40 (m, 2H), 4.09 – 3.99 (m, 3H), 3.86 (t, *J* = 6.9 Hz, 1H), 3.70 (t, *J* = 9.6 Hz, 1H), 3.48 – 3.41 (m, 1H), 2.42 (dd, *J* = 19.3, 8.8 Hz, 1H), 2.14 (s, 3H), 2.10 (s, 3H), 2.07 (d, *J* = 3.6 Hz, 1H), 2.04 (s, 6H), 2.02 (s, 6H), 1.95 (s, 3H), 1.93 – 1.88 (m, 1H), 1.84 – 1.74 (m, 2H), 1.74 – 1.66 (m, 2H), 1.65 – 1.36 (m, 4H), 1.33 – 1.17 (m, 7H), 1.06 (ddt, *J* = 12.3, 9.0, 3.3 Hz, 1H), 0.93 (m, 2H), 0.84 (s, 3H), 0.79 (s, 3H), 0.66 (td, *J* = 11.2, 3.9 Hz, 1H). **$^{13}C\{^{1}H\}$ NMR**: (126 MHz, $CDCl_3$) (major diastereomer) δ 221.3, 170.4, 170.4, 170.2, 170.1, 169.9, 169.6, 169.1, 101.1, 99.4, 79.7, 76.4, 72.9, 72.5, 71.9, 71.0, 70.7, 70.0, 69.1, 66.6, 60.8, 60.8, 54.4, 51.4, 47.8, 44.7, 36.9, 35.8, 35.7, 35.0, 34.6, 31.5, 30.9, 29.2, 28.5, 21.8, 20.9, 20.8, 20.8, 20.7, 20.6, 20.5, 20.5, 13.8, 12.2. (minor diastereomer) δ 221.4, 170.5, 170.4, 170.4, 170.2, 170.1, 169.6, 169.2, 101.2, 94.4, 78.4, 71.3, 71.1, 70.6, 70.0, 69.2, 68.1, 62.1, 60.8, 54.4, 51.4, 47.8, 45.0, 36.7, 35.8, 35.7, 34.6, 31.5, 30.9, 29.7, 27.7, 21.8, 21.0, 20.8, 20.7, 20.7, 20.5, 20.5, 13.8, 12.3. **FTIR** (thin film, cm^{-1}): 2931, 2855, 1740, 1434, 1367, 1215, 1173, 1044, 954, 901. **$[\alpha]_D^{20}$** = +33.1 (c = 0.3175 $CHCl_3$). **MP.** 126-128°C.



Glycoside product e **2.36:** Resin **2.17** (100 mg, 0.10 mmol, 2.0 eq), DCE (2.0 mL), and 4Å molecular sieves were added to a plastic vial. The resin was swelled at room temperature for 20 minutes. Glycosyl acceptor *trans*-androsterone (15 mg, 0.10 mmol, 1.0 eq) was added, and the reaction was heated to 80°C. $BF_3{\cdot}Et_2O$ (18 µL, 0.14 mmol, 1.5 eq) was added and the reaction

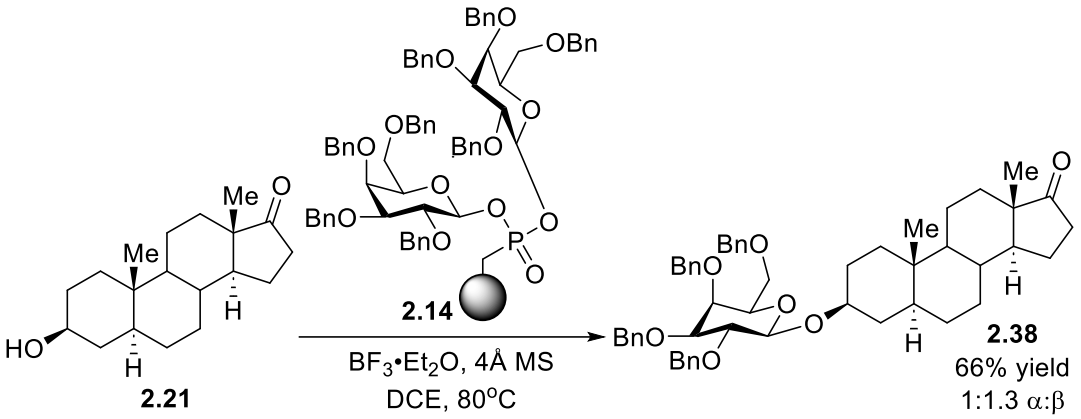
progress was monitored by TLC for 3 hours. Upon full consumption of the acceptor, the reaction mixture was filtered, and the resin was washed with CH_2Cl_2 (3x5 mL), EtOAc (3x5 mL), and CH_2Cl_2 (3x5 mL), and the filtrate was then quenched with Et_3N (50 µL). The filtrate was concentrated, and the crude residue was purified by flash column chromatography (15% EtOAc/hexanes) to afford **2.36** (24.9 mg, 3.1:1 α:β, 86% yield) as a white solid. **Major (α) diastereomer**: $\mathbf{R_f}$ = 0.34 (30% EtOAc/hexanes). **HRMS** (ESI-TOF) (m/z): $[M+Na]^+$ calcd for $C_{31}H_{46}O_9Na$ 585.3035, found 585.3030. **^{1}H NMR** (500 MHz, $CDCl_3$) δ 5.36 – 5.33 (m, 1H), 5.31 – 5.25 (m, 1H), 5.20 (d, *J* = 3.8 Hz, 1H), 5.04 (dd, *J* = 10.9, 3.8 Hz, 1H), 4.23 (q, *J* = 6.5 Hz, 1H), 3.48 (tt, *J* = 10.8, 4.8 Hz, 1H), 2.43 (dd, *J* = 19.3, 8.8 Hz, 1H), 2.16 (s, 3H), 2.07 (s, 3H), 2.05 – 2.00 (m, 1H), 1.98 (s, 3H), 1.92 (ddd, *J* = 12.1, 8.7, 5.9 Hz, 1H), 1.80 – 1.71 (m, 3H), 1.65 – 1.45 (m, 6H), 1.29 (dt, *J* = 12.9, 6.7 Hz, 6H), 1.23 (d, *J* = 2.3 Hz, 1H), 1.12 (d, *J* = 6.6 Hz, 3H), 1.10 – 0.92 (m, 2H), 0.85 (s, 3H), 0.83 (s, 3H), 0.68 (td, *J* = 12.1, 11.6, 4.1 Hz, 1H). **^{13}C{^{1}H} NMR** (126 MHz, $CDCl_3$) δ 221.3, 170.7, 170.5, 170.1, 94.6, 77.5, 71.3, 68.5, 68.1, 64.3, 54.4, 51.4, 47.8, 44.7, 37.0, 35.9, 35.0, 34.2, 31.6, 30.9, 29.7, 29.2, 28.5, 21.8, 20.9, 20.8, 20.7, 20.5, 15.9, 13.8, 12.3. **FTIR** (thin film, cm^{-1}): 2917, 2849, 1739, 1537, 1455, 1371, 1257, 1221, 1164, 1017, 978, 947, 800. **$[\alpha]_D^{20}$** = -29.4 (c=1.36, $CHCl_3$). **MP.** 138-139°C. **Minor (β) diastereomer**: $\mathbf{R_f}$ = 0.25 (30% EtOAc/hexanes). **HRMS** (ESI-TOF) (m/z): $[M+Na]^+$ calcd for $C_{31}H_{46}O_9Na$ 585.3035, found 585.3024. **^{1}H NMR** (500 MHz, $CDCl_3$) δ 5.22 (d, *J* = 3.5 Hz, 1H), 5.15 (dd, *J* = 10.4, 7.9 Hz, 1H), 5.01 (dd, *J* = 10.4, 3.5 Hz, 1H), 4.51 (d, *J* = 7.9 Hz, 1H), 3.78 (q, *J* = 6.4 Hz, 1H), 3.55 (tt, *J* = 10.9, 4.8 Hz, 1H), 2.43 (dd, *J* = 19.3, 8.8 Hz, 1H), 2.16 (s, 3H), 2.08 (t, *J* = 9.4 Hz, 1H), 2.04 (s, 3H), 1.98 (s, 3H), 1.92 (td, *J* = 10.8, 8.9, 6.1 Hz, 1H), 1.78 (ddd, *J* = 12.7, 5.7, 3.0 Hz, 2H), 1.76 – 1.60 (m, 2H),1.59 – 1.27 (m, 8H), 1.22 (d, *J* = 6.5 Hz, 3H), 1.10 (tt, *J* = 12.3, 3.6 Hz, 2H), 0.95 (dd, *J* = 12.7, 4.5 Hz, 2H), 0.89 (d, *J* = 6.5 Hz, 2H), 0.85 (s, 3H),

0.81 (s, 3H), 0.67 (td, *J* = 11.7, 11.3, 3.9 Hz, 1H). **$^{13}C\{^{1}H\}$ NMR** (126 MHz, $CDCl_3$) δ 221.4, 170.8, 170.3, 169.5, 100.1, 79.5, 71.4, 70.3, 69.3, 69.1, 54.5, 51.4, 47.8, 45.0, 36.8, 35.9, 35.7, 35.1, 31.6, 30.9, 29.7, 28.4, 28.1, 21.8, 20.9, 20.8, 20.7, 20.5, 16.3, 13.8, 12.3. **FTIR** (thin film, cm^{-1}): 1740, 1735, 1227, 1073, 1050, 1017. **$[\alpha]_D^{20}$** = +11.3 (c = 0.511, $CHCl_3$). **MP.** 182-186°C.



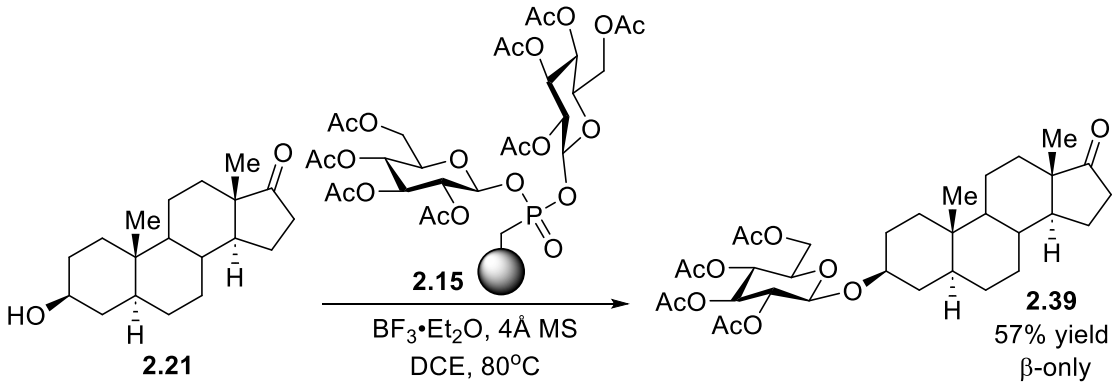
Glycoside product 2.37: Resin **2.13** (131 mg, 0.10 mmol, 2.0 eq), DCE (2.0 mL), and 4Å molecular sieves were added to a plastic vial. The resin was swelled at room temperature for 20 minutes. Glycosyl acceptor *trans*-androsterone (15 mg, 0.10 mmol, 1.0 eq) was added, and the reaction was heated to 80°C. $BF_3{\cdot}Et_2O$ (18 µL, 0.14 mmol, 1.5 eq) was added and the reaction progress was monitored by TLC for 1 hour. Upon full consumption of the acceptor, the reaction mixture was filtered, and the resin was washed with CH_2Cl_2 (3x5 mL), EtOAc (3x5 mL), and CH_2Cl_2 (3x5 mL), and the filtrate was then quenched with Et_3N (50 µL). The filtrate was concentrated, and the crude residue was purified by flash column chromatography (15% EtOAc/hexanes) to afford **2.37** (28.9 mg, 1:1.6 α:β, 69% yield) as a white solid. **Major (β) diastereomer**: **R_f =** 0.40 (20% EtOAc/hexanes). **HRMS** (ESI-TOF) (m/z): $[M+Na]^+$ calcd for $C_{53}H_{64}O_7Na$ 835.4545, found 835.4533. **^{1}H NMR**: (500 MHz, $CDCl_3$) δ 7.38 – 7.22 (m, 18H), 7.19 – 7.15 (m, 2H), 4.96 (d, *J* = 11.0 Hz, 1H), 4.91 (d, *J* = 10.9 Hz, 1H), 4.81 (d, *J* = 10.8 Hz, 1H), 4.78 (d, *J* = 10.9 Hz, 1H), 4.72 (d, *J* = 11.0 Hz, 1H), 4.60 (d, *J* = 12.2 Hz, 1H), 4.57 – 4.52 (m, 2H), 4.51 (d, *J* = 7.9 Hz, 1H), 3.74 (dd, *J* = 10.7, 1.9 Hz, 1H), 3.71 – 3.59 (m, 3H), 3.53 (t, *J*

= 9.3 Hz, 1H), 3.48 – 3.40 (m, 2H), 2.44 (dd, *J* = 19.2, 8.8 Hz, 1H), 2.16 – 1.87 (m, 3H), 1.83 – 1.57 (m, 8H), 1.55 – 1.43 (m, 1H), 1.43 – 1.18 (m, 6H), 1.14 – 1.05 (m, 1H), 1.03 – 0.91 (m, 2H), 0.86 (s, 3H), 0.85 (s, 3H), 0.68 (ddd, *J* = 12.1, 10.5, 4.0 Hz, 1H). **^{13}C{^{1}H} NMR** (126 MHz, $CDCl_3$) δ 221.4, 138.7, 138.6, 138.3, 138.1, 128.4, 128.4, 128.4, 128.3, 128.2, 128.0, 127.9, 127.8, 127.7, 127.7, 127.6, 127.6, 102.0, 84.9, 82.4, 78.9, 78.0, 75.7, 75.0, 74.9, 74.8, 73.4, 69.2, 54.5, 51.4, 47.8, 44.8, 37.0, 35.9, 35.8, 35.1, 34.7, 31.6, 30.9, 29.7, 28.5, 21.8, 20.5, 13.8, 12.3. **FTIR** (thin film, cm^{-1}): 3029, 2920, 2851, 1737, 1496, 1453, 1358, 1259, 1206, 1068, 1027, 733, 696. **$[\alpha]_D^{20}$** = +18.0 (c = 0.0575 $CHCl_3$). **Minor (α) diastereomer**: **R_f** = 0.44 (20% EtOAc/hexanes). **HRMS** (ESI-TOF) (m/z): $[M+Na]^+$ calcd for $C_{53}H_{64}O_7Na$ 835.4545, found 835.4541. **^{1}H NMR** (600 MHz, $CDCl_3$) δ 7.40 – 7.22 (m, 18H), 7.16 – 7.09 (m, 2H), 5.00 (d, *J* = 10.8 Hz, 1H), 4.92 (d, *J* = 3.7 Hz, 1H), 4.82 (dd, *J* = 14.9, 10.7 Hz, 2H), 4.77 (s, 1H), 4.65 (d, *J* = 11.9 Hz, 1H), 4.60 (d, *J* = 12.1 Hz, 1H), 4.47 (m, 2H), 3.99 (t, *J* = 9.3 Hz, 1H), 3.87 (d, *J* = 10.1 Hz, 1H), 3.72 (dd, *J* = 10.5, 3.9 Hz, 1H), 3.68 – 3.59 (m, 2H), 3.53 (ddd, *J* = 15.0, 10.5, 5.0 Hz, 2H), 2.44 (dd, *J* = 19.2, 8.8 Hz, 1H), 2.15 – 2.00 (m, 1H), 1.96 – 1.88 (m, 2H), 1.78 (m, 4H), 1.65 (d, *J* = 11.9 Hz, 1H), 1.54 – 1.42 (m, 3H), 1.33 – 1.19 (m, 7H), 1.08 (s, 1H), 0.95 – 0.87 (m, 1H), 0.86 (s, 3H), 0.83 (s, 3H), 0.70 – 0.64 (m, 1H). **^{13}C{^{1}H} NMR** (126 MHz, $CDCl_3$) δ 221.4, 139.0, 138.3, 138.0, 129.7, 128.5, 128.5, 128.4, 128.4, 128.4, 128.3, 128.3, 128.2, 128.2, 128.1, 128.0, 127.9, 127.9, 127.8, 127.7, 127.7, 127.6, 94.8, 82.1, 80.0, 77.9, 76.0, 75.7, 75.1, 73.4, 73.1, 73.1, 70.1, 68.7, 54.4, 51.5, 47.8, 45.1, 36.9, 35.9, 35.8, 35.1, 31.6, 30.9, 28.4, 27.3, 21.8, 20.5, 13.8, 12.4. **FTIR** (thin film, cm^{-1}): 3062, 3030, 2917, 2849, 1736, 1497, 1453, 1358, 1273, 1207, 1147, 1069, 1027, 734, 712, 696, 629. **$[\alpha]_D^{20}$** = +84.1 (c = 0.100 $CHCl_3$).



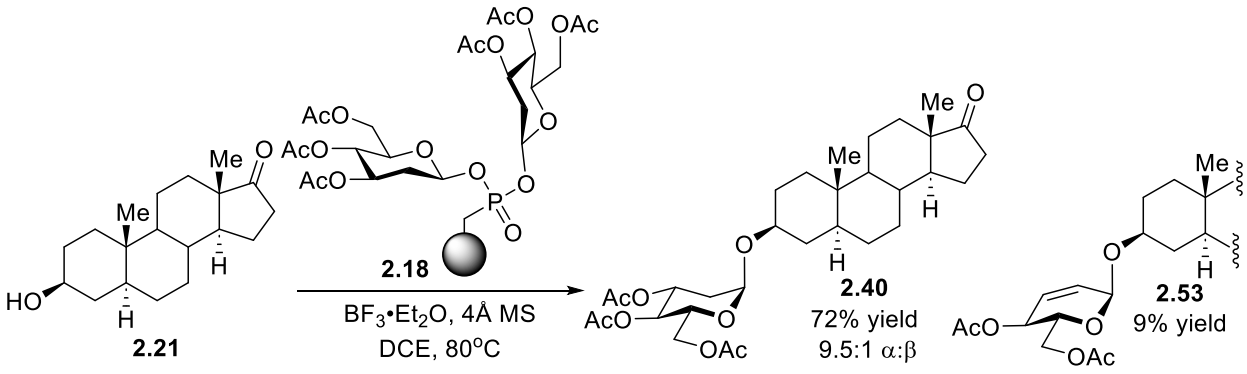
Glycoside product 2.38: Resin **2.14** (146 mg, 0.10 mmol, 2.0 eq), DCE (2.0 mL), and 4Å molecular sieves were added to a plastic vial. The resin was swelled at room temperature for 20 minutes. Glycosyl acceptor *trans*-androsterone (15 mg, 0.10 mmol, 1.0 eq) was added, and the reaction was heated to 80°C. $BF_3{\cdot}Et_2O$ (18 µL, 0.14 mmol, 1.5 eq) was added and the reaction progress was monitored by TLC for 1 hour. Upon full consumption of the acceptor, the reaction mixture was filtered, and the resin was washed with CH_2Cl_2 (3x5 mL), EtOAc (3x5 mL), and CH_2Cl_2 (3x5 mL), and the filtrate was then quenched with Et_3N (50 µL). The filtrate was concentrated, and the crude residue was purified by flash column chromatography (5% acetone/toluene) to afford **2.38** (27.8 mg, 1:1.3 α:β, 66% yield) as a white solid. $\mathbf{R_f}$ = 0.70 (30% EtOAc/hexanes) and characterized as a mixture of diastereomers. **HRMS** (ESI-TOF) (m/z): $[M+Na]^+$ calcd for $C_{53}H_{64}O_7Na$ 835.4545, found 835.4537. **^{1}H NMR**: (700 MHz, $CDCl_3$) δ7.46 – 7.22 (m, 40H), 4.99 (d, *J* = 3.8 Hz, 1H), 4.97 – 4.91 (m, 3H), 4.86 (d, *J* = 11.6 Hz, 1H), 4.81 – 4.66 m, 6H), 4.62 (d, *J* = 11.7 Hz, 1H), 4.57 (d, *J* = 11.5 Hz, 1H), 4.48 (d, J = 11.7 Hz, 1H), 4.46 (d, *J* = 7.7 Hz, 1H), 4.44 – 4.38 (m, 3H), 4.04 (t, *J* = 6.4 Hz, 1H), 4.02 (dd, *J* = 9.9, 3.8 Hz, 1H), 3.97 – 3.92 (m, 2H), 3.87 (dd, *J* = 3.0, 1.0 Hz, 1H), 3.79 (dd, *J* = 9.7, 7.7 Hz, 1H), 3.63 (tt, *J* = 11.2, 4.8 Hz, 1H), 3.57 (dd, *J* = 6.3, 1.7 Hz, 2H), 3.56 – 3.48 (m, 5H), 2.47 – 2.39 (m, 2H), 2.06 (dtd, *J* = 19.2, 9.1, 5.1 Hz, 2H), 1.97 – 1.88 (m, 3H), 1.86 – 1.82 (m, 1H), 1.82 – 1.61 (m, 10H),

1.61 – 1.42 (m, 7H), 1.39 – 1.17 (m, 12H), 1.14 – 1.02 (m, 2H), 0.99 – 0.87 (m, 6H), 0.86 (s, 6H), 0.83 (d, *J* = 1.6 Hz, 6H), 0.66 (tt, *J* = 12.2, 4.3 Hz, 2H). **$^{13}C\{^{1}H\}$ NMR** (176 MHz, CDCl3) δ 221.3, 139.0, 138.9, 138.73, 138.70, 138.69, 138.61, 138.1, 138.0, 128.40, 128.38, 128.33, 128.31, 128.28, 128.22, 128.21, 128.19, 128.12, 128.0, 127.8, 127.7, 127.62, 127.59, 127.57, 127.51, 127.49, 127.42, 127.40, 102.2, 95.6, 82.4, 79.7, 79.2, 78.6, 76.6, 76.1, 75.3, 75.2, 74.7, 74.4, 73.54, 73.51, 73.41, 73.37, 73.2, 73.14, 73..09, 69.34, 69.33, 69.1, 54.5, 54.4, 51.4, 47.8, 45.1, 44.8, 37.0, 36.9, 35.85, 35.80, 35.7, 35.0, 34.6, 31.6, 30.90, 30.89, 29.7, 29.5, 28.5, 28.4, 27.4, 21.8, 20.5, 13.8, 12.34, 12.27. **FTIR** (thin film, cm^{-1}): 2919, 2851, 1737, 1496, 1453, 1360, 1258, 1206, 1098, 1060, 1027, 733, 696. **$[\alpha]_D^{20}$** = +35.3 (c = 0.1175 $CHCl_3$).



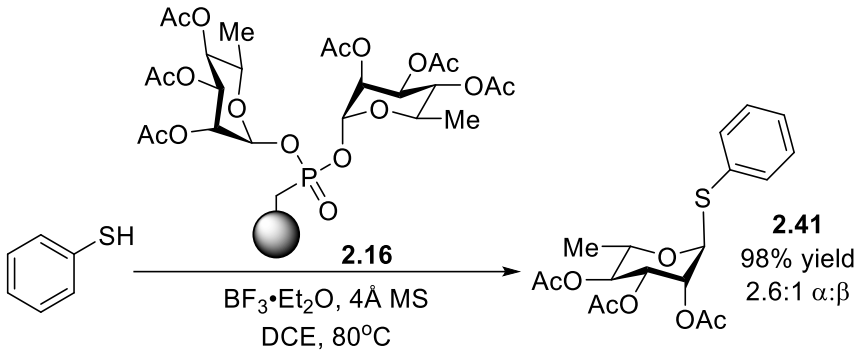
Glycoside product 2.39: Resin **2.15** (78 mg, 0.10 mmol, 2.0 eq), DCE (2.0 mL), and 4Å molecular sieves were added to a plastic vial. The resin was swelled at room temperature for 20 minutes. Glycosyl acceptor *trans*-androsterone (15 mg, 0.10 mmol, 1.0 eq) was added, and the reaction was heated to 80°C. $BF_3{\cdot}Et_2O$ (18 µL, 0.14 mmol, 1.5 eq) was added and the reaction progress was monitored by TLC for 1 hour. Upon full consumption of the acceptor, the reaction mixture was filtered, and the resin was washed with CH_2Cl_2 (3x5 mL), EtOAc (3x5 mL), and CH_2Cl_2 (3x5 mL), and the filtrate was then quenched with Et_3N (50 µL). The filtrate was concentrated, and the crude residue was purified by flash column chromatography (15% EtOAc/hexanes) to afford **2.39** (18.2 mg, β-only, 57% yield) as an off-white solid. **R_f** = 0.17

(30% EtOAc/hexanes). **HRMS** (ESI-TOF) (m/z): $[M+Na]^+$ calcd for $C_{33}H_{48}O_{11}Na$ 643.3089, found 643.3107. **^{1}H NMR**: (500 MHz, $CDCl_3$) δ 5.19 (t, *J* = 9.5 Hz, 1H), 5.07 (t, *J* = 9.7 Hz, 1H), 4.94 (dd, *J* = 9.7, 8.0 Hz, 1H), 4.59 (d, *J* = 8.0 Hz, 1H), 4.25 (dd, *J* = 12.2, 5.0 Hz, 1H), 4.11 (dd, *J* = 12.2, 2.5 Hz, 1H), 3.68 (ddd, *J* = 10.0, 4.9, 2.5 Hz, 1H), 3.55 (tt, *J* = 10.8, 4.8 Hz, 1H), 2.43 (dd, *J* = 19.2, 8.8 Hz, 1H), 2.10 – 2.08 (m, 1H), 2.07 (s, 3H), 2.04 (s, 3H), 2.02 (s, 3H), 2.00 (s, 3H), 1.96 – 1.84 (m, 1H), 1.79 (ddd, *J* = 12.3, 5.5, 3.2 Hz, 2H), 1.72 (dt, *J* = 13.3, 3.7 Hz, 1H), 1.68 – 1.43 (m, 4H), 1.34 – 1.17 (m, 7H), 1.14 – 1.04 (m, 1H), 1.02 – 0.91 (m, 2H), 0.85 (s, 3H), 0.81 (s, 3H), 0.71 – 0.62 (m, 1H). **^{13}C{^{1}H} NMR** (126 MHz, $CDCl_3$) δ 221.3, 170.7, 170.4, 169.4, 169.3, 99.6, 79.7, 72.9, 71.7, 71.6, 68.6, 62.2, 54.5, 51.4, 47.8, 44.8, 36.9, 35.9, 35.8, 35.0, 34.6, 31.6, 30.9, 29.2, 28.5, 21.8, 20.8, 20.8, 20.7, 20.6, 20.5, 13.8, 12.3. **FTIR** (thin film, cm^{-1}): 2922, 1734, 1734, 1369, 1240, 1229, 1169, 1091, 1038, 1020. **$[\alpha]_D^{20}$** = +11.3 (c = 0.511, $CHCl_3$). **MP.** 172-174°C.

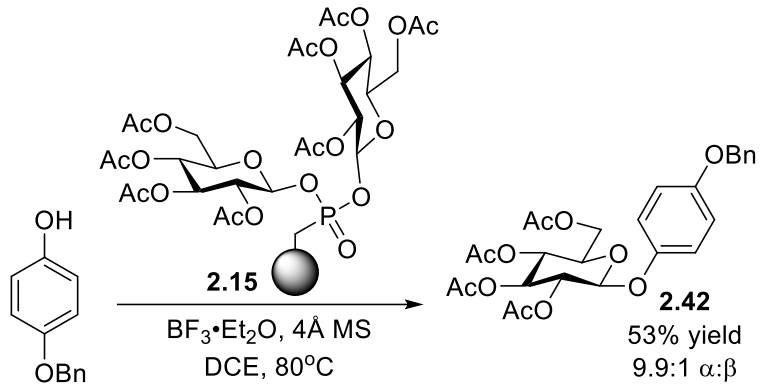


Glycoside product 2.40: Resin **2.18** (90 mg, 0.10 mmol, 2.0 eq), DCE (2.0 mL), and 4Å molecular sieves were added to a plastic vial. The resin was swelled at room temperature for 20 minutes. Glycosyl acceptor *trans*-androsterone **2.21** (15 mg, 0.05 mmol, 1.0 eq) was added, and the reaction was heated to 80°C. $BF_3{\cdot}Et_2O$ (10 µL, 0.08 mmol, 1.5 eq) was added and the reaction progress was monitored by TLC for 1 hour. Upon full consumption of the acceptor, the reaction mixture was filtered, and the resin was washed with CH_2Cl_2 (3x5 mL), EtOAc (3x5

mL), and CH_2Cl_2 (3x5 mL), and the filtrate was then quenched with Et_3N (50 µL). The filtrate was concentrated, and the crude residue was purified by flash column chromatography (10% EtOAc/hexanes) to afford **2.40 (**20.8 mg, 72% yield, 9.5:1 α:β) as a white solid. Byproduct **2.53** resulting from Ferrier glycosylation (2.5mg, 9% yield) was also isolated as a white solid. $\mathbf{R_f}$ = 0.66 (50% EtOAc/hexanes). **HRMS** (ESI-TOF) (m/z): $[M+Na]^+$ calcd for $C_{31}H_{46}O_9Na$ 585.3035, found 585.3006. **^{1}H NMR** (500 MHz, $CDCl_3$) δ 5.32 (ddd, *J* = 11.6, 9.4, 5.3 Hz, 1H), 5.09 (d, *J* = 3.6 Hz, 1H), 4.96 (t, *J* = 9.6 Hz, 1H), 4.31 – 4.21 (m, 1H), 4.10 – 3.99 (m, 2H), 3.49 (tt, *J* = 11.2, 4.8 Hz, 1H), 2.46 – 2.34 (m, 1H), 2.16 (ddd, J = 12.8, 5.4, 1.3 Hz, 1H), 2.07 (s, 3H), 2.06 – 2.04 (m, 1H), 2.02 (s, 3H), 1.99 (s, 3H), 1.95 – 1.87 (m, 1H), 1.85 – 1.75 (m, 4H), 1.72 (dt, *J* = 13.4, 3.9 Hz, 2H), 1.67 – 1.45 (m, 3H), 1.45 – 1.35 (m, 2H), 1.35 – 1.16 (m, 5H), 1.09 (ddt, *J* = 12.4, 9.5, 2.5 Hz, 1H), 1.00 – 0.90 (m, 2H), 0.84 (s, 3H), 0.82 (s, 3H), 0.71 – 0.62 (m, 1H). **(minor diastereomer)** 4.68 (dd, *J* = 9.8, 2.0 Hz, 1H). **^{13}C{^{1}H}** NMR (126 MHz, $CDCl_3$) **(major diastereomer)** δ 221.3, 170.8, 170.3, 170.0, 95.2, 76.7, 69.6, 69.2, 67.8, 62.5, 54.4, 51.4, 47.8, 45.0, 36.8, 35.8, 35.8, 35.6, 35.0, 31.5, 30.9, 28.5, 27.6, 21.8, 21.0, 20.8, 20.8, 20.5, 13.8, 12.3. **(minor diastereomer)** δ 221.3, 170.8, 170.4, 169.8, 97.6, 78.1, 71.9, 71.1, 70.8, 62.6, 54.5, 51.4, 44.9, 44.8, 38.1, 37.0, 35.0, 34.4, 33.9, 31.5, 29.7, 29.2, 28.4, 22.7, 20.9, 20.8, 20.7, 20.5, 14.1, 12.3. **FTIR** (thin film, cm^{-1}): 2933, 2850, 1736, 1451, 1366, 1223, 1128, 1091, 1030, 934. **$[\alpha]_D^{20}$** = +102.8 (c = 1.34 $CHCl_3$). **(Ferrier, 2.53) ^{1}H NMR** (500 MHz, $CDCl_3$) 5.87 (dt, *J* = 10.2, 1.3 Hz, 1H), 5.81 (ddd. *J* = 10.2, 2.7, 1.9 Hz, 1H), 5.35 - 5.25 (m, 1H), 5.16 (d, *J* = 2.7Hz, 1H), 4.30 – 4.13 (m, 3H), 3.70 – 3.55 (m, 1H), 2.49 – 2.38 (m, 1H), 2.09 (s, 3H), 2.07 (s, 3H), 1.98 – 1.63 (m, 10H), 1.56 – 1.38 (m, 4H), 1.36 – 1.19 (m, 4H), 1.17 – 1.00 (m, 4H), 0.97 (s, 3H), 0.95 (s, 3H), 0.72 – 0.54 (m, 1H).



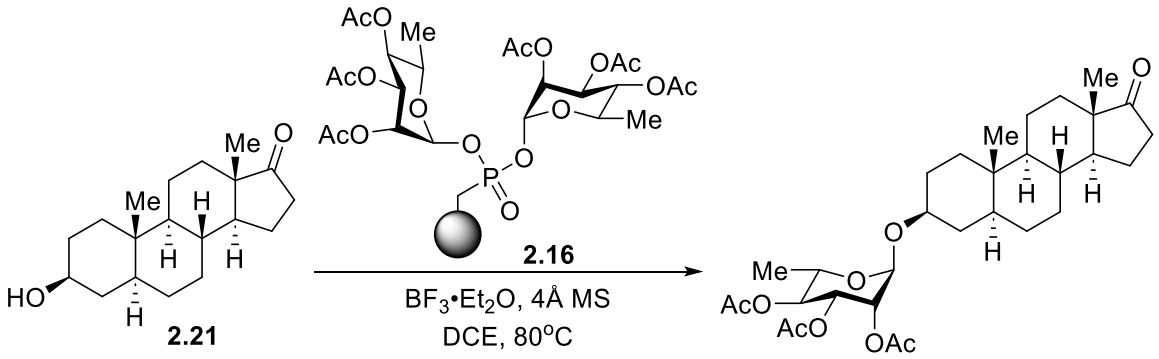
Glycoside product 2.41: Resin **2.16** (151 mg, 0.20 mmol, 2.0 eq), DCE (2.0 mL), and 4Å molecular sieves were added to a plastic vial. The resin was swelled at room temperature for 20 minutes. Glycosyl acceptor thiophenol (11 mg, 0.10 mmol, 1.0 eq) was added, and the reaction was heated to 80°C. $BF_3{\cdot}Et_2O$ (18 µL, 0.14 mmol, 1.5 eq) was added and the reaction progress was monitored by TLC for 1 hour. Upon full consumption of the acceptor, the reaction mixture was filtered, and the resin was washed with CH_2Cl_2 (3x5 mL), EtOAc (3x5 mL), and CH_2Cl_2 (3x5 mL), and the filtrate was then quenched with Et_3N (50 µL). The filtrate was concentrated, and the crude residue was purified by flash column chromatography (15% EtOAc/hexanes) to afford **2.41** (36.7 mg, 2.6:1 α:β, 98% yield) as a white solid. **(major diastereomer) ^{1}H NMR** (500 MHz, $CDCl_3$) δ 7.50 – 7.47 (m, 2H), 7.36 – 7.30 (m, 3H), 5.51 (dd, *J* = 3.4, 1.7 Hz, 1H), 5.43 (d, *J* = 1.7 Hz, 1H), 5.30 (dd, *J* = 10.0, 3.3 Hz, 1H), 5.16 (t, *J* = 9.9 Hz, 1H), 4.38 (dq, *J* = 9.7, 6.2 Hz, 1H), 2.16 (s, 3H), 2.09 (s, 3H), 2.03 (s, 3H), 1.26 (d, *J* = 6.4 Hz, 3H). **^{13}C{^{1}H} NMR** (126 MHz, $CDCl_3$) δ 170.0, 170.0, 169.9, 132.1, 131.8, 129.2, 129.1, 127.9, 85.7, 71.3, 71.1, 69.4, 67.8, 20.9, 20.8, 20.7, 17.3. **(minor diastereomer) ^{1}H NMR** (500 MHz, $CDCl_3$) δ 7.54 – 7.50 (m, 2H), 7.29 (t, *J* = 3.7 Hz, 3H), 5.67 (dd, *J* = 3.6, 1.2 Hz, 1H), 5.15 – 5.09 (m, 1H), 5.02 (dd, *J* = 10.2, 3.5 Hz, 1H), 4.92 (d, *J* = 1.2 Hz, 1H), 3.57 (dq, *J* = 9.5, 6.2 Hz, 1H), 2.22 (s, 3H), 2.06 (s, 3H), 2.00 (s, 3H), 1.33 (d, *J* = 6.2 Hz, 3H). **^{13}C{^{1}H} NMR** (126 MHz, $CDCl_3$) 170.3, 170.2, 169.8, 133.4, 133.3, 128.1, 127.9, 85.4, 75.0, 71.9. 71.1, 70.2, 20.8, 20.7, 20.6, 17.8.



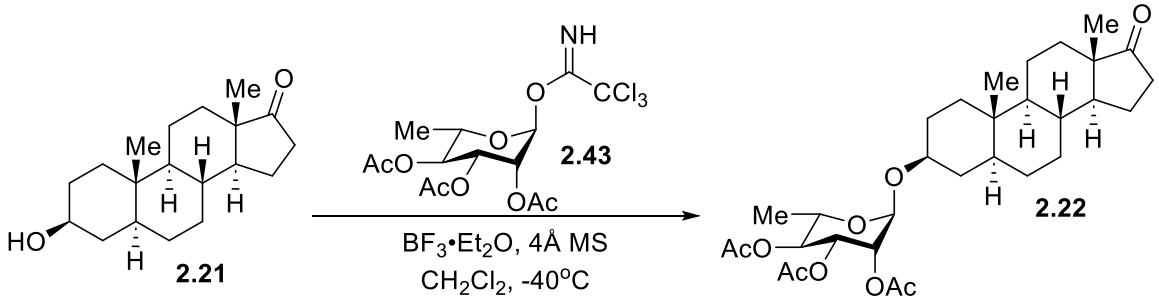
Glycoside product 2.42: Resin **2.15** (76 mg, 0.10 mmol, 2.0 eq), DCE (2.0vmL), and 4Å molecular sieves were added to a plastic vial. The resin was swelled at room temperature for 20 minutes. Glycosyl acceptor 4-benzyloxy-phenol (10 mg, 0.05 mmol, 1.0 eq) was added, and the reaction was heated to 80°C. $BF_3{\cdot}Et_2O$ (18 µL, 0.08 mmol, 1.5 eq) was added and the reaction progress was monitored by TLC for 1 hour. Upon full consumption of the acceptor, the reaction mixture was filtered, and the resin was washed with CH_2Cl_2 (3x5 mL), EtOAc (3x5 mL), and CH_2Cl_2 (3x5 mL), and the filtrate was then quenched with Et_3N (50 µL). The filtrate was concentrated, and the crude residue was purified by flash column chromatography (15% EtOAc/hexanes) to afford **2.42** (14.0 mg, 1:9.9 α:β, 53% yield) as a clear oil. **Major (β) diastereomer**: $\mathbf{R_f}$ = 0.19 (30% EtOAc/hexanes). **HRMS** (ESI-TOF) (m/z): $[M+Na]^+$ calcd for $C_{27}H_{30}O_{11}Na$ 553.1681, found 553.1730. **^{1}H NMR**: (500 MHz, $CDCl_3$) δ 7.45 – 7.35 (m, 4H), 7.35 – 7.30 (m, 1H), 6.97 – 6.84 (m, 4H), 5.34 – 5.20 (m, 2H), 5.16 (t, *J* = 9.3 Hz, 1H), 5.03 (s, 2H), 4.95 (d, *J* = 7.4 Hz, 1H), 4.28 (dd, *J* = 12.3, 5.2 Hz, 1H), 4.16 (dd, *J* = 12.2, 2.5 Hz, 1H), 3.80 (ddd, *J* = 10.0, 5.2, 2.4 Hz, 1H), 2.07 (s, 6H), 2.04 (s, 3H), 2.03 (s, 3H). **^{13}C{^{1}H} NMR**: (126 MHz, $CDCl_3$) δ 170.6, 170.3, 169.4, 169.3, 155.0, 151.1, 137.0, 128.6, 128.0, 127.5, 118.7, 115.7, 100.2, 72.8, 72.0, 71.2, 70.5, 68.3, 62.0, 29.7, 20.7, 20.7, 20.7, 20.6. **FTIR** (thin film, cm^{-1}): 1736, 1507, 1367, 1214, 1080, 1034, 832, 695. **$[\alpha]_D^{20}$** = +2.37 (c = 2.47 $CHCl_3$). **Minor (α) diastereomer**: $\mathbf{R_f}$ = 0.25 (30% EtOAc/hexanes). **HRMS** (ESI-TOF) (m/z): $[M+Na]^+$ calcd for

$C_{27}H_{30}O_{11}Na$ 553.1681, found 553.1640. **^{1}H NMR**: (500 MHz, $CDCl_3$) δ 7.45 – 7.28 (m, 5H), 7.00 (d, J = 9.2 Hz, 2H), 6.92 – 6.88 (m, 2H), 5.68 (t, J = 9.7 Hz, 1H), 5.62 (d, J = 3.6 Hz, 1H), 5.14 (t, J = 9.8 Hz, 1H), 5.01 (dd, J = 10.1, 3.6 Hz, 4H), 4.25 (dd, J = 12.3, 4.7 Hz, 1H), 4.20 – 4.13 (m, 1H), 4.07 (dd, J = 12.3, 2.2 Hz, 1H), 2.07 (s, 3H), 2.05 (s, 3H), 2.04 (s, 6H). **^{13}C{^{1}H} NMR**: (176MHz, $CDCl_3$): 170.6, 170.2, 169.6, 169.1, 154.6, 150.3 128.6, 128.0, 127.4, 117.8, 115.8, 95.00, 72.2, 70.5, 70.1, 68.4, 67.9, 61.7, 29.7, 20.8, 20.7, 20.6, 20.5. **FTIR** (thin film, cm^{-1}): 2917, 1737, 1509, 1456, 1364, 1225, 1211, 1128, 1100, 1031, 980, 954, 923, 818, 783, 740, 699, 660 . **$[\alpha]_D^{20}$** = +41.3 (c=0.17, $CHCl_3$).

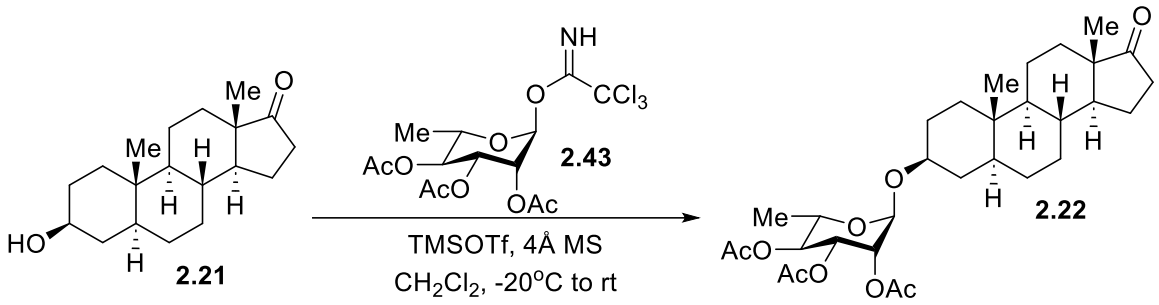
Comparison of Crude NMR reaction profiles (Error! Reference source not found.**)**



Studies in Error! Reference source not found.**B: Solid supported donor with BF_3·Et_2O.** Resin **2.16** (93 mg, 0.10 mmol, 2.0 equiv), DCE (2.0 mL), and 4Å molecular sieves were added to a plastic vial. The resin was swelled at room temperature for 20 minutes. Glycosyl acceptor *trans*-androsterone (15 mg, 0.05 mmol, 1.0equiv) was added, and the reaction was heated to 80 °C. BF_3·Et_2O (10 µL, 0.08 mmol, 1.5 equiv) was added and the reaction progress was monitored by TLC for 1 hour. Upon full consumption of the acceptor, the reaction mixture was filtered, and the resin was washed with CH_2Cl_2 (3x5 mL), EtOAc (3x5 mL), and CH_2Cl_2 (3x5 mL), and the filtrate was then quenched with Et_3N (50 µL). The filtrate was concentrated, and the crude residue was analyzed by ^{1}H NMR ($CDCl_3$, 500MHz).



Studies in Error! Reference source not found.**C: Solution donor with $BF_3{\cdot}Et_2O$.** Donor **2.43**[18] (45 mg, 0.10 mmol, 2.0 equiv), acceptor *trans*-androsterone (15.0 mg, 0.05 mmol, 1.0 equiv) and 4Å molecular sieves were added to a flame dried flask under N_2. The reaction was cooled to –40 ^oC, and CH_2Cl_2 (2.0 mL) was charged into the flask under N_2 and the reaction was stirred for 20 minutes. $BF_3{\cdot}Et_2O$ (6.4 µL, 0.05 mmol, 1.0 equiv) was added and the reaction was stirred at –40 ^oC for 2 hours. The reaction was quenched by addition of Et_3N (50 µL), filtered. The filtrate was concentrated, and the crude residue was analyzed by ^1H NMR ($CDCl_3$, 500MHz).



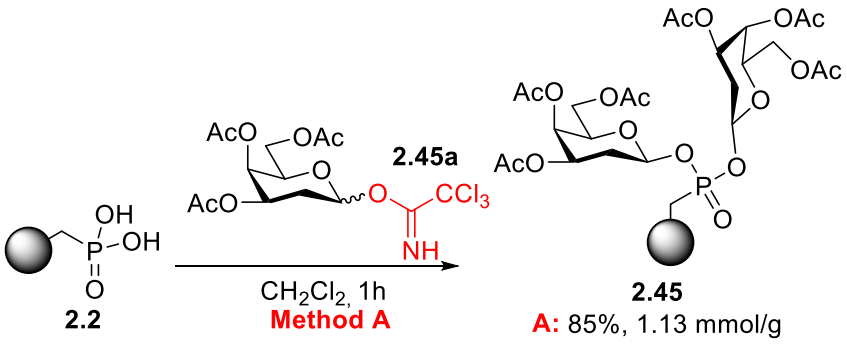
Studies in Error! Reference source not found.**D: Solution donor with TMSOTf.** Donor **2.43**[18] (27 mg, 0.06 mmol, 1.2 equiv), acceptor *trans*-androsterone (15.0 mg, 0.05 mmol, 1.0 equiv) and 4Å molecular sieves were added to a flame dried flask under N_2. The reaction was cooled to –20 ^oC and CH_2Cl_2 (2.0 mL) was charged into the flask under N_2 and the reaction was stirred for 20 minutes. TMSOTf (1.0 µL, 0.005 mmol, 0.1 equiv) was added and the reaction was stirred for 1 hour at –20 ^oC. The reaction was then warmed to room temperature and stirred for an additional

hour. The reaction was quenched by addition of Et_3N (50 µL), filtered. The filtrate was concentrated, and the crude residue was analyzed by ^1H NMR ($CDCl_3$, 500MHz).

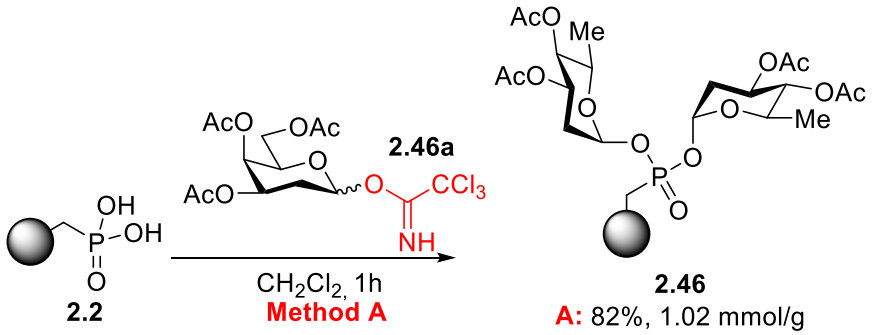
Resin Recycling (Studies in Figure 2.3)

A) Resin re-loading procedure. The washed recovered resin **2.2** (90 mg, 0.11 mmol, 1.0 equiv) was suspended in anhydrous DCM (2.0 mL). Rhamnosyl trichloroacetimidate **2.43**[18] (110 mg, 0.26 mmol, 2.2 equiv) was added and the reaction was stirred at room temperature for 18 hours. The reaction was filtered, washed with DCM (3x10 mL), and dried under vacuum to afford resin **2.16** (112 mg, 73%, 0.72 mmol/g).

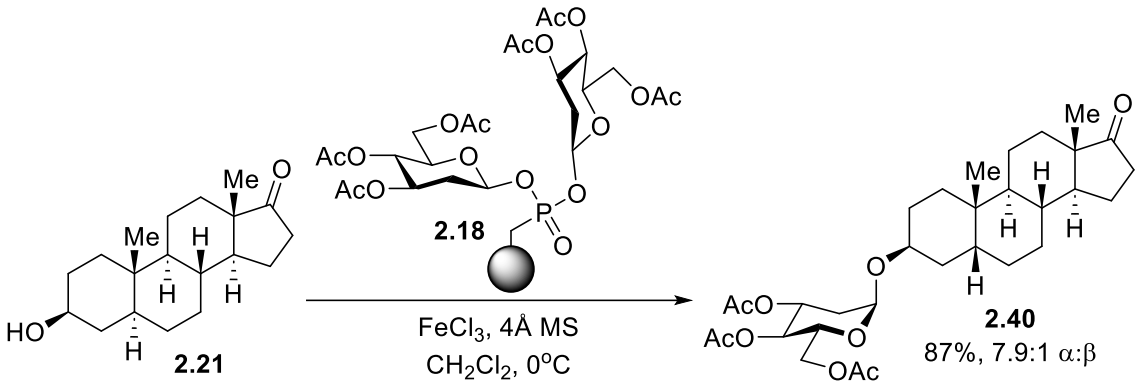
B) Recycled resin glycosylation procedure. The reloaded resin **2.16** (95 mg, 0.07 mmol, 2.0 equiv), DCE (2.0 mL), and 4Å molecular sieves were added to a plastic vial. The resin was swelled at room temperature for 20 minutes. Glycosyl acceptor *trans*-androsterone (10 mg, 0.04 mmol, 1.0 equiv) was added, and the reaction was heated to 80 °C. $BF_3{\cdot}Et_2O$ (6 µL, 0.06 mmol, 1.5 equiv) was added and the reaction progress was monitored by TLC for 1 hour. Upon full consumption of the acceptor, the reaction mixture was filtered, and the resin was washed with CH_2Cl_2 (3x5 mL), EtOAc (3x5 mL), and CH_2Cl_2 (3x5 mL), and the filtrate was then quenched with Et_3N (50 µL). The filtrate was concentrated, and the crude residue was purified by flash column chromatography (30% EtOAc/hexanes) to afford **2.22** (17.4 mg, α-only, 90% yield) as a white solid.



Resin 2.45: (Method A) Phosphonic acid resin **2.2** (550 mg, 0.72 mmol, 1.0 eq) was suspended in anhydrous CH_2Cl_2 (10 mL). 2-deoxygalactosyl trichloroacetimidate **2.45a**[67] (716 mg, 1.6 mmol, 2.2 eq) was added and the reaction was stirred at room temperature for 18 hours. The reaction was filtered, washed with CH_2Cl_2 (3x10 mL). The crude resin was suspended in the filtrate and stirred for an additional 18 hours at room temperature. The reaction was filtered, washed with CH_2Cl_2 (3x10 mL), and dried under vacuum to afford resin **2.45** (797 mg, 85%, 1.1 mmol/g) as a pale orange solid. **^{31}P NMR** (203 MHz, $CDCl_3$): δ 28.9. **FTIR** (thin film, cm^{-1}): 3025, 2917, 1743, 1493, 1452, 1422, 1368, 1232, 1039, 981, 855, 750, 698, 601, 572, 556, 540, 533, 526.

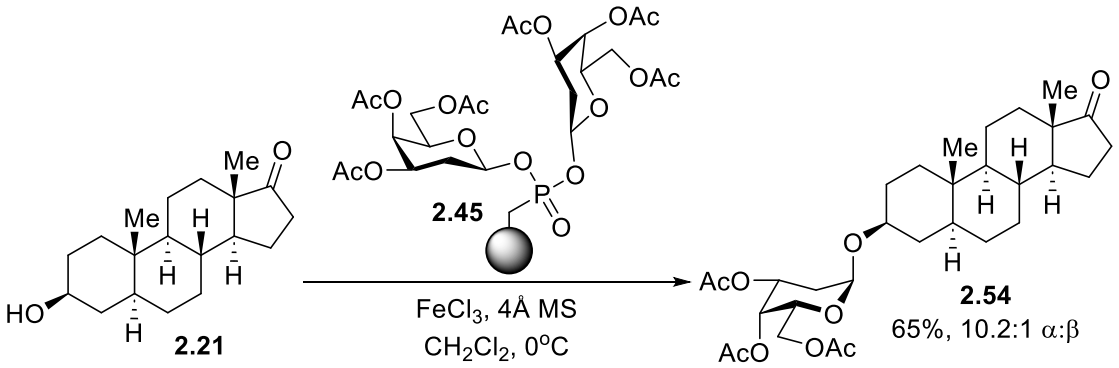


Resin 2.46: (Method A) Phosphonic acid resin **2.2** (550 mg, 0.72 mmol, 1.0 eq) was suspended in anhydrous CH_2Cl_2 (0.0 mL). 2-deoxyrhamnosyl trichloroacetimidate **2.46a**[68] (650 mg, 1.6 mmol, 2.2 eq) was added and the reaction was stirred at room temperature for 18 hours. The reaction was filtered, washed with CH_2Cl_2 (3x10 mL), and dried under vacuum to afford resin **2.46** (705 mg, 82%, 1.0 mmol/g) as a pale orange solid. **^{31}P NMR** (203 MHz, $CDCl_3$): δ 29.0. **FTIR** (thin film, cm^{-1}): 3025, 2917, 1738, 1493, 1452, 1422, 1369, 1240, 1166, 1046, 983, 845, 750, 698, 605, 571, 555, 546, 539, 532.



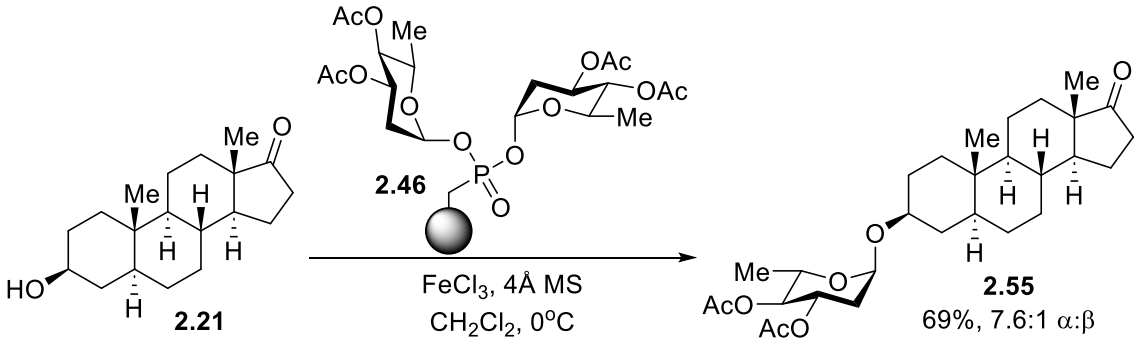
Glycoside product 2.40: Resin **2.18** (56 mg, 0.07 mmol, 2.0 eq), CH_2Cl_2 (2.0 mL), and 4Å molecular sieves were added to a plastic vial. The resin was swelled at room temperature for 20 minutes. Glycosyl acceptor *trans*-androsterone (10 mg, 0.03 mmol, 1.0 eq) was added, and the reaction was cooled to 0°C. $FeCl_3$ (7.3 mg, 0.05 mmol, 1.5 eq) was added and the reaction progress was monitored by TLC for 24 hours. Upon full consumption of the acceptor, the reaction mixture was filtered, and the resin was washed with CH_2Cl_2 (3x5 mL), EtOAc (3x5 mL), and CH_2Cl_2 (3x5 mL), and the filtrate was then quenched with Et_3N (50 mL). The filtrate was concentrated, and the crude residue was purified by flash column chromatography (15% EtOAc/hexanes) to afford **2.40** (16.8 mg, 7.9:1 α:β, 87% yield) as a white solid. $\mathbf{R_f}$ = 0.66 (50% EtOAc/hexanes). **HRMS** (ESI-TOF) (m/z): $[M+Na]^+$ calcd for $C_{31}H_{46}O_9Na$ 585.3035, found 585.3006. **^{1}H NMR** (500 MHz, $CDCl_3$) δ 5.32 (ddd, *J* = 11.6, 9.4, 5.3 Hz, 1H), 5.09 (d, *J* = 3.6 Hz, 1H), 4.96 (t, *J* = 9.6 Hz, 1H), 4.31 – 4.21 (m, 1H), 4.10 – 3.99 (m, 2H), 3.49 (tt, *J* = 11.2, 4.8 Hz, 1H), 2.46 – 2.34 (m, 1H), 2.16 (ddd, J = 12.8, 5.4, 1.3 Hz, 1H), 2.07 (s, 3H), 2.06 – 2.04 (m, 1H), 2.02 (s, 3H), 1.99 (s, 3H), 1.95 – 1.87 (m, 1H), 1.85 – 1.75 (m, 4H), 1.72 (dt, *J* = 13.4, 3.9 Hz, 2H), 1.67 – 1.45 (m, 3H), 1.45 – 1.35 (m, 2H), 1.35 – 1.16 (m, 5H), 1.09 (ddt, *J* = 12.4, 9.5, 2.5 Hz, 1H), 1.00 – 0.90 (m, 2H), 0.84 (s, 3H), 0.82 (s, 3H), 0.71 – 0.62 (m, 1H). **(minor diastereomer)** 4.68 (dd, *J* = 9.8, 2.0 Hz, 1H). **^{13}C{^{1}H}** NMR (126 MHz, $CDCl_3$) **(major diastereomer)** δ 221.3, 170.8, 170.3, 170.0, 95.2, 76.7, 69.6, 69.2, 67.8, 62.5, 54.4, 51.4, 47.8,

45.0, 36.8, 35.8, 35.8, 35.6, 35.0, 31.5, 30.9, 28.5, 27.6, 21.8, 21.0, 20.8, 20.8, 20.5, 13.8, 12.3. **(minor diastereomer)** δ 221.3, 170.8, 170.4, 169.8, 97.6, 78.1, 71.9, 71.1, 70.8, 62.6, 54.5, 51.4, 44.9, 44.8, 38.1, 37.0, 35.0, 34.4, 33.9, 31.5, 29.7, 29.2, 28.4, 22.7, 20.9, 20.8, 20.7, 20.5, 14.1, 12.3. **FTIR** (thin film, cm^{-1}): 2933, 2850, 1736, 1451, 1366, 1223, 1128, 1091, 1030, 934. **$[\alpha]_D^{20}$** = +102.8 (c = 1.34 $CHCl_3$). **(Ferrier, 2.53) ^{1}H NMR** (500 MHz, $CDCl_3$) 5.87 (dt, *J* = 10.2, 1.3 Hz, 1H), 5.81 (ddd. *J* = 10.2, 2.7, 1.9 Hz, 1H), 5.35 - 5.25 (m, 1H), 5.16 (d, *J* = 2.7Hz, 1H), 4.30 – 4.13 (m, 3H), 3.70 – 3.55 (m, 1H), 2.49 – 2.38 (m, 1H), 2.09 (s, 3H), 2.07 (s, 3H), 1.98 – 1.63 (m, 10H), 1.56 – 1.38 (m, 4H), 1.36 – 1.19 (m, 4H), 1.17 – 1.00 (m, 4H), 0.97 (s, 3H), 0.95 (s, 3H), 0.72 – 0.54 (m, 1H).



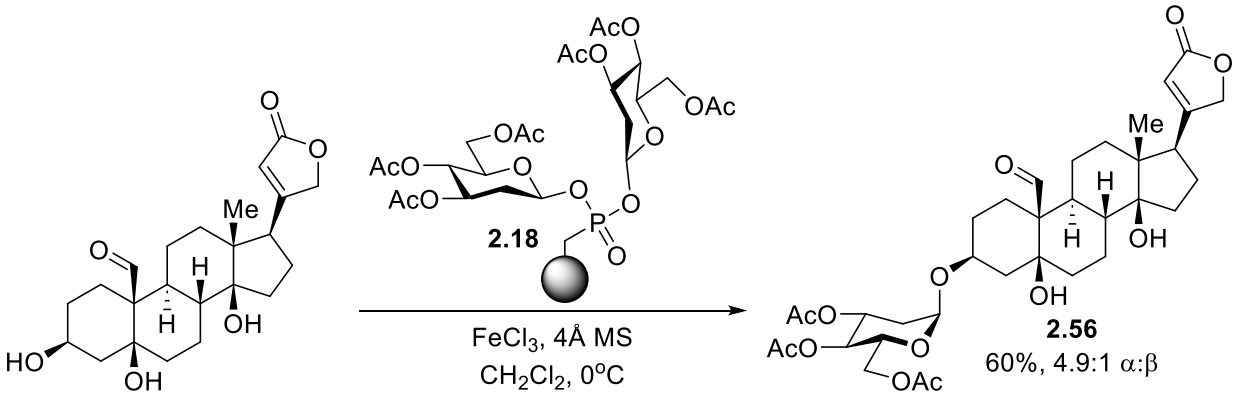
Glycoside product 2.54: Resin **2.45** (55 mg, 0.06 mmol, 2.0 eq), CH_2Cl_2 (2.0 mL), and 4Å molecular sieves were added to a plastic vial. The resin was swelled at room temperature for 20 minutes. Glycosyl acceptor *trans*-androsterone (9.0 mg, 0.03 mmol, 1.0 eq) was added, and the reaction was cooled to 0°C. $FeCl_3$ (7.5 mg, 0.05 mmol, 1.5 eq) was added and the reaction progress was monitored by TLC for 24 hours. Upon full consumption of the acceptor, the reaction mixture was filtered, and the resin was washed with CH_2Cl_2 (3x5 mL), EtOAc (3x5 mL), and CH_2Cl_2 (3x5 mL), and the filtrate was then quenched with Et_3N (50 mL). The filtrate was concentrated, and the crude residue was purified by flash column chromatography (15% EtOAc/hexanes) to afford **2.54** (11.1 mg, 10.2:1 α:β, 65% yield) as a white solid. **HRMS** (ESI-

TOF) (m/z): $[M+Na]^+$ calcd for $C_{31}H_{46}O_9Na$ 585.3035, found 585.3031. **^{1}H NMR** (500 MHz, $CDCl_3$) δ 5.36 – 5.27 (m, 2H), 5.16 (d, *J* = 3.4 Hz, 1H), 4.24 (t, *J* = 6.7 Hz, 1H), 4.11 – 4.00 (m, 2H), 3.51 (tt, *J* = 10.8, 4.8 Hz, 1H), 2.43 (dd, *J* = 19.3, 8.9 Hz, 1H), 2.12 (s, 3H), 2.11 – 2.05 (m, 3H), 2.04 (d, *J* = 2.3 Hz, 3H), 2.02 – 1.99 (m, 1H), 1.97 (s, 3H), 1.92 (ddd, *J* = 14.1, 8.6, 6.0 Hz, 2H), 1.87 – 1.25 (m, 1H), 1.16 – 0.89 (m, 5H), 0.85 (s, 3H), 0.83 (s, 3H), 0.69 (dtd, *J* = 16.0, 10.7, 9.6, 4.7 Hz, 1H). **^{13}C{^{1}H} NMR** (126 MHz, $CDCl_3$) δ 221.5, 170.6, 170.5, 170.3, 95.9, 76.8, 71.3, 67.0, 66.8, 66.5, 62.8, 54.6, 51.5, 47.9, 45.2, 38.2, 37.0, 36.0, 35.2, 31.7, 31.0, 28.6, 28.5, 27.8, 21.9, 21.0, 20.91, 20.89, 20.6, 13.9, 12.4. **FTIR** (thin film, cm^{-1}) 2293, 2852, 1737, 1500, 1451, 1369, 1226, 1161, 1120, 1079, 1020, 885, 713, 603, 571. **$[\alpha]_D^{24}$** = +142.6 (c = 0.45 CH_2Cl_2).



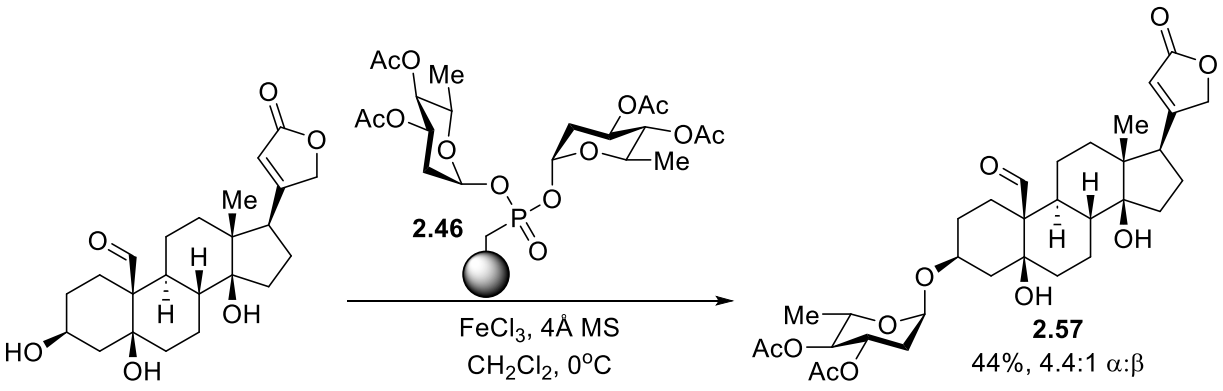
Glycoside product 2.55: Resin **2.46** (61 mg, 0.04 mmol, 1.3 eq), CH_2Cl_2 (2.0 mL), and 4Å molecular sieves were added to a plastic vial. The resin was swelled at room temperature for 20 minutes. Glycosyl acceptor *trans*-androsterone (9.0 mg, 0.03 mmol, 1.0 eq) was added, and the reaction was cooled to 0°C. $FeCl_3$ (7.5 mg, 0.05 mmol, 1.5 eq) was added and the reaction progress was monitored by TLC for 24 hours. Upon full consumption of the acceptor, the reaction mixture was filtered, and the resin was washed with CH_2Cl_2 (3x5 mL), EtOAc (3x5 mL), and CH_2Cl_2 (3x5 mL), and the filtrate was then quenched with Et_3N (50 mL). The filtrate was concentrated, and the crude residue was purified by flash column chromatography (10%

EtOAc/hexanes) to afford **2.55** (10.7 mg, 7.6:1 α:β, 69% yield) as a white solid. **HRMS** (ESI-TOF) (m/z): $[M+Na]^+$ calcd for $C_{29}H_{44}O_7Na$ 527.2980, found 527.2965. **^{1}H NMR** (500 MHz, $CDCl_3$) δ 5.28 (ddd, *J* = 11.6, 9.4, 5.3 Hz, 1H), 5.03 (d, *J* = 3.5 Hz, 1H), 4.71 (t, *J* = 9.6 Hz, 1H), 3.94 – 3.89 (m, 1H), 3.49 (tt, *J* = 11.1, 4.7 Hz, 1H), 2.42 (dd, *J* = 19.3, 8.8 Hz, 1H), 2.14 (ddd, *J* = 12.7, 5.3, 1.3 Hz, 1H), 2.10 – 2.05 (m, 1H), 2.04 (s, 3H), 1.99 (s, 3H), 1.95 – 1.84 (m, 1H), 1.80 – 1.76 (m, 3H), 1.74 – 1.59 (m, 2H), 1.56 – 1.45 (m, 2H), 1.32 – 1.27 (m, 2H), 1.25 – 1.19 (m, 2H), 1.15 (d, *J* = 6.3 Hz, 3H), 1.08 – 0.92 (m, 8H), 0.85 (s, 3H), 0.82 (s, 3H), 0.71 – 0.63 (m, 1H). **^{13}C{^{1}H} NMR** (126 MHz, $CDCl_3$) δ 221.6, 170.5, 170.4, 94.6, 75.8, 75.2, 69.4, 65.7, 54.6, 51.6, 47.9, 44.8, 37.2, 36.0, 35.2, 34.1, 31.7, 31.0, 29.3, 28.6, 27.6, 27.4, 27.0, 21.9, 21.0, 20.6, 17.7, 13.9, 12.4. **FTIR** (thin film, cm^{-1}) 2917, 2850, 1738, 1648, 1513, 1471, 1452, 1366, 1242, 1226, 1121, 1097, 1032, 994, 934, 899, 872, 826, 767, 652, 601, 534. **$[\alpha]_D^{24}$** = -5.57 (c = 0.11 CH_2Cl_2).



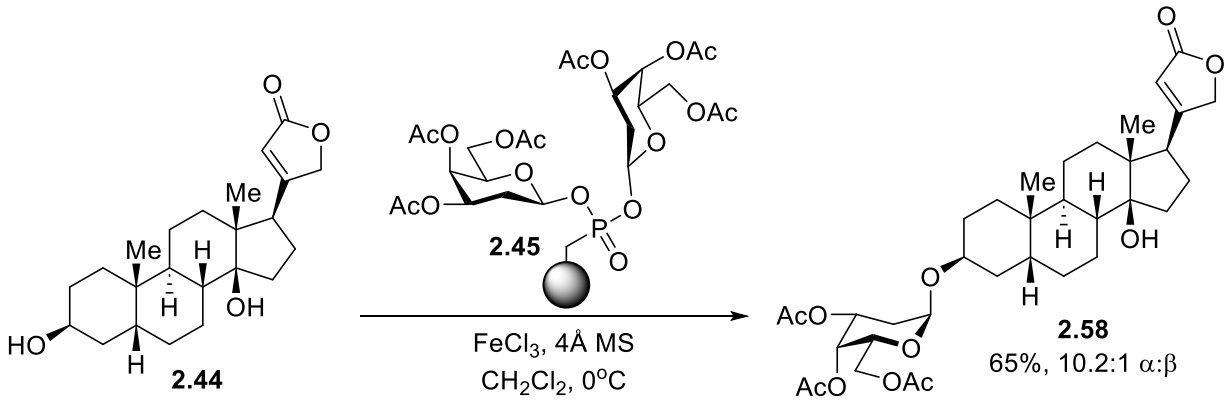
Glycoside product 2.56: Resin **2.18** (49 mg, 0.06 mmol, 2.0 eq), CH_2Cl_2 (2.0 mL), and 4Å molecular sieves were added to a plastic vial. The resin was swelled at room temperature for 20 minutes. Glycosyl acceptor strophanthidin (12 mg, 0.03 mmol, 1.0 eq) was added, and the reaction was cooled to 0°C. $FeCl_3$ (7.5 mg, 0.04 mmol, 1.5 eq) was added and the reaction progress was monitored by TLC for 0 hour. Upon full consumption of the acceptor, the reaction mixture was filtered, and the resin was washed with CH_2Cl_2 (3x5 mL), EtOAc (3x5 mL), and

CH_2Cl_2 (3x5 mL), and the filtrate was then quenched with Et_3N (50 mL). The filtrate was concentrated, and the crude residue was purified by flash column chromatography (50% EtOAc/hexanes) to afford **2.56** (12.0 mg, 4.9:1 α:β, 60% yield) as a white solid. **HRMS** (ESI-TOF) (m/z): $[M+Na]^+$ calcd for $C_{29}H_{44}O_7Na$ 699.2993, found 699.2977. **^{1}H NMR** (500 MHz, $CDCl_3$) δ 10.05 – 9.86 (m, 1H), 5.83 – 5.79 (m, 1H), 5.15 (ddd, *J* = 11.5, 9.4, 5.3 Hz, 1H), 5.07 – 5.00 (m, 1H), 4.98 – 4.91 (m, 1H), 4.89 (dd, *J* = 18.3, 2.1 Hz, 1H), 4.74 (ddd, *J* = 18.0, 5.5, 1.7 Hz, 1H), 4.30 – 3.83 (m, 4H), 2.70 (dt, *J* = 9.7, 4.7 Hz, 1H), 2.10-2.05 (m, 4H), 2.02 (s, 3H), 1.98 (s, 3H), 1.97 – 1.94 (m, 3H) 1.93 (s, 3H), 1.89 – 1.22 (m, 13H), 0.89 – 0.81 (m, 2H), 0.80 (s, 3H). 0.78 – 0.75 (m, 1H). **^{13}C{^{1}H} NMR** (126 MHz, $CDCl_3$) δ 207.8, 174.5, 170.8, 170.1, 170.0, 129.2, 128.4, 118.1, 94.0, 85.3, 73.6, 73.5, 71.0, 69.3, 68.7, 68.7, 62.4, 54.9, 50.5, 49.5, 41.9, 39.8, 39.5, 37.1, 36.0, 32.1, 29.8, 26.9, 24.3, 21.0, 20.9, 20.9, 20.8, 15.7, 15.7. **FTIR** (thin film, cm^{-1}) 2917, 2849, 1738, 1502, 1453, 1368, 1231, 1133, 1033, 890, 861, 793, 736, 696, 665, 605, 572, 557, 550, 536, 527. **$[\alpha]_D^{24}$** = +73.1 (c = 0.44 CH_2Cl_2).

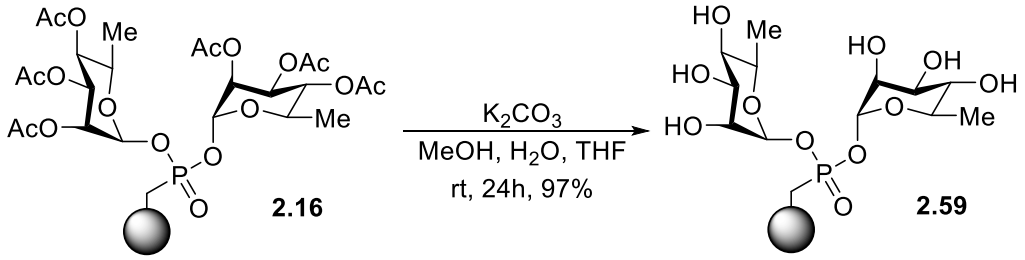


Glycoside product 2.57: Resin **2.46** (39 mg, 0.06 mmol, 2.0 eq), CH_2Cl_2 (2.0 mL), and 4Å molecular sieves were added to a plastic vial. The resin was swelled at room temperature for 20 minutes. Glycosyl acceptor strophanthidin (12 mg, 0.03 mmol, 1.0 eq) was added, and the reaction was cooled to 0°C. $FeCl_3$ (7.2 mg, 0.04 mmol, 1.5 eq) was added and the reaction progress was monitored by TLC for 24 hours. Upon full consumption of the acceptor, the

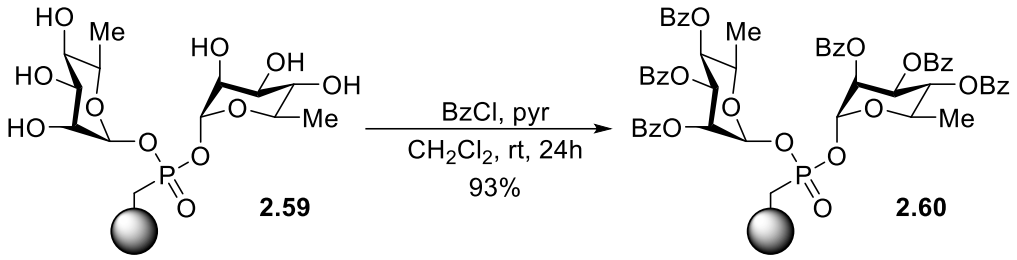
reaction mixture was filtered, and the resin was washed with CH_2Cl_2 (3x5 mL), EtOAc (3x5 mL), and CH_2Cl_2 (3x5 mL), and the filtrate was then quenched with Et_3N (50 mL). The filtrate was concentrated, and the crude residue was purified by flash column chromatography (30% EtOAc/hexanes) to afford **2.57** (7.0 mg, 4.4:1 α:β, 44% yield) as a white solid. **HRMS** (ESI-TOF) (m/z): $[M+H]^+$ calcd for $C_{29}H_{44}O_7H$ 619.3113, found 619.3120. **^{1}H NMR** (500 MHz, $CDCl_3$) δ 9.99 (s, 1H), 5.85 – 5.78 (m, 1H), 5.12 (ddt, *J* = 13.7, 7.1, 3.4 Hz, 1H), 4.99 (d, *J* = 3.8 Hz, 1H), 4.88 (dd, *J* = 18.0, 1.9 Hz, 1H), 4.73 (dd, *J* = 18.0, 1.8 Hz, 1H), 4.67 (td, *J* = 9.6, 1.9 Hz, 1H), 4.06 – 4.02 (m, 1H), 4.01 (s, 1H), 3.82 – 3.75 (m, 1H), 2.69 (dd, *J* = 9.7, 5.4 Hz, 1H), 2.05 – 2.01 (m, 1H), 1.99 (s, 3H), 1.96 – 1.94 1.93 (d, *J* = 1.8 Hz, 4H), 1.89 – 1.41 (m, 14H), 1.27 (d, *J* = 8.3 Hz, 3H), 1.17 – 1.13 (m, 4H), 1.11 (dd, *J* = 6.4, 1.8 Hz, 3H), 0.80 (d, *J* = 1.9 Hz, 3H). **^{13}C{^{1}H} NMR** (126 MHz, $CDCl_3$) δ 175.9, 174.6, 174.5, 170.4, 170.3, 118.0, 96.3, 85.5, 75.2, 74.2, 73.6, 73.2, 68.6, 67.2, 53.5, 50.5, 49.9, 41.1, 40.1, 39.6, 36.0, 35.5, 34.4, 32.5, 29.8, 26.9, 25.6, 23.9, 21.6, 21.1, 21.0, 17.6, 15.8. (during the course of acquiring the spectra, it appears the aldehyde was at least partially oxidized to carboxylic acid (δ 175.0ppm, aldehyde typically appears >200ppm). **FTIR** (thin film, cm^{-1}) 2929, 2850, 1731, 1502, 1452, 1377, 1243, 1166, 1125, 1095, 1030, 889, 862, 795, 736, 696, 604, 564, 556, 540, 531. **$[\alpha]_D^{24}$** = -26.9(c = 0.59 CH_2Cl_2).



Glycoside product 2.58: Resin **2.45** (52 mg, 0.06 mmol, 2.0 eq), CH_2Cl_2 (2.0 mL), and 4Å molecular sieves were added to a plastic vial. The resin was swelled at room temperature for 20 minutes. Glycosyl acceptor digitoxigenin (11 mg, 0.03 mmol, 1.0 eq) was added, and the reaction was cooled to 0°C. $FeCl_3$ (7.5 mg, 0.04 mmol, 1.5 eq) was added and the reaction progress was monitored by TLC for 24 hours. Upon full consumption of the acceptor, the reaction mixture was filtered, and the resin was washed with CH_2Cl_2 (3x5 mL), EtOAc (3x5 mL), and CH_2Cl_2 (3x5 mL), and the filtrate was then quenched with Et_3N (50 mL). The filtrate was concentrated, and the crude residue was purified by flash column chromatography (30% EtOAc/hexanes) to afford **2.58** (12.3 mg, 10.2:1 α:β, 65% yield) as a white solid. **HRMS** (ESI-TOF) (m/z): $[M+NH_4]^+$ calcd for $C_{29}H_{44}O_7Na$ 664.3691, found 664.3672. **^{1}H NMR** (500 MHz, $CDCl_3$) δ 5.87 (d, *J* = 1.8 Hz, 1H), 5.39 – 5.31 (m, 3H), 5.04 – 4.91 (m, 1H), 4.80 (dd, *J* = 18.0, 1.8 Hz, 1H), 4.40 (t, *J* = 6.5 Hz, 1H), 4.15 – 4.01 (m, 4H), 2.88 (s, 1H), 2.82 – 2.71 (m, 1H), 2.13 (s, 3H), 2.11 – 2.07 (m, 1H), 2.05 (s, 3H), 1.99 (s, 3H), 1.94 – 1.28 (m, 19H), 0.93 (d, *J* = 1.9 Hz, 3H), 0.87 (s, 3H), 0.85 – 0.76 (m, 2H). **^{13}C{^{1}H} NMR** (126 MHz, $CDCl_3$) δ 174.7, 170.8, 170.5, 170.4, 170.2, 117.8, 92.4, 73.6, 66.9, 65.9, 62.7, 51.0, 51.0, 49.7, 42.0, 40.2, 36.7, 35.8, 35.4, 33.3, 32.1, 32.0, 30.8, 30.3, 29.8, 27.0, 23.8, 21.3, 21.0, 20.9, 20.9, 20.9, 20.9, 20.8, 15.9. **FTIR** (thin film, cm^{-1}) 2921, 1738, 1501, 1449, 1368, 1224, 1157, 1022, 886, 603, 563, 535. **$[\alpha]_D^{24}$** = +91.8 (c = 0.38 CH_2Cl_2).

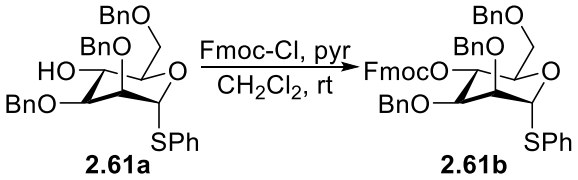


Resin 2.59: In a plastic vial, resin **2.16** (350 mg, 0.22 mmol, 1.0 eq) was swelled in a mixture of THF:MeOH:H_2O (1:1:1, 1.5mL) for 30 minutes at room temperature. K_2CO_3 (211 mg, 1.3 mmol, 6.0eq) was added and the reaction was stirred at room temperature overnight. The resin filtered and washed with H_2O (3x5 mL), CH_2Cl_2 (3x5 mL), MeOH (3x5 mL), and CH_2Cl_2, and resin was dried on high-vac for at least 8 hours. Resin **2.59** (308 mg, 97% yield, 0.55 mmol/g) was obtained as an off-white solid. **FTIR** (thin film, cm^{-1}): 2918, 1621, 1492, 1493, 1370, 1203, 1061, 977, 831, 756, 697, 592, 580, 572, 555, 539, 527.

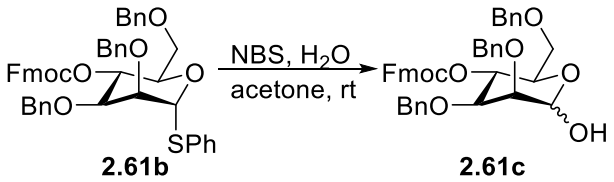


Resin 2.60: In a plastic vial, resin **2.59** (140 mg, 0.08 mmol, 1.0 eq) was swelled in CH_2Cl_2 (2.0 mL) for 30 minutes at room temperature. Pyridine (0.124 mL, 1.5 mmol, 20eq) and BzCl (0.190 mL, 0.15 mmol, 20eq) were added and the reaction was stirred at room temperature overnight. The resin filtered and washed with H_2O (3x5 mL), CH_2Cl_2 (3x5 mL), acetone (3x5 mL), H_2O (3x5 mL), and CH_2Cl_2, and resin was dried on high-vac for at least 8 hours. Resin **2.60** (153 mg, 93% yield, 0.35 mol/g) was obtained as an off-white solid. **^{31}P NMR:** (203 MHz, $CDCl_3$) 27.7. **FTIR** (thin film, cm^{-1}): 3024, 2917, 1709, 1493, 1451, 1240, 1174, 1046, 983, 846, 751, 697, 564, 539, 533.

Synthesis of Mannose Donor 2.61



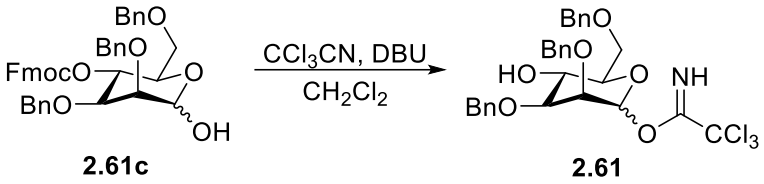
Intermediate 2.61b: Fmoc-Cl (0.36 g, 1.4 mmol, 1.3 eq) was to a solution of **2.61a**[69] (0.58 g, 1.1 mmol, 1.0 eq) in a mixture of pyridine:CH_2Cl_2 (1.3:7.5 mL). The reaction was stirred at room temperature for 24 hours. The solvents were removed under reduced pressure and the crude residue was taken up in H_2O (100 mL). The aqueous layer was extracted with EtOAc (3x50 mL), and the combined organic layers were dried over Na_2SO_4 and concentrated *in vacuo*. The crude material was purified by flash column chromatography (10% EtOAc/hexanes) to afford **2.61b** (0.47 g, 58% yield) as a white solid. **^{1}H NMR** (500 MHz, $CDCl_3$) δ 7.77 (d, *J* = 7.6 Hz, 2H), 7.60 (dd, *J* = 13.9, 7.6 Hz, 2H), 7.50 – 7.43 (m, 2H), 7.40 (t, *J* = 7.5 Hz, 2H), 7.36 – 7.18 (m, 20H), 5.56 (d, *J* = 1.7 Hz, 1H), 5.33 (t, *J* = 9.8 Hz, 1H), 4.70 (d, *J* = 12.3 Hz, 1H), 4.64 (d, *J* = 12.3 Hz, 1H), 4.59 – 4.51 (m, 3H), 4.51 – 4.45 (m, 2H), 4.42 – 4.30 (m, 2H), 4.18 (t, *J* = 7.3 Hz, 1H), 4.00 (dd, *J* = 3.1, 1.8 Hz, 1H), 3.89 (dd, *J* = 9.5, 3.1 Hz, 1H), 3.71 (qd, *J* = 10.9, 4.5 Hz, 2H).



2.61b **2.61c**

Intermediate 2.61c: NBS (0.21 g, 1.2 mmol, 2.0 eq) was added to a stirred solution of **2.61b** (0.45g, 0.59mmol, 1.0eq) in acetone:H_2O (20:2 mL) at room temperature. The reaction was stirred at room temperature for 24 hours. The solvent was evaporated under reduced pressure and the crude residue was purified by flash column chromatography (25% EtOAc/hexanes) to afford **2.61c** (280 mg, 73% yield) as a white solid. **^{1}H NMR** (500 MHz, $CDCl_3$) δ 7.76 (d, *J* = 7.6 Hz, 2H), 7.57 (dd, *J* = 12.1, 7.5 Hz, 2H), 7.39 (t, *J* = 7.5 Hz, 2H), 7.36 – 7.18 (m, 12H), 5.28 – 5.19 (m, 2H), 4.78 (d, *J* = 12.4 Hz, 1H), 4.69 (d, *J* = 12.4 Hz, 1H), 4.62 – 4.52 (m, 4H), 4.34 (dd, *J* =

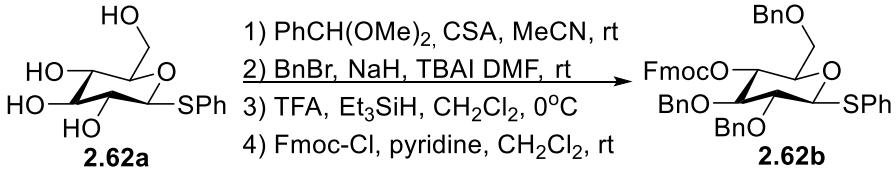
7.4, 2.4 Hz, 2H), 4.22 – 4.10 (m, 2H), 4.00 (dd, *J* = 9.7, 3.0 Hz, 1H), 3.88 – 3.79 (m, 1H), 3.71 – 3.55 (m, 2H).



2.61c **2.61**

Trichloroacetimidate 2.61: CCl_3CN (0.13 mL, 1.2 mmol, 3.0 eq) was added to a stirred solution of **2.61c** (0.28 g, 0.42 mmol, 1.0 eq) and DBU (0.020 mL, 0.013 mmol, 0.3 eq) in CH_2Cl_2 (2 mL). The reaction was stirred at room temperature for 24 hours. The reaction mixture was concentrated, and the crude residue was purified by flash column chromatography (30-50% EtOAc/hexanes + 5% Et_3N) to afford **2.61** (247 mg, >99% yield, 3.2:1 mixture of diastereomers) as an amber oil. **^{1}H NMR** (500 MHz, $CDCl_3$) δ 8.55 (s, 1H), 7.41 – 7.37 (m, 2H), 7.35 – 7.26 (m, 11H), 6.36 (d, *J* = 1.9 Hz, 1H), 4.76 (d, *J* = 12.1 Hz, 1H), 4.69 – 4.51 (m, 5H), 4.21 (t, *J* = 9.7 Hz, 1H), 3.96 (dt, *J* = 9.3, 4.3 Hz, 1H), 3.88 (dd, *J* = 3.2, 2.0 Hz, 1H), 3.84 – 3.72 (m, 3H).

Synthesis of Glucose Donor 2.62



2.62a **2.62b**

Intermediate 2.62b: Benzaldehyde dimethylacetal (0.67 mL, 4.4 mol, 1.2 eq) was added dropwise to a solution of **2.62a**[70] (1.0 g, 3.7 mmol, 1.0 eq) and (+)-CSA (0.22 g, 0.93 mmol, 0.25 eq) in MeCN (15 mL) at room temperature. The reaction was stirred for 24 hours at room temperature. Upon completion, the reaction was quenched by addition of Et_3N (1.0 mL), diluted with H_2O (100 mL), extracted with EtOAc (3x100 mL), and washed with brine (100 mL). The

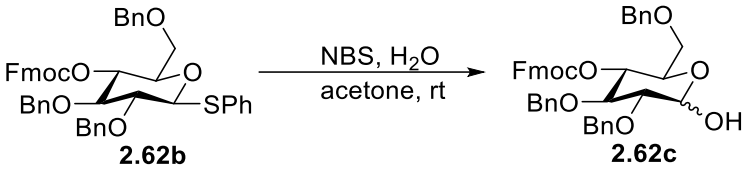
combined organic layers were dried over Na_2SO_4 and concentrated *in vacuo*. The crude product was used in the next step without further purification.

The crude residue was dissolved in DMF (10 mL) and NaH (60% in mineral oil, 0.74 g, 18 mmol, 5.0 eq) and TBAI (0.14 g, 0.37 mmol, 0.1 eq) were added to the reaction at room temperature. The reaction was stirred for one hour until gas evolution ceased. Benzyl bromide (2.2 mL, 18 mmol, 5.0 eq) was added and the reaction was stirred for 24 hours at room temperature. The reaction was diluted with H_2O (100 mL) and extracted with EtOAc (3x100 mL). The combined organic layers were washed with 1N HCl (100 mL), dried over Na_2SO_4, and concentrated *in vacuo* and used in the next step without further purification.

The crude residue was dissolved in CH_2Cl_2 and cooled to 0 ^oC in an ice bath. Triethylsilane (2.9mL, 18mmol, 5.0eq) was added in one portion at 0 ^oC. Trifluoroacetic acid (1.4 mL, 18 mmol, 5.0eq) was added dropwise at 0 ^oC. The reaction warmed to room temperature and was stirred at room temperature for four hours. The reaction was quenched with Et_3N (5 mL) and the volatiles were removed under reduced pressure. The crude product was used in the next step without further purification.

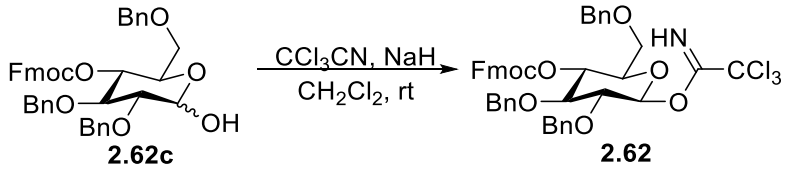
The crude residue was dissolved in pyridine (10 mL) and Fmoc-Cl (1.9 g, 7.4 mmol, 2.0eq) was added in one portion. The reaction was stirred at room temperature for 24 hours. The solvents were removed under reduced pressure and the crude residue was taken up in H_2O (100 mL). The aqueous layer was extracted with EtOAc (3x50 mL), and the combined organic layers were dried over Na_2SO_4 and concentrated *in vacuo*. The crude material was purified by flash column chromatography (20% EtOAc/hexanes) to afford **2.62b** (0.40 g, 14% yield) as a white solid. **HRMS (ESI-TOF)** (m/z): $[M+NH_4]+$ calcd for $C_{48}H_{44}O_7SNH_4$ 782.3146, found 782.3130. **^{1}H NMR** (500 MHz, $CDCl_3$) δ 7.75 (d, *J* = 7.5 Hz, 2H), 7.66 – 7.43 (m, 4H), 7.44 – 7.11 (m, 22H),

4.88 (dt, *J* = 9.8, 4.4 Hz, 2H), 4.81 (dd, *J* = 11.3, 3.3 Hz, 1H), 4.75 – 4.65 (m, 3H), 4.52 (d, *J* = 3.3 Hz, 2H), 4.37 – 4.24 (m, 2H), 4.12 (t, *J* = 7.4 Hz, 1H), 3.75 (td, *J* = 9.1, 3.3 Hz, 1H), 3.71 – 3.60 (m, 3H), 3.55 (td, *J* = 9.3, 3.3 Hz, 1H).



2.62b **2.62c**

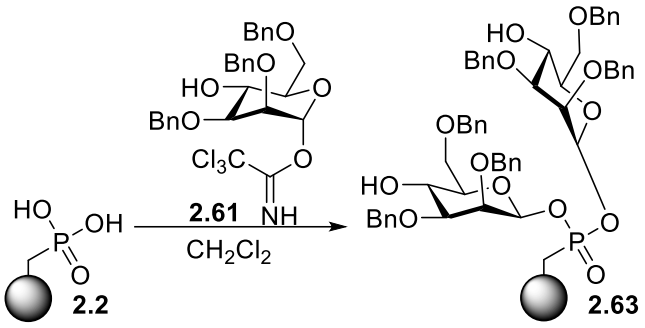
Intermediate 2.62c: NBS (0.29 g, 1.6 mmol, 1.5 eq) was added to a stirred solution of **2.62b** (0.73 g, 1.1 mmol, 1.0 eq) in acetone:H_2O (20:2 mL) at room temperature. The reaction was stirred at room temperature for 24 hours. The solvent was evaporated under reduced pressure and the crude residue was purified by flash column chromatography to afford **2.62c** (390 mg, 62% yield) as a white solid. **^{1}H NMR** (400 MHz, $CDCl_3$) δ 7.8 (d, *J* = 7.6 Hz, 2H), 7.5 (dt, *J* = 12.8, 6.6 Hz, 2H), 7.3 (ddt, *J* = 44.5, 22.3, 8.2 Hz, 19H), 5.2 (d, *J* = 3.5 Hz, 1H), 4.9 – 4.6 (m, 6H), 4.6 – 4.4 (m, 2H), 4.4 – 4.0 (m, 5H), 3.7 – 3.5 (m, 4H).



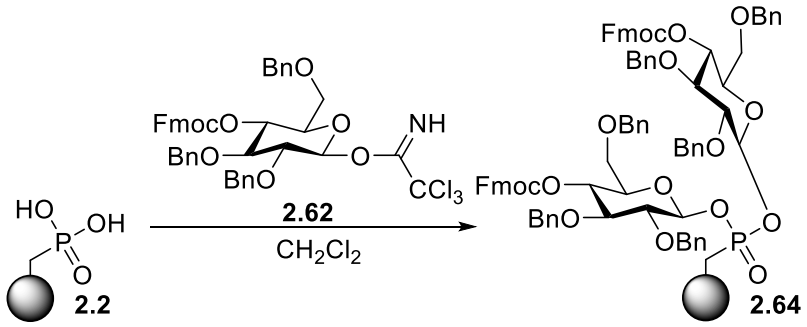
2.62c **2.62**

Trichloroacetimidate 2.62: CCl_3CN (0.11 mL, 1.0 mmol, 3.0 eq) was added to a stirred solution of **2.62d** (0.11 g, 0.35 mmol, 1.0 eq) and NaH (60% in mineral oil, 0.004 g, 0.10 mmol, 0.3 eq) in CH_2Cl_2 (5 mL). The reaction was stirred at room temperature for 24 hours. The reaction mixture was concentrated, and the crude residue was purified by flash column chromatography (10-50% EtOAc/hexanes) to afford **2.62** (225mg, 80% yield, 3.2:1 mixture of diastereomers) as an amber oil. **^{1}H NMR** (401 MHz, CDCl3) δ 8.75 (minor, s, 0H), 8.63 (s, 1H), 7.76 (d, *J* = 7.6 Hz, 2H), 7.56 (dd, *J* = 14.1, 7.6 Hz, 2H), 7.41 – 7.34 (m, 2H), 7.34 – 7.12 (m, 17H), 6.51 (d, *J* = 3.4 Hz, 1H), 5.85 (minor, d, *J* = 3.6 Hz, 0H), 5.08 (t, *J* = 9.9 Hz, 1H), 4.88 (q, *J* = 11.5, 10.9 Hz,

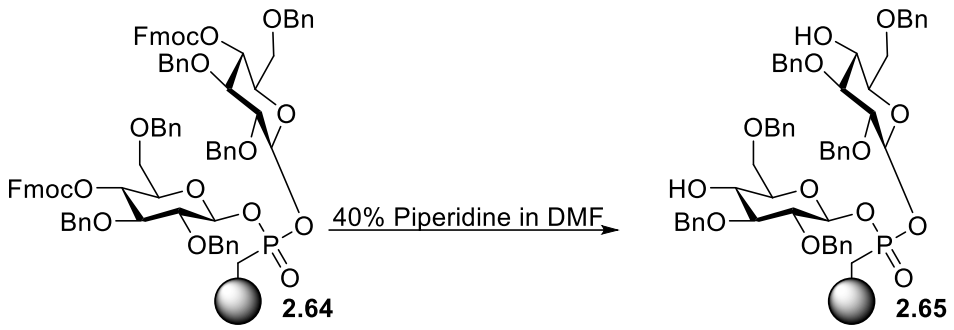
1H), 4.78 – 4.63 (m, 3H), 4.54 – 4.42 (m, 3H), 4.33 (dd, *J* = 7.2, 2.7 Hz, 1H), 4.19 – 4.02 (m, 3H), 3.86 – 3.79 (m, 1H), 3.60 (qd, *J* = 11.1, 3.5 Hz, 2H).



Resin 2.63: Phosphonic acid resin **2.2** (145 mg, 0.20 mmol, 1.0 eq) was suspended in CH_2Cl_2 (2.0 mL) and stirred at room temperature for 30 minutes. Donor **2.61** was added, and the suspension was stirred at room temperature for 24 hours. The suspension was filtered, and the resin was washed with CH_2Cl_2 (10x5 mL) and dried thoroughly under vacuum. Resin **2.63** (229 mg, 74% yield, 0.84 mmol/g) was afforded as an orange solid.

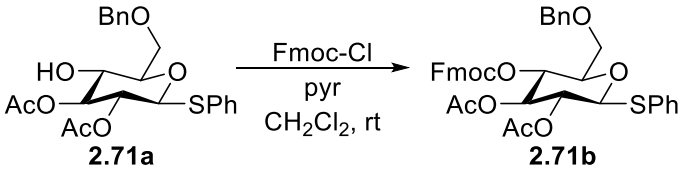


Resin 2.64: Phosphonic acid resin **2.2** (100 mg, 0.13 mmol, 1.0 eq) was suspended in CH_2Cl_2 (2.0 mL) and stirred at room temperature for 30 minutes. Donor **2.62** (230 mg, 0.29 mmol, 2.2 eq) was added and the suspension was stirred at room temperature for 24 hours. The suspension was filtered, and the resin was washed with CH_2Cl_2 (10x5 mL) and dried thoroughly under vacuum. Resin **2.64** (177 mg, 65% yield, 0.66 mmol/g) was afforded as an orange solid.



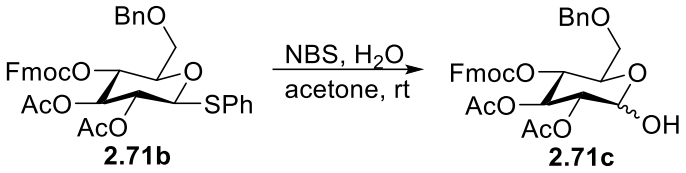
Resin 2.65: Resin **2.64** (177 mg, 0.12 mmol, 1.0 eq) was stirred in a 40% solution of piperidine in DMF (2.0 mL) for one hour. The resin was filtered washed extensively with CH_2Cl_2 (10x5 mL) and dried thoroughly under vacuum. Resin **2.64** (137 mg, 91%, 0.63 mmol/g) was afforded as a dark orange. Cleavage of the Fmoc group was confirmed by HRMS detection of dibenzofulvene in the filtrate after washing: **HRMS** (ESI-TOF) (m/z): [M+H]+ calcd for $C_{14}H_{10}H$ 179.0856, found 179.0851.

Synthesis of glucose donor 2.71



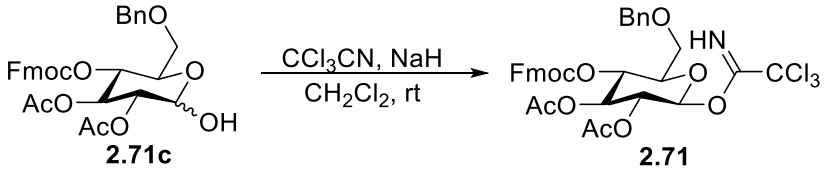
Intermediate 2.71b: Fmoc-Cl (0.83 g, 1.8 mmol, 2.0 eq) was added to a solution of **2.71a**[72] (0.40 g, 0.90 mmol, 1.0 eq) and pyridine (2.0 mL, 26 mmol, 30 eq) in CH_2Cl_2 (10 mL). The reaction was stirred at room temperature for 24 hours. The solvents were removed under reduced pressure and the crude residue was taken up in H_2O (100 mL). The aqueous layer was extracted with EtOAc (3x50 mL), and the combined organic layers were dried over Na_2SO_4 and concentrated *in vacuo*. The crude material was purified by flash column chromatography (20% EtOAc/hexanes) to afford **2.713b** (400 mg, 67% yield). **HRMS (ESI-TOF)** (m/z): [M+Na]+ calcd for 691.1973, found 691.1967. $C_{38}H_{36}O_9SNa$ **^{1}H NMR** (500 MHz, $CDCl_3$) δ 7.76 (d, *J* = 7.2 Hz, 3H), 7.64 – 7.60 (m, 2H), 7.55 – 7.49 (m, 4H), 7.40 (d, *J* = 7.8 Hz, 4H), 7.30 (dd, *J* = 6.8,

1.9 Hz, 5H), 5.35 (t, *J* = 9.2 Hz, 1H), 5.00 (t, *J* = 9.7 Hz, 1H), 4.90 (t, *J* = 9.8 Hz, 1H), 4.75 (d, *J* = 10.1 Hz, 1H), 4.38 (dq, *J* = 23.0, 5.2 Hz, 5H), 4.24 (dt, *J* = 18.4, 7.3 Hz, 2H), 3.89 – 3.84 (m, 1H), 2.10 (s, 3H), 1.94 (s, 3H).



2.71b **2.71c**

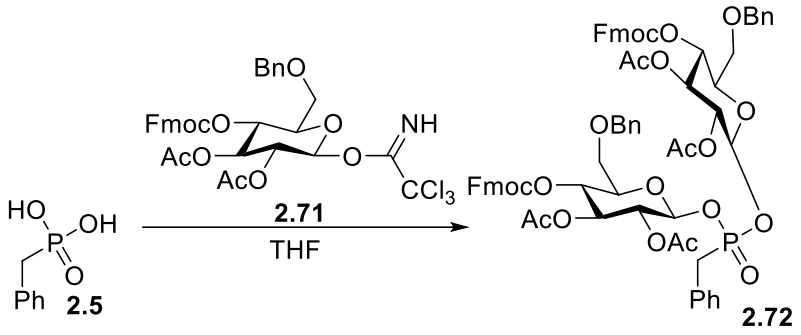
Intermediate 2.63c: NBS (0.29 g, 1.6 mmol, 1.5 eq) was added to a stirred solution of **2.71b** (0.73 g, 1.1 mmol, 1.0 eq) in acetone:H_2O (20:2 mL) at room temperature. The reaction was stirred at room temperature for 24 hours. The solvent was evaporated under reduced pressure and the crude residue was purified by flash column chromatography to afford **2.71c** (390 mg, 62% yield) as a white solid. **^{1}H NMR** (400 MHz, $CDCl_3$) δ 7.77 (d, *J* = 7.5 Hz, 2H), 7.55 (q, *J* = 6.9 Hz, 2H), 7.41 (t, *J* = 7.3 Hz, 2H), 7.37 – 7.11 (m, 7H), 5.65 (t, *J* = 9.9 Hz, 1H), 5.47 (t, *J* = 3.6 Hz, 1H), 5.04 – 4.85 (m, 2H), 4.54 (q, *J* = 12.3 Hz, 2H), 4.43 – 4.08 (m, 4H), 3.63 (dd, *J* = 11.4, 4.4 Hz, 2H), 2.08 (d, *J* = 1.0 Hz, 3H), 1.97 (t, *J* = 1.6 Hz, 3H).



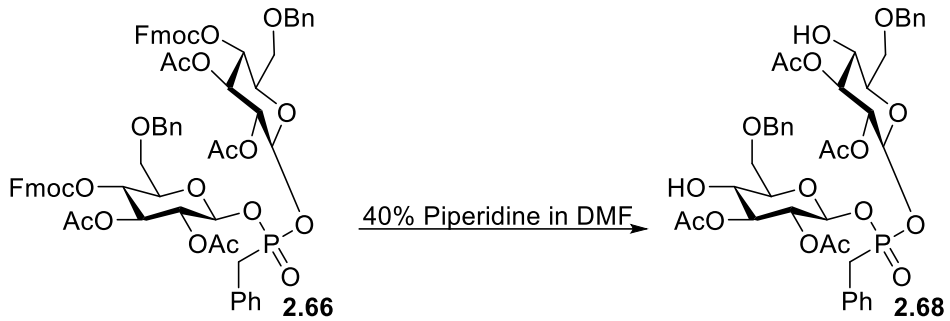
2.71c **2.71**

Trichloroacetimidate 2.71: CCl_3CN (0.35 mL, 3.5 mmol, 3.0 eq) was added to a stirred solution of **2.63c** (0.67 g, 1.2 mmol, 1.0 eq) and NaH (60% in mineral oil, 0.014 g, 0.35 mmol, 0.3 eq) in CH_2Cl_2 (5 mL). The reaction was stirred at room temperature for 24 hours. The reaction mixture was concentrated, and the crude residue was purified by flash column chromatography (10-50% EtOAc/hexanes) to afford **2.63** (430 mg, 51% yield, 1:1 mixture of diastereomers) as an amber oil. **HRMS (ESI-TOF)** (m/z): [M+Na]+ calcd for $C_{34}H_{32}Cl_3NO_{10}Na$ 744.0955, found 744.0962. **^{1}H NMR** (500 MHz, $CDCl_3$) δ 8.73 (s, 1H), 8.67 (s, 1H), 7.77 (d, *J* = 7.5 Hz, 5H), 7.62 – 7.51

(m, 5H), 7.41 (t, *J* = 7.5 Hz, 5H), 7.30 (d, *J* = 12.5 Hz, 12H), 7.21 (t, *J* = 5.8 Hz, 2H), 6.59 (d, *J* = 3.7 Hz, 1H), 5.91 (d, *J* = 8.0 Hz, 1H), 5.70 (t, *J* = 10.1 Hz, 1H), 5.40 (t, *J* = 9.2 Hz, 1H), 5.30 (t, *J* = 8.6 Hz, 1H), 5.15 (ddd, *J* = 21.5, 18.0, 9.7 Hz, 3H), 4.61 – 4.46 (m, 4H), 4.42 – 4.36 (m, 2H), 4.31 – 4.23 (m, 3H), 4.17 (q, *J* = 7.3 Hz, 2H), 3.97 (dd, *J* = 9.3, 4.7 Hz, 1H), 3.74 – 3.64 (m, 4H), 2.02 (s, 3H), 2.01 (s, 3H), 1.99 (s, 5H), 1.98 (s, 3H).

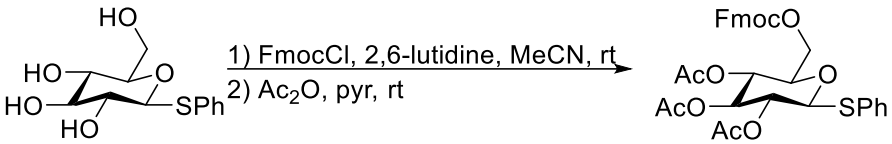


Phosphonate 2.72: Benzylphosphonic acid **2.5** (10 mg, 0.13 mmol, 1.0eq) was suspended in THF (1.0mL) with activated 4Å molecular sieves and stirred at room temperature for 30 minutes under N_2. Donor **2.71** was added, and the solution was stirred at room temperature for 24 hours. The reaction was filtered through Celite^{TM} and concentrated under reduced pressure. The crude residue was purified by flash column chromatography (10% MeOH/CH_2Cl_2) to afford **2.72** (33mg, 44% yield) as a white solid**. HRMS** (ESI-TOF) (m/z): [M+Na]+ calcd for $C_{71}H_{69}PO_{21}Na$ 1311.3961, found 1311.3951.



Phosphonate 2.73: Bisfunctionalized benzylphosphonate **2.72** (32 mg, 0.025 mmol, 1.0 eq) was stirred in a 15% solution of Et_3N in pyridine (1.0 mL) for 18 hours. The solvents were removed under reduced pressure and the crude residue was purified by flash column chromatography (50-100% EtOAc/hexanes). Bisfunctionalized benzylphosphonate **2.73** (10 mg, 48%) was afforded as a white solid. **HRMS** (ESI-TOF) (m/z): [M+Na]+ calcd for $C_{41}H_{49}PO_{17}Na$ 867.2760, found 867.2688.

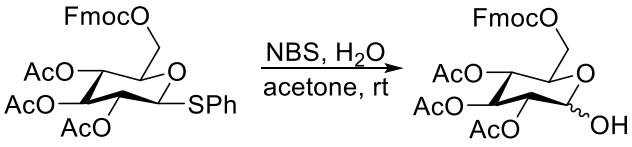
Synthesis of glucose donor 2.78



2.62a **2.78a**

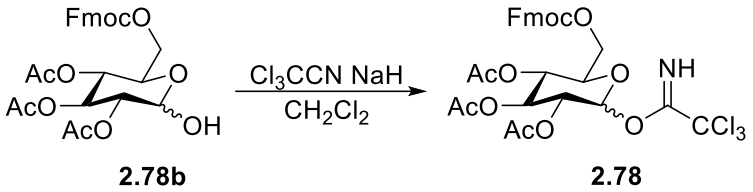
Intermediate 2.75a: Fmoc chloride (1.4 g, 5.5 mmol, 1.5 eq) was added portion wise to a stirred suspension of **2.62a**[70] (1.0 g, 3.7 mmol, 1.0 eq) and 2,6-lutidine (0.85 mL, 7.3 mmol, 2.0 eq) in MeCN (25 mL) at room temperature. The reaction was stirred at room temperature for 18 hours. The reaction was quenched by addition of MeOH (10 mL), and the solvents were removed under reduced pressure. The crude residue was dissolved in pyridine (20 mL) and Ac_2O (3.5 mL, 37 mmol, 10 eq) was added in one portion at room temperature. The reaction was stirred for 18 hours at room temperature. The solvent was evaporated under reduced pressure, the crude residue was diluted with 1N HCl (100 mL) and extracted with EtOAc (3x100 mL). The combined organic layers were washed with brine, dried over Na_2SO_4, and concentrated *in vacuo*. The crude residue was purified by flash column chromatography (20% EtOAc/hexanes) to afford **2.75a** (1.5 g, 66% yield) as a white solid. **HRMS (ESI-TOF)** (m/z): [M+Na]+ calcd for $C_{32}H_{30}O_{10}SNa$ 643.1609, found 643.1598. **^{1}H NMR** (500 MHz, $CDCl_3$) δ 7.78 (d, *J* = 7.6 Hz, 2H), 7.68 – 7.60 (m, 2H), 7.50 (tt, *J* = 4.5, 2.5 Hz, 2H), 7.42 (t, *J* = 7.5 Hz, 2H), 7.36 – 7.27 (m,

5H), 5.24 (q, *J* = 9.6 Hz, 1H), 5.09 – 4.94 (m, 2H), 4.71 (dd, *J* = 10.1, 5.7 Hz, 1H), 4.50 – 4.37 (m, 2H), 4.35 – 4.18 (m, 3H), 3.77 (ddd, *J* = 9.4, 5.9, 2.9 Hz, 1H), 2.10 (s, 3H), 2.01 (s, 3H), 2.00 (s, 3H). **^{13}C{^{1}H} NMR** (126 MHz, $CDCl_3$) NMR δ 170.2, 169.5, 169.3, 154.8, 143.3, 143.2, 141.3, 133.1, 133.0, 131.7, 129.0, 129.0, 128.4, 127.9, 127.2, 125.2, 125.2, 120.1, 85.8, 75.6, 73.8, 70.1, 69.9, 68.6, 66.1, 46.7, 20.8, 20.6, 20.6.



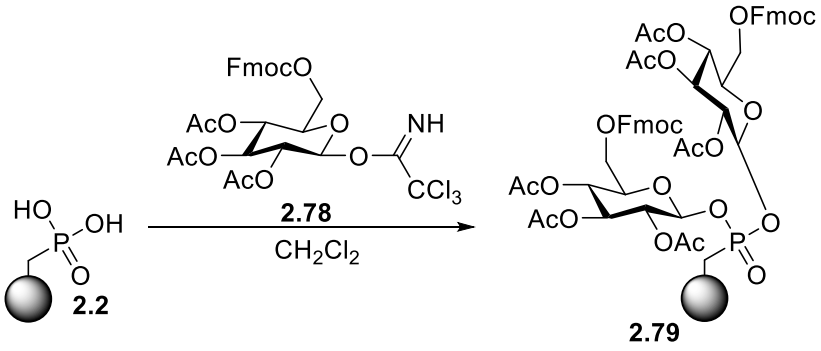
2.78a **2.78b**

Intermediate 2.78b: Thioglycoside **2.78a** (1.4 g, 2.3 mmol, 1.0eq) was dissolved in an acetone (40 mL)/H_2O (4 mL) mixture. NBS (0.80 g, 4.6 mmol, 2 eq) was added and the reaction was stirred at 35 ^{o}C for 18 hours. The solvent was evaporated, the residue was dissolved in CH_2Cl_2 (100 mL) and washed with H_2O (2x50 mL). The organic fraction was dried over Na_2SO_4 and concentrated *in* vacuo. The crude residue was purified by flash column chromatography (25-50% EtOAc/hexanes) to afford **2.78b** (0.90 g, 74% yield) as a white solid. **HRMS (ESI-TOF)** (m/z): $[M+Na]^+$ calcd for $C_{27}H_{28}O_{11}Na$ 551.1524, found 551.1515. **^{1}H NMR** (500 MHz, $CDCl_3$) δ 7.73 (d, *J* = 7.6 Hz, 2H), 7.59 (t, *J* = 6.9 Hz, 2H), 7.37 (t, *J* = 7.5 Hz, 2H), 7.30 (td, *J* = 7.4, 1.2 Hz, 2H), 5.56 (t, *J* = 9.8 Hz, 1H), 5.46 (t, *J* = 3.6 Hz, 1H), 5.10 (t, *J* = 9.8 Hz, 1H), 4.92 – 4.88 (m, 1H), 4.65 (d, *J* = 4.1 Hz, 1H), 4.46 – 4.32 (m, 2H), 4.32 – 4.18 (m, 3H), 2.05 (s, 3H), 2.01 (d, *J* = 1.5 Hz, 3H), 2.00 (s, 3H). **^{13}C{^{1}H} NMR** (126 MHz, $CDCl_3$) δ 170.2, 170.1, 169.7, 155.0, 143.4, 143.2, 141.3, 127.9, 127.2, 125.3, 125.2, 120.1, 90.2, 71.0, 70.2, 69.7, 68.8, 67.3, 65.9, 46.7, 20.75, 20.73, 20.66



2.78b **2.78**

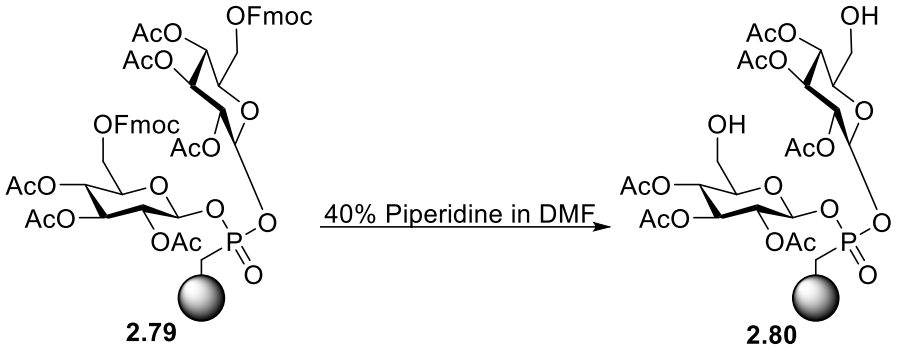
Trichloroacetimidate 2.78: NaH (60% dispersion in mineral oil, 2.2 mg, 0.057 mmol, 0.10 eq) was added to a stirred solution of **2.78b** (300 mg, 0.57 mmol, 1.0 eq) and Cl_3CCN (1.1 mL, 11 mmol, 20eq) in CH_2Cl_2 (5 mL). The reaction was stirred at room temperature for 18 hours. The solvent was evaporated, and the crude residue was purified by flash column chromatography (20% EtOAc/hexanes) to afford **2.78** (250 mg, 65% yield, 5.5:1α:β) as a white solid. **HRMS (ESI-TOF)** (m/z): [M+Na]+ calcd for $C_{29}H_{28}O_{11}NCl_3Na$ 696.0591, found 696.0576. **^{1}H NMR** (500 MHz, $CDCl_3$) (major, α-anomer) δ 8.69 (s, 1H), 7.77 (d, *J* = 7.5 Hz, 2H), 7.68 – 7.58 (m, 2H), 7.41 (t, *J* = 7.5 Hz, 2H), 7.33 (tt, *J* = 7.5, 1.4 Hz, 2H), 6.59 (d, *J* = 3.7 Hz, 1H), 5.60 (t, *J* = 9.8 Hz, 1H), 5.23 (t, *J* = 9.7 Hz, 1H), 5.17 (dd, *J* = 10.2, 3.7 Hz, 1H), 4.42 (dd, *J* = 10.3, 7.4 Hz, 1H), 4.37 – 4.32 (m, 2H), 4.31 – 4.23 (m, 3H), 2.06 (s, 3H), 2.05 (s, 3H), 2.03 (s, 3H);. **^{13}C{^{1}H} NMR** (126 MHz, $CDCl_3$) (major, α-anomer) δ 170.0, 169.9, 169.6, 160.8, 154.8, 143.4, 143.2, 141.3, 127.92, 127.91, 127.2, 125.3, 125.2, 120.1, 120.0, 92.8, 90.7, 77.2, 70.3, 69.9, 69.8, 69.7, 68.1, 65.2, 46.6, 20.7, 20.6, 20.5.



2.79

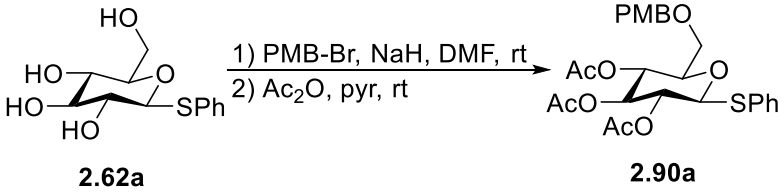
Resin 2.79: Phosphonic acid resin **2.2** (134 mg, 0.17 mmol, 1.0 eq) was suspended in CH_2Cl_2 (2.0 mL) and stirred at room temperature for 30 minutes. Donor **2.78** (258 mg, 0.38 mmol, 2.2

eq) was added, and the suspension was stirred at room temperature for 24 hours. The suspension was filtered, and the resin was washed with CH_2Cl_2 (10x5 mL) and dried thoroughly under vacuum. Resin **2.79** (223mg, 70% yield, 0.76mmol/g) was afforded as an orange solid.



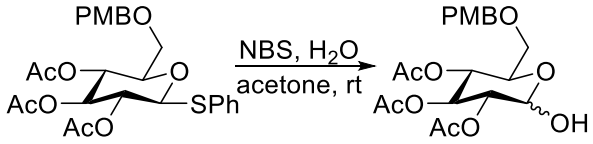
Resin 2.80: Resin **2.79** (213 mg, 0.17mmol, 1.0 eq) was swelled in a 40% solution of piperidine in DMF (2.0 mL) for one hour. The resin was filtered washed extensively with CH_2Cl_2 (10x5 mL) and dried thoroughly under vacuum. Resin **2.77** (163mg, 92%, 0.63mmol/g) was afforded as a dark orange. Cleavage of the Fmoc group was confirmed by HRMS detection of dibenzofulvene in the filtrate after washing: **HRMS** (ESI-TOF) (m/z): [M+H]+ calcd for $C_{14}H_{10}H$ 179.0856, found 179.0855.

Synthesis of glucose donor 2.90



Intermediate 2.90a: NaH (60% in mineral oil, 0.74 g, 19 mmol, 4.0 eq) was added portion wise to a stirred suspension of **2.62a** (1.3 g, 4.6 mmol, 1.0 eq) in DMF (40 mL) at room temperature. The reaction was stirred for one hour, until the gas evolution ceased. Freshly prepared PMB-Br[74] (1.2 g, 6.0 mmol, 1.3 eq) was added dropwise to the reaction at room temperature. The reaction was stirred for one hour at room temperature. Ac_2O (3.5 mL, 37 mmol, 8.0 eq) was added and

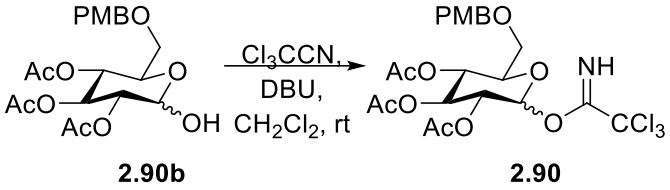
the reaction was stirred for two additional hours. The solvent was removed under reduced pressure and the crude residue was purified by flash column chromatography (20-50% EtOAc/hexanes) to afford **2.90a** (0.84 g, 35%) as white solid. **HRMS** (ESI-TOF) (m/z): $[M+Na]^+$ calcd for $C_{26}H_{30}O_9SNa$ 541.1497, found 541.1498. **^{1}H NMR** (500 MHz, $CDCl_3$) δ 7.50 (dd, *J* = 7.7, 1.7 Hz, 2H), 7.34 – 7.27 (m, 3H), 7.23 (d, J = 8.6 Hz, 2H), 6.90 – 6.83 (m, 2H), 5.21 (t, *J* = 9.3 Hz, 1H), 5.03 (t, *J* = 9.8 Hz, 1H), 4.98 (t, *J* = 9.6 Hz, 1H), 4.72 (d, *J* = 10.1 Hz, 1H), 4.45 (q, *J* = 11.5 Hz, 2H), 3.81 (s, 4H), 3.69 (dt, *J* = 10.0, 4.3 Hz, 1H), 3.56 (d, *J* = 4.2 Hz, 2H), 2.08 (s, 3H), 1.98 (s, 3H), 1.93 (s, 3H)..0, 4.3 Hz, 1H), 3.6 (d, *J* = 4.2 Hz, 2H), 2.1 (s, 3H), 2.0 (s, 3H), 1.9 (s, 3H). **^{13}C{^{1}H} NMR** (126 MHz, $CDCl_3$) δ 170.3, 169.5, 169.3, 159.3, 132.7, 132.2, 129.9, 129.5, 129.0, 128.2, 113.8, 85.8, 77.5, 74.1, 73.3, 70.1, 69.1, 68.8, 55.3, 20.8, 20.7.



2.90a **2.90b**

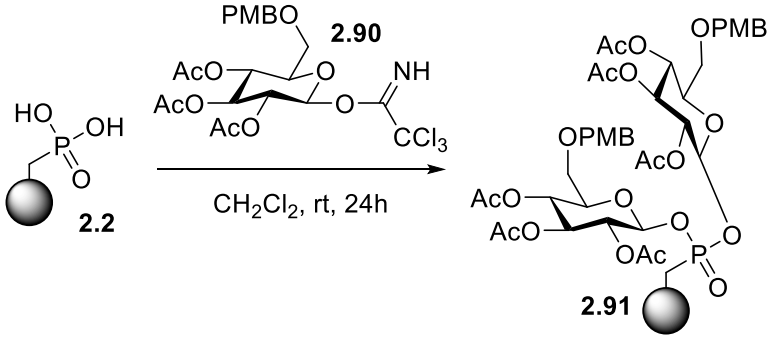
Intermediate 2.90b: NBS (0.11 g, 0.64 mmol, 2 eq) was added to a solution of **2.90a** (0.17 g, 0.32 mmol, 1.0 equiv) in an acetone:DCM:H_2O (5:1:0.5 mL) mixture. and the reaction was stirred at room temperature for 18 hours. The solvent was evaporated, the residue was dissolved in CH_2Cl_2 (100 mL) and washed with H_2O (2x50 mL). The organic fraction was dried over Na_2SO_4 and concentrated *in* vacuo. The crude residue was purified by flash column chromatography (50% EtOAc/hexanes) to afford **2.90b** (0.056 g, 41% yield) as a white solid. **HRMS** (ESI-TOF) (m/z): $[M+Na]^+$ calcd for $C_{20}H_{26}O_{10}Na$ 449.1418, found 449.1401. **^{1}H NMR** (500 MHz, $CDCl_3$) δ 7.23 (d, *J* = 3.0 Hz, 2H), 6.90 – 6.85 (m, 2H), 5.52 (t, *J* = 9.8 Hz, 1H), 5.43 (d, *J* = 3.7 Hz, 1H), 5.07 – 5.00 (m, 1H), 4.89 (dt, *J* = 9.8, 3.0 Hz, 1H), 4.53 – 4.47 (m, 1H), 4.42 (d, *J* = 11.6 Hz, 1H), 4.22 (ddd, *J* = 10.3, 5.0, 3.3 Hz, 1H), 3.80 (s, 3H), 3.51 – 3.45 (m, 2H),

2.07 (s, 3H), 2.00 (s, 3H), 1.94 (s, 3H). **$^{13}C\{^{1}H\}$ NMR** (126 MHz, $CDCl_3$) δ 170.3, 170.2, 169.8, 159.4, 129.7, 129.5, 113.8, 90.0, 73.2, 71.2, 70.1, 69.3, 68.3, 68.2, 55.3, 29.6, 29.6, 20.8, 20.7, 20.7.

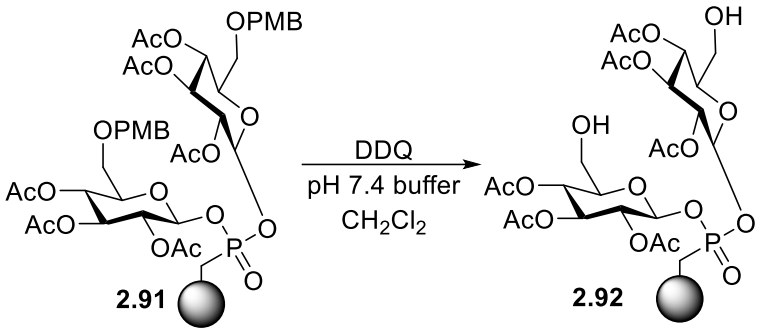


2.90b **2.90**

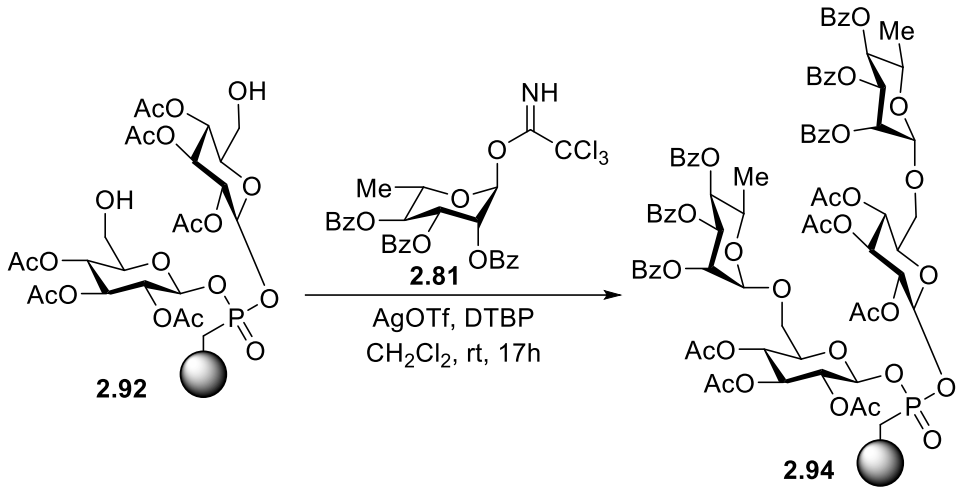
Trichloroacetimidate 2.90:. CCl_3CN (1.2 mL, 12 mmol, 10 equiv) was added to a stirred solution of **2.90b** (0.52 g, 1.2 mmol, 1.0 equiv) and DBU (0.055 mL, 0.37 mmol, 0.3 equiv) in CH_2Cl_2 (12 mL). The reaction was stirred at room temperature for 24 hours. The reaction mixture was concentrated, and the crude residue was purified by flash column chromatography (15-50% EtOAc/hexanes) to afford **2.90** (288 mg, 41% yield) as an amber oil. **HRMS** (ESI-TOF) (m/z): $[M+Na]^+$ calcd for $C_{22}H_{26}Cl_3NO_{10}Na$ 592.0514, found 592.0517. **^{1}H NMR** (500 MHz, $CDCl_3$) δ 8.65 (s, 1H), 7.22 (d, *J* = 8.6 Hz, 2H), 6.86 (d, *J* = 8.6 Hz, 2H), 6.57 (d, *J* = 3.7 Hz, 1H), 5.54 (t, *J* = 9.9 Hz, 1H), 5.27 (t, *J* = 9.9 Hz, 1H), 5.12 (dd, *J* = 10.2, 3.7 Hz, 1H), 4.51 (d, *J* = 11.7 Hz, 1H), 4.38 (d, *J* = 11.7 Hz, 1H), 4.15 (dt, *J* = 10.3, 3.4 Hz, 1H), 3.80 (s, 3H), 3.59 – 3.46 (m, 2H), 2.03 (s, 3H), 2.00 (s, 3H), 1.92 (s, 3H). **$^{13}C\{^{1}H\}$ NMR** (126 MHz, $CDCl_3$) δ 170.2, 169.9, 169.5, 160.9, 159.3, 129.6, 113.8, 93.1, 90.8, 73.1, 71.2, 70.1, 69.9, 68.5, 67.3, 55.3, 46.1, 20.8, 20.6, 20.5.



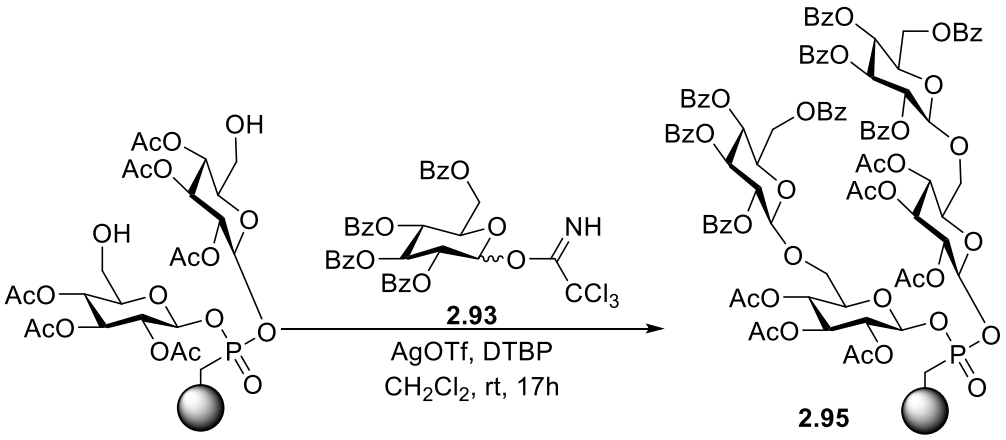
Resin 2.91: Phosphonic acid resin **2.2** (50 mg, 0.07 mmol, 1.0 equiv) was suspended in anhydrous CH_2Cl_2 (2.0 mL). Glucosyl trichloroacetimidate **2.90** (76 mg, 0.13 mmol, 2.1 equiv) was added and the reaction was stirred at room temperature for 18 hours. The reaction was filtered, washed with DCM (3x10 mL), and dried under vacuum to afford resin **2.91** (71 mg, 68%, 0.71 mmol/g) as an orange solid.



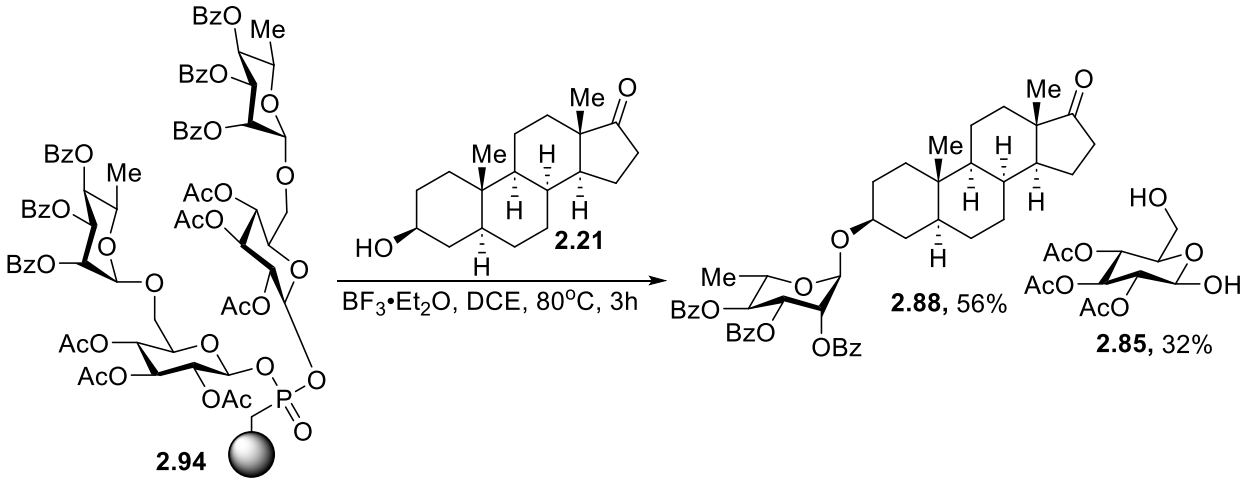
Resin 2.92: Resin **2.91** (71 mg, 0.05 mmol, 1.0 equiv) was swelled in CH_2Cl_2 for 30 minutes. Aqueous pH 7 buffer (0.2 mL) (Honeywell, cat #33646) was added followed by DDQ (17 mg, 0.08 mmol, 1.5 equiv) and the reaction was stirred at room temperature for 4 hours. The resin was filtered and washed extensively with DCM (10x5 mL) and dried thoroughly under vacuum) to afford **2.92** (61 mg, 94%, 0.62 mmol/g) as a light brown solid. Cleavage of the PMB group was confirmed by the formation of *p*-methoxybenzaldehyde (HRMS (ESI-TOF) (m/z): $[M+H]^+$ calcd for $C_8H_8O_2H$ 137.0597, found 137.0624)



Resin 2.94: Resin **2.92** (61 mg, 0.04 mmol, 1.0 equiv) was suspended in anhydrous CH_2Cl_2 (2.0 mL) for 20 minutes. Rhamnosyl trichloroacetimidate **2.81**[26] (118 mg, 0.19 mmol, 5.0 equiv), AgOTf (49 mg, 0.19 mmol, 5.0 equiv) and 2,6-di-*tert*-butyl-pyridine (82 µL, 0.38 mmol, 10.0 equiv) were added to the resin suspension and the reaction was stirred at room temperature for 17 hours. The reaction was filtered and washed extensively with CH_2Cl_2 (20x5 mL) to ensure all excess donor and base were removed. The resin was dried under vacuum to afford **2.94** (90.4 mg, 115%, 0.48mmol/g) as a brown solid. Full removal of the excess donor was confirmed by TLC, and the excess weight of the resin is likely resultant of an insoluble Ag-impurity that was not removed by filtration. The resin was carried forward without further purification. Attempts to remove Ag-impurities via basic wash (NH_3/H_2O or KCN/H_2O) were unsuccessful.

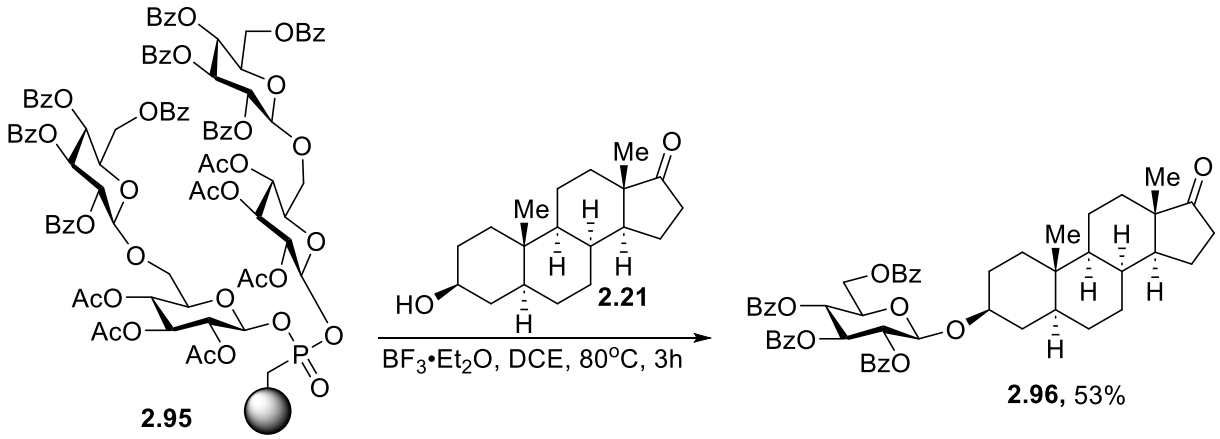


Resin 2.95: Resin **2.92** (90 mg, 0.02 mmol, 1.0 equiv) was suspended in anhydrous CH_2Cl_2 (2.0 mL) for 20 minutes. Rhamnosyl trichloroacetimidate **2.93**[75] (64 mg, 0.09 mmol, 5.0 equiv), AgOTf (22 mg, 0.09 mmol, 5.0 equiv) and 2,6-di-*tert*-butyl-pyridine (37 µL, 0.17 mmol, 10.0 equiv) were added to the resin suspension and the reaction was stirred at room temperature for 17 hours. The reaction was filtered and washed extensively with CH_2Cl_2 (20x5 mL) to ensure all excess donor and base were removed. The resin was dried under vacuum to afford **2.95** (100 mg, 99%, 0.17mmol/g) as a brown solid. Full removal of the excess donor was confirmed by TLC, and the excess weight of the resin is likely resultant of an insoluble Ag-impurity that was not removed by filtration. The resin was carried forward without further purification. Attempts to remove Ag-impurities via basic wash (NH_3/H_2O or KCN/H_2O) were unsuccessful.



Glycoside product 2.88: Resin **2.94** (90.4 mg, 0.04 mmol, 2.0 equiv), DCE (2.0 mL), and 4Å molecular sieves were added to a plastic vial. The resin was swelled at room temperature for 20 minutes. Glycosyl acceptor *trans*-androsterone (5.5 mg, 0.02 mmol, 1.0 equiv) was added, and the reaction was heated to 80°C. $BF_3{\cdot}Et_2O$ (4 µL, 0.03 mmol, 1.5 equiv) was added and the reaction progress was monitored by TLC for 3 hours. Upon full consumption of the acceptor, the reaction mixture was filtered, and the resin was washed with CH_2Cl_2 (3x5 mL), EtOAc (3x5

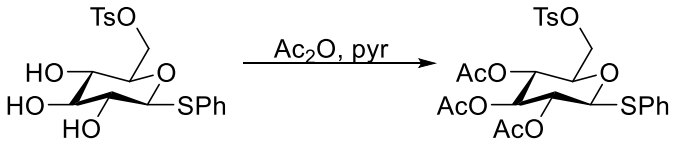
mL), and CH_2Cl_2 (3x5 mL), and the filtrate was then quenched with Et_3N (50 µL). The filtrate was concentrated, and the crude residue was purified by flash column chromatography (30% EtOAc/hexanes) to afford **2.88** (7.9 mg, 56% yield) and **2.85**[76] (3.7 mg, 32% yield). **2.88**: $\mathbf{R_f}$ = 0.84 (50% EtOAc/hexanes). **HRMS** (ESI-TOF) (m/z): $[M+Na]^+$ calcd for $C_{46}H_{52}O_9Na$ 771.3504, found 771.3495. **^{1}H NMR** (500 MHz, $CDCl_3$) δ 8.10 (d, *J* = 8.4 Hz, 3H), 7.98 (d, *J* = 7.8 Hz, 2H), 7.82 (d, *J* = 7.9 Hz, 2H), 7.61 (t, *J* = 7.5 Hz, 1H), 7.51 (dt, *J* = 14.7, 7.7 Hz, 4H), 7.40 (q, *J* = 8.8, 7.7 Hz, 3H), 5.85 (dd, *J* = 10.2, 3.3 Hz, 1H), 5.66 (t, *J* = 10.0 Hz, 1H), 5.59 (s, 1H), 5.17 (s, 1H), 4.26 (dq, *J* = 12.2, 7.0 Hz, 1H), 3.65 (dq, *J* = 10.8, 5.3, 4.7 Hz, 1H), 2.44 (dd, *J* = 19.4, 8.9 Hz, 1H), 2.13 – 2.02 (m, 1H), 1.93 (dd, *J* = 13.5, 5.9 Hz, 2H), 1.85 – 1.46 (m, 8H), 1.44 – 1.39 (m, 1H), 1.35 (s, 3H), 1.32 (s, 1H), 1.15 – 0.93 (m, 3H), 0.89 (s, 3H), 0.88 – 0.86 (m, 6H), 0.82 (d, *J* = 14.5 Hz, 1H), 0.73 (d, *J* = 11.9 Hz, 1H). **2.85:** R_f = 0.42 (50% EtOAc/hexanes). ^{1}H NMR (500 MHz, CDCl3) δ 5.47 (s, 1H), 4.87 (s, 1H), 4.70 – 4.59 (m, 3H), 4.10 (d, *J* = 7.9 Hz, 1H), 3.81 (t, *J* = 7.0 Hz, 1H), 2.18 (s, 3H), 2.15 (s, 3H), 2.12 (s, 3H).



Glycoside product 2.96[77]: Resin **2.95** (90 mg, 0.044mmol, 1.0 eq) was swelled in DCE (2.0 mL) for 30 minutes at room temperature with 4Å molecular sieves and *trans*-androsterone **2.21** (12.7 mg, 0.044 mmol, 1.0 eq). $BF_3{\cdot}Et_2O$ (0.0081 mL, 0.066 mmol, 1.5 eq) was added and the reaction was heated to 80 °C and stirred for three hours, at which time all starting material was consumed

by TLC. No steroidal disaccharide was isolated; however, it was detected by **HRMS** (ESI-TOF) (m/z): [M+Na]+ calcd for$C_{65}H_{72}O_{19}Na$: 1179.4560, found 1179.4627). **2.96** was the major steroidal glycoside isolated (8.0mg, 53%), **2.93**: **HRMS** (ESI-TOF) (m/z): [M+Na]+ calcd for $C_{53}H_{56}O_{11}Na$891.3715, found 891.3714. **^{1}H NMR** (700 MHz, $CDCl_3$) δ 8.01 (d, *J* = 7.7 Hz, 2H), 7.96 (d, *J* = 7.8 Hz, 2H), 7.90 (d, *J* = 7.8 Hz, 2H), 7.83 (d, *J* = 7.7 Hz, 2H), 7.52 (dq, *J* = 23.5, 7.4 Hz, 3H), 7.43 (t, *J* = 7.5 Hz, 1H), 7.39 (td, *J* = 7.5, 4.7 Hz, 4H), 7.34 (s, 1H), 7.28 (t, *J* = 7.7 Hz, 2H), 7.16 (dd, *J* = 15.8, 7.6 Hz, 1H), 5.89 (t, *J* = 9.6 Hz, 1H), 5.62 (t, *J* = 9.7 Hz, 1H), 5.48 (dd, *J* = 9.8, 7.9 Hz, 1H), 4.94 (d, *J* = 7.8 Hz, 1H), 4.60 (dd, *J* = 12.0, 3.3 Hz, 1H), 4.53 (dd, *J* = 12.0, 6.0 Hz, 1H), 4.15 (ddd, *J* = 9.9, 6.0, 3.4 Hz, 1H), 3.59 (tt, *J* = 11.2, 5.3 Hz, 1H), 2.43 (dt, *J* = 18.8, 8.7 Hz, 1H), 2.19 – 2.01 (m, 2H), 1.94 – 1.86 (m, 2H), 1.81 – 1.76 (m, 2H), 1.74 – 1.71 (m, 1H), 1.69 – 1.29 (m, 7H), 1.18 (ddd, *J* = 25.6, 14.3, 8.8 Hz, 2H), 1.02 – 0.93 (m, 2H), 0.91 – 0.87 (m, 2H), 0.83 (s, 3H), 0.71 (s, 3H), 0.60 (td, *J* = 11.1, 3.8 Hz, 1H).

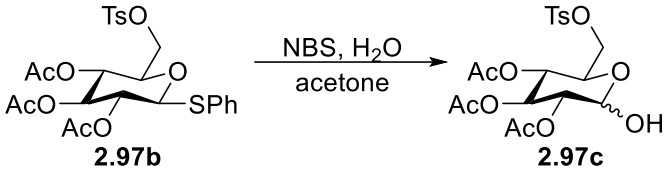
Synthesis of glucose donor 2.97.



2.97a **2.97b**

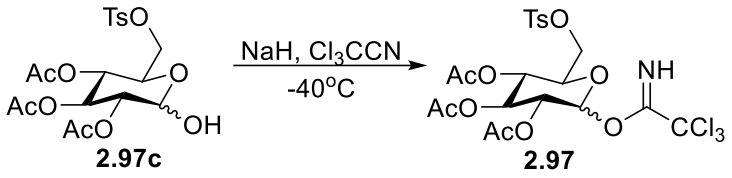
Intermediate 2.97b: Ac_2O (1.5 mL, 17 mmol, 6.0 eq) was added to a stirred solution of **2.97a**[78] (1.2 g, 2.8 mmol, 1.0 eq) in pyridine (5.0ml) and the reaction was stirred for three hours at room temperature. The reaction mixture was quenched with sat. aq. $NaHCO_3$ (250 mL) and extracted with EtOAc (3x100 mL). The combined organic fractions were washed with 1N HCl (aq) (2x100 mL), dried over Na_2SO_4, and concentrated *in vacuo*. The product **2.97b** (1.0 g, 65%) was obtained and used without further purification. **HRMS** (ESI-TOF) (m/z): [M+Cs]+ calcd for $C_{25}H_{28}O_{10}S_2Cs$ 685.0173, found 685.0187 **^{1}H NMR** (500 MHz, $CDCl_3$) δ 7.78 (d, *J* = 8.3 Hz, 2H), 7.41 (dd, *J* = 8.0, 1.6 Hz, 2H), 7.34 – 7.28 (m, 3H), 5.18 (t, *J* = 9.3 Hz, 1H), 4.92 – 4.86 (m,

2H), 4.65 (d, *J* = 10.1 Hz, 1H), 4.15 (d, *J* = 2.7 Hz, 0H), 4.06 (dd, *J* = 11.0, 6.1 Hz, 1H), 3.79 – 3.70 (m, 1H), 2.44 (s, 3H), 2.07 (s, 3H), 2.00 (s, 3H), 1.97 (s, 3H). **^{13}C NMR** (126 MHz, $CDCl_3$) δ 170.2, 169.6, 169.3, 145.3, 133.1, 132.5, 131.6, 130.1, 129.2, 128.6, 128.3, 85.8, 75.6, 73.8, 69.8, 68.5, 67.8, 21.8, 20.9, 20.9, 20.9, 20.7, 20.7. **FTIR** (thin film, cm^{-1}): 2941, 1747, 1598, 1482, 1440, 1366, 1341, 1234, 1211, 1190, 1172, 1088, 1034, 995. 967, 939, 912, 809, 782, 747. 689, 610, 597, 567, 551, 532..

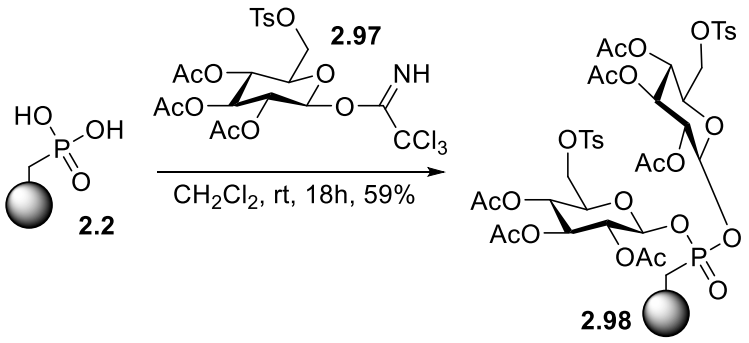


2.97b **2.97c**

Intermediate 2.97c: NBS (0.29 g, 1.6 mmol, 2.0 eq) was added to a solution of **2.97b** (0.45 g, 0.81 mmol, 1.0 eq) in an acetone (8 mL)/H_2O (0.8 mL) mixture. The reaction was stirred at room temperature for 18 hours while excluding light. The solvent was then evaporated, the residue was dissolved in CH_2Cl_2 (100 mL) and washed with H_2O (2x 50mL). The organic fraction was dried over Na_2SO_4 and concentrated *in* vacuo. The crude residue was purified by flash column chromatography (30-50% EtOAc/hexanes) to afford **2.97c** (0.18 g, 47% yield) as a white solid. **HRMS** (ESI-TOF) (m/z): $[M+NH_4]+$ calcd for $C_{25}H_{28}O_{10}S_2NH_4$ 478.1377, found 478.1369. **^{1}H NMR** (500 MHz, $CDCl_3$) ^{1}H NMR (500 MHz, $cdcl_3$) δ 7.79 (dd, *J* = 8.2, 2.1 Hz, 2H), 7.35 (d, *J* = 7.9 Hz, 2H), 5.48 (t, *J* = 9.8 Hz, 1H), 5.38 (s, 1H), 5.02 – 4.89 (m, 1H), 4.88 – 4.73 (m, 1H), 4.28 (ddd, *J* = 10.6, 5.5, 2.4 Hz, 1H), 4.11 – 3.98 (m, 2H), 2.46 (d, *J* = 2.2 Hz, 3H), 2.07 (d, *J* = 1.9 Hz, 3H), 2.05 (d, *J* = 1.8 Hz, 3H), 2.00 (s, 3H). **^{13}C{^{1}H} NMR** (126 MHz, $CDCl_3$) δ 170.2, 170.1, 169.6, 145.2, 132.5, 129.9, 128.1, 90.0, 70.8, 69.6, 68.7, 67.8, 67.1, 21.7, 20.7, 20.7, 20.6. (extra peaks in ^{13}C NMR δ 177.2, 29.6 correspond to succinimide by-product).

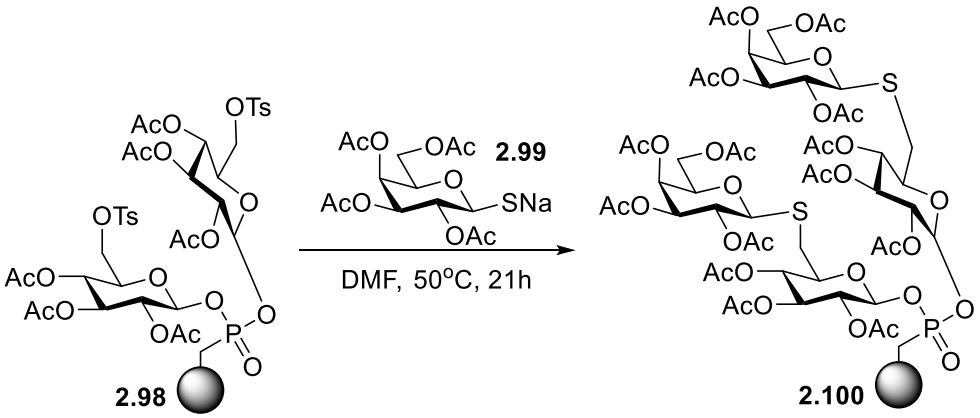


Trichloroacetimidate 2.97: NaH (60% dispersion in mineral oil, 0.12 g, 3.0 mmol, 8.0 eq) was added to a stirred solution of **2.97c** (0.17 g, 0.37 mmol, 1.0 eq) in Cl_3CCN (2.0 mL, 20 mmol, 55 eq) at -40 ^oC. The reaction was warmed to room temperature and stirred for one hour. The reaction then was quenched with sat. aq. $NaHCO_3$ (50 mL) and extracted with CH_2Cl_2 (3x25 mL). The combined organic layers were dried over Na_2SO_4 and concentrated *in vacuo*. The crude residue was purified by flash column chromatography (10% EtOAc/hexanes + 1% Et_3N) to afford **2.97** (0.16 g, 73% yield) as a white solid. **HRMS** (ESI-TOF) (m/z): $[M+NH_4]+$ calcd for $C_{25}H_{28}O_{10}S_2NH_4$ 621.0474, found 621.0477. **^{1}H NMR** (500 MHz, $CDCl_3$) δ 8.60 (s, 1H), 7.71 (d, *J* = 8.2 Hz, 2H), 7.18 (d, *J* = 0.5 Hz, 2H), 6.40 (d, *J* = 3.6 Hz, 1H), 5.50 – 5.40 (m, 1H), 5.02 (t, *J* = 9.9 Hz, 1H), 4.94 (dd, *J* = 10.2, 3.7 Hz, 1H), 4.08 – 4.05 (m, 3H), 2.38 (s, 3H), 1.97 (s, 3H), 1.95 (s, 3H), 1.94 (s, 3H).



Resin 2.98: Resin **2.2** (100 mg, 0.13 mmol, 1.0 equiv) was suspended in anhydrous CH_2Cl_2 (2.0 mL). Glucosyl trichloroacetimidate **2.97** (163 mg, 0.27 mmol, 2.1 equiv) was added and the reaction was stirred at room temperature for 18 hours. The reaction was filtered, washed with CH_2Cl_2 (3x10 mL), and dried under vacuum to afford resin **2.98** (128 mg, 59%, 0.49 mmol/g) as

a pale orange solid. **FTIR** (thin film, cm^{-1}): 3025, 2919, 1662, 1601, 1492, 1451, 1365, 1178, 1043, 906, 840, 755, 696, 548.



Resin 2.100: Resin **2.98** (128 mg, 0.062mmol, 1.0 eq) was swelled in DMF (2.0 mL) at room temperature for 30 minutes. The reaction was heated to 50°C and glucosyl thiolate **2.99**[79] (32.5mg, 0.084 mmol, 1.4eq) was added to the swelled resin. The reaction was stirred at 50°C for 18 hours. The resin was filtered, washed with CH_2Cl_2 (3x5 mL), H_2O (3x5 mL), and CH_2Cl_2 (3x5 mL) and dried under high-vac for 18 hours. The resin **2.97** (136mg, 96%) was compared by FTIR spectroscopy with the starting resin **2.98** and C6-tosyl-thioglycoside **2.97b**. It was determined that the reaction was incomplete as by the presence of the S=O stretch of the tosylate observed at $1365cm^{-1}$. **FTIR** (thin film, cm^{-1}): 3025, 2918, 1601, 1493, 1452, 1365, 1180, 1044, 907, 843, 756, 697, 592, 576, 545.

2.8 References

(1) Schuerch, C.; Frechet, J. M. Solid-Phase Synthesis of Oligosaccharides. I. Preparation of the Solid Support. Poly[p-(1-Propen-3-Ol-1-Yl)Styrene]. *J. Am. Chem. Soc.* **1971**, *93* (2), 492–496. https://doi.org/10.1021/ja00731a031.

(2) Seeberger, P. H.; Haase, W.-C. Solid-Phase Oligosaccharide Synthesis and Combinatorial Carbohydrate Libraries. *Chem Rev.* **2000**. *100 (12).* 4349–4394. https://doi.org/10.1021/cr9903104.

(3) Bennett, C. S. Principles of Modern Solid-Phase Oligosaccharide Synthesis. *Org. Biomol. Chem.* **2014**, *12* (11), 1686–1698. https://doi.org/10.1039/C3OB42343C.

(4) Plante, O. J.; Palmacci, E. R.; Seeberger, P. H. Automated Solid-Phase Synthesis of Oligosaccharides. *Science* **2001**, *291* (5508), 1523–1527. https://doi.org/10.1126/science.1057324.

(5) Ganesh, N.V.; Fujikawa, K.; Tan, Y. H.; Stine, K. J.; Demchenko, A. V. HPLC-Assisted Automated Oligosaccharide Synthesis. *Org. Lett*. **2012**. *14 (12)*. 3036–3039. https://doi.org/10.1021/ol301105y.

(6) Zhang, J.; Chen, C.; Gadi, M. R.; Gibbons, C.; Guo, Y.; Cao, X.; Edmunds, G.; Wang, S.; Liu, D.; Yu, J.; Wen, L.; Wang, P. G. Machine-Driven Enzymatic Oligosaccharide Synthesis by Using a Peptide Synthesizer. *Angewandte Chemie International Edition* **2018**, *57* (51), 16638–16642. https://doi.org/10.1002/anie.201810661.

(7) Yao, W.; Xiong, D.-C.; Yang, Y.; Geng, C.; Cong, Z.; Li, F.; Li, B.-H.; Qin, X.; Wang, L.-N.; Xue, W.-Y.; Yu, N.; Zhang, H.; Wu, X.; Liu, M.; Ye, X.-S. Automated Solution-Phase Multiplicative Synthesis of Complex Glycans up to a 1,080-Mer. *Nat. Synth* **2022**, *1* (11), 854–863. https://doi.org/10.1038/s44160-022-00171-9.

(8) Hsu, C.-H.; Hung, S.-C.; Wu, C.-Y.; Wong, C.-H. Toward Automated Oligosaccharide Synthesis. *Angew Chem Int Ed.* **2011**, *50* (50), 11872–11923. https://doi.org/10.1002/anie.201100125.

(9) Wen, L.; Edmunds, G.; Gibbons, C.; Zhang, J.; Gadi, M. R.; Zhu, H.; Fang, J.; Liu, X.; Kong, Y.; Wang, P. G. Toward Automated Enzymatic Synthesis of Oligosaccharides. *Chem Rev.* **2018**. *118 (17)*, 8151–8187. https://doi.org/10.1021/acs.chemrev.8b00066.

(10) Panza, M.; Pistorio, S. G.; Stine, K. J.; Demchenko, A. V. Automated Chemical Oligosaccharide Synthesis: Novel Approach to Traditional Challenges. *Chem. Rev.* **2018**, *118* (17), 8105–8150. https://doi.org/10.1021/acs.chemrev.8b00051.

(11) Gubermann, M.; Seeberger, P. H. Automated Glycan Assembly: A Perspective. *J. Am. Chem. Soc*. **2019**, *141 (14)*, 5581–5592. https://doi.org/10.1021/jacs.9b00638.

(12) DeYong, A. E.; Rudich, M. L.; Pohl, N. L. B. 2.21 - Synthesis of Carbohydrate Building Blocks for Automated Oligosaccharide Construction. In *Comprehensive Glycoscience (Second Edition)*; Barchi, J. J., Ed.; Elsevier: Oxford, 2021; pp 637–659. https://doi.org/10.1016/B978-0-12-819475-1.00109-7.

(13) Li, X.; Yang, Y. Automated Chemical Solid-Phase Synthesis of Glycans. *Chinese Journal of Chemistry* **2022**, *40* (14), 1714–1728. https://doi.org/10.1002/cjoc.202200183.

(14) Geyer, K.; Seeberger, P. H. Optimization of Glycosylation Reactions in a Microreactor. *Helvetica Chimica Acta* **2007**, *90* (2), 395–403. https://doi.org/10.1002/hlca.200790046.

(15) Cancogni, D.; Lay, L. Exploring Glycosylation Reactions under Continuous-Flow Conditions. *Synlett* **2014**, *25* (20), 2873–2878. https://doi.org/10.1055/s-0034-1379471.

(16) Xolin, A.; Stévenin, A.; Pucheault, M.; Norsikian, S.; Boyer, F.-D.; Beau, J.-M. Glycosylation with N-Acetyl Glycosamine Donors Using Catalytic Iron(III) Triflate: From Microwave Batch Chemistry to a Scalable Continuous-Flow Process. *Org. Chem. Front.* **2014**, *1* (8), 992–1000. https://doi.org/10.1039/C4QO00183D.

(17) Matthies, S.; McQuade, D. T.; Seeberger, P. H. Homogeneous Gold-Catalyzed Glycosylations in Continuous Flow. *Org. Lett.* **2015**, *17* (15), 3670–3673. https://doi.org/10.1021/acs.orglett.5b01584.

(18) Konishi, N.; Shirahata, T.; Yokoyama, M.; Katsumi, T.; Ito, Y.; Hirata, N.; Nishino, T.; Makino, K.; Sato, N.; Nagai, T.; Kiyohara, H.; Yamada, H.; Kaji, E.; Kobayashi, Y. Synthesis of Bisdesmosidic Oleanolic Acid Saponins via a Glycosylation-Deprotection Sequence under Continuous Microfluidic/Batch Conditions. *J. Org. Chem.* **2017**, *82* (13), 6703–6719. https://doi.org/10.1021/acs.joc.7b00841.

(19) Sun, Z.; Winschel, G. A.; Borovika, A.; Nagorny, P. Chiral Phosphoric Acid-Catalyzed Enantioselective and Diastereoselective Spiroketalizations. *J. Am. Chem. Soc.* **2012**, *134* (19), 8074–8077. https://doi.org/10.1021/ja302704m.

(20) Mensah, E.; Camasso, N.; Kaplan, W.; Nagorny, P. Chiral Phosphoric Acid Directed Regioselective Acetalization of Carbohydrate-Derived 1,2-Diols. *Angewandte Chemie International Edition* **2013**, *52* (49), 12932–12936. https://doi.org/10.1002/anie.201304298.

(21) Wang, S.; Zhelavskyi, O.; Lee, J.; Argüelles, A. J.; Khomutnyk, Y. Ya.; Mensah, E.; Guo, H.; Hourani, R.; Zimmerman, P. M.; Nagorny, P. Studies of Catalyst-Controlled Regioselective Acetalization and Its Application to Single-Pot Synthesis of Differentially Protected Saccharides. *J. Am. Chem. Soc.* **2021**, *143* (44), 18592–18604. https://doi.org/10.1021/jacs.1c08448.

(22) Kim, S.; Khomutnyk, Y.; Bannykh, A.; Nagorny, P. Synthesis of Glycosyl Fluorides by Photochemical Fluorination with Sulfur(VI) Hexafluoride. *Org. Lett.* **2021**, *23* (1), 190–194. https://doi.org/10.1021/acs.orglett.0c03915.

(23) Kim, S.; Nagorny, P. Electrochemical Synthesis of Glycosyl Fluorides Using Sulfur(VI) Hexafluoride as the Fluorinating Agent. *Org. Lett.* **2022**, *24* (12), 2294–2298. https://doi.org/10.1021/acs.orglett.2c00431.

(24) Tay, J.-H.; Argüelles, A. J.; DeMars, M. D. I.; Zimmerman, P. M.; Sherman, D. H.; Nagorny, P. Regiodivergent Glycosylations of 6-Deoxy-Erythronolide B and Oleandomycin-Derived Macrolactones Enabled by Chiral Acid Catalysis. *J. Am. Chem. Soc.* **2017**, *139* (25), 8570–8578. https://doi.org/10.1021/jacs.7b03198.

(25) Lee, J.; Borovika, A.; Khomutnyk, Y.; Nagorny, P. Chiral Phosphoric Acid-Catalyzed Desymmetrizative Glycosylation of 2-Deoxystreptamine and Its Application to

Aminoglycoside Synthesis. *Chem. Commun.* **2017**, *53* (64), 8976–8979. https://doi.org/10.1039/C7CC05052F.

(26) Tay, J.-H.; Dorokhov, V.; Wang, S.; Nagorny, P. Regioselective Single Pot C3-Glycosylation of Strophanthidol Using Methylboronic Acid as a Transient Protecting Group. *J Antibiot* **2019**, *72* (6), 437–448. https://doi.org/10.1038/s41429-019-0172-1.

(27) Schmidt, R. R.; Stumpp, M.; Michel, J. α- and β-d-Glucopyranosyl Phosphates from 0-α-D-Glucoypyranosyl Trichloroacetimidates. *Tetrahedron Letters* **1982**, *23* (4), 405–408. https://doi.org/10.1016/S0040-4039(00)86843-4.

(28) Plante, O. J.; Andrade, R. B.; Seeberger, P. H. Synthesis and Use of Glycosyl Phosphates as Glycosyl Donors. *Org. Lett.* **1999**. *1 (2)*, 211–214. https://doi.org/10.1021/ol9905452.

(29) Hunt, D. K.; Seeberger, P. H. Linker Influence on the Stereochemical Outcome of Glycosylations Utilizing Solid Support-Bound Glycosyl Phosphates. *Org. Lett.* **2002**, *4* (16), 2751–2754. https://doi.org/10.1021/ol026276o.

(30) Lukashova, M. S. Merrifield Resin Modified with Thiacalixarene-Tetraphosphonates: Synthesis, Characterization and Europium Sorption. *Funct.Mater.* **2016**, *23* (1), 111–119. https://doi.org/10.15407/fm23.01.111.

(31) Abderrahim, O.; Ferrah, N.; Didi, M. A.; Villemin, D. A New Sorbent for Europium Nitrate Extraction: Phosphonic Acid Grafted on Polystyrene Resin. *J Radioanal Nucl Chem* **2011**, *290* (2), 267–275. https://doi.org/10.1007/s10967-011-1243-3.

(32) Ferrah, N.; Abderrahim, O.; Didi, M. A.; Villemin, D. Sorption Efficiency of a New Sorbent towards Uranyl: Phosphonic Acid Grafted Merrifield Resin. *J Radioanal Nucl Chem* **2011**, *289* (3), 721–730. https://doi.org/10.1007/s10967-011-1172-1.

(33) Głowińska, A.; Trochimczuk, A. W. Polymer-Supported Phosphoric, Phosphonic and Phosphinic Acids—From Synthesis to Properties and Applications in Separation Processes. *Molecules* **2020**, *25* (18), 4236. https://doi.org/10.3390/molecules25184236.

(34) Al-Riyami, L.; Pineda, M. A.; Rzepecka, J.; Huggan, J. K.; Khalaf, A. I.; Suckling, C. J.; Scott, F. J.; Rodgers, D. T.; Harnett, M. M.; Harnett, W. Designing Anti-Inflammatory Drugs from Parasitic Worms: A Synthetic Small Molecule Analogue of the Acanthocheilonema Viteae Product ES-62 Prevents Development of Collagen-Induced Arthritis. *J. Med. Chem.* **2013**, *56* (24), 9982–10002. https://doi.org/10.1021/jm401251p.

(35) Khaled, A.; Gravier-Pelletier, C.; Le Merrer, Y. Synthesis of Bis-(2,3,4,6-Tetra-O-Acetyl-α-d-Mannopyranosyl)-l-Serinyl Phosphate, as a Prodrug of Mannose-1-Phosphate. *Tetrahedron: Asymmetry* **2007**, *18 (18)*, 2121–2124. https://doi.org/10.1016/j.tetasy.2007.09.023.

(36) Sjölin, P.; Kihlberg, J. Use of Fluorobenzoyl Protective Groups in Synthesis of Glycopeptides: β-Elimination of O-Linked Carbohydrates Is Suppressed. *J. Org. Chem.* **2001**. *66 (9)*, 2957–2965. https://doi.org/10.1021/jo001584q.

(37) Samoshina, N. F.; Denisenko, V. A.; Novikov, V. L.; Uvarova, N. I. Catalytic Rearrangement Ofα-D-Glucose 1,2-Orthoacetate Derivatives of Pregnenolone and 16-Dehydropregnenolone. *Chem Nat Compd* **1984**, *20* (2), 177–182. https://doi.org/10.1007/BF00579479.

(38) Sati, G. C.; Martin, J. L.; Xu, Y.; Malakar, T.; Zimmerman, P. M.; Montgomery, J. Fluoride Migration Catalysis Enables Simple, Stereoselective, and Iterative Glycosylation. *J. Am. Chem. Soc.* **2020**, *142* (15), 7235–7242. https://doi.org/10.1021/jacs.0c03165.

(39) Martin, J. L.; Sati, G. C.; Malakar, T.; Hatt, J.; Zimmerman, P. M.; Montgomery, J. Glycosyl Exchange of Unactivated Glycosidic Bonds: Suppressing or Embracing Side Reactivity in Catalytic Glycosylations. *J. Org. Chem.* **2022**, *87 (9)*, 5817–5826. https://doi.org/10.1021/acs.joc.2c00132.

(40) Ruiz, M. C. del R.; Amer, H.; Stanetty, C.; Beseda, I.; Czollner, L.; Shah, P.; Jordis, U.; Kueenburg, B.; Claßen-Houben, D.; Hofinger, A.; Kosma, P. Efficient Synthesis of Glycyrrhetinic Acid Glycoside/Glucuronide Derivatives Using Silver Zeolite as Promoter. *Carbohydrate Research **2009**, 344 (9)*, 1063–1071. https://doi.org/10.1016/j.carres.2009.04.015.

(41) Bennett, C. S.; Galan, M. C. Methods for 2-Deoxyglycoside Synthesis. *Chem Rev.* **2018**. *118 (17)*, 7931–7985. https://doi.org/10.1021/acs.chemrev.7b00731.

(42) Elshahawi, S. I.; Shaaban, K. A.; Kharel, M. K.; Thorson, J. S. A Comprehensive Review of Glycosylated Bacterial Natural Products. *Chem. Soc. Rev.* **2015**, *44* (21), 7591–7697. https://doi.org/10.1039/C4CS00426D.

(43) Carney, N.; Perry, N.; Garabedian, J.; Nagorny, P. Development of α-Selective Glycosylation with l-Oleandral and Its Application to the Total Synthesis of Oleandrin. *Org. Lett.* **2023**, *25* (6), 966–971. https://doi.org/10.1021/acs.orglett.2c04358.

(44) Chatterjee, S.; Moon, S.; Hentschel, F.; Gilmore, K,; Seeberger, P. H. An Empirical Understanding of the Glycosylation Reaction. *J. Am. Chem. Soc.* **2018**. *140 (38)*, 11942–11953. https://doi.org/10.1021/jacs.8b04525.

(45) Das, R.; Mukhopadhyay, B. Chemical O-Glycosylations: An Overview. *ChemistryOpen* **2016**, *5* (5), 401–433. https://doi.org/10.1002/open.201600043.

(46) Nguyen, S. H.; Trotta, A. H.; Cao, J.; Straub, T. J.; Bennett, C. S. Direct O-Glycosidation of Resin Bound Thioglycosides. *Org. Biomol. Chem.* **2012**, *10* (12), 2373–2376. https://doi.org/10.1039/C2OB06883D.

(47) Joseph, A. A.; Pardo-Vargas, A.; Seeberger, P. H. Total Synthesis of Polysaccharides by Automated Glycan Assembly. *J. Am. Chem. Soc.* **2020**, *142* (19), 8561–8564. https://doi.org/10.1021/jacs.0c00751.

(48) Li, Y.; Yang, Y.; Yu, B. An Efficient Glycosylation Protocol with Glycosyl Ortho-Alkynylbenzoates as Donors under the Catalysis of Ph3PAuOTf. *Tetrahedron Letters* **2008**, *49* (22), 3604–3608. https://doi.org/10.1016/j.tetlet.2008.04.017.

(49) Tang, Y.; Li, J.; Zhu, Y.; Li, Y.; Yu, B. Mechanistic Insights into the Gold(I)-Catalyzed Activation of Glycosyl Ortho-Alkynylbenzoates for Glycosidation. *J. Am. Chem. Soc.* **2013**, *135* (49), 18396–18405. https://doi.org/10.1021/ja4064316.

(50) Zhang, Y.-M.; Mallet, J.-M.; Sinaÿ, P. Glycosylation Using a One-Electron-Transfer, Homogeneous Reagent. Application to an Efficient Synthesis of the Trimannosyl Core of N-Glycosylproteins. *Carbohydrate Research* **1992**, *236*, 73–88. https://doi.org/10.1016/0008-6215(92)85007-M.

(51) Mootoo, D. R.; Konradsson, Peter.; Udodong, Uko.; Fraser-Reid, Bert. Armed and Disarmed N-Pentenyl Glycosides in Saccharide Couplings Leading to Oligosaccharides. *J. Am. Chem. Soc.* **1988**, *110* (16), 5583–5584. https://doi.org/10.1021/ja00224a060.

(52) Yoshiharu Sawada; Naoki Nanboku; Emiko Yanase; Shin-ichi Nakatsuka. Selective Protection of Hydroxy Group at C6 Position of Glucose Derivatives. *Heterocyclic Communications* **2010**, *16* (1), 21–24. https://doi.org/10.1515/HC.2010.16.1.21.

(53) Yang, W.; Yang, B.; Ramadan, S.; Huang, X. Preactivation-Based Chemoselective Glycosylations: A Powerful Strategy for Oligosaccharide Assembly. *Beilstein J. Org. Chem.* **2017**, *13* (1), 2094–2114. https://doi.org/10.3762/bjoc.13.207.

(54) Wright, J. A.; Yu, J.; Spencer, J. B. Sequential Removal of the Benzyl-Type Protecting Groups PMB and NAP by Oxidative Cleavage Using CAN and DDQ. *Tetrahedron Letters* **2001**, *42* (24), 4033–4036. https://doi.org/10.1016/S0040-4039(01)00563-9.

(55) Zhang, G.-L.; Gadi, M. R.; Cui, X.; Liu, D.; Zhang, J.; Saikam, V.; Gibbons, C.; Wang, P. G.; Li, L. Protecting-Group-Free S-Glycosylation towards Thioglycosides and Thioglycopeptides in Water. *Green Chem.* **2021**, *23* (8), 2907–2912. https://doi.org/10.1039/D1GC00098E.

(56) Zhong, W.; Kuntz, D. A.; Ember, B.; Singh, H.; Moremen, K. W.; Rose, D. R.; Boons, G.-J. Probing the Substrate Specificity of Golgi α-Mannosidase II by Use of Synthetic Oligosaccharides and a Catalytic Nucleophile Mutant. *J. Am. Chem. Soc.* **2008**, *130* (28), 8975–8983. https://doi.org/10.1021/ja711248y.

(57) Preindl, J.; Jouvin, K.; Laurich, D.; Seidel, G.; Fürstner, A. Gold- or Silver-Catalyzed Syntheses of Pyrones and Pyridine Derivatives: Mechanistic and Synthetic Aspects. *Chemistry – A European Journal* **2016**, *22* (1), 237–247. https://doi.org/10.1002/chem.201503403.

(58) Weck, S.; Opatz, T. β-Selective C-Mannosylation of Electron-Rich Phenols. *Synthesis* **2010**, *2010* (14), 2393–2398. https://doi.org/10.1055/s-0029-1218772.

(59) Dong, H.; Du, W.; Yao, Z.; Wu, M.; Luo, H.; He, Y.; Cao, S. First Total Syntheses of Two Natural Glycosides. *Carbohydrate Research* **2021**, *499*, 108200. https://doi.org/10.1016/j.carres.2020.108200.

(60) Chen, J.; Tang, Y.; Yu, B. A Mild Glycosylation Protocol with Glycosyl 1-Methylimidazole-2-Carboxylates as Donors. *European Journal of Organic Chemistry* **2021**, *2021* (30), 4333–4344. https://doi.org/10.1002/ejoc.202100677.

(61) Bucher, C.; Gilmour, R. Fluorine-Directed Glycosylation. *Angewandte Chemie International Edition* **2010**, *49* (46), 8724–8728. https://doi.org/10.1002/anie.201004467.

(62) Chambers, R. D.; Nakano, T.; Parsons, M.; Sandford, G.; Batsanov, A. S.; Howard, J. A. K. Elemental Fluorine: Part 22. Fluorination of 3β-Acetoxy-5α-Androstan-17-One Using Fluorine and Selectfluor®. *Journal of Fluorine Chemistry* **2008**, *129* (9), 811–816. https://doi.org/10.1016/j.jfluchem.2008.04.010.

(63) Direct Glycosylation of Unprotected and Unactivated Sugars Using Bismuth Nitrate Pentahydrate. *Journal of Carbohydrate Chemistry* **2015**, *34* (4), 196–205. https://doi.org/10.1080/07328303.2015.1028585.

(64) Jalsa, N. K. Regioselective Removal of the Anomeric O-Benzyl from Differentially Protected Carbohydrates. *Tetrahedron Letters* **2011**, *52* (49), 6587–6590. https://doi.org/10.1016/j.tetlet.2011.09.130.

(65) Mukherjee, M. M.; Ghosh, R. Synthetic Routes toward Acidic Pentasaccharide Related to the O-Antigen of E. Coli 120 Using One-Pot Sequential Glycosylation Reactions. *J. Org. Chem.* **2017**, *82* (11), 5751–5760. https://doi.org/10.1021/acs.joc.7b00561.

(66) Donahue, M. G.; Johnston, J. N. Preparation of a Protected Phosphoramidon Precursor via an H-Phosphonate Coupling Strategy. *Bioorganic & Medicinal Chemistry Letters* **2006**, *16* (21), 5602–5604. https://doi.org/10.1016/j.bmcl.2006.08.024.

(67) Durantie, E.; Bucher, C.; Gilmour, R. Fluorine-Directed β-Galactosylation: Chemical Glycosylation Development by Molecular Editing. *Chemistry – A European Journal* **2012**, *18* (26), 8208–8215. https://doi.org/10.1002/chem.201200468.

(68) Aiguabella, N.; Holland, M. C.; Gilmour, R. Fluorine-Directed 1,2-Trans Glycosylation of Rare Sugars. *Org. Biomol. Chem.* **2016**, *14* (24), 5534–5538. https://doi.org/10.1039/C6OB00025H.

(69) Manabe, S.; Ito, Y. Hafnium(IV) Tetratriflate in Selective Reductive Carbohydrate Benzylidene Acetal Opening Reaction and Direct Silylation Reaction. *Tetrahedron Letters* **2013**, *54* (50), 6838–6840. https://doi.org/10.1016/j.tetlet.2013.10.011.

(70) Novoa, A.; Barluenga, S.; Serba, C.; Winssinger, N. Solid Phase Synthesis of Glycopeptides Using Shoda's Activation of Unprotected Carbohydrates. *Chem. Commun.* **2013**, *49* (69), 7608–7610. https://doi.org/10.1039/C3CC43458C.

(71) Trinderup, H. H.; Sandgaard, T. L. P.; Juul-Madsen, L.; Jensen, H. H. Anomeric Thioglycosides Give Different Anomeric Product Distributions under NIS/TfOH Activation. *J. Org. Chem.* **2022**, *87* (6), 4154–4167. https://doi.org/10.1021/acs.joc.1c03001.

(72) Naïtaleb, R.; Denys, A.; Allain, F.; Ausseil, J.; Toumieux, S.; Kovensky, J. Synthesis of New Sulfated Disaccharides for the Modulation of TLR4-Dependent Inflammation. *Org. Biomol. Chem.* **2021**, *19* (19), 4346–4351. https://doi.org/10.1039/D1OB00692D.

(73) Li, L.; Gong, T.; Lu, X.; Xiao, B.; Fu, Y. Nickel-Catalyzed Synthesis of 1,1-Diborylalkanes from Terminal Alkenes. *Nat Commun* **2017**, *8* (1), 345. https://doi.org/10.1038/s41467-017-00363-4.

(74) Brian, P. M.; Musau, P. Synthesis, Reactivity and Stability of Aryl Halide Protecting Groups towards Di-Substituted Pyridines. *Indonesian Journal of Chemistry* **2018**, *16* (1), 53–58. https://doi.org/10.22146/ijc.21177.

(75) Montel, E.; Hrmova, M.; Fincher, G. B.; Driguez, H.; Cottaz, S. A Chemoenzymatic Route to Conjugatable β(1→3)-Glucan Oligosaccharides*. *Aust. J. Chem.* **2009**, *62* (6), 575–584. https://doi.org/10.1071/CH08517.

(76) Dijcks, F. A.; Veeneman, G. H.; Peters, J. L. M. Isoxazole Derivatives Used as Oestrogen Modulators. WO2012052395A1, April 26, 2012.

(77) Liang, H.; Ma, L.; Li, C.; Peng, Q.; Wang, Z.; Zhang, Z.; Yu, L.; Liu, H.; An, F.; Xue, W. Efficient Glycosylation with Glycosyl Ortho-Allylbenzoates as Donors. *Tetrahedron Letters* **2019**, *60* (1), 84–87. https://doi.org/10.1016/j.tetlet.2018.11.061.

(78) Airoldi, C.; Palmioli, A.; D'Urzo, A.; Colombo, S.; Vanoni, M.; Martegani, E.; Peri, F. Glucose-Derived Ras Pathway Inhibitors: Evidence of Ras–Ligand Binding and Ras–GEF (Cdc25) Interaction Inhibition. *ChemBioChem* **2007**, *8* (12), 1376–1379. https://doi.org/10.1002/cbic.200700185.

(79) Repetto, E.; Manzano, V. E.; Uhrig, M. L.; Varela, O. Synthesis of Branched Dithiotrisaccharides via Ring-Opening Reaction of Sugar Thiiranes. *J. Org. Chem.* **2012**. *77 (1).* 253–265. https://doi.org/10.1021/jo2018685.

Chapter 3 Introduction to Synthesis of Bufadienolide Natural Products

3.1 Introduction to bufadienolides

The natural sources of bufadienolides have been used in traditional medicine for thousands of years.[1] Scillarenin **3.1** (Figure 3.1), a component ancient Egyptian squill, was the first bufadienolide structure to be explicitly assigned in 1933.[2] Over the next 60 years, thanks to significant improvements in separation and analytical technologies, over 250 unique members of the bufadienolide family were isolated and characterized.[3] In animals, bufadienolides are commonly found as aglycones, however, in plants, their glycosides are more prevalent.[4] Bufadienolides, like their cardenolide counterparts, have shown a wide range of biological activites.[5,6] Bufalin **3.3**, resibufagenin **3.5**, and cinobufagin **3.6** (Figure 3.1) are naturally occurring bufadienolides and are some of the active components of Ch'an Su and Senso.[7] These traditional Chinese medicines, derived from the dried venom of toads in the genus *Bufo*, have been used as cardiotonic, diuretic, anti-tumor, and local anesthetic agents.[8] Their cardiotonic activity, as with the cardenolides, is due to the inhibition of Na/K ATPase.[9] Bufadienolide glycosides, including **3.2** and **3.4**, have been isolated from several plant extracts,[3,4] and have shown promise as potential therapeutics.[10,11] However, their low natural abundance from isolation and narrow therapeutic index had made it challenging for them to find success as clinical therapeutics.[3,4]

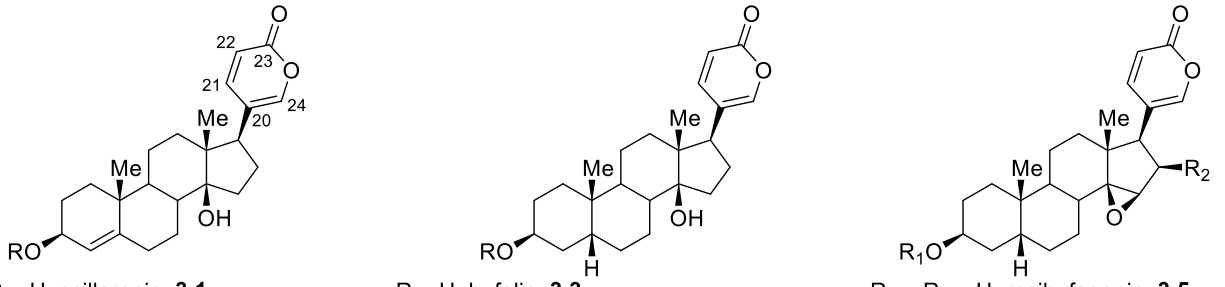
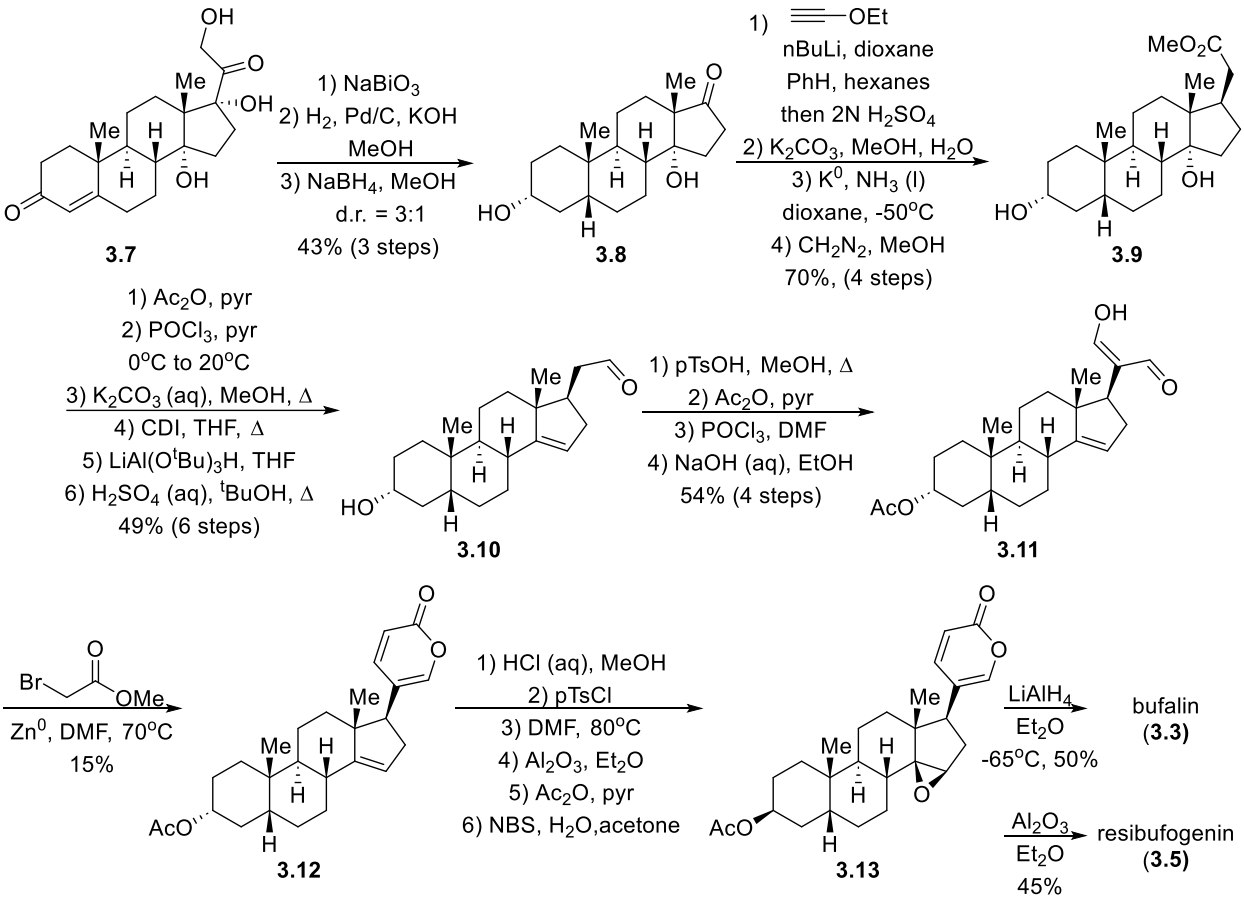


Figure 3.1: Selected examples of naturally occurring bufadienolides

Even though many syntheses of cardenolides have been reported in recent years taking advantage of modern synthetic techniques,[12-20] most of the reported syntheses of bufadienolides were reported between the 1960s and 1980s, and typically were lengthy, inefficient semisynthetic routes.[21-23] However, in recent years, Inoue,[24] Li,[25] and Nagorny[26] have completed elegant syntheses of bufadienolides, and Li's synthesis was the first to begin from a non-steroidal starting material.[25] The recent progress of efficient, divergent approaches to the synthesis of bufadienolides will enable further exploration of these natural products as therapeutic agents.

3.2 Synthesis of bufadienolides

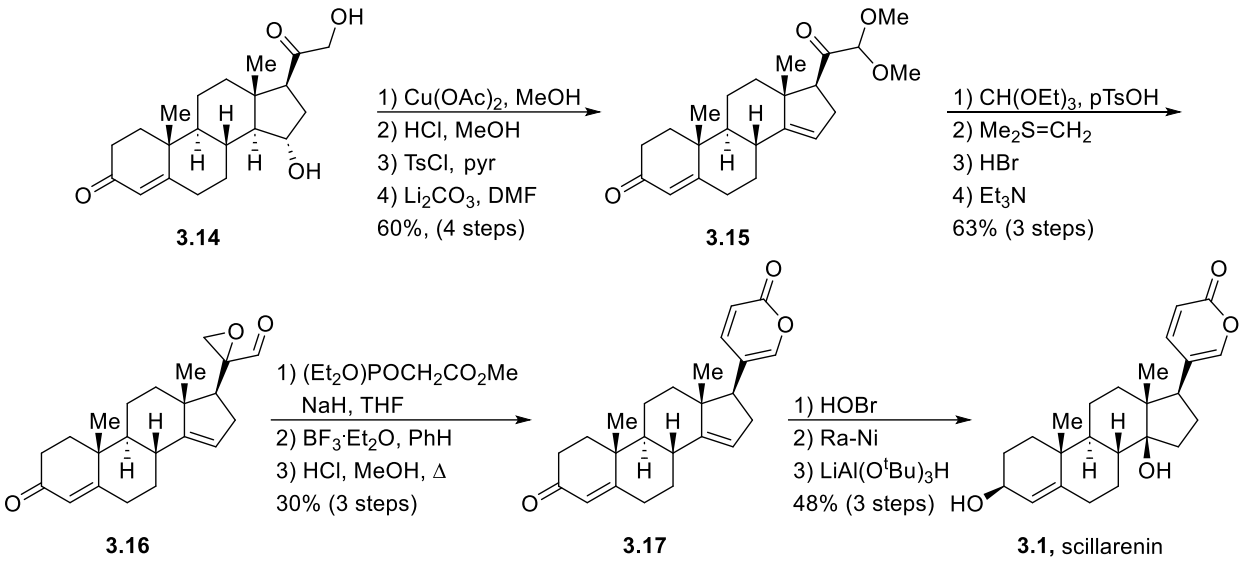
Bufalin **3.3** and resibufagenin **3.5** are two naturally occurring bufadienolides that are active components in the traditional Chinese medicine Ch'an Su.[7] The first synthesis of a natural product bufadienolide was completed by Sondheimer and coworkers in 1969.[27] The syntheses of bufalin **3.3** and resibufagenin **3.5** were each achieved in 24 steps starting from 14α-hydroxycortexolone **3.7** (Scheme 3.1).



Scheme 3.1: Sondheimer's semisynthesis of bufalin **3.3** and resibufagenin **3.5** from 14α-hydroxycortexolone **3.7**

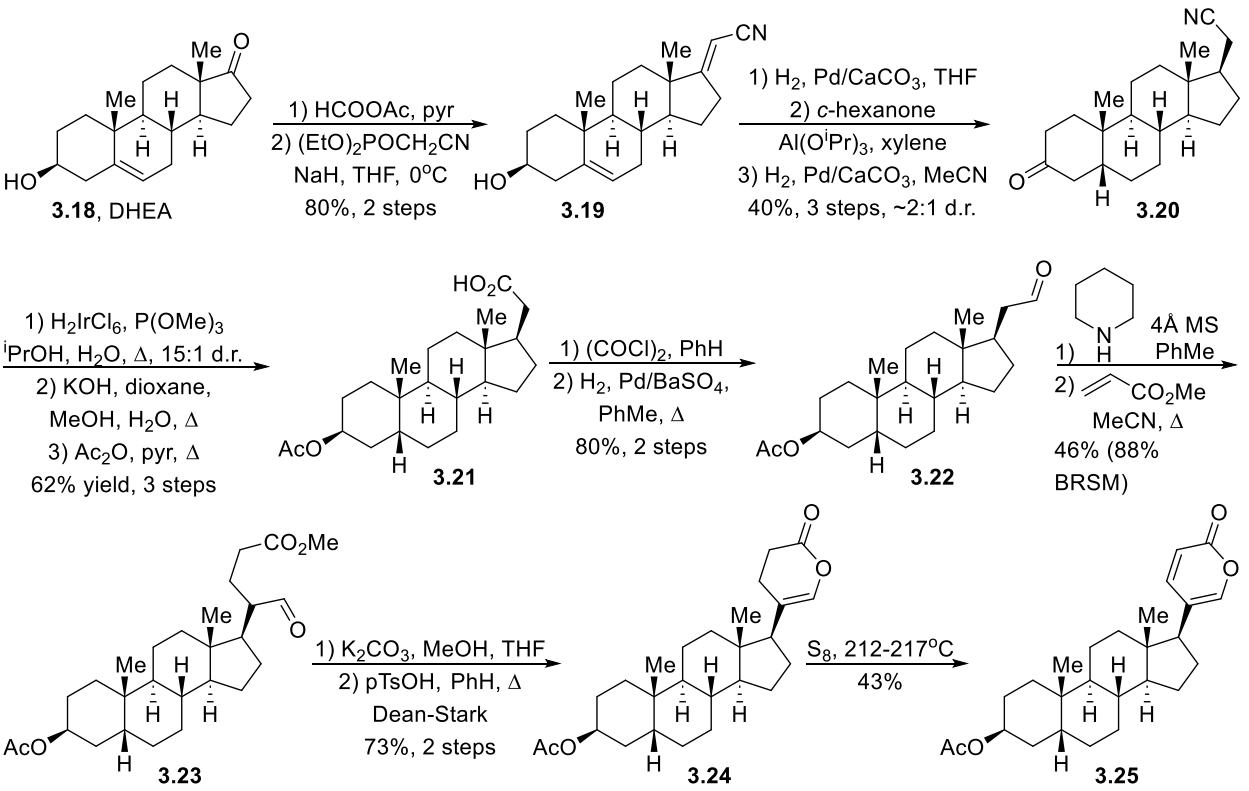
Sondheimer's synthesis[27] (Scheme 3.1) began by oxidative cleavage of the side chain from C17 with $NaBiO_3$ to afford a diketone. The enone functionality was reduced by hydrogenation with KOH over 10% palladium on charcoal to provide primarily the *cis*-ring junction, and the C3 ketone was reduced to the alcohol with $NaBH_4$ to afford **3.8.** Ethoxy acetylene was deprotonated with nBuLi and added to the C17 ketone, then the tertiary propargyl alcohol was treated with dilute H_2SO_4 to hydrate the alkyne and form an unsaturated ester. Saponification of the ester revealed the free carboxylic acid, the alkene functionality was reduced under Birch conditions (K^0, NH_3), and the methyl ester was reformed by treatment with diazomethane in methanol to afford **3.9.** The C3 alcohol was acetylated and the C14 alcohol was eliminated to form the $\Delta^{14,15}$ double bond. Saponification of the methyl ester revealed the

carboxylic acid, which was reduced to the aldehyde first by treatment with 1,1'-carbonyldiimidazole (CDI), then $LiAl(O^tBu)_3H$, and the mixed aminal product was converted to the aldehyde by treatment with dilute H_2SO_4 to afford **3.10**. Aldehyde **3.10** was converted to dimethylacetal by treatment with *p*-TsOH in methanol. The C3 alcohol was reacetylated, and the resulting product was subjected to Vilsmeier–Haack conditions to form the conjugate methyl enol ether, which was hydrolyzed to Z-enolate **3.11** by treatment with NaOH. The key reaction to Sondheimer's formation of the α-pyrone moiety was the Reformatsky reaction of **3.11** and methyl bromoacetate, which afforded bufadienolide **3.12** in 15% yield. The stereochemistry of the C3 alcohol was inverted by a five-step sequence of 1) deacetylation, 2) tosylation, 3) S_N2-reaction with DMF to form the formate ester, 4) deformylation, and 5) acetylation. Bromohydrin formation and *in situ* substitution afford bufadienolide-epoxide **3.13**. Concomitant epoxide opening and deacetylation of **3.13** provided bufalin **3.3**. Resibufagenin **3.5** was obtained after deacetylation of **3.13** with basic alumina. Sondheimer's approach was fundamental, and his strategy for late-stage installation of the C14 alcohol would be adapted in many other bufadienolide syntheses.



Scheme 3.2: Stache's synthesis of scillarenin **3.1** from a cortisone derivative **3.14**

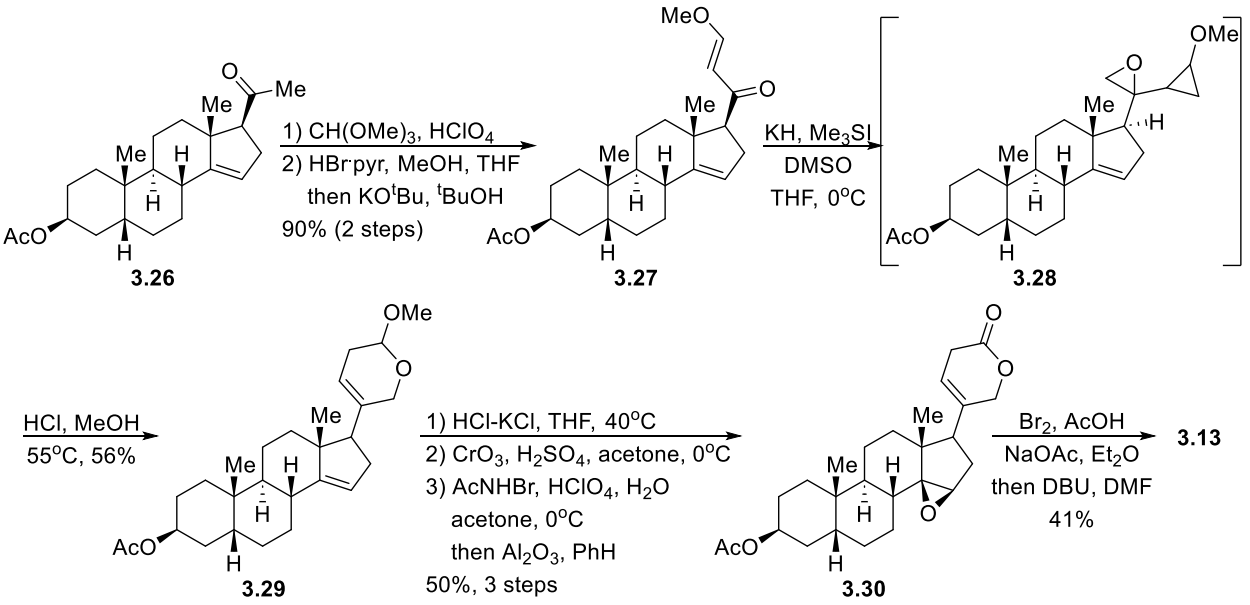
The synthesis of scillarenin **3.1** from cortisone derivative **3.14** was accomplished by Stache and coworkers (Scheme 3.2) in 1969.[28,29] The C21 primary alcohol was first oxidized to an aldehyde with $Cu(OAc)_2$ in methanol. The aldehyde was converted into a dimethyl acetal, and the second alcohol was eliminated to form the $\Delta^{14,15}$ double bond by a two-step sequence of tosylation followed by elimination to provide **3.15.** The C3 ketone was protected as an ethyl enol ether by treatment with triethyl orthoformate. The ketone was converted to an epoxide under Corey-Chaykovsky conditions. The acetal and enol ether moieties were converted back to their respected carbonyls after exposure to aqueous HBr, which also opened the epoxide to form a bromohydrin. The epoxide was reformed by treating the bromohydrin with triethylamine, providing epoxide **3.16**. A Horner-Wadsworth-Emmons reaction of the aldehyde moiety of **3.16** afforded the epoxy ester, then House-Meinwald rearrangement transformed the epoxide to an aldehyde, and acid catalyzed enol lactonization provided pyrone **3.17.** The synthesis of scillarenin **3.1** was completed by a three-step sequence of bromohydrin formation, reductive removal of the bromide with Raney-Ni, and reduction of the C3 ketone with $LiAl(O^tBu)_3H$.



Scheme 3.3: Pettit's synthesis of a 5β,14α-bufadienolide

In the early 1970's, Pettit and coworkers worked extensively on the synthesis of bufadienolides.[30] Pettit's work began with the semisynthesis of steroidal 5β,14α-bufadienolide **3.25** from DHEA **3.18** (Scheme 3.3). [31-33] DHEA was formylated with acetic formic anhydride to provide C3-formyl-DHEA. Horner-Wadsworth-Emmons olefination of the C17 ketone with provided vinyl nitrile **3.19**. Chemoselective catalytic hydrogenation of the conjugated vinyl nitrile occurred opposite the C18 methyl group. Oppenauer oxidation, deacylation of the formyl group, and olefin migration of the $\Delta^{5,6}$ double bond to the $\Delta^{4,5}$ double bond was achieved with catalytic aluminum (III) tri-isopropoxide in refluxing xylenes with cyclohexanone as a sacrificial ketone. Hydrogenation of the $\Delta^{4,5}$ double bond with a second catalytic hydrogenation afforded **3.20** in 40% yield over three steps. The diastereoselectivity of the hydrogenation of the $\Delta^{4,5}$ double bond was 55:34 favoring the desired *cis* ring junction. The C3 ketone was reduced

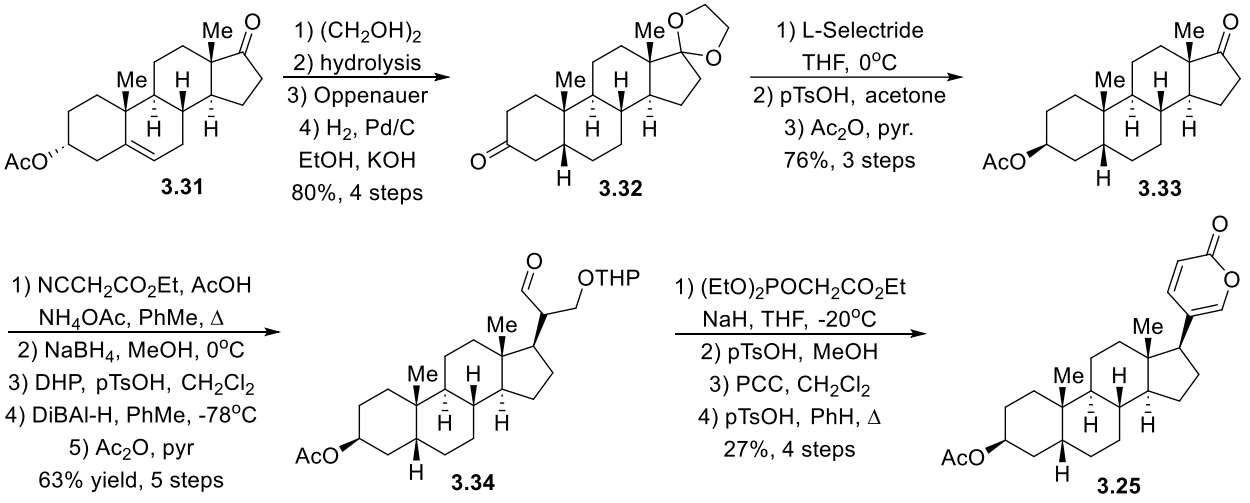
diastereoselectively (15:1 d.r.) to afford the axial alcohol via the Hembest[34] method with chloroiridic acid and trimethylphosphite in refluxing aqueous *iso*-propanol. The nitrile was then hydrolyzed to a carboxylic acid by treatment with aqueous potassium hydroxide in a solution of dioxane and methanol, and the C3 alcohol was capped as an acetate ester to afford **3.21**. Conversion of the carboxylic acid **3.21** to the acid chloride and subsequent Rosemund reduction[35] afford aldehyde **3.22**. Aldehyde **3.22** was condensed to an enamine by treatment with piperidine under anhydrous conditions (4Å molecular sieves). Subsequent Michael addition to methyl acrylate and hydrolysis of the enamine afforded aldehyde **3.23**. Saponification of the ester to the carboxylic acid and acid catalyzed enol cyclization afford bufenolide **3.24**. The final $\Delta^{20,21}$ double bond was installed by dehydrogenation in molten sulfur to provide 5β,14α-bufadienolide **3.25** in 43% yield.



Scheme 3.4: Yoshii's synthesis of bufalin **3.3** and resibufagenin **3.5** via transient epoxy cyclopropane **1.33**

Yoshii envisioned an approach to bufadienolides proceeding through a transient epoxy cyclopropane intermediate.[36] Pregnenolone derivative **1.31**[37] was treated with trimethyl orthoformate for homologation, and the resulting conjugated aldehyde was converted to the

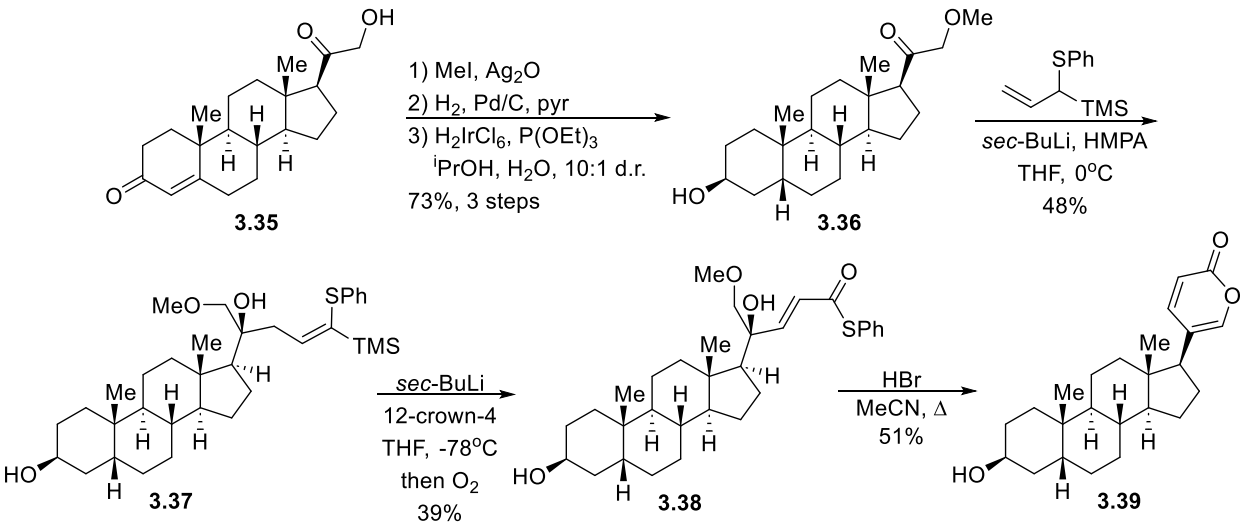
conjugated ketone **3.27** (Scheme 3.4). Double methylene transfer to the dienyl alkenes of **3.27** afforded transient epoxy cyclopropane intermediate **3.28**. Treatment of **3.28** with HCl in methanol afforded methoxydihydropyran **3.29**. Acetal **3.29** was hydrolyzed to its corresponding lactol, and the lactol was oxidized under Jones conditions to yield the lactone. Bromohydrin formation and *in situ* substitution facilitated by basic alumina provided epoxide **3.30**. The alkene of the dihydropyrone moiety was dibrominated with elemental bromine. Double elimination of the dibromide with DBU in DMF provided α-pyrone **3.13**. Using the same conditions as Sondheimer[27] (*cf.* Scheme 3.1), they completed the synthesis of bufalin **3.3** and resibufagenin **3.5**.



Scheme 3.5: Wicha's synthesis of 3β-acetoxy-14α-H bufadienolide **3.25**

Wicha and coworkers developed a synthesis of 3β-acetoxy-14α-H bufadienolide **3.25** from acetlyated androsterone derivative **3.31**[38] (Scheme 3.5). A four step sequence of 1) ketalization with ethylene glycol, 2) hydrolysis of the C3 acetate, 3) Openhauer oxidation and double bond migration of the $\Delta^{5,6}$ double bond to the $\Delta^{4,5}$ bond, and 4) diastereoselective hydrogentation with palladium on charcoal in EtOH with potassium hydroxide afford steroid **3.32** with a *cis*-A,B-ring junction. Diastereoselective ketone reduction with L-selectride afforded

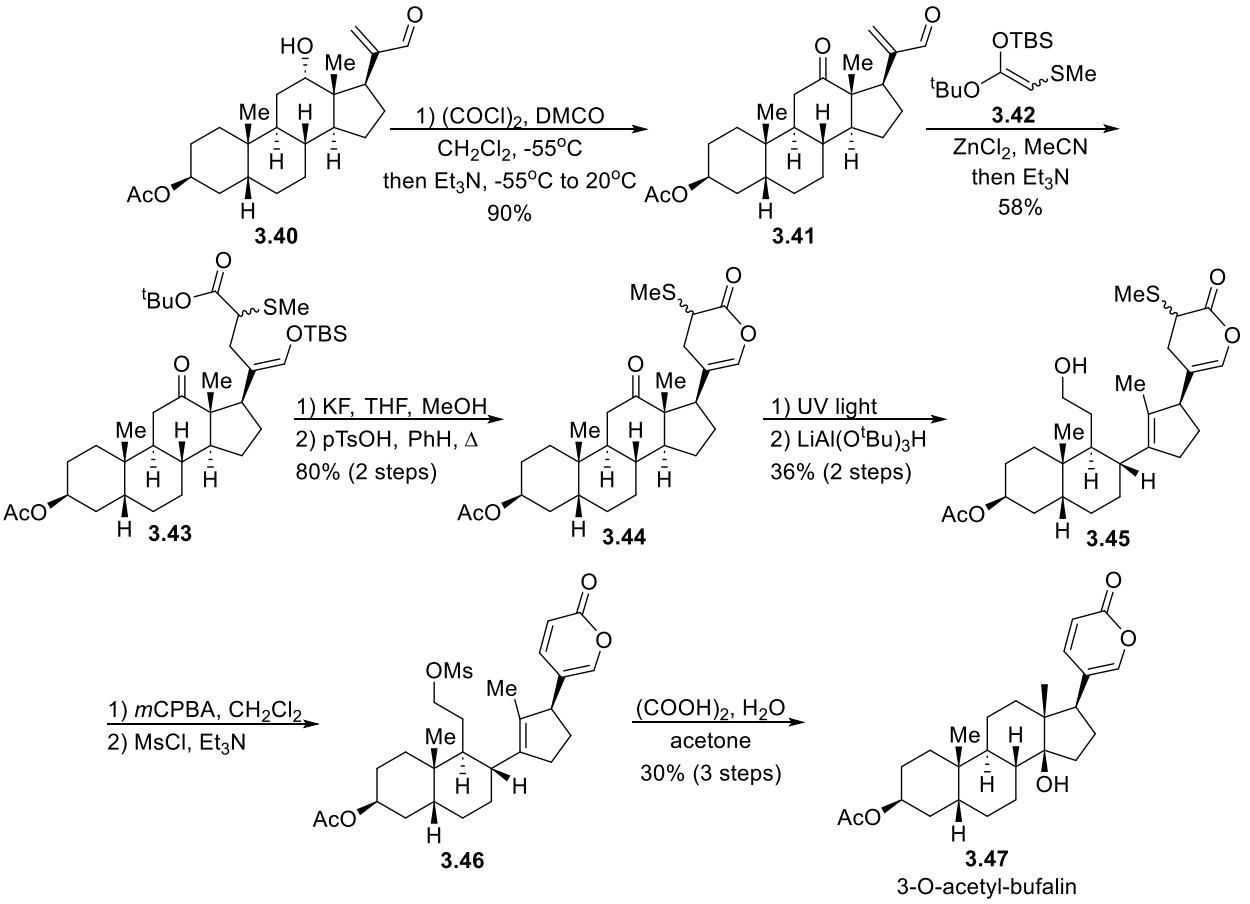
the C3 axial alcohol. Ketal deprotection and acetylation of the C3 alcohol afforded **3.33**. Knoevenagel-type condensation of **3.33** with cyanoethylacetate gave a mixture of E/Z alkenes which were reduced with $NaBH_4$ to the desired C17 diastereomer; reduction of the ethyl ester to the primary alcohol was also achieved under these conditions. The newly formed primary alcohol was capped as a tetrahydropyranyl mixed acetal. Reduction of the nitrile to the aldehyde with DiBAl-H was accompanied by C3 deacylation. Reinstallation of the C3 acetate afforded aldehyde **3.34** in 63% yield over five steps. Horner-Wadsworth-Emmons olefination of **3.34** with triethyl acetophosphonate afforded the *E*-alkene. Removal of the THP group and oxidation of the primary alcohol to the aldehyde with PCC also resulted in olefin migration to afford the conjugated aldehyde. Final acid-catalyzed enol lactonization afforded bufadienolide **3.25** in 27% yield over the final four steps.



Scheme 3.6: Watt's synthesis of bufadienolide **3.39**

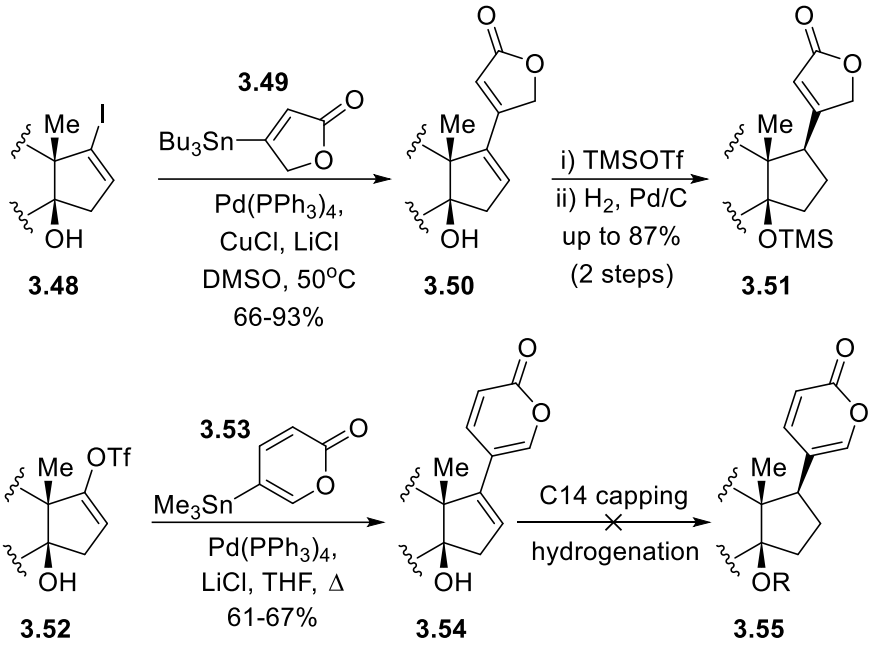
Watt and coworkers developed a short and concise method to bufadienolide **3.39** from deoxycorticosterone **3.35**[39] (Scheme 3.6). Watt's primary aim was to eliminate the dehydrogenation step needed to convert a dihydropyrone to a pyrone, which had previously been carried out in molten sulfur in low to moderate yields (Scheme 3.3). Deoxycorticosterone **3.35**

was converted to **3.36** via a three step sequence of 1) methylation of the C21 primary alcohol, 2) diastereoselective reduction of the $\Delta^{4,5}$ double bond to afford the *cis*-ring junction, and 3) diastereoselective reduction of the C3 alcohol via the Hembest method[34] to afford the axial alcohol. Formal allyation of **3.36** at the C20 ketone with 1-(phenylthio)-1-trimethylsilyl-2-propene homoenolate afforded the tertiary alcohol **3.37**. Treatment of **3.37** with *sec*-butyllithium afforded a lithium trianion, which reacted with oxygen selectively at C24 through a radical-anion process,[39] and after loss of trimethylsilanol, provided thioester **3.38** in 39% yield. Finally, acid promoted cyclization afforded bufadienolide **3.39** in 51% yield. Watt's route is one the shortest methods to install the α-pyrone moiety, and the lithium-oxidation step is tolerant of several unprotected functionalities.



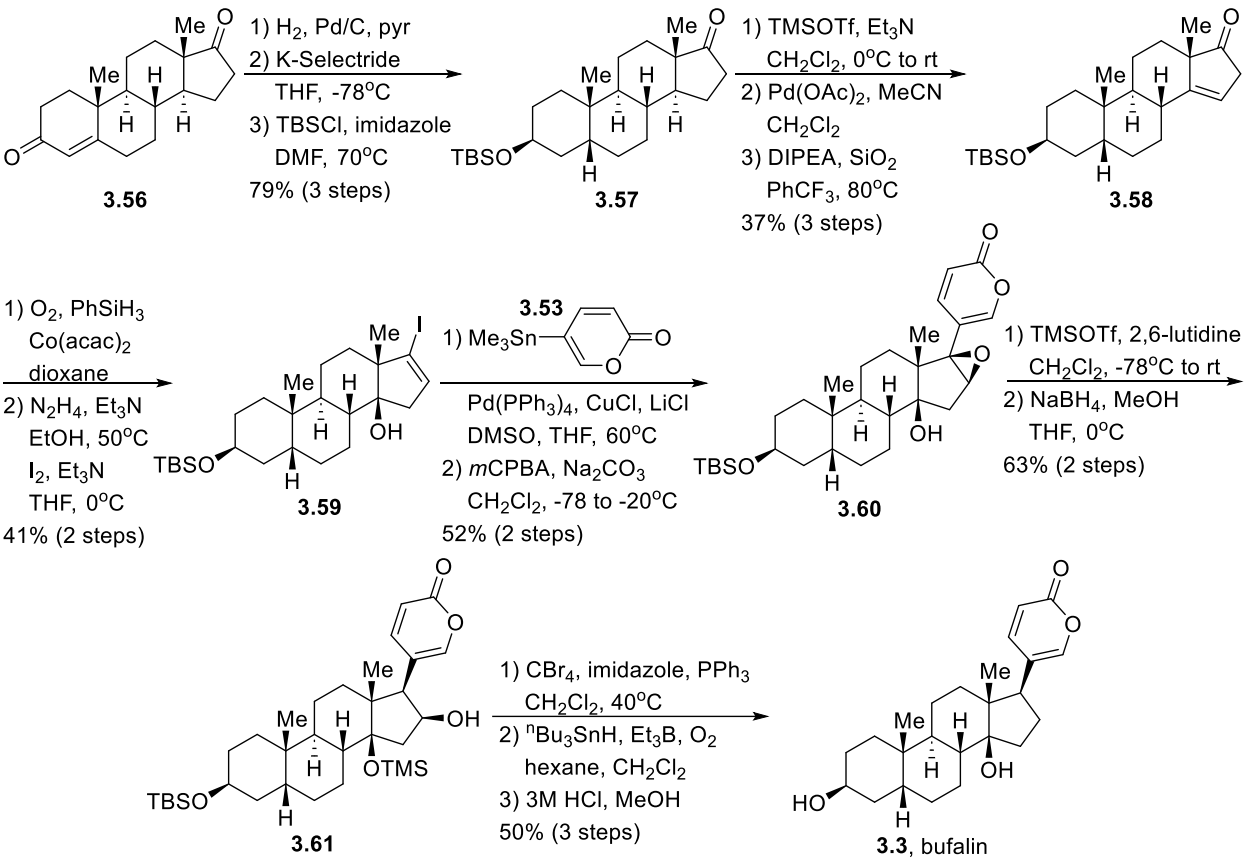
Scheme 3.7: Welzel's synthesis of 3-*O*-acetyl bufalin **3.47** from deoxycholic acid

Welzel completed the synthesis of 3-*O*-acetyl-bufalin from deoxycholic acid (Scheme 3.7) by relying on a stepwise Mukaiyama Michael reaction followed by enol lactonization.[40] Conjugated aldehyde **3.40** was prepared in four steps from deoxycholic acid as previously described.[41] Swern oxidation of the secondary alcohol of **3.40** afforded the C11 ketone **3.41**. Zinc-catalyzed Mukaiyama-Michael addition of silyl ketene acetal **3.42** to the enal of **3.41** afforded silyl enol ether **3.43**. Removal of the silyl group and acid catalyzed enol lactonization afforded dihydropyrone **3.44**. Irradiation of the carbonyl with UV light led to ring fragmentation to form the C12 aldehyde, which was promptly reduced to primary alcohol **3.45** with $LiAl(O^tBu)_3H$. Oxidation of the thioether and elimination of the sulfoxide resulted in pyrone formation, and the primary alcohol was then capped as a mesylate to provide **3.46**. Solvolysis under Masamune's conditions[42] provided 3-*O*-acetyl bufalin **3.47**. Welzel later developed a concerted process to form dihydropyrone **3.44** via $Eu(fod)_3$ catalyzed [4+2] cycloadddtion between enal **3.41** and silyl ketene acetal **3.42**, followed by hydrolysis of the resulting ortho ester to the desired lactone.[43,44] Oxidation of the thioether and elimination of the sulfoxide afforded the desired bufadienolides. The direct application of the cycloaddition process to the synthesis of a natural product bufadienolide had not been reported.



Scheme 3.8: Synthesis of butenolides and bufadienolides by cross coupling and hydrogenation

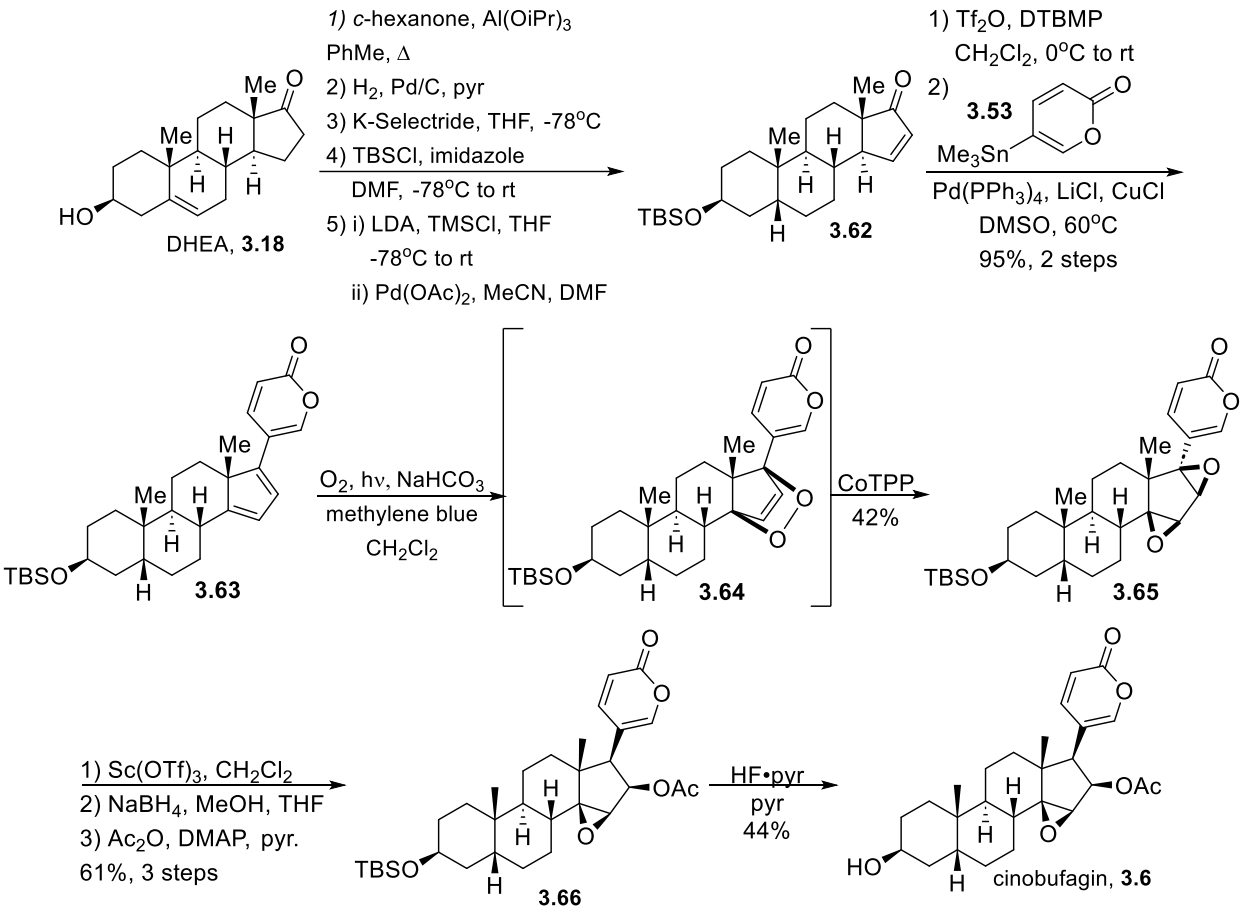
Direct installation of the α-pyrone has historically been difficult on the cardiotonic steroid core due to the steric congestion around C17.[22] In recent reports on the total synthesis of cardenolides,[12-20] the butenolide heterocycle at C17 was installed via cross coupling of steroidal vinyl halide **3.48** and vinyl stannane **3.49**. The resulting $\Delta^{16,17}$ double bond of **3.50** was then saturated with catalytic hydrogenation to afford the desired diastereomer **3.51** in good yields (Scheme 3.8). Application of this cross coupling strategy to α-pyrone stannanes[24,45] or boronic acids[25,26,46,47] has been successful. However, while the cross coupling can proceed nicely in good yields for both the Stille[24,26,45] or Suzuki reactions,[25,46,47] regioselective reduction of the $\Delta^{16,17}$ double bond in the presence of the α-pyrone has not been accomplished when the C14-β-OH is present,[45,48] To circumvent this challenge, Inoue,[24] Nagorny,[26] and Li[25] have each taken unique approaches to remove the $\Delta^{16,17}$ double bond after cross coupling. Inoue's and Nagorny's approach will be discussed in this section, Li's will be discussed in the following section with the synthesis of bufogaragizins.



Scheme 3.9: Inoue's synthesis of bufalin **3.3**

Inoue and coworkers reported the unified total synthesis of five bufadienolides in 2020.[24] Inoue's synthesis began from diketone **3.56** (Scheme 3.9). Diastereoselective reduction of the $\Delta^{4,5}$ double bond to form the *cis*-ring junction was achieved by hydrogenation with palladium on carbon in pyridine. The C3 ketone was reduced to the axial alcohol in a diastereoselective manner by employing sterically bulky reducing agent K-Selectride. The newly formed alcohol was capped as a silyl ether to afford **3.57**. The $\Delta^{15,16}$ double bond was installed by Saegusa-Ito oxidation, and deconjugation of the $\Delta^{15,16}$ to the $\Delta^{14,15}$ was carried out according the conditions reported by Baran[19] to provide **3.58**. The C14-OH was installed diastereoselectivity (2.3:1 d.r.) by Mukaiyama hydration,[49] and the ketone was converted to vinyl iodide **3.59** by Barton's conditions.[50] The α-pyrone was incorporated via Stille coupling of vinyl iodide **3.59** and vinyl stannane **3.53**; the $\Delta^{16,17}$ double bond was converted to epoxide **3.60** with *m*CPBA. The

diastereoselectivity was directed by the C14 alcohol.[24] Stereoselective House-Meinwald rearrangement converted the epoxide to C16 ketone, which was subsequently reduced to the alcohol **3.61**. During the House-Meinwald rearrangement, the C14 alcohol was silylated. Oxygenation at C16 was removed by a two-step sequence consisting of Appel bromination followed by radical dehalogenation. The silyl groups were removed by treatment with HCl to afford bufalin **3.3** in 15 steps from diketone **3.56**. Using this methodology, Inoue was able to prepare five different bufadienolides. Inoue's work was able to overcome the challenging cross coupling of the α-pyrone to the steroid core. Previous work by our group had shown reduction of the $\Delta^{16,17}$ double bond in the presence of both C14 alcohol and C17 α-pyrone was nearly impossible to perform selectively;[48] Inoue was able to circumvent this challenging reduction by performing epoxidations and formal deoxygenation.



Scheme 3.10: Nagorny's synthesis of cinobufagin **3.6**

In 2023, Nagorny and coworkers completed the first synthesis of cinobufagin **3.6** from commercially available DHEA **3.18**[26] (Scheme 3.10). Through a five step sequence previously developed in our group,[48,51] DHEA **3.18** was transformed into **3.62.** First, Oppenauer oxidation converted the C3 alcohol to the ketone, and migrated the $\Delta^{5,6}$ double bond to the $\Delta^{4,5}$ double bond. Catalytic hydrogenation over palladium on carbon in anhydrous pyridine afforded a mixture of diastereomers favoring the *cis* ring junction. Regio- and diastereoselective reduction of the C3 ketone provided the axial alcohol, which was immediately capped as the TBS ether. Conversion of the C17 ketone to the $\Delta^{16,17}$ silyl enol ether and subsequent Saegusa-Ito oxidation afforded steroid **3.62**. Triflation of the vinylogous enolate and subsequent Stille coupling with pyrone stannane **3.53** afforded diene **3.63**. Cycloaddition of **3.63** with singlet oxygen[52] and

methylene blue as the photosensitizer afforded a diastereomeric mixture of *endo*-peroxides **3.64**, which were opened to provide a diastereomeric mixture of bisepoxides that favored the desired isomer **3.65** (56% total yield, 3.2:1 d.r., 42% yield desired diastereomer **3.65**). House-Meinwald rearrangement catalyzed by scandium (III) triflate provided the C16 ketone, and the desired orientation of the C17 α-pyrone. Reduction of the ketone with $NaBH_4$ and capping of the resulting alcohol with acetic anhydride provided acetate **3.66** in 61% yield over three steps. Final deprotection of the C3-TBS group afforded cinobufagin **3.6** in 44% yield. This pioneering work described the first synthesis of cinobufagin, and detailed an exquisite synthesis of the highly oxygenated D-ring.

3.2.1 Conversion of butenolides to bufadienolides

The synthesis of cardenolide aglycones has many more examples than bufadienolide aglycones, but most of the strategies have not been repurposed or are not compatible for the synthesis of bufadienolides. Most bufadienolides found in animals are present as the aglycones, but in plants, the glycosides are much more prevalent.[21] Many cardenolides and bufadienolides share the same tetracyclic steroidal core, and many have similar oxygenation patterns, differing only by the heterocyclic moiety at the C17 position (Figure 3.2).

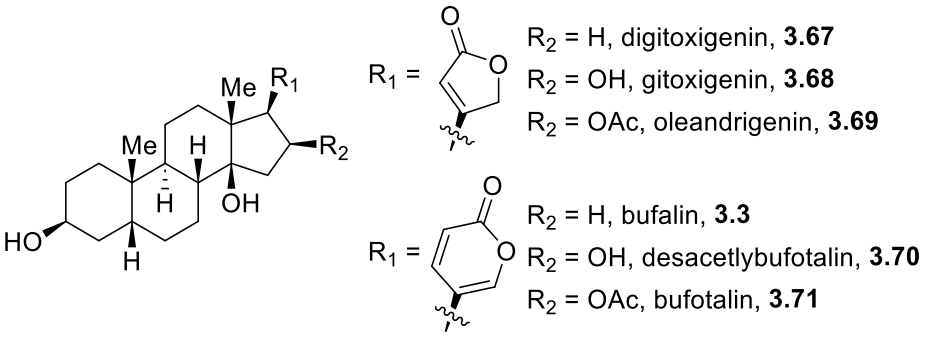
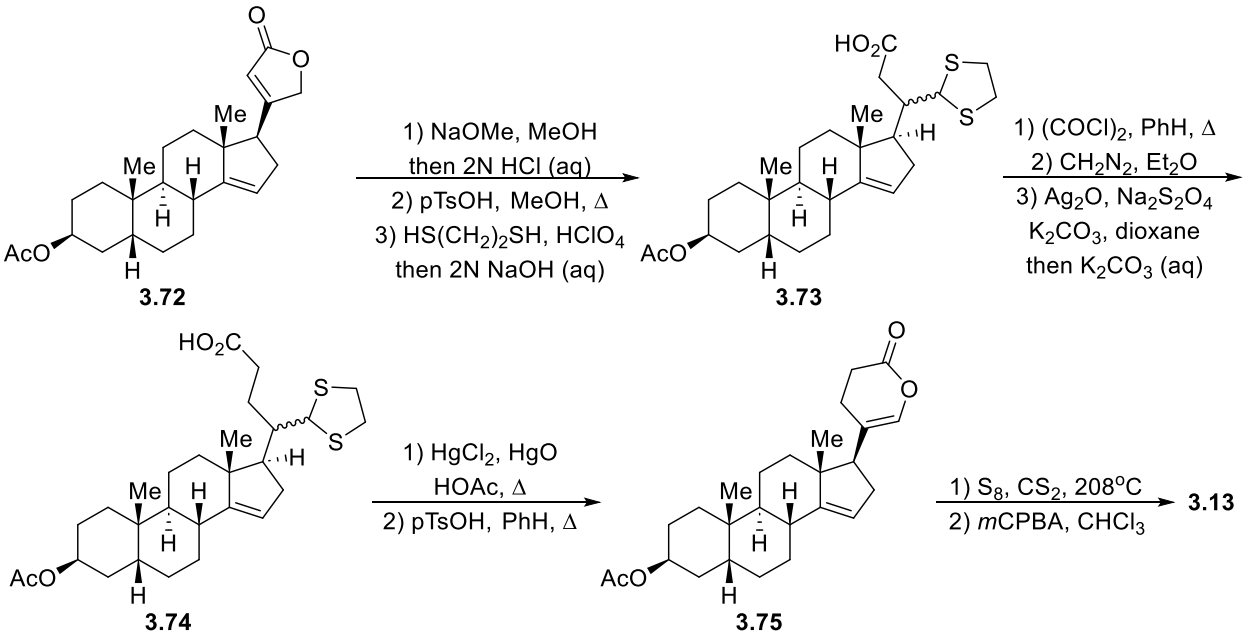


Figure 3.2: Cardenolides and bufadienolides with similar steroidal oxygenation patterns.

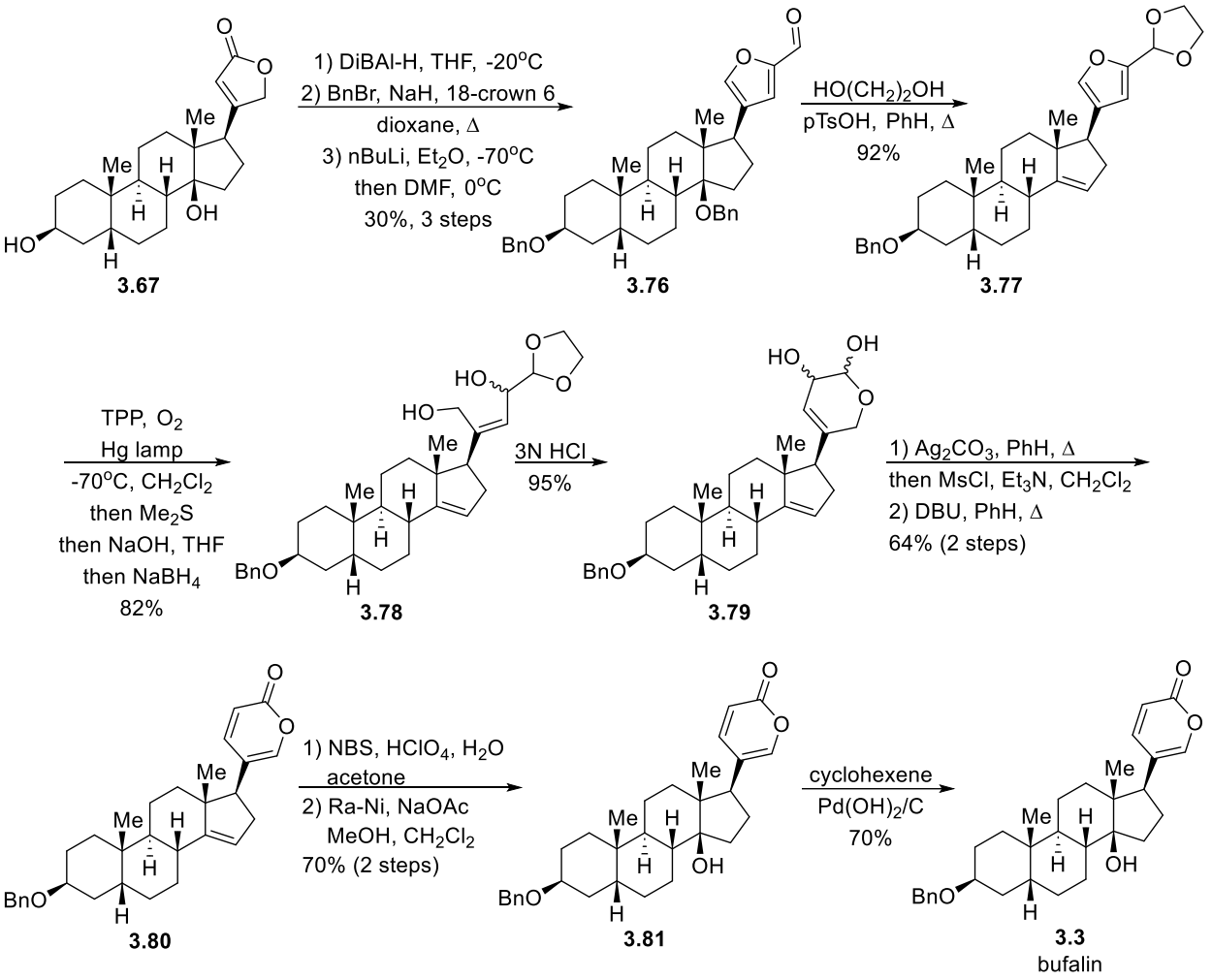
Due to the relatively greater natural sources of cardenolides compared to bufadienolides,[7,53,54] a simple method to transform the butenolide ring into an α-pyrone greatly increases the diversity of bufadienolides that can be prepared, with minimal steps involved. The Petit[55-56] and Weiser[57-62] groups have demonstrated the conversion of butenolides into α-pyrones, however both require the removal and future reinstallation of the C14 alcohol. The C5 tertiary hydroxyl and other hydroxy functionalities would likely also not be compatible with these previous synthetic routes. Studies by our group towards the conversion of butenolides to bufadienolides will be covered in Chapter 4 of this thesis.



Scheme 3.11: Pettit's semisynthesis of bufalin **3.3** and resibufagenin **3.5** from digitoxin

Pettit and coworkers completed the synthesis of bufalin (Scheme 3.11) from digitoxin in 1970.[55] Digitoxin was converted to the C3 acetate **3.72** in three steps;[56] 1) hydrolysis of the tri-digitoxose moiety at C3, 2) acetylation of the C3 alcohol, and 3) dehydration of the C14 alcohol to form the $\Delta^{14,15}$ double bond. The butenolide **3.72** was treated with NaOMe in methanol to deconjugate the butenolide and form the resulting lactol upon acidic work up. Methanolysis of

the resulting lactol converted the lactone to the methyl ester and the lactol to the dimethyl acetal. the acetal methyl ester, subsequently the acetal was converted to dithiane by treatment with ethanedithiol and perchloric acid. Following saponification of the methyl ester afforded carboxylic acid **3.73**. Acid **3.73** was first converted to acid chloride by treatment with oxalyl chloride. The acid chloride was subjected to homologation via Arndt-Eistert conditions (CH_2N_2, then Ag_2O) to provide **3.74**. The dithioacetal was removed with $HgCl_2$, and subsequent enol lactonization afforded **3.75**. Oxidation of the lactone ring to the α-pyrone was achieved by heating with elemental sulfur. Finally, epoxidation of the $\Delta^{14,15}$ double bond with mCPBA afforded **3.13**. Using the same conditions previously reported by Sondheimer,[27] they completed the synthesis of bufalin **3.3** and resibufagenin **3.5**.



Scheme 3.12: Wiesner's synthesis of bufalin **3.3** from digitoxigenin **3.67**

Wiesner also developed an effective method for the conversion of digitoxigenin to bufalin (Scheme 3.12).[57-59] Digitoxigenin **3.67** was first converted to aldehyde **3.76** by a three step sequence[60-62] of 1) reduction of the butenolide to the furan with DiBAl-H, 2) bis-benzylation of the C3 and C14 alcohols, and 3) formylation of the lithiated furan with DMF. The aldehyde was protected as cyclic acetal **3.77** by refluxing ethylene glycol in benzene with catalytic *p*-TsOH. The C14 benzyl ether was also eliminated, furnishing the $\Delta^{14,15}$ double bond. Photochemical singlet oxygen cycloaddition formed an *endo*-peroxide from furan **1.37** with *meso*-tetraphenylporphyrine (TPP) as the sensitizing agent. The *endo*-peroxide was opened by

treatment with dimethyl sulfide to furnish a dicarbonyl. The dicarbonyl intermediate was immediately reduced with $NaBH_4$ to afford diol **3.78.** Acid-catalyzed acetal deprotect and lactolization provided **3.79.** This lactol was oxidized to a lactone with Fetizon's reagent, and the neighboring alcohol was capped as a mesylate. Elimination of the mesylate was achieved by refluxing with DBU in benzene to afford **3.80.** The alcohol was reinstalled at C14 by bromohydrin formation, and subsequent reductive removal of bromine with Raney-Ni provided **3.81**. Final benzyl deprotection of **1.81** afforded bufalin **1.3** in 11 steps from digitoxigenin **3.67**.

3.2.2 Synthesis of bufogargarizins

Bufogargarizins A **3.82**, B **3.83**, and C **3.84** (Figure 3.3) are *abeo*-steroids with unusual carbon skeletons that were isolated from the venom of *Bufo bufo gargarizans*,[63,64] which has been used as the traditional Chinese medicine Ch'an Su for the treatment of various ailments.[7] In contrast to the usual 6/6/6/5 tetracyclic ring structure of bufadienolide cardiotonic steroids, bufogargarizins A **3.82** and C **3.84** possess a 7/5/6/5 ring structure, and bufogargarizin B **3.83** has a 5/7/6/5 ring structure. Unlike bufalin and similar bufadienolides, **3.82** and **3.83** were not cytotoxic to HeLa or HepG 2 cells at concentrations up to 100μM, suggesting that the unusual ring structure of the bufogargarizins could reduce the cytotoxic activity of this class of compounds.[63] Due to the low natural abundance of these compounds (8.0mg **3.82** or 5.5mg **3.83** per 1.5kg toad venom), [63] the development of efficient synthetic access to this class of compounds is crucial to continue evaluation of their biological activity.

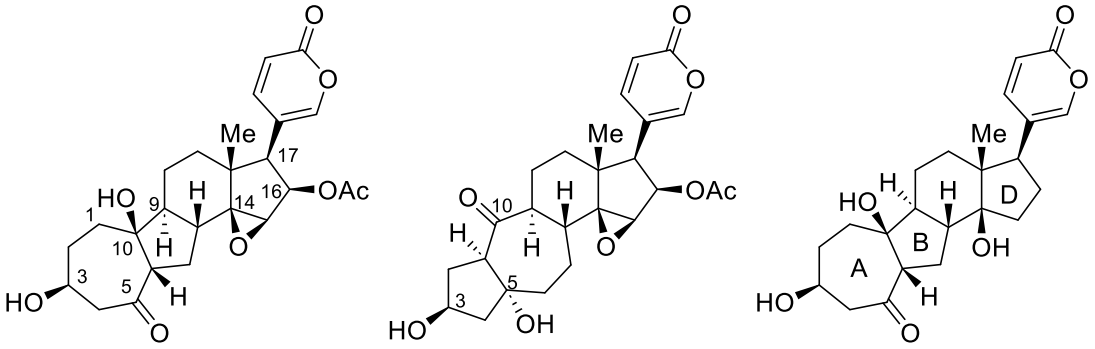
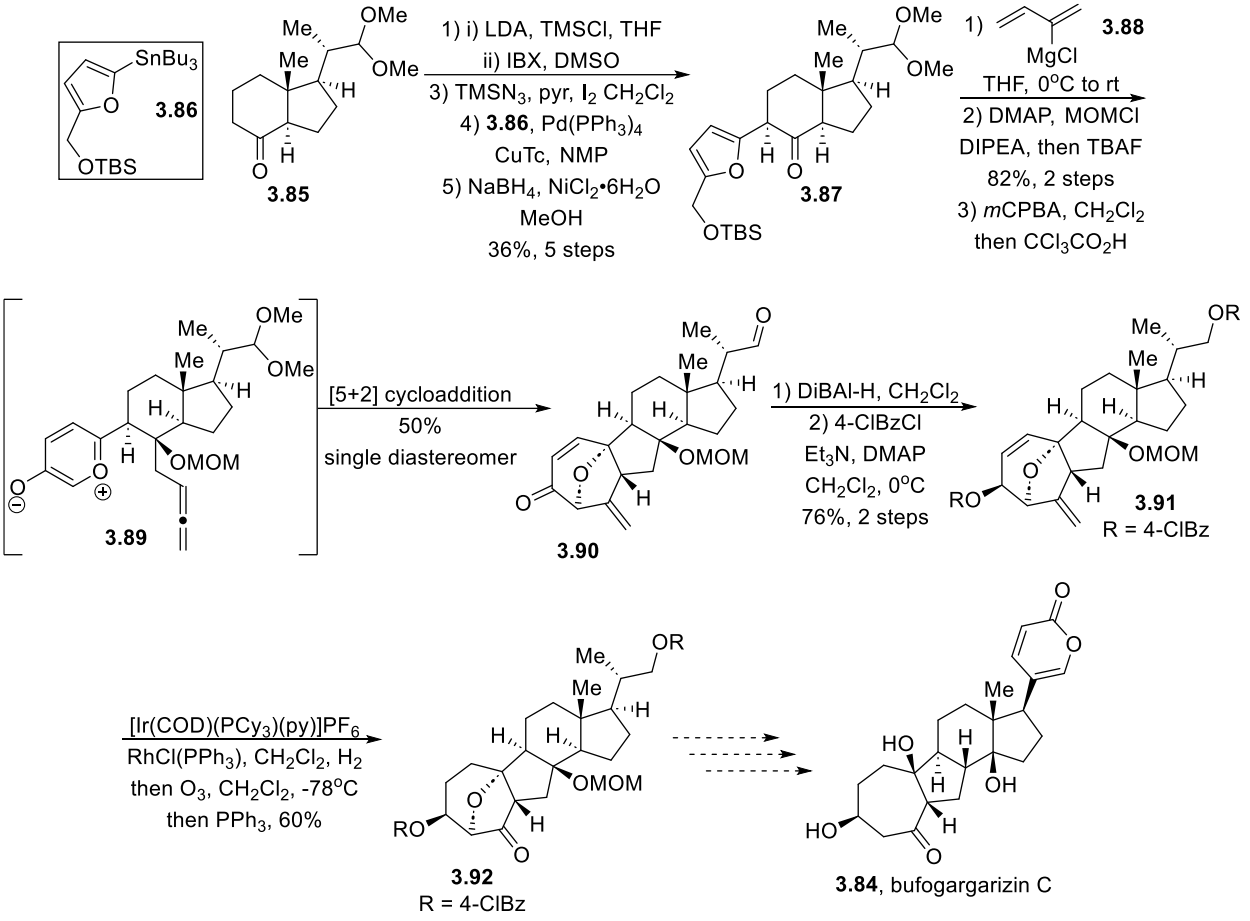


Figure 3.3: Bufogargarizins A-C, *abeo*-steroids with unusual carbon skeletons

Li and coworkers first set out to construct the 7/6/6/5 core ring structure of bufogargarizin C (Scheme 3.13).[65] Beginning from **3.85**, the ketone was converted to the enone via silyl enol ether formation followed by dehydration with IBX. The α-vinyl iodide was installed via treatment of the enone with elemental iodine, pyridine and $TMSN_3$. Stille cross coupling of the vinyl iodide with furanyl stannane **3.86** was achieved with $Pd(PPh_3)_4$ as the catalyst. Final conjugate reduction of the enone to the saturated ketone was carried out with *in situ* generated $Ni_2(BH_4)$[66] to provide **3.87** in 36% yield over 5 steps. Addition of Grignard reagent **3.3.88** to **3.87** furnished a single diastereomer of the tertiary alcohol. Capping of the tertiary alcohol as a methoxymethyl (MOM) ether provided the key intermediate for the desired [5+2] cycloaddition to form the 5/7 A/B ring system of the natural product. First, treatment of the furanyl compound with *m*CPBA initiated the Achmatowicz rearrangement to form the lactol, which when treated with mild acid, eliminated H_2O and tautomerized to zwitterionic oxidopyrylium ylide **3.89**, which underwent [5+2] cycloaddition with the allene to afford oxa-bridged cycloheptanone product **3.90** in 50% yield as a single diastereomer. Global reduction of the carbonyls and subsequent protection of the alcohols with 4-chlorobenzoyl chloride afforded **3.91**, which was recrystallized to determine its absolute configuration. In the presence of Crabtree's ($[Ir(COD)(PCy_3)(py)]PF_6$) and Wilkinson's ($RhCl(PPh_3)$) catalysts, the endocyclic

alkene was selectively hydrogenated, then the exocyclic alkene was oxidatively cleaved via ozonolysis to the give ketone **3.92**. This tetracyclic core of bufogargarizin C had desirable functional groups and the intended stereochemistry at the C3, C6, C9, C13, and C17 positions, and could be applied to a future total synthesis of bufogargarizin C **3.84**.

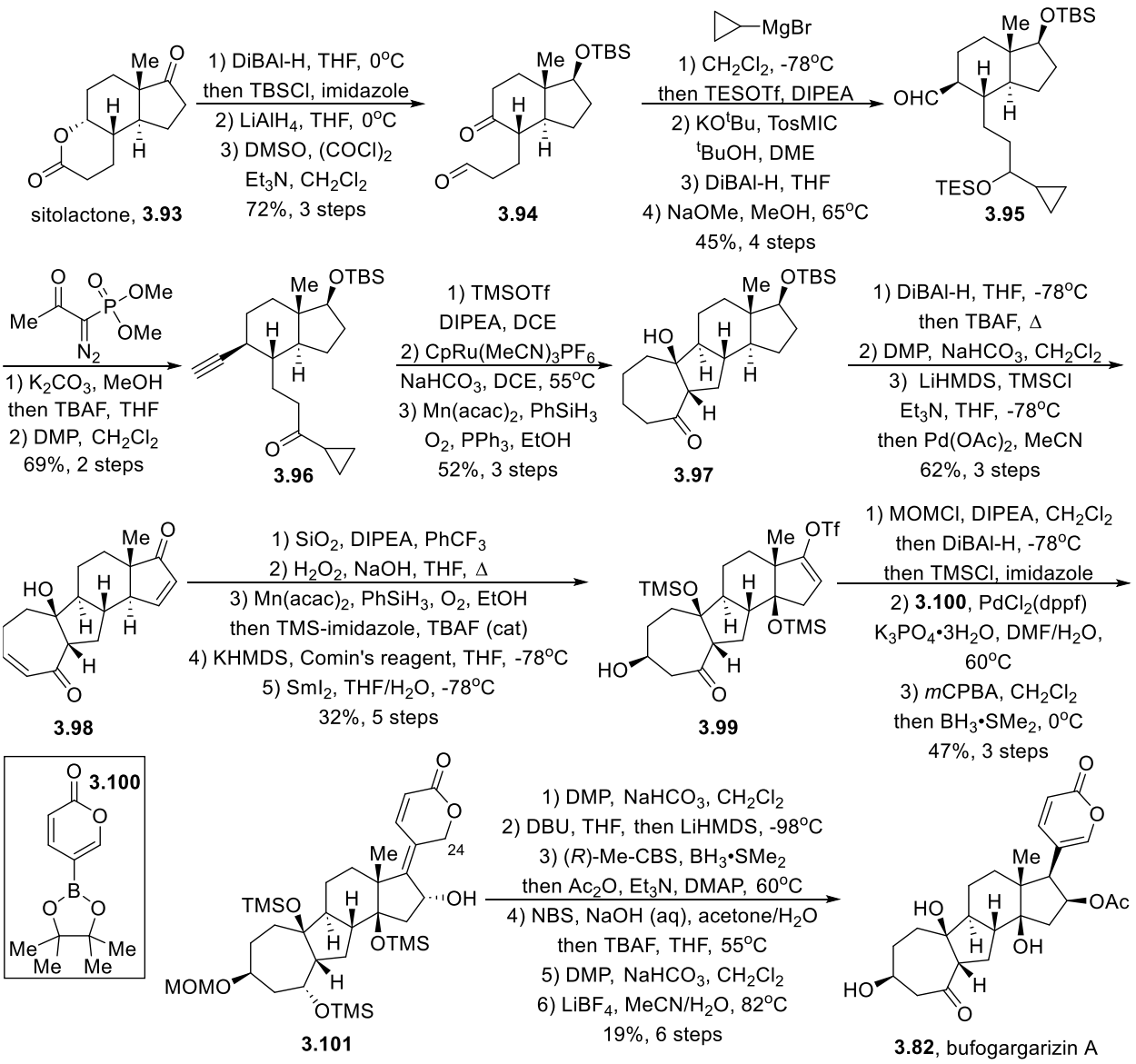


Scheme 3.13: Li's synthesis of the tetracyclic core of bufogargarizin C **3.84**

Li next reported the syntheses of bufogargarizins A[25] **3.82** (Scheme 3.14) and B[25] **3.83** (Scheme 3.15) using a modified version of the [5+2] cycloaddition that was developed for the synthesis of the bufogargarizin C core[65]. Li initially targeted bufogargarizin A **3.82** starting from commercially available sitolactone[25] **3.93** (Scheme 3.14). The ketone was reduced diastereoselectively with DiBAl-H to afford the secondary alcohol, which was immediately protected as a TBS ether. The lactone moiety was reduced to the diol with $LiAlH_4$, and then both

alcohols were oxidized via Swern conditions to afford compound **3.94**. Chemoselective addition of cyclopropyl magnesium bromide to the aldehyde of **3.94** and one-pot capping of the resulting alkoxide afforded the protected secondary alcohol. A van Leusen reaction[67] was used to convert the ketone into a nitrile, which was reduced to the aldehyde by treatment with DiBAl-H (1.5:1 d.r. at C9). The stereocenter was equilibrated by treatment with sodium methoxide in refluxing methanol to give **3.95** in 45% yield over four steps (>8:1 d.r. at C9). Aldehyde **3.95** was treated with the Ohira-Bestmann reagent to furnish the terminal alkyne, which was subjected to TBAF to remove the TES ether in a one-pot fashion. The revealed secondary alcohol was oxidized to the ketone with Des Martin periodinane (DMP) to furnish **3.96** in 69% yield over two steps. The ketone was converted to its corresponding silyl enol ether by treatment with TMSOTf and DIPEA. The silyl enol ether was subjected to the optimized conditions for the rhodium-catalyzed [5+2] cycloaddition to afford the 7/5/6/5 tetracycle[25]. The tetracyclic product was subjected to Mukaiyama hydration conditions to afford **3.97** bearing the C10 tertiary alcohol as the desired diastereomer. The ketone of **3.97** was reduced to the secondary alcohol, then TBAF was added to remove the secondary TBS ether in a one pot manner to afford the C5,C11 diol. Oxidation of both alcohols with DMP afforded the diketone, which were both converted to silyl enol ethers and subjected to Saegusa-Ito oxidation to afford bis-enone **3.98**. The $\Delta^{15,16}$ double bond was migrated to the $\Delta^{14,15}$ double bond by treatment with silica gel in a mixture of DIPEA and α,α,α-trifluorotoluene[19]. The A-ring enone alkene was converted to the epoxide by reaction with sodium peroxide generated *in situ*. Subsequent Mukaiyama hydration of the $\Delta^{14,15}$ double bond provided the tertiary C14 alcohol as the desired diastereomer, and then the tertiary C10 and C14 alcohols were protected as TMS ethers in one-pot. The C17 ketone was then converted to the $\Delta^{16,17}$ vinyl triflate, and the C3-C4 epoxide was reductively opened with samarium diiodide to

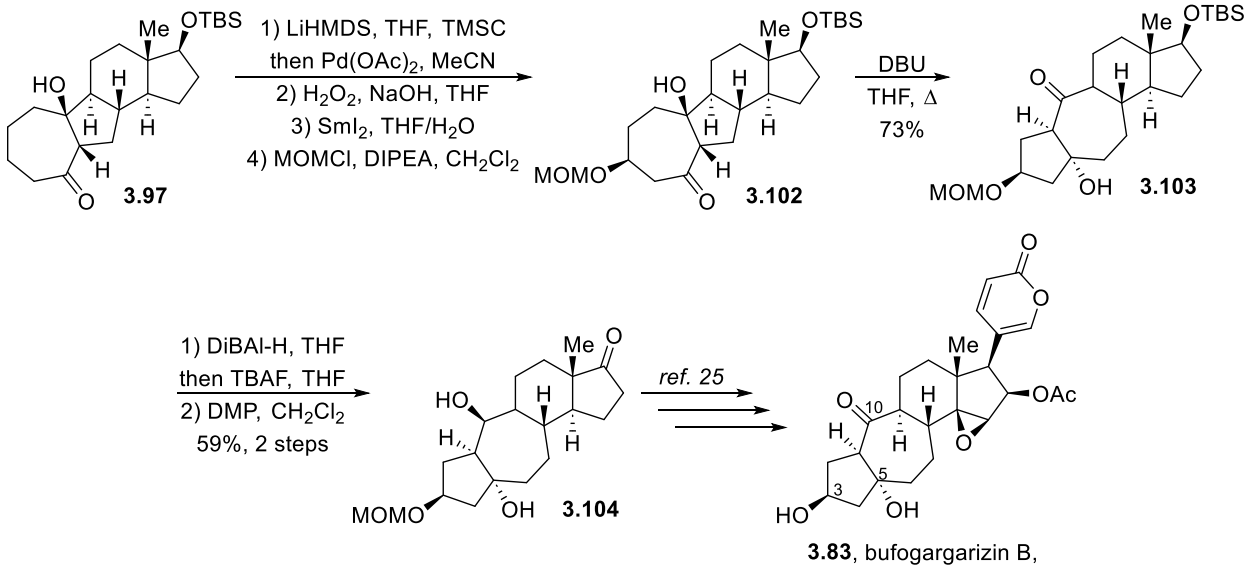
afford **3.99** bearing the C3 alcohol. The C3 alcohol was protected as the methoxymethyl ether, then the C5 ketone was reduced to the secondary alcohol with DiBAl-H and resulting alcohol was protected as a TMS ether. Suzuki cross coupling of tetracyclic vinyl triflate and boronic ester **3.100** afforded the desired α-pyrone product. Epoxidation with *m*CPBA occurred selectively at the $\Delta^{16,17}$ double bond, and the resulting epoxide was opened via S_N2'-like addition of hydride from borane-dimethyl sulfide at the C24 position of the pyrone to afford alcoholic bufenolide **3.101**. The C16 alcohol was oxidized to the ketone, and the $\Delta^{17,20}$ double bond rearranged to the $\Delta^{20,24}$ double bond under basic conditions to reform the α-pyrone. Under these conditions, the C14 OTMS was eliminated to form the $\Delta^{14,15}$ double bond. Equilibration of the C17 stereocenter with LiHMDS afforded the desired diastereomer. The C16 ketone was diastereoselectively reduced with Corey-Bakashi-Shibata reduction[68] to afford the desired alcohol as a single isomer. The newly formed alcohol was acetylated in a one-pot protocol following the reduction. Diastereoselective epoxidation of the $\Delta^{14,15}$ double bond was accomplished with NBS and water in an aqueous solution of NaOH. Global TMS deprotection unmasked the C5 and C10 alcohols. The C5 alcohol was oxidized to the ketone by reaction with DMP. Final removal of the methoxymethyl ether at C3 to furnish the secondary alcohol and completed the synthesis of bufogargarizin A **3.82** in 28 steps from sitolactone. This marked the first total synthesis of a bufadienolide from a non-steroidal starting material.



Scheme 3.14: Li's synthesis of bufogargarizin A **3.82**

Having completed the synthesis of bufogargarizin A **3.82** (Scheme 3.14), Li and coworkers set to finish the synthesis of bufogargarizin B **3.83** (Scheme 3.15). Initial attempts to convert **3.82** to **3.83** via a retroaldol-tautomerization-aldol cascade proved ineffective, and led primarily to the formation of undesired C6 or C10 diastereomers or decomposition of **3.82**. Ultimately, the retro aldol cascade was carried out on an earlier intermediate (Scheme 3.15): compound **3.97**, the product from the [5+2] cycloaddition (Scheme 3.14), prior to Mukayiama

oxidation. The C3 alcohol was installed in a four step sequence of 1) silyl enol ether formation and Saegusa-Ito oxidation, 2) epoxidation with *in situ* generated sodium peroxide, 3) reductive peroxide opening with samarium diiodide, and 4) MOM protection of the newly formed secondary alcohol to provide cascade reaction substrate **3.102**. The retro-aldol-transannular-aldol cascade was achieved on substrate **3.102** by treatment with DBU (15 equivalents) in refluxing THF to provide 5/7/6/5 core structure **3.103** in 73% yield (Scheme 3.15). The C10 ketone was reduce diastereoselectively with DiBAl-H, then the C17 TBS ether was removed by treatment with TBAF. Oxidation of the C17 alcohol to the ketone was achieved with DMP to afford **3.104** in 59% yield over two steps. **3.104** was elaborated to bufogargarizin B **3.83** following the same methods for D-ring modification as described for bufogargarizin A (Scheme 3.14). The synthesis bufogargarizin B **3.83** was completed in 30 steps from sitolactone.



Scheme 3.15: Li's synthesis of bufogargarizin B **3.83**

Li's syntheses of bufogargarizins marked an important milestone in bufadienolide synthesis. The first total syntheses of a bufadienolide natural products, nearly a century after the first bufadienolide was characterized, was no small feat. Current work in our lab is also focused on the synthesis of bufogargarizins with the 5/7/6/5 or 7/5/6/5 core via a transannular aldol

approach (akin to Li's strategy for **3.83**, Scheme 3.15), and the highly oxygenated D-ring would be prepared via the singlet oxygen cycloaddition strategy that was described for cinobufagin[26] (Scheme 3.10). With efficient strategies for bufadienolide aglycones being developed, and the identification and synthesis of the less cytotoxic bufogargarizin subclass of bufadienolides, the possibility of developing a therapeutic from this promising natural product class is much more hopeful.

3.3 Conclusions

The semisynthesis of bufadienolides from other steroids was first reported in the late 1960's. Many of these strategies involved first forming a partially saturated lactone, then performing dehydration or elimination to access the desired α-pyrone, and the C14 oxygenation commonly found in bufadienolide natural products was typically installed after the pyrone was formed. Weisner and Petit were able to successfully convert naturally abundant butenolides to bufadienolides, however these protocols required redundant redox manipulations to remove and reinstall the desired natural oxidation patterns. Watt and coworkers developed a short protocol to generate the α-pyrone moiety from a hydroxy ketone intermediate, and Welzel discovered an efficient cycloaddition to access the 6-membered lactone. Bufogargarizins, a newer class of bufadienolides, had recently been synthesized by the Li group, and the methods to access these *abeo*-steroids creatively circumvented previous challenges encountered during the synthesis of traditional bufadienolides. Nagorny's synthesis of cinobufagin and Inoue's synthesis of bufalin also contained unique approaches toward the α-pyrone installation and subsequent oxygenations. Based on the challenges to access bufadienolides via total synthesis, and relatively small number of analogs prepared via previous semi-synthetic campaigns, we envisioned that a simple and

mild method for the conversion of butenolides to bufadienolides and other similar heterocycles would be of great importance to probe the therapeutic effects of this class of compounds.

3.4 References

(1) Baumgarten, G. Die Herzwirksamen Glykoside : Herkunft, Chemie Und Grundlagen Ihrer Pharmakologischen Und Klinischen Wirkung; *Thieme*, **1963**.

(2) Stoll, A.; Suter, E.; Kreis, W.; Bussemaker, B. B.; Hofmann, A. Die Herzaktiven Substanzen Der Meerzwiebel. Scillaren A. *Helvetica Chimica Acta* **1933**, 16 (1), 703–733. https://doi.org/10.1002/hlca.19330160198.

(3) Krenn, L.; Kopp, B. Bufadienolides from Animal and Plant Sources. *Phytochemistry* **1998**, 48 (1), 1–29. https://doi.org/10.1016/S0031-9422(97)00426-3.

(4) Steyn, P. S.; Heerden, F. R. van. Bufadienolides of Plant and Animal Origin. *Nat. Prod. Rep*. **1998**, 15 (4), 397–413. https://doi.org/10.1039/A815397Y.

(5) Gao, H.; Popescu, R.; Kopp, B.; Wang, Z. Bufadienolides and Their Antitumor Activity. *Nat. Prod. Rep*. **2011**, 28 (5), 953–969. https://doi.org/10.1039/C0NP00032A.

(6) Zou, D.; Wang, Q.; Chen, T.; Sang, D.; Yang, T.; Wang, Y.; Gao, M.; He, F.; Li, Y.; He, L.; Longzhu, D. Bufadienolides Originated from Toad Source and Their Anti-Inflammatory Activity. *Frontiers in Pharmacology*. **2022**, 13.

(7) Yang, Z.; Luo, H.; Wang, H.; Hou, H. Preparative Isolation of Bufalin and Cinobufagin from Chinese Traditional Medicine ChanSu. *Journal of Chromatographic Science*. **2008**, 46 (1), 81–85. https://doi.org/10.1093/chromsci/46.1.81.

(8) Chen, K. K.; Jensen, H. Crystalline Principles From Ch'an Su, the Dried Venom of the Chinese Toad. *Proceedings of the Society for Experimental Biology and Medicine*. **1929**, 26 (5), 378–380. https://doi.org/10.3181/00379727-26-4311.

(9) Laursen, M.; Gregersen, J. L.; Yatime, L.; Nissen, P.; Fedosova, N. U. Structures and Characterization of Digoxin- and Bufalin-Bound Na+,K+-ATPase Compared with the Ouabain-Bound Complex. *Proceedings of the National Academy of Sciences*. **2015**, 112 (6), 1755–1760. https://doi.org/10.1073/pnas.1422997112.

(10) Da Costa, E. M.; Armaos, G.; McInnes, G.; Beaudry, A.; Moquin-Beaudry, G.; Bertrand-Lehouillier, V.; Caron, M.; Richer, C.; St-Onge, P.; Johnson, J. R.; Krogan, N.; Sai, Y.; Downey, M.; Rafei, M.; Boileau, M.; Eppert, K.; Flores-Díaz, E.; Haman, A.; Hoang, T.; Sinnett, D.; Beauséjour, C.; McGraw, S.; Raynal, N. J.-M. Heart Failure Drug Proscillaridin A Targets MYC Overexpressing Leukemia through Global Loss of Lysine Acetylation. *Journal of Experimental & Clinical Cancer Research*. **2019**, 38 (1), 251. https://doi.org/10.1186/s13046-019-1242-8.

(11) Gould, L.; Fisch, S.; Cherbakoff, A.; DeGraff, A. C. Clinical Studies on Proscillaridin a New Squill Glycoside. *J Clin Pharmacol New Drugs*. **1971**, 11 (2), 135–145. https://doi.org/10.1177/009127007101100209.

(12) Khatri, H. R.; Carney, N.; Rutkoski, R.; Bhattarai, B.; Nagorny, P. Recent Progress in Steroid Synthesis Triggered by the Emergence of New Catalytic Methods. *European Journal of Organic Chemistry*. **2020**, 2020 (7), 755–776. https://doi.org/10.1002/ejoc.201901466.

(13) Cichowicz, N. R.; Kaplan, W.; Khomutnyk, Y.; Bhattarai, B.; Sun, Z.; Nagorny, P. Concise Enantioselective Synthesis of Oxygenated Steroids via Sequential Copper(II)-Catalyzed Michael Addition/Intramolecular Aldol Cyclization Reactions. *J. Am. Chem. Soc*. **2015**, 137 (45), 14341–14348. https://doi.org/10.1021/jacs.5b08528.

(14) Kaplan, W.; Khatri, H. R.; Nagorny, P. Concise Enantioselective Total Synthesis of Cardiotonic Steroids 19-Hydroxysarmentogenin and Trewianin Aglycone. *J. Am. Chem. Soc*. **2016**, 138 (22), 7194–7198. https://doi.org/10.1021/jacs.6b04029.

(15) Bhattarai, B.; Nagorny, P. Enantioselective Total Synthesis of Cannogenol-3-O-α-l-Rhamnoside via Sequential Cu(II)-Catalyzed Michael Addition/Intramolecular Aldol Cyclization Reactions. *Org. Lett*. **2018**, 20 (1), 154–157. https://doi.org/10.1021/acs.orglett.7b03513.

(16) Khatri, H. R.; Bhattarai, B.; Kaplan, W.; Li, Z.; Long, M. J. C.; Aye, Y.; Nagorny, P. Modular Total Synthesis and Cell-Based Anticancer Activity Evaluation of Ouabagenin and Other Cardiotonic Steroids with Varying Degrees of Oxygenation. *J. Am. Chem. Soc.* **2019**, *141* (12), 4849–4860. https://doi.org/10.1021/jacs.8b12870.

(17) Urabe, D.; Nakagawa, Y.; Mukai, K.; Fukushima, K.; Aoki, N.; Itoh, H.; Nagatomo, M.; Inoue, M. Total Synthesis and Biological Evaluation of 19-Hydroxysarmentogenin-3-O-α-l-Rhamnoside, Trewianin, and Their Aglycons. J. Org. Chem. 2018, 83 (22), 13888–13910. https://doi.org/10.1021/acs.joc.8b02219.

(18) Zhang, H.; Sridhar Reddy, M.; Phoenix, S.; Deslongchamps, P. Total Synthesis of Ouabagenin and Ouabain. *Angewandte Chemie International Edition*. **2008**, 47 (7), 1272–1275. https://doi.org/10.1002/anie.200704959.

(19) Renata, H.; Zhou, Q.; Baran, P. S. Strategic Redox Relay Enables A Scalable Synthesis of Ouabagenin, A Bioactive Cardenolide. **Science**. *2013*, 339 (6115), 59–63. https://doi.org/10.1126/science.1230631.

(20) Watanabe, S.; Nishikawa, T.; Nakazaki, A. Total Synthesis of the Cardiotonic Steroid (+)-Cannogenol. *J. Org. Chem*. **2021**, 86 (4), 3605–3614. https://doi.org/10.1021/acs.joc.0c02966.

(21) Heasley, B. Chemical Synthesis of the Cardiotonic Steroid Glycosides and Related Natural Products. *Chemistry – A European Journal*. **2012**, 18 (11), 3092–3120. https://doi.org/10.1002/chem.201103733.

(22) Michalak, M.; Michalak, K.; Wicha, J. The Synthesis of Cardenolide and Bufadienolide Aglycones, and Related Steroids Bearing a Heterocyclic Subunit. *Nat. Prod. Rep*. **2017**, 34 (4), 361–410. https://doi.org/10.1039/C6NP00107F.

(23) Zhong, Y.-; Zhao, C.-; Wu, W.-Y.; Fan, T.-Y.; Li, N.-G.; Chen, M.-; Duan, J.-A.; Shi, Z.-H. Total Synthesis, Chemical Modification and Structure-Activity Relationship of Bufadienolides. *European Journal of Medicinal Chemistry*. **2020**, 189, 112038. https://doi.org/10.1016/j.ejmech.2020.112038.

(24) Shimizu, S.; Hagiwara, K.; Itoh, H.; Inoue, M. Unified Total Synthesis of Five Bufadienolides. Org. Lett. 2020, 22 (21), 8652–8657. https://doi.org/10.1021/acs.orglett.0c03251.

(25) Zhong, L.-P.; Feng, R.; Wang, J.-J.; Li, C.-C. Asymmetric Total Synthesis of Twin Bufogargarizins A and B. *J. Am. Chem. Soc*. **2023**, 145 (4), 2098–2103. https://doi.org/10.1021/jacs.2c13494.

(26) Tichvon, C.; Zviagin, I.; Nagorny, P. Efficient Synthesis of Cinobufagin. *Manuscript in Preparation*. **2023**.

(27) Sondheimer, F.; McCrae, W.; Salmond, W. G. Synthesis of Bufadienolides. Synthesis of Bufalin and Resibufogenin. *J. Am. Chem. Soc*. **1969**, 91 (5), 1228–1230. https://doi.org/10.1021/ja01033a039.

(28) Stache, U.; Radscheit, K.; Fritsch, W.; Kohl, H.; Haede, W.; Ruschig, H. Synthesen von Bufadienoliden Synthese von Scillarenin. *Tetrahedron Letters* **1969**, 10 (35), 3033–3038. https://doi.org/10.1016/S0040-4039(01)88337-4.

(29) Stache, U.; Radscheit, K.; Fritsch, W.; Haede, W.; Kohl, H.; Ruschig, H. Herstellung von ungesättigten Lactonen der Steroidreihe, VII. Synthese von 4(5)-Dehydro-bufadienoliden. *Justus Liebigs Annalen der Chemie* **1971**, 750 (1), 149–164. https://doi.org/10.1002/jlac.19717500117.

(30) Pettit, G. R.; Fessler, D. C.; Paull, K. D.; Hofer, P.; Knight, J. C. Synthesis of buf-20(21)-enolides and bufa-20,22-dienolides. *Can. J. Chem*. **1969**, 47 (13), 2511–2513. https://doi.org/10.1139/v69-416.

(31) Pettit, G. R.; Knight, J. C.; Herald, C. L. Steroids and Related Natural Products. LIII. Bufadienolides. 6. Synthesis of 17.Beta.-(6-.Alpha.-Pyronyl)Androstanes. *J. Org. Chem*. **1970**, 35 (5), 1393–1398. https://doi.org/10.1021/jo00830a030.

(32) Pettit, G. R.; Fessler, D. C.; Paull, K. D.; Hofer, P.; Knight, J. C. Steroids and Related Natural Products. LIV. Bufadienolides. 7. Synthesis of 3.Beta.-Acetoxy-5.Alpha.-L4.Alpha.-Bufa-20,22-Dienolide. *J. Org. Chem*. **1970**, 35 (5), 1398–1404. https://doi.org/10.1021/jo00830a031.

(33) Pettit, G. R.; Dias, J. R. Bufadienolides. 13. Conversion of 3.Beta.-Hydroxy-17-Oxoandrost-5-Ene to 3.Beta.-Acetoxy-5.Beta.,14.Alpha.-Bufa-20,22-Dienolide. *J. Org. Chem.* **1971**, 36 (21), 3207–3211. https://doi.org/10.1021/jo00820a028.

(34) Haddad, Y. M. Y.; Henbest, H. B.; Husbands, J.; Mitchell, T. R. B. Reduction of Cyclohexanones to Axial Alcohols via Iridium-Containing Catalysts. *Proc. Chem. Soc.* **1964**, 361.

(35) Über eine neue Methode zur Darstellung von Aldehyden. 1. Mitteilung - Rosenmund - 1918 - Berichte der deutschen chemischen Gesellschaft - Wiley Online Library. https://chemistry-europe.onlinelibrary.wiley.com/doi/abs/10.1002/cber.19180510170 (accessed 2023-11-02).

(36) Yoshii, E.; Oribe, T.; Koizumi, T.; Hayashi, I.; Tumura, K. Studies on the Synthesis of Cardiotonic Steroids. III. New and Effective Route to Bufadienolides. *Chemical & Pharmaceutical Bulletin* **1977**, 25 (9), 2249–2256. https://doi.org/10.1248/cpb.25.2249.

(37) 英一吉井; 保三輪; 徹小泉; 栄太郎北辻. Facile Preparation of Pregn-14-Ene-20, 21-Diones. *Chemical & Pharmaceutical Bulletin* **1975**, 23 (2), 462–464. https://doi.org/10.1248/cpb.23.462.

(38) Kabat, M. M.; Kurek, A.; Wicha, J. Cardiotonic Steroids. 5. A Synthesis of Bufadienolides and Cardenolides from 3.Beta.-Acetoxy-5-Androsten-17-One via Common Intermediates. *J. Org. Chem.* **1983**, 48 (23), 4248–4251. https://doi.org/10.1021/jo00171a018.

(39) Bauer, P. E.; Kyler, K. S.; Watt, D. S. A Synthesis of 3.Beta.-Hydroxy-5.Beta.,14.Alpha.-Bufa-20,22-Dienolide from Deoxycorticosterone. *J. Org. Chem.* **1983**, 48 (1), 34–39. https://doi.org/10.1021/jo00149a007.

(40) Hoppe, H.-W.; Welzel, P. A Synthesis of Bufalin from Deoxycholic Acid. *Tetrahedron Letters* **1986**, 27 (22), 2459–2462. https://doi.org/10.1016/S0040-4039(00)84555-4.

(41) Welzel, P.; Stein, H.; Milkova, T. 14β-Hydroxysteroide, VII. Synthese von Digoxigenin und Digitoxigenin aus Desoxycholsäure. *Liebigs Annalen der Chemie* **1982**, 1982 (12), 2119–2134. https://doi.org/10.1002/jlac.198219821203.

(42) Murai, A.; Sato, S.; Masamune, T. π-Cyclization: The Synthesis of (±)-Solavetivone and (±)-Hinesol. *Tetrahedron Letters* **1981**, 22 (11), 1033–1036. https://doi.org/10.1016/S0040-4039(01)82858-6.

(43) Hoppe, H. W.; Kaiser, M.; Müller, D.; Welzel, P. An Approach to Bufadienolides from Deoxycholic Acid-1: Strategy and Synthesis of a Model Bufadienolide. *Tetrahedron* **1987**, 43 (9), 2045–2057. https://doi.org/10.1016/S0040-4020(01)86786-7.

(44) Hoppe, H.-W.; Stammen, B.; Werner, U.; Stein, H.; Welzel, P. An Approach to Bufadienolides from Deoxycholic Acid. Reactions of a Steroidal Aβ-Unsaturated

Aldehyde with Some O-Silylated Ketene Acetals. *Tetrahedron* **1989**, 45 (12), 3695–3710. https://doi.org/10.1016/S0040-4020(01)89231-0.

(45) Liu, Z.; Meinwald, J. 5-(Trimethylstannyl)-2H-Pyran-2-One and 3-(Trimethylstannyl)-2H-Pyran-2-One: New 2H-Pyran-2-One Synthons. *J. Org. Chem*. **1996**, 61 (19), 6693–6699. https://doi.org/10.1021/jo951394t.

(46) Gravett, E. C.; Hilton, P. J.; Jones, K.; Péron, J.-M. A New Route to 5-Aryl and 5-Heteroaryl-2-Pyrones via Suzuki Coupling of a 2-Pyrone-5-Boronate Ester. *Synlett* **2003**, 2003 (2), 253–255. https://doi.org/10.1055/s-2003-36789.

(47) Gravett, E. C.; Hilton, P. J.; Jones, K.; Romero, F. A Suzuki Coupling Approach to Bufadienolides. *Tetrahedron Letters* **2001**, 42 (51), 9081–9084. https://doi.org/10.1016/S0040-4039(01)01980-3.

(48) Fejedelem, Z.; Carney, N.; Nagorny, P. Synthesis of Cardiotonic Steroids Oleandrigenin and Rhodexin B. *J. Org. Chem*. **2021**, 86 (15), 10249–10262. https://doi.org/10.1021/acs.joc.1c00985.

(49) Isayama, S.; Mukaiyama, T. A New Method for Preparation of Alcohols from Olefins with Molecular Oxygen and Phenylsilane by the Use of Bis(Acetylacetonato)Cobalt(II). *Chem. Lett.* **1989**, 18 (6), 1071–1074. https://doi.org/10.1246/cl.1989.1071.

(50) Barton, D. H. R.; O'Brien, R. E.; Sternhell, S. 88. A New Reaction of Hydrazones. *J. Chem. Soc*. **1962**, No. 0, 470–476. https://doi.org/10.1039/JR9620000470.

(51) Carney, N.; Perry, N.; Garabedian, J.; Nagorny, P. Development of α-Selective Glycosylation with l-Oleandral and Its Application to the Total Synthesis of Oleandrin. *Org. Lett*. **2023**, 25 (6), 966–971. https://doi.org/10.1021/acs.orglett.2c04358.

(52) Orfanopoulos, M. Singlet Oxygen: Discovery, Chemistry, C60-Sensitization†. *Photochemistry and Photobiology* **2021**, 97 (6), 1182–1218. https://doi.org/10.1111/php.13486.

(53) Petschenka, G.; Züst, T.; Hastings, A. P.; Agrawal, A. A.; Jander, G. Chapter Ten - Quantification of Plant Cardenolides by HPLC, Measurement of Na+/K+-ATPase Inhibition Activity, and Characterization of Target Enzymes. In Methods in Enzymology; Jez, J., Ed.; *Biochemical Pathways and Environmental Responses in Plants: Part B*; Academic Press, **2023**; Vol. 680, pp 275–302. https://doi.org/10.1016/bs.mie.2022.08.003.

(54) Harry, R. Extraction and Isolation of Digitoxin. *US2449673A*, September 21, **1948**. https://patents.google.com/patent/US2449673A/en (accessed 2023-11-02).

(55) Pettit, G. R.; Houghton, L. E.; Knight, J. C.; Bruschweiler, F. Bufadienolides. 11. Bufalin and Resibufogenin. *J. Org. Chem*. **1970**, 35 (9), 2895–2898. https://doi.org/10.1021/jo00834a008.

(56) Bach, G.; Capitaine, J.; Engel, Ch. R. Steroids and Related Products. XXV. Cardiotonic Steroids. II. The Synthesis of 17β-Substituted 14(15)-Unsaturated Steroids of the A/B-Cis Series. Part I. *Can. J. Chem*. **1968**, 46 (5), 733–749. https://doi.org/10.1139/v68-123.

(57) Tsai, T. Y. R.; Wiesner, K. On Cardioactive Steroids. IX. The Conversion of Digitoxigenin to Bufalin. *Can. J. Chem*. **1982**, 60 (16), 2161–2163. https://doi.org/10.1139/v82-309.

(58) Wiesner, K.; Tsai, T. Y. R.; Jäggi, F. J.; Tsai, C. S. J.; Gray, G. D. On Cardioactive Steroids. VIII. The Synthesis of Bufalin and Resibufogenin Isomers. *Helvetica Chimica Acta* **1982**, 65 (7), 2049–2060. https://doi.org/10.1002/hlca.19820650712.

(59) Wiesner, K.; Tsai, T. Y. R.; Sen, A.; Kumar, R.; Tsubuki, M. On Cardioactive Steroids. XII. The Synthesis of (Natural) Bufalin and A′-Isobufalin. *Helvetica Chimica Acta* **1983**, 66 (8), 2632–2640. https://doi.org/10.1002/hlca.19830660831.

(60) Minato, H.; Nagasaki, T. A New Method for the Synthesis of Furan Compounds. *J. Chem. Soc. C.* **1966**, No. 0, 377–379. https://doi.org/10.1039/J39660000377.

(61) Ferland, J. M.; Lefebvre, Y.; Deghenghi, R.; Wiesner, K. Synthetic New Cardenolides. *Tetrahedron Letters* **1966**, 7 (30), 3617–3620. https://doi.org/10.1016/S0040-4039(01)82838-0.

(62) Wiesner, K.; Josef J拡gi, F.; Y. R. Tsai, T. On Cardioactive Steroids VII. The Conversion of Digitoxigenin to Isomers of Natural Bufalin and Resibufogenin. *HETEROCYCLES* **1982**, 19 (4), 647. https://doi.org/10.3987/R-1982-04-0647.

(63) Tian, H.-Y.; Wang, L.; Zhang, X.-Q.; Wang, Y.; Zhang, D.-M.; Jiang, R.-W.; Liu, Z.; Liu, J.-S.; Li, Y.-L.; Ye, W.-C. Bufogargarizins A and B: Two Novel 19-Norbufadienolides with Unprecedented Skeletons from the Venom of Bufo Bufo Gargarizans. *Chemistry – A European Journal* **2010**, 16 (36), 10989–10993. https://doi.org/10.1002/chem.201000847.

(64) New Cytotoxic 19-Norbufadienolide and Bufogargarizin Isolated from Chan Su. *Fitoterapia* **2015**, 104, 1–6. https://doi.org/10.1016/j.fitote.2015.05.011.

(65) Fan, J.-H.; Hu, Y.-J.; Guo, Q.; Li, S.; Zhao, J.; Li, C.-C. Asymmetric Synthesis of the Tetracyclic Core of Bufogargarizin C by an Intramolecular [5 + 2] Cycloaddition. *Org. Chem. Front*. **2018**, 6 (1), 22–26. https://doi.org/10.1039/C8QO01089G.

(66) Dhawan, D.; Grover, S. K. Facile Reduction of Chalcones to Dihydrochalcones with NaBH4/Ni2+ System. *Synthetic Communications* **1992**, 22 (16), 2405–2409. https://doi.org/10.1080/00397919208019098.

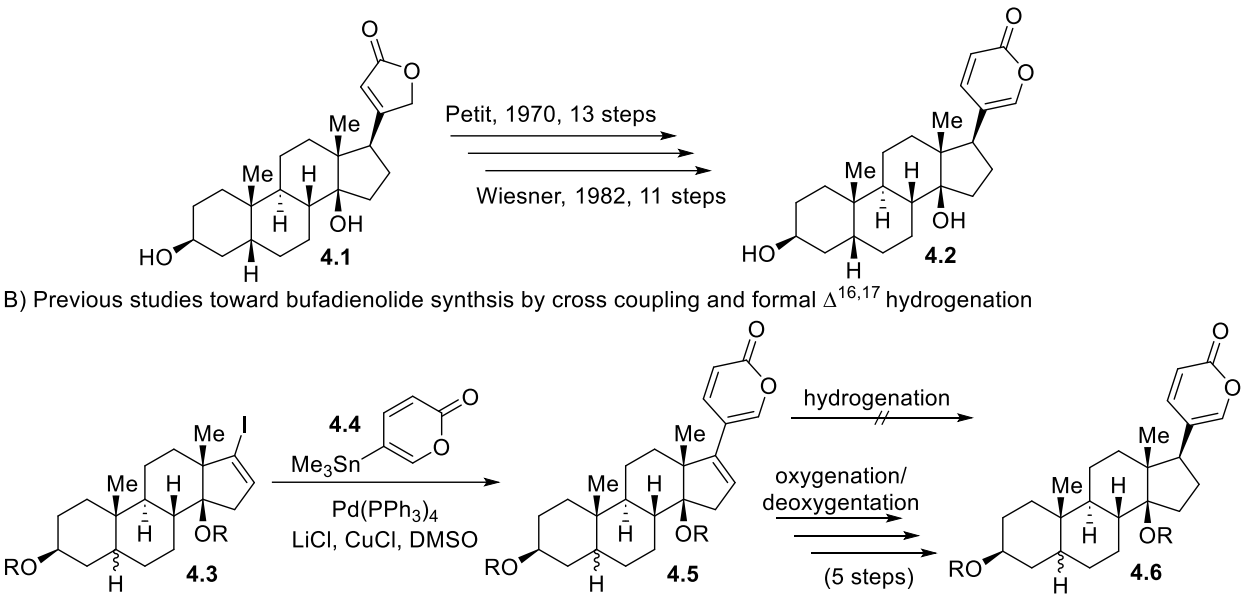
(67) Chemistry of sulfonylmethyl isocyanides. 13. A general one-step synthesis of nitriles from ketones using tosylmethyl isocyanide. Introduction of a one-carbon unit | The *Journal of Organic Chemistry*. https://pubs.acs.org/doi/10.1021/jo00439a002 (accessed 2023-11-02).

(68) Corey, E. J.; Bakshi, R. K.; Shibata, S. Highly Enantioselective Borane Reduction of Ketones Catalyzed by Chiral Oxazaborolidines. Mechanism and Synthetic Implications. *J. Am. Chem. Soc*. **1987**, 109 (18), 5551–5553. https://doi.org/10.1021/ja00252a056.

Chapter 4 Studies Towards the Synthesis of Bufadienolides

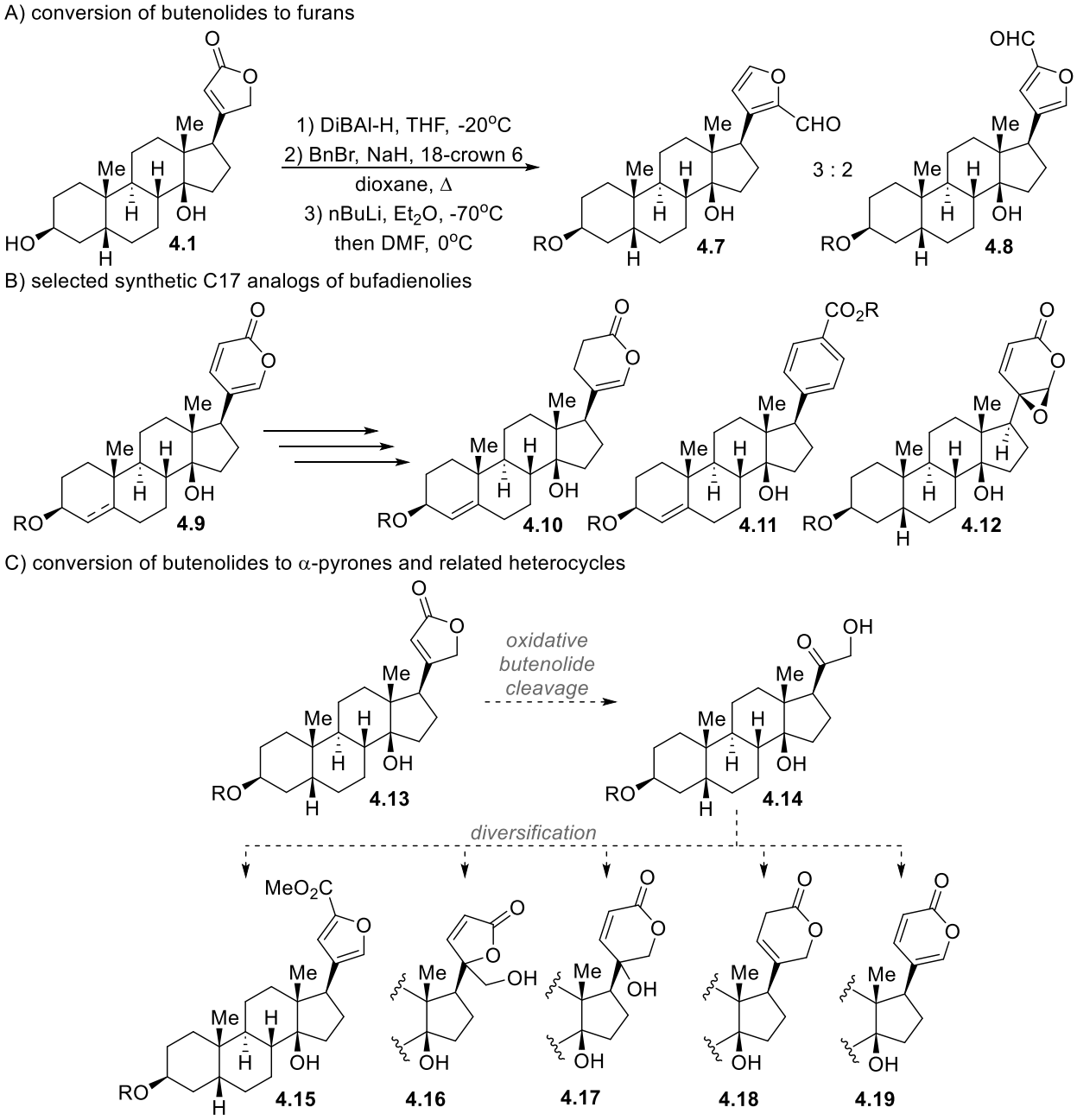
4.1 Introduction

Bufadienolides have been used in traditional medicine for thousands of years as the active components of Chinese medicines derived from toad venom such as Ch'an su and Senso.[1,2] These natural products have relatively low natural abundance, and until recently, they had only been prepared by lengthy semi-synthetic procedures.[3-5] Petit[6] and Weisner[7,8] each independently prepared the bufadienolide bufalin **4.2** in a semi synthetic manner from the cardenolide digitoxigenin **4.1**, which shares the same core steroidal structure, and only differs by the C17 heterocycle. Their syntheses required 13- and 11- steps, respectively, and during the process, the C14 tertiary alcohol was eliminated and had to be reinstalled (Scheme 4.1A). Several other groups have reported the semisynthesis of bufadienolides, and these were often lengthy, and resulted in low yields of the pyrone installation step.[3-5] Several groups had reported the cross coupling of α-pyrone stannanes (e.g. **4.4**) with steroidal vinyl iodides (e.g. **4.3**).[9-13] However, extensive studies by our group found that selective hydrogenation of the $\Delta^{16,17}$ of **4.5** was challenging, and resulted in products of over-reduction, hydrogenolysis, and olefin migration (Scheme 4.1B).[12] Recently, a convergent strategy for the synthesis of bufadienolides, including bufalin was reported by Inoue, where the $\Delta^{16,17}$ of **4.5** was removed via an epoxidation of the $\Delta^{16,17}$ and four additional steps to remove the newly installed oxygen (Scheme 4.1B) to provide bufadienolide **4.6**.[11] Through these methods, the synthesis of bufadienolides had been achieved, but very few analogs had been prepared for medicinal chemistry studies.[5]



Scheme 4.1: Selected previous syntheses towards bufadienolides

Butenolides have previously been converted to furans (Scheme 4.2A),[7,14-16] and the furan derivatives (**4.7**, **4.8**) on the digitoxigenin backbone (**4.8**) were shown to have increased binding affinity to the Na/K ATPase in a computational binding study.[17] Previous synthesis of the carbonylated furan derivates was limited by the formation of multiple regioisomeric products (**4.7**, **4.8**). Bufadienolide analogs have been prepared from the modification of naturally extracted bufadienolides.[5] Unnatural bufadienolide analogs have not been previously prepared from total synthesis. Some exploration of modifications (Scheme 4.2B) to the C17 heterocycle provided **4.12**, which had high affinity as a IL-6 receptor antagonist.[18] Overactivation of IL-6 receptor is involved in the onset and progression of certain cancers.[19,20] Semi-hydrogenated analog **4.10** and phenyl derivative **4.11** showed improved safety profiles in animal models.[21-25] The limited supply and low selectivity for the transformations has made deep exploration of C17 heterocyclic analogs of bufadienolides challenging.

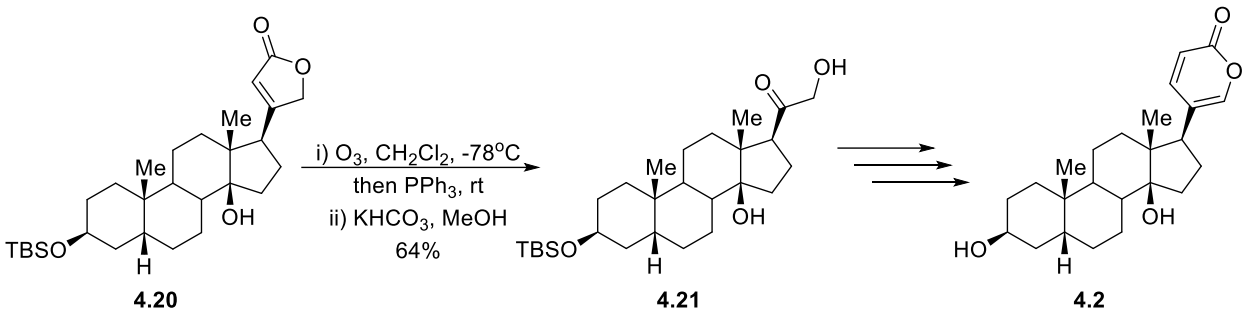


Scheme 4.2: Synthesis of C17 heterocyclic analogs of butenolides and bufadienolides

A short, simple protocol for the conversion of butenolides (**4.13**) to bufadienolides would greatly benefit and expedite medicinal chemistry studies of these compounds. Facile oxidative cleavage of the butenolide would afford hydroxy ketone **4.14**, which could be elaborated to various heterocycles (e.g. **4.15-4.18**) (Scheme 4.2C). This intermediate could serve as a key diversification point for the synthesis of bufadienolides (**4.19**) from butenolides.

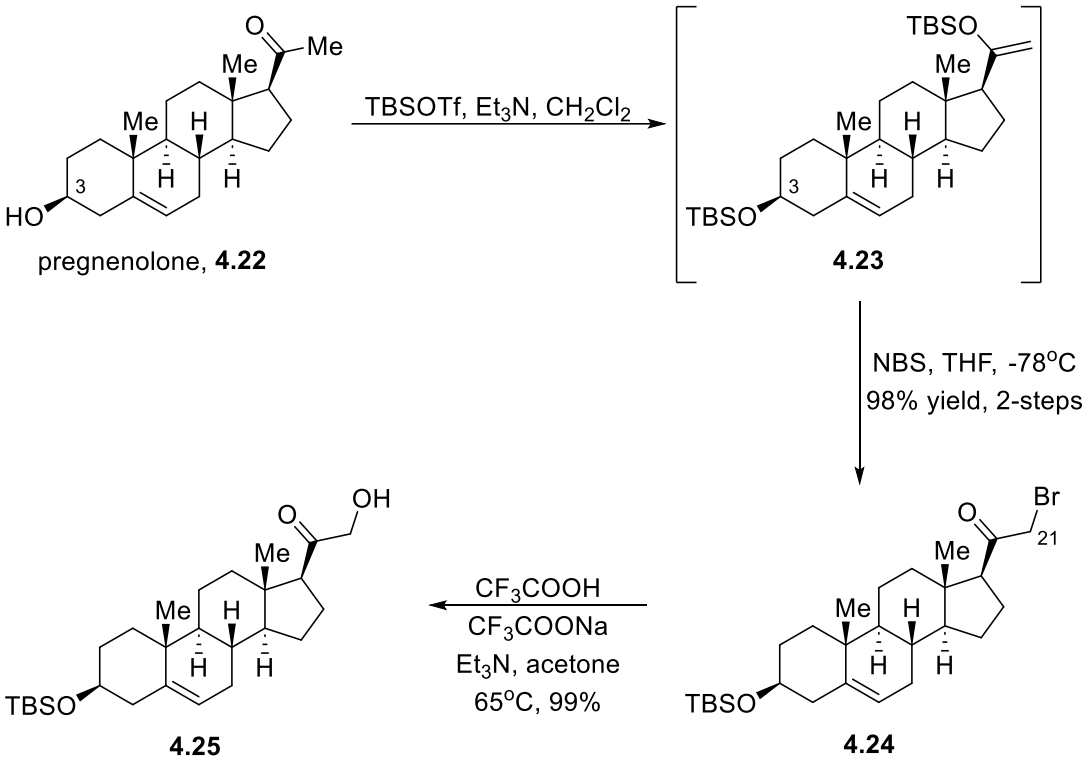
4.2 Oxidative butenolide cleavage and model substrate synthesis

We envisioned proceeding from butenolides to α-pyrones through hydroxy and related heterocycles through ketone intermediate **4.21** (Scheme 4.2), similar to intermediate **3.36** employed in Watt's bufadienolide synthesis (Scheme 3.6).[26] Oxidative cleavage of butenolides had been previously reported,[27-34] and the method was adapted for the conversion of silylated digitoxigenin analog **4.20** to hydroxyketone **4.21** (Scheme 4.3). With the proof of concept oxidative cleavage in hand we began to explore methods for pyrone formation on a model substrate **4.25**.



Scheme 4.3: Oxidative cleavage of butenolides to access key hydroxy ketone intermediate **4.2**[a]
[a]ozonolysis (i) was carried on 0.20 mmol **4.20** with PPh_3 (0.40 mmol, 2.0 equiv). hydrolysis (ii) was carried with 10:1 MeOH:sat. aq. $KHCO_3$ (5.0:0.5 mL).

Model substrate **4.25** was prepared in three steps from pregnenolone **4.22** (Scheme 4.4). First, treatment of pregnenolone **4.22** with TBSOTf and Et_3N afford the C3-TBS ether and $\Delta^{20,21}$ silyl enol ether **4.23**. Selective bromination of the $\Delta^{20,21}$ silyl enol ether afforded pregnenolone bromide **4.24**. A one-pot protocol of S_N2 displacement of the bromide with trifluoroacetate and *in situ* deacylation afforded pregnenolone derived hydroxy ketone **4.25**. This method was quite efficient, high yielding (97% over 3 steps), and provided multi-gram quantities of hydroxy ketone **4.25**.



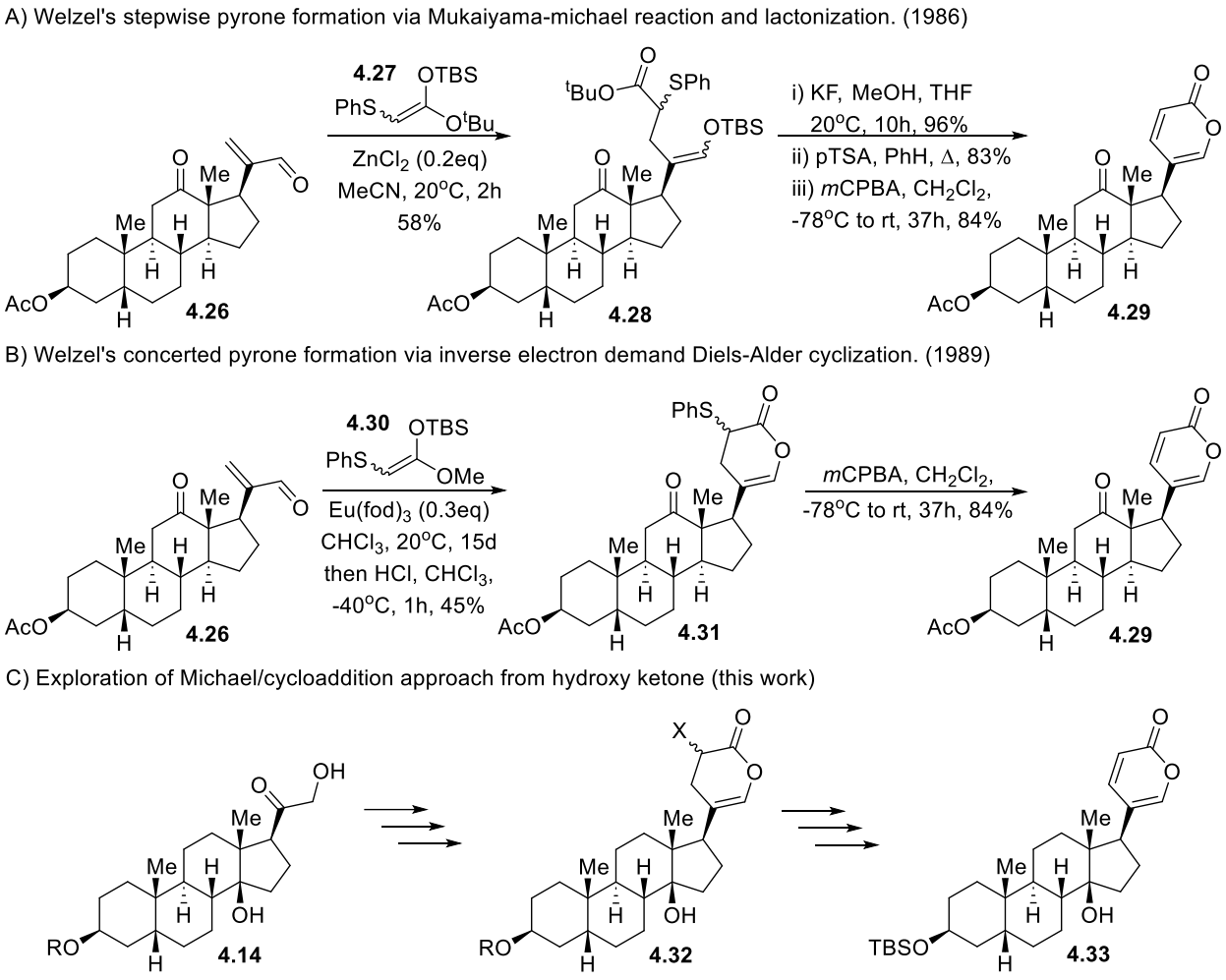
Scheme 4.4: Synthesis of model pregnenolone-derived hydroxy ketone **4.25**.[a]
[a]Preparation of hydroxy ketone **4.25** was carried from 5.0 g (16 mmol) **4.22**.

The desired hydroxy ketone **4.25** could also be prepared in a five step sequence of 1) TBS protection of C3 alcohol, 2) $\Delta^{20,21}$ silyl enol ether formation , 3) bromination of the silyl enol ether with NBS, 4) S_N2 displacement of the bromide with sodium benzoate/acetate and 5) deacylation. This sequence provided hydroxy ketone **4.25** in 86% yield over the five steps. With the desired model substrate in hand, exploration of α-pyrone formation was investigated next.

4.3 Intermolecular 1,4-addition and cycloaddition strategies

Welzel's methodology for the synthesis of bufadienolides via an inverse-electron demand Diels-Alder cycloaddition caught our attention as a promising avenue to begin our studies.[35-38] Welzel's exploration began with the Michael reaction and subsequent acid-catalyzed lactonization to form the dihydropyrone moiety (Scheme 3.7). Attempts of standard Michael reaction of **4.25** with *tert*-butyl methylsulfanyl acetate with sodium methoxide as the base

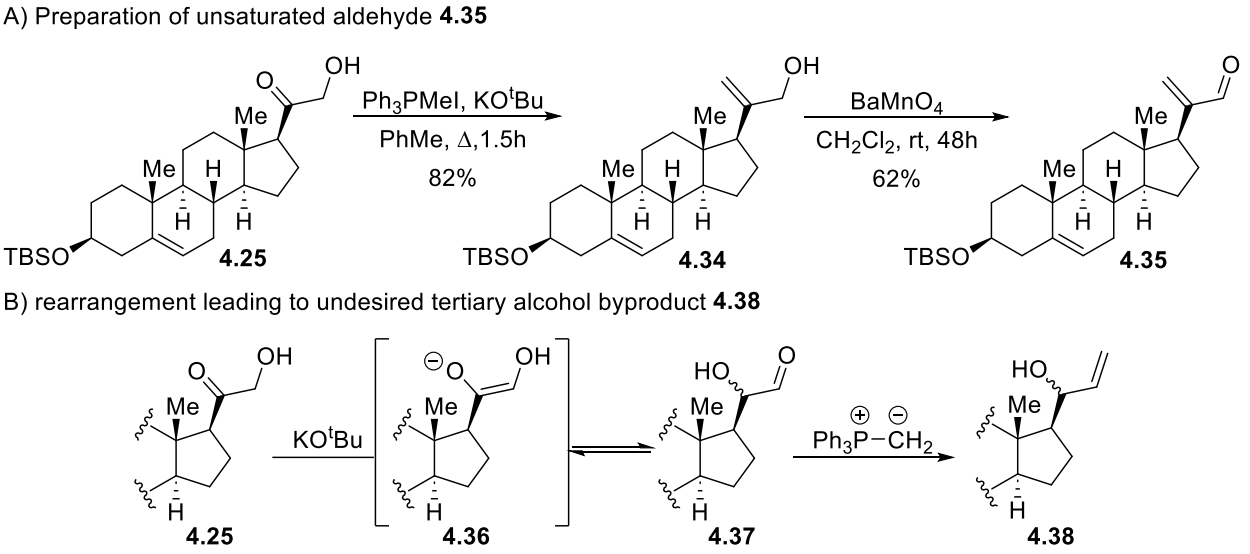
provided the 1,4-addition product in 38% yield, but were accompanied by aldol condensation (8%) and dimerization (5%) byproducts.[37]



Scheme 4.5: Previous studies of pyrone formation via cycloaddition and oxidation

The Mukaiyama Michael reaction of silyl ketene acetal **4.27** with Michael acceptor **4.26** afforded the desired 1,4-addition product **4.28** in 58% yield (Scheme 4.5A).[36] The Michael adduct was progressed to α-pyrone **4.29** through a three step sequence of 1) desilylation, 2) acid catalyzed enol lactonization, and 3) oxidative eliminate of the thioether. Through optimization of the Lewis acid promoter, they were able to favor the concerted [4+2] reaction pathway to provide the orthoester intermediate (Scheme 4.5B).[38] The orthoester was unstable, and was immediately converted to bufenolide **4.31** by treatment with anhydrous hydrochloric acid. Subsequent

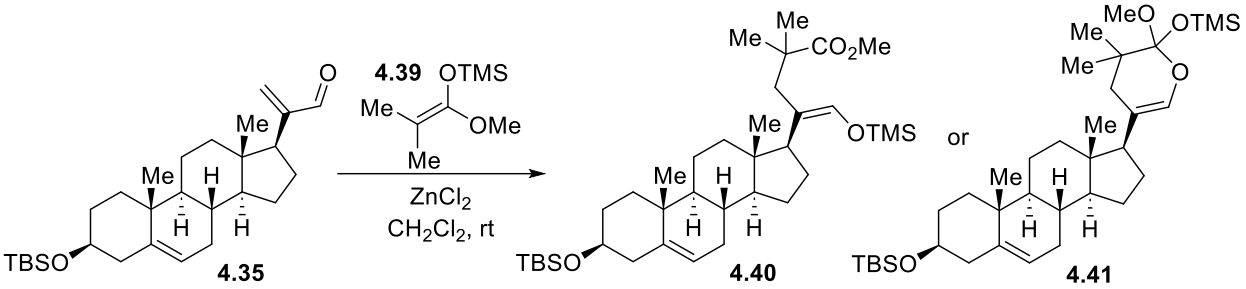
oxidative elimination of the thioether provided α-pyrone **4.29**. We envisioned that optimization of the reaction conditions (catalyst, solvent, temperature) would improve the efficiency (yield and reaction time) of both the Michael reaction and cycloaddition (Scheme 4.5C).



Scheme 4.6: Synthesis of unsaturated aldehyde **4.35**
A) Wittig olefination was carried with 1.0 g (2.3 mmol) **4.25**. Oxidation of the allylic alcohol was to **4.35** was carried with 0.20 g (0.45 mmol) **4.34**.

Starting from our model hydroxy ketone **4.25**, we carried out a two-step procedure of Wittig-methylenation and oxidation of the allylic alcohol to access the desired unsaturated aldehyde **4.25** (Scheme 4.6A). Close monitoring of the Wittig reaction was crucial to avoid the formation of byproduct **4.38**, which was the result of deprotonation of the C21-α-H. The hydrogen bond-stabilized enolate **4.36** could be re-protonated at the C20-position, to form aldehyde **4.37**. Wittig olefin of the aldehyde resulted in formation of tertiary alcohol byproduct **4.38**, which was observed during prolonged exposure of the ketone to the reaction conditions (Scheme 4.6B). With the optimized condition (PhMe, 110^{o}C, 1.5 h) the desired allylic alcohol was prepared in good yields (82% with Ph_3PMeI, or 76% with Ph_3PMeBr). Desired allylic alcohol **4.34** was oxidized with $BaMnO_4$ to afford conjugated aldehyde **4.35** (Scheme 4.6B). Oxidation of the allylic alcohol could also be carried with DMP (CH_2Cl_2, 71%) or MnO_2

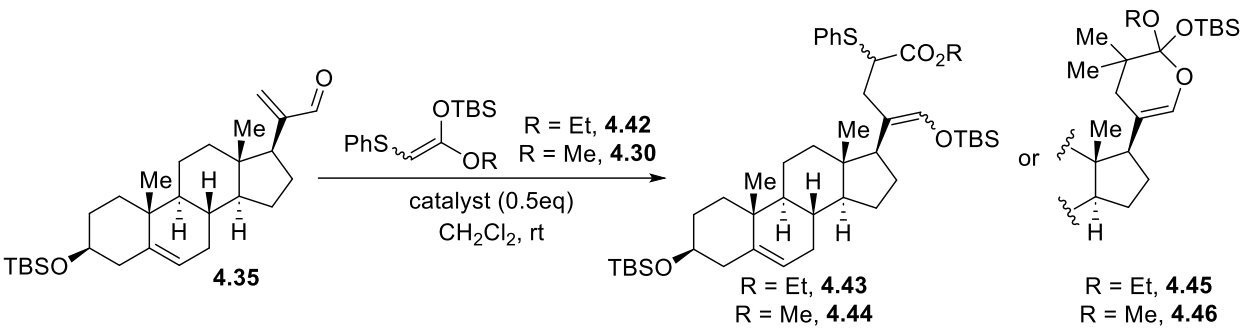
(acetone, 50%). The conjugated aldehyde **4.35** was employed as the diene (or Michael acceptor) in the subsequent studies (Scheme 4.7, Table 4.1, Scheme 4.9).



Scheme 4.7: Preliminary reaction study of aldehyde **4.35** with silyl ketene acetal **4.39**.[a]
[a]**4.35** (20 µmol, 1.0 eq), **4.39** (40 µmol, 2.0 equiv), $ZnCl_2$ (10 µmol, 0.5 equiv), CH_2Cl_2 (0.4 mL), rt, 5h.

We began by investigating the reaction between conjugated aldehyde **4.35** with commercially available silyl ketene acetal **4.39** (Scheme 4.7). The uncatalyzed thermal reaction of **4.35** and **4.39** resulted in neither the Michael product **4.40** nor the cycloaddition product **4.41**, and the starting aldehyde **4.35** was quantitatively recovered. The reaction of **4.35** and **4.39** with $Eu(fod)_3$ in CH_2Cl_2 resulted in only trace formation of the Michael adduct **4.40** and the orthoester **4.41**, even over prolonged reaction times (>4 days), and most of the starting aldehyde **4.35** was recovered (>95%). The reaction of **4.35** and **4.39** promoted by zinc (II) chloride led to full consumption of aldehyde **4.35** and exclusive formation of the 1,4-addition product **4.40** in 90% yield (Scheme 4.7). Attempts to directly cyclize the enol ether **4.40** to the enol lactone (pTsOH, rt or 80^{o}C) led to complex mixture of products, including only trace amounts of the desired lactone.

Table 4.1: Reaction screening of aldehyde **4.35** with 2-sulfanyl silylketene acetals **4.42** and **4.30.**[a]

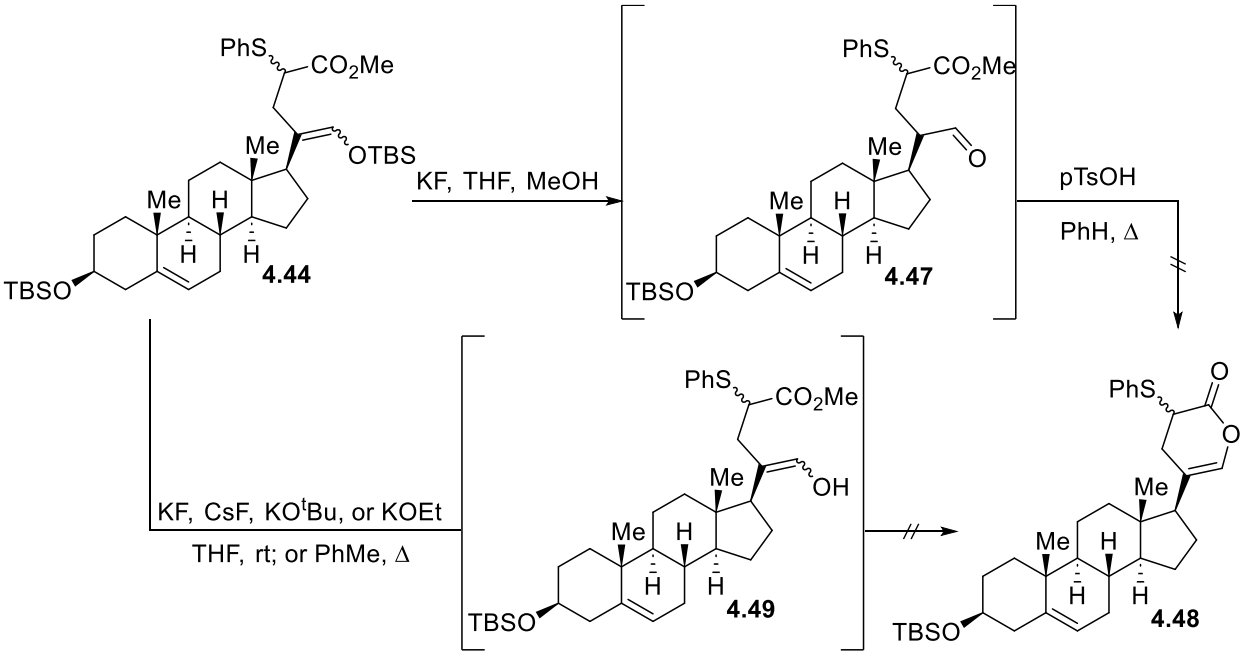


Entry	dienophile	catalyst	time	yield
1	**4.42**	-	4d	trace
2	**4.42**	$Eu(fod)_3$	4d	trace
3	**4.42**	$ZnCl_2$	4d	trace
4	**4.30**	$Eu(fod)_3$	4d	trace
5	**4.30**	$ZnCl_2$	17h	83% (**4.43)**
6	**4.30**	$ZnCl_2$[b]	30h	trace

[a]reactions were carried with **4.35** (20 µmol, 1.0 eq), **4.30** or **4.42** (40 µmol, 2.0 equiv), promoter (10 µmol, 0.5 equiv), CH_2Cl_2 (0.4 mL), rt. Yields reported are of isolated products after flash column chromatography. Trace yield is < 5% as judged by ^1H NMR.

Next, cycloadditions with 2-sulfanyl silylketene acetals **4.42** and **4.30** were investigated (Table 4.1). The uncatalyzed (entry 1), $Eu(fod)_3$ (entry 2) and $ZnCl_2$-catalyzed (entry 3) reactions of ethyl silyl ketene acetal **4.42** with conjugated aldehyde **4.35** produced only trace amounts of the Michael (**4.43)** and cycloaddition (**4.45**) products. The $Eu(fod)_3$-catalyzed reaction (entry 4) of methyl silyl ketene acetal **4.30** with conjugated aldehyde **4.35** resulted in only trace amounts of products **4.44** and **4.46**. In all of these aforementioned trials (Table 4.1, entry 1-4), the starting aldehyde **4.35** was nearly quantitatively recovered (>95%). To our delight, employing $ZnCl_2$ as the catalyst with methyl silyl ketene acetal **4.30** afforded the 1,4-addition product **4.44** in 83% yield. This was a significant improvement from the yield seen by Welzel (58%, Scheme 4.5A). Finally, we envisioned that transfer of the silyl group could be suppressed by the use non-polar solvents (Table 4.1, entry 5). Instead, however, the reaction progress was suppressed and only trace amounts of the 1,4-addition addition product **4.44** was observed. This observation may

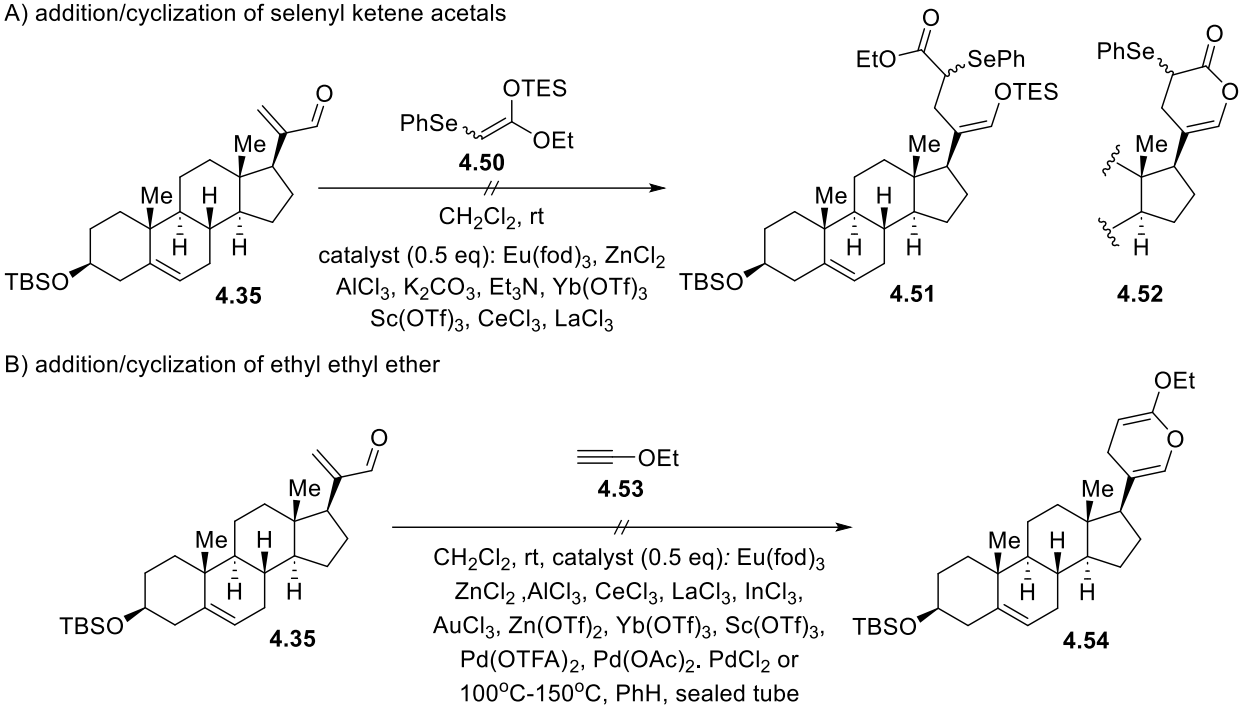
confirm Welzel's hypothesis that the silyl migration is the driving force of the reaction, rather than simply a symptom of it.[38]



Scheme 4.8: Enol lactonization studies of **4.44**[a]
[a]desilylations were carried on 13 µmol scale of **4.44** and 54 µmol (4.0 equiv) CsF/KF or 14 µmol (1.1 equiv) KO^{t}Bu/KOEt.

We next explored the cyclization of **4.44** to bufenolide **4.48**. Following Welzel's initial model,[35] the enol ether was liberated to form aldehyde **4.47** by treatment with potassium fluoride in methanol. The inorganic salts were removed by filtration and the solvents were removed under reduced pressure. Acid-catalyzed enol lactonization with *p*-TsOH only led to a complex mixture of products resulting from the decomposition of aldehyde **4.47**. We attempted direct formation of bufenolide **4.48** via enolate intermediate **4.49**. Desilylation in aprotic solvents was carried out to prevent protonation of the enolate. Anionic fluorides (KF[37], CsF[39]) and strong bases (KOEt, KO^{t}Bu)[40] were employed to drive formation of the enolate, however, only trace amounts of cyclized product **4.48** were observed. There was also only minimal aldehyde **4.47** observed, which resulted from protonation of enolate intermediate **4.49**. Ultimately, even at prolonged reaction times (>3 days) and elevated temperatures (>100 ^{o}C), mainly the starting enol ether **4.44**

was recovered (>90%). We next turned out attention to exploring alternative dienophiles for the cycloaddition.



Scheme 4.9: Cyclization with selenyl ketene acetal **4.50** and ethyl ethynyl ether **4.53**[a]
[a]reactions were carried on 20 µmol scale of **4.35** with 40 µmol (2.0 equiv) **4.50**/**4.53** and 10 µmol (50 mol%) of promoter.

Conjugated aldehyde **4.35** was reacted with **s**elenyl ketene acetal **4.50** in the presence of Lewis acid ($Eu(fod)_3$,[38,41,42] $ZnCl_2$,[36] $AlCl_3$,[43] $CeCl_3$,[44] $LaCl_3$,[44] $Yb(OTf)_3$,[41] $Sc(OTf)_3$[41]) or base (K_2CO_3,[45] Et_3N[46]) (Scheme 4.9A). The progress of the reaction was slow across all promoters, and only trace amounts of the 1,4-addition product **4.51** and cycloaddition product **4.52** were observed, and most of the starting conjugated aldehyde was recovered (>95%). Cycloaddition of conjugated aldehyde **4.35** and ethyl ethynyl ether **4.53** was carried out with an array of Lewis acid promoters and thermal conditions (Scheme 4.9B). Reactions with Lewis acid promoters ($Eu(fod)_3$,[38,41,42] $ZnCl_2$,[36] $AlCl_3$,[43] $CeCl_3$,[44] $LaCl_3$,[44] $InCl_3$,[47] $AuCl_3$,[48] $Yb(OTf)_3$,[41] $Sc(OTf)_3$[41]) and acetylides formed from CuTc[49] and $Zn(OTf)_2$[50] afforded only trace amounts of the bis-enol product **4.54**; most of the starting conjugated aldehyde **4.35** was recovered (>95%). The Pd(II)-

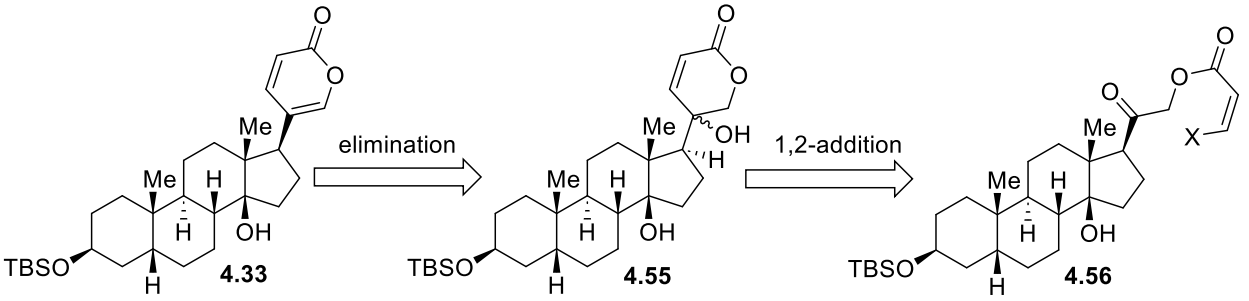
catalyzed reactions ($Pd(OTFA)_2$, $Pd(OAc)_2$, $PdCl_2$)[51] led to decomposition of the starting conjugated aldehyde **4.35**. Uncatalyzed reactions under thermal conditions and elevated pressures (100-150ºC, sealed tube)[43,52] resulted in only trace formation of the bis-enol ether **4.54**, and the starting conjugate aldehyde was recovered (>95%). Having struggled with the cycloaddition and enol lactonization, we next turned our efforts towards another strategy based on intermolecular esterification, followed by intramolecular C-C bond formation.

4.4 Intramolecular 1,2-addition strategies for bufadienolide synthesis

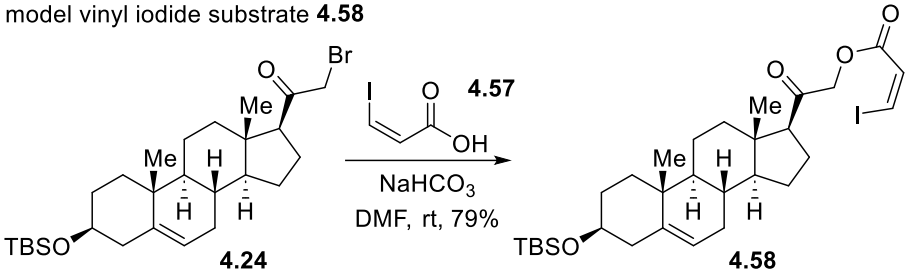
4.4.1 Studies of 1,2-addition via metal-halogen exchange

We next investigated the intramolecular 1,2-addtion of nucleophiles to the C20-ketone as the key ring closing step to form dihydropyrone **4.55** (Scheme 4.10A). The final bufadienolide **4.33** could then be accessed by elimination of water to install the desired final degree of unsaturation. The vinyl halide substrate **4.56** would undergo metal halogen exchange, then the organometallic species would undergo 6-*exo*-trig cyclization to afford dihydropyrone **4.55**. The allylic C20 alcohol may undergo more facile elimination than the C14 alcohol, affording α-pyrone **4.33**.

A) retrosynthetic strategy for pyrone formation via intramolecular addition to C20 ketone



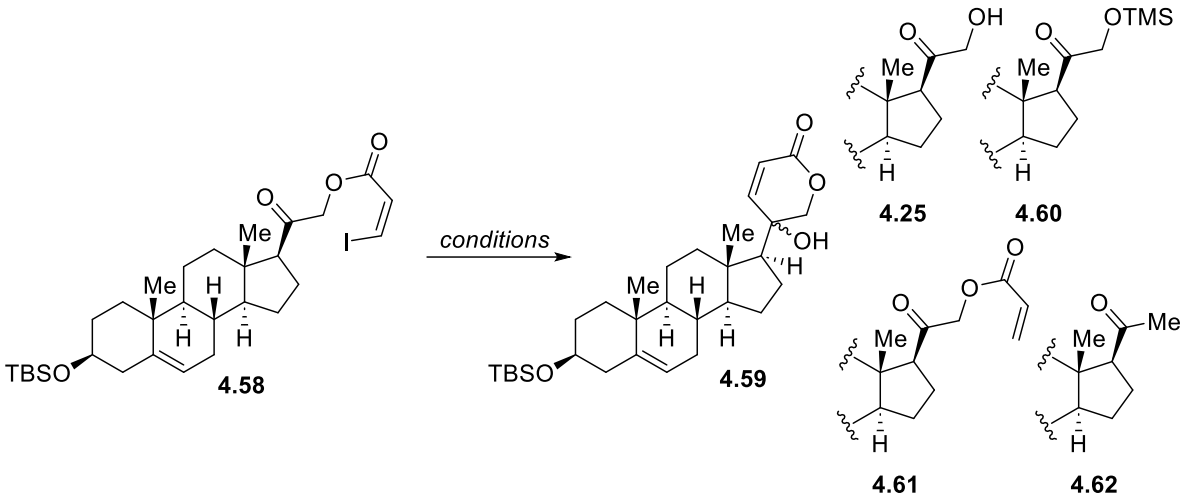
B) synthesis of model vinyl iodide substrate **4.58**



Scheme 4.10: Strategy and substrate for intramolecular cyclization via 1,2-addition
B) **4.24** (2.3 mmol, 1.0 equiv), **4.57** (3.4mmol, 1.5 equiv), $NaHCO_3$ (4.5 mmol, 2.0 equiv), DMF (30 mL), rt, 18h.

First, the model vinyl iodide **4.58** was prepared to evaluate various conditions or metal-halogen exchange and intramolecular cyclization (Scheme 4.10B). The bromide of pregnenolone derivative **4.35** underwent S_N2 displacement with *Z*-iodoacrylate (generated *in situ* by deprotonation of *Z*-iodoacrylic acid **4.57**) to afford the vinyl iodide substrate **4.58** in 79% yield. When the S_N2 reaction was carried out with stronger bases than sodium bicarbonate (K_2CO_3, DIPEA, pKa > 10), the C21-propiolate ester **4.67** (*cf.* Scheme 4.12) was formed as the major product. With vinyl iodide substrate **4.58** in hand, we began investigation of the intramolecular cyclization reaction (Table 4.2).

Table 4.2: Investigation of intramolecular 6-*exo*-trig cyclization via 1,2-carbonyl addition[a]



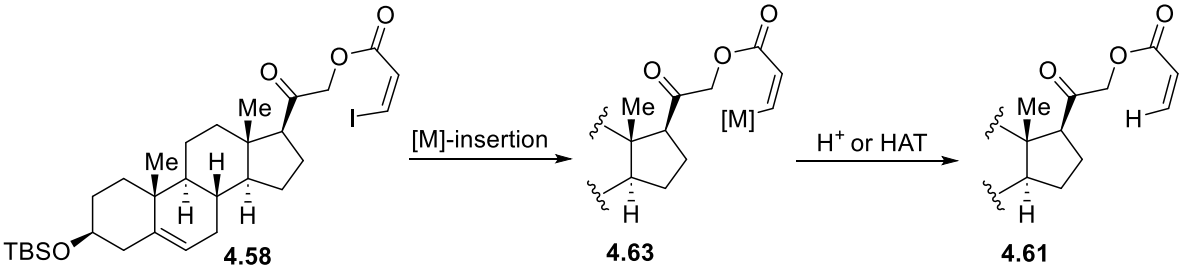
Entry	Title	conditions	conversion	yield
1	Grignard	Mg^0, $CeCl_3$, THF, -40 to -20°C, 24h	<5%	n.r
2	Turbo	^{i}PrMgCl , LiCl, THF, -40 to -20°C, 24h	*>95%*	n.d.
3	[Li]	nBuLi, THF, -78°C, 2h	*50%*	n.d.
4	[Zn]	Zn^0, NH_4Cl (aq):THF, rt, 24h	*78%*	67% **4.61**
5	[Mn]	Mn^0, THF, 0°C, rt, 24h	*<5%*	n.r.
6	[Ni]	$Ni(COD)_2$, 2,2'-bpy, Mn^0, $MgCl_2$, DMF, 60°C, 24h	*~25%*	n.d.
7	[Sn]	$Me_3SiSnBu_3$, CsF, DMF, rt, 16h	*>95%*	48% **4.60**
8	[Pd]	$Pd(PPh_3)_4$, Et_3N, DMF, 110°C, 18h	*>95%*	55% **4.25**
9	[SmI_2]	SmI_2, ^{t}BuOH, THF:HMPA, rt, 24h	*<5%*	n.r
10	NHK	$NiCl_2$, $CrCl_2$, DMF, rt, 14h	*93%*	65% **4.25**, 1% **4.61,** 4% **4.62**

[a]reactions were carried on 0.10 mmol scale of **4.58**. Yields reported are of isolated products after flash column chromatography. n.d. = none detected. n.r. = no reaction.

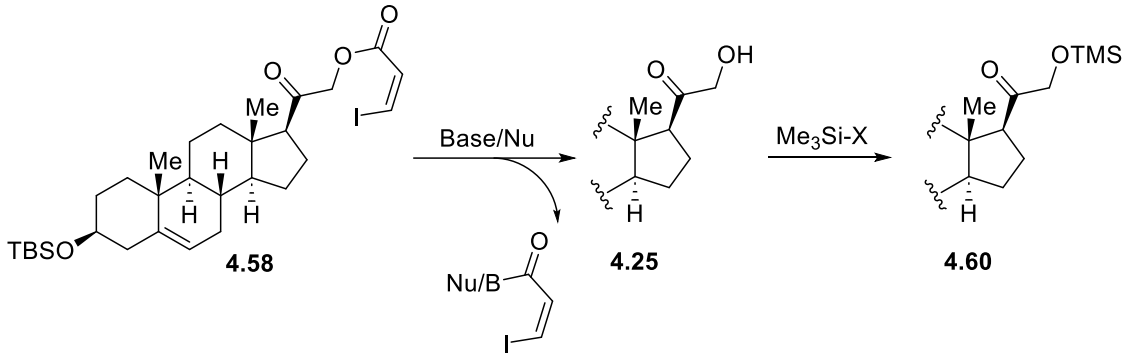
We began our studies with a tried and true method for carbonyl addition, magnesium halogen exchange (i.e., Grignard reaction, Table 4.2, entry 1). Under standard conditions[53] with the vinyl iodide **4.58** and freshly ground magnesium turnings and catalytic cerium (III) chloride, no reaction was observed, and the starting material was recovered. Turbo Grignard reagent (LiCl•^{i}PrMgCl) is known to accelerate the magnesium-halogen exchange process.[54,55] With Turbo Grignard, full consumption of vinyl iodide **4.58** was achieved, however, a complex mixture of products was formed, and no desired cyclization was found (entry 2). Lithium halogen exchange[56] led to incomplete conversion of a complex mixture of products (entry 3). The zinc-promoted Barbier reaction[57] (entry 4) led to formation of C21-*O*-acrylate byproduct

4.61 in 67% yield. The acrylate byproduct **4.61** was formed by protonation or hydrogen atom transfer (HAT) of/to the *in situ* formed organometallic (*i.e.* vinyl zinc) intermediate **4.63** (Scheme 4.11A).[58] The cyclization of **4.58** via an organo-manganese reagent[59] (Table 4.2, entry 5) was unsuccessful with powdered Mn^0 and led to full recovery of vinyl iodide **4.58**, due to unsuccessful oxidative addition of Mn^0 to the carbon-iodine bond. Reductive Ni^0-catalyzed cyclization[60] (entry 6) resulted in low conversion (~25%), and no desired cyclization product **4.59** was observed. Cyclization via organo-tin reagent generated from **4.58** and $Bu_3SnSiMe_3$[61] (entry 7) did not lead to any desired product, but instead led to the formation of C21-OTMS byproduct **4.60** (Scheme 4.11B). The C21 ester of **4.58** was first hydrolyzed to reveal the free alkoxide, and the alkoxide was capped by TMS to afford **4.60**.[61] The palladium-catalyzed addition of the vinyl iodide to the carbonyl[62] (Table 4.2, entry 8) led only to byproduct **4.25** (Scheme 4.11B) via removal of the C21-acyl group by Et_3N.[63] Radical coupling of the vinyl iodide and carbonyl promoted by SmI_2[64](Table 4.2, entry 9) resulted in only trace formation of products, and the starting materially was recovered (>90%). Nozaki-Hiyama-Kishi (NHK) reaction[65](entry 10) of **4.58** resulted in full consumption of the vinyl iodide **4.58**, but led to a mix of products **4.25**, **4.61**, and **4.62**. The deoxygenation product **4.62** could be formed by a one- or two- electron reduction mechanism (Scheme 4.11C).[66-74]

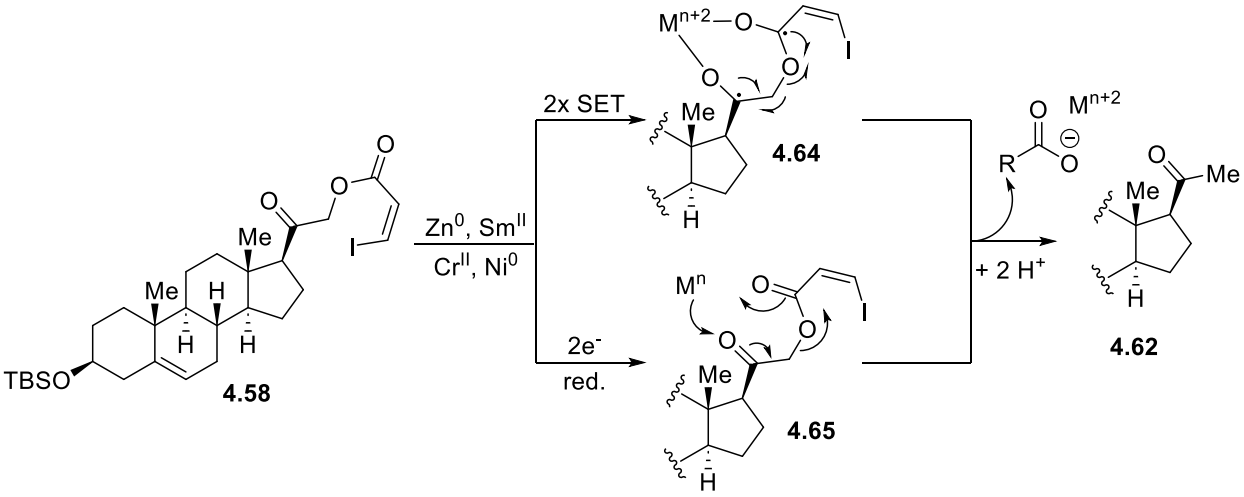
A) proposed mechanism for the formation of C21-O-acrylate byproduct **4.61**



B) proposed mechanism for formation of byproducts **4.25** and **4.60**

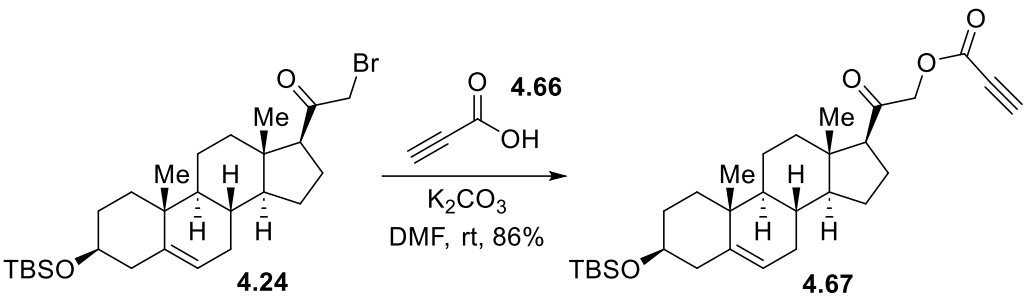


C) proposed mechanism for the formation of byproduct **4.62**



Scheme 4.11: Proposed mechanisms for the formation of byproducts **4.25**, and **4.60**-**4.62**.

After exhaustive screening of organometallic additions, only trace amounts of the desired cyclization product **4.59** was observed, and only byproducts **4.25**, **4.60**, **4.61**, and **4.62** were obtained after isolation. The formation of product **4.61** was evidence that the organometallic species were being formed, but intramolecular addition to the C20 ketone was a challenging step in the transformation.

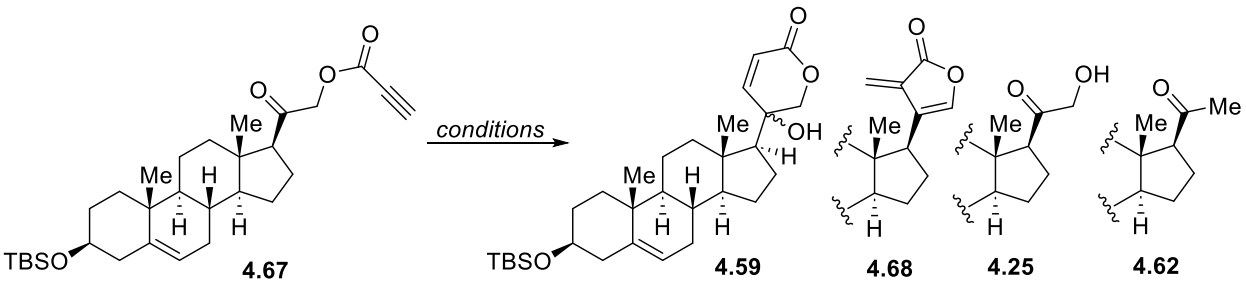


Scheme 4.12: Synthesis of propiolate ester substrate **4.67**.[a]

[a]**4.24** (1.0mmol, 1.0 equiv), **4.66** (1.5 mmol, 1.5 equiv), K_2CO_3 (2.0 mmol, 2.0 equiv), rt, 20h.

We prepared propiolate ester substrate **4.67** from pregnenolone bromide **4.24** in 86% yield (Scheme 4.12). We envisioned the reduction of the C20 ketone to the ketyl radical, and subsequent 6-*endo*-dig cyclization[75] would afford 6-membered lactone **4.59**, which could be advanced to the α-pyrone via elimination of the C20-tertiary alcohol (*cf* Scheme 4.10A). Propiolate ester **4.67** was subjected to reductions with Zn^0 and SmI_2 (Table 4.3).

Table 4.3: Reductive cyclizations of propiolate ester **4.67**.[a]



Entry	*conditions*	yield
1	Zn^0, H_2O, MeCN, rt, 24h	complex mix containing **4.62**, **4.25**
2	SmI_2 , THF:H_2O, rt, 24h	55% **4.62,** 40% **4.25**, <1% **4.68**

[a]reactions were carried on 0.20 mmol scale of **4.67**. Yields reported are of isolated products after flash column chromatography.

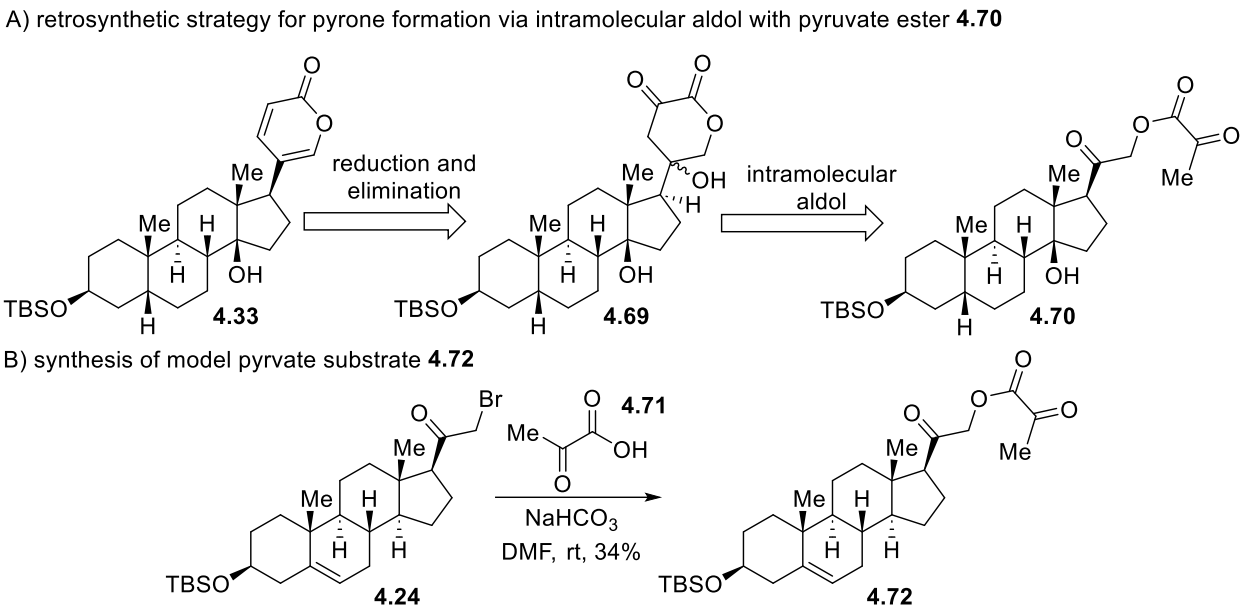
Reductive cyclization with elemental zinc dust[76] led to full consumption of starting propiolate ester **4.67**, but resulted in a complex mixture of products containing **4.25** and **4.62**, which were the result of hydrolysis (*cf* Scheme 4.11B) and an undesired deoxygenation pathway (*cf* Scheme 4.11C), respectively. Reductive cyclization of propiolate ester **4.67** with samarium (II) iodide[77] primarily resulted in the formation of products **4.62** (55%) and **4.25** (40%). A small amount (<1%) of 5-*exo*-dig cyclization product **4.68** was observed by ^{1}H NMR and HRMS, but

isolation of the material was challenging. Due to the low yield, and propensity of the starting α-acyl ketone to undergo α-deoxygenation, further optimization of this strategy was not explored.

The congested steric environment around the C20-ketone[69] may hinder the addition of the larger organometallic species and its ability to undergo intramolecular 6-*endo*-dig cyclization. from the ketyl radical with the vinyl iodide (Table 4.2, entry 9) or alkyne (Table 4.3). To combat this problem, we looked to employ smaller nucleophiles, such as lithium enolates, for an intramolecular aldol addition reaction (Scheme 4.13).

4.4.2 Studies of 1,2-addition via the intramolecular aldol reaction with pyruvate enolates

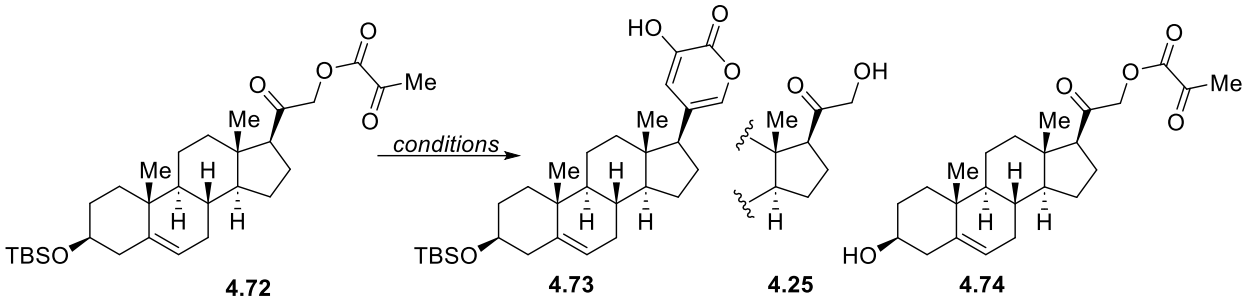
We envisioned the pyrone **4.33** could be prepared by the intramolecular aldol reaction of pyruvate ester **4.70** to form lactone **4.69** (Scheme 4.13A). Reduction of the ketone to the alcohol, and elimination of C20 and C23 alcohols would furnish the α-pyrone **4.33**. We prepared model pregnenolone derived pyruvate **4.72** from pregnenolone bromide **4.24** by S_N2 displacement of the C21 bromide with sodium pyruvate (generated by *in situ* deprotonation of pyruvic acid **4.71**) (Scheme 4.13B). The choice of base was important, as stronger bases (K_2CO_3, DBU) led to hydrolysis of the pyruvate to afford hydroxy ketone **4.25**. With pyruvate ester **4.72** in hand, we began investigation of the intramolecular aldol reaction (Table 4.4).



Scheme 4.13: Pyruvate aldol strategy for α-pyrone synthesis
B) **4.24** (2.0 mmol, 1.0 equiv), **4.71** (2.9 mmol, 1.5 equiv), $NaHCO_3$ (3.9 mmol, 2.0 equiv), DMF (10 mL), rt, 18 h.

We first investigated the addition of the enolate of the pyruvate moiety of **4.72** to the C20 ketone. Aldol reaction with various bases (LiHMDS, DBU,[78] Table 4.4, entry 1-3) led to hydrolysis of the pyruvate (*cf* Scheme 4.11B) to provide hydroxy ketone **4.25** in 31-99% yield. Acid catalyzed aldol reaction with pTsOH (Table 4.4, entry 4) did not lead to any desired lactone or pyrone product **4.73**. Due to the sensitivity of the pyruvate to strong bases and Bronsted acids, the Lewis acid catalyzed intramolecular Mukaiyama aldol reaction of **4.24** was attempted (Table 4.4, entry 5). The silyl enol ether of the pyruvate **4.24** was prepared by treatment with TMSCl and Et_3N in CH_2Cl_2. The silyl enol ether was treated with BF_3•Et_2O to initiate the Mukaiyama aldol reaction, but instead only led to cleavage of the silyl enol ether and the C3 TBS ether to provide **4.74** in quantitative yield. Finally, to minimize the competitive hydrolysis if the C21 pyruvate, we attempted the intermolecular addition of methyl pyruvate to hydroxy ketone **4.25** (entry 6), however, no desired addition or cyclization products were observed, and the starting hydroxy ketone **4.25** was recovered quantitatively.

Table 4.4: Investigations of the intramolecular aldol reaction of pyruvate ester **4.72**.[a]



4.72 **4.73** **4.25** **4.74**

entry	conditions	yield
1	LiHMDS, THF, -78°C, 18h	31% **4.25**
2	DBU, THF, rt, 18h	48% **4.25**
3	DBU, THF, 66°C, 40h	99% 4.**25**
4	pTsOH, MeCN, 55°C, 48h	n.d.
5	i) Et_3N, TMSCl, CH_2Cl_2, 0°C to rt, 18h ii) BF_3•Et_2O, CH_2Cl_2, rt, 18h	99% **4.74**
6[b]	Methyl pyruvate, DBU, THF, rt to 60°C, 48h	n.r.

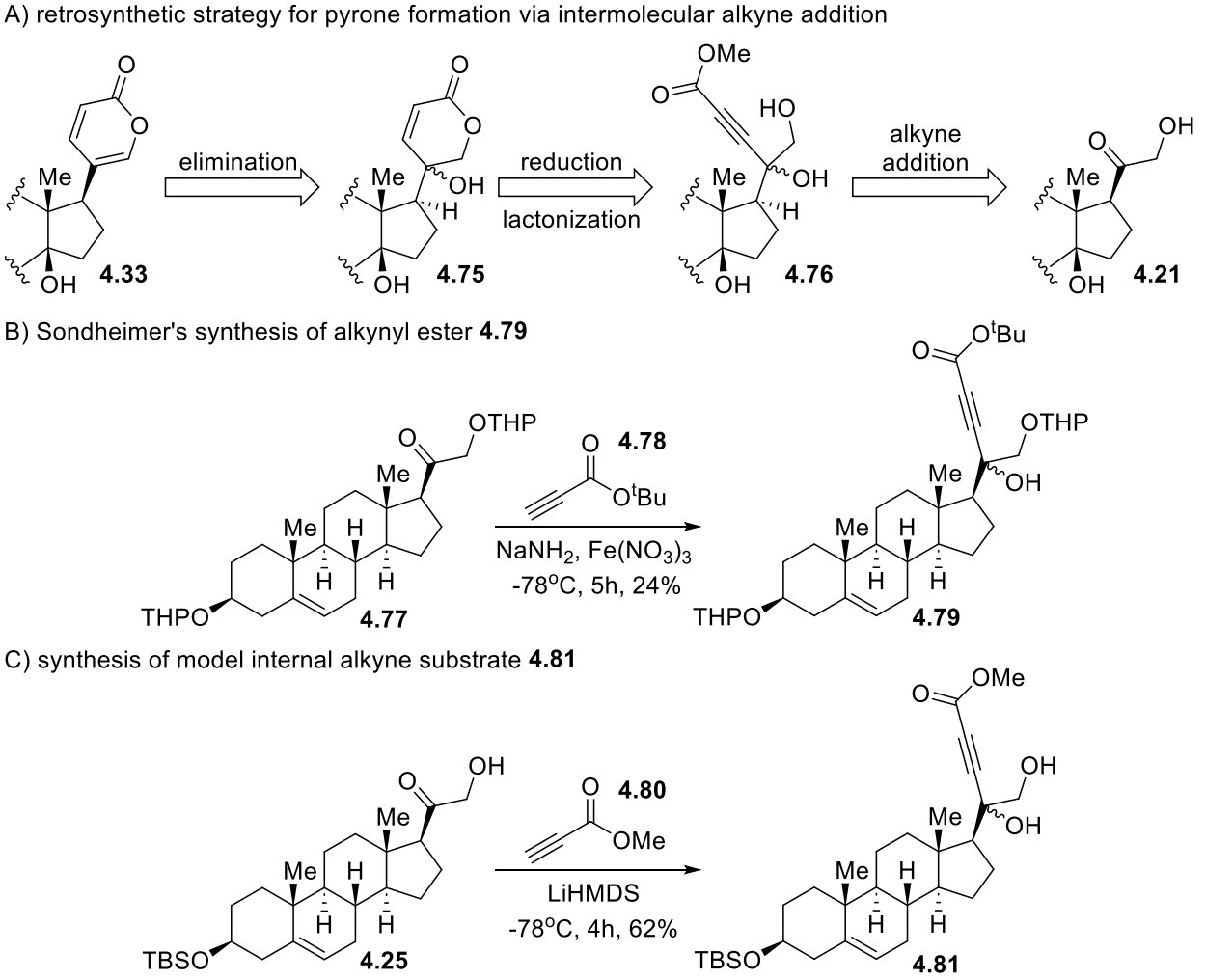
[a]reactions were carried on 0.10 mmol scale of **4.72**. Yields reported are of isolated products after flash column chromatography. [b]intermolecular aldol of methyl pyruvate (0.12 mmol, 1.1 equiv) with hydroxyketone **4.25** (0.11 mmol, 1.0 equiv) and DBU (0.22 mmol, 2.0 equiv) in THF (1.0mL) at rt for 48 h. n.d. = none detected. n.r. = no reaction.

Ultimately, the intramolecular addition to the C20 carbonyl was a challenging endeavor. The steric congestion around the C20 ketone prevented the addition of the larger organometallic species (Table 4.2). Reductive cyclizations from the formation of the C20 ketyl radical led to deoxygenation of C21-O acyl moiety (Table 4.3). The intramolecular aldol cyclization of pyruvates was hampered by competitive hydrolysis of the pyruvate ester (Table 4.4). Due to the difficulty of intramolecular addition, we next explore intermolecular carbonyl addition, followed by intramolecular lactonization.

4.5 Reaction of internal alkynes toward the synthesis of bufadienolides

Addition of terminal alkyne nucleophiles to hydroxy ketone **4.21** would furnish the internal alkyne **4.76** (Scheme 4.14A). Reduction of the internal alkyne and lactonization would form the 6-membered lactone **4.75**. Final elimination of C20 alcohol would lead to α-pyrone **4.33**. We envisioned the reduction of the alkyne to the Z-alkene and lactonization to form the 6-memebered lactone **4.75** over the 5-membered lactone to be key steps for this sequence. A

pregnenolone derived alkynyl ester **4.79** was previously prepared[79] in low yields by nucleophilic addition of *tert*-butyl propiolate **4.78** to the protected hydroxy ketone **4.77** (Scheme 4.14B). In Sondheimer's subsequent studies,[79] reduction of the alkyne to the Z-alkene and cleavage of the THP ethers provided the triol in 61% yield, but attempts to form the 6-membered lactone from the *tert*-butyl ester resulted in a complex mixture of products. We prepared alkynyl ester **4.81** by nucleophilic addition of methyl propiolate **4.80** to the hydroxy ketone **4.25** in 62% with LiHMDS as the base (Scheme 4.14C). We envisioned the methyl ester to be more stable than the *tert*-butyl ester to acidic lactonization conditions, and would allow for a more controlled lactonization event.

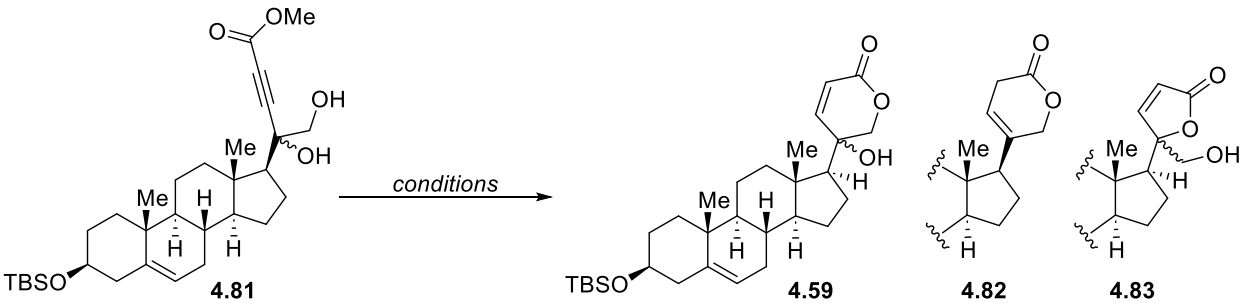


Scheme 4.14: Alkyne reduction and lactonization strategy towards the synthesis of α-pyrones.
C) **4.80** (1.74 mmol, 3.0 equiv), LiHMDS (1.74 mmol, 3.0 equiv), THF (1.0 mL), -78 °C, 1 h, then add **4.25** (0.58 mmol, 1.0 equiv) in THF (1.0 mL), -78 °C, 2h.

Next, the semi hydrogenation of the internal alkyne of **4.81** was explored. Re-employing Sondheimer's method[79] of Lindlar reduction[80] with H_2 and palladium on calcium (II) carbonate (poisoned with lead) and catalytic quinoline, the desired 6-membered lactone **4.59** was formed in 23% yield as the major isolated product (Table 4.5, entry 1). The reduction was also accompanied by-products resulting from over reduction of the alkyne and hydrolysis of the methyl ester. An alternative Lindlar-like reduction with palladium on barium (II) sulfate[81] (entry 2) failed to produce any semi-reduced product and the starting alkyne was recovered (>95%).

Reduction with *in situ* generated Brown's P2-nickel[82,83] (entry 3) resulted in a complex mixture of semi- and over-reduction products. Reductions by the Hansen-modification to the Boland reduction[84] (entry 4), stoichiometric Stryker's reagent[85] (entry 5), and hydrozirconation-protonation[86] (entry 6) did not result in any productive reaction, and the starting alkyne was recovered quantitatively. The reduction with catalytic Stryker's reagent and pinacol borane[87] (entry 7) provided the 5-membered lactone **4.83** in 28% yield as the major isolated product. Nickel-catalyzed transfer hydrogenation[88] (entry 8) provided over-reduced product **4.82** in 22% yield. Palladium-catalyzed transfer hydrogenations[89,90] (entry 9-11) resulted in complex mixtures of semi- and over-reduced products including **4.59, 4.82,** and **4.83**. Palladium-catalyzed hydrosilylation[91] (entry 12) led to a complex mixture of reduction products. Finally, reduction with *in situ* generated copper-nanoparticles[92] (entry 13) did not lead to any reduction, and the starting alkyne was quantitatively recovered. The reductions of diol **4.81** were generally unselective for the semi-reduction product compared to the over-reduction products. Lactonization of the diol occurred spontaneously under the reaction conditions, and often was concurrent with alkyne reduction, which complicated the monitoring of the reduction reaction. Next, a protecting group for the diol (Scheme 4.15) was employed so that the alkyne reduction could be more accurately monitored (Table 4.6).

Table 4.5: Semi-hydrogenations of internal alkyne **4.81**.[a]

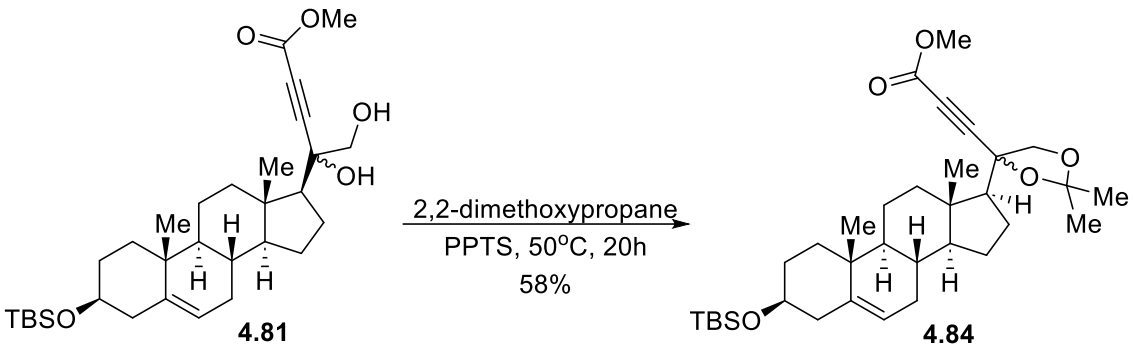


4.81 **4.59** **4.82** **4.83**

entry	conditions	yield
1	H_2 , $Pd/CaCO_3$, quinoline, EtOAc , rt,1h	23% **4.59**
2	H_2, $Pd/BaSO_4$, quinoline, EtOAc, rt,1h	n.r.
3	H_2, $Ni(OAc)_2•7H_2O$, $NaBH_4$, $(CH_2NH_2)_2$, EtOH, rt, 18h	n.d.
4	Zn(CuAg), TMSCl, H_2O:MeOH, rt, 18h	n.r.
5	$[(PPh_3)CuH]_6$, PhMe, -78 to 0^oC, 3d	n.r.
6	Cp_2ZrHCl, THF, rt, 2h	n.r.
7	$[(PPh_3)CuH]_6$, HBPin, PPh_3, THF, 0^oC, 6h	28% **4.83**
8	$NiBr_2$, Zn^0, HCO_2H, dioxane, 120^oC sealed tube, 22h	22% **4.82**
9	$PdCl_2$, HCO_2H, K_2CO_3, dioxane, 80^oC, 17h	n.d.
10	$Pd(OAc)_2$, NaOAc, TEOA, EtOH, THF, 140^oC, sealed tube, 16h	<5% **4.59**
11	$Pd(OAc)_2$, Mn, H_2O, MeCN, rt, 5h	<5% **4.83**
12	$Pd(dba)_2$, PCy_3, Et_3SiH, PhMe, rt, 14h	n.d.
13	$CuSO_4$, BH_3NH_3, EtOH, 40^oC, 3h	n.r.

[a]semi-reductions were carried on 40 µmol of **4.81**. Yields reported are of isolated products after flash column chromatography. n.d. = none detected. n.r. = no reaction.

The diol moiety of **4.81** was converted into the corresponding acetonide **4.84** by stirring in 2,2-dimethoxy propane with catalytic pyridinium *para*-toluene sulfonate (PPTS) at 50^{o}C for 20 hours (Scheme 4.15). The acetonide **4.84** was prepared in 58% yield. With the acetonide in hand, we investigated the *Z*-selective semi-hydrogenation of **4.84** (Table 4.6).

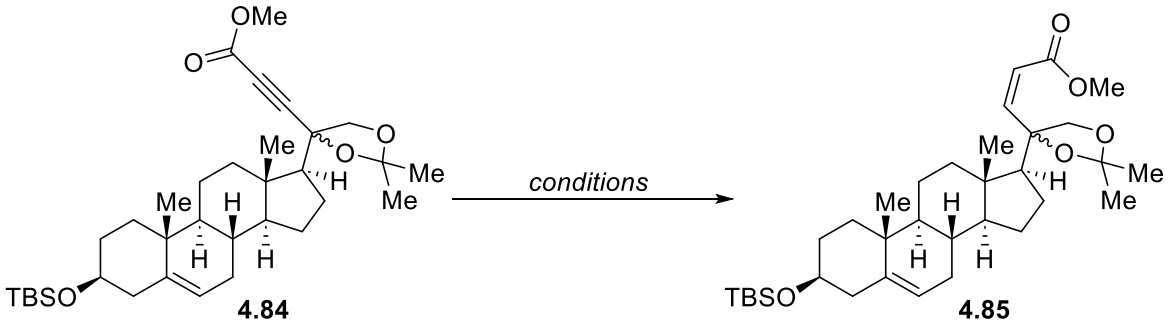


Scheme 4.15: Acetonide protection of diol **4.81**.[a]

[a]**4.81** (150 µmol, 1.0 equiv), pyridinium *para*-toluene sulfonate (30 µmol, 0.2 equiv), 2,2-dimethoxypropane (1.5 mL), 50 °C, 20h.

With Sondheimer's method[79] of Lindlar reduction[80] with H_2 and palladium on calcium (II) carbonate (poisoned with lead) and catalytic quinoline (Table 4.6,entry 1), the desired *Z*-alkene **4.85** was not observed, however, products resulting from the over-reduction of the alkyne were detected by ^{1}H NMR and HRMS analysis. An alternative Lindlar-like reduction with palladium on barium (II) sulfate[81] (entry 2) provided the desired *Z*-alkene **4.85** in near quantitative yield (97%). Careful monitoring of the reaction by HRMS was required to prevent over reduction to the alkane. Reduction with *in situ* generated Brown's P2-nickel[82,83] (entry 3) afforded the *Z*-alkene **4.85** in 72% yield. Reduction with the Hansen-modification to the Boland reduction[84] (entry 4), provided the desired *Z*-alkene **4.85** in 22% yield, and the starting material was recovered (>99% brsm). Reduction by stoichiometric Stryker's reagent[85] (entry 5) and hydrozirconation-protonation[86] (entry 6) did not afford any of the desired *Z*-alkene, and by products resulting from over reduction were observed. The alternative Lindlar reduction with the Rosemund catalyst ($Pd/BaSO_4$) selectively provided the *Z*-alkene on up to 50 milligram scale. With an efficient route to the desired *Z*-alkene **4.85**, optimal conditions for acetonide removal and selective formation of the 6-membered lactone **4.59** were investigated (Table 4.7).

Table 4.6: Semi-reduction of pregnenolone-alkynyl-acetonide **4.84**.[a]



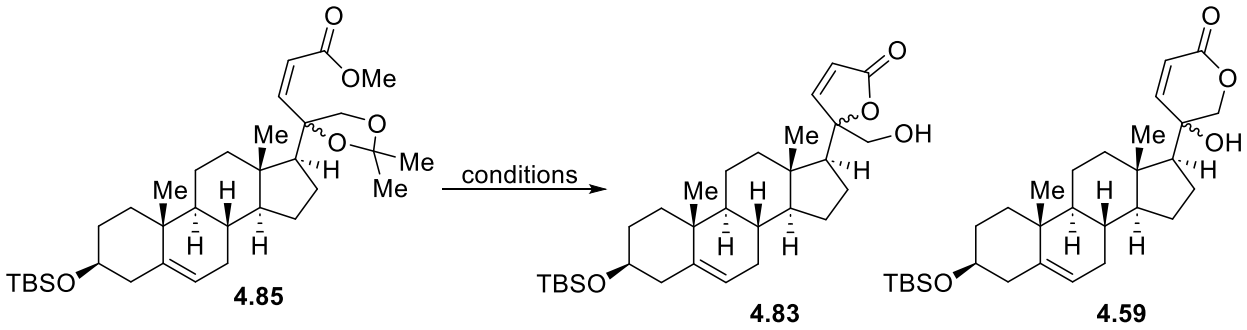
4.84 **4.85**

entry	conditions	yield
1	H_2, $Pd/CaCO_3$, quinoline, EtOAc, rt,1h	n.d
2	H_2, $Pd/BaSO_4$, quinoline, EtOAc, rt,1h	97%
3	H_2, $Ni(OAc)_2 \cdot 7H_2O$, $NaBH_4$, $(CH_2NH_2)_2$, EtOH, rt, 18h	72%
4	Zn(CuAg), TMSCl, H_2O:MeOH, rt, 18h	22%
5	$[(PPh_3)CuH]_6$, PhMe, -40°C, 3d	n.d.
6	Cp_2ZrHCl, THF, rt, 2h	n.d.

[a]semi-reductions were carried on 18 µmol of **4.84**. Yields reported are of isolated products after flash column chromatography. n.d. = none detected.

In Sondheimer's previous work on a non-steroidal model substrate, lactonization had favored the formation of the 5-membered lactone. We envisioned a protocol where, under kinetic control, the acetonide is opened from the C21 primary alcohol,[93] and lactonization occurs immediately, followed by complete removal of the resulting mixed acetal at the C20 tertiary alcohol. We initially looked into mild acidic conditions for the removal of the acetonide and subsequent lactonization (Table 4.7).

Table 4.7: Optimization of acetonide removal and intramolecular lactonization.[a]

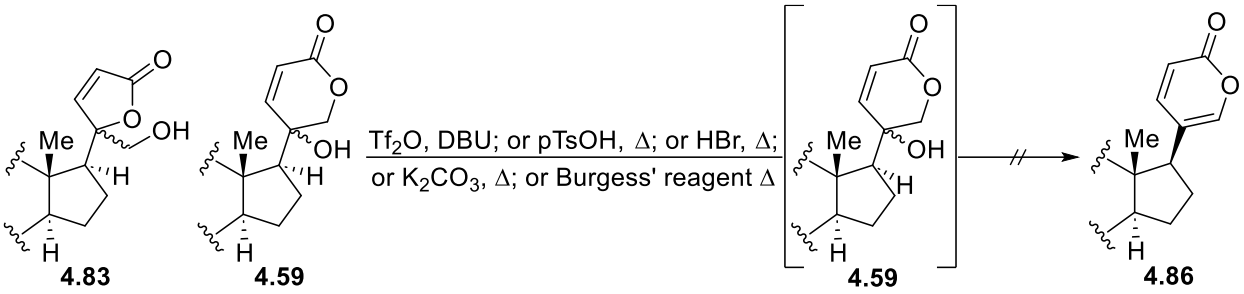


entry	conditions	yield
1	$FeCl_3$•SiO_2, $CHCl_3$, rt, 22h	52%, 4.8:1 **4.83:4.49**
2	$FeCl_3$•SiO_2, $CHCl_3$, rt, 48h	74% **4.83**
3	$BiCl_3$, CH_2Cl_2, rt, 16h	75%, 2.2:1 **4.83:4.59**
4	$BiCl_3$, CH_2Cl_2, -78°C, 24h	n.r.
5	$CeCl_3$•$7H_2O$, $(COOH)_2$, MeCN, rt, 5h	n.r.

[a]reactions were carried on 13-61 µmol scale of **4.85**. Yields reported are of isolated products after flash column chromatography. Ratio of products **4.83** and **4.59** were determined by ^{1}H NMR analysis of the crude reaction mixture. n.r. = no reaction.

Iron (III) chloride adsorbed on silica gel ($FeCl_3$•SiO_2)[94] was previously developed as mild condition for the selective removal of acetonides in the presence of silyl ethers. The stirring of **4.85** with $FeCl_3$•SiO_2 for 22 hours (Table 4.7, entry 1) provided a 4.8:1 mixture of 5- and 6-membered lactones **4.83** and **4.59** in 52% yield. Prolonged stirring (48 hours) with $FeCl_3$•SiO_2 (entry 2) led to exclusive formation of the 5-membered lactone **4.83** in 74% yield. This finding confirmed the 5-membered lactone to be the thermodynamic product. Treatment of acetonide **4.85** with catalytic $BiCl_3$[95] (entry 3) formed a 2.2:1 mixture of 5- and 6- membered lactones **4.83** and **4.59** in 75% yield. This procedure showed more favorability for the 6-membered lactone than reactions with $FeCl_3$•SiO_2. The temperature of the reaction was lowered to -78°C (entry 4) in an effort to favor the kinetic opening of the acetonide, but the reaction failed to proceed at the lower temperature and the starting material was recovered (>95%). Final attempts to open the acetonide with oxalic acid and cerium (III) chloride[96] (entry 5) were unable to open the acetonide. The lactones **4.83** and **4.59** were separable by flash column chromatography, and we

next explored the conversion of the 5-membered lactone **4.83** to 6-membered lactone **4.59**, and the subsequent dehydration of **4.59** to form pyrone **4.86** (Scheme 4.16).



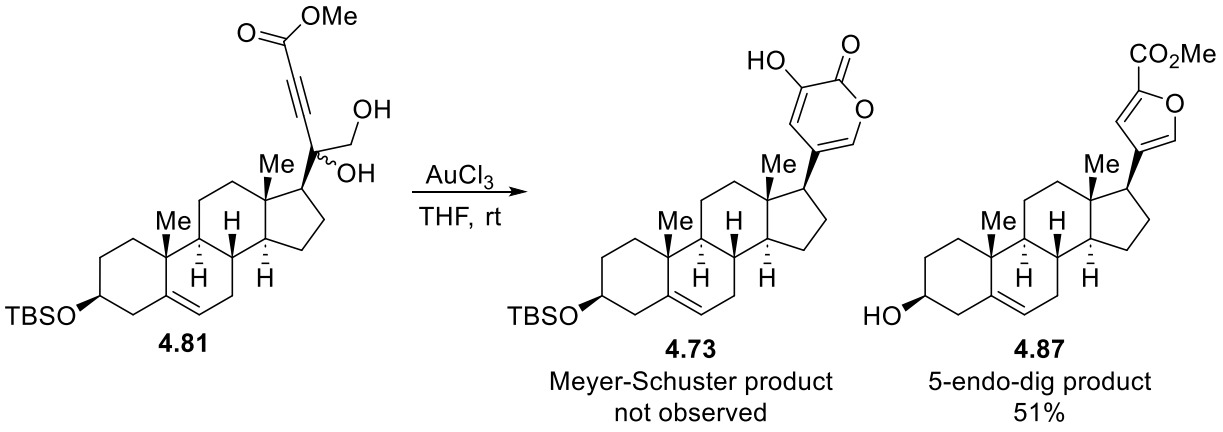
Scheme 4.16: Studies of isomerization and dehydration of lactones **4.83** and **4.59** to α-pyrone **4.86**.

Treatment of the lactones **4.83** and **4.59** with various acids (*p*-TsOH; HBr), bases (K_2CO_3; DBU), and dehydrating agents (Tf_2O, DBU; Burgess reagent) resulted in a complex mixture of products that did not contain α-pyrone **4.86** (Scheme 4.16). With *p*-TsOH, the 6-membered lactone **4.59** was converted to the 5-membered lactone **4.83**. Ultimately, the alkyne reduction-lactonization strategy was unable to produce the α-pyrone **4.86** in meaningful yields. Using this methodology, cardenolide (**4.83**) and bufadienolide (**4.59**, **4.83**) analogs were prepared in low-to-moderate yields. Previous studies[21-25] indicated that semi-reduced analogs of bufadienolides showed improved safety and larger therapeutic indices, and this method could be adapted for the synthesis of cardenolide and bufadienolide analogs for medicinal chemistry studies. Moving forward, we looked for methods to remove the C20 alcohol prior to the lactonization step, so that the 6-membered lactone would be formed exclusively.

4.5.1 Rearrangements of propargyl alcohols towards the synthesis of bufadienolides

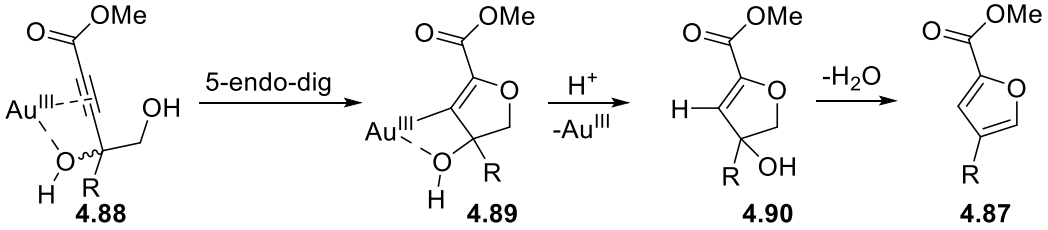
The Meyer-Schuster rearrangement of propargylic alcohols has been used in various natural product syntheses.[97] The Meyer-Schuster rearrangement and lactonization of **4.81** would provide pyrone product **4.73** (Scheme 4.17). Treatment of **4.81** with various Lewis acids

($AgSbF_6$,[98] $Cu(OTf)_2$,[99] $FeCl_3$[100]) failed to initiate the rearrangement. Employing the π-acid $AuCl_3$[101] provided the furan product **4.87** in 51% yield (Scheme 4.17).



Scheme 4.17: Au-catalyzed rearrangement of propargylic alcohol **4.81**.
[a]**4.81** (9.4 µmol, 1.0 equiv), $AuCl_3$ (4.7 µmol, 50 mol%), THF (100 µL), rt, 18h.

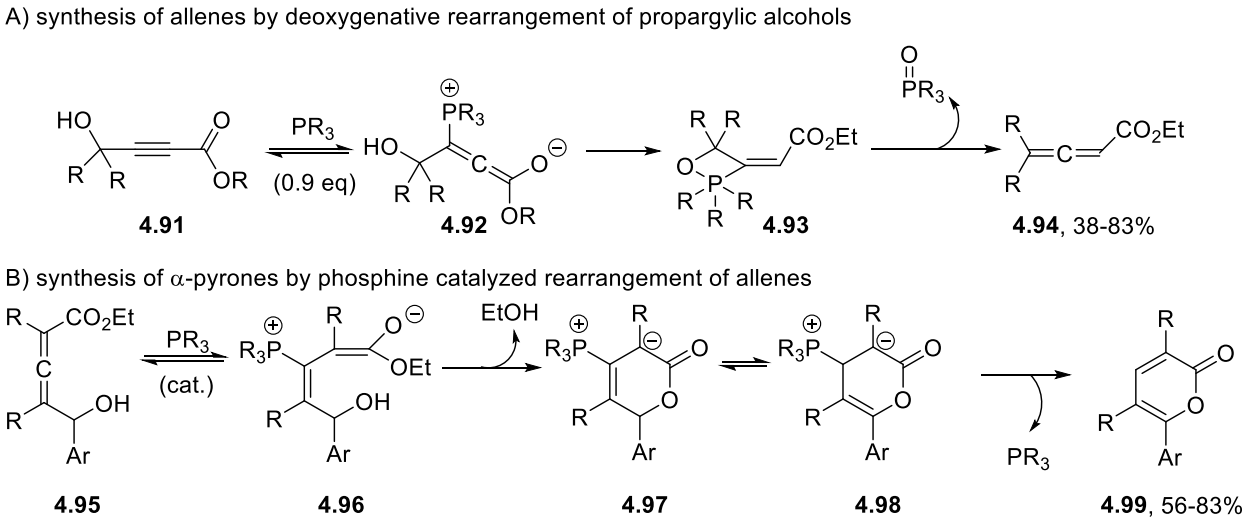
The furan product **4.87** was formed via a competing 5-*exo*-dig reaction pathway (Scheme 4.18).[102] The gold catalyst coordinated to the alkyne, and then the primary hydroxyl added via a 5-*exo*-dig pathway to form intermediate **4.89**. Protonation of intermediate **4.89** released the gold-catalyst to form dihydrofuran **4.90.** Subsequent dehydration of the tertiary alcohol afforded furan **4.87**. The cationic rearrangement of alkynyl diol **4.81** led to exclusive formation of the 5-*exo*-dig product which converged to furan **4.87**. We next explored the reactions of alkynyl diol **4.81** with Lewis bases to furnish allenes and pyrones (Scheme 4.19).



Scheme 4.18: Mechanism for formation of furan **4.87**.

The reaction of propargyl alcohols with phosphines to form allenes was reported in 2013 (Scheme 4.19A).[103] The phosphine underwent 1,4-addition to the conjugated alkyne **4.91** to form

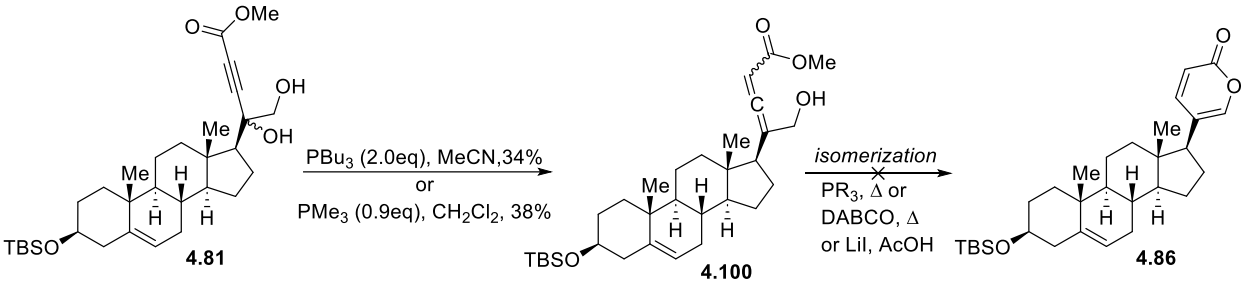
zwitterionic species **4.92**. Transfer of the anionic charge to the more electronegative hydroxyl led to the formation of oxaphosphetane **4.93**. Decomposition of the oxaphosphetane then lead to the formation of allene **4.94**. Importantly, if any excess of the phosphine was used, the allene would decompose to a conjugated diene.[103] The synthesis of α-pyrones from allenoates has been reported via a phosphine-promoted cyclization and rearrangement (Scheme 4.19B).[104,105] Conjugate addition of the phosphine to allene **4.95** afforded enolate **4.96.** Intramolecular lactonization and anionic charge transfer resulted in zwitterionic intermediate **4.97**. Migration of the double bond through a series of proton transfer events[104] provided intermediate **4.98**. Final elimination of the phosphine resulted in the formation of pyrone **4.99**. The structure and nucleophilicity of the phosphine played an important role in optimization of the synthesis and reaction of allenes (Scheme 4.19). We envisioned the tandem phosphine-promoted formation of allenes and subsequent rearrangement to be an interesting avenue to obtain bufadienolides (Scheme 4.20).



Scheme 4.19: Phosphine promoted synthesis of allenes and α-pyrones

Treatment of alkynyl diol **4.81** with alkyl phosphines PMe_3 and PBu_3 led to formation of the desired allene **4.100** in 38% and 34% yield, respectively (Scheme 4.20). Performing the

reaction in a solvent where the starting alkyne **4.81** was barely soluble (CH_2Cl_2, MeCN) was important to minimize byproducts resulting from the formyl expulsion of methyl propiolate (e.g., **4.25**) or cyclization resulting from demethylation of the methyl ester (e.g **4.83)**. With a procedure for the synthesis of allene **4.100** in hand, we explored various Lewis bases for the isomerization of allene **4.100** to pyrone **4.86**. Phosphines (PMe_3, PBu_3, PCy_3, PPh_3) were unable to promote the desired rearrangement and cyclization and instead led to the formation of the 5-membered lactone **4.83** possibly through demethylation of the ester and subsequent cyclization. The phosphine-catalyzed rearrangement may have been hampered by the lack of an aryl group at the C5-position of the pyrone. In previous studies, allenes with a C5 aryl group provided higher yields of their corresponding pyrones (60-90%) compared to substrates with C5 alkyl groups (30-40%).[104,105] The cyclization of allenes with a primary alcohol at the C5 position had not been previously explored. Other methods for conjugate addition, cyclization, and elimination sequences (DABCO, EtOH, Δ;[106] LiI, AcOH, hydroquinone[107]) failed to react with allene **4.100**.



Scheme 4.20: Studies of allene formation and rearrangements toward the synthesis of bufadienolides.[a]
[a]**4.81** (19 µmol, 1.0 equiv), PBu_3 (38 µmol, 2.0 equic), MeCN (2.0mL), rt, 18h. or **4.81** (19 µmol, 1.0 equiv), PMe_3 (18 µmol, 0.9 equiv), CH_2Cl_2 (0.4 mL), rt, 18h.

Rearrangements of the alkynyl diol **4.81** allowed for the expedient synthesis of furan **4.87** and allene **4.100** in moderate yields. Furan heterocycles like **4.87** have been reported to have higher binding affinity to the Na/K ATPase than the native cardenolides, however, previous synthetic strategies to access these types compounds from their parent cardenolides were

unselective and produced a mixture of products. Allene **4.100** is a unique intermediate in the transformation of cardenolides to various heterocycles. While these initial attempts at cyclizing the allene to the corresponding pyrone were unsuccessful, future implementation of this intermediate to the synthesis of various 5- and 6-membered heterocycles may prove useful for medicinal chemistry studies.

4.6 Conclusions

We conducted extensive studies on the transformation of cardenolides to various heterocycles proceeding through a key hydroxy ketone intermediate. Preliminary studies were carried out on pregnenolone derived hydroxy ketone **4.25**, which was prepared in 97% yield (3 steps) at multigram scale. Initial studies towards the synthesis of α-pyrones involved employing an inverse electron demand hetero Diels-Alder reaction, which had previously been used by Welzel in their synthesis of bufadienolides. In two steps, the hydroxy ketone was converted to the conjugated aldehyde which would serve as the diene. The Diels-Alder reaction was very sluggish, and only trace amounts of product were observed even after prolonged reaction times (<4 days) with various dienophiles (silyl ketene acetals, ethynyl ethers). We successfully furnished the 1,4-addition product by employing $ZnCl_2$ as catalyst, however, attempts as enol lactonization were unsuccessful, and let to decomposition of the starting material. Moving forward, We began to investigate intramolecular additions to the C20 ketone as the ring closing step, rather than enol lactonization, which generally required harsh conditions of refluxing the substrate in acidic media. We prepared steroidal 21-*O*-*Z*-iodoacyrlate **4.58**, 21-*O*-pyruvate **4.72**, and 21-*O*-propiolate **4.67** to explore the intramolecular cyclization. Metalation of the *Z*-iodoacrylate and addition of the organometallic intermediates to the C20 ketone did not lead to any of the desired 6-membered lactone **4.59**. Metal insertion to the carbon-halogen bond was

successful, however, the organometallic species favored unproductive side reactions over the desired cyclization. The pyruvate esters proved to be especially susceptible to basic hydrolysis, and the pyruvate esters were frequently cleaved to their corresponding alcohols under the reaction conditions for the intramolecular aldol reactions. Further exploration into olefination pyruvate derived Wittig reagents may help achieve the desired cyclization. The reduction of the C20-ketone to the ketyl radical did not result in 6-*endo*-dig cyclization with the propiolate alkyne, but instead resulted in deoxygenation of the C21 alcohol. We returned to intramolecular lactonization as the ring forming step, but looked for alternatives to acid-catalyzed enol lactonizations. Addition of acetylide anion derived from deprotonation of methyl propiolate afforded the internal alkyne diol **4.81** in 62% yield. Direct semi-hydrogenation of the alkyne to the *Z*-alkene provided lactone products **4.59** (23%, H_2, Pd/$CaCO_3$, quinoline), **4.82** (22%, $NiBr_2$, Zn, HCO_2H), and **4.83** (28%, Stryker's reagent, HBPin, PPh_3). The direct diol hydrogenation reaction mixtures were complex mixtures containing by-products from over reduction of the alkyne. The diol was trapped as an acetonide, and semi-hydrogenation of the alkynyl acetonide to the *Z*-alkene **4.85** was achieved in 97% yield with H_2 and palladium on $BaSO_4$ (unreduced) that was poisoned with quinoline. Previous studies had suggested that, under thermodynamic conditions, the 5-membered lactone **4.83** would be the favored lactonization product, not the desired 6-membered lactone **4.59**. We were able to form the 6-membered lactone **4.59** in 23% (75% yield, 2.2:1 **4.83:4.59**) yield with $BiCl_3$ to facilitate the acetonide removal and lactonization. Further attempts to eliminate the C20 tertiary alcohol resulted in decomposition of the lactone. Lactones **4.59** and **4.83** are novel heterocyclic scaffolds for the cardiotonic steroid skeleton, and their exploration as therapeutic agents may help improve the safety profile of this class of compounds. Cationic rearrangement of the alkyne via the Meyer-Schuster reaction

proved unsuccessful, but a 5-*exo*-dig cyclization cleanly afforded steroidal furan **4.87** in 51% yield. This heterocycle had shown promise in computational screening of cardenolides analog binding of the Na/K ATPase, and more steroidal skeletons with this moiety could prove valuable for potential therapeutics. Attempts to form the pyrone via the phosphine-promoted rearrangements we partially successfully. The alkynyl diol **4.81** was successfully transformed to the allene **4.100** in up to 38% yield. Extensive screening of the solvent, temperature, and phosphine was conducted, and for higher yields, an alternative procedure for the allene formation could be explored. Reactions to form the allene directly from the hydroxy ketone, such as olefination with vinyl- phosphonates or -phosphoranes could provide the desired allenes. Alternatively, the allenylation of terminal alkyne (ATA) reaction could also provide a more expedient synthesis of allene **4.100**. Isomerization of the allenes to α-pyrones was unsuccessful in our hands, however, the allene intermediate can be used a diversification point towards the synthesis of other heterocycles. Moving forward, the chemistry and analogs developed from these studies can be applied to natural product derivatization and medicinal chemistry studies of C17 heterocyclic analogs of cardiotonic steroids.

4.7 Experimental

4.7.1 General Methods

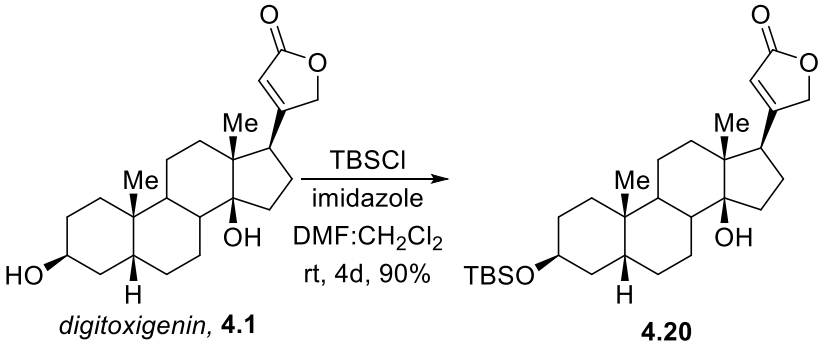
All reagents and solvents were purchased from commercial sources and were used as received without further purification unless otherwise specified. CH_2Cl_2, DMF, Et_2O, THF, PhMe, were purified by Innovative Technology's Pure-Solve System using basic alumina. All reactions were carried out under a positive pressure of nitrogen in flame- or oven-dried glassware with magnetic stirring. Reactions were cooled using a cryocooler or external cooling baths (ice water (0 °C), sodium chloride/ice water (–20 °C), dry ice/acetonitrile (–40 °C), or dry ice/acetone (–78 °C).

Heating was achieved by use of a silicone oil bath with heating controlled by an electronic contact thermometer. Deionized water was used in the preparation of all aqueous solutions and for all aqueous extractions. Solvents used for extraction and chromatography were ACS or HPLC grade. Purification of reaction mixtures was performed by flash chromatography using SiliCycle SiliaFlash P60 (230-400 mesh). Yields indicate the isolated yield of the title compound with ≥95% purity as determined by ^{1}H NMR analysis. Diastereomeric ratios were determined by ^{1}H NMR analysis. ^{1}H NMR spectra were recorded on a Varian vnmrs 700 (700 MHz), 600 (600 MHz), 500 (500 MHz), 400 (400 MHz), Varian Inova 500 (500 MHz), 400 (400 MHz), or a Bruker Avance Neo 500 (500 MHz) spectrometer and chemical shifts (δ) are reported in parts per million (ppm) with solvent resonance as the internal standard ($CDCl_3$ at δ 7.26, D_3COD at δ 3.31, C_6D_6 at δ 7.16). Tabulated ^{1}H NMR Data are reported as s = singlet, d = doublet, t = triplet, q = quartet, qn = quintet, sext = sextet, m = multiplet, ovrlp = overlap, and coupling constants in Hz. Proton-decoupled ^{13}C NMR spectra were recorded on Varian vnmrs 700 (700 MHz) spectrometer and chemical shifts (δ) are reported in ppm with solvent resonance as the internal standard ($CDCl_3$ at δ 77.16, D_3COD at δ 49.0, C_6D_6 at δ 128.06). High resolution mass spectra (HRMS) were performed and recorded on Agilent 6230 TOF or VG (Micromass) 70-250-S Magnetic sector mass spectrometers in the University of Michigan mass spectrometry laboratory. Infrared (IR) spectra were recorded as thin films a Perkin Elmer Spectrum BX FT-IR spectrometer. Absorption peaks are reported in wavenumbers (cm^{-1}). Optical rotations were measured at room temperature in CH_2Cl_2, $CHCl_3$ or H_3COH on a Jasco P-2000 polarimeter. Structural assignments were made with additional information from COSY, HSQC, and HMBC. Ozone was generated with an Azcozon Ozone Generator (Model #RMU16-16) graciously loaned to us by the Montgomery group at the University of Michigan.

4.7.2 Preparation of known compounds

Compounds **4.1**,[108] **4.30**,[38] **4.42**,[109] **4.50a**,[109] **4.57**,[110] and **$FeCl_3$•SiO_2**[111] were prepared according to the previously reported procedures. The spectra of the prepared compounds matched the reported spectra data.

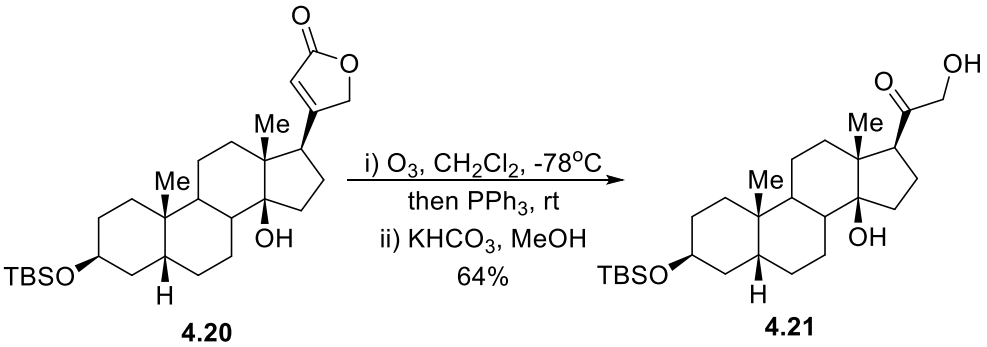
4.7.3 Preparation of new compounds



digitoxigenin, **4.1** **4.20**

Cardenolide 4.20: TBSCl (79 mg, 0.52 mmol, 1.5 eq) was added to a stirred solution of digitoxigenin[108] **4.1** (130 mg, 0.35mmol, 1.0 eq) and imidazole (71 mg, 1.0 mmol, 3.0 eq) in CH_2Cl_2:DMF (3 mL:3 mL). The reaction was stirred at room temperature for 24 hours, at which time an additional aliquot of TBSCl (79 mg, 0.52 mmol, 1.5 eq) in DMF (3 mL) was added and the reaction was stirred for an additional three days. The reaction was diluted with H_2O (20 mL), and extracted with CH_2Cl_2 (3x10 mL). The combined organics were dried over Na_2SO_4 and concentrated *in vacuo*. The crude residue was purified by flash column chromatography (20% EtOAc/hexanes) to afford **4.20** (152 mg, 90%) as a white solid. **HRMS** (ESI-TOF) (m/z): $[M+Na]^+$ calcd for $C_{29}H_{48}O_4SiNa$ 511.3214, found 511.3209. **^{1}H NMR** (500 MHz, $CDCl_3$) δ 5.87 (d, *J* = 1.8 Hz, 1H), 4.99 (dd, *J* = 18.1, 1.8 Hz, 1H), 4.80 (dd, *J* = 18.1, 1.8 Hz, 1H), 4.21 – 3.84 (m, 1H), 2.77 (dd, *J* = 8.9, 5.4 Hz, 1H), 2.26 – 2.02 (m, 2H), 1.86 (dddd, *J* = 13.9, 11.6, 8.1, 5.0 Hz, 2H), 1.80 – 1.72 (m, 2H), 1.67 (dddd, *J* = 17.4, 11.4, 7.8, 2.9 Hz, 2H), 1.61 – 1.46 (m,

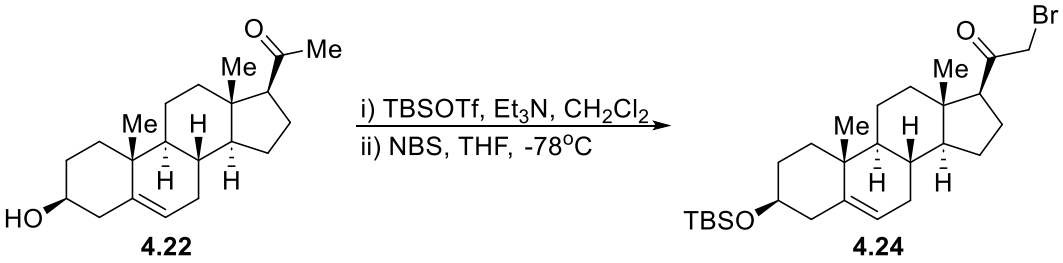
5H), 1.46 – 1.31 (m, 4H), 1.22 (ddt, *J* = 17.6, 9.5, 5.9 Hz, 5H), 0.92 (s, 3H), 0.88 (s, 9H), 0.87 (s, 3H), 0.01 (d, *J* = 1.0 Hz, 6H). **$^{13}C\{^{1}H\}$ NMR** (126 MHz, $CDCl_3$) δ 174.7, 174.7, 117.8, 85.8, 73.6, 67.3, 51.1, 49.7, 42.1, 40.3, 36.1, 35.8, 35.4, 34.4, 33.3, 29.8, 28.8, 27.0, 26.9, 26.0, 24.0, 21.7, 21.4, 18.2, 15.9, -4.7, -4.7. **FTIR** (thin film, cm^{-1}): 3526, 2928, 2887, 2856, 1788, 1752, 1714, 1628, 1470, 1447, 1375, 1361, 1349, 1250, 1187, 1161, 1072, 1060, 1031, 1007, 995, 955, 926, 893, 868, 835, 810, 774, 740, 686, 645, 601, 539, 532. **$[\alpha]_D^{24}$** = +19.8 (c = 0.72, CH_2Cl_2).



4.20 **4.21**

Hydroxy ketone 4.21: Ozone was bubbled through a solution of **4.20** (100 mg, 0.20 mmol, 1.0 eq) in CH_2Cl_2 (15 mL) at -78 °C for approximately ten minutes until the deep blue color was persistent throughout the solution. The reaction was stirred at -78 °C for an additional four hours. The now pale blue solution was sparged with N_2 to remove excess ozone, and the reaction was warmed to room temperature. PPh_3 (107 mg, 0.41 mmol, 2.0 eq) was added and the reaction was stirred for 15 hours at room temperature. The solvent was then removed under reduced pressure, the crude residue was taken up in MeOH (5 mL), and sat. aq. $KHCO_3$ (0.5 mL) was added to the mixture. The reaction was stirred for an additional three hours. MeOH was removed *in vacuo*, and the resulting aqueous mixture was diluted with water (1 mL) and extracted with EtOAc (3x5 mL). The combined organics were dried over Na_2SO_4 and concentrated *in vacuo*. The crude residue was purified by flash column chromatography (30-100% EtOAc/hexanes) to afford **4.21** (61 mg, 64%) as a white solid. **HRMS** (ESI-TOF) (m/z): $[M+Na]^+$ calcd for $C_{27}H_{48}O_4SiNa$

487.3214, found 487.3232. **^{1}H NMR** (700 MHz, $CDCl_3$) δ 4.29 (q, *J* = 20.0 Hz, 2H), 4.04 (s, 1H), 2.72 (dd, *J* = 9.8, 4.4 Hz, 1H), 2.22 – 2.14 (m, 1H), 2.08 – 1.99 (m, 1H), 1.95 – 1.75 (m, 6H), 1.65 – 1.31 (m, 10H), 1.27 – 1.13 (m, 4H), 0.93 (s, 3H), 0.91 (s, 3H), 0.88 (s, 9H), 0.01 (s, 6H). **^{13}C{^{1}H} NMR** (126 MHz, $CDCl_3$) δ 217.4, 85.2, 70.3, 67.4, 58.1, 50.0, 40.3, 39.5, 36.2, 35.5, 35.3, 34.4, 34.1, 29.9, 28.9, 26.9, 26.0, 25.1, 24.1, 21.9, 21.1, 18.2, 15.5, -4.7, -4.7. **FTIR** (thin film, cm^{-1}): 3417, 2927, 2856, 1752, 1628, 1447, 1375, 1361, 1250, 1163, 1061, 1007, 956, 893, 835, 811, 774, 687, 601. **$[\alpha]_D^{24}$** = +33.0 (c = 3.71, CH_2Cl_2).

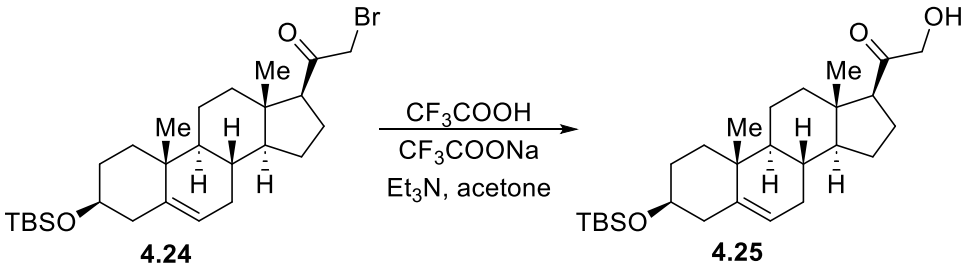


4.22 4.24

Intermediate 4.24: TBSOTf (10.9 mL, 47.4 mmol, 2.2 eq) was added dropwise to a solution of pregnenolone **4.22** (5.0 g, 15.8 mmol, 1.0 eq) in a CH_2Cl_2:Et_3N mixture (60 mL:30 mL) at room temperature. Upon complete addition, the reaction was stirred for an additional one hour at room temperature. The reaction was diluted with sat. aq. $NaHCO_3$ (250 mL) and extracted with CH_2Cl_2 (3x100 mL). The combined organics were dried over Na_2SO_4 and concentrated *in vacuo*. The formation of the $\Delta^{20\text{-}21}$ silylenolether was confirmed by ^{1}H NMR. The crude material was used in the next step without further purification.

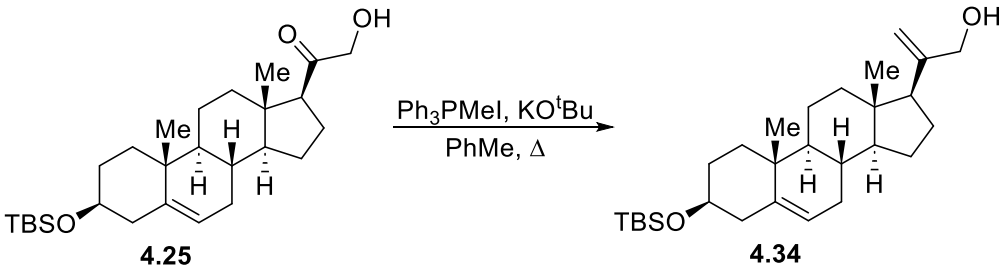
The crude residue was taken up in THF (50 mL) and cooled to -78 ^{o}C. NBS (3.1 g, 17.4 mmol, 1.1 eq) in THF (50 mL) was added dropwise at -78 ^{o}C. The reaction was stirred for four hours at -78 ^{o}C. The reaction was diluted with sat. aq. $NaHCO_3$ (250 mL), warmed to room temperature, and extracted with EtOAc (3x100 mL). The combined organics were dried over Na_2SO_4 and concentrated *in vacuo*. The crude residue was purified by flash column chromatography (1%

EtOAc/hexanes) to afford **4.24** (8.1 g, 99%) as a white solid. **^{1}H NMR** (500 MHz, $CDCl_3$) δ 5.40 – 5.26 (m, 1H), 3.96 – 3.85 (m, 2H), 3.48 (tt, *J* = 11.0, 4.7 Hz, 1H), 2.83 (t, *J* = 8.8 Hz, 1H), 2.32 – 2.13 (m, 3H), 2.03 – 1.93 (m, 2H), 1.87 – 1.69 (m, 4H), 1.67 – 1.44 (m, 6H), 1.32 – 1.23 (m, 1H), 1.17 (ddd, *J* = 12.5, 10.3, 6.4 Hz, 1H), 1.09 – 1.02 (m, 1H), 1.00 (s, 3H), 0.89 (s, 9H), 0.66 (s, 3H), 0.06 (s, 6H). **^{13}C{^{1}H} NMR** (126 MHz, $CDCl_3$) δ 202.2, 141.7, 120.9, 72.6, 60.5, 57.0, 50.1, 45.0, 42.9, 38.9, 37.5, 36.8, 36.1, 32.2, 32.1, 31.9, 26.1, 24.7, 23.9, 21.2, 19.6, 18.4, 13.6, -4.4. **FTIR** (thin film, cm^{-1}): 2928, 2855, 1753, 1705, 1471, 1383, 1360, 1250, 1188, 1061, 1005, 956, 887, 869, 836, 775, 686, 644. **$[\alpha]_D^{24}$** = +31.8 (c = 0.467, CH_2Cl_2).



Intermediate 4.25: Trifluoroacetic acid (11.9 mL, 0.16 mol, 10 eq) was added slowly to a solution of E_3N (38 ml, 0.20 mol, 13eq) in acetone (0.35 L) at 0 ^{o}C. The mixture was slowly brought to room temperature while stirring over 10 minutes. Pregnenolone bromide **4.24** (8.0 g, 0.16 mol, 1.0 eq) in acetone (0.05 L) was added to the reaction at room temperature. The reaction was placed in an oil bath, and heated to 65 ^{o}C for one hour. At this time, sodium trifluoroacetate (31.8 g, 0.23 mol, 15 eq) was added and the reaction was stirred at 65 ^{o}C for an additional 16 hours. Full consumption of the **4.24** was confirmed by TLC analysis, the reaction was cooled to room temperature and then concentrated under reduced pressure. The crude residue was diluted with H_2O (300 mL) and extracted with CH_2Cl_2 (3x100 mL). the combined organics were dried over Na_2SO_4 and concentrated *in vacuo*. The crude residue was purified by flash column chromatography (5%-30% EtOAc/hexanes) to afford **4.25** (6.1 g, 98%) as a white solid. **HRMS**

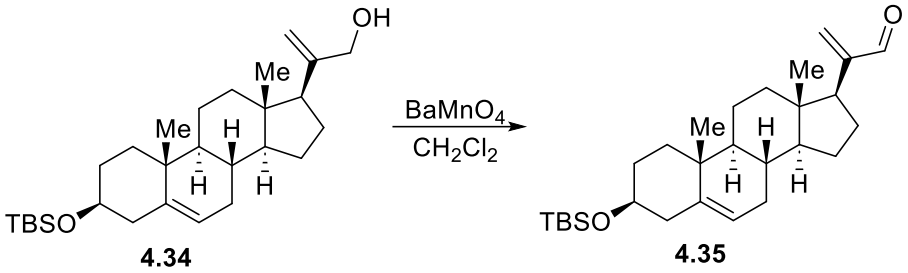
(ESI-TOF) (m/z): $[M+Na]^+$ calcd for $C_{27}H_{46}O_3SiNa$ 469.3108, found 469.3080. **^{1}H NMR** (500 MHz, $CDCl_3$) δ 5.38 – 5.22 (m, 1H), 4.26 – 4.08 (m, 2H), 3.48 (ddt, *J* = 15.7, 10.7, 4.7 Hz, 1H), 3.26 (s, 1H), 2.46 (t, *J* = 9.0 Hz, 1H), 2.31 – 2.13 (m, 4H), 2.05 – 1.95 (m, 1H), 1.92 (dt, *J* = 11.9, 3.4 Hz, 1H), 1.81 (dt, *J* = 13.0, 3.5 Hz, 1H), 1.78 – 1.68 (m, 3H), 1.66 – 1.23 (m, 8H), 1.15 (ddd, *J* = 12.6, 10.4, 6.5 Hz, 1H), 1.05 (td, *J* = 13.6, 3.8 Hz, 1H), 1.00 (s, 3H), 0.89 (s, 9H), 0.65 (s, 3H), 0.06 (s, 6H). **^{13}C{^{1}H} NMR** (126 MHz, $CDCl_3$) δ 210.4, 141.7, 120.9, 120.8, 72.6, 69.6, 59.4, 57.1, 50.1, 44.9, 42.9, 38.7, 37.5, 36.7, 32.1, 32.0, 31.9, 26.1, 24.7, 23.1, 21.1, 19.6, 18.4, 13.5, -4.5. **FTIR** (thin film, cm^{-1}): 2928, 2856, 1705, 1471, 1383, 1252, 1083, 1062, 1004, 958, 887, 869, 836, 803, 770, 670. **$[\alpha]_D^{25}$** = +11.4 (c = 0.147, CH_2Cl_2).



4.25 **4.34**

Intermediate 4.34: PPh_3MeI (3.6 g, 9.0 mmol, 4.0 eq) was added to a suspension of KO^tBu (1.0 g, 9.0 mmol, 4.0 eq) in PhMe (25 mL) under N_2. The reaction was heated to 110 ^oC and stirred for one hour, at which time the reaction mixed became a bright yellow color suspension. **4.25** (1.0 g , 2.3 mmol, 1.0 eq) was added and the reaction was stirred for an additional 1.5 hours at 110 ^oC. The reaction was cooled to room temperature, H_2O (100 mL) was added, and the reaction was stirred for an additional 18 hours. The layers were separated and the aqueous layer was extracted with EtOAc (3x25 mL). The combined organics were dried over Na_2SO_4 and concentrated *in vacuo*. The crude residue was purified by flash column chromatography (10-20% EtOAc/hexanes) to afford **4.34** (0.82 g, 82%) as a white solid. **HRMS** (ESI-TOF) (m/z): $[M+Na]^+$ calcd for $C_{28}H_{48}O_2SiNa$ 467.3316, found 467.3417. **^{1}H NMR** (700 MHz, $CDCl_3$) δ

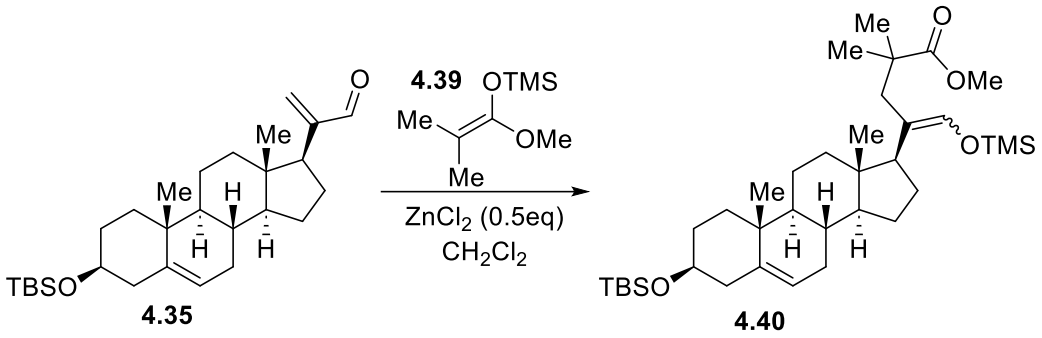
5.32 (d, *J* = 4.3 Hz, 1H), 5.20 (s, 1H), 4.95 (s, 1H), 4.12 (d, *J* = 14.3 Hz, 1H), 4.03 (d, *J* = 14.1 Hz, 1H), 3.47 (d, *J* = 12.5 Hz, 1H), 2.27 (t, *J* = 12.4 Hz, 1H), 2.22 – 2.15 (m, 1H), 2.10 (t, *J* = 9.8 Hz, 1H), 2.00 (d, *J* = 17.6 Hz, 1H), 1.86 – 1.65 (m, 6H), 1.59 – 1.40 (s, 5H), 1.26 – 1.18 (m, 2H), 1.16 – 1.02 (m, 2H), 1.00 (s, 3H), 0.98 – 0.92 (m, 1H), 0.89 (s, 9H), 0.60 (s, 3H), 0.06 (s, 6H). **^{13}C NMR** (126 MHz, $CDCl_3$) δ 149.1, 141.8, 121.1, 109.8, 72.7, 67.1, 56.8, 53.4, 50.4, 43.2, 43.0, 38.6, 37.5, 36.8, 32.5, 32.2, 32.0, 26.1, 25.9, 24.3, 21.2, 19.6, 18.4, 12.9, -4.4. **FTIR** (thin film, cm^{-1}): 2929, 2856, 1705. 1471, 1383, 1252, 1195, 1083, 1004, 958, 886, 869, 836, 803, 772, 670, 603. **$[\alpha]_D^{25}$** = -12.6 (c = 0.127, CH_2Cl_2).



4.34 **4.35**

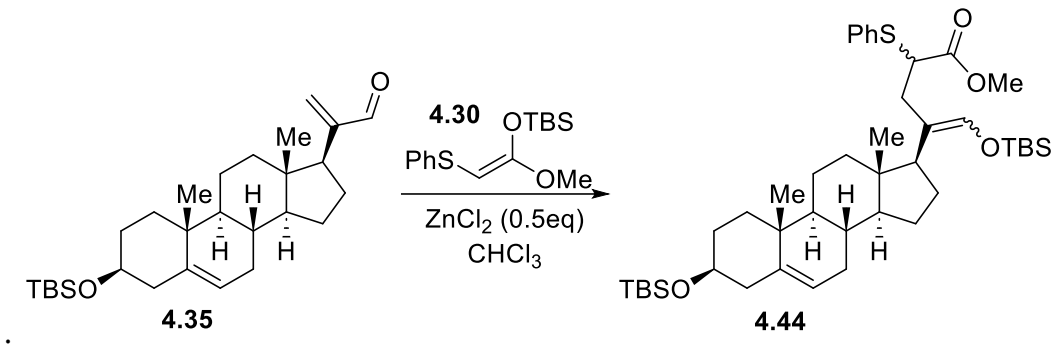
Conjugated aldehyde 4.35: $BaMnO_4$ (1.15 g, 4.5 mmol, 10 eq) was added to a solution of **4.34** (200 mg, 0.45 mmol, 1.0 eq) in CH_2Cl_2 (10 mL). The reaction was stirred at room temperature for 48 hours, then was filtered through celite, and the solvent was removed under reduced pressure. The crude residue was purified by flash column chromatography (2-10% EtOAc/hexanes) to afford **4.35** (151 mg, 76%) as a white solid. **HRMS** (ESI-TOF) (m/z): $[M+Na]^+$ calcd for $C_{28}H_{46}O_2SiNa$ 465.3159, found 365.3156. **^{1}H NMR** (500 MHz, $CDCl_3$) δ 9.56 (s, 1H), 6.28 (s, 1H), 6.11 (s, 1H), 5.32 (dt, *J* = 5.0, 2.1 Hz, 1H), 3.48 (tt, *J* = 11.0, 4.7 Hz, 1H), 2.78 (t, *J* = 9.1 Hz, 1H), 2.26 (ddd, *J* = 13.8, 10.5, 2.4 Hz, 1H), 2.17 (ddd, *J* = 13.3, 5.0, 2.3 Hz, 1H), 2.01 (dtd, *J* = 17.3, 5.1, 2.7 Hz, 1H), 1.88 – 1.67 (m, 5H), 1.63 – 1.42 (m, 5H), 1.41 – 1.22 (m, 5H), 1.05 (td, *J* = 14.1, 4.2 Hz, 2H), 0.99 (s, 3H), 0.89 (s, 9H), 0.53 (s, 3H), 0.06 (s, 6H). **^{13}C{^{1}H} NMR** (126 MHz, $CDCl_3$) δ 194.3, 148.7, 140.7, 134.1, 119.9, 71.6, 55.6, 49.2,

45.8, 42.3, 41.8, 36.7, 36.3, 35.6, 31.5, 31.0, 30.8, 24.9, 24.9, 23.4, 19.9, 18.4, 17.2, 11.8, 0.0, -5.6. **FTIR** (thin film, cm^{-1}): 2928, 1705, 1383, 1252, 1082, 887, 869, 836, 772, 670. $[\alpha]_D^{25}$ = -33.7 (c = 0.153, CH_2Cl_2).



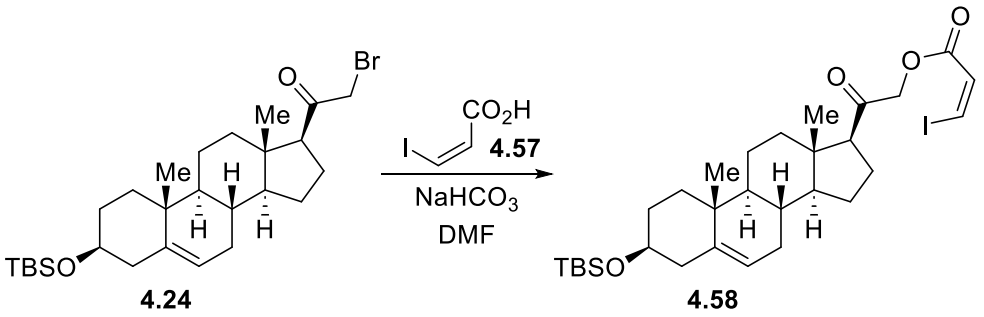
Michael adduct 4.40: Commercially available silyl ketene acetal **4.39** (61% purity, 8.9 mg, 0.04 mmol, 2.0 eq) was added to a stirred solution of $ZnCl_2$ (1.2 mg, 0.01 mmol, 0.5 eq) and **4.35** (8.0 mg, 0.02 mmol, 1.0 eq) in CH_2Cl_2 (0.5 mL) under N_2. The reaction was stirred for three hours at room temperature. Upon full consumption of **4.35** as judged by TLC analysis, the reaction was quenched by addition of Et_3N (10 µL), and the solvent were removed under reduced pressure. The crude residue was purified by flash column chromatography (1-10% EtOAc/hexanes) to afford **4.40** (10.0 mg, 90%) as a white solid. **HRMS** (ESI-TOF) (m/z): $[M+Na]^+$ calcd for $C_{36}H_{64}O_4Si_2Na$ 639.4235, found 639.4230. **^{1}H NMR** (500 MHz, $CDCl_3$) δ 6.09 (s, 1H), 5.31 (dt, *J* = 4.5, 2.0 Hz, 1H), 3.64 (s, 3H), 3.54 – 3.36 (m, 1H), 2.28 (tdd, *J* = 13.7, 8.0, 2.7 Hz, 2H), 2.20 – 2.13 (m, 2H), 2.11 – 2.04 (m, 2H), 1.99 (dtd, *J* = 17.4, 5.2, 2.6 Hz, 1H), 1.80 (dt, *J* = 13.3, 3.6 Hz, 1H), 1.74 – 1.58 (m, 3H), 1.52 (ddt, *J* = 13.9, 7.5, 3.7 Hz, 2H), 1.42 (tt, *J* = 15.8, 6.0 Hz, 2H), 1.28 – 1.17 (m, 2H), 1.16 (s, 3H), 1.11 (s, 3H), 1.10 – 1.00 (m, 2H), 0.99 (s, 3H), 0.97 – 0.92 (m, 1H), 0.89 (s, 9H), 0.63 (s, 3H), 0.14 (s, 9H), 0.07 (d, *J* = 3.0 Hz, 3H), 0.06 (s, 6H). **^{13}C{^{1}H} NMR** (126 MHz, $CDCl_3$) δ 178.8, 141.8, 138.1, 121.3, 115.8, 72.8, 55.7, 52.6, 51.7,

50.7, 46.2, 43.7, 43.6, 43.0, 38.7, 37.6, 36.9, 32.3, 32.3, 32.2, 26.1, 26.1, 25.1, 25.0, 23.6, 21.0, 19.6, 18.4, 13.4, -0.4, -4.4.

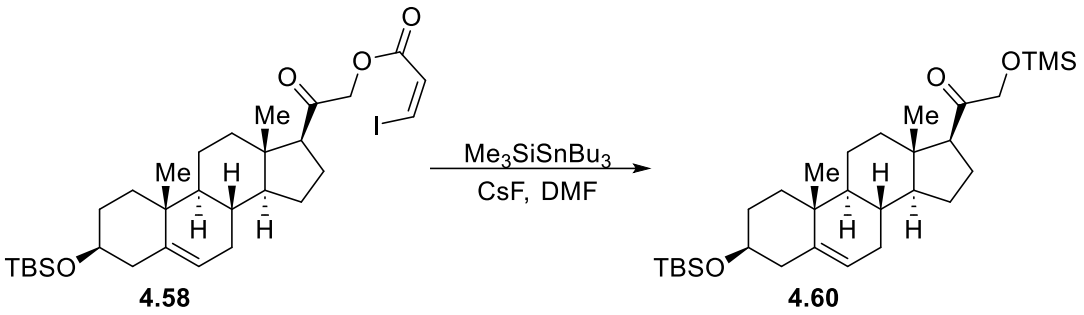


Michael Adduct 4.44: Silyl ketene acetal **4.30**[38] (77% purity, 67 mg, 0.22 mmol, 2.0 eq) was added to a stirred solution of $ZnCl_2$ (8.0 mg, 0.06 mmol, 0.5 eq) and **4.35** (50 mg, 0.11 mmol, 1.0 eq) in CH_2Cl_2 (1.0 mL) under N_2. The reaction was stirred for 18 hours at room temperature. Upon full consumption of **4.35** as judged by TLC analysis, the reaction was quenched by addition of Et_3N (10 µL), and the solvent were removed under reduced pressure. The crude residue was purified by flash column chromatography (1-10% EtOAc/hexanes) to afford **4.44** (69 mg, 83%) as a white solid. **HRMS** (ESI-TOF) (m/z): $[M+H]^+$ calcd for $C_{43}H_{70}O_4SSi_2H$ 739.4607, found 739.4649. **^{1}H NMR** (500 MHz, $CDCl_3$) δ 7.50 – 7.40 (m, 2H), 7.35 – 7.26 (m, 3H), 6.22 (s, 1H), 5.39 – 5.26 (m, 1H), 3.79 – 3.73 (m, 1H), 3.65 (dd, *J* = 10.7, 4.3 Hz, 1H), 3.59 (s, 3H), 3.53 – 3.41 (m, 1H), 2.58 – 2.39 (m, 2H), 2.35 – 2.20 (m, 3H), 2.17 (ddd, *J* = 13.1, 5.0, 2.2 Hz, 1H), 1.99 (dtq, *J* = 16.5, 5.1, 2.7 Hz, 1H), 1.86 – 1.35 (m, 10H), 1.29 – 1.01 (m, 3H), 0.99 (d, *J* = 1.7 Hz, 3H), 0.96 – 0.91 (m, 1H), 0.89 – 0.87 (m, 18H), 0.59 (s, 3H), 0.07 – 0.01 (m, 12H). **^{13}C{^{1}H} NMR** (126 MHz, $CDCl_3$) δ 172.7, 141.8, 139.5, 133.5, 132.6, 129.1, 129.0, 128.2, 121.3, 115.5, 72.8, 72.8, 55.5, 52.1, 51.6, 51.3, 50.9, 50.6, 48.7, 46.3, 46.0, 43.0, 38.5, 37.6, 36.9, 36.9, 34.4, 32.3, 32.2, 26.1, 25.8, 25.0, 25.0, 24.3, 20.9, 19.6, 18.4, 13.6, 13.2, 1.2, -4.4, -5.1, -5.3. **FTIR** (thin film, cm^{-1}): 2929, 2856, 1742, 1705, 1653, 1471, 1437, 1382, 1252,

1201, 1159, 1084, 1005, 958, 939, 888, 868, 835, 804, 772, 746, 689, 666, 604. **[α]$_D^{25}$** = -60.8 (c = 0.947, CH_2Cl_2).

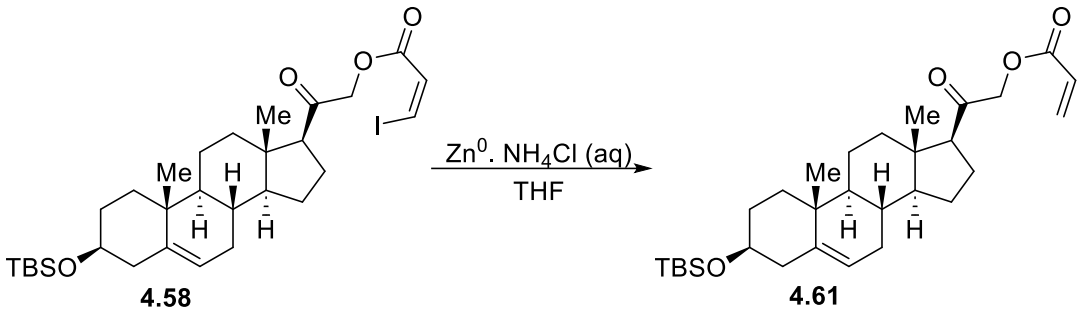


Vinyl iodide 4.58: $NaHCO_3$ (0.38 g, 4.5 mmol, 2.0 eq) was added to a stirred solution of *Z*-iodoacrylic acid **4.57** (0.67 g, 3.4 mmol, 1.5 eq) and **4.24** (1.15 g, 2.3 mmol, 1.0 eq) in DMF (30mL) at room temperature. The reaction was stirred for 18 hours at room temperature. The reaction was diluted with 50% sat. aq. NaCl (300 mL) and extracted with EtOAc (3x100 mL). The combined organics were dried over Na_2SO_4 and concentrated *in vacuo*. The crude residue was purified by flash column chromatography (5% EtOAc/hexanes) to afford **4.58** (1.1 g, 79%) as a white solid. **HRMS** (ESI-TOF) (m/z): $[M+Na]^+$ calcd for $C_{30}H_{47}O_4ISiNa$ 649.2180, found 649.2176. **^{1}H NMR** (500 MHz, $CDCl_3$) δ 7.58 (d, *J* = 9.0 Hz, 1H), 7.05 (d, *J* = 9.0 Hz, 1H), 5.31 (dt, *J* = 5.4, 1.9 Hz, 1H), 4.83 (d, *J* = 16.8 Hz, 1H), 4.67 (d, *J* = 16.8 Hz, 1H), 3.48 (tt, *J* = 11.0, 4.7 Hz, 1H), 2.54 (t, *J* = 8.9 Hz, 1H), 2.31 – 2.13 (m, 3H), 2.10 – 1.95 (m, 2H), 1.82 (dt, *J* = 13.2, 3.5 Hz, 1H), 1.77 – 1.68 (m, 3H), 1.65 – 1.36 (m, 6H), 1.34 – 1.23 (m, 1H), 1.16 (dddd, *J* = 15.0, 11.4, 7.3, 3.7 Hz, 1H), 1.06 (td, *J* = 13.7, 3.9 Hz, 1H), 1.00 (s, 3H), 0.99 – 0.92 (m, 1H), 0.89 (s, 9H), 0.69 (s, 3H), 0.06 (s, 6H). **^{13}C{^{1}H} NMR** (126 MHz, $CDCl_3$) δ 203.3, 163.8, 141.7, 129.1, 120.9, 96.9, 72.7, 69.3, 59.6, 57.3, 50.2, 44.9, 42.9, 38.8, 37.5, 36.8, 32.2, 32.0, 31.9, 26.1, 24.8, 23.0, 21.2, 19.6, 18.4, 13.4, -4.4. **FTIR** (thin film, cm^{-1}): 2959, 2928, 2896, 2857, 1734, 1714, 1598, 1471, 1451, 1383, 1364, 1319, 1255, 1194, 1157, 1082, 1003, 956, 938, 887, 870, 836, 804, 769, 670, 631, 603, 550. **[α]$_D^{25}$** = +32.5 (c = 1.33, CH_2Cl_2).

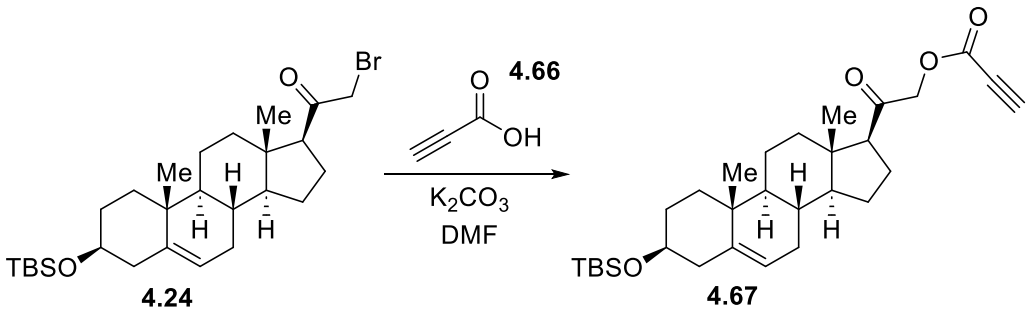


4.58 **4.60**

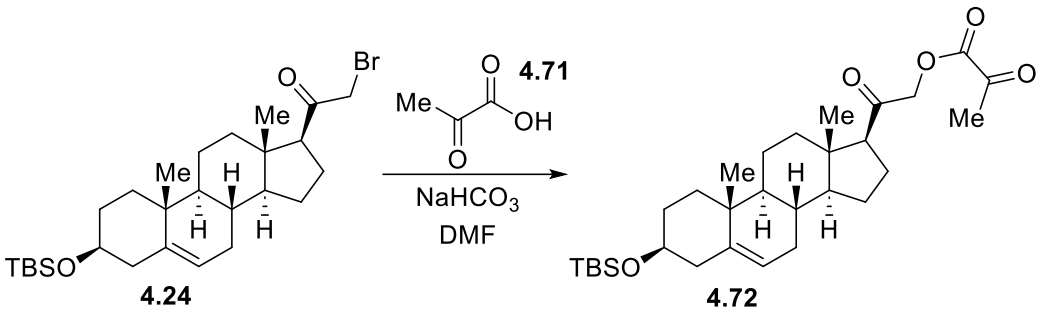
Byproduct 4.60: $Me_3SiSnBu_3$ (70 µL, 0.20 mol, 2.0 eq) was added to a stirred solution of CsF (30.3 mg, 0.20 mmol, 2.0 eq) and **4.58** (62.6 mg, 0.10 mmol, 1.0 eq) in DMF (1.0 mL) at room temperature. The reaction was stirred at room temperature for 16 hours at room temperature. The reaction was diluted with sat. aq. NH_4Cl (10 mL) and extracted with EtOAc (3x5 mL). The crude residue was purified by flash column chromatography (5% EtOAc/hexanes) to afford **4.60** (24.9 mg, 48%) as a white solid. **HRMS** (ESI-TOF) (m/z): $[M+Na]^+$ calcd for $C_{30}H_{54}O_3Si_2Na$ 541.3503, found 541.3536. **^{1}H NMR** (500 MHz, $CDCl_3$) δ 5.31 (dd, *J* = 5.8, 2.9 Hz, 1H), 4.71 (d, *J* = 16.8 Hz, 1H), 4.52 (d, *J* = 16.8 Hz, 1H), 3.48 (tt, *J* = 10.5, 4.7 Hz, 1H), 2.66 – 2.55 (m, 1H), 2.51 (t, *J* = 8.9 Hz, 1H), 2.29 – 2.13 (m, 2H), 2.06 – 1.96 (m, 1H), 1.81 (dt, *J* = 13.4, 3.5 Hz, 1H), 1.70 (dq, *J* = 13.5, 7.7 Hz, 2H), 1.54 – 1.37 (m, 4H), 1.29 (dq, *J* = 14.7, 7.4 Hz, 5H), 1.08 – 1.02 (m, 1H), 0.99 (s, 3H), 0.90 (s, 3H), 0.89 (d, *J* = 1.2 Hz, 12H), 0.87 (s, 3H), 0.67 (s, 3H), 0.06 (s, 6H). **^{13}C{^{1}H} NMR** (126 MHz, $CDCl_3$) δ 204.1, 141.7, 120.9, 72.7, 69.3, 59.5, 57.3, 50.2, 44.9, 42.9, 38.7, 37.5, 36.8, 32.2, 32.0, 32.0, 31.2, 29.3, 27.5, 26.1, 24.8, 23.0, 21.2, 19.6, 18.4, 13.9, 13.2, 9.0, 3.3, -4.4. **FTIR** (thin film, cm^{-1}): 2928, 2898, 2856, 1731, 1716, 1598, 1471, 1436, 1410, 1383, 1364, 1319, 1255, 1194, 1157, 1083, 1003, 956, 938, 938, 887, 835, 804, 770, 726, 669, 632, 602, 548, 533. **$[\alpha]_D^{25}$** = +19.9 (c = 0.573, CH_2Cl_2).



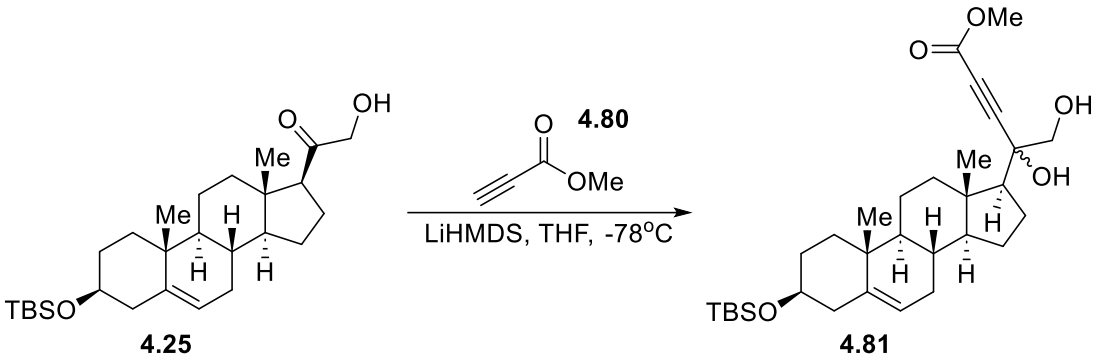
Acrylate 4.61: NH_4Cl (sat. aq. 0.8 mL) was added to a stirred suspension of Zn^0 (13.1 mg, 0.20 mmol, 2.0 eq) and **4.58** (62.6 mg, 0.10 mmol, 1.0eq) in THF (0.2 mL) under argon. The reaction was stirred for 16 hours at room temperature. The reaction was diluted with sat. aq. NH_4Cl (10 mL) and extracted with EtOAc (3x5mL). The combined organics were dried over Na_2SO_4 and concentrated. The crude residue was purified by flash column chromatography (5% EtOAc/hexanes) to afford **4.61** (33.6 mg, 67%) as a white solid. Starting material **4.58** (13.5 mg, 22%) was also recovered. **4.61: HRMS** (ESI-TOF) (m/z): $[M+Na]^+$ calcd for $C_{30}H_{48}O_4SiNa$ 523.3214, found 523.3217. **^{1}H NMR** (500 MHz, $CDCl_3$) δ 6.49 (dd, *J* = 17.3, 1.3 Hz, 1H), 6.22 (dd, *J* = 17.3, 10.5 Hz, 1H), 5.91 (dd, *J* = 10.5, 1.4 Hz, 1H), 5.31 (dd, *J* = 4.9, 2.4 Hz, 1H), 4.80 (d, *J* = 16.8 Hz, 1H), 4.61 (d, *J* = 16.8 Hz, 1H), 3.48 (tt, *J* = 11.1, 4.7 Hz, 1H), 2.53 (t, *J* = 8.8 Hz, 1H), 2.32 – 2.12 (m, 3H), 2.10 – 1.92 (m, 2H), 1.81 (dt, *J* = 13.3, 3.6 Hz, 1H), 1.71 (tdd, *J* = 10.9, 9.1, 7.5, 4.2 Hz, 3H), 1.66 – 1.36 (m, 6H), 1.34 – 1.22 (m, 1H), 1.20 – 1.10 (m, 1H), 1.05 (td, *J* = 13.8, 3.9 Hz, 1H), 0.99 (s, 3H), 0.98 – 0.92 (m, 1H), 0.88 (s, 7H), 0.68 (s, 3H), 0.05 (s, 6H). **^{13}C{^{1}H} NMR** (126 MHz, $CDCl_3$) δ 203.7, 165.5, 141.7, 132.1, 127.7, 120.9, 72.7, 69.4, 59.5, 57.3, 50.2, 44.9, 42.9, 38.8, 37.5, 36.8, 32.2, 32.0, 32.0, 26.1, 24.8, 23.0, 21.2, 19.6, 18.4, 13.3, -4.4. **FTIR** (thin film, cm^{-1}): 2928, 2897, 2857, 1733, 1715, 1598, 1471, 1410, 1383, 1363, 1319, 1255, 1193, 1157, 1082, 1003, 956, 887, 869, 836, 803, 769, 670, 631, 603, 551. **$[\alpha]_D^{25}$** = +17.3 (c = 0.980, CH_2Cl_2).



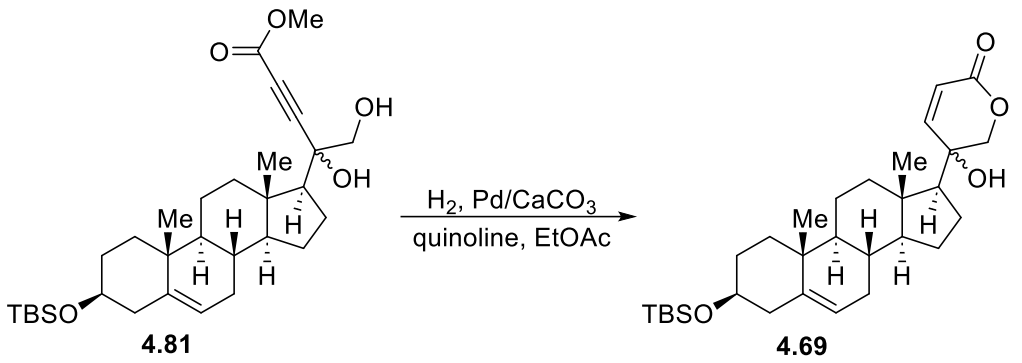
Propiolate 4.67: Propiolic acid **4.66** (0.093 mL, 1.5 mmol, 1.5 eq) was added to a stirred mixture of K_2CO_3 (0.27 g, 2.0 mmol, 2.0 eq) and **4.24** (0.50 g, 1.0 mmol, 1.0 eq) in DMF (5mL) at room temperature. The reaction was stirred for 24 hours at room temperature. The reaction was diluted with 50% sat. aq. NaCl (100 mL) and extracted with EtOAc (3x50 mL). The combined organics were dried over Na_2SO_4 and concentrated *in vacuo*. The crude residue was purified by flash column chromatography (5-30% EtOAc/hexanes) to afford **4.67** (0.43 g, 86%) as a white solid. **HRMS** (ESI-TOF) (m/z): $[M+Na]^+$ calcd for $C_{30}H_{46}O_4SiNa$ 521.3057, found 521.3048. **^{1}H NMR** (401 MHz, CDC_3) δ 5.31 (d, *J* = 5.0 Hz, 1H), 4.80 (d, *J* = 16.6 Hz, 1H), 4.65 (d, *J* = 16.6 Hz, 1H), 3.47 (dt, *J* = 10.5, 4.9 Hz, 1H), 2.96 (s, 1H), 2.51 (t, *J* = 8.7 Hz, 1H), 2.34 – 2.12 (m, 4H), 2.06 – 1.95 (m, 1H), 1.85 – 1.76 (m, 1H), 1.76 – 1.22 (m, 10H), 1.19 – 1.02 (m, 2H), 1.00 (s, 3H), 0.98 – 0.93 (m, 1H), 0.89 (s, 9H), 0.67 (s, 3H), 0.06 (s, 6H). **^{13}C{^{1}H} NMR** (126 MHz, $CDCl_3$) δ 202.2, 152.0, 141.7, 120.9, 76.2, 74.1, 72.7, 70.2, 59.4, 57.2, 50.1, 45.0, 42.9, 38.8, 37.5, 36.8, 32.2, 32.0, 31.9, 26.1, 24.7, 23.0, 21.2, 19.6, 18.4, 13.3, -4.4. **FTIR** (thin film, cm^{-1}): 2928, 2899, 2857, 2125, 1714, 1598, 1470, 1411, 1383, 1365, 1319, 1254, 1226, 1194, 1157, 1083, 1003, 956, 887, 869, 836, 803, 770, 670, 631, 603. **$[\alpha]_D^{25}$** = +54.7 (c = 0.707, CH_2Cl_2).



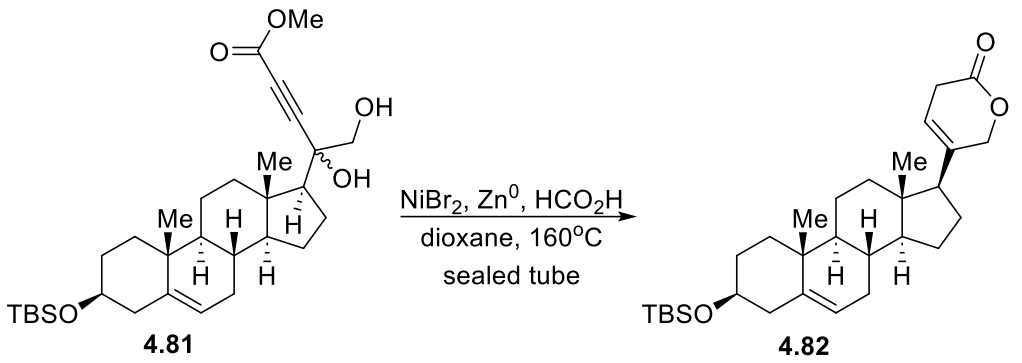
Pyruvate 4.72: Pyruvic acid **4.71** (0.21 mL, 2.9 mmol, 1.5 eq) was added to a stirred mixture of $NaHCO_3$ (0.33 g, 3.9 mmol, 2.0 eq) and **4.24** (1.0 g, 2.0 mmol, 1.0 eq) in DMF (10 mL) at room temperature. The reaction was stirred for 24 hours at room temperature. The reaction was diluted with 50% sat. aq. NaCl (100 mL) and extracted with EtOAc (3x50 mL). The combined organics were dried over Na_2SO_4 and concentrated *in vacuo*. The crude residue was purified by flash column chromatography (5% EtOAc/hexanes) to afford **4.72** (373 mg, 34%) as a white solid. **HRMS** (ESI-TOF) (m/z): $[M+Na]^+$ calcd for $C_{30}H_{48}O_5SiNa$ 539.3163, found 539.3138. **^{1}H NMR** (500 MHz, C_6D_6) δ 5.3 (dt, *J* = 5.1, 1.9 Hz, 1H), 4.9 (d, *J* = 16.5 Hz, 1H), 4.7 (d, *J* = 16.5 Hz, 1H), 3.5 (tt, *J* = 11.0, 4.7 Hz, 1H), 2.5 (s, 4H), 2.3 – 2.1 (m, 3H), 2.0 (ddt, *J* = 19.3, 7.5, 2.8 Hz, 2H), 1.8 (dt, *J* = 13.3, 3.6 Hz, 1H), 1.8 – 1.7 (m, 3H), 1.7 – 1.4 (m, 5H), 1.4 – 1.2 (m, 2H), 1.2 (ddd, *J* = 12.6, 10.2, 6.4 Hz, 1H), 1.1 (td, *J* = 12.2, 10.6, 2.7 Hz, 1H), 1.0 (s, 3H), 1.0 – 0.9 (m, 1H), 0.9 (s, 9H), 0.7 (s, 3H), 0.1 (s, 6H). **^{13}C{^{1}H} NMR** (126 MHz, $CDCl_3$) δ 201.8, 191.2, 159.9, 141.7, 120.9, 72.7, 70.4, 59.5, 57.3, 50.1, 45.1, 42.9, 38.8, 37.5, 36.8, 32.2, 32.0, 31.9, 27.0, 26.1, 24.7, 23.0, 21.2, 19.6, 18.4, 13.3, -4.4. **FTIR** (thin film, cm^{-1}): 2928, 2897, 2857, 1733, 1712, 1598, 1471, 1410, 1383, 1362, 1319, 1255, 1194, 1157, 1082, 1003, 956, 887, 870, 836, 803, 769, 670, 632. **$[\alpha]_D^{25}$** = +44.3 (c = 0.747, CH_2Cl_2).



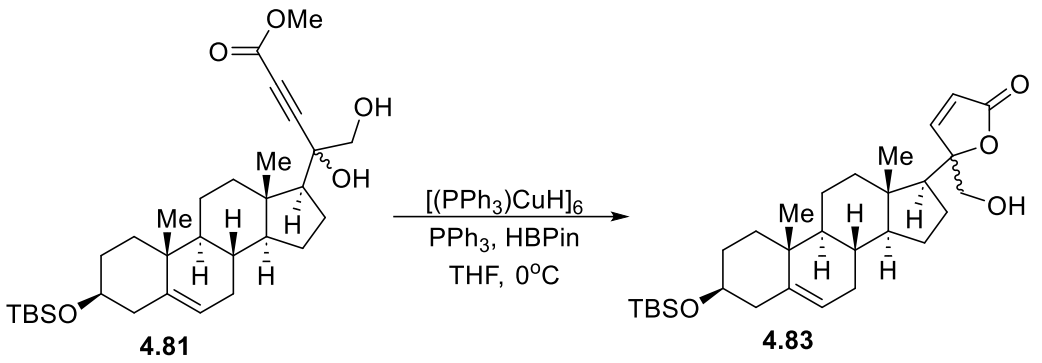
Internal alkyne 4.81: Methyl propiolate **4.80** (0.156 mL, 1.75 mmol, 3.0 eq) was added slowly, dropwise to a stirred solution of LiHMDS (293 mg, 1.75 mmol, 3.0 eq) in THF (2.0 mL) at -78 ^{o}C. The reaction was stirred at -78 ^{o}C for one hour. At this time, **4.25** (280 mg, 0.63 mmol, 1.0 eq) in THF (2.0 mL) was added slowly, dropwise at -78 ^{o}C. After the reaction was stirred for two hours at -78 ^{o}C, then the reaction was diluted with sat. aq. NH_4Cl (10 mL) and H_2O (10 mL) and extracted with EtOAc (3x10 mL). The combined organics were dried over Na_2SO_4 and concentrated *in vacuo*. The crude residue was purified by flash column chromatography (10-20% EtOAc/hexanes) to afford **4.81** (190 mg, 62%) as a white solid. **HRMS** (ESI-TOF) (m/z): $[M+Na]^+$ calcd for $C_{31}H_{50}O_5SiNa$ 553.3320, found 553.3322. **^{1}H NMR** (600 MHz, $CDCl_3$) δ 5.31 (d, *J* = 5.1 Hz, 1H), 3.78 (s, 3H), 3.70 (d, *J* = 11.1 Hz, 1H), 3.47 (dq, *J* = 10.6, 5.0 Hz, 2H), 2.79 (s, 1H), 2.33 – 2.22 (m, 1H), 2.21 – 2.14 (m, 2H), 1.99 (d, *J* = 2.9 Hz, 0H), 1.80 (dd, *J* = 13.3, 3.6 Hz, 1H), 1.76 – 1.63 (m, 2H), 1.60 – 1.38 (m, 8H), 1.33 – 1.14 (m, 2H), 1.09 – 1.02 (m, 1H), 1.01 (s, 3H), 1.00 (s, 3H), 0.96 – 0.90 (m, 1H), 0.89 (s, 9H), 0.85 (d, *J* = 9.4 Hz, 1H), 0.05 (s, 6H). . **^{13}C{^{1}H} NMR** (126 MHz, $CDCl_3$) δ 153.9, 141.9, 121.0, 88.3, 79.6, 75.2, 72.8, 70.4, 56.1, 54.7, 53.0, 50.3, 43.8, 42.9, 40.0, 37.5, 36.8, 32.2, 32.0, 31.6, 29.9, 26.1, 24.6, 24.5, 20.9, 19.6, 18.4, 13.8, -4.4. **FTIR** (thin film, cm^{-1}): 3529, 2929, 2897, 2857, 1717, 1597, 1471, 1430, 1383, 1362, 1318, 1255, 1195, 1157, 1083, 1003, 956, 887, 870, 836, 804, 770, 749, 670, 639. **$[\alpha]_D^{26}$** = -0.606 (c = 0.275, 3:1 CH_2Cl_2:MeOH).



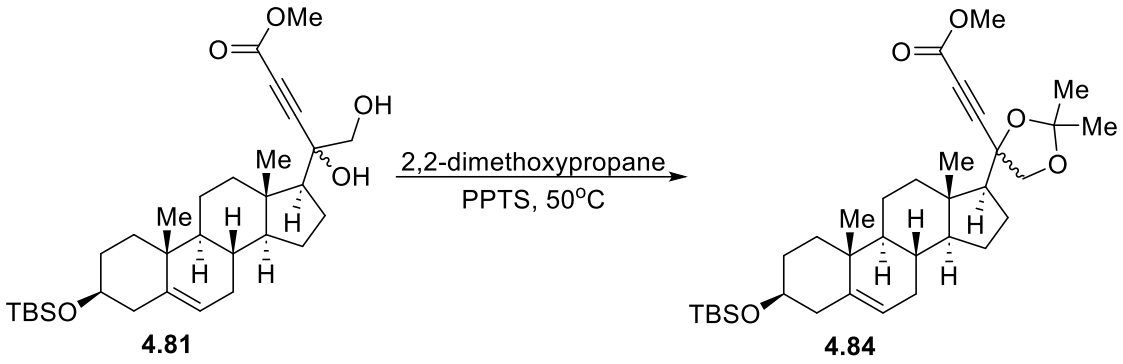
Lactone 4.69: Quinoline (0.015 mL, 0.17 mmol, 4.5 eq) was added to a mixture of **4.81** (20.0 mg, 0.04 mmol, 1.0 eq) and 5 wt% Pd on $CaCO_3$, poisoned with lead (40 mg, 10 wt%) in EtOAc (1.0 mL). The reaction mixture was sparged with N_2 for 30 seconds, then H_2 (balloon) for 5 minutes. The reaction was sealed, and stirred under H_2 atmosphere (balloon, ~1 bar) for 16 hours. The reaction was filtered through celite, washed with CH_2Cl_2 (~10 mL), and concentrated *in vacuo*. The crude residue was purified by flash column chromatography (5-30% EtOAc/hexanes) and **4.69** (4.4 mg, 23%) was obtained as the major identifiable product. **HRMS** (ESI-TOF) (m/z): $[M+Na]^+$ calcd for $C_{30}H_{48}O_4SiNa$ 523.3214, found 523.3241. **^{1}H NMR** (500 MHz, $CDCl_3$) δ 6.89 (d, *J* = 10.0 Hz, 1H), 5.94 (d, *J* = 10.0 Hz, 1H), 5.31 (dt, *J* = 4.7, 2.0 Hz, 1H), 4.43 – 4.31 (m, 2H), 3.47 (tt, *J* = 10.9, 4.7 Hz, 1H), 2.30 – 2.22 (m, 1H), 2.00 – 1.46 (m, 17H), 1.19 – 1.01 (m, 4H), 0.97 (s, 3H), 0.96 (s, 3H), 0.88 (s, 9H), 0.05 (s, 6H). **FTIR** (thin film, cm^{-1}): 2928, 2857, 1716, 1598, 1471, 1383, 1364, 1319, 1255, 1194, 1156, 1083, 1004, 956, 887, 870, 837, 804, 770, 670, 636. **$[\alpha]_D^{26}$** = -34.2 (c = 0.046, CH_2Cl_2).



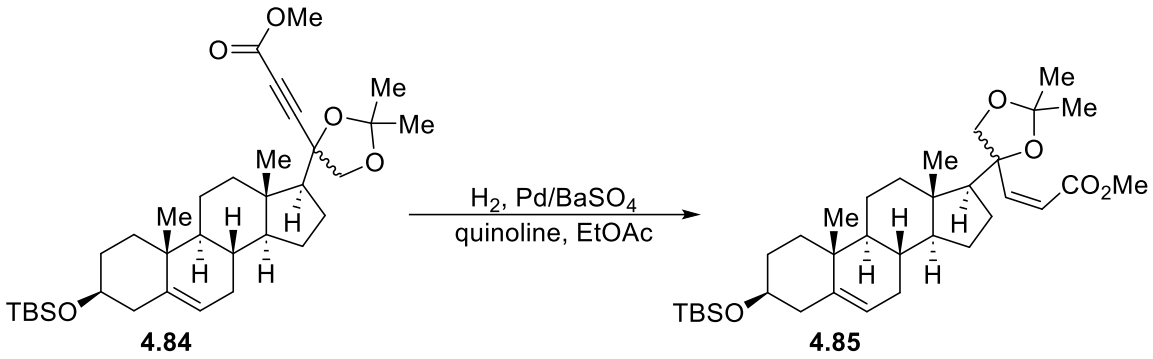
Lactone 4.82: $NiBr_2$ (0.8 mg, 0.004 mmol, 0.1 eq), Zn^0 (12.3 mg, 0.19 mmol, 5.0 eq), formic acid (7.1 µL, 0.19 mmol, 5.0 eq), **4.81** (20.0 mg, 0.04 mmol, 1.0 eq) and dioxane (0.4 mL) were charged into a 5mL-schlenk tube equipped with a magnetic stir bar. The tube was sealed, and placed in an oil bath behind a blast shield. The reaction was heated to a bath temperature of 160 °C and stirred at 160 °C for 22 hours. The reaction was cooled to room temperature, then filtered through celite, washed with CH_2Cl_2 (~10 mL), and concentrated *in vacuo*. The crude residue was purified by flash column chromatography (5-30% EtOAc/hexanes) and **4.82** (4.1 mg, 22%) was obtained as the major identifiable product. **HRMS** (ESI-TOF) (m/z): $[M+Na]^+$ calcd for $C_{30}H_{48}O_3SiNa$ 507.3265, found 507.3373. **^{1}H NMR** (500 MHz, $CDCl_3$) δ 5.84 (d, *J* = 1.8 Hz, 1H), 5.32 (d, *J* = 5.0 Hz, 1H), 4.82 (dd, *J* = 17.4, 1.8 Hz, 1H), 4.69 (d, *J* = 17.2 Hz, 1H), 3.48 (tt, *J* = 10.9, 4.8 Hz, 1H), 2.36 (t, *J* = 9.6 Hz, 1H), 2.27 (t, *J* = 11.4 Hz, 2H), 2.23 – 2.10 (m, 1H), 2.01 (td, *J* = 14.3, 6.0 Hz, 3H), 1.90 – 1.66 (m, 2H), 1.60 – 1.14 (m, 11H), 1.13 – 1.03 (m, 1H), 1.01 (s, 3H), 0.89 (s, 9H), 0.71 (t, *J* = 7.6 Hz, 1H), 0.64 (s, 3H), 0.06 (d, *J* = 5.5 Hz, 6H). **^{13}C{^{1}H} NMR** (126 MHz, $CDCl_3$). **FTIR** (thin film, cm^{-1}): 2926, 2850, 1715, 1598, 1459, 1383, 1365, 1318, 1256, 1194, 1156, 1083, 1004, 956, 887, 870, 836, 804, 770, 726, 670, 637, 604. **$[\alpha]_D^{26}$** = -18.8 (c = 0.091, CH_2Cl_2).



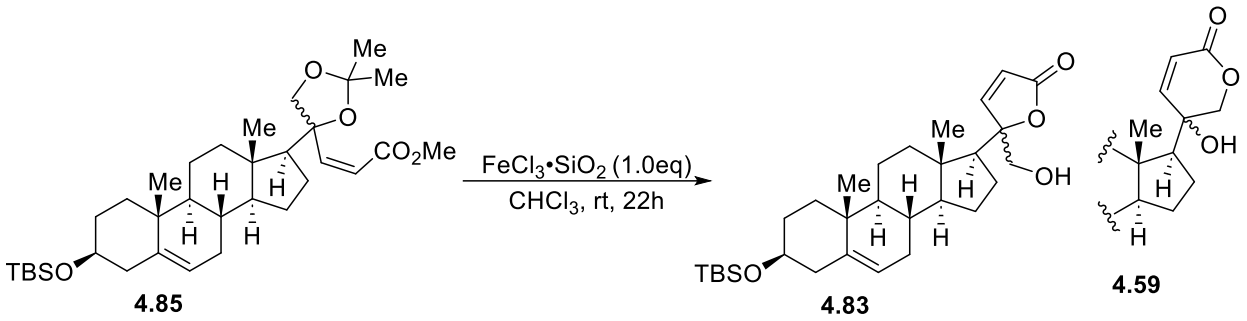
Lactone 4.83: Pinacolborane (4.5 µL, 31 µmol, 1.1 eq) was added to solution of Stryker's reagent (1.1 mg, 0.57 µmol, 0.02 eq), PPh_3 (0.2 mg, 0.57 µmol, 0.02 eq) and **4.81** (15 mg, 28 µmol, 1.0 eq) in THF (0.2mL) at 0°C. The reaction was stirred at 0 °C for six hours. The solvent was removed under reduced pressure, and the crude residue was purified by flash column chromatography (5-30% EtOAc/hexanes) and **4.83** (4.0 mg, 28%) was obtained as the major identifiable product. **HRMS** (ESI-TOF) (m/z): $[M+Na]^+$ calcd for $C_{30}H_{48}O_4SiNa$ 523.3214, found 523.3228. **^{1}H NMR** (600 MHz, $CDCl_3$) δ 7.40 (d, *J* = 5.7 Hz, 1H), 6.11 (d, *J* = 5.7 Hz, 1H), 5.30 (dt, *J* = 4.9, 2.0 Hz, 1H), 3.95 (dd, *J* = 12.0, 4.5 Hz, 1H), 3.71 (dd, *J* = 12.2, 5.9 Hz, 1H), 3.55 – 3.40 (m, 1H), 2.26 (tq, *J* = 11.0, 2.7 Hz, 1H), 2.16 (ddd, *J* = 13.3, 5.0, 2.3 Hz, 1H), 2.03 – 1.91 (m, 3H), 1.79 (dt, *J* = 13.1, 3.4 Hz, 2H), 1.75 – 1.36 (m, 9H), 1.29 (dd, *J* = 12.8, 4.3 Hz, 1H), 1.16 (tt, *J* = 11.1, 5.7 Hz, 1H), 1.09 – 1.01 (m, 2H), 0.98 (s, 3H), 0.96 – 0.90 (m, 1H), 0.88 (s, 9H), 0.75 (s, 3H), 0.05 (s, 6H). **^{13}C{^{1}H} NMR** (151 MHz, $CDCl_3$) δ 173.0, 157.8, 141.7, 121.9, 120.7, 94.0, 72.5, 65.5, 56.6, 52.4, 50.0, 42.9, 42.8, 39.4, 37.3, 36.6, 32.0, 31.6, 31.4, 29.7, 25.9, 23.8, 22.8, 20.8, 19.4, 18.3, 14.3, -4.6. **FTIR** (thin film, cm^{-1}): 2917, 2849, 1717, 1461, 1382, 1254, 1083, 957, 887, 871, 835, 805, 771. **$[\alpha]_D^{26}$** = -27.0 (c = 0.033, CH_2Cl_2).



Acetonide 4.84: PPTS (7.5 mg, 0.028 mmol, 0.2 eq) was added a stirred solution of **4.81** (75 mg, 0.14 mmol, 1.0 eq) in dimethoxypropene (1.5 mL). The reaction was heated to 50 ^{o}C and stirred at that temperature for 20 hours. The solvent was removed under reduced pressure, and the crude residue was purified by flash column chromatography to afford **4.84** (47 mg, 58%) a white solid. **HRMS** (ESI-TOF) (m/z): $[M+Na]^+$ calcd for $C_{34}H_{54}O_5SiNa$ 593.3633, found 593.3647. **^{1}H NMR** (400 MHz, $CDCl_3$) δ 5.31 (d, *J* = 5.1 Hz, 1H), 4.13 (d, *J* = 8.4 Hz, 1H), 3.86 (d, *J* = 8.4 Hz, 1H), 3.76 (s, 3H), 3.47 (tt, *J* = 10.6, 4.7 Hz, 1H), 2.32 – 2.11 (m, 3H), 1.97 (d, *J* = 16.3 Hz, 1H), 1.80 (dd, *J* = 13.3, 3.5 Hz, 1H), 1.76 – 1.64 (m, 5H), 1.59 – 1.50 (m, 3H), 1.49 (s, 3H), 1.48 – 1.40 (m, 2H), 1.39 (s, 3H), 1.33 – 1.02 (m, 5H), 1.00 (s, 3H), 0.93 (s, 3H), 0.89 (s, 9H), 0.06 (s, 6H). **^{13}C{^{1}H} NMR** (126 MHz, $CDCl_3$) δ 154.0, 141.9, 121.0, 111.4, 89.1, 79.4, 78.5, 76.0, 72.7, 57.8, 56.2, 52.8, 50.4, 43.6, 43.0, 39.7, 37.5, 36.8, 32.2, 32.1, 31.6, 29.9, 26.8, 26.1, 26.1, 24.5, 24.4, 20.8, 19.6, 18.4, 13.7, -4.4. **FTIR** (thin film, cm^{-1}): 2928, 2986, 2855, 2226, 1711, 1439, 1380, 1367, 1254, 1159, 1089, 1005, 958, 904, 887, 869, 836, 808, 780, 753, 670, 638. **$[\alpha]_D^{26}$** = -10.5 (c = 0.793, CH_2Cl_2).

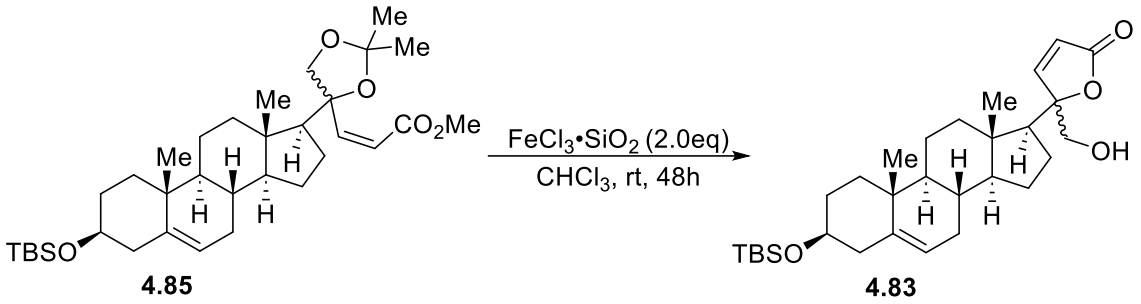


Acetonide 4.85: Quinoline (0.015 mL, 0.017 mmol, 0.1 eq) was added to a mixture of **4.84** (10.0 mg, 0.017 mmol, 1.0 eq) and 5wt% Pd on $BaSO_4$, unreduced (40 mg, 10 wt%) in EtOAc (1.0 mL). The reaction mixture was sparged with N_2 for 30 seconds, then H_2 (balloon) for 5 minutes. The reaction was sealed, and stirred under H_2 atmosphere (balloon, ~1 bar) for 16 hours. The reaction was filtered through celite, washed with CH_2Cl_2 (~10 mL), and concentrated *in vacuo*. The crude residue was purified by flash column chromatography (5% EtOAc/hexanes) and **4.85** (9.7 mg, 97%) was obtained a white solid. **HRMS** (ESI-TOF) (m/z): $[M+Na]^+$ calcd for $C_{34}H_{56}O_5SiNa$ 595.3789, found 595.3786. **^{1}H NMR** (600 MHz, $CDCl_3$) δ 6.42 (d, *J* = 12.7 Hz, 1H), 5.73 (d, *J* = 12.7 Hz, 1H), 5.30 (dd, *J* = 5.2, 2.3 Hz, 1H), 4.43 (d, *J* = 9.3 Hz, 1H), 3.97 (d, *J* = 9.3 Hz, 1H), 3.71 (s, 3H), 3.47 (ddd, *J* = 11.1, 6.3, 4.6 Hz, 1H), 2.30 – 2.21 (m, 1H), 2.20 – 2.06 (m, 3H), 1.95 (dtd, *J* = 17.2, 5.1, 2.7 Hz, 1H), 1.80 (dt, *J* = 13.3, 3.6 Hz, 1H), 1.75 – 1.66 (m, 3H), 1.64 – 1.57 (m, 1H), 1.56 (s, 1H), 1.54 – 1.44 (m, 4H), 1.44 (s, 3H), 1.42 (d, *J* = 10.9 Hz, 1H), 1.35 – 1.29 (m, 1H), 1.28 (s, 3H), 1.11 (ddd, *J* = 13.3, 7.8, 2.5 Hz, 1H), 1.04 – 1.00 (m, 1H), 0.99 (s, 3H), 0.95 – 0.90 (m, 1H), 0.88 (s, 9H), 0.81 (s, 3H), 0.05 (s, 6H). **^{13}C{^{1}H} NMR** (126 MHz, $CDCl_3$) δ 166.5, 141.8, 121.1, 117.8, 108.3, 86.4, 72.8, 72.4, 57.2, 56.2, 51.6, 50.3, 43.0, 43.0, 39.9, 37.5, 36.7, 32.2, 31.9, 31.7, 26.6, 26.1, 25.3, 24.1, 24.0, 21.0, 19.6, 18.4, 14.4, -4.4. **FTIR** (thin film, cm^{-1}): 2916, 2849, 1735, 1712, 1461, 1379, 1254, 1192, 1159, 1084, 958, 887, 870, 836, 804, 773, 558. **$[\alpha]_D^{26}$** = -34.1 (c = 0.033, CH_2Cl_2).



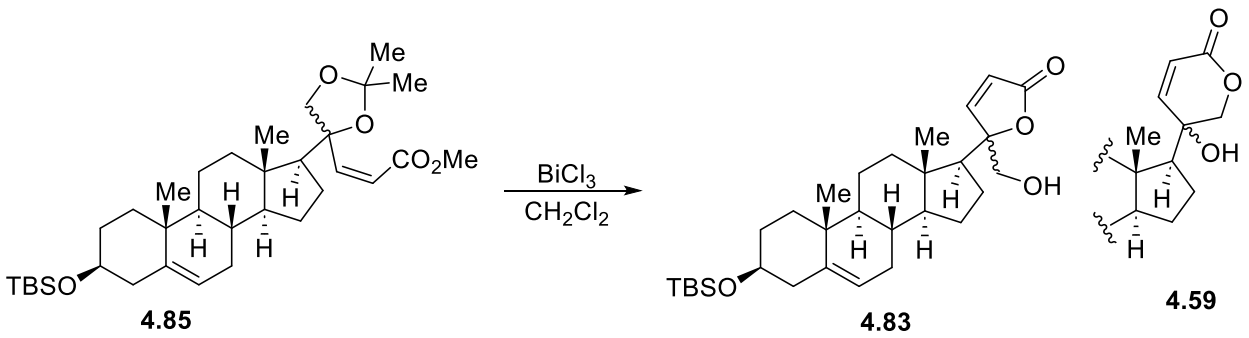
Lactones 4.83 and **4.59**: $FeCl_3•SiO_2$[111] (2.0 mg, 0.017mmol, 1.0 eq) was added to a stirred solution of **4.85** (9.7 mg, 0.017 mmol, 1.0 eq) in $CHCl_3$. The reaction was stirred at room temperature until full consumption of **4.85** was determined by TLC analysis. Upon completion (22 h), the reaction was filtered, and the filtrate was collected and concentrated *in vacuo.* The crude residue was purified by flash column chromatography (10-30% EtOAc/hexanes) to afford **4.83** (3.7 mg, 43%) and **4.59** (0.8 mg, 9%). **4.83**: **HRMS** (ESI-TOF) (m/z): $[M+Na]^+$ calcd for $C_{30}H_{48}O_4SiNa$ 523.3214, found 523.3228. **^{1}H NMR** (600 MHz, $CDCl_3$) δ 7.40 (d, *J* = 5.7 Hz, 1H), 6.11 (d, *J* = 5.7 Hz, 1H), 5.30 (dt, *J* = 4.9, 2.0 Hz, 1H), 3.95 (dd, *J* = 12.0, 4.5 Hz, 1H), 3.71 (dd, *J* = 12.2, 5.9 Hz, 1H), 3.55 – 3.40 (m, 1H), 2.26 (tq, *J* = 11.0, 2.7 Hz, 1H), 2.16 (ddd, *J* = 13.3, 5.0, 2.3 Hz, 1H), 2.03 – 1.91 (m, 3H), 1.79 (dt, *J* = 13.1, 3.4 Hz, 2H), 1.75 – 1.36 (m, 9H), 1.29 (dd, *J* = 12.8, 4.3 Hz, 1H), 1.16 (tt, *J* = 11.1, 5.7 Hz, 1H), 1.09 – 1.01 (m, 2H), 0.98 (s, 3H), 0.96 – 0.90 (m, 1H), 0.88 (s, 9H), 0.75 (s, 3H), 0.05 (s, 6H). **^{13}C{^{1}H} NMR** (151 MHz, $CDCl_3$) δ 173.0, 157.8, 141.7, 121.9, 120.7, 94.0, 72.5, 65.5, 56.6, 52.4, 50.0, 42.9, 42.8, 39.4, 37.3, 36.6, 32.0, 31.6, 31.4, 29.7, 25.9, 23.8, 22.8, 20.8, 19.4, 18.3, 14.3, -4.6. **FTIR** (thin film, cm^{-1}): 2917, 2849, 1717, 1461, 1382, 1254, 1083, 957, 887, 871, 835, 805, 771. **$[\alpha]_D^{26}$** = -27.0 (c = 0.033, CH_2Cl_2). **4.59**: **HRMS** (ESI-TOF) (m/z): $[M+Na]^+$ calcd for $C_{30}H_{48}O_4SiNa$ 523.3214, found 523.3241. **^{1}H NMR** (500 MHz, $CDCl_3$) δ 6.89 (d, *J* = 10.0 Hz, 1H), 5.94 (d, *J* = 10.0 Hz, 1H), 5.31 (dt, *J* = 4.7, 2.0 Hz, 1H), 4.43 – 4.31 (m, 2H), 3.47 (tt, *J* = 10.9, 4.7 Hz, 1H), 2.30 – 2.22 (m, 1H), 2.00 – 1.46 (m, 17H), 1.19 – 1.01 (m, 4H), 0.97 (s, 3H), 0.96 (s, 3H), 0.88 (s, 9H), 0.05 (s,

6H). **FTIR** (thin film, cm^{-1}): 2928, 2857, 1716, 1598, 1471, 1383, 1364, 1319, 1255, 1194, 1156, 1083, 1004, 956, 887, 870, 837, 804, 770, 670, 636. **$[\alpha]_D^{26}$** = -34.2 (c = 0.046, CH_2Cl_2).

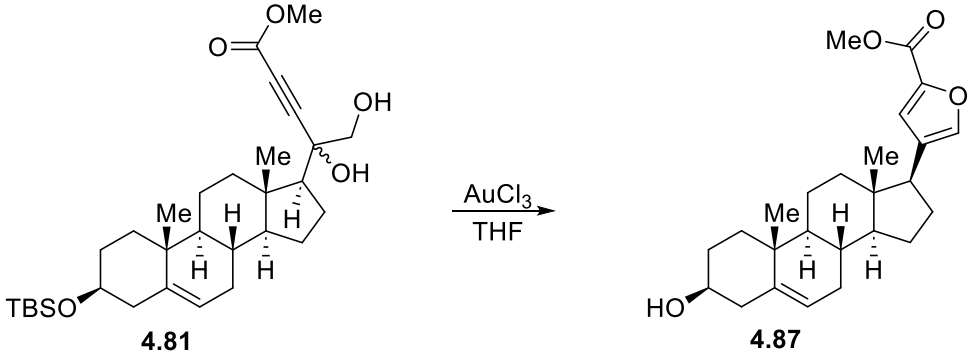


Lactone 4.83: $FeCl_3$•SiO_2[111] (15.0 mg, 0.061 mmol, 1.0 eq) was added to a stirred solution of **4.85** (35.0 mg, 0.061 mmol, 1.0 eq) in $CHCl_3$. The reaction was stirred at room temperature for 48 hours. The reaction was filtered, and the filtrate was collected and concentrated *in vacuo.* The crude residue was purified by flash column chromatography (10-30% EtOAc/hexanes) to afford **4.83** (22.6 mg, 74%). **HRMS** (ESI-TOF) (m/z): $[M+Na]^+$ calcd for $C_{30}H_{48}O_4SiNa$ 523.3214, found 523.3228. **^{1}H NMR** (600 MHz, $CDCl_3$) δ 7.40 (d, *J* = 5.7 Hz, 1H), 6.11 (d, *J* = 5.7 Hz, 1H), 5.30 (dt, *J* = 4.9, 2.0 Hz, 1H), 3.95 (dd, *J* = 12.0, 4.5 Hz, 1H), 3.71 (dd, *J* = 12.2, 5.9 Hz, 1H), 3.55 – 3.40 (m, 1H), 2.26 (tq, *J* = 11.0, 2.7 Hz, 1H), 2.16 (ddd, *J* = 13.3, 5.0, 2.3 Hz, 1H), 2.03 – 1.91 (m, 3H), 1.79 (dt, *J* = 13.1, 3.4 Hz, 2H), 1.75 – 1.36 (m, 9H), 1.29 (dd, *J* = 12.8, 4.3 Hz, 1H), 1.16 (tt, *J* = 11.1, 5.7 Hz, 1H), 1.09 – 1.01 (m, 2H), 0.98 (s, 3H), 0.96 – 0.90 (m, 1H), 0.88 (s, 9H), 0.75 (s, 3H), 0.05 (s, 6H). **^{13}C{^{1}H} NMR** (151 MHz, $CDCl_3$) δ 173.0, 157.8, 141.7, 121.9, 120.7, 94.0, 72.5, 65.5, 56.6, 52.4, 50.0, 42.9, 42.8, 39.4, 37.3, 36.6, 32.0, 31.6, 31.4, 29.7, 25.9, 23.8, 22.8, 20.8, 19.4, 18.3, 14.3, -4.6 **FTIR** (thin film, cm^{-1}): 2917, 2849, 1717, 1461,

1382, 1254, 1083, 957, 887, 871, 835, 805, 771. **$[\alpha]_D^{26}$** = -27.0 (c = 0.033, CH_2Cl_2).

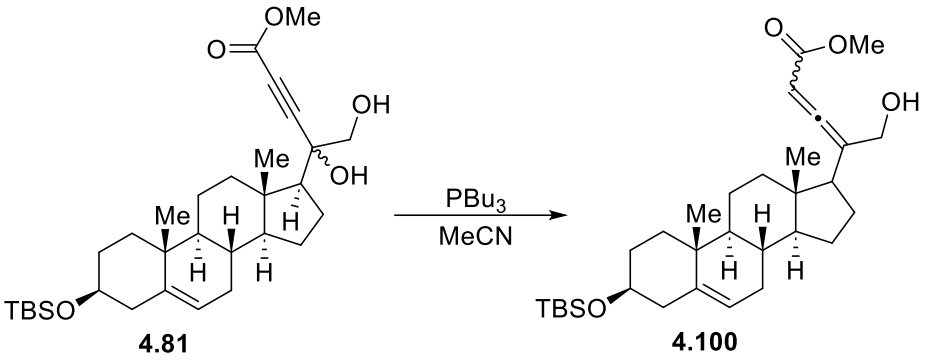


Lactones 4.83 and **4.59**: $BiCl_3$ (0.2 mg, 0.0006 mmol, 0.05 eq) was added to a stirred solution of **4.85** (7.2 mg, 0.013 mmol, 1.0 eq) in $CHCl_3$. The reaction was stirred at room temperature until full consumption of **4.85** was determined by TLC analysis. Upon completion (22 h), the reaction was filtered, and the filtrate was collected and concentrated *in vacuo.* The crude residue was purified by flash column chromatography (10-30% EtOAc/hexanes) to afford **4.83 and 4.59** (4.7 mg, 43%, 2.2:1 **4.83**:**4.59**.



Furan 4.87: Alkyne **4.81** (5.0 mg, 0.009 mmol, 1.0 eq) was added to a stirred solution of $AuCl_3$ (1.4 mg, 0005 mmol, 0.5 eq) in THF (0.2 mL). The reaction was stirred at room temperature for 24 hours. The solvent was removed under reduced pressure and the crude residue was purified by flash column chromatography (30-50% EtOAc/hexanes) to afford **4.87** (1.9 mg, 51%) as a white solid. **HRMS** (ESI-TOF) (m/z): $[M+H]^+$ calcd for $C_{25}H_{35}O_4H$ 399.2530, found 399.2538. **^{1}H NMR** (600 MHz, $CDCl_3$) δ 7.40 (d, *J* = 5.7 Hz, 1H), 6.11 (d, *J* = 5.7 Hz, 1H), 5.30 (dt, *J* = 4.9,

2.0 Hz, 1H), 3.95 (dd, *J* = 12.0, 4.5 Hz, 1H), 3.71 (dd, *J* = 12.2, 5.9 Hz, 1H), 3.55 – 3.40 (m, 1H), 2.26 (tq, *J* = 11.0, 2.7 Hz, 1H), 2.16 (ddd, *J* = 13.3, 5.0, 2.3 Hz, 1H), 2.03 – 1.91 (m, 3H), 1.79 (dt, *J* = 13.1, 3.4 Hz, 2H), 1.75 – 1.36 (m, 10H), 1.29 (dd, *J* = 12.8, 4.3 Hz, 1H), 1.16 (tt, *J* = 11.1, 5.7 Hz, 1H), 1.09 – 1.01 (m, 2H), 0.98 (s, 3H), 0.96 – 0.90 (m, 1H), 0.88 (s, 10H), 0.75 (s, 3H), 0.05 (s, 6H). **^{13}C{^{1}H} NMR** (126 MHz, $CDCl_3$) δ 159.5, 144.3, 143.4, 141.0, 128.0, 121.6, 119.3, 71.9, 56.1, 52.0, 50.4, 47.3, 43.5, 42.4, 37.7, 37.4, 36.8, 32.4, 32.0, 31.8, 29.9, 27.1, 24.6, 20.9, 19.6, 12.9. **FTIR** (thin film, cm^{-1}): 3142, 2918, 2849, 1731, 1709, 1598, 1517, 1439, 1365, 1332, 1318, 1278, 1231, 1202, 1132, 1111, 1044, 1028, 978, 954, 914, 897, 850, 834, 809, 776, 762, 737, 634, 606. **$[\alpha]_D^{26}$** = -35.4 (c = 0.100, CH_2Cl_2).



4.81 **4.100**

Allene 4.100: PBu_3 (9.3µL, 0.038 mmol, 2.0 eq) was added to a stirred solution of alkyne **4.81** (10.0 mg, 0.019 mmol, 1.0 eq) in MeCN (2.0 mL). The reaction was stirred at room temperature for 18 hours. The solvent was removed under reduced pressure and the crude residue was purified by flash column chromatography (5-20% EtOAc/hexanes) to afford **4.100** (3.3 mg, 34%) as a white solid. **HRMS** (ESI-TOF) (m/z): $[M+H]^+$ calcd for $C_{30}H_{48}O_4H$ 537.3371, found 537.3370. **^{1}H NMR** (500 MHz, $CDCl_3$) ^{1}H NMR (500 MHz, $CDCl_3$) δ 5.81 (q, *J* = 2.8 Hz, 1H), 5.31 (dt, *J* = 5.1, 2.1 Hz, 1H), 4.26 (dd, *J* = 13.4, 2.8 Hz, 1H), 4.10 (dd, *J* = 13.4, 3.1 Hz, 1H), 3.72 (s, 3H), 3.48 (tt, *J* = 11.0, 4.7 Hz, 1H), 2.27 (ddd, *J* = 13.6, 10.9, 2.8 Hz, 1H), 2.17 (ddd, *J* = 13.3, 5.0, 2.2 Hz, 1H), 2.07 – 1.94 (m, 2H), 1.84 (ddt, *J* = 27.4, 13.2, 3.7 Hz, 3H), 1.75 – 1.41

(m, 7H), 1.19 (dt, *J* = 17.4, 5.5 Hz, 1H), 1.14 – 1.04 (m, 2H), 1.00 (s, 3H), 0.95 (ddd, *J* = 12.2, 10.8, 4.8 Hz, 1H), 0.89 (s, 9H), 0.73 (s, 3H), 0.05 (s, 6H). . **$^{13}C\{^{1}H\}$ NMR** (126 MHz, $CDCl_3$) δ 210.0, 167.1, 141.8, 121.0, 112.2, 91.7, 72.7, 62.8, 56.3, 52.1, 50.3, 50.0, 43.9, 42.9, 38.6, 37.5, 36.8, 32.5, 32.2, 31.9, 29.8, 27.1, 26.1, 24.4, 21.2, 19.6, 18.4, 13.2, -4.4. **FTIR** (thin film, cm^{-1}): 3452, 2928, 2855, 1957, 1727, 1703, 1435, 1379, 1274, 1249, 1203, 1151, 1089, 1041, 958, 940, 888, 870, 834, 801, 773, 726, 669, 601, 531. **$[\alpha]_D^{26}$** = +9.30 (c = 0.560, CH_2Cl_2).

4.8 References

(1) Steyn, P. S.; Heerden, F. R. van. Bufadienolides of Plant and Animal Origin. *Nat. Prod. Rep.* **1998**, *15* (4), 397–413. https://doi.org/10.1039/A815397Y.

(2) Krenn, L.; Kopp, B. Bufadienolides from Animal and Plant Sources. *Phytochemistry* **1998**, *48* (1), 1–29. https://doi.org/10.1016/S0031-9422(97)00426-3.

(3) Heasley, B. Chemical Synthesis of the Cardiotonic Steroid Glycosides and Related Natural Products. *Chemistry – A European Journal* **2012**, *18* (11), 3092–3120. https://doi.org/10.1002/chem.201103733.

(4) Michalak, M.; Michalak, K.; Wicha, J. The Synthesis of Cardenolide and Bufadienolide Aglycones, and Related Steroids Bearing a Heterocyclic Subunit. *Nat. Prod. Rep.* **2017**, *34* (4), 361–410. https://doi.org/10.1039/C6NP00107F.

(5) Zhong, Y.-; Zhao, C.-; Wu, W.-Y.; Fan, T.-Y.; Li, N.-G.; Chen, M.-; Duan, J.-A.; Shi, Z.-H. Total Synthesis, Chemical Modification and Structure-Activity Relationship of Bufadienolides. *European Journal of Medicinal Chemistry* **2020**, *189*, 112038. https://doi.org/10.1016/j.ejmech.2020.112038.

(6) Pettit, G. R.; Houghton, L. E.; Knight, J. C.; Bruschweiler, F. Bufadienolides. 11. Bufalin and Resibufogenin. *J. Org. Chem.* **1970**, *35* (9), 2895–2898. https://doi.org/10.1021/jo00834a008.

(7) Tsai, T. Y. R.; Wiesner, K. On Cardioactive Steroids. IX. The Conversion of Digitoxigenin to Bufalin. *Can. J. Chem.* **1982**, *60* (16), 2161–2163. https://doi.org/10.1139/v82-309.

(8) Wiesner, K.; Tsai, T. Y. R.; Jäggi, F. J.; Tsai, C. S. J.; Gray, G. D. On Cardioactive Steroids. VIII. The Synthesis of Bufalin and Resibufogenin Isomers. *Helvetica Chimica Acta* **1982**, *65* (7), 2049–2060. https://doi.org/10.1002/hlca.19820650712.

(9) Liu, Z.; Meinwald, J. 5-(Trimethylstannyl)-2H-Pyran-2-One and 3-(Trimethylstannyl)-2H-Pyran-2-One: New 2H-Pyran-2-One Synthons. *J. Org. Chem.* **1996**, *61* (19), 6693–6699. https://doi.org/10.1021/jo951394t.

(10) Gravett, E. C.; Hilton, P. J.; Jones, K.; Romero, F. A Suzuki Coupling Approach to Bufadienolides. *Tetrahedron Letters* **2001**, *42* (51), 9081–9084. https://doi.org/10.1016/S0040-4039(01)01980-3.

(11) Shimizu, S.; Hagiwara, K.; Itoh, H.; Inoue, M. Unified Total Synthesis of Five Bufadienolides. *Org. Lett.* **2020**, *22* (21), 8652–8657. https://doi.org/10.1021/acs.orglett.0c03251.

(12) Synthesis of Cardiotonic Steroids Oleandrigenin and Rhodexin B and Studies Toward the Synthesis of Bufalin. Thesis, University of Michigan, Ann Arbor, MI, 2021. https://dx.doi.org/10.7302/2822.

(13) Tichvon, C.; Zviagin, I.; Nagorny, P. Efficient Synthesis of Cinobufagin. *Manuscript in Preparation* **2023.**

(14) Minato, H.; Nagasaki, T. A New Method for the Synthesis of Furan Compounds. *J. Chem. Soc. C* **1966**, No. 0, 377–379. https://doi.org/10.1039/J39660000377.

(15) Ferland, J. M.; Lefebvre, Y.; Deghenghi, R.; Wiesner, K. Synthetic New Cardenolides. *Tetrahedron Letters* **1966**, *7* (30), 3617–3620. https://doi.org/10.1016/S0040-4039(01)82838-0.

(16) Wiesner, K.; Josef J拡gi, F.; Y. R. Tsai, T. On Cardioactive Steroids VII. The Conversion of Digitoxigenin to Isomers of Natural Bufalin and Resibufogenin. *HETEROCYCLES* **1982**, *19* (4), 647. https://doi.org/10.3987/R-1982-04-0647.

(17) Bohl, M.; Ponsold, K.; Reck, G. Quantitative Structure-Activity Relationships of Cardiotonic Steroids Using Empirical Molecular Electrostatic Potentials and Semiempirical Molecular Orbital Calculations. *Journal of Steroid Biochemistry* **1984**, *21* (4), 373–379. https://doi.org/10.1016/0022-4731(84)90299-1.

(18) Boos, T. L.; Cheng, K.; Greiner, E.; Deschamps, J. R.; Jacobson, A. E.; Rice, K. C. Configurational Reassignment and Improved Preparation of the Competitive IL-6 Receptor Antagonist 20R,21R-Epoxyresibufogenin-3-Formate. *J. Nat. Prod.* **2012**, *75* (4), 661–668. https://doi.org/10.1021/np2008957.

(19) Johnson, D. E.; O'Keefe, R. A.; Grandis, J. R. Targeting the IL-6/JAK/STAT3 Signalling Axis in Cancer. *Nat Rev Clin Oncol* **2018**, *15* (4), 234–248. https://doi.org/10.1038/nrclinonc.2018.8.

(20) Jones, S. A.; Jenkins, B. J. Recent Insights into Targeting the IL-6 Cytokine Family in Inflammatory Diseases and Cancer. *Nat Rev Immunol* **2018**, *18* (12), 773–789. https://doi.org/10.1038/s41577-018-0066-7.

(21) 仁作榊原; 淳森; 慎一永井; 芳弘堀田; 和視竹谷. 強心性植物成分の研究(第4報). 日本薬理学雑誌 **1987**, *90* (2), 115–123. https://doi.org/10.1254/fpj.90.115.

(22) Mori, J.; Nagai, S.-I.; Sakakibara, J.; Takeya, K.; Hotta, Y.; Ando, H. Studies on Cardiac Ingredients of Plants. III. Structural Confirmation and Biological Activity of Reduced Proscillaridins. *Chemical & Pharmaceutical Bulletin* **1987**, *35* (5), 1839–1846. https://doi.org/10.1248/cpb.35.1839.

(23) Mori, J.; Nagai, S.-I.; Sakakibara, J.; Takeya, K.; Hotta, Y. Studies on Cardiac Ingredients of Plants. V. : Chemical Transformation of Proscillaridin and Biological Activities of Derivaties. *Chemical & Pharmaceutical Bulletin* **1988**, *36* (1), 48–59. https://doi.org/10.1248/cpb.36.48.

(24) Murakami, N.; Tanase, T.; Nagai, S.; Sato, Y.; Ueda, T.; Sakakibara, J.; Ando, H.; Hotta, Y.; Takeya, K. Studies on Cardiac Ingredients of Plants. VII : Chemical Transformation of Proscillaridin by Means of the Diels-Alder Reaction and Biological Activities of Its Derivatives. *Chemical & Pharmaceutical Bulletin* **1991**, *39* (8), 1962–1966. https://doi.org/10.1248/cpb.39.1962.

(25) Tanase, T.; Murakami, N.; Nagai, S.; Ueda, T.; Sakakibara, J.; Ando, H.; Hotta, Y.; Takeya, K. Studies on Cardiac Ingredients of Plants. IX. Chemical Transformation of Proscillaridin by Utilizing Its 1, 4-Cycloadducts as Key Compounds and Biological Activities of Their Derivatives. *Chemical & Pharmaceutical Bulletin* **1992**, *40* (2), 327–332. https://doi.org/10.1248/cpb.40.327.

(26) Bauer, P. E.; Kyler, K. S.; Watt, D. S. A Synthesis of 3.Beta.-Hydroxy-5.Beta.,14.Alpha.-Bufa-20,22-Dienolide from Deoxycorticosterone. *J. Org. Chem.* **1983**, *48* (1), 34–39. https://doi.org/10.1021/jo00149a007.

(27) Lardon, A. Partial Synthesis of Cortisone and Related Substances from Sarmentogenin. *Pharmaceutica acta Helvetiae* **1952**, *27*, 287–302.

(28) Templeton, J. F.; Ling, Y.; Jin, J.; Boehmer, M. A.; Zeglam, T. H.; LaBella, F. S. Synthesis of 3β,14-Dihydroxy-5β,14β-Pregnan-20-One C-3 Derivatives: Ozonolysis of Digitoxin and Digitoxigenin and Their Derivatives Followed by Zinc–Acetic Acid Reduction to the C-21 Methyl Ketone. *J. Chem. Soc., Perkin Trans. 1* **1991**, No. 4, 823–829. https://doi.org/10.1039/P19910000823.

(29) Templeton, J. F.; Ling, Y.; Zeglam, T. H.; LaBella, F. S. Synthesis of 20-Hydroxy-, 20-Amino-, and 20-Nitro-14-Hydroxy-21-nor-5.Beta.,14.Beta.-Pregnane C-3 Glycosides and Related Derivatives: Structure-Activity Relationships of Pregnanes That Bind to the Digitalis Receptor. *J. Med. Chem.* **1993**, *36* (1), 42–45. https://doi.org/10.1021/jm00053a006.

(30) Kuate, S. P.; Pádua, R. M.; Poumale, H. M. P.; Kreis, W. Synthesis of a Putative Substrate for Malonyl-Coenzyme A: 21-Hydroxypregnane 21-O-Malonyltransferase and Development of an HPLC Method for the Quantification of the Enzyme Reaction.

Journal of Chromatography B **2007**, *860* (2), 195–201. https://doi.org/10.1016/j.jchromb.2007.10.038.

(31) Pádua, R. M.; Waibel, R.; Kuate, S. P.; Schebitz, P. K.; Hahn, S.; Gmeiner, P.; Kreis, W. A Simple Chemical Method for Synthesizing Malonyl Hemiesters of 21-Hydroxypregnanes, Potential Intermediates in Cardenolide Biosynthesis. *Steroids* **2008**, *73* (4), 458–465. https://doi.org/10.1016/j.steroids.2007.12.012.

(32) Zhang, H.; Sridhar Reddy, M.; Phoenix, S.; Deslongchamps, P. Total Synthesis of Ouabagenin and Ouabain. *Angewandte Chemie International Edition* **2008**, *47* (7), 1272–1275. https://doi.org/10.1002/anie.200704959.

(33) Reddy, M. S.; Zhang, H.; Phoenix, S.; Deslongchamps, P. Total Synthesis of Ouabagenin and Ouabain. *Chemistry – An Asian Journal* **2009**, *4* (5), 725–741. https://doi.org/10.1002/asia.200800429.

(34) Syeda, S. S.; Sanchez, G.; Hong, K. H.; Hawkinson, J. E.; Georg, G. I.; Blanco, G. Design, Synthesis, and in Vitro and in Vivo Evaluation of Ouabain Analogues as Potent and Selective Na,K-ATPase α4 Isoform Inhibitors for Male Contraception. *J. Med. Chem.* **2018**. *61 (5).* 1800–1820. https://doi.org/10.1021/acs.jmedchem.7b00925.

(35) Welzel, P.; Stein, H.; Milkova, T. 14β-Hydroxysteroide, VII. Synthese von Digoxigenin und Digitoxigenin aus Desoxycholsäure. *Liebigs Annalen der Chemie* **1982**, *1982* (12), 2119–2134. https://doi.org/10.1002/jlac.198219821203.

(36) Hoppe, H.-W.; Welzel, P. A Synthesis of Bufalin from Deoxycholic Acid. *Tetrahedron Letters* **1986**, *27* (22), 2459–2462. https://doi.org/10.1016/S0040-4039(00)84555-4.

(37) Hoppe, H. W.; Kaiser, M.; Müller, D.; Welzel, P. An Approach to Bufadienolides from Deoxycholic Acid-1: Strategy and Synthesis of a Model Bufadienolide. *Tetrahedron* **1987**, *43* (9), 2045–2057. https://doi.org/10.1016/S0040-4020(01)86786-7.

(38) Hoppe, H.-W.; Stammen, B.; Werner, U.; Stein, H.; Welzel, P. An Approach to Bufadienolides from Deoxycholic Acid. Reactions of a Steroidal Aβ-Unsaturated Aldehyde with Some O-Silylated Ketene Acetals. *Tetrahedron* **1989**, *45* (12), 3695–3710. https://doi.org/10.1016/S0040-4020(01)89231-0.

(39) Anisfeld, S. T.; Lansbury, P. T. Jr. A Convergent Approach to the Chemical Synthesis of Asparagine-Linked Glycopeptides. *J. Org. Chem.* **1990**, *55* (21), 5560–5562. https://doi.org/10.1021/jo00308a009.

(40) Duhamel, P.; Cahard, D.; Poirier, J.-M. Unprecedented Route to Enolates from Silyl Enol Ethers and Enol Acetates: Reaction with Hard and Soft Electrophiles. *J. Chem. Soc., Perkin Trans. 1* **1993**, No. 21, 2509–2511. https://doi.org/10.1039/P19930002509.

(41) Werner, U.; Möller, U.; Wagner, P.; Welzel, P.; Zylka, C.; Mechmann, S.; Pusch, H.; Glitsch, H. G. Synthese Und Pharmakologische Eigenschaften Eines Neuartigen

Herzwirksamen Steroids. *Angewandte Chemie* **1989**, *101* (10), 1417–1419. https://doi.org/10.1002/ange.19891011029.

(42) Armstrong, A.; Ashraff, C.; Chung, H.; Murtagh, L. Oxidative Rearrangement of 2-Alkoxy-3,4-Dihydro-2H-Pyrans: Stereocontrolled Synthesis of 4,5-Cis-Disubstituted Tetrahydrofuranones Including Whisky and Cognac Lactones and Crobarbatic Acid. *Tetrahedron* **2009**, *65* (23), 4490–4504. https://doi.org/10.1016/j.tet.2009.04.013.

(43) Yamamoto, Y.; Suzuki, H.; Moro-Oka, Y. MoO2(Acac)2 CATALYZED HETERO DIELS–ALDER REACTION OF BENZYL PROP-1-EN-1-YL ETHER WITH METHACROLEIN. *Chemistry Letters* **1986**, *15* (1), 73–76. https://doi.org/10.1246/cl.1986.73.

(44) Spino, C.; Clouston, L. L.; Berg, D. J. Lanthanide Catalysts for the Hetero Diels–Alder Reaction: Effect of Ligand Structure and Acidity. *Can. J. Chem.* **1997**, *75* (8), 1047–1054. https://doi.org/10.1139/v97-125.

(45) Cuzzupe, A. N.; Hutton, C. A.; Lilly, M. J.; Mann, R. K.; McRae, K. J.; Zammit, S. C.; Rizzacasa, M. A. Total Synthesis of the Epidermal Growth Factor Inhibitor (−)-Reveromycin B. *J. Org. Chem.* **2001**, *66* (7), 2382–2393. https://doi.org/10.1021/jo001646c.

(46) Neokosmidi, A.; Ragoussis, V.; Zikos, C.; Paravatou-Petsotas, M.; Livaniou, E.; Ragoussis, N.; Evangelatos, G. Synthesis of Haptens and Development of an Immunoassay for the Olive Fruit Fly Pheromone. *J. Agric. Food Chem.* **2004**, *52* (14), 4368–4374. https://doi.org/10.1021/jf0497758.

(47) Lin, L.; Kuang, Y.; Liu, X.; Feng, X. Indium(III)-Catalyzed Asymmetric Hetero-Diels–Alder Reaction of Brassard-Type Diene with Aliphatic Aldehydes. *Org. Lett.* **2011**, *13* (15), 3868–3871. https://doi.org/10.1021/ol2013999.

(48) Pertschi, R.; Wagner, P.; Ghosh, N.; Gandon, V.; Blond, G. Gold(I)-Catalyzed Synthesis of Furopyrans: Insight into Hetero-Diels–Alder Reactions. *Org. Lett.* **2019**, *21* (15), 6084–6088. https://doi.org/10.1021/acs.orglett.9b02228.

(49) Liyanage Perera, E.; Lee, D. Synthesis of 4-Pyrones by Formal Hydration of 1,3-Diynones Promoted by 1,4-Addition of Piperidine. *Org. Lett.* **2022**, *24* (38), 7042–7046. https://doi.org/10.1021/acs.orglett.2c02914.

(50) Frantz, D. E.; Fässler, R.; Tomooka, C. S.; Carreira, E. M. The Discovery of Novel Reactivity in the Development of C−C Bond-Forming Reactions: In Situ Generation of Zinc Acetylides with ZnII/R3N. *Acc. Chem. Res.* **2000**, *33* (6), 373–381. https://doi.org/10.1021/ar990078o.

(51) Oi, S.; Terada, E.; Ohuchi, K.; Kato, T.; Tachibana, Y.; Inoue, Y. Asymmetric Hetero Diels−Alder Reaction Catalyzed by Chiral Cationic Palladium(II) and Platinum(II) Complexes. *J. Org. Chem.* **1999**, *64* (23), 8660–8667. https://doi.org/10.1021/jo9906680.

(52) Zhu, S.; Jin, G.; Peng, W.; Huang, Q. Cycloaddition Reactions of β-Trifluoroacetylvinyl Ethers. *Tetrahedron* **2003**, *59* (16), 2899–2905. https://doi.org/10.1016/S0040-4020(03)00344-2.

(53) Mori, K.; Matsushima, Y. Synthesis of Mono- and Sesquiterpenoids; XXIV: (-)-Homogynolide A, an Insect Antifeedant Isolated from Homogyne Alpina. *Synthesis* **1995**, *1995* (7), 845–850. https://doi.org/10.1055/s-1995-4004.

(54) Ziegler, D. S.; Wei, B.; Knochel, P. Improving the Halogen–Magnesium Exchange by Using New Turbo-Grignard Reagents. *Chemistry – A European Journal* **2019**, *25* (11), 2695–2703. https://doi.org/10.1002/chem.201803904.

(55) Hermann, A.; Seymen, R.; Brieger, L.; Kleinheider, J.; Grabe, B.; Hiller, W.; Strohmann, C. Comprehensive Study of the Enhanced Reactivity of Turbo-Grignard Reagents**. *Angewandte Chemie International Edition* **2023**, *62* (25), e202302489. https://doi.org/10.1002/anie.202302489.

(56) Piers, E.; Boulet, S. L. Use of the Bifunctional Reagent (Z)-4-Iodo-1-(Tributylstannyl)but-1-Ene: A New Cyclohexenone Annulation Method. *Synlett* **1998**, *1998* (5), 516–518. https://doi.org/10.1055/s-1998-1707.

(57) Bernhardt, S.; Metzger, A.; Knochel, P. Direct Addition of Functionalized Organozinc Reagents to Carbon Dioxide, Ketones, and Aldehydes in the Presence of MgCl2. *Synthesis* **2010**, *2010* (22), 3802–3810. https://doi.org/10.1055/s-0030-1258314.

(58) Gore, M. P.; Nanjappan, P.; Hoops, G. C.; Woodard, R. W. Synthesis of (E)- and (Z)-3-Deuteriophosphoenolpyruvate. *J. Org. Chem.* **1990**, *55* (2), 758–760. https://doi.org/10.1021/jo00289a063.

(59) Kakiya, H.; Nishimae, S.; Shinokubo, H.; Oshima, K. Preparation of Organomanganese Reagents from Organic Halides with Activated Manganese. *Tetrahedron* **2001**, *57* (42), 8807–8815. https://doi.org/10.1016/S0040-4020(01)00864-X.

(60) Zhou, P.; Xu, T. Nickel-Catalyzed Intramolecular Desymmetrization Addition of Aryl Halides to 1,3-Diketones. *Chem. Commun.* **2020**, *56* (59), 8194–8197. https://doi.org/10.1039/D0CC00457J.

(61) Mori, M.; Isono, N.; Kaneta, N.; Shibasaki, M. Novel Cyclization by Stannyl Anion Generated from (Trimethylsilyl)Tributylstannane (Me3SiSnBu3) and Fluoride Ion. Application to Natural Product Synthesis. *J. Org. Chem.* **1993**, *58* (11), 2972–2976. https://doi.org/10.1021/jo00063a012.

(62) Saadi, J.; Bentz, C.; Redies, K.; Lentz, D.; Zimmer, R.; Reissig, H.-U. Stereoselective synthesis of tricyclic compounds by intramolecular palladium-catalyzed addition of aryl iodides to carbonyl groups. *Beilstein J. Org. Chem.* **2016,** *12*, 1236–1242. https://doi.org/10.3762/bjoc.12.118

(63) Tsuzuki, K.; Nakajima, Y.; Watanabe, T.; Yanagiya, M.; Matsumoto, T. Total Synthesis of D1 Pedaldehyde. *Tetrahedron Letters* **1978**, *19* (11), 989–992. https://doi.org/10.1016/S0040-4039(01)85432-0.

(64) Abe, K. Radical Coupling of β-Bromostyrene with Carbonyl Compounds Promoted by Samarium (II) Diiodide. *Chemistry Express* **1991**, *6* (3), 189–192.

(65) Xu, D.; Drahl, M. A.; Williams, L. J. Toward an Integrated Route to the Vernonia Allenes and Related Sesquiterpenoids. *Beilstein J. Org. Chem.* **2011**, *7* (1), 937–943. https://doi.org/10.3762/bjoc.7.104.

(66) Nes, W. R.; Mason, H. L. The Action of Zinc on the 20,21-Ketol Acetate Group of a Δ16-Pregnene. *J. Am. Chem. Soc.* **1951**. *73 (10)*, 4765–4766. https://doi.org/10.1021/ja01154a085.

(67) Rosenfeld, R. S. Tertiary Hydroxyl Group Elimination in Steroid Ketols1. *J. Am. Chem. Soc.* **1957**, *79* (20), 5540–5542. https://doi.org/10.1021/ja01577a056.

(68) USKOKOVIć, M.; DORFMAN, R. I.; GUT, M. A Preparation of 3β-Hydroxypregn-5-En-20-One-4-C14. *J. Org. Chem.* **1958**, *23* (12), 1947–1951. https://doi.org/10.1021/jo01106a037.

(69) Somaiah, R.; Ravindar, K.; Cencic, R.; Pelletier, J.; Deslongchamps, P. Synthesis of the Antiproliferative Agent Hippuristanol and Its Analogues from Hydrocortisone via Hg(II)-Catalyzed Spiroketalization: Structure–Activity Relationship. *J. Med. Chem.* **2014**, *57* (6), 2511–2523. https://doi.org/10.1021/jm401799j.

(70) Hachiya, I.; Inagaki, T.; Ishihara, Y.; Shimizu, M. Titanium Tetraiodide-Promoted Reductive Enolate Formation of α-Tosyloxy Ketone Derivatives and Aldol Reaction with Aldehydes. *BCSJ* **2011**, *84* (4), 419–421. https://doi.org/10.1246/bcsj.20100363.

(71) Danishefsky, S.; Schuda, P.; Kato, K. Synthesis of Vernolepin. Diels-Alder Approach to the Angularly Functionalized AB System. *J. Org. Chem.* **1976**, *41* (7), 1081–1088. https://doi.org/10.1021/jo00869a001.

(72) House, H. O.; Carlson, R. G. Perhydroindanone Derivatives. IV. The 1,1a,4,4a-Tetrahydrofluoren-9-One System1a. *J. Org. Chem.* **1964**, *29* (1), 74–78. https://doi.org/10.1021/jo01024a016.

(73) Paquette, L. A.; Ross, R. J.; Shi, Y. J. Regioselective Routes to Nucleophilic Optically Active 2- and 3-Carene Systems. *J. Org. Chem.* **1990**, *55* (5), 1589–1598. https://doi.org/10.1021/jo00292a039.

(74) Yao, Z.; Ye, D.; Liu, H.; Chen, K.; Jiang, H. Transformation of Aryl Acyloin O-Alkyl and O-Phenyl Derivatives to Ketones. *Synthetic Communications* **2007**, *37* (1), 149–156. https://doi.org/10.1080/00397910600978564.

(75) 真和宗野. ヨウ化サマリウムを用いた6-Endo-Trig 型の環化反応によるヒドリンダノン類縁体の合成. *Yakugaku Zasshi* **2003**, *123* (8), 653–663. https://doi.org/10.1248/yakushi.123.653.

(76) Yeh, C.-H.; Korivi, R. P.; Cheng, C.-H. Ene-Carbonyl Reductive Coupling Mediated by Zinc and Ammonia for the Synthesis of γ-Hydroxybutyric Acid Derivatives. *Advanced Synthesis & Catalysis* **2013**, *355* (7), 1338–1344. https://doi.org/10.1002/adsc.201300073.

(77) Parmar, D.; Matsubara, H.; Price, K.; Spain, M.; Procter, D. J. Lactone Radical Cyclizations and Cyclization Cascades Mediated by SmI2–H2O. *J. Am. Chem. Soc.* **2012**, *134* (30), 12751–12757. https://doi.org/10.1021/ja3047975.

(78) Chen, H.; Ma, X.; Li, Z.; Wang, Q.; Tao, F. Approach to Novel Isotetronic Acid Derivatives: DBU-Et3N-Mediated Aldol/Lactonization/O-Protection Sequence of 2-Oxocarboxylic Esters. *Arkivoc* **2009**, *2009* (10), 87–105. https://doi.org/10.3998/ark.5550190.0010.a10.

(79) SONDHEIMER, F.; STJERNSTRÖM, N.; ROSENTHAL, D. Syntheses in the Cardiac Aglycone Field. I. The Condensation of α-Ketol Tetrahydropyranyl Ethers with Acetylene and with Propiolic Esters. *J. Org. Chem.* **1959**, *24* (9), 1280–1284. https://doi.org/10.1021/jo01091a031.

(80) Kumar, K. S.; Reddy, C. S. Total synthesis of (+)-anamarine. *Org. Biomol. Chem.* **2012**. *10 (13),* 2647–2655. https://doi.org/10.1039/C2OB06940G.

(81) Clive, D. L. J.; Tao, Y.; Bo, Y.; Hu, Y.-Z.; Selvakumar, N.; Sun, S.; Daigneault, S.; Wu, Y.-J. Synthetic Studies on calicheamicinγ1I—Synthesis of (−)-Calicheamicinone and Models Representing the Four Sugars Andthe Aromatic System. *Chem. Commun.* **2000**, No. 15, 1341–1350. https://doi.org/10.1039/B001204L.

(82) Kyle, A. F.; Jakubec, P.; Cockfield, D. M.; Cleator, E.; Skidmore, J.; Dixon, D. J. Total Synthesis of (−)-Nakadomarin A. *Chem. Commun.* **2011**, *47* (36), 10037–10039. https://doi.org/10.1039/C1CC13665H.

(83) Zhang, X.; Liu, J.; Sun, X.; Du, Y. An Efficient Cis-Reduction of Alkyne to Alkene in the Presence of a Vinyl Iodide: Stereoselective Synthesis of the C22–C31 Fragment of Leiodolide A. *Tetrahedron* **2013**, *69* (5), 1553–1558. https://doi.org/10.1016/j.tet.2012.12.008.

(84) Mohamed, Y. M. A.; Hansen, T. V. Z-Stereoselective Semi-Reduction of Alkynes: Modification of the Boland Protocol. *Tetrahedron* **2013**, *69* (19), 3872–3877. https://doi.org/10.1016/j.tet.2013.03.038.

(85) Chiu, P.; Leung, S. K. Stoichiometric and Catalytic Reductive Aldol Cyclizations of Alkynediones Induced by Stryker's Reagent. *Chem. Commun.* **2004**, No. 20, 2308–2309. https://doi.org/10.1039/B407842J.

(86) Zhang, D.; Ready, J. M. Directed Hydrozirconation of Propargylic Alcohols. *J. Am. Chem. Soc.* **2007**, *129* (40), 12088–12089. https://doi.org/10.1021/ja075215o.

(87) Lipshutz, B. H.; Bošković, Ž. V.; Aue, D. H. Synthesis of Activated Alkenylboronates from Acetylenic Esters by CuH-Catalyzed 1,2-Addition/Transmetalation. *Angewandte Chemie* **2008**, *120* (52), 10337–10340. https://doi.org/10.1002/ange.200804912.

(88) Richmond, E.; Moran, J. Ligand Control of E/Z Selectivity in Nickel-Catalyzed Transfer Hydrogenative Alkyne Semireduction. *J. Org. Chem.* **2015**. *80 (13),* 6922–6929. https://doi.org/10.1021/acs.joc.5b01047.

(89) Wang, C.; Dong, J.; Li, T.; Zhao, X.; Xu, D. Palladium-Catalyzed Semihydrogenation of Alkynes with EtOH: Highly Stereoselective Synthesis of E- and Z-Alkenes. *Synthesis* **2022**, *54* (11), 2687–2695. https://doi.org/10.1055/a-1736-8721.

(90) Iwasaki, R.; Tanaka, E.; Ichihashi, T.; Idemoto, Y.; Endo, K. Semireduction of Alkynes Using Formic Acid with Reusable Pd-Catalysts. *J. Org. Chem.* **2018**, *83* (21), 13574–13579. https://doi.org/10.1021/acs.joc.8b02169.

(91) Sumida, Y.; Kato, T.; Yoshida, S.; Hosoya, T. Palladium-Catalyzed Regio- and Stereoselective Hydrosilylation of Electron-Deficient Alkynes. *Org. Lett.* **2012**, *14* (6), 1552–1555. https://doi.org/10.1021/ol300279c.

(92) Park, B. Y.; Lim, T.; Han, M. S. A Simple and Efficient in Situ Generated Copper Nanocatalyst for Stereoselective Semihydrogenation of Alkynes. *Chem. Commun.* **2021**, *57* (56), 6891–6894. https://doi.org/10.1039/D1CC02685B.

(93) Rychnovsky, S. D.; Kim, J. Regiospecificity of Acetal Cleavage to an Enol Ether Using a Carbon-13 Labeled Acetonide. *Tetrahedron Letters* **1991**, *32* (49), 7223–7224. https://doi.org/10.1016/0040-4039(91)80481-K.

(94) Evans, D. A.; Ng, H. P.; Rieger, D. L. Total Synthesis of the Macrolide Antibiotic Rutamycin B. *J. Am. Chem. Soc.* **1993**, *115* (24), 11446–11459. https://doi.org/10.1021/ja00077a049.

(95) Swamy, N. R.; Venkateswarlu, Y. A Mild and Efficient Method for Chemoselective Deprotection of Acetonides by Bismuth(III) Trichloride. *Tetrahedron Letters* **2002**, *43* (42), 7549–7552. https://doi.org/10.1016/S0040-4039(02)01809-9.

(96) Xiao, X.; Bai, D. An Efficient and Selective Method for Hydrolysis of Acetonides. *Synlett* **2001**, *2001* (4), 535–537. https://doi.org/10.1055/s-2001-12340.

(97) Justaud, F.; Hachem, A.; Grée, R. Recent Developments in the Meyer-Schuster Rearrangement. *European Journal of Organic Chemistry* **2021**, *2021* (4), 514–542. https://doi.org/10.1002/ejoc.202001494.

(98) Naveen, N.; Ramesh, G.; Balamurugan, R. Silver-Catalyzed Synthesis of Enones/α-Iodoenones from Tertiary Propargyl Alcohols. *ChemistrySelect* **2019**, *4* (46), 13610–13614. https://doi.org/10.1002/slct.201903568.

(99) Arai, S.; Nakajima, M.; Nishida, A. A Concise and Versatile Synthesis of Alkaloids from Kopsia Tenuis: Total Synthesis of (±)-Lundurine A and B. *Angewandte Chemie International Edition* **2014**, *53* (22), 5569–5572. https://doi.org/10.1002/anie.201400464.

(100) El Douhaibi, A. S.; Judeh, Z. M. A.; Basri, H.; Moussa, Z.; Messali, M.; Qi, G. Iron(III) Chloride–Promoted Isomerization of Propargyl Alcohols to α,β-Unsaturated Carbonyl Compounds. *Synthetic Communications* **2011**, *41* (4), 533–540. https://doi.org/10.1080/00397911003611810.

(101) Kadiyala, V.; Bharath Kumar, P.; Balasubramanian, S.; Karunakar, G. V. Gold-Catalyzed Synthesis of 6-Hydroxyindoles from Alkynylcyclohexadienones and Substituted Amines. *J. Org. Chem.* **2019**, *84* (18), 12228–12236. https://doi.org/10.1021/acs.joc.9b02023.

(102) Hosseyni, S.; Su, Y.; Shi, X. Gold Catalyzed Synthesis of Substituted Furan by Intermolecular Cascade Reaction of Propargyl Alcohol and Alkyne. *Org. Lett.* **2015**, *17* (24), 6010–6013. https://doi.org/10.1021/acs.orglett.5b02980

(103) Kim, H.; Jin, K. Y.; Ha, T. H.; Yu, C.-M. A Convenient Method for the Synthesis of Allenoates from 4-Hydroxyalk-2-Ynoates with PPh_3. *Bulletin of the Korean Chemical Society* **2013**, *34* (3), 719–720. https://doi.org/10.5012/bkcs.2013.34.3.719.

(104) Zhu, X.-F.; Schaffner, A.-P.; Li, R. C.; Kwon, O. Phosphine-Catalyzed Synthesis of 6-Substituted 2-Pyrones: Manifestation of E/Z-Isomerism in the Zwitterionic Intermediate. *Org. Lett.* **2005**, *7* (14), 2977–2980. https://doi.org/10.1021/ol050946j.

(105) Selig, P.; Turočkin, A.; Raven, W. Guanidine-Catalyzed γ-Selective Morita–Baylis–Hillman Reactions on α,γ-Dialkyl-Allenoates: Access to Densely Substituted Heterocycles. *Synlett* **2013**, *24* (19), 2535–2539. https://doi.org/10.1055/s-0033-1339471.

(106) Dong, W.; Hu, P.; Hu, J.; Tong, X. Lewis Base-Catalyzed Divergent Isomerizations of 5-Hydroxyl-2,3-Dienoate. *Tetrahedron Letters* **2014**, *55* (10), 1682–1685. https://doi.org/10.1016/j.tetlet.2013.10.059.

(107) Jana, S.; Roy, A.; Lepore, S. D. Diversification Reactions of γ-Silyl Allenyl Esters: Selective Conversion to All-Carbon Quaternary Centers and γ-Allene Dicarbinols. *Chem. Commun.* **2017**, *53* (37), 5125–5127. https://doi.org/10.1039/C7CC01708A.

(108) Doss, S. H.; Wardakhan, W. W.; Louca, N. A. The Reaction of Digitoxin and Digoxin with Cyanoacetic Acid Hydrazide: Synthesis of Coumarin, Thiazole, Thiophene and Pyridine Derivatives with Potential Biological Activities. *Arch Pharm Res* **2001**, *24* (5), 377–384. https://doi.org/10.1007/BF02975179.

(109) Tappin, N. D. C.; Renaud, P. Methyl Radical Initiated Kharasch and Related Reactions. *Advanced Synthesis & Catalysis* **2021**, *363* (1), 275–282. https://doi.org/10.1002/adsc.202001000.

(110) Dai, Y.; Wang, F.; Zhu, S.; Chu, L. Selective Ni-catalyzed cross-electrophile coupling of alkynes, fluoroalkyl halides, and vinyl halides. *Chinese Chem Lett.* **2022**. *33 (8)*, 4074–4078. https://doi.org/10.1016/j.cclet.2021.12.050.

(111) Kim, K. S.; Song, Y. H.; Lee, B. H.; Hahn, C. S. Efficient and Selective Cleavage of Acetals and Ketals Using Ferric Chloride Adsorbed on Silica Gel. *J. Org. Chem.* **1986**, *51* (3), 404–407. https://doi.org/10.1021/jo00353a027.

Chapter 5 Summary and Future Directions

The studies reported in this thesis developed new methods for the synthesis of carbohydrate containing bioactive compounds. Chapter 1 provided an extensive overview of solid support carbohydrate synthesis and the synthesis of glycosylated cardiotonic steroids. Chapter 1 described the development of a novel solid supported glycosyl donor and its application toward the synthesis of carbohydrate containing natural products and studies toward the synthesis of polysaccharides. The results obtained from the studies in Chapter 1 were published in the *Journal of Organic Chemistry* (https://doi.org/10.1021/acs.joc.3c01985). Chapter 3 described previous syntheses of bufadienolide natural products and the novel methodologies developed for the synthesis of the α-pyrone moiety. Chapter 1 described the studies towards the synthesis of bufadienolides and related heterocyclic analogs of cardenolides and bufadienolides. Appendix A: described collaborative medicinal chemistry studies of natural and unnatural cardiotonic steroid analogs as anti-inflammatory agents with the Sadagurki group at Wayne State University. The results obtained from these studies have been accepted for publication in *ACS Medicinal Chemistry Letters*. Appendix B: described a collaborative study of the mechanistic factors that determine the stereoselectivity of the galactosylation reaction with the Marianski group at Hunter College.

In Chapter 1, we developed novel solid supported glycosyl donors that allowed for the glycosylation of natural products with cleaner crude reaction profiles than traditional methods. The solid supported leaving groups were recyclable, and their use in solid-supported

polysaccharide synthesis was investigated. We developed a decagram synthesis of recyclable polystyrene-based phosphonic acid resin **2.2** from commercially available Merrifield's resin. The immobilized donors could be prepared from their corresponding trichloroacetimidates or hemiacetals to furnish phosphonate donors **2.13**-**2.20**. These glycosylphosphonate-containing resins were obtained in 59-96% yields and were found to be bench-stable at room temperature for periods of at least four years. Optimization of the reaction conditions to transfer the solid supported donors to natural product-like aglycones. Ultimately, these donors could be activated using trifluoroborane etherate at 80 ºC to react with various alcohol and thiol-based acceptors to provide 17 different glycosides in good-to-excellent yields (53-98%). The crude reaction profiles with the solid supported donors were cleaner than traditional trichloroacetimidate donors in solution. To develop a broadly applicable application of these solid supported, the glycosylation of resin-bound 2-deoxyglycosylphosphonates was developed. Additional reaction condition screening identified $FeCl_3$ at 0ºC to be the optimal condition to maximize yield and diastereoselectivity while minimizing undesired byproducts formed due to the competing Ferrier-rearrangement reaction pathway. Resin-bound 2-deoxyglycosylphosphonates were used to transfer 2-deoxy-glucosides, 2-deoxy-glacatosides, and 2-deoxy rhamnosides to natural product and natural product like aglycones in good to excellent yields (44-87%) and good diastereoselectivity for the α-glycoside (up to 10.2:1 α:β). Three protected glycosylated cardiotonic steroids (**2.56**-**2.58**) were prepared using the optimized conditions. In addition, it was demonstrated that **2.2** could be recovered and recycled multiple times without significant decrease in the yields for the subsequent steps. Extensive investigation into the use of the phosphonate resins for solid phase polysaccharide synthesis was performed. Frist, resin bound monosaccharides bearing a temporary Fmoc protecting group were installed to the solid support

in good yields (65-91%). Removal of the Fmoc was quick and facile and proceeded in high yields (91-92%), and was monitored by the release of dibenzofulvene (^{1}H NMR, HRMS). Glycosylation of the resin bound monosaccharide acceptor to from a resin bound disaccharide could be achieved with various glycosyl donors (**2.6**, **2.43**, **2.66**, **2.67**, **2.74**, **2.81**) and promoters (Table 2.3-Table 2.5), however, competitive cleavage of the resulting disaccharide was observed under the reaction conditions. Attempts to transfer the disaccharide attached to the solid support to an acceptor proceeded in low yields, possibility to the trace amounts of base from the Fmoc deprotection interfering with the reaction promoter. Use of PMB as the temporary protecting allow for base-free on-resin deprotection, and conversion of the deprotection reaction was also monitored by the release of *p*-anisaldehyde (^{1}H NMR, HRMS). On-resin glycosylation with glycosyl trichloroacetimidates (**2.81**, **2.93**) proceeded in high yields (<90%) determined by increase in resin mass. Suppression of the cleavage of the disaccharide from the solid support was achieved by using AgOTf as a mild promoter and adding stoichiometric DTBP to neutralize any strong acid formed during the reaction. Transfer of the newly formed disaccharide was found to be challenging and led to the cleavage of newly formed glycosidic linkage. Further efforts to optimize the transfer of the on-resin formed disaccharide can minimize the deglycosylation pathway; the use of the 2-deoxy glycosides as the resin bound monosaccharide acceptor and subsequent cleavage of the 2-deoxy sugar containing disaccharide with $FeCl_3$ may prove fruitful for the elongation and disaccharide transfer. Additionally, the mild conditions and good selectivity for 2-deoxyglycoside transfers offers an enticing approach for the synthesis of natural products bearing similar motifs. The heterogenous nature of the solid support allows for future applications in flow chemistry and automated synthesis. A column packed with phosphonic acid resin **2.2** could be loaded by continuous flow of a solution of 2-deoxy-

glycosyltrichloroacetimidate bearing a PMB temporary protecting group. The PMB could be removed and the cleavage could be monitored by in-line UV-Vis spectroscopy. The resin could then be subjected to glycosylation to grow the carbohydrate chain on the solid support, and final transfer of the resin-bound polysaccharide could be achieved with a saturated solution of $FeCl_3$. Careful consideration for regent solubility must be taken to avoid mechanical issues within the flow system. As method for singular glycosylation, the α-selective glycosylation with 2-deoxyglycosides has been notoriously challenging, and a simple high yielding protocol utilizing the solid supported donors could simplify the synthesis for future medicinal chemistry studies. Given then simple preparation of the solid support and the relatively high loadings achieved for glycoside immobilization (up to 1.1mmol/g), the resins could be used for gram scale synthesis of glycosylated natural products or polysaccharides.

In Chapter 1, we conducted extensive studies on the transformation of cardenolides to various heterocycles proceeding through a key hydroxy ketone intermediate. Preliminary studies were carried out on pregnenolone derived hydroxy ketone **4.25**, which was prepared in 97% yield (3 steps) at multigram scale. Initial studies towards the synthesis of α-pyrones involved employing an inverse electron demand hetero Diels-Alder reaction, which had previously been used by Welzel in their synthesis of bufadienolides. In two steps, the hydroxy ketone was converted to the conjugated aldehyde which would serve as the diene. The Diels-Alder reaction was very sluggish, and only trace amounts of product were observed even after prolonged reaction times (<4 days) with various dienophiles (silyl ketene acetals, ethynyl ethers). We successfully furnished the 1,4-addition product by employing $ZnCl_2$ as catalyst, however, attempts as enol lactonization were unsuccessful, and let to decomposition of the starting material. Moving forward, We began to investigate intramolecular additions to the C20 ketone as

the ring closing step, rather than enol lactonization, which generally required harsh conditions of refluxing the substrate in acidic media. We prepared steroidal 21-*O*-*Z*-iodoacyrlate **4.58**, 21-*O*-pyruvate **4.72**, and 21-*O*-propiolate **4.67** to explore the intramolecular cyclization. Metalation of the *Z*-iodoacrylate and addition of the organometallic intermediates to the C20 ketone did not lead to any of the desired 6-membered lactone **4.59**. Metal insertion to the carbon-halogen bond was successful, however, the organometallic species favored unproductive side reactions over the desired cyclization. The pyruvate esters proved to be especially susceptible to basic hydrolysis, and the pyruvate esters were frequently cleaved to their corresponding alcohols under the reaction conditions for the intramolecular aldol reactions. Further exploration into olefination pyruvate derived Wittig reagents may help achieve the desired cyclization. The reduction of the C20-ketone to the ketyl radical did not result in 6-*endo*-dig cyclization with the propiolate alkyne, but instead resulted in deoxygenation of the C21 alcohol. We returned to intramolecular lactonization as the ring forming step, but looked for alternatives to acid-catalyzed enol lactonizations. Addition of acetylide anion derived from deprotonation of methyl propiolate afforded the internal alkyne diol **4.81** in 62% yield. Direct semi-hydrogenation of the alkyne to the *Z*-alkene provided lactone products **4.59** (23%, H_2, $Pd/CaCO_3$, quinoline), **4.82** (22%, $NiBr_2$, Zn, HCO_2H), and **4.83** (28%, Stryker's reagent, HBPin, PPh_3). The direct diol hydrogenation reaction mixtures were complex mixtures containing by-products from over reduction of the alkyne. The diol was trapped as an acetonide, and semi-hydrogenation of the alkynyl acetonide to the *Z*-alkene **4.85** was achieved in 97% yield with H_2 and palladium on $BaSO_4$ (unreduced) that was poisoned with quinoline. Previous studies had suggested that, under thermodynamic conditions, the 5-membered lactone **4.83** would be the favored lactonization product, not the desired 6-membered lactone **4.59**. We were able to form the 6-membered lactone **4.59** in 23%

(75% yield, 2.2:1 **4.83:4.59**) yield with $BiCl_3$ to facilitate the acetonide removal and lactonization. Further attempts to eliminate the C20 tertiary alcohol resulted in decomposition of the lactone. Lactones **4.59** and **4.83** are novel heterocyclic scaffolds for the cardiotonic steroid skeleton, and their exploration as therapeutic agents may help improve the safety profile of this class of compounds. Cationic rearrangement of the alkyne via the Meyer-Schuster reaction proved unsuccessful, but a 5-*exo*-dig cyclization cleanly afforded steroidal furan **4.87** in 51% yield. This heterocycle had shown promise in computational screening of cardenolides analog binding of the Na/K ATPase, and more steroidal skeletons with this moiety could prove valuable for potential therapeutics. Attempts to form the pyrone via the phosphine-promoted rearrangements we partially successfully. The alkynyl diol **4.81** was successfully transformed to the allene **4.100** in up to 38% yield. Extensive screening of the solvent, temperature, and phosphine was conducted, and for higher yields, an alternative procedure for the allene formation could be explored. Reactions to form the allene directly from the hydroxy ketone, such as olefination with vinyl- phosphonates or -phosphoranes could provide the desired allenes. Alternatively, the allenylation of terminal alkyne (ATA) reaction could also provide a more expedient synthesis of allene **4.100**. Isomerization of the allenes to α-pyrones was unsuccessful in our hands, however, the allene intermediate can be used a diversification point towards the synthesis of other heterocycles. Moving forward, the chemistry and analogs developed from these studies can be applied to natural product derivatization and medicinal chemistry studies of C17 heterocyclic analogs of cardiotonic steroids.

In Appendix A:, we developed a method for the regioselective glycosylation of natural product polyols, and explored the anti-inflammatory activity of these prepared and some related compounds in an *in vitro* assay with several known inflammatory cytokines. We developed a

direct strategy for achieving C3-(α)-L-rhamnosylation of common polyhydroxylated cardenolide aglycones **A.1–A.3** containing a primary C19-hydroxyl group. Based on the computational predictions suggesting that the reaction of **A.1–A.3** with boronic acids would favor the formation of the cyclic C5/C19 or C1/C19 esters, we have developed one pot glycosylation protocols that directly lead to strophanthidol-3-(α)-*L*-rhamnoside **A.16**, and unnatural steroid *anhydro*-ouabagenin-3-(α)-*L*-rhamnoside **A.20**. Despite the promising computational predictions, the attempts to achieve selective glycosylation of ouabagenin **A.1** failed due to its low solubility in organic solvents coupled with the propensity to form *bis*-boronates. The potential of 200 nM solutions of synthetic C3-(a)-*L*-rhamnosides **A.16** and **A.20**, C19-(a)-*L*-rhamnoside **A.21**, *anhydro*-ouabagenin **A.2**, ouabain **A.24** and digoxin to reduce LPS-induced neuroinflammation was subsequently investigated using primary murine glial cells. While the C3-glycosylated steroids reduced the expression of inflammatory IL-1, IL-6, TNFa and IKBKE, the co-administration of unnatural C19-glycoside **A.21** or aglycone **A.2** resulted in enhanced inflammation. In addition to glycosylation, the oxidation of the cardenolide skeleton was found to play a significant role in determining the extent of the *anti*-inflammatory activity exhibited by the steroids. Surprisingly, the previously unexplored unnatural *anhydro*-ouabagenin-3-(a)-*L*-rhamnoside **A.20** was found to exhibit the highest levels of *anti*-inflammatory activity. Further exploration of *anhydro*-ouabagenin glycosides and related synthetic derivatives of ouabain may lead to the analogs with enhanced *anti*-inflammatory properties and is currently the subject of ongoing studies in our laboratories.

In Appendix B:, in collaboration with the Marianski group, we explored the factors that contribute to the stereoselectivity of the galactosylation reaction by preparing several novel galactoside donors and evaluating the diastereoselectivity of their glycosylation with

cyclohexanol. The relative stability of reaction intermediates of the galactosylation reaction were assessed by DFT calculation. Based on DFT calculations, it became evident that the thermal stability of the dioxolenium intermediates could be affected by the electron donating/withdrawing substituents of benzoate protecting groups. Thus, if the thermal stability of the intermediates drives the selectivity, then the glycosylation with galactose donors could be altered by the electronic nature of benzoate groups at the C2 and C4 positions. We developed and prepared in five steps from a commercial thioglycoside **B.1**, two novel galactose donors (**B.8**, **B.11**) with C2 and C4 benzoate protecting groups with varying electronic properties about the benzoates. Glycosylation of cyclohexanol with donors **B.8**/**B.11** and NIS and TMSOTf as promoters led to the exclusive formation of the β-glycosides with both donors. Glycosylation of cyclohexanol with donor **B.11** and TolSCl and $AgSbF_6$ as promoters did not form any of the desired glycosidic product, but instead provided products resulting from side reaction of the glycosyl oxocarbenium intermediate. From these results, it appears that the thermal stability of the intermediates is not enough to alter the selectivity. Likely, the barriers leading to the formation of the intermediates play a deciding role. With the Marianski group, further exploration and calculations of the energies of these barriers can be explored to probe their effects on galactosylation stereoselectivity. Additionally, the additive effect of electron donor/withdrawing groups on the benzoates may be explored to greater the energy difference between the dioxolenium intermediates, and possibly switch the selectivity. The counterion effects may also be playing a role, and a deeper investigation into their effects can provide more information to the reaction mechanism. We have conducted experimental validation for a computationally predicted reaction outcome, and have developed a greater understanding for the driving forces of stereoselectivity of galactosylation reactions.

Moving forward, the glycosylation methodology reported in Chapter 1 can be used to prepared novel carbohydrate containing compounds for biological study. Notably, the solid supported glycosyl donors can transfer 2-deoxy glycosides with high α-selectivity under mild conditions, can may be used for the synthesis of natural product-like glycosides in continuous flow or by automated synthesis. The resins may also be employed for solid-supported oligosaccharide synthesis; however, more optimization of the reaction conditions is required to suppress the undesired deglycosylation pathway that occurred with the currently developed conditions.

The methodology developed in Chapter 1 can be applied for the synthesis of novel C17 heterocycles of cardiotonic steroids starting from naturally isolated cardenolides. The 4-5 step procedure to make various lactones or furans is simple and tolerant to sensitive functional groups. Additional studies of the reactivity of the steroidal allenes may provide additional heterocycles (dihydrofurans or α-pyrones). Synthesis of the allenes could be improved, possibly by avoiding the alkyne addition/phosphine rearrangement sequence and instead forming the allene via olefination with vinyl phosphonates/phosphoranes or allenylation of terminal alkynes. These novel heterocyclic analogs may also be glycosylated using the resins developed in Chapter 1.

The compounds evaluated in Appendix A:, namely *anhydro*-ouabain, may be further progressed as anti-inflammatory agents. Neuroinflammation has been linked to numerous diseases, including cancer and neurodegenerative disorders, and agents with promise in this therapeutic area could provide critical relief to suffering patients. The glycosylation of ouabagenin was challenging due to its poor solubility in organic solvent and unselective formation of multiple boronate esters. Further optimization of the glycosylation conditions

(solvent/temp) may improve the solubility and reactivity of ouabagenin, and perhaps implantation of other transient protecting groups or organocatalysts may improve the regioselectivity of the glycosylation.

The studies in Appendix B: provided a greater understanding of the mechanism of the galactosylation reaction. While in these cases, the electronic effects of the benzoates were not enough to sway the selectivity, further exploration of other factors may provide more insights. Other sugar donors, such as glycals, may have lower barriers to form each of the respective dioxolenium-type ions, and in these substrates the electronic effects of the esters may have a stronger effect on the diastereoselectivity.

Appendices

Appendix A: Synthesis and Evaluation of Ouabagenin and Ouabain Analogs and Anti-inflammatory Agents

This chapter in part was published in:

Rutkoski, R.; Debarba, L. K.; Stilgenbauer, L; Rosenthal, T.; Sadagurski, M.; Nagorny, P. *ACS Med. Chem. Lett.* Accepted. 2023.

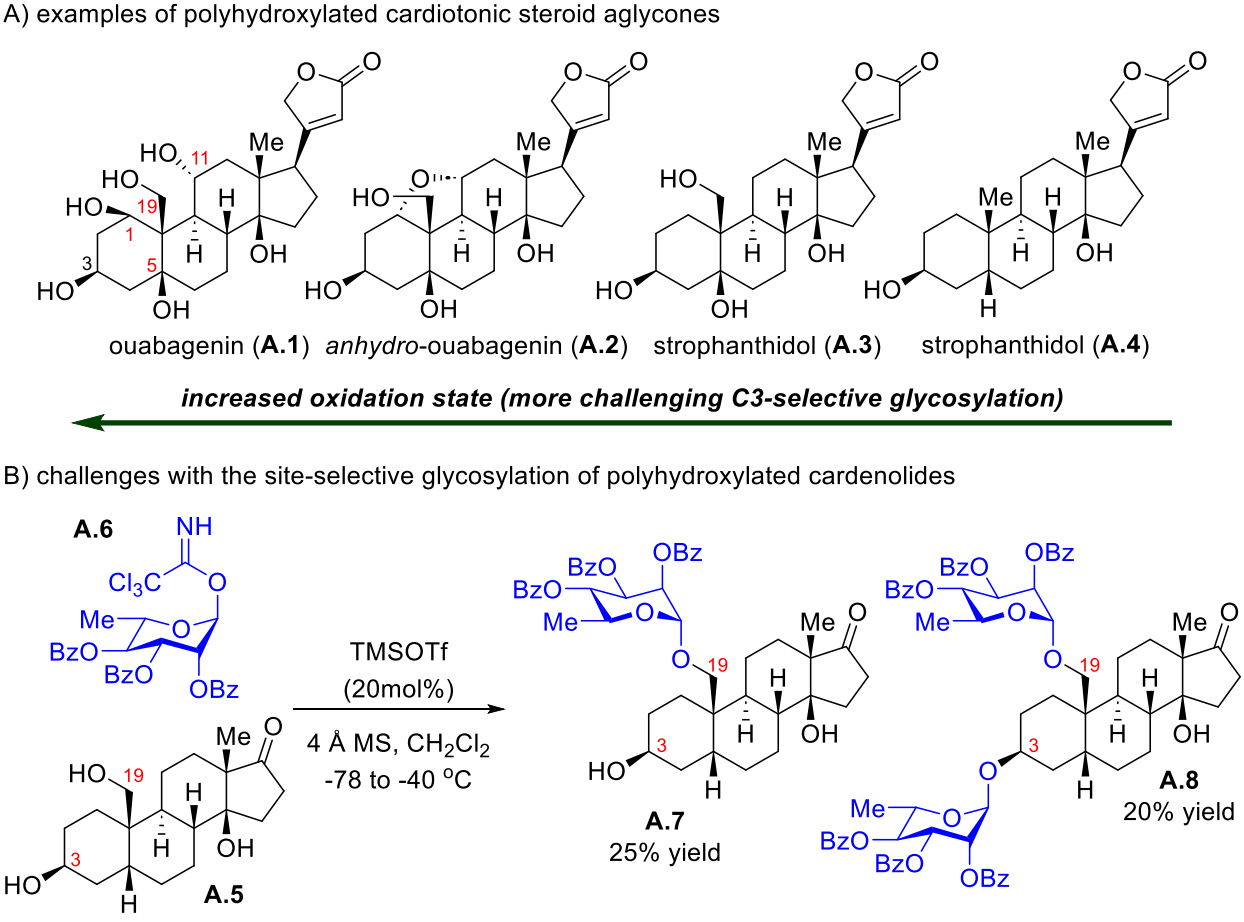
Compounds **A.1**, **A.2**, and **A.14-A.21** were prepared by Dr. Tay Rosenthal.

The biological evaluations of digoxin, **A.2**, **A.16**, **A.20**, **A.21**, and **A.24** as anti-inflammatory agents were conducted by Lucas Debarba, Dr. Lukas Stilgenbauer, and Dr. Marianna Sadagurski of Wayne State University.

A.1 Introduction

Cardenolides represent a broad family of glycosylated steroids found in animals and plants such as oleander, foxglove, lily of the valley, red squill, dogbane. etc.[1,2] For centuries, herbal remedies containing cardenolides as active ingredients have been used to treat various conditions such as edema or "dropsy".[3] Cardenolides are known to serve as inotropic agents and they are known to reversibly inhibit the Na,K-ATPase pump, which increases intracellular sodium and decreases intracellular potassium levels, which, in turn, results in intracellular accumulation of calcium. Due to this effect, cardiotonic steroids digoxin and digitoxin have been essential therapeutics for the treatment of heart failure and arrhythmia.[2,4-7] However, the biological activity of cardenolides extends well beyond their cardiotonic activity. Among numerous other applications, cardiotonic steroids have been explored as potential therapeutic agents for the treatment of cancer,[8-10] viral infections,[11,12] neurodegenerative diseases,[13,14]

stroke,[15-17] and as anti-inflammatory[12,18,19] and senolytic[20] agents. Particularly interesting are the recent reports indicating that cardiotonic steroids such as ouabain and digoxin may influence the peripheral and central nervous systems. Ouabain is an endogenous cardiotonic steroid produced by mammalians in subnanomolar concentrations by the adrenal gland, hypothalamus, and pituitary.[21-24] Several recent *in vivo* studies demonstrated ouabain has an anti-inflammatory effect in the rat hippocampus and that ouabain demonstrated neuroprotection against liposaccharide (LPS) induced inflammation.[25-28] This neuroprotective effect was attributed to the ability of ouabain to promote membrane lipid remodeling and increase the expression of glutamate transporter EAAT4, which helps to mitigate the oxidative stress induced by LPS. This effect is not limited to ouabain as cardiotonic steroids oleandrin and digoxin demonstrated neuroprotection for oxygen and glucose deprivation in ischemia models.[15-17]



Appendix Figure A.1: Polyhydroxylated cardiotonic steroid aglycones and challenges with site-selective glycosylation

While these prior examples suggest that cardenolides may exhibit neuroprotective properties, the specific structural features that are essential for these effects are unknown. It has been observed that both the carbohydrate structure and skeletal oxidation (Appendix Figure A.1A) may impact the biological activity of cardenolides; however, no comparative study evaluating neuroprotective properties of cardenolides across a group of cardiotonic steroids with different oxidation patterns and glycosylation sites has been carried to date. We investigated the selective (a)-*L*-rhamnosylation and subsequent exploration of C19-hydroxylated cardenolides with different oxidation patterns (**A.1**-**A.3**). The potential of the synthetic and natural steroids to reduce LPS-caused neuroinflammation was investigated at 200 nM concentration using primary microglia cells derived from neonatal 1-2 days old mice. The effect of steroids was monitored

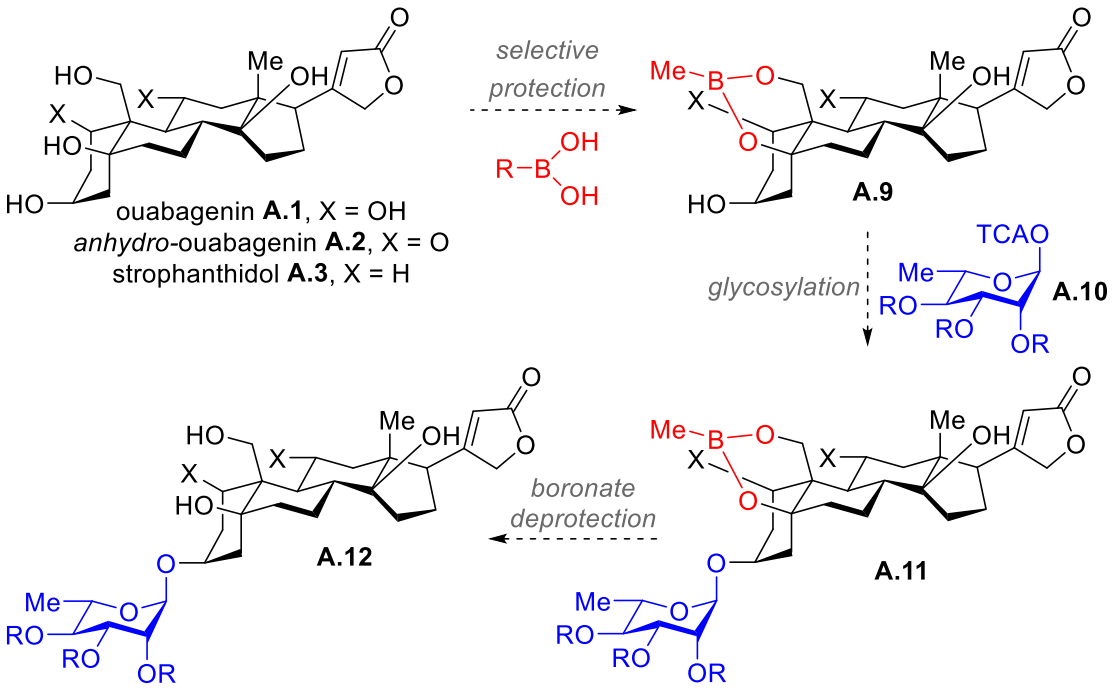
using the inflammation markers IL-1, IL-6, TNFα, and IKBKE, and several significantly differing responses were observed. The synthetic and natural 3-(a)-*L*-rhamnosides of **A.1**-**A.3** as well as digitoxigenin were found to significantly reduce the LPS-induced inflammation with the synthetic analog *anhydro*-ouabagenin 3-(a)-*L*-rhamnoside (**A.20**) exhibiting the most significant effect. At the same time, the aglycone of **A.20**, *anhydro*-ouabagenin (**A.2**) significantly enhanced the inflammation levels.

The Nagorny group has long-standing interests in streamlining the medicinal chemistry exploration of cardiotonic steroids by developing new strategies for the aglycone synthesis and their selective glycosylation.[29-32] Previously we described strategies for the installation of native (a)-*L*-rhamnoside moiety at the C3-position of various cardiotonic steroids.[33-35] It was observed that cardiotonic steroids such as **A.5** containing C3 and C19 oxidation undergo competitive C19 glycosylation that produces a complex mixture of products such as **A.7** and **A.8** (Appendix Figure A.1B).[33] While this challenge could be overcome by selective introduction of a C19-protecting group such as methoxyacetate[33] or *para*-bromobenzoate this may require significant protecting group optimization and might be problematic for the substrates that have additional hydroxyl groups such as **A.1**–**A.3** (Appendix Figure A.1).[36-38]

A.2 Regioselective synthesis of strophanthidol, anhydro-ouabagenin, and ouabagenin

In the context of their studies focused on regioselective glycosylation of 6-deoxyerythronolide B,[39] the Nagorny group utilized boronic acid esters as the traceless protecting groups.[40-43] *In situ* protection of the 1,3-diol moiety of 2-deoxyerythronolide B (6-dEB) was followed by the addition of glycosyl trichloroacetimidate and TMSOTf as the promoter to accomplish selective glycosylation. The basic reaction work up was used to remove

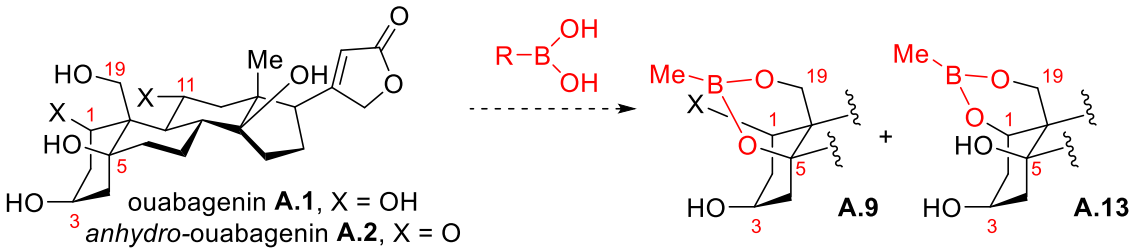
the boronic acid and produce the desired glycoside as the single regioisomer. This concept could be applied to highly oxidized cardiotonic steroids **A.1–A.3** containing 1,3,5-hydroxyl groups (Appendix Scheme A.1).[34]



Appendix Scheme A.1: Traceless boronic acid protecting group for the selective protection of the C19 position of cardiotonic steroids

Unlike the previous glycosylation developed for 6-dEB, the presence of multiple hydroxyl groups may lead to several regioisomeric protection products in addition to the desired boronic acid. ester **A.9**. This would lead to multiple regioisomeric glycosylation products in addition to **A.9**. Assuming that boronic acid formation is a reversible process and the most thermodynamically stable boronate is formed under the protection conditions, the regioselectivity of boronic acid ester formation could be assessed computationally. The results of these computations (DFT, B3LYP, 6-31+G*) are summarized in Appendix Table A.1.

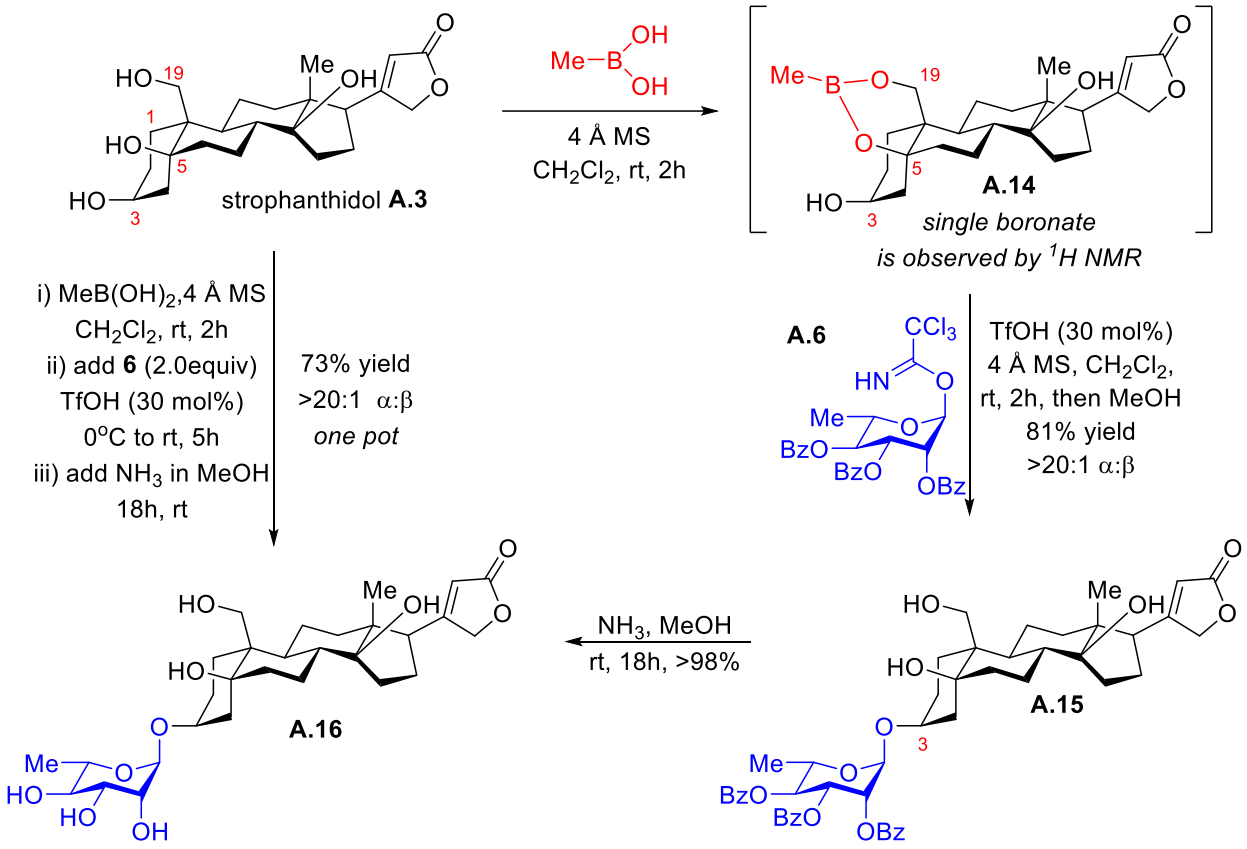
Appendix Table A.1: Computed relative stabilities of methyl boronic acid esters derived from steroids 1–3 (DFT, B3LYP, 6-31+G*)



scaffold	relative energy for the regioisomeric boronates (DFR, B3LYP, 6-31+G*) (kcal/mol)							
	C1/C3	C1/C5	C1/C11	C1/C19	C3/C5	C3/C19	C5/C19	C11/C19
A.1[a]	+8.3	+8.9	+7.6	0	+7.8	+18.3	+2.3	+7.6
A.2[b]	-	-	-	-	+1.9	+22.2	0	-
A.3[c]	-	-	-	-	+1.7	+17.2	0	-

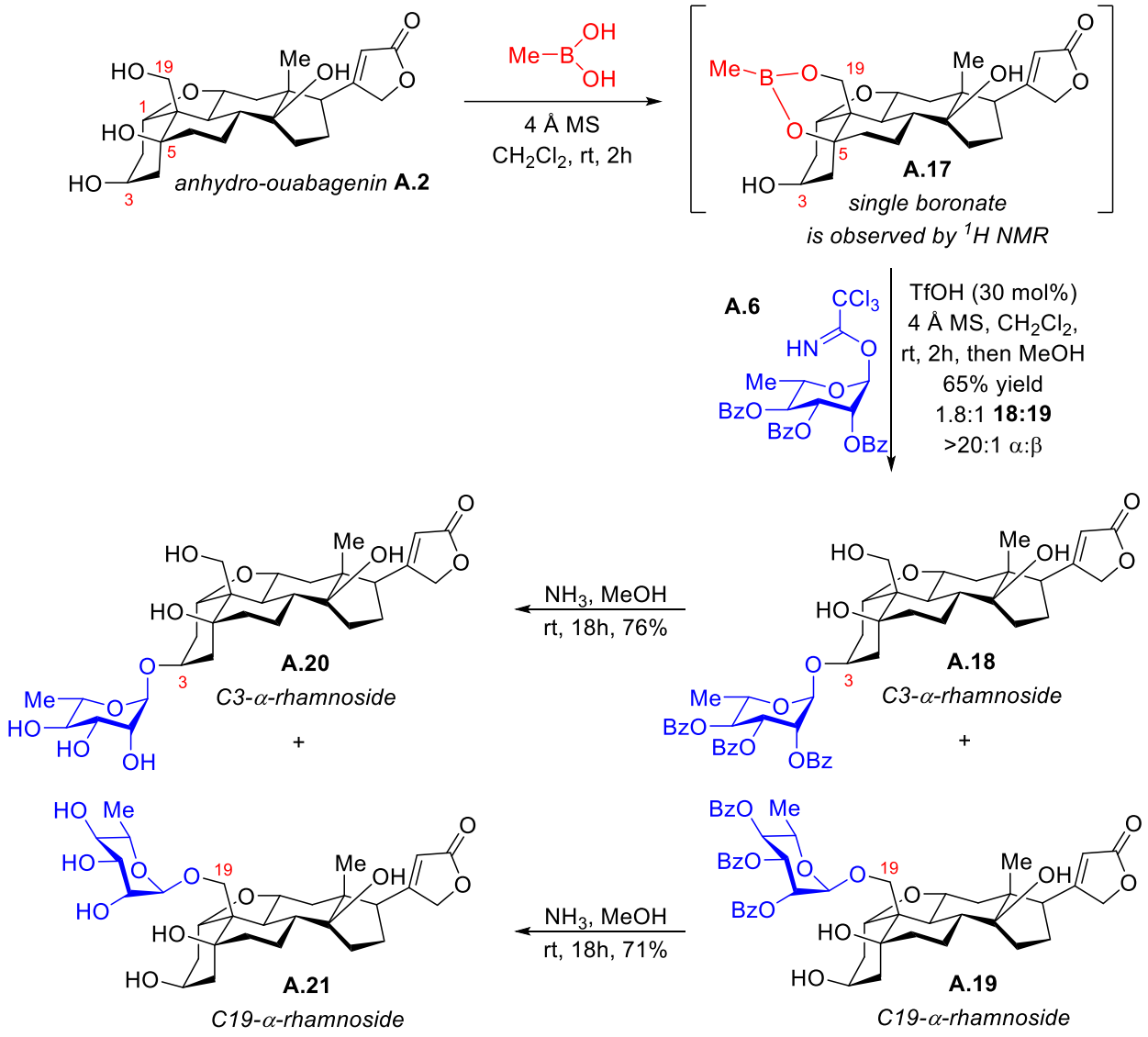
[a]Referenced to the energy of cyclic C3/C5 boronate derived of **1**. [b]Referenced to the energy of cyclic C5/C19 boronate of **2**. [c]Referenced to the energy of cyclic C5/C19 boronate derived from **3**.

Ouabagenin **A.1** contains 5 hydroxyl groups that may participate in boronic acid ester formation and may form 8 potential products. The C1/C19 boronic acid ester **A.13** was found to have the lowest energy with 2.3 kcal/mol higher stability than the second most stable C5/C19 boronate **A.9**. Only 3 cyclic boronates are possible in the case of *anhydro*-ouabagenin **A.2** and strophanthidol **A.3**. In both cases, the most stable ester is formed by the complexation of the C5/C19 sites, and the formation of the second most stable C3/C5 boronate would be disfavored by 1.9 kcal/mol **A.2** or 1.7 kcal/mol **A.1**. The results in Appendix Table A.1 suggest that the reaction of methyl boronic acid with **A.2** and **A.3** should lead to clean protection of the C5 and C19 positions and only the C3 alcohols would be available to react. At the same time, the reaction of ouabagenin will result in a selective protection of the C1 and C19 alcohols, and the C3 and C11 alcohols can be potentially glycosylated. Indeed, when strophanthidol **A.3** was treated with methyl boronic acid in the presence of 4Å MS, exclusive formation of boronate **A.14** was observed by NMR (Appendix Scheme A.2).



Appendix Scheme A.2: C3-selective (α)-L-rhamnosylation of strophanthidol **A.3**

The reaction of **A.14** with trichloroacetimidate **A.6** required optimization.[34] Under the optimized conditions, that included using two equivalents of **A.6**, activation with triflic acid (30 mol%), 4 Å MS at 0 ºC to room temperature resulted in the efficient formation of the glycosylated product. The subsequent removal of the boronic acid ester with methanol resulted in 81% yield of the desired a-product **A.15**. The benzoyl protecting groups present on the rhamnose moiety of **A.15** were selectively removed with saturated solution of ammonia in methanol (18 hours) to provide the desired deprotection product in the quantitative yield. This procedure was subsequently optimized to be performed as a one-pot telescoped operation to provide **α-A.16** directly from **A.3** in 73% overall yield.

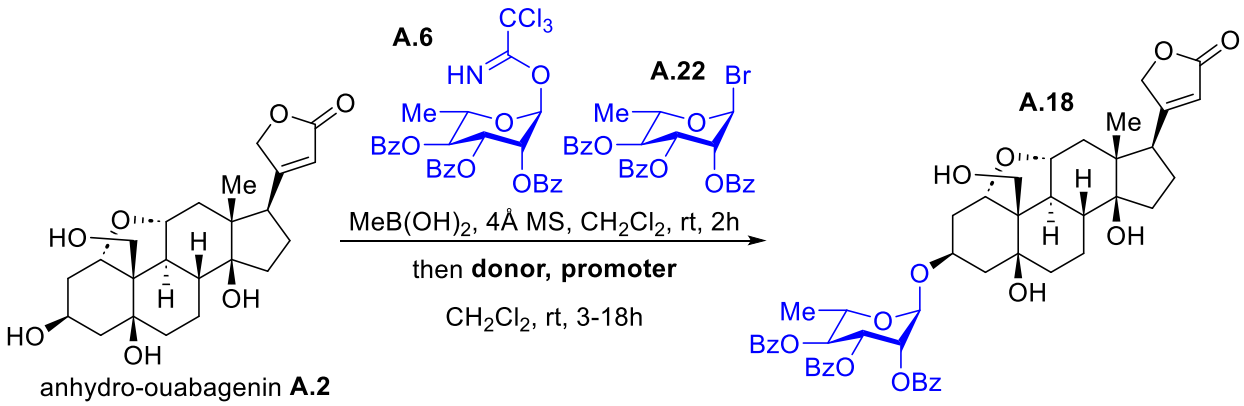


Appendix Scheme A.3: Initial studies on C3-selective (a)-*L*-rhamnosylation of anhydro-ouabagenin **A.2**

Our subsequent studies focused on investigating the C3-selective (a)-*L*-rhamnosylation of *anhydro*-ouabagenin (**A.2**) (Appendix Scheme A.3). *Anhydro*-ouabagenin (**A.2**) is a known degradation product of ouabain.[44-46] While this compound carries all the major structural features present in ouabagenin **A.1** and strophanthidol **A.3**, the glycosylated variants of these compound have not been previously synthesized and evaluated. As in the case of **A.3**, computational studies (Appendix Table A.1), predicted selective formation of the C5/C19 boronate. Indeed, upon exposure to methylboronic acid, single boronate **A.17** was observed by ^{1}H NMR. However,

subjecting **A.17** to reaction with **A.6** under previously developed conditions resulted in 1.8:1 mixture of the C3- and C19-glycosylated products **A.18** and **A.19** in 65% yield. Both **A.18** and **A.19** were separated and subsequently deprotected to provide regioisomeric glycosides **A.20** and **A.21**.

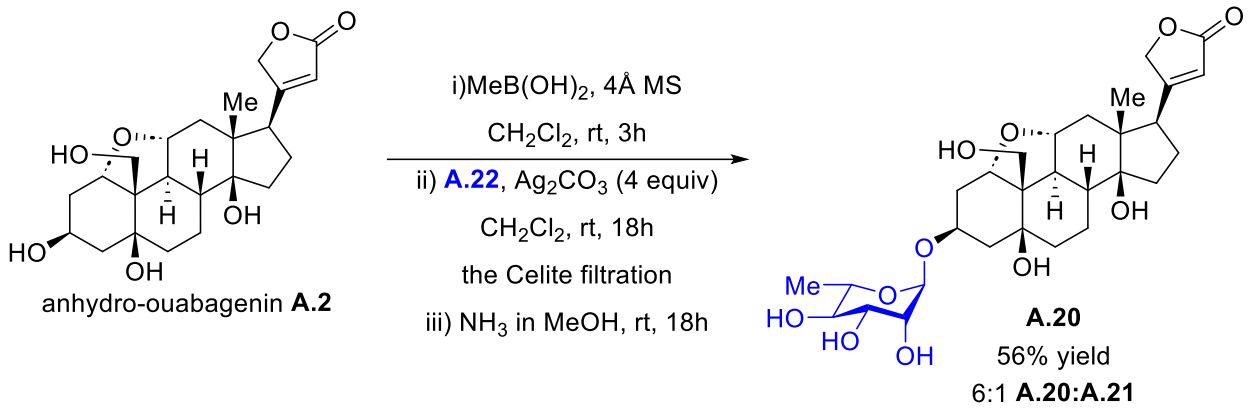
Appendix Table A.2 Optimization of regioselective rhamnosylation of anhydro-ouabagenin



entry	donor	promoter	r.r. **A.18:A.19**	yield **A.18+A.19**
1	**A.6**	TfOH	1.8:1	65%
2	**A.22**	$AgBF_4$	-	-
3	**A.22**	AgOTf	-	-
4	**A.22**	AgOTf, DTBP	1.8:1	49%
5	**A.22**	Ag_2CO_3	7.5:1	69%

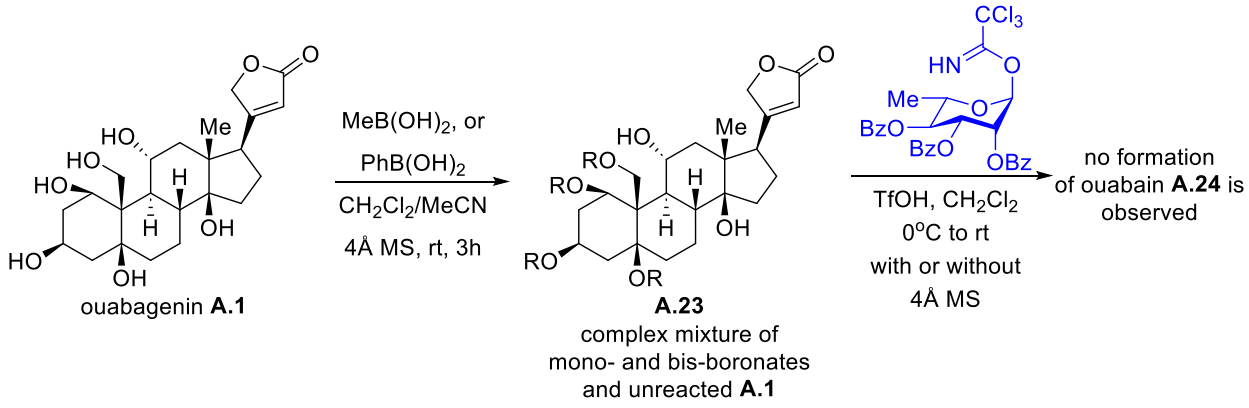
The eroded selectivity could be attributed to *in situ* boronate isomerization under the acidic conditions, which is more favored for the conformationally restricted **A.2**. To avoid the isomerization of **A.17**, a base promoted glycosylation was investigated (Appendix Table A.2 Optimization of regioselective rhamnosylation of anhydro-ouabagenin). The boronate **A.17** was formed from **A.2** by the established conditions. Glycosylation of **A.17** boronate with glycosyl bromide donor **A.22** and $AgBF_4$ (entry 2) ang AgOTf (entry 3) failed to provide any of the desired glycosylation product. To neutralize the triflic acid generated during the reaction with AgOTf, di-*tert*-butyl pyridine (DTBP) was added as an acid scavenger (entry 4), this tactic led to the formation of α-glycosides **A.18** and **A.19** as a 1.8:1 mixture of regioisomers. Turing to a

more basic counterion for the silver(I) salt, the reaction with Ag_2CO_3 provided α-glycosides **A.18** and **A.19** as a 7.5:1 mixture of regioisomers. With an optimal promoter for the regioselective glycosylation in hand, we carried out the process as a one pot procedure (Appendix Scheme A.4).



Appendix Scheme A.4: One-pot regioselective glycosylation of anhydro-ouabagenin **A.2**

Cyclic boronate **A.17** was formed *in situ* and the resultant crude reaction mixture was subjected to glycosylation with glycosyl bromide **A.22** in the presence of silver carbonate. The resultant mixture was filtered through celite to remove excess of Ag(I) salts and treated with ammonia in methanol to provide 6:1 mixture of **20** and **21** in 56% yield (Appendix Scheme A.4).



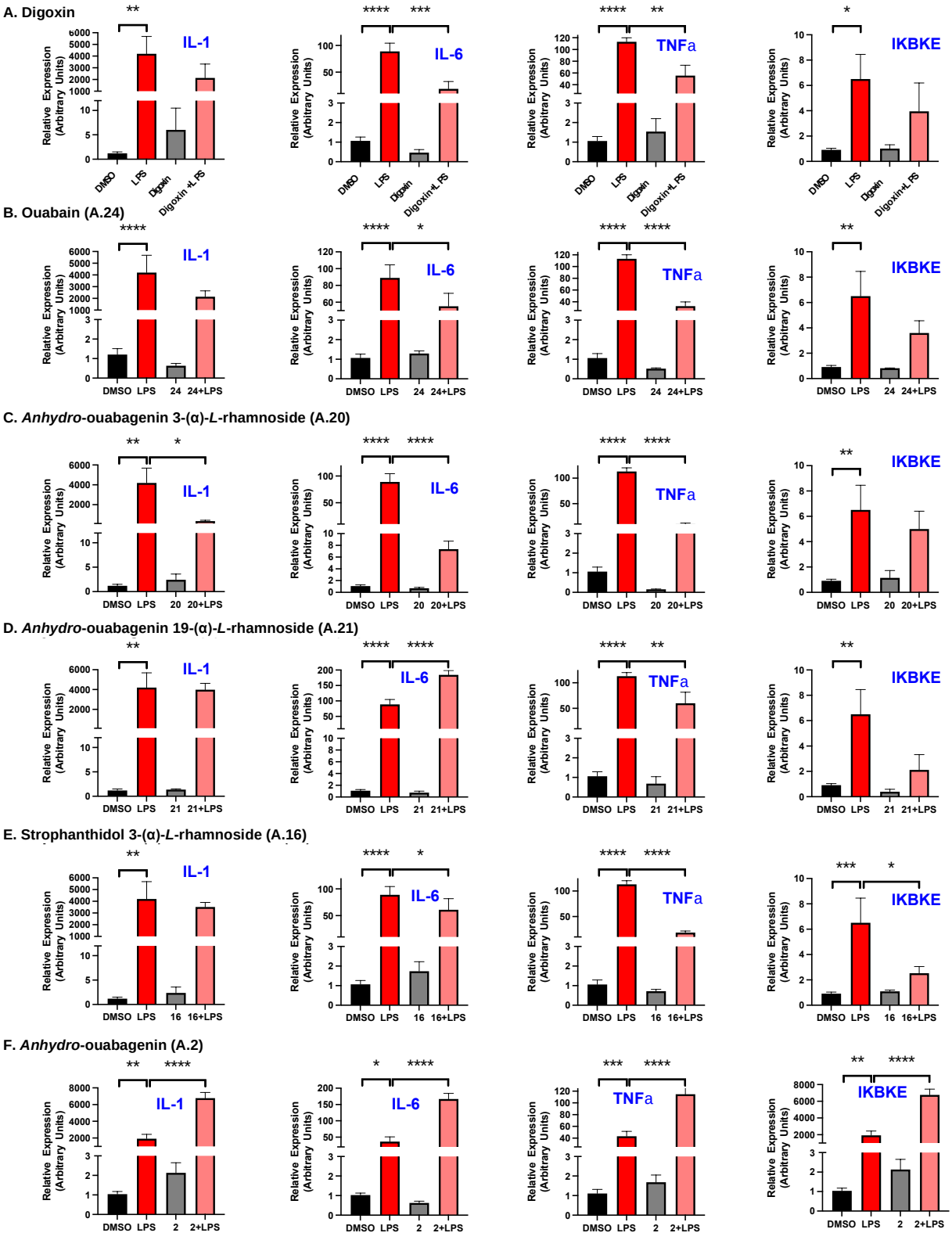
Appendix Scheme A.5: Attempts to accomplish the C3-selective glycosylation of ouabagenin **A.1**

Unlike **A.2** and **A.3**, ouabagenin **A.1** is expected to form a C1/C19 boronate (*cf.* Appendix Table A.1). However, low solubility of **A.1** in dichloromethane prevented this reaction

(Appendix Scheme A.5). The addition of acetonitrile as a co-solvent seemed to aid the formation of boronic acid esters; however, complexation with either methyl or phenyl boronic acids resulted in the formation of multiple *mono*- and *bis*-protected esters. Subjecting these mixtures to the acid-catalyzed glycosylation with **A.6** did not lead to the formation of ouabain **A.24**, and multiple decomposition products were isolated along with unreacted **A.1**.

A.3 Biological evaluation of anti-inflammatory activity

With the access to the synthetic aglycones **A.2** and **A.3**, and their (a)-*L*-rhamnosides **A.16**, **A.20** and **A.21**, our subsequent studies focused on exploring neuroprotective properties of these derivatives along with natural cardenolides digoxin and ouabain (Appendix Figure A.2).



Appendix Figure A.2: Evaluation of anti-inflammatory activity of 200 nM solutions of digoxin and prepared compounds **A.2**, **A.16**, **A.20**, **A.21**, **A.24.**

(A) Digoxin; (B) ouabain (**A.1**); (C) *anhydro*-ouabagenin-3-(α)-*L*-rhamnoside (**A.20**); (D) *anhydro*-ouabagenin-19-(α)-*L*-rhamnoside (**A.21**); (E) strophanthidol-3-(α)-*L*-rhamnoside (**A.16**); and (F) *anhydro*-ouabagenin (**A.2**) during 24 hours in the primary glial cell culture. The inflammatory gene expression of IL-1, IL-6, TNFα, and IKBKE was stimulated using LPS (250 ng/ml), and DMSO was used as a negative control. Data were expressed as the mean ± SEM and analyzed by two-way ANOVA followed by Newman-Keuls post hoc analysis. (*$p < 0.05$; **$p < 0.01$; ***$p < 0.001$; ****$p < 0.0001$).

A primary glial culture extracted from the whole brain was used to assess the potential neuroprotective properties of cardiotonic steroids. The whole brain from 1-2 day-old C57BL/6J mice neonatal mice was collected, without the meninges, placed in HBSS modified medium without calcium or magnesium (Gibco 14190144), and processed following the standard protocol to separate the oligodendrocytes and neurons from the glial cell culture. The primary glial cells were grown in 24-well plates as described above and were treated with 200 nM solution of cardiotonic steroids and stimulated with LPS (250 ng/mL), known to stimulate inflammatory cytokines gene expression in microglia cells, which was used as a positive control. DMSO was used as a negative control. The cells were harvested in Trizol and processed for the total RNA isolation. The IL-1, IL-6, TNF-α, and IKBKE gene expression were determined using qPCR. The fold change of mRNA in the unknown sample relative to the control group was determined by 2-ΔΔCT, group following a known procedure. Data are shown as mRNA expression levels relative to the DMSO control treatment.

The results of these experiments are depicted in Appendix Figure A.2. In all the described cases, administration of LPS has elicited strong inflammation that manifested itself in significant production of IL-1, IL-6, TNF-α as well as IKBKE markers relative to the control experiment with DMSO. In contrast, the treatment of the microglia cells with buffered solutions of digoxin, and compounds **A.2**, **A.16**, **A.20**, **A.21**, and **A.24** did not result in significant inflammation levels. When microglia cells were co-treated with LPS and 200 nM solutions of strophanthidol-3-(α)-*L*-rhamnoside **A.16**, ouabain **A.24,** *anhydro*-ouabain **A.20** and digoxin, a

significant reduction in the expression of all four inflammation genes was observed with *anhydro*-ouabain **A.20** demonstrating the strongest effect. In contrast, the use of the unnatural C19-glycoside **A.21**, did not result in a significant reduction of IL-1 and surprisingly enhanced the expression of IL-6. At the same time, reduced production of TNFα as well as IKBKE markers was noted for **A.21**. Finally, the co-administration of unglycosylated *anhydro*-ouabagenin **A.2** led to significant inflammation enhancement, and all four genes were expressed at significantly higher levels than when microglia were treated with LPS alone.

The results above suggest that the structural features such as the presence of glycosylation, its position, and the oxidation patterns present in cardiotonic steroid may play a significant impact on the ability of cardenolides to reduce neuroinflammation in microglia cells. The lack of the C3-glycosylation may play a dramatic role as the unglycosylated *anhydro*-ouabagenin **A.2** was found to enhance rather than reduce neuroinflammation. Similarly, moving the glycosylation site from the C3- position in compound **A.20** to the C19-position in **A.21** resulted in a significantly enhanced production of the IL-1, IL-6 and TNFα cytokines. Finally, the oxidation state of the steroidal skeleton was found to have an impact on the overall anti-inflammatory activity of the C3-glycosylated cardenolides as evidenced by comparing **A.16**, **A.20**, and **A.24**. Ouabain **A.24** contains hydroxyl groups at the C1/C11 positions while the strophanthidol skeleton of **A.16** lacks these hydroxyl groups. The unnatural glycoside **A.20** represents a hybrid of these two structures, and it features a C1/C11 ether bridge that gives rigidity to otherwise conformationally flexible A/B ring system of cardenolides. The direct comparison of the glycosylated strophanthidol derivative **A.16**, *anhydro*-ouabagenin derivative **A.20**, and ouabain **A.24**) indicates that **A.20** has the highest levels of *anti*-inflammatory activity across all four inflammation markers. It also seems that the lack of the C1/C11 oxidation in **A.16**

enhances the expression of the IL-1 and IL-6 genes but does not impact the expression of the TNFα and IKBKE, which suggests that there are several different inflammation pathways that may get impacted by cardenolides.

A.4 Conclusions

In summary, we developed a direct strategy for achieving C3-(α)-L-rhamnosylation of common polyhydroxylated cardenolide aglycones **A.1–A.3** containing a primary C19-hydroxyl group. Based on the computational predictions suggesting that the reaction of **A.1–A.3** with boronic acids would favor the formation of the cyclic C5/C19 or C1/C19 esters, we have developed one pot glycosylation protocols that directly lead to strophanthidol-3-(α)-*L*-rhamnoside **A.16**, and unnatural steroid *anhydro*-ouabagenin-3-(α)-*L*-rhamnoside **A.20**. Despite the promising computational predictions, the attempts to achieve selective glycosylation of ouabagenin **A.1** failed due to its low solubility in organic solvents coupled with the propensity to form *bis*-boronates.

The potential of 200 nM solutions of synthetic C3-(a)-*L*-rhamnosides **A.16** and **A.20**, C19-(a)-*L*-rhamnoside **A.21**, *anhydro*-ouabagenin **A.2**, ouabain **A.24** and digoxin to reduce LPS-induced neuroinflammation was subsequently investigated using primary murine glial cells. While the C3-glycosylated steroids reduced the expression of inflammatory IL-1, IL-6, TNFα and IKBKE, the co-administration of unnatural C19-glycoside **A.21** or aglycone **A.2** resulted in enhanced inflammation. In addition to glycosylation, the oxidation of the cardenolide skeleton was found to play a significant role in determining the extent of the *anti*-inflammatory activity exhibited by the steroids. Surprisingly, the previously unexplored unnatural *anhydro*-ouabagenin-3-(a)-*L*-rhamnoside **A.20** was found to exhibit the highest levels of *anti*-inflammatory activity. Further exploration of *anhydro*-ouabagenin glycosides and related

synthetic derivatives of ouabain may lead to the analogs with enhanced *anti*-inflammatory properties and is currently the subject of ongoing studies in our laboratories

A.5 Experimental

General Methods

All reagents and solvents were purchased from commercial sources and were used as received without further purification unless otherwise specified. CH_2Cl_2 and PhME were purified by Innovative Technology's Pure-Solve System using basic alumina. 4Å molecular sieves were activated prior to use by heating under reduced pressure. Cooling was achieved by use of Cryocool machine or ice bath. Heating was achieved by use of a silicone oil bath with heating controlled by an electronic contact thermometer. Deionized water was used in the preparation of all aqueous solutions and for all aqueous extractions. Solvents used for extraction and chromatography were ACS or HPLC grade. Purification of reactions mixtures was performed by flash chromatography using SiliCycle SiliaFlash P60 (230-400 mesh). Yields indicate the isolated yield of the title compound with ≥95% purity as determined by ^{1}H NMR analysis. Diastereomeric ratios were determined by ^{1}H NMR or ^{13}C NMR analysis; the α-diastereomer was assigned to J^{C-H} of approximately 170Hz, and the β-diastereomer was assigned to J^{C-H} of approximately 160Hz. Structural assignments were made with additional information from gHMBC experiments. Compounds tested *in vitro* were 95% pure by HPLC.

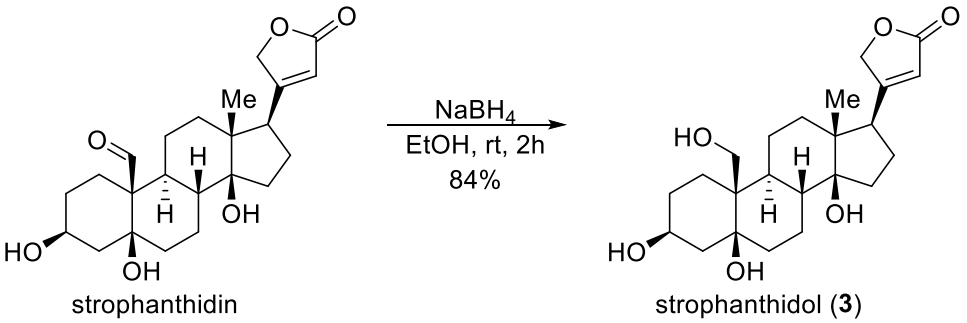
^{1}H NMR spectra were recorded on Varian vnmrs 700 (700 MHz), Varian vnmrs 500 (500 MHz), Varian INOVA 500 (500 MHz), Varian MR400 (400 MHz), Bruker Avance Neo 500 (500 MHz) spectrometers and chemical shifts (δ) are reported in parts per million (ppm) with solvent resonance as the internal standard ($CDCl_3$ at δ 7.26, CD_3OD at δ 3.31, C_6D_6 at δ 7.16). Data are reported as (br = broad, s = singlet, d = doublet, t = triplet, q = quartet, m = multiplet; coupling

constant(s) in Hz; integration). Proton-decoupled 13C NMR spectra were recorded on Varian vnmrs 700 (700 MHz), Varian vnmrs 500 (500 MHz), Varian INOVA 500 (500 MHz) or Varian MR400 (400 MHz) spectrometers and chemical shifts (δ) are reported in ppm with solvent resonance as the internal standard (CDCl3 at δ 77.16, CD3OD at 49.0, C6D6 at 128.06). High resolution mass spectra (HRMS) were recorded on Agilent 6230 TOF or VG (Micromass) 70-250-S Magnetic sector mass spectrometers in the University of Michigan mass spectrometry laboratory. Infrared (FTIR) spectra were recorded as thin film on a Perkin Elmer Spectrum BX FT-IR spectrometer. Absorption peaks were reported in wavenumbers (cm^{-1}). Optical rotations were measured in a solvent of choice on a JASCO P-2000 or Autopol III digital polarimeter at 589 nm (D-line). High performance liquid chromatography (HPLC) chromatograms were obtained on Shimadzu HPLC system at 233nm via a photodiode array detector.

Preparation of previously reported compounds

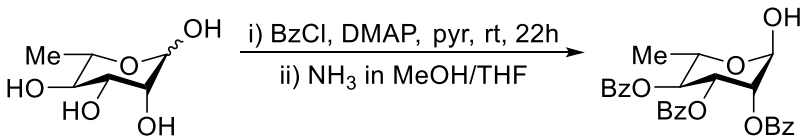
Compounds **A.1**,[31,47] **A.5**,[33] **A.7**,[33] and **A.8**[33] were prepared according to the previously reported procedures. Compounds **A.2**, **A.14-A.21** were prepared by Dr. Tay Rosenthal and the characterization data of these compounds were reported in his dissertation.[48] The spectra of the prepared compounds matched the reported spectra data.

Preparation of new compounds.



Strophanthidol A.3: $NaBH_4$ (95 mg, 2.48 mmol, 2.0 eq) was added to a stirred solution of strophanthidin (500 mg, 1.24 mmol, 1.0 eq) in EtOH (8.3 mL) at room temperature. The reaction

was stirred for two hours at room temperature. The reaction was diluted with sat. aq. NH_4Cl (50 mL) and EtOAc (50 mL) and was stirred for an additional 18 hours. The layers were separated, and the organic layer was concentrated *in vacuo*. The crude residue was purified by flash column chromatography (5-10% MeOH/CH_2Cl_2) to afford strophanthidol **3** (423 mg, 84%) as a white solid. **HRMS** [ESI-TOF] (m/z): $[M+Na]^+$ calcd. for $C_{23}H_{34}O_6$, 429.2247; found, 429.2248. **^{1}H NMR** (700 MHz, $CDCl_3$): δ 5.87 (s, 1H), 5.75 (s, 1H), 4.97 (d, *J* = 18.2 Hz, 1H), 4.80 (d, *J* = 17.9 Hz, 1H), 4.70 (d, *J* = 7.5 Hz, 1H), 4.37 (d, *J* = 11.2 Hz, 1H), 4.20 (d, *J* = 4.1 Hz, 1H), 4.07 (d, *J* = 4.6 Hz, 1H), 3.47 (dd, *J* = 11.4, 7.5 Hz, 1H), 2.76 (dd, *J* = 9.8, 5.5 Hz, 1H), 2.55 (td, *J* = 14.7, 4.1 Hz, 1H), 2.15 (dt, *J* = 13.6, 10.0 Hz, 1H), 2.09 (dd, *J* = 15.0, 3.1 Hz, 1H), 2.05 – 1.98 (m, 1H), 1.97 – 1.91 (m, 3H), 1.86 (dtd, *J* = 14.4, 9.3, 5.4 Hz, 1H), 1.79 – 1.63 (m, 4H), 1.64 – 1.45 (m, 5H), 1.41 – 1.31 (m, 2H), 1.25 – 1.17 (m, 2H), 0.85 (s, 3H). **^{13}C{^{1}H}** NMR (176 MHz, $CDCl_3$): δ 174.8, 174.7, 117.9, 85.5, 78.2, 73.7, 67.9, 65.7, 50.7, 49.6, 42.3, 40.6, 40.2, 39.0, 36.9, 35.5, 32.7, 27.7, 26.9, 24.0, 21.4, 19.2, 15.9. **FTIR** (thin film, cm^{-1}): 3323, 2939, 1779, 1731, 1619, 1450, 1025. **$[\alpha]_D^{20}$:** +30.6 (c = 1.0 in $CHCl_3$).

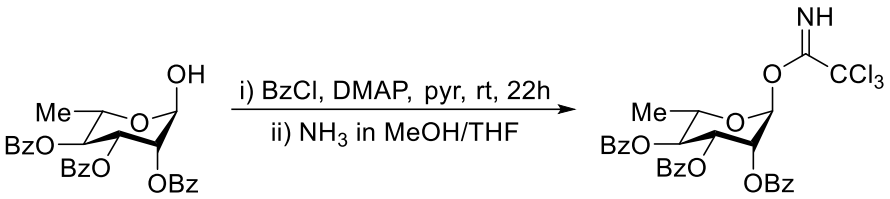


A.6a **A.6b**

Glycosyl hemiacetal A.6b: Benzoyl chloride (3.54 mL, 30 mmol, 5.0 eq) was added slowly to a stirred solution of L-rhamnose **A.6a** (1.0 g, 6.0 mmol, 1.0 eq) and DMAP (0.30 g, 2.4 mmol, 0.4 eq) in pyridine (30 mL, 0.2 M). The reaction was stirred at room temperature for 15 hours, then was quenched by addition of cold H_2O (100 mL), and extracted with EtOAc (3x100 mL). The combined organics were washed with cold 1N aq. HCl (3x75 mL), sat. aq. $NaHCO_3$ (100 mL), and

sat. aq. NaCl (75 mL) then dried over Na_2SO_4 and concentrated *in vacuo*. The crude residue was used in the next step without further purification.

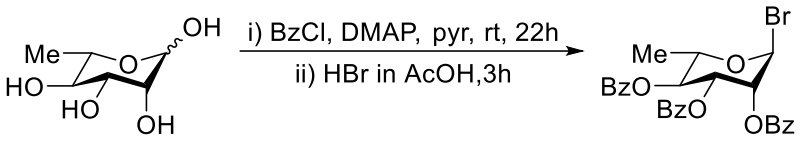
The crude residue from above was dissolved in MeOH:THF (15 mL :35 mL) and NH_3 gas was bubbled through the solution for 20 minutes at 0°C. The reaction was sealed and slowly warmed to room temperature while stirring over 21 hours. NH_3 gas was bubbled through the reaction mixture for an additional 20 minutes, and stirred at room temperature for three hours. The crude reaction mixture was concentrated under reduced pressure and purified by flash column chromatography (30% EtOAc/hexanes) to afford **A.6b** (1.6 g, 56%) as a white solid. The product was confirmed by comparing with reported spectra.[49] **^{1}H NMR** (600 MHz, $CDCl_3$) δ 8.11 (dd, J = 8.0, 1.4 Hz, 2H), 8.00 – 7.92 (m, 2H), 7.85 – 7.77 (m, 2H), 7.64 – 7.58 (m, 1H), 7.51 (dt, J = 14.0, 7.6 Hz, 3H), 7.43 – 7.36 (m, 3H), 7.26 (t, J = 7.3 Hz, 2H), 5.92 (dd, J = 10.1, 3.4 Hz, 1H), 5.72 – 5.66 (m, 2H), 5.46 (s, 1H), 4.45 (dq, J = 9.8, 6.3 Hz, 1H), 1.37 (d, J = 6.2 Hz, 3H).



A.6b **A.6**

Glycosyl trichloroacetimidate donor A.6: CCl_3CN (1.8 mL, 18 mmol, 30 eq) was added dropwise to a solution of **A.6b** (28 0mg, 0.59 mmol, 1.0 eq) and DBU (0.030 mL, 0.18 mmol, 0.3 eq) in CH_2Cl_2 (5 mL) at 0°C. The reaction was warmed to rt and stirred for 18 hours. The reaction mixture was concentrated, and the crude mixture was purified by flash column chromatography (15% EtOAc/hexanes + 2% Et_3N) to afford **A.6** (300 mg, 82% yield) as a white solid. The product was confirmed by comparing to reported spectra.[37] **^{1}H NMR** (500 MHz, $CDCl_3$) δ 8.82 (s, 1H), 8.13 – 8.09 (m, 2H), 8.01 – 7.95 (m, 2H), 7.82 (dd, J = 8.4, 1.4 Hz, 2H), 7.66 – 7.61 (m, 1H), 7.57 – 7.49 (m, 3H), 7.46 – 7.36 (m, 3H), 7.28 (t, J = 7.8 Hz, 2H), 6.49 (d, J = 1.6 Hz, 1H), 5.99 – 5.85

(m, 2H), 5.77 (ddd, J = 11.4, 9.7, 1.5 Hz, 1H), 4.40 (dq, J = 9.9, 6.2 Hz, 1H), 1.42 (d, J = 6.2 Hz, 3H).



A.6a **A.22**

Glycosyl bromide donor A.22: Benzoyl chloride (2.0 mL, 14 mmol, 6.0 eq) was added slowly to a stirred solution of L-rhamnose monohydrate **A.6a** (0.50 g, 2.7 mmol, 1.0 eq) and DMAP (0.13 g, 1.1 mmol, 0.4 eq) in pyridine (14 mL, 0.2 M). The reaction was stirred at room temperature for 22 hours, then was quenched by addition of H_2O (30 mL), and extracted with EtOAc (3x30 mL). The combined organics were washed with cold 1N aq. HCl (3x30 mL), sat. aq. $NaHCO_3$ (30 mL), and sat. aq. NaCl (30 mL) then dried over Na_2SO_4 and concentrated *in vacuo*. The crude residue was used in the next step without further purification.

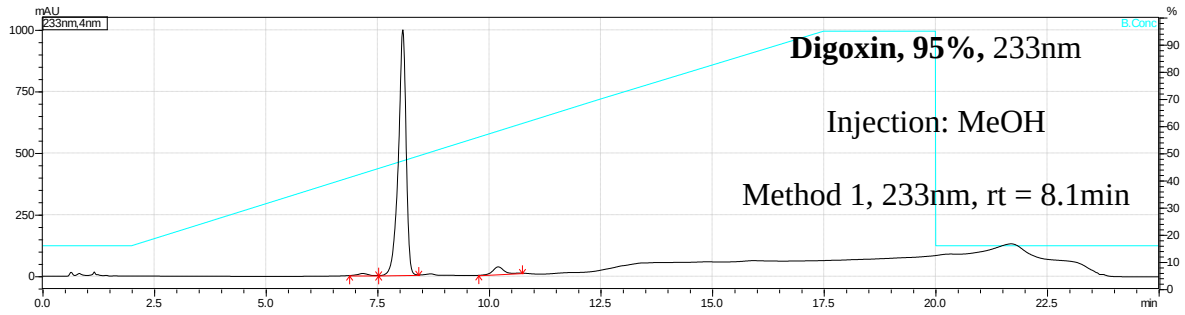
The crude residue from above was dissolved in CH_2Cl_2 (9.0 mL), and 33% HBr in AcOH (2.0 mL) was added dropwise at room temperature. The reaction was stirred at room temperature for three hours, then was quench by the slow addition of sat. aq. $NaHCO_3$ (50 mL). The layers were separated, and the organic layer was washed with sat. aq. $NaHCO_3$ (2x50 mL) and brine (50mL) then were dried over Na_2SO_4 and concentrated *in vacuo*. The crude residue was purified by flash column chromatography (5-10% EtOAc/hexanes) to afford **A.22** (0.82g, 55%) as a white solid. The product was confirmed by comparing with reported spectra.[37] **^{1}H NMR** (500 MHz, $CDCl_3$) δ 8.10 – 8.03 (m, 2H), 8.03 – 7.96 (m, 2H), 7.88 – 7.79 (m, 2H), 7.69 – 7.60 (m, 1H), 7.55 – 7.49 (m, 3H), 7.42 (dt, *J* = 13.3, 7.8 Hz, 3H), 7.28 (d, *J* = 7.6 Hz, 2H), 6.55 (d, *J* = 1.6 Hz, 1H), 6.19 (dd, *J* = 10.2, 3.4 Hz, 1H), 5.87 (dd, *J* = 3.6, 1.6 Hz, 1H), 5.77 (t, *J* = 10.1 Hz, 1H), 4.43 (dq, *J* = 9.8, 6.3 Hz, 1H), 1.43 (d, *J* = 6.2 Hz, 3H).

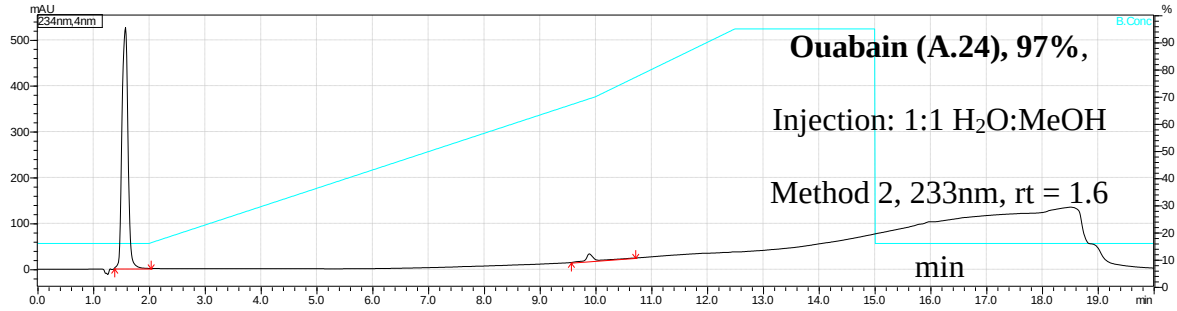
HPLC data for compounds tested *in vitro*

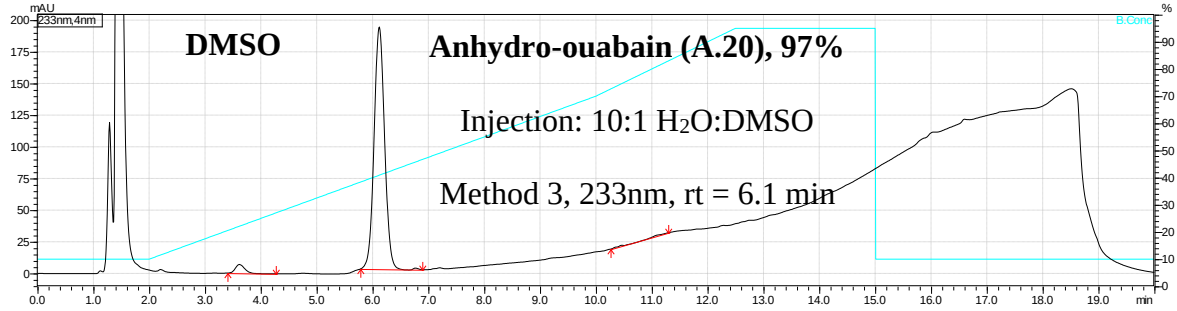
HPLC Method 1: Instrument: Shimadzu HPLC, photodiode array detector; Column: NovaPack C18, 3.9x150mm, Part No. WAT086344. 20 minute run time: 0 to 2min, 16% solvent B:solvent A, 2 to 17.5min 16 → 95% solvent B:solvent A, 17.5 to 20min 95% solvent B:solvent A, then 5 minute wash 16% solvent B:solvent A; Solvents: solvent A: 0.1% CF_3CO_2H in water (v/v), solvent B: 0.1% CF_3CO_2H in acetonitrile; Injection volume 20µL; UV detection array 190-800nm; flow rate: 1.0mL/min. rt = retention time.

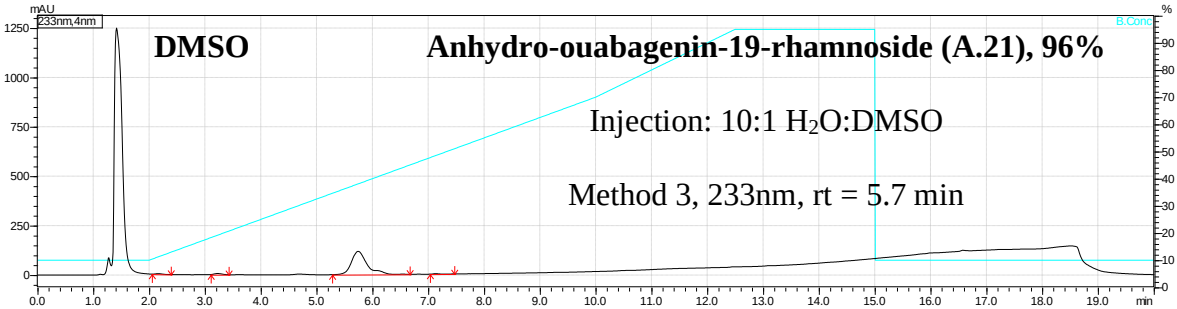
HPLC Method 2: Instrument: Shimadzu HPLC, photodiode array detector; Column: NovaPack C18, 3.9x150mm, Part No. WAT086344. 15 minute run time: 0 to 2min, 16% solvent B:solvent A, 2 to 10 min 16 → 70% solvent B:solvent A, 10 to 12.5min 70 → 95% solvent B:solvent A, 12.5 to 15 min. then 5 minute wash 16% solvent B:solvent A; Solvents: solvent A: 0.1% CF_3CO_2H in water (v/v), solvent B: 0.1% CF_3CO_2H in acetonitrile; Injection volume 20µL; UV detection array 190-800nm; flow rate: 1.0mL/min. rt = retention time.

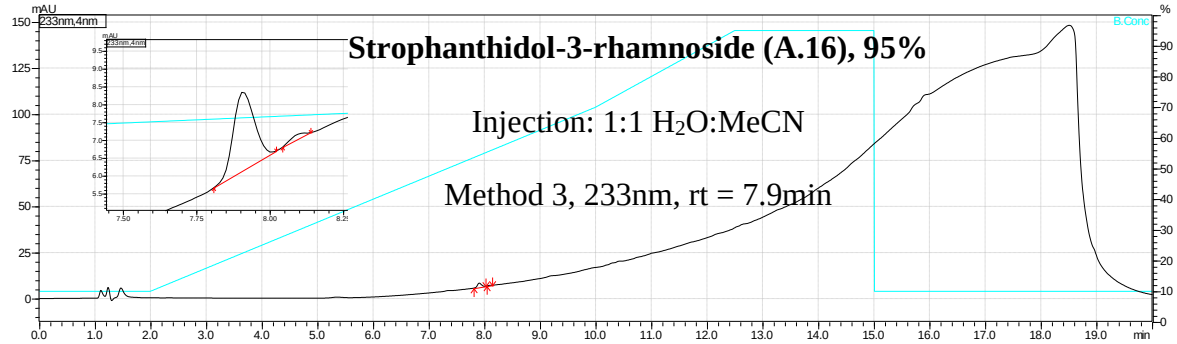
HPLC Method 3: Instrument: Shimadzu HPLC, photodiode array detector; Column: NovaPack C18, 3.9x150mm, Part No. WAT086344. 15 minute run time: 0 to 2min, 10% solvent B:solvent A, 2 to 10 min 10 → 70% solvent B:solvent A, 10 to 12.5min 70 → 95% solvent B:solvent A, 12.5 to 15 min. then 5 minute wash 10% solvent B:solvent A; Solvents: solvent A: 0.1% CF_3CO_2H in water (v/v), solvent B: 0.1% CF_3CO_2H in acetonitrile; Injection volume 20µL; UV detection array 190-800nm; flow rate: 1.0mL/min; rt = retention time.

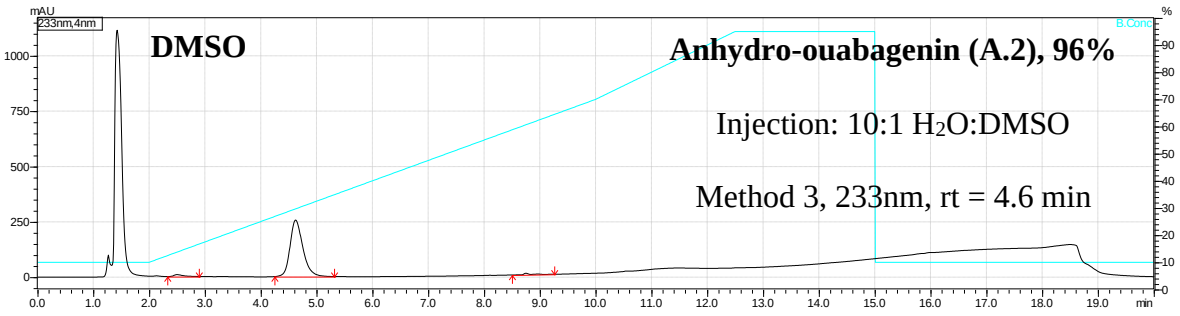



Ouabain (A.24), 97%,
Injection: 1:1 H_2O:MeOH
Method 2, 233nm, rt = 1.6 min


DMSO
Anhydro-ouabain (A.20), 97%
Injection: 10:1 H_2O:DMSO
Method 3, 233nm, rt = 6.1 min


DMSO
Anhydro-ouabagenin-19-rhamnoside (A.21), 96%
Injection: 10:1 H_2O:DMSO
Method 3, 233nm, rt = 5.7 min

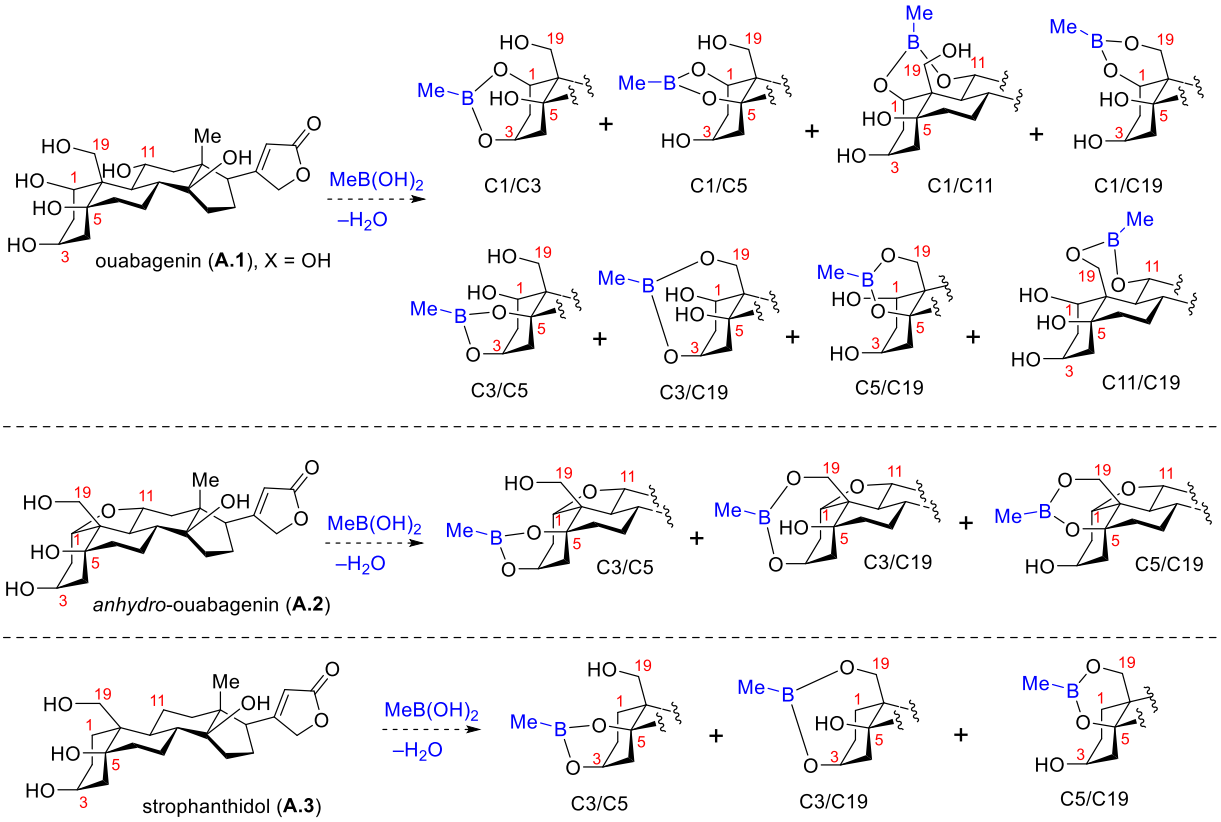

Strophanthidol-3-rhamnoside (A.16), 95%
Injection: 1:1 H_2O:MeCN
Method 3, 233nm, rt = 7.9min


mAU
233nm,4nm
DMSO
Anhydro-ouabagenin (A.2), 96%
Injection: 10:1 H2O:DMSO
Method 3, 233nm, rt = 4.6 min
B.Conc
%
min

Computed relative stabilities of methyl boronic acid esters derived from steroids 1–3 (DFT, B3LYP, 6-31+G*).

The geometry optimization studies summarized in Table 1 were carried using Spartan 20 (DFT, B3LYP, 6-31+G* in Gas Phase) using geometry optimization. The absolute computed energies are provided below.

Appendix Table A.3: Computed energies for the regioisomeric boronates



aglycone	absolute computed energies for the regioisomeric boronates (DFT, B3LYP, 6-31+G*) (kcal/mol)							
	C1/C3	C1/C5	C1/C11	C1/C19	C3/C5	C3/C19	C5/C19	C11/C19
A.1	-980413.96	-980413.36	-980414.61	-980422.23	-980414.41	-980403.95	-980419.98	-980414.63
A.2	–	–	–	–	–932459.98	-932439.70	-932461.91	–
A.3	–	–	–	–	-886021.08	-886005.49	-886022.71	–

Animal models

Adult male and female C57BL/6J (stock 000664) mice were acquired from the Jackson Laboratory and bred to generate wild-type litters. Post-natal day 1-2 mice were euthanized and their brain tissue collected for primary glial cell culture studies. All mice had ad libitum access to a standard chow diet (Purina Lab Diet 5001) and were housed in temperature-controlled rooms on a 12-hour light–12-hour dark cycle. The procedures conducted in this study were approved by the Wayne State University Institutional Animal Care and Use Committee (IACUC).

Primary glia culture[50]

The whole brain from neonatal 1-2 days pups was collected, excluding the meninges. It was then placed in a modified HBSS medium without calcium or magnesium (Gibco 14190144) and processed following the instructions provided by Miltenyi Biotech. The resulting supernatant was discarded, and the pellet was re-suspended in 2 mL of complete medium comprising Dulbecco's Modified Eagle Medium/Nutrient Mixture F-12, without phenol red (DMEM/F-12) (Gibco 21041025), supplemented with 10% inactivated fetal bovine serum (FBS) (Thermo Fischer 10082147) and 1% Antibiotic-Antimycotic (Thermo Fischer 15240062). Following homogenization, the cells were cultured in Nunc™ Cell Culture Treated Flasks with Filter Caps (Thermo Fischer, 178905) containing 10 mL of complete medium within a 5% CO_2 incubator (Galaxy 170R, Eppendorf) at 37°C. Medium replacement, constituting 50% of the total, occurred at 48 and 72-hour intervals. Once the cells reached 80% confluence, they were incubated in a shaker at 200 rpm for 2 hours at 37°C to separate the oligodendrocytes and neurons from the glial cell culture. The cells in suspension were then discarded, and the adhered cells were rinsed with 1 mL of Dulbecco's Phosphate-Buffered Saline without calcium or magnesium (DPBS) (Gibco 14190144). Cell harvesting was performed using 5 mL of 1x trypsin (Thermo Fischer 15400054),

and trypsin activity was neutralized using an equal amount of complete medium. Subsequently, the cells were seeded in 24-well plates and treated for 24 hours with 200 nM of cardiotonic steroids. Upon reaching confluence and complete attachment, they were stimulated with LPS (250 ng/mL). The cardiotonic steroids, LPS (positive control), 0.005% DMSO (negative control), and a combination of cardiotonic steroids with LPS were all diluted in complete medium. Following treatment, the cells were washed with cold 1X DPBS, and total RNA extraction was carried out using Trizol.

Quantitative real-time PCR

Total RNA was isolated from primary glial cell culture using TRIzol reagent (Invitrogen, #15596026). A concentration of 1000 ng of RNA was utilized for complementary DNA (cDNA) synthesis employing the High Capacity cDNA Reverse Transcription Kit (Bio-Rad, #1708891). To detect contaminated DNA, negative controls were processed without the reverse transcriptase enzymes. Quantitative real-time PCR was conducted using the Applied Biosystems 7500 Real-Time PCR and specific primers: Il-1b (Forward) TGGACCTTCCAGGATGAGGACA (Reverse) GTTCATCTCGGAGCCTGTAGTG, Il-6 (Forward) TACCACTTCACAAGTCGGAGGC (Reverse) CTGCAAGTGCATCATCGTTGTTC, TNFα (Forward) GGTGCCTATGTCTCAGCCTCTT (Reverse) GCCATAGAACTGATGAGAGGGAG, IKBKE (Forward) CCCAAAGTTCGTCCCTAAGGTTG (Reverse) ATCAACGCCTGTCCATCCAGCA. Each PCR reaction was performed in duplicate. As negative controls, water was used instead of the cDNA, and β-actin was measured in each cDNA sample as the housekeeping gene. The ΔΔCT method was applied to determine the gene transcripts in each sample. For each sample, the cycle threshold (CT) was measured and normalized to the average of the housekeeping gene (ΔCT = CT gene of interest − CT housekeeping gene). The fold change

of mRNA in the DMSO control group was determined by 2−ΔΔCT. The data are presented as mRNA expression levels relative to the vehicle-treated controls.

A.6 References

(1) Wasserstrom, J. A.; Aistrup, G. L. Digitalis: New Actions for an Old Drug. *American Journal of Physiology-Heart and Circulatory Physiology* **2005**, *289* (5), H1781–H1793. https://doi.org/10.1152/ajpheart.00707.2004.

(2) Nesher, M.; Shpolansky, U.; Rosen, H.; Lichtstein, D. The Digitalis-like Steroid Hormones: New Mechanisms of Action and Biological Significance. *Life Sciences* **2007**, *80* (23), 2093–2107. https://doi.org/10.1016/j.lfs.2007.03.013.

(3) Senthilkumaran, S.; Meenakshisundaram, R.; Thirumalaikolundusubramanian, P. Chapter 5 - Plant Toxins and the Heart. In *Heart and Toxins*; Ramachandran, M., Ed.; Academic Press: Boston, 2015; pp 151–174. https://doi.org/10.1016/B978-0-12-416595-3.00005-0.

(4) Schoner, W.; Schneiner-Bobis, G. Endogenous and Exogenous Cardiac Glycosides: Their Roles in Hypertension, Salt Metabolism, and Cell Growth. *J. Physiol. Cell Physiol.* **2007**, *293* (2), C509–C536. https://doi.org/10.1152/ajpcell.00098.2007.

(5) Prassas, I.; Diamandis, E. P. Novel Therapeutic Applications of Cardiac Glycosides. *Nat. Rev. Drug. Discov.* **2008**, *7*, 926–935. https://doi.org/10.1038/nrd2682.

(6) Bagrov, A. Y.; Shapiro, J. I.; Fedorova, O. V. Endogenous Cardiotonic Steroids: Physiology, Pharmacology, and Novel Therapeutic Targets. *Pharmacol Rev* **2009**, *61* (1), 9–38. https://doi.org/10.1124/pr.108.000711.

(7) Ren, J.; Gao, X.; Guo, X.; Wang, N.; Wang, X. Research Progress in Pharmacological Activities and Applications of Cardiotonic Steroids. *Frontiers in Pharmacology* **2022**, *13*.

(8) Mijatovic, T.; Van Quaquebeke, E.; Delest, B.; Debeir, O.; Darro, F.; Kiss, R. Cardiotonic Steroids on the Road to Anti-Cancer Therapy. *Biochimica et Biophysica Acta (BBA) - Reviews on Cancer* **2007**, *1776* (1), 32–57. https://doi.org/10.1016/j.bbcan.2007.06.002.

(9) Babula, P.; Masarik, M.; Adam, V.; Provaznik, I.; Kizek, R. From Na+/K+-ATPase and Cardiac Glycosides to Cytotoxicity and Cancer Treatment. *Anti-Cancer Agents in Medicinal Chemistry 13* (7), 1069–1087.

(10) *Molecules | Free Full-Text | Anticancer and Immunogenic Properties of Cardiac Glycosides*. https://www.mdpi.com/1420-3049/22/11/1932 (accessed 2023-11-30).

(11) Jin, Y.-H.; Jeon, S.; Lee, J.; Kim, S.; Jang, M. S.; Park, C. M.; Song, J. H.; Kim, H. R.; Kwon, S. Broad Spectrum Antiviral Properties of Cardiotonic Steroids Used as Potential

Therapeutics for Emerging Coronavirus Infections. *Pharmaceutics* **2021**, *13* (11), 1839. https://doi.org/10.3390/pharmaceutics13111839.

(12) El-Seedi, H. R.; Yosri, N.; El-Aarag, B.; Mahmoud, S. H.; Zayed, A.; Du, M.; Saeed, A.; Musharraf, S. G.; El-Garawani, I. M.; Habib, M. R.; Tahir, H. E.; Hegab, M. M.; Zou, X.; Guo, Z.; Efferth, T.; Khalifa, S. A. M. Chemistry and the Potential Antiviral, Anticancer, and Anti-Inflammatory Activities of Cardiotonic Steroids Derived from Toads. *Molecules* **2022**, *27* (19), 6586. https://doi.org/10.3390/molecules27196586.

(13) Eid, S.; Zerbes, T.; Williams, D.; Wang, X.; Sackmann, C.; Meier, S.; Dulin, N. O.; Nagorny, P.; Schmitt-Ulms, G. Identification of a Cardiac Glycoside Exhibiting Favorable Brain Bioavailability and Potency for Reducing Levels of the Cellular Prion Protein. *International Journal of Molecular Sciences* **2022**, *23* (23), 14823. https://doi.org/10.3390/ijms232314823.

(14) Markina, A. A.; Kazanskaya, R. B.; Timoshina, J. A.; Zavialov, V. A.; Abaimov, D. A.; Volnova, A. B.; Fedorova, T. N.; Gainetdinov, R. R.; Lopachev, A. V. Na+,K+-ATPase and Cardiotonic Steroids in Models of Dopaminergic System Pathologies. *Biomedicines* **2023**, *11* (7), 1820. https://doi.org/10.3390/biomedicines11071820.

(15) Kaur, S.; Rehni, A. K.; Singh, N.; Jaggi, A. S. Studies on Cerebral Protection of Digoxin against Ischemia/Reperfusion Injury in Mice. *Yakugaku Zasshi* **2009**, *129* (4), 435–443. https://doi.org/10.1248/yakushi.129.435.

(16) Dunn, D. E.; He, D. N.; Yang, P.; Johansen, M.; Newman, R. A.; Lo, D. C. In Vitro and in Vivo Neuroprotective Activity of the Cardiac Glycoside Oleandrin from Nerium Oleander in Brain Slice-Based Stroke Models. *J Neurochem* **2011**, *119* (4), 805–814. https://doi.org/10.1111/j.1471-4159.2011.07439.x.

(17) Kanegan, M. J. V.; He, D. N.; Dunn, D. E.; Yang, P.; Newman, R. A.; West, A. E.; Lo, D. C. BDNF Mediates Neuroprotection against Oxygen-Glucose Deprivation by the Cardiac Glycoside Oleandrin. *J. Neurosci.* **2014**, *34* (3), 963–968. https://doi.org/10.1523/JNEUROSCI.2700-13.2014.

(18) Orellana, A. M.; Kinoshita, P. F.; Leite, J. A.; Kawamoto, E. M.; Scavone, C. Cardiotonic Steroids as Modulators of Neuroinflammation. *Frontiers in Endocrinology* **2016**, *7*.

(19) Leite, J. A.; Cavalcante-Silva, L. H. A.; Ribeiro, M. R.; de Morais Lima, G.; Scavone, C.; Rodrigues-Mascarenhas, S. Neuroinflammation and Neutrophils: Modulation by Ouabain. *Frontiers in Pharmacology* **2022**, *13*.

(20) Smer-Barreto, V.; Quintanilla, A.; Elliott, R. J. R.; Dawson, J. C.; Sun, J.; Campa, V. M.; Lorente-Macías, Á.; Unciti-Broceta, A.; Carragher, N. O.; Acosta, J. C.; Oyarzún, D. A. Discovery of Senolytics Using Machine Learning. *Nat Commun* **2023**, *14* (1), 3445. https://doi.org/10.1038/s41467-023-39120-1.

(21) Hamlyn, J. M.; Blaustein, M. P.; Bova, S.; DuCharme, D. W.; Harris, D. W.; Mandel, F.; Matthews, W. R.; Ludens, J. H. Identification and Characterization of a Ouabain-like

Compound from Human Plasma. *PNAS* **1991**, *88* (14), 6259–6263. https://doi.org/10.1073/pnas.88.14.6259.

(22) Tymiak, A. A.; Norman, J. A.; Bolgar, M.; DiDonato, G. C.; Lee, H.; Parker, W. L.; Lo, L. C.; Berova, N.; Nakanishi, K.; Haber, E. Physicochemical Characterization of a Ouabain Isomer Isolated from Bovine Hypothalamus. *Proceedings of the National Academy of Sciences* **1993**, *90* (17), 8189–8193. https://doi.org/10.1073/pnas.90.17.8189.

(23) Ferrandi, M.; Manunta, P.; Balzan, S.; Hamlyn, J. M.; Bianchi, G.; Ferrari, P. Ouabain-like Factor Quantification in Mammalian Tissues and Plasma. *Hypertension* **1997**, *30* (4), 886–896. https://doi.org/10.1161/01.HYP.30.4.886.

(24) Blaustein, M. P.; Hamlyn, J. M. Ouabain, Endogenous Ouabain and Ouabain-like Factors: The Na+ Pump/Ouabain Receptor, Its Linkage to NCX, and Its Myriad Functions. *Cell Calcium* **2020**, *86*, 102159. https://doi.org/10.1016/j.ceca.2020.102159.

(25) Kinoshita, P. F.; Yshii, L. M.; Vasconcelos, A. R.; Orellana, A. M. M.; Lima, L. de S.; Davel, A. P. C.; Rossoni, L. V.; Kawamoto, E. M.; Scavone, C. Signaling Function of Na,K-ATPase Induced by Ouabain against LPS as an Inflammation Model in Hippocampus. *Journal of Neuroinflammation* **2014**, *11* (1), 218. https://doi.org/10.1186/s12974-014-0218-z.

(26) Garcia, I. J. P.; Kinoshita, P. F.; de Oliveira Braga, I.; Parreira, G. M.; Mignaco, J. A.; Scavone, C.; Barbosa, L. A.; de Lima Santos, H. Ouabain Attenuates the Oxidative Stress Induced by Lipopolysaccharides in the Cerebellum of Rats. *Journal of Cellular Biochemistry* **2018**, *119* (2), 2156–2167. https://doi.org/10.1002/jcb.26377.

(27) Garcia, I. J. P.; Kinoshita, P. F.; Silva, L. N. D. e; De Souza Busch, M.; Atella, G. C.; Scavone, C.; Cortes, V. F.; Barbosa, L. A.; De Lima Santos, H. Ouabain Attenuates Oxidative Stress and Modulates Lipid Composition in Hippocampus of Rats in Lipopolysaccharide-Induced Hypocampal Neuroinflammation in Rats. *Journal of Cellular Biochemistry* **2019**, *120* (3), 4081–4091. https://doi.org/10.1002/jcb.27693.

(28) Pereira Garcia, I. J.; Kinoshita, P. F.; de Moura Valadares, J. M.; Drumond de Carvalho, L. E.; Cortes, V. F.; Barbosa, L. A.; Scavone, C.; de Lima Santos, H. Effect of Ouabain on Glutamate Transport in the Hippocampus of Rats with LPS-Induced Neuroinflammation. *Biomedicines* **2023**, *11* (3), 920. https://doi.org/10.3390/biomedicines11030920.

(29) Cichowicz, N. R.; Kaplan, W.; Khomutnyk, Y.; Bhattarai, B.; Sun, Z.; Nagorny, P. Concise Enantioselective Synthesis of Oxygenated Steroids via Sequential Copper(II)-Catalyzed Michael Addition/Intramolecular Aldol Cyclization Reactions. *J. Am. Chem. Soc.* **2015**, *137* (45), 14341–14348. https://doi.org/10.1021/jacs.5b08528.

(30) Kaplan, W.; Khatri, H. R.; Nagorny, P. Concise Enantioselective Total Synthesis of Cardiotonic Steroids 19-Hydroxysarmentogenin and Trewianin Aglycone. *J. Am. Chem. Soc.* **2016**, *138* (22), 7194–7198. https://doi.org/10.1021/jacs.6b04029.

(31) Khatri, H. R.; Bhattarai, B.; Kaplan, W.; Li, Z.; Long, M. J. C.; Aye, Y.; Nagorny, P. Modular Total Synthesis and Cell-Based Anticancer Activity Evaluation of Ouabagenin and Other Cardiotonic Steroids with Varying Degrees of Oxygenation. *J. Am. Chem. Soc.* **2019**, *141* (12), 4849–4860. https://doi.org/10.1021/jacs.8b12870.

(32) Fejedelem, Z.; Carney, N.; Nagorny, P. Synthesis of Cardiotonic Steroids Oleandrigenin and Rhodexin B. *J. Org. Chem.* **2021**, *86* (15), 10249–10262. https://doi.org/10.1021/acs.joc.1c00985.

(33) Bhattarai, B.; Nagorny, P. Enantioselective Total Synthesis of Cannogenol-3-O-α-l-Rhamnoside via Sequential Cu(II)-Catalyzed Michael Addition/Intramolecular Aldol Cyclization Reactions. *Org. Lett.* **2018**, *20* (1), 154–157. https://doi.org/10.1021/acs.orglett.7b03513.

(34) Tay, J.-H.; Dorokhov, V.; Wang, S.; Nagorny, P. Regioselective Single Pot C3-Glycosylation of Strophanthidol Using Methylboronic Acid as a Transient Protecting Group. *J Antibiot* **2019**, *72* (6), 437–448. https://doi.org/10.1038/s41429-019-0172-1.

(35) Carney, N.; Perry, N.; Garabedian, J.; Nagorny, P. Development of α-Selective Glycosylation with l-Oleandral and Its Application to the Total Synthesis of Oleandrin. *Org. Lett.* **2023**, *25* (6), 966–971. https://doi.org/10.1021/acs.orglett.2c04358.

(36) Hong, B.-C.; Kim, S.; Kim, T.-S.; Corey, E. J. Synthesis and Properties of Several Isomers of the Cardioactive Steroid Ouabain. *Tetrahedron Letters* **2006**, *47* (16), 2711–2715. https://doi.org/10.1016/j.tetlet.2006.02.089.

(37) Zhang, H.; Sridhar Reddy, M.; Phoenix, S.; Deslongchamps, P. Total Synthesis of Ouabagenin and Ouabain. *Angewandte Chemie International Edition* **2008**, *47* (7), 1272–1275. https://doi.org/10.1002/anie.200704959.

(38) Urabe, D.; Nakagawa, Y.; Mukai, K.; Fukushima, K.; Aoki, N.; Itoh, H.; Nagatomo, M.; Inoue, M. Total Synthesis and Biological Evaluation of 19-Hydroxysarmentogenin-3-O-α-l-Rhamnoside, Trewianin, and Their Aglycons. *J. Org. Chem.* **2018**, *83* (22), 13888–13910. https://doi.org/10.1021/acs.joc.8b02219.

(39) Tay, J.-H.; Argüelles, A. J.; DeMars, M. D. I.; Zimmerman, P. M.; Sherman, D. H.; Nagorny, P. Regiodivergent Glycosylations of 6-Deoxy-Erythronolide B and Oleandomycin-Derived Macrolactones Enabled by Chiral Acid Catalysis. *J. Am. Chem. Soc.* **2017**, *139* (25), 8570–8578. https://doi.org/10.1021/jacs.7b03198.

(40) Píš, J.; Hykl, J.; Buděšinský, M.; Harmatha, J. Regioselective Synthesis of 20-Hydroxyecdysone Glycosides. *Tetrahedron* **1994**, *50* (32), 9679–9690. https://doi.org/10.1016/S0040-4020(01)85536-8.

(41) (Fenger, T. H.; Madsen, R. Regioselective Glycosylation of Unprotected Phenyl 1-Thioglycopyranosides with Phenylboronic Acid as a Transient Masking Group. *Eur. J. Org. Chem.* **2013**, *2013* (26), 5923–5933. https://doi.org/10.1002/ejoc.201300723.

(42) Kaji, E.; Nishino, T.; Ishige, K.; Ohya, Y.; Shirai, Y. Regioselective Glycosylation of Fully Unprotected Methyl Hexopyranosides by Means of Transient Masking of Hydroxy Groups with Arylboronic Acids. *Tetrahedron Letters* **2010**, *51* (12), 1570–1573. https://doi.org/10.1016/j.tetlet.2010.01.048.

(43) Mancini, R. S.; Lee, J. B.; Taylor, M. S. Boronic Esters as Protective Groups in Carbohydrate Chemistry: Processes for Acylation, Silylation and Alkylation of Glycoside-Derived Boronates. *Org. Biomol. Chem.* **2017**, *15* (1), 132–143. https://doi.org/10.1039/C6OB02278B.

(44) Sneeden, R. P. A.; Turner, R. B. *Ouabagenin. I. The Relationship between Ouabagenin Monoacetonide and "Anhydroöuabagenin"1*. ACS Publications. https://doi.org/10.1021/ja01110a059.

(45) Volpp, G.; Tamm, Ch. 1α, 11α-Oxido-Strophanthidol (Monoanhydro-Ouabagenin) Sowie Weitere 1α, 11α-Oxido-Steroide Aus Ouabagenin. *Helvetica Chimica Acta* **1963**, *46* (1), 219–237. https://doi.org/10.1002/hlca.19630460122.

(46) Volpp, G.; Tamm, Ch. 1α-11α-Epoxy-Steroids from Ouabagenin by Transannular Substitution. *Tetrahedron Letters* **1960**, *1* (48), 31–36. https://doi.org/10.1016/S0040-4039(01)99410-9.

(47) Mukai, K.; Kasuya, S.; Nakagawa, Y.; Urabe, D.; Inoue, M. A Convergent Total Synthesis of Ouabagenin. *Chem. Sci.* **2015**, *6* (6), 3383–3387. https://doi.org/10.1039/C5SC00212E.

(48) Rosenthal, T. Chiral Bronsted Acid: Innovations and Application to Regiodivergent Glycosylations. Thesis, 2018. http://deepblue.lib.umich.edu/handle/2027.42/145997 (accessed 2023-12-02).

(49) Zhang, M.; Du, Y.; Kong, F. Practical Synthesis of a Tetrasaccharide Derivative Corresponding to Ristomycin A and Ristocetin A. *Carbohydr. Res.* **2001**, *330* (3), 319–324. https://doi.org/10.1016/S0008-6215(00)00303-7.

(50) Awada, A. A.; Zhang, K.; Klueh, U.; Sadagurski, M. Acarbose Protects from Central and Peripheral Metabolic Imbalance Induced by Benzene Exposure. *Brain, Behavior, and Immunity* **2020**, *89*, 87–99. https://doi.org/10.1016/j.bbi.2020.05.073.

Appendix B: Probing the Effect on Remote Participation for Galactosylation

This appendix is part of an ongoing collaboration between the Nagorny group and Asst. Prof. Mateusz Marianski's group at Hunter College. Calculations and computational modeling of the reaction intermediates and mechanism was performed by Dr. Marianski and Ryan Kwok of Hunter College.

B.1 Introduction

Carbohydrates play an essential role in biological process including metabolism, energy storage, intercellular communication and immunorecognition.[1] From 2015-2020, of the over 200 FDA approved new small molecule drugs, less than 5% contained a carbohydrate unit.[2] Carbohydrate drugs and vaccines remain niche due to their complex and labor intensive synthesis, which requires careful regio- and stereo- control of the glycosidic bond formation.[3]

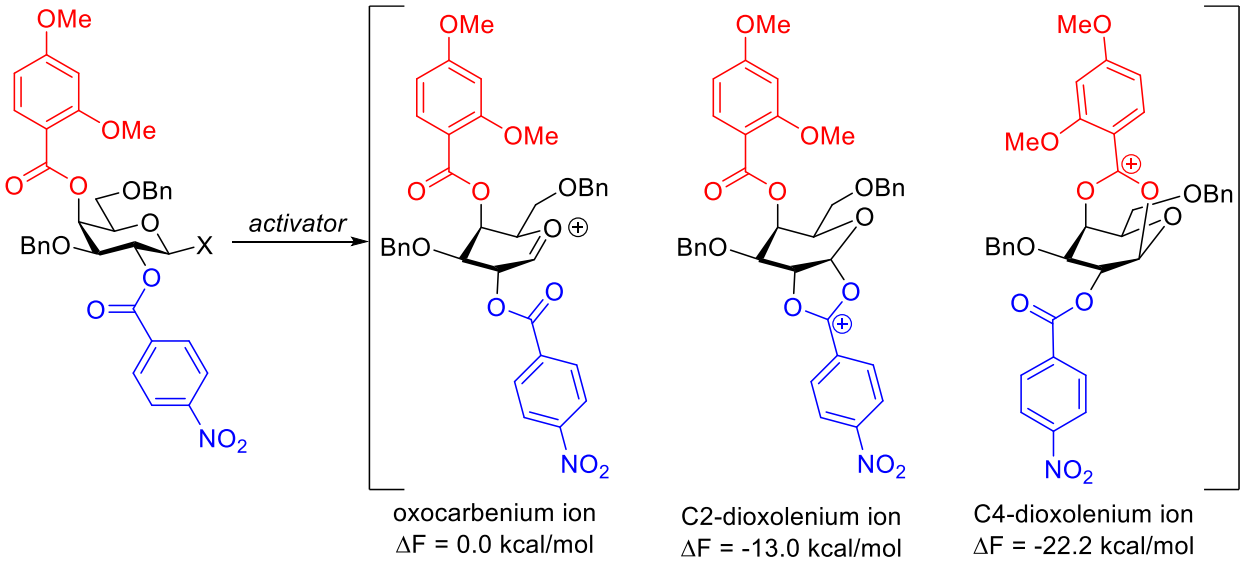
The glycosylation reaction involved the coupling of a glycosyl donor to an acceptor that proceeds through a complex glycosyl donor intermediate. This intermediate likely exists as a distribution over a continuum of potential covalent and ionic intermediates, rather than as a single, well defined structure.[4] The dominant structure will then drive the reaction mechanism, and define the stereochemistry of the product. Thus, methods to influence the dominant glycosyl intermediates will greatly benefit the selectivity of the reaction. This can be achieved by stabilization of desired intermediates through specialize tailoring of the glycosyl donor, nucleophilicity of the glycosyl acceptor, the nature of the activator, or optimization of reaction conditions including solvent and temperature.[5,6] Due to the instability and short lived nature of

the glycosyl cations, the mechanistic impact of the factors that affect the glycosylation mechanism is poorly understood.

Direct observation of these intermediates is only possible with specialized chemical derivatives or in strongly stabilizing environments, such as in super acids or as gas-phase ions.[7-9] However, these conditions can cause the donor to behave vastly different than in the standard solution phase reaction. A tool to empirically model and optimize the glycosylation reaction may be helpful to elucidate substrates or conditions to favor the desired intermediates. Density-functional theory (DFT) has been an appealing alternative to experimental methods in the investigation of the glycosylation reaction. As computational tool, DFT has been used to model the mechanisms of various chemical reaction including S_NAr substitutions,[10] [2+2) photochemical cycloaddition,[11] and the Diels-Alder reaction.[12] It has also been previously employed to study carbohydrate systems,[13] including the prediction of rearrangement products[14,15] and the investigation of the reaction in solution[16] and at the enzymatic catalytic site.[17] DFT simulations have been conducted previously to validate various glycosylation mechansisms,[18-26] however, few studies aim to garner a greater understanding of the factors determine the reaction outcome.[16,27-29] The Marianski group employed DFT calculations to obtain insights into the thermodynamics and kinetics of the protecting group participation effects that influence the reaction stereoselectivity.[30] Notably, they aimed glean insight to the importance and effect of the stability of the dioxolenium ions for the protecting group participation mechanism. By gaining this understanding, the glycosyl donors could be more productively optimized to provide specific stereoselective products.[31-33]

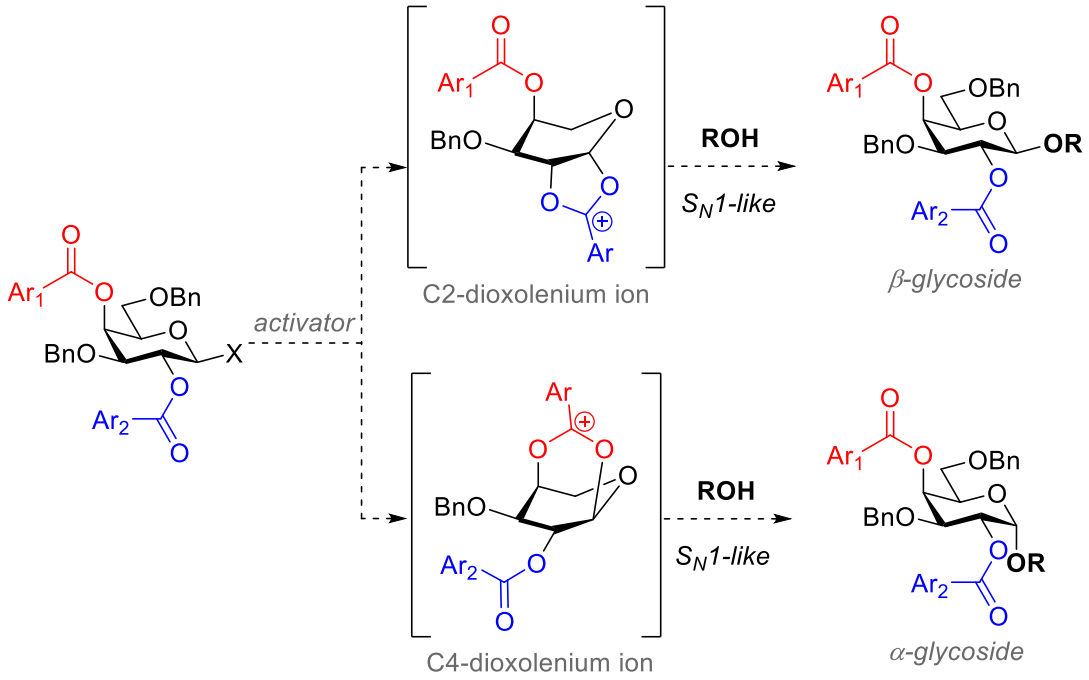
Glycosylation stereochemistry can be guided through various intermediates resulting from the activation of the glycosyl donor (*cf.* Scheme 1.2). With the combined use of cryogenic

IR spectroscopy and DFT the Marianski and coworkers demonstrated that C2-neighboring protecting groups (acetyl or benzoyl) adopt a dioxolenium type structure by forming a covalent bond between the anomeric carbon and the carbonyl oxygen of the acetyl group, which lead to formation of a 1,2-*trans* glycoside.[9,34-35] The effect of remote participating groups on the stereoselectivity of galactosylation reactions was also investigated with the combined use of cryogenic IR spectroscopy and DFT.[4] The C4 acetate of the galactose donor was found to form a dioxolenium type intermediate in the gas phase, which led to the formation of the 1,2-*cis* galactoside product. Recently, Pagel and coworkers demonstrated in galactosides that increasing the electron density of the C4 participating group led to higher selectivity for the 1,2-*cis* galactoside product.[36-40] This finding may suggest that the 1,2-*cis* glycoside is formed through the bridged dioxolenium type intermediate, however, the exact mechanism by which distal protecting participate in the reaction is unconfirmed and a hot button debate within the scientific community. It has been argued that the formation of the dioxolenium ion is kinetically unfavorable due to several high-energy steps required for their formation, and that the observation is of these ions in the gas phase is not indicative of their behavior a solution phase reaction.[5,41,42] Instead, the selectivity arises from the electron withdrawing properties of the protecting group destabilizing the oxocarbenium-type intermediate, which causes the reaction to proceed through a more S_N2-like mechanism.



Appendix Scheme B.1: Computed energies of dioxolenium-type intermediates of galactosylation with C2 and C4 benzoate protecting groups

Marianski and coworkers has investigated the effect of the electron withdrawing group on the potential reaction mechanism, and the anticipated reaction outcome.[30] All calculations were performed using the PBE0+D3/6-311+G(d,p) level of theory in Gaussian16. They have shown that the stability of the dioxolenium ion intermediates increases with the electron donating strength of the protecting group (based on the Hammet parameter). Additionally, they found that for galactosyl donors with both C2 and C4 benzoate, the more electron rich benzoate forms the more stable dioxolenium-type intermediate (Appendix Scheme B.1).



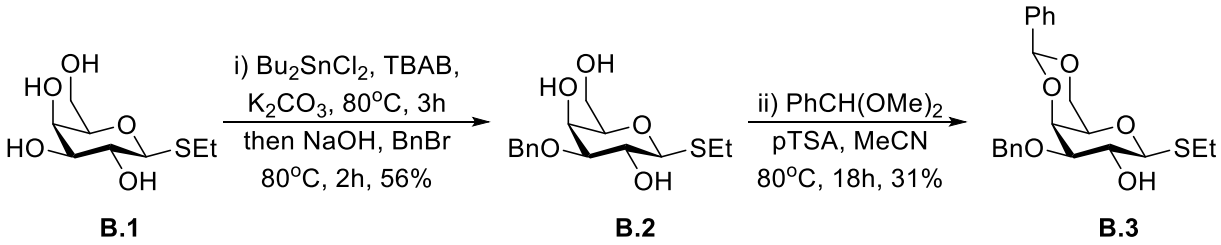
Appendix Scheme B.2: Possible mechanisms for directing group participation in galactosides

Based on this observation, a substrate that has a C4 protecting group with a strong electron donating group, and a C2 protecting group with a strong electron withdrawing group could switch the mechanism from the C2-participation to C4-participation (Appendix Scheme B.2). To validate the computed reaction pathways and determine the experimental utility of protecting group drive reaction diversification, we prepared galactose donors with C2 and C4 benzoates with electron donation (OMe) and electron withdrawing (CF_3) groups.

B.2 Synthesis of galactosyl donors and studies on galactosylation diastereoselectivity

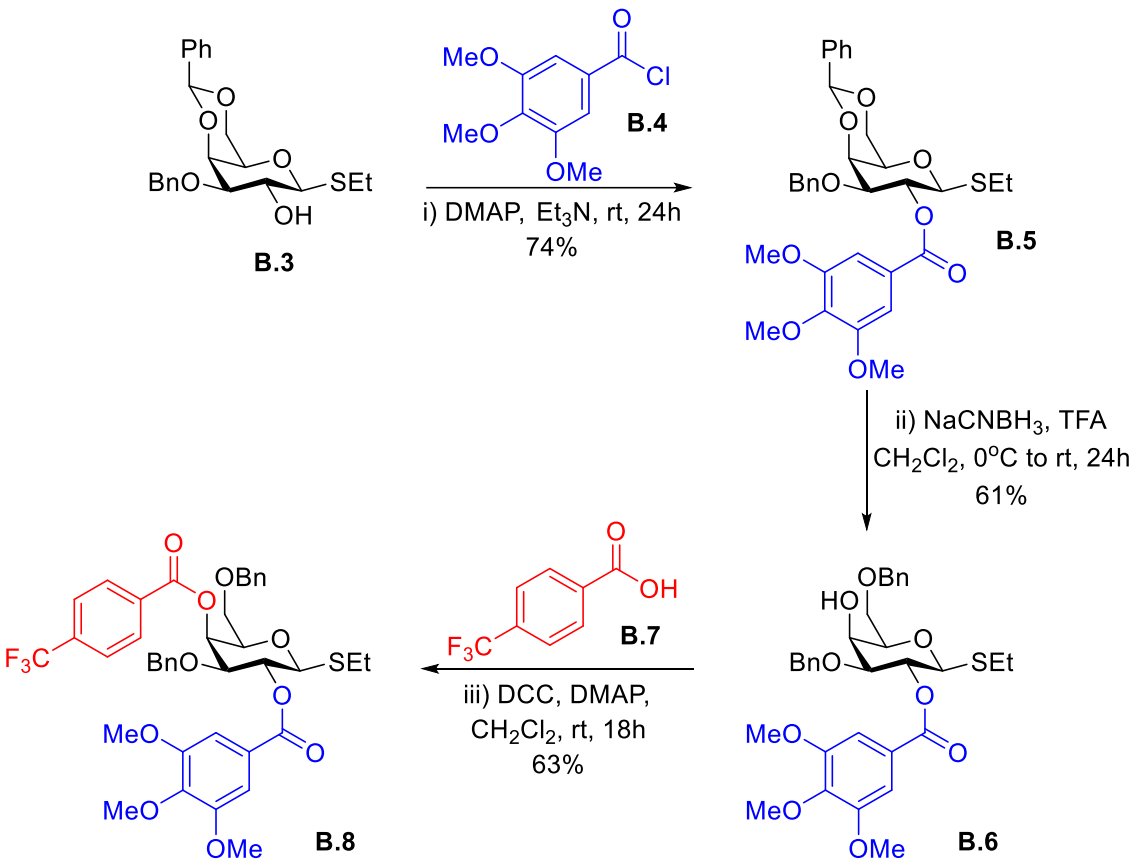
We prepared galactosyl donors **B.8** and **B.11** from commercially available ethyl-β-D-thiogalactopyranoside **B.1** (Appendix Scheme B.3-Appendix Scheme B.5). The common C3-*O*-benzyl, C4,C6-*O*-benzylidene intermediated **B.3** was prepared in two steps from **B.1** (Appendix Scheme B.3). The C3-*O*-benzyl group was regioselectively installed in 51% yield by employing

the organotin reagent dibutyltin dichloride.[Ref] The C4,C6-*O*-benzylidene was installed by treatment with **B.2** with benzylidene dimethyl acetal and CSA to afford **B.3** in 31% yield.



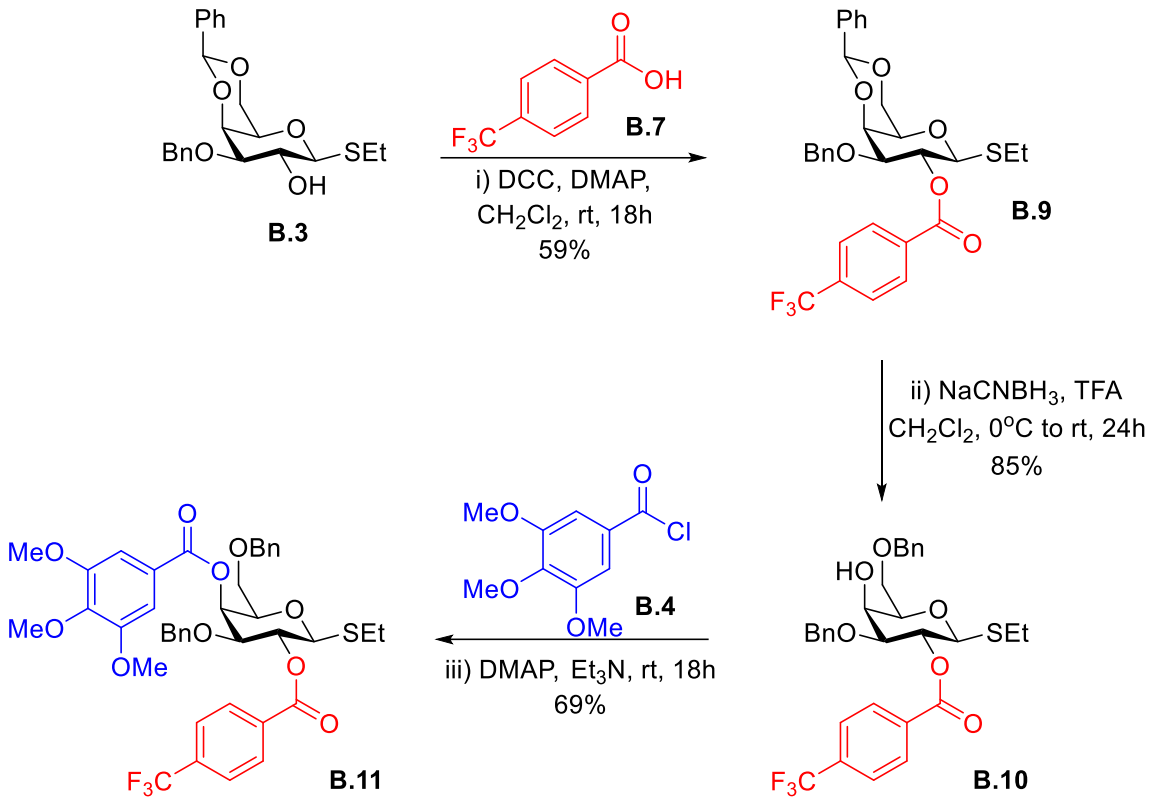
Appendix Scheme B.3: Synthesis of galactose benzylidene intermediate **B.3**
[i)] **B.1** (2.2 mmol, 1.0eq), Bu_2SnCl_2 (0.22 mmol, 10 mol%), tetrabutylammonium bromide (TBAB, 0.22 mmol, 10mol%), K_2CO_3 (3.4 mmol, 1.5eq), BnBr (4.5 mmol, 2.0 eq), MeCN:DMF (10:1 mL), 80 °C, 3 h, then add BnBr (4.5 mmol, 2.0 eq), NaOH (3.4 mmol, 1.5 eq), 80 °C, 2 h, 56%; ii) **B.2** (1.6 mmol, 1.0 eq), benzaldehyde dimethyl acetal (2.4 mmol, 1.5 eq), *para*-toluenesulfonyl chloride (pTSA, 0.11 mmol, 7.5 mol%), MeCN (3.0 mL), 80°C, 18 h, 21%.

Benzylidene intermediate **B.3** was elaborated to galactosyl donors **B.8** (Appendix Scheme B.4) and **B.11** (Appendix Scheme B.5) via a three step sequence of 1) C2 acylation, 2) regioselective reductive benzylidene opening, and 3) C4 acylation. First, we targeted thioglycoside donor **B.8** with an electron rich benzoate at C2 and an electron poor benzoate at C4 (Appendix Scheme B.4). Benzylidene **B.3** was treated with 3,4,5-trimethoxybenzoyl chloride **B.4** in Et_3N with catalytic DMAP to provide C2-benzoate **B.5** in 74% yield. Regioselective reductive opening of the benzylidene of **B.5** with $NaCNBH_3$ and TFA in CH_2Cl_2 provided the C4-secondary free alcohol galactoside **B.6** in 61% yield. Attempts to open the benzylidene with Et_3SiH and TFA in CH_2Cl_2 provided a complex mixture of products including complete removal of the C4,C6-benzylidene and hydrolysis of the C2-benzoate. Final esterification of the C4-alcohol of **B.6** with 4-trifluoromethylbenzoic acid **B.7** and DCC and DMAP as activators provided thioglycoside donor **B.8** in 63% yield.



Appendix Scheme B.4: Synthesis of galactosyl donor **B.8**.
i) **B.3 (**110 µmol, 1.0 eq), 3,4,5-tri-methoxybenzoyl chloride **B.4** (46 µmol, 4.0 eq), 4-dimethylaminopyridine (DMAP, 20 µmol, 20 mol%), Et_3N (0.5 mL), rt, 24 h, 74%; ii) **B.5** (84 µmol, 1.0 eq), trifluoroacetic acid (TFA, 1700 µmol, 20 eq), $NaCNBH_3$ (840 µmol, 10 eq), Et_2O:CH_2Cl_2 (0.3:0.6 mL), 0 °C to rt, 24 h, 61%; iii) **B.6** (50 µmol, 1.0 eq), 4-trifluoromethylbenzoic acid **B.7** (100 µmol, 2.0 eq), dicyclohexylcarbodiimide (DCC, 150 µmol, 3.0 eq), DMAP (10 µmol, 20 mol%), CH_2Cl_2 (1.0 mL), rt, 18 h, 63%.

We next prepared thioglycoside donor **B.11** with an electron poor benzoate at C2 and an electron rich benzoate at C4 (Appendix Scheme B.5). Benzylidene **B.3** was treated with 4-trifluoromethylbenzoic acid **B.7**, DCC, and DMAP as activators to provide C2-benzoate **B.9** in 59% yield. Regioselective reductive opening of the benzylidene of **B.9** with $NaCNBH_3$ and TFA in CH_2Cl_2 provided the C4-secondary free alcohol galactoside **B.10** in 85% yield. Final esterification of the C4-alcohol of **B.10** with 3,4,5-trimethoxybenzoyl chloride **B.4** in Et_3N and CH_2Cl_2 with catalytic DMAP provided thioglycoside donor **B.11** in 69% yield. With glycosyl donors **B.8** and **B.11** in hand, we next looked at the effect of the electronic nature of the C2 and C4 benzoates on the diastereoselectivity of the galactosylation reaction.

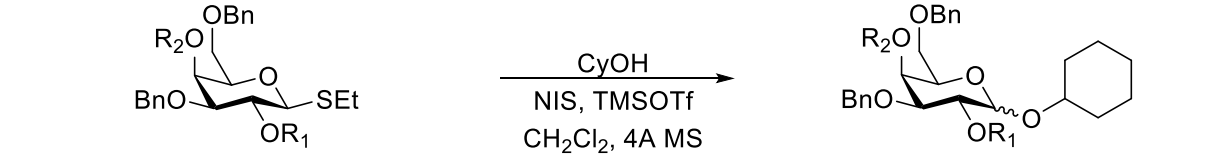


Appendix Scheme B.5: Synthesis of galactosyl donor **B.11**
i) **B.3** (124 µmol, 1.0 eq), 4-trifluoromethylbenzoic acid **B.7** (249 µmol, 2.0 eq), dicyclohexylcarbodiimide (DCC, 373 µmol, 3.0 eq), DMAP (25 µmol, 20 mol%), CH_2Cl_2 (1.0 mL), rt, 18 h, 59%; ii) **B.9** (70 µmol, 1.0 eq), trifluoroacetic acid (TFA, 1400 µmol, 20 eq), $NaCNBH_3$ (700 µmol, 10 eq), CH_2Cl_2 (1.0 mL), 0 °C to rt, 24 h, 85%; iii) **B.10** (121 µmol, 1.0 eq), 3,4,5-tri-methoxybenzoyl chloride **B.4** (486 µmol, 4.0 eq), 4-dimethylaminopyridine (DMAP, 486 µmol, 4.0 eq), Et_3N:CH_2Cl_2 (2:2 mL), rt, 18 h, 69%.

We evaluated each of the prepared donors in the simple glycosylation with cyclohexanol via activation with NIS and TMSOTf (Appendix Table B.1). Glycosylation of cyclohexanol with donor **B.8** provided exclusively the β-glycoside in 79% yield (Appendix Table B.1, entry 1). This result was expected based on the preliminary calculations of the Marianski group.[30] The β-glycoside **B.12** was formed due to anchimeric assistance controlling the selectivity, and the glycosylation proceeded to for the 1,2-*trans* (β) glycoside (*cf.* Appendix Scheme B.3 and Scheme 1.2B). Glycosylation of cyclohexanol with donor **B.11** also provided the β-glycoside **B.13** exclusively in 67% yield (Appendix Table B.1, entry 2). This result indicated that even when the bridged dioxolenium ion from the C4-benzoate is more stable than the dioxolenium resulting

from the C2-benzoate, anchimeric assistance from the C2-benzoate still controlled the diastereoselectivity. This may be caused by 1) under the reaction conditions, a covalent intermediate is formed instead of the dioxolenium ion, and an S_N2 like mechanism predominates and leads to the β-glycoside, or 2) the energy barriers for the formation of the dioxolenium intermediates may be quite large, and the barriers for the intermediates may be a greater factor than the stability of the intermediates themselves. To probe for the possibility of a covalent intermediate leading to the observed selectivity, we attempted glycosylation with donor **B.11** under conditions that are unlikely to form a covalent intermediate (Appendix Scheme B.6).

Appendix Table B.1: Glycosylation of thioglycoside donors **B.8** and **B.11**



R_1 = 3,4,5-OMe-Bz, R_2 = 4-CF_3-Bz, **B.8**
R_1 = 4-CF_3-Bz, R_2 = 3,4,5-OMe-Bz, **B.11**

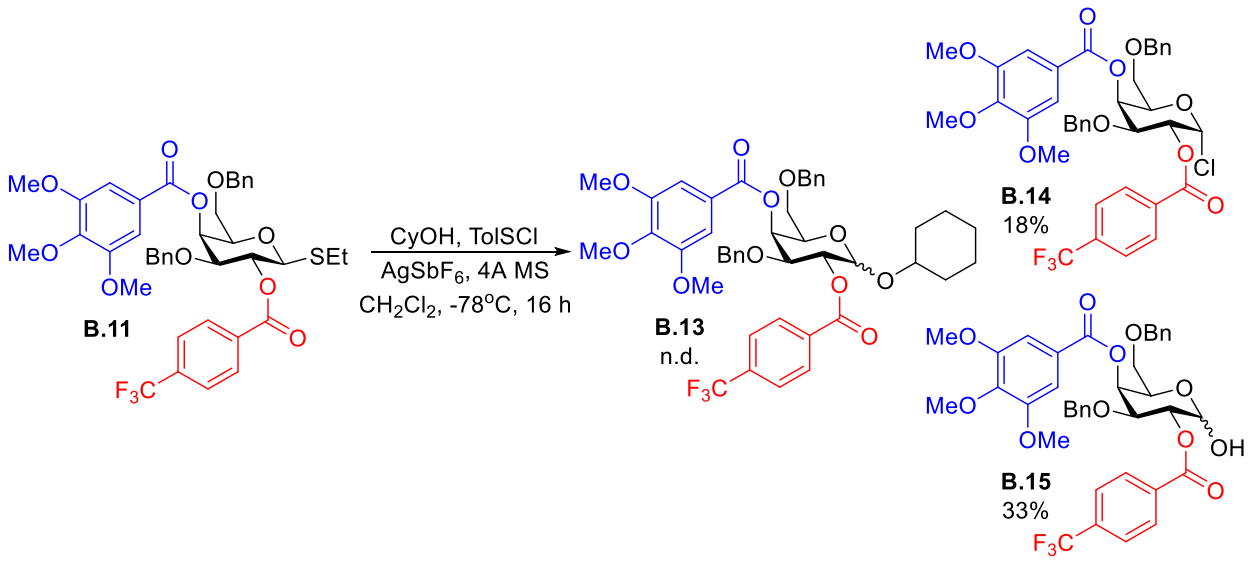
R_1 = 3,4,5-OMe-Bz, R_2 = 4-CF_3-Bz, **B.12**
R_1 = 4-CF_3-Bz, R_2 = 3,4,5-OMe-Bz, **B.13**

entry	donor	R_1	R_2	conversion	yield	d.r. (α:β)
1	**B.8**	3,4,5-OMe-Bz	4-CF_3-Bz	>95%	79% **B.12**	β-only
2	**B.11**	4-CF_3-Bz	3,4,5-OMe-Bz	>95%	67% **B.13**	β-only

entry 1) **B.8** (13 µmol, 1.0 eq), cyclohexanol (CyOH, 26 µmol, 2.0 eq), NIS (20 µmol, 1.5 eq), TMSOTf (3.0 µmol, 20 mol%), 4Å molecular sieves (100 mg), CH_2Cl_2 (0.5 mL), -15 °C, 0.5 h.; entry 2) **B.11** (1.3 µmol, 1.0 eq), cyclohexanol (CyOH, 2.6 µmol, 2.0 eq), NIS (2.0 µmol, 1.5 eq), TMSOTf (0.3 µmol, 20 mol%), 4Å molecular sieves (50 mg), CH_2Cl_2 (0.5 mL), -15 °C, 0.5 h. Conversions, yields, and diastereomeric ratios (d.r.) were determined by ^{1}H NMR analysis of the crude reaction mixtures with CH_2Br_2 (5.0 µL) as internal standard.

Hexafluoroantimonate (SbF_6^-) has been used as a non-coordinating counterion in glycosylation reactions[43,44] and transition metal catalysis.[45] With toluene sulfenyl chloride (TolSCl) as the thiophilic activator and $AgSbF_6$ as promoter, the glycosylation with donor **B.11** failed to provide any of the desired cyclohexyl glycoside **B.13** (Appendix Scheme B.6). Instead, glycosyl chloride **B.14** and hydrolysis byproduct **B.15** were formed in 18% and 33% yield, respectively. With the strong electron withdrawing group at the C2 position, the oxocarbenium

ion pair became too unstable, and instead of reaction with cyclohexanol, the intermediate was captured by chloride or water.[46]



Appendix Scheme B.6: Glycosylation with an activator with a non-coordinating counterion.[a]
[a]**B.11** (13 µmol, 1.0 eq), cyclohexanol (CyOH, 26 µmol, 2.0 eq), $AgSbF_6$ (20 µmol, 1.5 eq), TolSCl (16 µmol, 1.2 eq), 4Å molecular sieves (100 mg), CH_2Cl_2 (0.5 mL), -78 °C, 0.5 h. Conversions, yields, and diastereomeric ratios (d.r.) were determined by 1H NMR analysis of the crude reaction mixtures with CH_2Br_2 (5.0 µL) as internal standard.

The use of a non-coordinating anion did not lead to selective formation of either glycosidic product. From this, we cannot rule out the possibility of a covalent intermediate as the cause for the selectivity observed in previous glycosylations (Appendix Table B.1). However, these results suggest that the thermal stability of the dioxolenium intermediate is not enough to alter the selectivity expected by anchimeric assistance (Scheme 1.2B).

B.3 Conclusions

The Marianski group explored the relative stability of reaction intermediates of the galactosylation reaction. Based on DFT calculations, the thermal stability of the dioxolenium intermediates can be affected by the electron donating/withdrawing substituents of benzoate protecting groups. Thus, if the thermal stability of the intermediates drives the selectivity, then the glycosylation with galactose donors could be altered by the electronic nature of benzoate

groups at the C2 and C4 positions. We developed and prepared in five steps from a commercial thioglycoside **B.1**, two novel galactose donors (**B.8**, **B.11**) with C2 and C4 benzoate protecting groups with varying electronic properties about the benzoates. Glycosylation of cyclohexanol with donors **B.8**/**B.11** and NIS and TMSOTf as promoters led to the exclusive formation of the β-glycosides with both donors. Glycosylation of cyclohexanol with donor **B.11** and TolSCl and $AgSbF_6$ as promoters did not form any of the desired glycosidic product, but instead provided products resulting from side reaction of the glycosyl oxocarbenium intermediate. From these results, it appears that the thermal stability of the intermediates is not enough to alter the selectivity. Likely, the barriers leading to the formation of the intermediates play a deciding role. With the Marianski group, further exploration and calculations of the energies of these barriers can be explored to probe their effects on galactosylation stereoselectivity. Additionally, the additive effect of electron donor/withdrawing groups on the benzoates may be explored to greater the energy difference between the dioxolenium intermediates, and possibly switch the selectivity. The counterion effects may also be playing a role, and a deeper investigation into their effects can provide more information to the reaction mechanism. We have conducted experimental validation for a computationally predicted reaction outcome, and have developed a greater understanding for the driving forces of stereoselectivity of galactosylation reactions.

B.4 Experimental

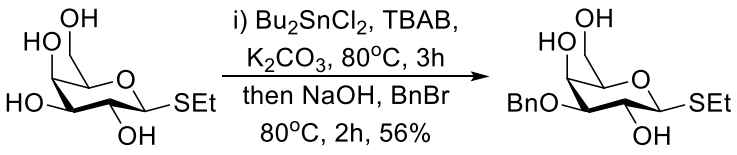
General Methods

All reagents and solvents were purchased from commercial sources and were used as received without further purification unless otherwise specified. Ethyl-β-D-thiogalactopyranoside **(B.1)** was purchased from Combi-Blocks (Lot #B48996). CH_2Cl_2, Et_2O, DMF, PhMe. and THF were purified by Innovative Technology's Pure-Solve System using basic alumina. 4Å molecular

sieves were activated prior to use by heating under reduced pressure. Cooling was achieved by use of Cryocool machine or ice/salt bath. Heating was achieved by use of a silicone oil bath with heating controlled by an electronic contact thermometer. Deionized water was used in the preparation of all aqueous solutions and for all aqueous extractions. Solvents used for extraction and chromatography were ACS or HPLC grade. Purification of reactions mixtures was performed by flash chromatography using SiliCycle SiliaFlash P60 (230-400 mesh). Yields indicate the isolated yield of the title compound with ≥95% purity as determined by ^{1}H NMR analysis. Diastereomeric ratios were determined by ^{1}H NMR analysis. Structural assignments were made with additional information from gHMBC experiments.

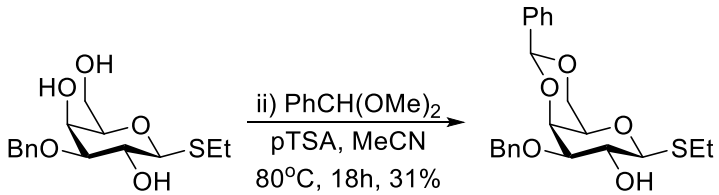
^{1}H NMR spectra were recorded on Varian vnmrs 700 (700 MHz), Varian vnmrs 500 (500 MHz), Varian MR400 (400 MHz), Bruker Avance Neo 500 (500 MHz) spectrometers and chemical shifts (δ) are reported in parts per million (ppm) with solvent resonance as the internal standard ($CDCl_3$ at δ 7.26, C_6D_6 at δ 7.16). Data are reported as (br = broad, s = singlet, d = doublet, t = triplet, q = quartet, m = multiplet; coupling constant(s) in Hz; integration). Proton-decoupled 13C NMR spectra were recorded on Varian vnmrs 700 (700 MHz), Varian vnmrs 500 (500 MHz), or Varian MR400 (400 MHz) spectrometers and chemical shifts (δ) are reported in ppm with solvent resonance as the internal standard ($CDCl_3$ at δ 77.16, C_6D_6 at 128.06). High resolution mass spectra (HRMS) were recorded on Agilent 6230 TOF or VG (Micromass) 70-250-S Magnetic sector mass spectrometers in the University of Michigan mass spectrometry laboratory. Optical rotations were measured in a solvent of choice on a JASCO P-2000 polarimeter at 589 nm (D-line).

Preparation of new compounds



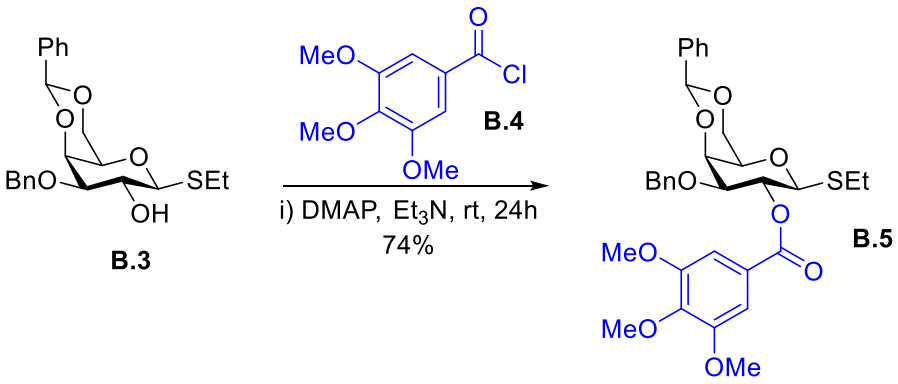
B.1 **B.2**

Ethyl-3-*O*-benzyl-β-D-thiogalactopyranoside (B.2): Ethyl-β-D-thiogalactopyranoside **B.1** (500 mg, 2.23 mmol, 1.0 eq) was added to a suspension of Bu_2SnCl_2 (68 mg, 0.223 mmol, 0.1 eq), K_2CO_3 (476 mg, 3.44 mmol, 1.5 eq), benzyl bromide (BnBr, 0.5 3mL, 4.45 mmol, 2.0 eq) and tetrabutylammonium bromide (TBAB, 52 mg, 0.223 mmol, 0.1 eq) in MeCN:DMF (10 mL:1 mL). The reaction was heated to 80 °C and stirred for three hours. Additional BnBr (0.53 mL, 4.45 mmol, 2.0 eq) and NaOH (138 mg, 3.44 mmol, 1.5 eq) was added to the reaction was stirred for an additional two hours at 80 °C. Upon completion determined by TLC, the solvents were removed *in vacuo*, and the crude residue was purified by flash column chromatography (50-75% EtOAc/hexanes) to afford **B.2** (395 mg, 56%) as a white solid. **HRMS** (ESI-TOF) (m/z): [M+Na]+ calcd for $C_{15}H_{22}O_5S$ 337.1080, found 337.1061. **^{1}H NMR** (700 MHz, $CDCl_3$) δ 7.47 – 7.31 (m, 5H), 4.83 – 4.70 (m, 2H), 4.31 (d, *J* = 9.7 Hz, 1H), 4.05 (s, 1H), 3.83 (t, *J* = 9.4 Hz, 1H), 3.80 (ddd, *J* = 12.3, 8.6, 4.4 Hz, 1H), 3.54 (t, *J* = 5.6 Hz, 1H), 3.45 (dd, *J* = 9.0, 3.2 Hz, 1H), 2.75 (qq, *J* = 13.5, 7.5 Hz, 2H), 2.59 (d, *J* = 1.9 Hz, 1H), 2.14 (dd, *J* = 8.6, 4.2 Hz, 1H), 1.31 (t, *J* = 7.4 Hz, 3H). **^{13}C NMR** (176 MHz, $CDCl_3$) δ 137.8, 128.8, 128.3, 128.1, 86.4, 81.4, 78.5, 72.4, 69.5, 67.7, 63.0, 24.3, 15.5.



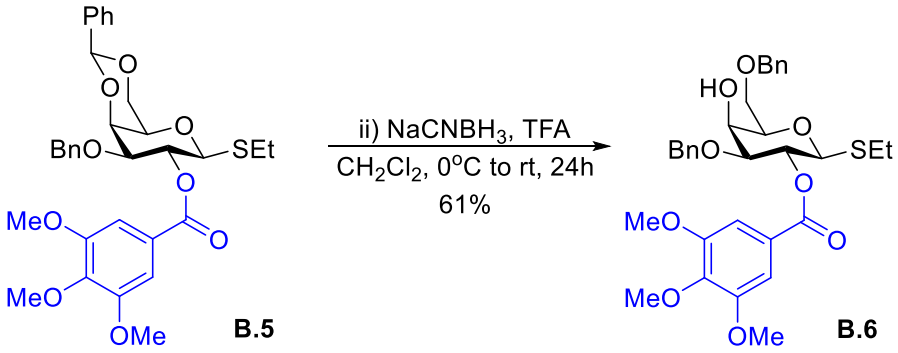
B.2 **B.3**

Ethyl-3-*O*-benzyl-4,6-*O*-benzylidene-β-D-thiogalactopyranoside (B.3): Benzaldehyde dimethyl acetal (0.36 mL, 2.38 mmol, 1.5 eq) was added dropwise to a solution of **B.2** (500 mg, 1.59 mmol, 1.0eq) and *para*-toluenesulfonic acid (pTSA, 23 mg, 0.119 mmol, 0.075 eq) in MeCN (3.0 mL, 0.5 M). The reaction was heated to reflux (80 ^{o}C) and stirred for 18 hours. The reaction was quenched by addition of Et_3N (0.10 mL) and the solvents were removed *in vacuo*. The crude residue was purified by flash column chromatography (10-30% EtOAc/hexanes) to afford **B.3** (197 mg, 31%) as a white solid. **HRMS** (ESI-TOF) (m/z): [M+Na]+ calcd for $C_{22}H_{26}O_5S$ 425.1393, found 425.1391. **^{1}H NMR** (400 MHz, $CDCl_3$) δ 7.50 (dd, *J* = 7.3, 2.3 Hz, 2H), 7.45 – 7.27 (m, 8H), 5.45 (s, 1H), 4.78 (d, *J* = 2.4 Hz, 2H), 4.34 (dd, *J* = 14.3, 11.0 Hz, 2H), 4.19 (d, *J* = 3.4 Hz, 1H), 4.07 (t, *J* = 9.4 Hz, 1H), 3.98 (dd, *J* = 12.4, 1.8 Hz, 1H), 3.50 (dd, *J* = 9.3, 3.3 Hz, 1H), 3.42 (s, 1H), 2.91 – 2.70 (m, 2H), 2.53 (s, 1H), 1.33 (t, *J* = 7.5 Hz, 3H). **^{13}C NMR** (101 MHz, cdcl$_3$) δ 137.8, 129.0, 128.5, 128.2, 127.9, 126.4, 101.3, 85.3, 80.3, 73.5, 71.5, 70.1, 69.4, 68.0, 22.9, 15.3. NMR spectra were in agreement with reported data.[47]



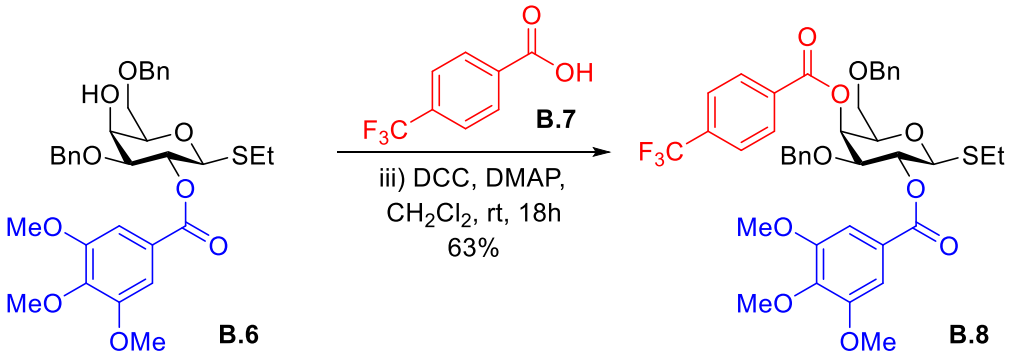
Ethyl-2-*O*-(3,4,5-trimethoxybenzoyl)-3-*O*-benzyl-4,6-*O*-benzylidene-β-D-thiogalactopyranoside (B.5): To a solution of **B.3** (46 mg, 0.114 mmol, 1.0 eq) and 4-dimethylaminopyridine (DMAP, 3 mg, 0.023 mmol, 0.2 eq) in Et_3N (0.5 mL) was added 3,4,5-trimethoxybenzoyl chloride **B.4** (106 mg, 0.458 mmol, 4.0 eq) and the reaction was stirred at room temperature for 24 hours. The reaction was quenched by addition of 5mL sat. aq. $NaHCO_3$,

and was then extracted with CH_2Cl_2 (3x5 mL). The combined organics were dried over Na_2SO_4 and concentrated *in vacuo*. The crude residue was purified by flash column chromatography (10-30% EtOAc/hexanes) to afford **B.5** (51 mg, 74%) as a white solid. **HRMS** (ESI-TOF) (m/z): [M+Na]+ calcd for $C_{32}H_{36}O_9S$ 619.1972, found 619.1961. **^{1}H NMR** (500 MHz, $CDCl_3$) δ 7.50 (dd, *J* = 7.6, 2.1 Hz, 2H), 7.42 – 7.26 (m, 10H), 5.45 (s, 1H), 4.77 (d, *J* = 3.0 Hz, 2H), 4.38 – 4.29 (m, 2H), 4.19 (dd, *J* = 3.5, 1.1 Hz, 1H), 4.07 (t, *J* = 9.4 Hz, 1H), 3.96 (s, 1H), 3.92 (s, 9H), 3.50 (dd, *J* = 9.2, 3.4 Hz, 1H), 3.42 (d, *J* = 1.4 Hz, 1H), 2.93 – 2.71 (m, 2H), 1.33 (t, *J* = 7.4 Hz, 3H). **^{13}C NMR** (126 MHz, $CDCl_3$) δ 162.3, 153.2, 143.9, 138.1, 137.8, 129.0, 128.5, 128.2, 127.9, 127.9, 126.4, 123.5, 107.9, 101.3, 85.3, 80.3, 73.6, 71.6, 70.2, 69.5, 68.0, 61.1, 56.4, 22.9, 15.3.



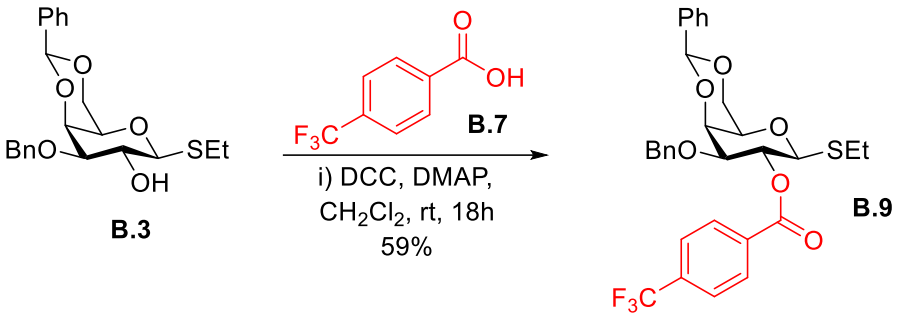
Ethyl-2-*O*-(3,4,5-trimethoxybenzoyl)-3,6-di-*O*-benzyl-β-D-thiogalactopyranoside (B.6): TFA (0.128 mL, 1.68 mmol, 20 eq) was added dropwise to a solution of **B.5** (50 mg, 0.084 mmol, 1.0 eq) and $NaCNBH_3$ (53 mg, 0.838 mmol, 10 eq) in Et_2O:CH_2Cl_2 (0.3 mL:0.6 mL) at 0 °C. The reaction was stirred for 24 hours while slowly warming to room temperature. The reaction was diluted with EtOAc (5 mL) and diluted with sat. aq. $NaHCO_3$ (10 mL). The organic layer was separated, and the aqueous layer was extracted with EtOAc (2x5 mL). The combined organic layers were washed with brine, then dried over Na_2SO_4 and concentrated *in vacuo*. The crude residue was purified by flash column chromatography (25-50% EtOAc/hexanes) to afford

B.6 (31 mg, 61%) as a white solid. **HRMS** (ESI-TOF) (m/z): [M+Na]+ calcd for $C_{32}H_{38}O_9S$ 621.2129, found 621.2159. **^{1}H NMR** (500 MHz, $CDCl_3$) δ 7.30 – 7.08 (m, 12H), 5.44 (t, *J* = 9.7 Hz, 1H), 4.62 (d, *J* = 12.4 Hz, 1H), 4.53 (s, 2H), 4.51 – 4.40 (m, 2H), 4.13 (d, *J* = 3.1 Hz, 1H), 3.85 (s, 3H), 3.82 (s, 6H), 3.79 – 3.67 (m, 2H), 3.65 – 3.53 (m, 2H), 2.72 – 2.59 (m, 2H), 1.16 (t, *J* = 7.4 Hz, 3H). **^{13}C NMR** (126 MHz, $CDCl_3$) δ 162.3, 153.2, 143.9, 138.1, 137.8, 129.0, 128.5, 128.2, 127.9, 127.9, 126.4, 123.5, 107.9, 101.3, 85.3, 80.3, 73.6, 71.6, 70.2, 69.5, 68.0, 61.1, 56.4, 22.9, 15.3.



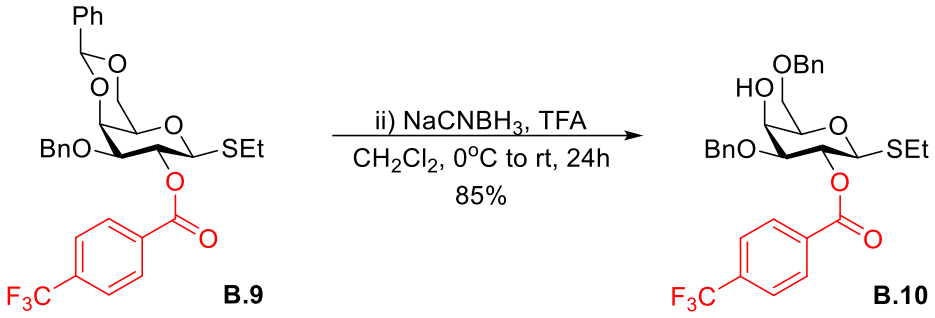
Ethyl-2-*O*-(3,4,5-trimethoxybenzoyl)-3,6-di-*O*-benzyl-4-*O*-(4-trifluoromethylbenzoyl)-β-D-thiogalactopyranoside (B.8): DMAP (1.0 mg, 0.01 mmol, 0.2 eq) was added to a solution of 4-(trifluoromethyl)benzoic acid **B.7** (19 mg, 0.10 mmol, 2.0 eq) and dicyclohexylcarbodiimide (DCC, 31 mg, 0.15 mmol, 3.0 eq) in CH_2Cl_2 (1.0 mL). The reaction was stirred for one hour at room temperature. **B.6** (30 mg, 0.05 mmol, 1.0 eq) was added in one portion and the reaction was stirred at room temperature for 18 hours. The reaction was filtered through Celite™ and the filtrate was concentrated *in vacuo*. The crude residue was purified by flash column chromatography (20-30% EtOAc) to afford **B.8** (24 mg, 63%) as a white solid. **HRMS** (ESI-TOF) (m/z): [M+Na]+ calcd for $C_{40}H_{41}O_{10}F_3S$ 793.2265, found 793.2248. **^{1}H NMR** (500 MHz, $CDCl_3$) δ 8.24 (d, *J* = 8.1 Hz, 2H), 7.78 (d, *J* = 8.2 Hz, 2H), 7.34 – 7.19 (m, 8H), 7.18 – 7.09 (m, 4H), 6.02 (d, *J* = 3.3 Hz, 1H), 5.55 (t, *J* = 9.8 Hz, 1H), 4.75 (d, *J* = 12.8 Hz, 1H), 4.68 (d, *J* =

10.1 Hz, 1H), 4.57 (dd, *J* = 12.3, 9.0 Hz, 2H), 4.47 (d, *J* = 11.8 Hz, 1H), 4.01 (d, *J* = 6.7 Hz, 1H), 3.98 (s, 3H), 3.92 (s, 6H), 3.85 (dd, *J* = 9.6, 3.3 Hz, 1H), 3.72 (dd, *J* = 9.4, 5.6 Hz, 1H), 3.62 (dd, *J* = 9.4, 7.5 Hz, 1H), 2.94 – 2.73 (m, 2H), 1.33 (t, *J* = 7.5 Hz, 3H). **^{13}C NMR** (126 MHz, $CDCl_3$) δ 165.0, 164.6, 152.9, 142.5, 137.3, 137.2, 134.7 (q, *J* = 32.7 Hz), 132.9, 130.4, 128.4, 128.3, 128.1, 128.0, 127.9, 127.7, 125.6 (q, *J* = 3.8 Hz), 124.6, 107.2, 83.9, 76.2, 73.8, 70.8, 69.6, 67.7, 67.6, 61.0, 56.3, 24.0, 15.0. **^{19}F NMR** (471 MHz, $CDCl_3$) δ -63.1. **$[\alpha]_D^{24}$** = + 67.2 (*c* = 0.17, CH_2Cl_2).



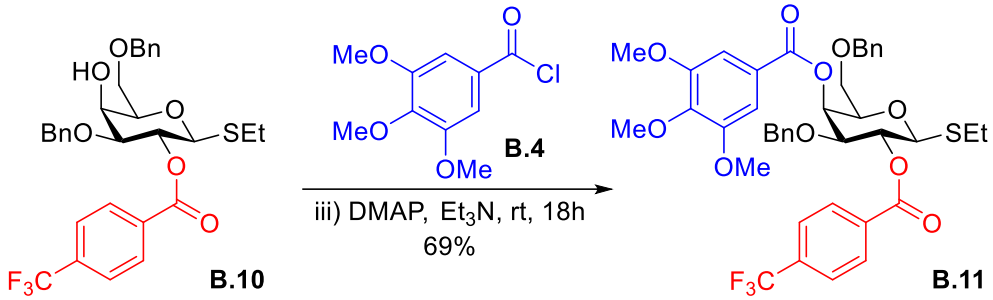
Ethyl-2-*O*-(4-trifluoromethylbenzoyl)-3-*O*-benzyl-4,6-*O*-benzylidene-β-D-thiogalactopyranoside (B.9): DMAP (3.0 mg, 0.025 mmol, 0.2 eq) was added to a solution of 4-(trifluoromethyl)benzoic acid **B.7** (47 mg, 0.249 mmol, 2.0 eq) and dicyclohexylcarbodiimide (DCC, 77 mg, 0.373 mmol, 3.0 eq) in CH_2Cl_2 (1.0 mL). The reaction was stirred for one hour at room temperature. **B.3** (50 mg, 0.124 mmol, 1.0 eq) was added in one portion and the reaction was stirred at room temperature for 18 hours. The reaction was filtered through Celite™ and the filtrate was concentrated *in vacuo*. The crude residue was purified by flash column chromatography (10-30% EtOAc) to afford **B.9** (42 mg, 59%) as a white solid. **HRMS** (ESI-TOF) (m/z): [M+Na]+ calcd for $C_{30}H_{29}O_6F_3S$ 597.1529, found 597.1559. **^{1}H NMR** (500 MHz, $CDCl_3$) δ 8.11 (d, *J* = 8.1 Hz, 2H), 7.72 (d, *J* = 8.2 Hz, 2H), 7.61 – 7.52 (m, 2H), 7.44 – 7.34 (m, 3H), 7.23 – 7.12 (m, 4H), 5.72 (t, *J* = 9.7 Hz, 1H), 5.52 (s, 1H), 4.69 (d, *J* = 12.8 Hz, 1H), 4.59 (d, *J* = 12.8 Hz, 1H), 4.54 (d, *J* = 9.8 Hz, 1H), 4.37 (dd, *J* = 12.4, 1.6 Hz, 1H), 4.30 (d, *J* = 3.7

Hz, 1H), 4.03 (dd, *J* = 12.4, 1.7 Hz, 1H), 3.75 (dd, *J* = 9.6, 3.4 Hz, 1H), 3.51 – 3.47 (m, 1H), 2.91 (dq, *J* = 12.3, 7.5 Hz, 1H), 2.76 (dq, *J* = 12.2, 7.4 Hz, 1H), 1.28 (t, *J* = 7.7 Hz, 3H). **^{13}C NMR** (126 MHz, $CDCl_3$) δ 164.2, 137.8 (d, *J* = 2.0 Hz), 134.5 (q, *J* = 32.7 Hz), 133.4, 130.3, 129.2, 128.5, 128.4, 128.0, 127.8, 126.6, 125.5 (q, *J* = 3.7 Hz), 101.5, 82.8, 78.2, 73.4, 71.1, 70.3, 69.5, 69.4, 33.9, 22.9, 15.0. **^{19}F NMR** (471 MHz, $CDCl_3$) δ -63.1.



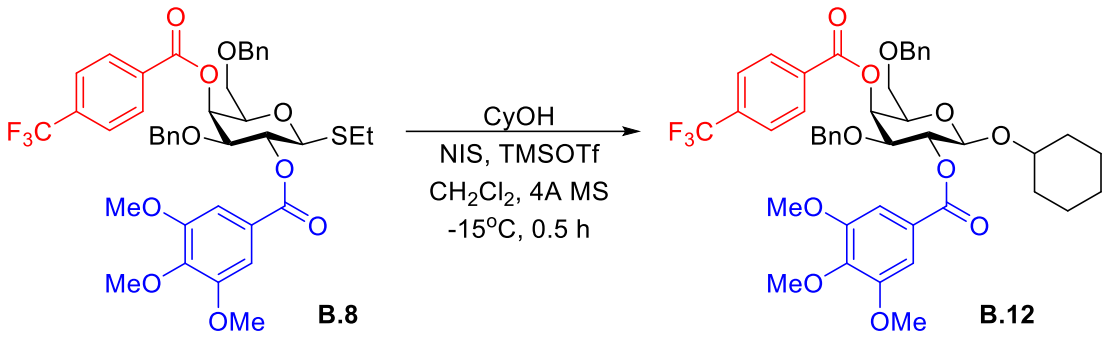
Ethyl-2-*O*-(4-trifluoromethylbenzoyl)-3,6-di-*O*-benzyl-β-D-thiogalactopyranoside (B.10): TFA (0.135 mL, 1.4 mmol, 20 eq) was added dropwise to a solution of **B.9** (40 mg, 0.070 mmol, 1.0 eq) and $NaCNBH_3$ (44 mg, 0.70 mmol, 10 eq) in CH_2Cl_2 (1.0 mL) at 0 °C. The reaction was stirred for 24 hours while slowly warming to room temperature. The reaction was diluted with EtOAc (5 mL) and diluted with sat. aq. $NaHCO_3$ (10 mL). The organic layer was separated, and the aqueous layer was extracted with EtOAc (2x5 mL). The combined organic layers were washed with brine, then dried over Na_2SO_4 and concentrated *in vacuo*. The crude residue was purified by flash column chromatography (5-20% EtOAc/hexanes) to afford **B.10** (34 mg, 85%) as a white solid. **HRMS** (ESI-TOF) (m/z): [M+Na]+ calcd for $C_{30}H_{31}O_6F_3S$ 599.1686, found 599.1729. **^{1}H NMR** (500 MHz, $CDCl_3$) δ 8.08 (d, *J* = 8.1 Hz, 2H), 7.71 (d, *J* = 8.1 Hz, 2H), 7.40 – 7.28 (m, 5H), 7.22 – 7.04 (m, 5H), 5.52 (t, *J* = 9.6 Hz, 1H), 4.69 (d, *J* = 12.3 Hz, 1H), 4.60 (s, 2H), 4.57 – 4.45 (m, 2H), 4.21 (d, *J* = 3.2 Hz, 1H), 3.83 (dd, *J* = 9.8, 6.3 Hz, 1H), 3.79 (s, 0H), 3.69 (t, *J* = 6.0 Hz, 1H), 3.65 (dd, *J* = 9.3, 3.2 Hz, 1H), 2.81 – 2.65 (m, 2H), 2.64 (d, *J* = 5.8 Hz, 1H), 1.22 – 1.12 (m, 3H). **^{13}C NMR** (126 MHz, $CDCl_3$) δ 164.4, 138.0, 137.2, 134.7 (q, *J* = 32.6

Hz), 133.3, 130.4, 128.6 (d, *J* = 3.3 Hz), 128.2, 128.0, 125.5 (q, *J* = 3.7 Hz), 83.4, 79.4, 73.9, 71.4, 70.2, 69.1, 66.4, 29.5, 23.8, 15.0. **^{19}F NMR** (471 MHz, $CDCl_3$) δ -63.1.

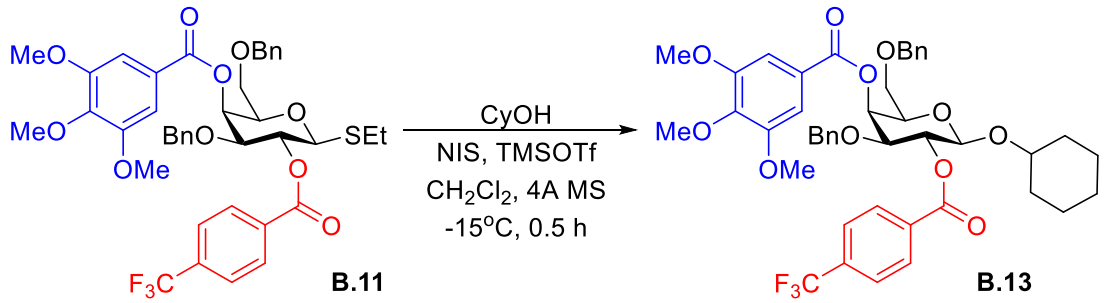


Ethyl-2-*O*-(4-trifluoromethylbenzoyl)-3,6-di-*O*-benzyl-4-*O*-(3,4,5-trimethoxybenzoyl)-β-D-thiogalactopyranoside (B.11): To a solution of **B.10** (70 mg, 0.121 mmol, 1.0 eq) and 4-dimethylaminopyridine (DMAP, 55 mg, 0.486 mmol, 4.0 eq) in 1:1 Et_3N/CH_2Cl_2 (4.0 mL) was added 3,4,5-trimethoxybenzoyl chloride **B.4** (112 mg, 0.486 mmol, 4.0 eq) and the reaction was stirred at room temperature for 18 hours. The reaction was quenched by addition of 5mL sat. aq. $NaHCO_3$, and was then extracted with CH_2Cl_2 (3x5 mL). The combined organics were dried over Na_2SO_4 and concentrated *in vacuo*. The crude residue was purified by flash column chromatography (10-30% EtOAc/hexanes) to afford **B.11** (64 mg, 69%) as a white solid. **HRMS** (ESI-TOF) (m/z): [M+Na]+ calcd for $C_{40}H_{41}O_{10}F_3S$ 793.2265, found 793.2273. **^{1}H NMR** (500 MHz, $CDCl_3$) δ 8.05 (dd, *J* = 8.1, 0.0 Hz, 2H), 7.71 (d, *J* = 8.2 Hz, 2H), 7.37 (s, 2H), 7.33 – 7.22 (m, 4H), 7.19 – 7.15 (m, 1H), 7.14 – 7.03 (m, 4H), 5.94 (d, *J* = 3.1 Hz, 1H), 5.59 (t, *J* = 9.8 Hz, 1H), 4.70 (d, *J* = 12.8 Hz, 1H), 4.61 – 4.40 (m, 4H), 3.94 (d, *J* = 4.0 Hz, 9H), 3.77 (dd, *J* = 9.6, 3.2 Hz, 1H), 3.69 (dd, *J* = 9.5, 5.7 Hz, 1H), 3.59 (dd, *J* = 9.5, 7.2 Hz, 1H), 2.89 – 2.69 (m, 2H), 1.25 (t, *J* = 7.6 Hz, 3H). **^{13}C NMR** (126 MHz, $CDCl_3$) δ 165.6, 164.3, 142.7, 137.6, 137.4, 130.4, 128.6, 128.4, 128.2, 128.0, 127.9, 125.52, 125.49, 125.46, 124.8, 107.3, 83.4, 77.3, 76.5, 73.9, 70.8, 69.8, 68.2, 67.2, 61.1, 56.3, 23.4, 14.9. **$[\alpha]_D^{24}$** = + 104.5 (*c* = 0.67, CH_2Cl_2).

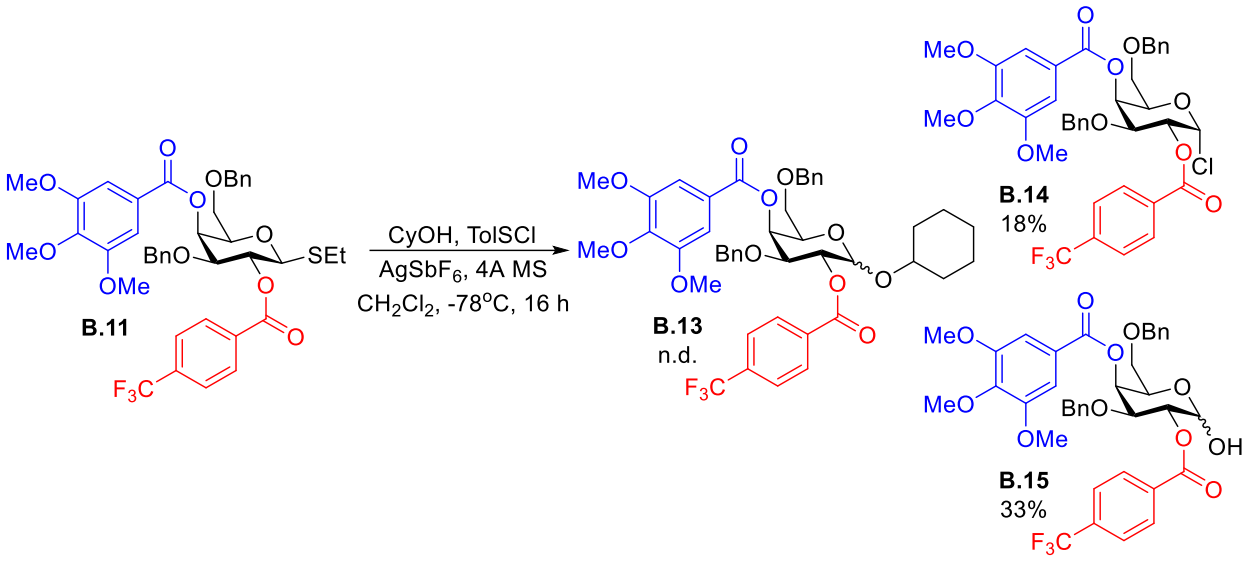
Studies of C2/C4 directed glycosylation of thiogalactosides



Glycosylation with C2-EDG,C4-EWG Thioglycloisde B.12: Thioglycoside **B.8** (10 mg, 0.013 mmol, 1.0 eq) was added to a flame dried flask with freshly activated 4Å molecular sieves (100 mg) and the flask was purged with N_2 for five minutes. Anhydrous CH_2Cl_2 (0.5 mL) was charged into the flask, and the mixture was stirred for 30 minutes at room temperature. The mixture was cooled to -15 ^oC (3:1 ice:NaCl) and CyOH (3 µL, 0.026 mmol, 2.0 eq) was added. The mixture was stirred for an additional five minutes, then NIS (4.4 mg, 0.020 mmol, 1.5 eq) and TMSOTf (0.5 µL, 0.003 mmol, 0.2 eq) were added to the reaction at -15 ^oC under N_2 atmosphere. The reaction was stirred for 30 minutes at -15 ^oC, at which time complete consumption of **B.8** was observed by TLC (30% EtOAc/hexanes) and HRMS. The reaction was quenched with Et_3N (20 µL) at -15 ^oC, then was warmed to room temperature. The crude reaction was filtered through Celite^{TM}, and the filtrate was concentrated in vacuo. The crude residue was dissolved in $CDCl_3$ (0.6 mL) and CH_2Br_2 (2 µL, internal standard) was added. The NMR-yield (**B.12,** 79%) and diastereomeric ratio (β-only) were determined by ^{1}H-NMR analysis.



Glycosylation with C2-EWG,C4-EDG Thioglycloisde B.13: Thioglycoside **B.11** (0.8 mg, 0.0013 mmol, 1.0 eq) was added to a flame dried flask with freshly activated 4Å molecular sieves (50 mg) and the flask was purged with N_2 for five minutes. Anhydrous CH_2Cl_2 (0.5 mL) was charged into the flask, and the mixture was stirred for 30 minutes at room temperature. The mixture was cooled to -15 ^oC (3:1 ice:NaCl) and CyOH (0.3 µL, 0.0026 mmol, 2.0 eq) was added. The mixture was stirred for an additional five minutes, then NIS (0.4 mg, 0.0020 mmol, 1.5 eq) and TMSOTf (0.1 µL, 0.0006 mmol, 0.5 eq) were added to the reaction at -15 ^oC under N_2 atmosphere. The reaction was stirred for 30 minutes at -15 ^oC, at which time complete consumption of **B.11** was observed by TLC (30% EtOAc/hexanes) and HRMS. The reaction was quenched with Et_3N (20µL) at -15^oC, then was warmed to room temperature. The crude reaction was filtered through Celite^{TM}, and the filtrate was concentrated in vacuo. The crude residue was dissolved in $CDCl_3$ (0.6 mL) and CH_2Br_2 (5 µL, internal standard) was added. The NMR-yield (**B.13**, 67%) and diastereomeric (β -only) ratio were determined by ^{1}H-NMR analysis.



Glycosylation with C2-EWG,C4-EDG Thioglycloisde B.11: Thioglycoside **B.11** (10 mg, 0.013 mmol, 1.0 eq) and $AgSbF_6$ (5.0 mg, 0.020 mmol, 1.5 eq) were added to a flame dried flask

with freshly activated 4Å molecular sieves (100 mg) and the flask was purged with N_2 for five minutes. Anhydrous mixture of Et_2O:CH_2Cl_2 (3:1) (0.5 mL) was charged into the flask, and the mixture was stirred for 30 minutes at room temperature. The mixture was cooled to -78 ^oC (Neslab Cryobath C8-80) and CyOH (3 µL, 0.026 mmol, 2.0 eq) was added. The mixture was stirred for an additional five minutes, then TolSCl (2.5 µL, 0.016 mmol, 1.2 eq) was added to the reaction at -78 ^oC under N_2 atmosphere. The reaction was stirred for 16 hours at -78 ^oC. The reaction was quenched with Et_3N (20 µL) at -78 ^oC, then was warmed to room temperature. The crude reaction was filtered through Celite^{TM}, and the filtrate was concentrated in vacuo. The crude residue was dissolved in C_6D_6 (0.6 mL) and CH_2Br_2 (2 µL, internal standard) was added. The yield of observed major products (**B.14,** 18% and **B.15**, 33%) were determined by ^{1}H-NMR analysis.

B.5 References

(1) Jiang, H.; Qin, X.; Wang, Q.; Xu, Q.; Wang, J.; Wu, Y.; Chen, W.; Wang, C.; Zhang, T.; Xing, D.; Zhang, R. Application of Carbohydrates in Approved Small Molecule Drugs: A Review. *European Journal of Medicinal Chemistry* **2021**, *223*, 113633. https://doi.org/10.1016/j.ejmech.2021.113633.

(2) Bhutani, P.; Joshi, G.; Raja, N.; Bachhav, N.; Rajanna, P. K.; Bhutani, H.; Paul, A. T.; Kumar, R. U.S. FDA Approved Drugs from 2015–June 2020: A Perspective. *J. Med. Chem.* **2021**. *64 (5),* 2339–2381. https://doi.org/10.1021/acs.jmedchem.0c01786.

(3) Wang, J.; Zhang, Y.; Lu, Q.; Xing, D.; Zhang, R. Exploring Carbohydrates for Therapeutics: A Review on Future Directions. *Frontiers in Pharmacology* **2021**, *12*.

(4) Marianski, M.; Mucha, E.; Greis, K.; Moon, S.; Pardo, A.; Kirschbaum, C.; Thomas, D. A.; Meijer, G.; von Helden, G.; Gilmore, K.; Seeberger, P. H.; Pagel, K. Remote Participation during Glycosylation Reactions of Galactose Building Blocks: Direct Evidence from Cryogenic Vibrational Spectroscopy. *Angewandte Chemie International Edition* **2020**, *59* (15), 6166–6171. https://doi.org/10.1002/anie.201916245.

(5) Hettikankanamalage, A. A.; Lassfolk, R.; Ekholm, F. S.; Leino, R.; Crich, D. Mechanisms of Stereodirecting Participation and Ester Migration from Near and Far in Glycosylation and Related Reactions. *Chem Rev.* **2020**. *120 (15),* 7104–7151. https://doi.org/10.1021/acs.chemrev.0c00243.

(6) Adero, P. O.; Amarasekara, H.; Wen, P.; Bohé, L.; Crich, D. The Experimental Evidence in Support of Glycosylation Mechanisms at the SN1–SN2 Interface. *Chem. Rev.* **2018**, *118* (17), 8242–8284. https://doi.org/10.1021/acs.chemrev.8b00083.

(7) Martin, A.; Arda, A.; Désiré, J.; Martin-Mingot, A.; Probst, N.; Sinaÿ, P.; Jiménez-Barbero, J.; Thibaudeau, S.; Blériot, Y. Catching Elusive Glycosyl Cations in a Condensed Phase with HF/SbF5 Superacid. *Nature Chem* **2016**, *8* (2), 186–191. https://doi.org/10.1038/nchem.2399.

(8) Hashimoto, Y.; Tanikawa, S.; Saito, R.; Sasaki, K. β-Stereoselective Mannosylation Using 2,6-Lactones. *J. Am. Chem. Soc.* **2016**, *138* (45), 14840–14843. https://doi.org/10.1021/jacs.6b08874.

(9) Mucha, E.; Marianski, M.; Xu, F.-F.; Thomas, D. A.; Meijer, G.; von Helden, G.; Seeberger, P. H.; Pagel, K. Unravelling the Structure of Glycosyl Cations via Cold-Ion Infrared Spectroscopy. *Nat Commun* **2018**, *9* (1), 4174. https://doi.org/10.1038/s41467-018-06764-3.

(10) Kwan, E. E.; Zeng, Y.; Besser, H. A.; Jacobsen, E. N. Concerted Nucleophilic Aromatic Substitutions. *Nature Chem* **2018**, *10* (9), 917–923. https://doi.org/10.1038/s41557-018-0079-7.

(11) Ha, S.; Lee, Y.; Kwak, Y.; Mishra, A.; Yu, E.; Ryou, B.; Park, C.-M. Alkyne–Alkene [2 + 2] Cycloaddition Based on Visible Light Photocatalysis. *Nat Commun* **2020**, *11* (1), 2509. https://doi.org/10.1038/s41467-020-16283-9.

(12) Loco, D.; Chataigner, I.; Piquemal, J.-P.; Spezia, R. Efficient and Accurate Description of Diels-Alder Reactions Using Density Functional Theory**. *ChemPhysChem* **2022**, *23* (18), e202200349. https://doi.org/10.1002/cphc.202200349.

(13) Marianski, M.; Supady, A.; Ingram, T.; Schneider, M.; Baldauf, C. Assessing the Accuracy of Across-the-Scale Methods for Predicting Carbohydrate Conformational Energies for the Examples of Glucose and α-Maltose. *J. Chem. Theory Comput.* **2016**, *12* (12), 6157–6168. https://doi.org/10.1021/acs.jctc.6b00876.

(14) Greis, K.; Kirschbaum, C.; Leichnitz, S.; Gewinner, S.; Schöllkopf, W.; von Helden, G.; Meijer, G.; Seeberger, P. H.; Pagel, K. Direct Experimental Characterization of the Ferrier Glycosyl Cation in the Gas Phase. *Org. Lett.* **2020**, *22* (22), 8916–8919. https://doi.org/10.1021/acs.orglett.0c03301.

(15) Bhuma, N.; Lebedel, L.; Yamashita, H.; Shimizu, Y.; Abada, Z.; Ardá, A.; Désiré, J.; Michelet, B.; Martin-Mingot, A.; Abou-Hassan, A.; Takumi, M.; Marrot, J.; Jiménez-Barbero, J.; Nagaki, A.; Blériot, Y.; Thibaudeau, S. Insight into the Ferrier Rearrangement by Combining Flash Chemistry and Superacids. *Angewandte Chemie International Edition* **2021**, *60* (4), 2036–2041. https://doi.org/10.1002/anie.202010175.

(16) Fu, Y.; Bernasconi, L.; Liu, P. Ab Initio Molecular Dynamics Simulations of the SN1/SN2 Mechanistic Continuum in Glycosylation Reactions. *J. Am. Chem. Soc.* **2021**, *143* (3), 1577–1589. https://doi.org/10.1021/jacs.0c12096.

(17) Petschenka, G.; Züst, T.; Hastings, A. P.; Agrawal, A. A.; Jander, G. Chapter Ten - Quantification of Plant Cardenolides by HPLC, Measurement of Na+/K+-ATPase Inhibition Activity, and Characterization of Target Enzymes. In *Methods in Enzymology*; Jez, J., Ed.; Biochemical Pathways and Environmental Responses in Plants: Part B; Academic Press, 2023; Vol. 680, pp 275–302. https://doi.org/10.1016/bs.mie.2022.08.003.

(18) Vorm, S. van der; Hansen, T.; Hengst, J. M. A. van; Overkleeft, H. S.; Marel, G. A. van der; Codée, J. D. C. Acceptor Reactivity in Glycosylation Reactions. *Chem. Soc. Rev.* **2019**, *48* (17), 4688–4706. https://doi.org/10.1039/C8CS00369F.

(19) Li, G.; Luo, Y.; Mo, J.; Noguchi, M.; Jing, J.; Luo, Z.; Shoda, S.; Ye, X.-S. Hydrogen Bond-Assisted 1,2-Cis O-Glycosylation under Mild Hydrogenolytic Conditions. *Chinese Chemical Letters* **2023**, *34* (4), 107754. https://doi.org/10.1016/j.cclet.2022.107754.

(20) Gou, X.-Y.; Li, Y.; Shi, W.-Y.; Luan, Y.-Y.; Ding, Y.-N.; An, Y.; Huang, Y.-C.; Zhang, B.-S.; Liu, X.-Y.; Liang, Y.-M. Ruthenium-Catalyzed Stereo- and Site-Selective Ortho- and Meta-C−H Glycosylation and Mechanistic Studies. *Angewandte Chemie International Edition* **2022**, *61* (32), e202205656. https://doi.org/10.1002/anie.202205656.

(21) Pal, K. B.; Guo, A.; Das, M.; Báti, G.; Liu, X.-W. Superbase-Catalyzed Stereo- and Regioselective Glycosylation with 2-Nitroglycals: Facile Access to 2-Amino-2-Deoxy-O-Glycosides. *ACS Catal.* **2020**, *10* (12), 6707–6715. https://doi.org/10.1021/acscatal.0c00753.

(22) Colombo, M. I.; Rúveda, E. A.; Stortz, C. A. Regioselectivity of the Glycosylation of N-Dimethylmaleoyl-Protected Hexosamine Acceptors. An Experimental and DFT Approach. *Org. Biomol. Chem.* **2011**, *9* (8), 3020–3025. https://doi.org/10.1039/C1OB00021G.

(23) Elferink, H.; Mensink, R. A.; Castelijns, W. W. A.; Jansen, O.; Bruekers, J. P. J.; Martens, J.; Oomens, J.; Rijs, A. M.; Boltje, T. J. The Glycosylation Mechanisms of 6,3-Uronic Acid Lactones. *Angewandte Chemie International Edition* **2019**, *58* (26), 8746–8751. https://doi.org/10.1002/anie.201902507.

(24) Huang, M.; Garrett, G. E.; Birlirakis, N.; Bohé, L.; Pratt, D. A.; Crich, D. Dissecting the Mechanisms of a Class of Chemical Glycosylation Using Primary 13C Kinetic Isotope Effects. *Nature Chem* **2012**, *4* (8), 663–667. https://doi.org/10.1038/nchem.1404.

(25) Vorm, S. van der; Hansen, T.; Overkleeft, H. S.; Marel, G. A. van der; Codée, J. D. C. The Influence of Acceptor Nucleophilicity on the Glycosylation Reaction Mechanism. *Chem. Sci.* **2017**, *8* (3), 1867–1875. https://doi.org/10.1039/C6SC04638J.

(26) Tanaka, M.; Nakagawa, A.; Nishi, N.; Iijima, K.; Sawa, R.; Takahashi, D.; Toshima, K. Boronic-Acid-Catalyzed Regioselective and 1,2-Cis-Stereoselective Glycosylation of Unprotected Sugar Acceptors via SNi-Type Mechanism. *J. Am. Chem. Soc.* **2018**, *140* (10), 3644–3651. https://doi.org/10.1021/jacs.7b12108.

(27) Whitfield, D. M.; Nukada, T. DFT Studies of the Role of C-2–O-2 Bond Rotation in Neighboring-Group Glycosylation Reactions. *Carbohydrate Research* **2007**, *342* (10), 1291–1304. https://doi.org/10.1016/j.carres.2007.03.030.

(28) Moon, S.; Chatterjee, S.; Seeberger, P. H.; Gilmore, K. Predicting Glycosylation Stereoselectivity Using Machine Learning. *Chem. Sci.* **2021**, *12* (8), 2931–2939. https://doi.org/10.1039/D0SC06222G.

(29) Alibay, I.; Bryce, R. A. Ring Puckering Landscapes of Glycosaminoglycan-Related Monosaccharides from Molecular Dynamics Simulations. *J. Chem. Inf. Model.* **2019**, *59* (11), 4729–4741. https://doi.org/10.1021/acs.jcim.9b00529.

(30) Kwok, R. W.; Marianski, M. On the Remote Group Participation Mechanism in Glycosylation Reaction. *Manuscript in Preparation* **2023**.

(31) Pardo-Vargas, A.; Delbianco, M.; Seeberger, P. H. Automated Glycan Assembly as an Enabling Technology. *Current Opinion in Chemical Biology* **2018**, *46*, 48–55. https://doi.org/10.1016/j.cbpa.2018.04.007.

(32) Wen, L.; Edmunds, G.; Gibbons, C.; Zhang, J.; Gadi, M. R.; Zhu, H.; Fang, J.; Liu, X.; Kong, Y.; Wang, P. G. Toward Automated Enzymatic Synthesis of Oligosaccharides. *Chem Rev.* **2018**. *118 (17)*, 8151–8187. https://doi.org/10.1021/acs.chemrev.8b00066.

(33) Chen, J.; Zhai, Z.; Edgar, K. J. Recent Advances in Polysaccharide-Based in Situ Forming Hydrogels. *Current Opinion in Chemical Biology* **2022**, *70*, 102200. https://doi.org/10.1016/j.cbpa.2022.102200.

(34) Crich, D.; Dai, Z.; Gastaldi, S. On the Role of Neighboring Group Participation and Ortho Esters in β-Xylosylation: 13C NMR Observation of a Bridging 2-Phenyl-1,3-Dioxalenium Ion. *J. Org. Chem.* **1999**, *64* (14), 5224–5229. https://doi.org/10.1021/jo990424f.

(35) Pittman, C. U.; McManus, S. P.; Larsen, J. W. 1,3-Dioxolan-2-Ylium and Related Heterocyclic Cations. *Chem. Rev.* **1972**, *72* (4), 357–438. https://doi.org/10.1021/cr60278a003.

(36) Greis, K.; Kirschbaum, C.; Fittolani, G.; Mucha, E.; Chang, R.; von Helden, G.; Meijer, G.; Delbianco, M.; Seeberger, P. H.; Pagel, K. Neighboring Group Participation of Benzoyl Protecting Groups in C3- and C6-Fluorinated Glucose. *European Journal of Organic Chemistry* **2022**, *2022* (15), e202200255. https://doi.org/10.1002/ejoc.202200255.

(37) Greis, K.; Leichnitz, S.; Kirschbaum, C.; Chang, C.-W.; Lin, M.-H.; Meijer, G.; von Helden, G.; Seeberger, P. H.; Pagel, K. The Influence of the Electron Density in Acyl Protecting Groups on the Selectivity of Galactose Formation. *J. Am. Chem. Soc.* **2022**, *144* (44), 20258–20266. https://doi.org/10.1021/jacs.2c05859.

(38) Demchenko, A. V.; Rousson, E.; Boons, G.-J. Stereoselective 1,2-Cis-Galactosylation Assisted by Remote Neighboring Group Participation and Solvent Effects. *Tetrahedron Letters* **1999**, *40* (36), 6523–6526. https://doi.org/10.1016/S0040-4039(99)01203-4.

(39) Gerbst, A. G.; Ustuzhanina, N. E.; Grachev, A. A.; Tsvetkov, D. E.; Khatuntseva, E. A.; Nifant'ev, N. E. Effect of the Nature of Protecting Group at O-4 on Stereoselectivity of Glycosylation by 4-O-Substituted 2,3-Di-O-Benzylfucosyl Bromides. *Mendeleev Communications* **1999**, *9* (3), 114–116. https://doi.org/10.1070/MC1999v009n03ABEH001073.

(40) Gerbst, A. G.; Ustuzhanina, N. E.; Grachev, A. A.; Khatuntseva, E. A.; Tsvetkov, D. E.; Whitfield, D. M.; Berces, A.; Nifantiev, N. E. Synthesis, Nmr, and Conformational Studies of Fucoidan Fragments. Iii.[1] Effect of Benzoyl Group at O-3 on Stereoselectivity of Glycosylation by 3-O- and 3,4-Di-O-Benzoylated 2-O-Benzylfucosyl Bromides. *Journal of Carbohydrate Chemistry* **2001**, *20* (9), 821–831. https://doi.org/10.1081/CAR-100108659.

(41) Crich, D. En Route to the Transformation of Glycoscience: A Chemist's Perspective on Internal and External Crossroads in Glycochemistry. *J. Am. Chem. Soc.* **2021**, *143* (1), 17–34. https://doi.org/10.1021/jacs.0c11106.

(42) Ande, C.; Crich, D. Stereodirecting Effect of Esters at the 4-Position of Galacto- and Glucopyranosyl Donors: Effect of 4-C-Methylation on Side-Chain Conformation and Donor Reactivity, and Influence of Concentration and Stoichiometry on Distal Group Participation. *J. Org. Chem.* **2023**, *88* (19), 13883–13893. https://doi.org/10.1021/acs.joc.3c01496.

(43) Zhang, Y.-M.; Mallet, J.-M.; Sinaÿ, P. Glycosylation Using a One-Electron-Transfer, Homogeneous Reagent. Application to an Efficient Synthesis of the Trimannosyl Core of N-Glycosylproteins. *Carbohydrate Research* **1992**, *236*, 73–88. https://doi.org/10.1016/0008-6215(92)85007-M.

(44) Zhang, Y.; Chen, C.; Gao, Y.; Yang, M.; He, Z.; Zhang, B.; Gu, G.; Tang, B.; Cai, F. β-l-Rhamnosylation and β-d-Mannosylation Mediated by 4-O-Ester Groups in a Weakly Nucleophilic Environment. *Org. Lett.* **2023**, *25* (39), 7120–7125. https://doi.org/10.1021/acs.orglett.3c02566.

(45) Bhattarai, B.; Nagorny, P. Enantioselective Total Synthesis of Cannogenol-3-O-α-l-Rhamnoside via Sequential Cu(II)-Catalyzed Michael Addition/Intramolecular Aldol Cyclization Reactions. *Org. Lett.* **2018**, *20* (1), 154–157. https://doi.org/10.1021/acs.orglett.7b03513.

(46) Franconetti, A.; Ardá, A.; Asensio, J. L.; Blériot, Y.; Thibaudeau, S.; Jiménez-Barbero, J. Glycosyl Oxocarbenium Ions: Structure, Conformation, Reactivity, and Interactions. *Acc. Chem. Res.* **2021**, *54* (11), 2552–2564. https://doi.org/10.1021/acs.accounts.1c00021.

(47) Mandal, S. S.; Liao, G.; Guo, Z. Chemical Synthesis of the Tumor-Associated Globo H Antigen. *RSC Adv.* **2015**, *5* (30), 23311–23319. https://doi.org/10.1039/C5RA00759C.